THE UNIVERSITY OF ADELAIDE

PHYSICAL AGEING AND DIMENSIONAL CHANGES OF ACRYLATE POLYMERS

A thesis submitted for the Degree of Doctor
of Philosophy in the Departments of Chemical Engineering
and Physical and Inorganic Chemistry.
June 1992

CHEE-HOONG LAI
B.Sc. (Hons.)

If a man is called to be a streetsweeper, he should sweep streets as Michelangelo painted, or Beethoven composed music, or Shakespeare wrote poetry. He should sweep streets so well that all the hosts of heaven and earth will pause to say, here lived a great streetsweeper who did his job well.

Martin Luther King Jr.

TABLE OF CONTENTS

SUMMARY vii

STATEMENT viii

ACKNOWLEDGEMENTS ix

CHAPTER 1

1.1 INTRODUCTION 1

BIBLIOGRAPHY 5

CHAPTER 2

LITERATURE REVIEW

2.1 PHYSICAL AGEING 9

2.2 FREE VOLUME MODELS

2.2.1 The Williams-Landel-Ferry (WLF) Model 11

2.2.2 The Simha-Boyer Model 15

2.2.3 The Struik Model 18

2.3 BASIC ASPECTS OF PHYSICAL AGEING

2.3.1 Physical Ageing Occurs Generally 21

2.3.2 The Timescale of Physical Ageing 22

2.3.3 The Thermoreversibility of Physical Ageing 24

2.3.4 The Temperature Range of Physical Ageing 24

2.3.5 The Non-Linearity and Asymmetry of Physical Ageing 27

2.3.6 The Single-Parameter Model for Volume Recovery 29

2.3.7 The Two-Parameter Model for Volume Recovery 31

2.3.8 The Multi-Parameter Model for Volume Recovery 33

2.3.9 Molecular Motions of Poly(Methyl Methacrylate) and Poly(*n*-Alkyl Methacrylates) 35

2.3.10 Mechanical Modelling of Molecular Behaviour 38

2.3.11 Physical Ageing and Residual Stresses 40

2.3.12 Physical Ageing and The Glass Transition 47

2.3.14 Physical Ageing and The Thermal Expansion Coefficient 51

BIBLIOGRAPHY 58
GLOSSARY OF SYMBOLS 67

CHAPTER 3

EXPERIMENTAL AND VALIDITY OF MEASURING TECHNIQUE

3.1 MATERIALS: DESCRIPTION 69

3.2 POLYMER CURING AND CASTING 70

3.3 THERMOMECHANICAL ANALYSER (TMA) 71

3.4 VALIDITY OF MEASURING TECHNIQUE
- 3.4.1 Dimensional Chages Arising From Residual Stresses and Physical Ageing 73
- 3.4.2 Dimensional Changes Arising From the Sorption and Desorption of Diluents 77
- 3.4.3 Dimensional Changes Arising From Viscoelastic Deformation 77
- 3.4.4 Dimensional Changes Arising From Molecular Deformation 77

SUMMARY 78

BIBLIOGRAPHY 79

CHAPTER 4

PHYSICAL AGEING IN PMMA

4.1 INTRODUCITON 81

4.2 SAMPLE PREPARATION AND EXPERIMENTAL 82

4.3 LENGTH CONTRACTION AS A QUANTITATIVE MEASURE OF FREE VOLUME 83

4.4 RESULTS AND DISCUSSION
- 4.4.1 Free Volume Fraction 84
- 4.4.2 Temperature Range for Length Contraction 88
- 4.4.3 Thermal Expansion Coefficient 91
- 4.4.4 Relaxation Times for Length Contraction 96

4.4.5 Gruneisen Constant for Poly(Methyl Methacrylate) 97

4.5 SUMMARY 99

BIBLIOGRAPHY 100
GLOSSARY OF SYMBOLS 104

CHAPTER 5

ISOTHERMAL PHYSICAL AGEING OF PMMA

5.1 INTRODUCTION 106

5.2 EXPERIMENTAL 107

5.3 RESULTS AND DISCUSSION
5.3.1 Isothermal Ageing
Length Contraction 108
Relaxation Rates and Relaxation Times 111
Activation Energy for Physical Ageing 116
5.3.2 Sequential Ageing
Length Contraction 119
Relaxation Rates 120

5.4 SUMMARY 122

BIBLIOGRAPHY 123
GLOSSARY OF SYMBOLS 126

CHAPTER 6

RANDOMISATION AND PHYSICAL AGEING IN ORIENTED PMMA

6.1 INTRODUCTION 127

6.2 EXPERIMENTAL 129

6.3 RESULTS AND DISCUSSION
6.3.1 Quenched Oriented PMMA
Dimensional Changes 129
Thermal Expansion Coefficient 132

6.3.2 Slow-Cooled Oriented PMMA
Length Changes Under a Constant Heating Rate 133
Length Changes During Sequential Ageing 134
Relaxation Times and Free Volume Fraction 135
Activation Energy of Randomisation 135

6.4 SUMMARY 137

BIBLIOGRAPHY 138
GLOSSARY OF SYMBOLS 140

CHAPTER 7
PHYSICAL AGEING AND MOLECULAR WEIGHT

7.1 INTRODUCTION 141

7.2 EXPERIMENTAL 143

7.3 RESULTS AND DISCUSSION
7.3.1 Viscosity-Molecular Weight Relationship 144
7.3.2 Free Volume Fraction 146
7.3.3 Length Contraction At a Constant Rate of Heating 149
7.3.4 Dimensional Changes of Low Molecular Weight PMMA 149
Free Volume Fraction 151
Relaxation Times and Activation Energy 152

7.4 SUMMARY 153

APPENDIX
Measurement of Viscosity 154
Determination of Molecular Weight 154

BIBLIOGRAPHY 156
GLOSSARY OF SYMBOLS 158

CHAPTER 8
PHYSICAL AGEING AND PLASTICISATION

8.1 INTRODUCTION 160

8.2 EXPERIMENTAL 161

8.3 RESULTS AND DISCUSSION
8.3.1 Length Contraction At a Constant Heating Rate 163
8.3.2 Glass Transition Temperature of PMMA Plasticised With DBP 164
8.3.3 Free Volume Fraction of Plasticised PMMA 167
8.3.4 Thermal Expansion Coefficient of Plasticised PMMA 170
8.3.5 Isothermal Ageing of Quenched PMMA Plasticised With DBP 172
Length Contraction and Free Volume Fraction 172
Rates of Relaxation and Activation Energies 173

8.4 SUMMARY 176

BIBLIOGRAPHY 177
GLOSSARY OF SYMBOLS 180

CHAPTER 9
PHYSICAL AGEING IN CROSSLINKED POLYMERS

9.1 INTRODUCTION 181

9.2 EXPERIMENTAL 184

9.3 RESULTS AND DISCUSSION
9.3.1 Length Contraction 186
9.3.2 Thermal Expansion Coefficient 188

9.4 SUMMARY 192

BIBLIOGRAPHY 193
GLOSSARY OF SYMBOLS 197

CHAPTER 10
PHYSICAL AGEING IN POLY(2-HYDROXYETHYL METHACRYLATE)

10.1 INTRODUCTION 198

10.2 EXPERIMENTAL
10.2.1 Preparation of PHEMA Specimens 202

10.2.2 Hydration of PHEMA Specimens 202
10.2.3 Preparation of PHEMA-KBr Specimens 203
10.2.4 Preparation of Poly(HEMA-co-EGDMA) Specimens 204

10.3 RESULTS AND DISCUSSION
10.3.1 Physical Ageing of Dry and Partially-Hydrated PHEMA 204
10.3.2 Effect of Crosslinking on Physical Ageing of Dry PHEMA 207
10.3.3 Physical Ageing of Dry PHEMA-KBr Polymers 208

10.4 SUMMARY 210

BIBLIOGRAPHY 210
GLOSSARY OF SYMBOLS 215

CHAPTER 11

EFFECT OF SUBSTITUENTS ON PHYSICAL AGEING OF ACRYLATE POLYMERS

11.I INTRODUCTION 216

11.2 EXPERIMENTAL 217

11.3 RESULTS AND DISCUSSION
11.3.1 Length Contraction 217
11.3.2 Thermal Expansion Coefficient 220

11.4 SUMMARY 222

BIBLIOGRAPHY 223

CONCLUSION 225

SUMMARY OF THESIS FOR THE DEGREE OF DOCTOR OF PHILOSOPHY

Chee-Hoong Lai
Department of Physical and Inorganic Chemistry
University of Adelaide
South Australia

PHYSICAL AGEING AND DIMENSIONAL CHANGES OF ACRYLATE POLYMERS

A novel technique for investigating the nature and structure of glassy acrylic polymers, in particular poly(methyl methacrylate) (PMMA), has been developed by studying the dimensional changes of these polymers using a thermomechanical analyser (TMA).

Physical ageing describes a complex process in which an amorphous material in a non-equilibrium state undergoes spontaneous and gradual changes in properties (e.g. decrease in specific volume, increase in creep retardation times, reduction in internal energy, etc.) towards attaining an equilibrium structure. In this work, physical ageing is characterised by length contraction in the glass transition region. The contraction is associated with the collapse of free volume, which is a hypothetical concept used to explain the observed changes during physical ageing. These contractions deviate from the idealised volume-temperature curves which portray T_g as the intersection of the extrapolated liquid and glass lines. The magnitude of length contraction provided a quantitative measure of free volume fraction (f), in which values of f for quenched polymers were found to range from 0.08 to 0.26, but decreased to 0.05-0.06 for slow-cooled PMMA. In addition, free volume fraction was also found to be affected by changes in molecular weight, plasticisation, side-group and main-chain substituents and crosslinking. These variations in free volume fraction leads to the conclusion that a single, "universal" value, as proposed by the Simha-Boyer and Williams-Landel-Ferry theories, is unlikely.

This thesis also investigates of the effects of molecular orientation and residual stresses on the dimensional changes of PMMA. A preliminary study on the dimensional instability of hydrated poly(2-hydroxyethyl methacrylate) (PHEMA) is also presented, in which length measurements may represent a potentially useful tool in elucidating the distribution of water in PHEMA.

STATEMENT

The candidate, Chee-Hoong Lai, declares that:

(a) this thesis contains no material which has been accepted for the award of any other degree and diploma in any University, and that, to the best of the candidate's knowledge and belief, the thesis contains no material previously published or written by another person except where due reference is made in the text of the thesis; and

(b) the author consents to the thesis being made available for photocopying and loan if applicable if accepted for the award of the degree.

Chee-Hoong Lai

June 1992

ACKNOWLEDGEMENTS

The completion of this thesis signifies the end of my active involvement with the University of Adelaide which has spanned a period of more than eight years. Throughout the duration of my study and the preparation of this manuscript, I have received a lot of help from many sources, to whom I am always grateful.

My foremost thanks and gratitude go to my supervisors, Dr. Peter E.M. Allen and Dr. David R.G. Williams, for their continued support, guidance and assistance throughout the course of my studies. In particular, I wish to thank my supervisors for their comments and critical assessment of preliminary drafts of this thesis.

My association with the Departments of Physical and Inorganic Chemistry and Chemical Engineering also extends to other members of the teaching staff and the workshop, to whom I thank for their assistance. I would like to acknowledge my friends in both departments, in particular Dr. Darrell Bennett, Tony Clayton and Darren Miller, for their friendship and unique contribution to my life. I must also mention Dr. "Chrus" Adams, with whom I had many titanic battles on the squash court.

A number of people have also contributed generously with their time and resources. In particular, I wish to thank the Crouch family for their warmth and the loan of a car, and Alison for her love, encouragement and prayers. Kerry Beaumont also deserves special mention for her word processing skills and all-round help during the final stages of this work. I am fortunate to have had a long and happy stay at Lincoln College, and I wish to thank Dr. Geoffrey Scott and other members of the administrative staff for their help and care over the years. I am grateful for the fellowship and memories of many friends, some of whom have since returned to their home countries, while there are others who are still completing their studies. I would like to thank my friends and the pastoral staff at the Austral-Asian Christian Church at Kent Town.

Finally, I would not have been able to arrive at this level of tertiary study without the unfailing love and financial support of my parents and family. A special thanks go to my parents, for the many sacrifices they had to make to ensure that I had the opportunity to study overseas. I am also grateful for the award of a postgraduate scholarship at the University of Adelaide.

CHAPTER 1

1.1 INTRODUCTION

The purpose of this research is to investigate the nature and structure of glassy polymers by studying linear dimensional changes using a thermomechanical analyser (TMA). The increasing use of polymers in engineering and biomedical industries imposes stringent demands on the dimensional stability of polymeric structures and products as a desired property. For example, the application of large space structures (e.g. Space Telescope, Mars Observer Optical Bench, etc.) in the aerospace industry requires high structural precision and long-term dimensional stability of polymer materials incorporated into these structures [1]. Extensive literature reports [1-31] alluding to the study of the effects of dimensional instability on polymer properties testify to the interest and significance of maintaining the dimensional integrity of a material over long periods of time.

The main source of dimensional instability in polymers arises from physical ageing [21, 32], which constitutes a process where an amorphous material undergoes spontaneous and gradual structural rearrangement towards attaining an equilibrium structure. The rearrangement arises from the non-equilibrium nature of the glassy state, therefore physical ageing takes place as long as the material is cooled rapidly past T_g and remains at a temperature below T_g. During cooling from above to below T_g the material solidifies and hardens, but the rate of cooling period is too fast for the material to make the necessary adjustments to reduce its excess volume and entropy, which become frozen-in at T_g. Volume relaxation studies [18-20] have revealed that the molecular mobility below T_g is not zero, and consequently there is a slow and gradual reduction in these properties towards equilibrium values.

Physical ageing is an important phenomenon because it affects the mechanical [2-9], electrical [10-12] and calorimetric [13-17] properties of polymers. Some of the effects of ageing include decreases in internal energy, creep rate, stress relaxation rate and dielectric relaxation, while increases in elastic modulus, yield strength, density and relaxation times are observed. A striking illustration of the ageing effect in poly(vinyl chloride) (PVC) is shown in Figure 1.1, which shows that for a change in ageing time from 0.03 to 1000 days the creep is retarded by a factor of 10^4-10^5 [21]. Since the working temperatures of most glassy polymers

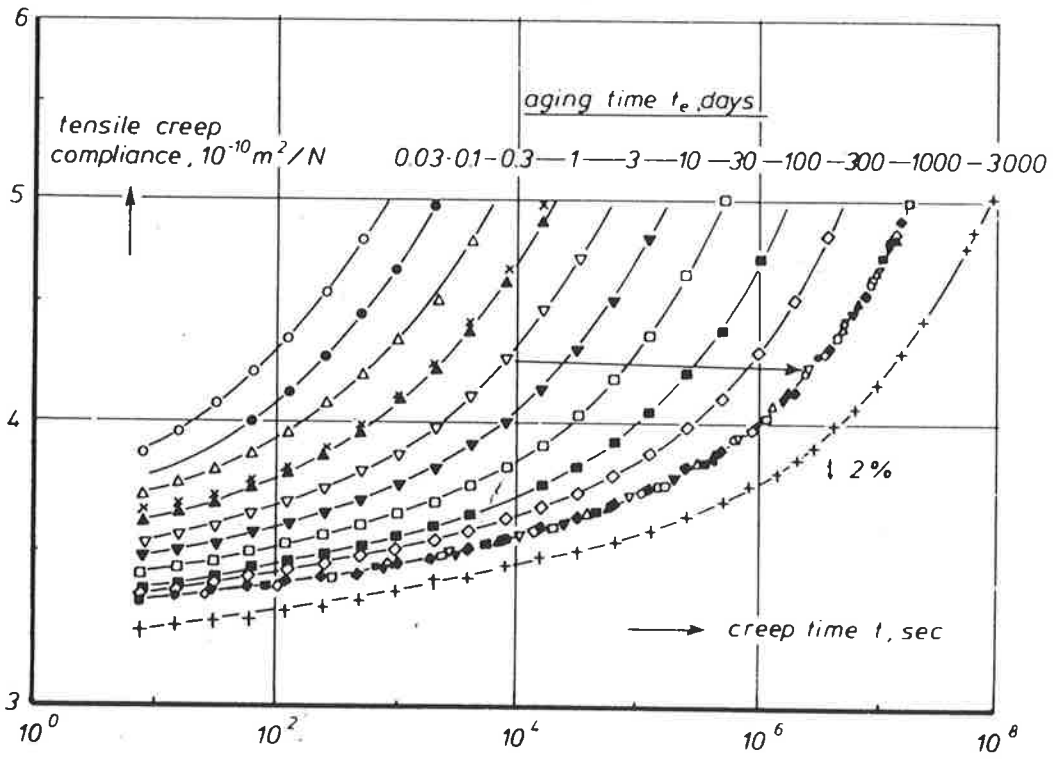

Figure 1.1 Small-strain creep curves of rigid PVC quenched from 90 C (i.e. about 10 C above T_g) to 40 C and kept at 40 C for a period of four years. The different curves were measured for various times t_e elapsed after the quench. An increase in the ageing time from 0.03 days to 1000 days resulted in a change in the creep retardation by a factor of 10^4 - 10^5 (reproduced from [21]).

are normally below their glass transition, physical ageing has to be considered in the prediction of their long-term behaviour and performance. However, although the phenomenon of physical ageing has been studied extensively, the mechanism of ageing is not well understood. In view of the importance of dimensional stability in the long-term performance of a material, a detailed investigation is necessary to characterise dimensional changes which arise from physical ageing. One of the aims of this work will be to distinguish and separate the changes associated with physical ageing from those associated with different processes, for example, randomisation, viscous flow and the relieve of internal stresses.

It been known for many years that most amorphous materials are unstable in their glass states [18-21, 33-34], where the specific volume of glassy polymers has been observed to spontaneously decrease below T_g [18-31]. Jones [34] reported "anomalies" in the form of a contraction in property-temperature relationships of rapidly cooled polymers when determined near T_g. A "general hysteresis phenomena" was observed by Rehage and Borchard [35], when a material, after cooling from the melt to below T_g, is reheated. The heating curve does not retrace the cooling curve but instead lies below it (Fig. 1.2). The heating and cooling curves later rejoins at some temperature above T_g. However, the hysteresis was predicted by Volkenshtein and Ptitsyn [36] to be small, and a number of authors [6, 37-38] could find no discernible hysteresis effect from their experiments. A number of researchers [18-20, 32] realised that a comprehensive and detailed study of physical ageing in amorphous polymers was necessary. Struik's extensive treatise [32] on the subject shows that physical ageing is a very complex process and it affects a number of polymer properties. Physical ageing must not be confused with chemical ageing, which affects the chemical structure of the material, usually by decomposition or degradation.

The free volume concept [39-43] has been utilised to explain experimental observations. However, a unified free volume theory has not been established because it is still a matter of debate whether the formation of the glass-rubber transition is a kinetic [18-21, 26-27, 32] or a thermodynamic [22, 44-47] phenomenon. Experiments to resolve these arguments have been considered to be infeasible because equilibrium at a temperature just a few degrees below T_g cannot be reached within a reasonable experimental timescale [19]. In spite of the advancements made in the understanding of ageing, many textbooks [e.g. 48-49] and reviews [50] continue to present volume-temperature curves which do not show any manifestation of

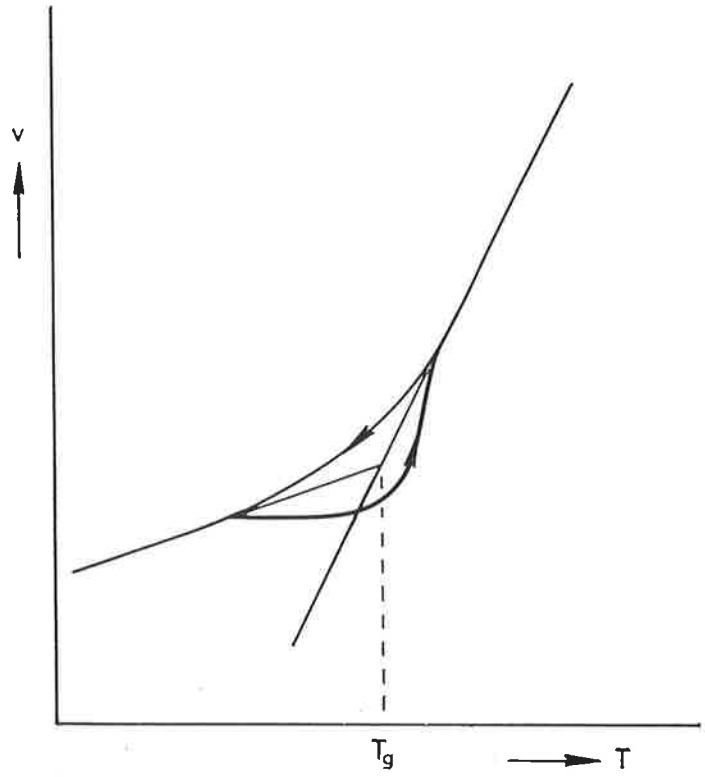

Figure 1.2 Volume hysteresis in amorphous polymers: after cooling from above to below T_g, the heating curve does not retrace the cooling curve. Physical ageing in glassy amorphous polymers results in a lowering of the specific volume (v) as the glass transition is approached (reproduced from [35]).

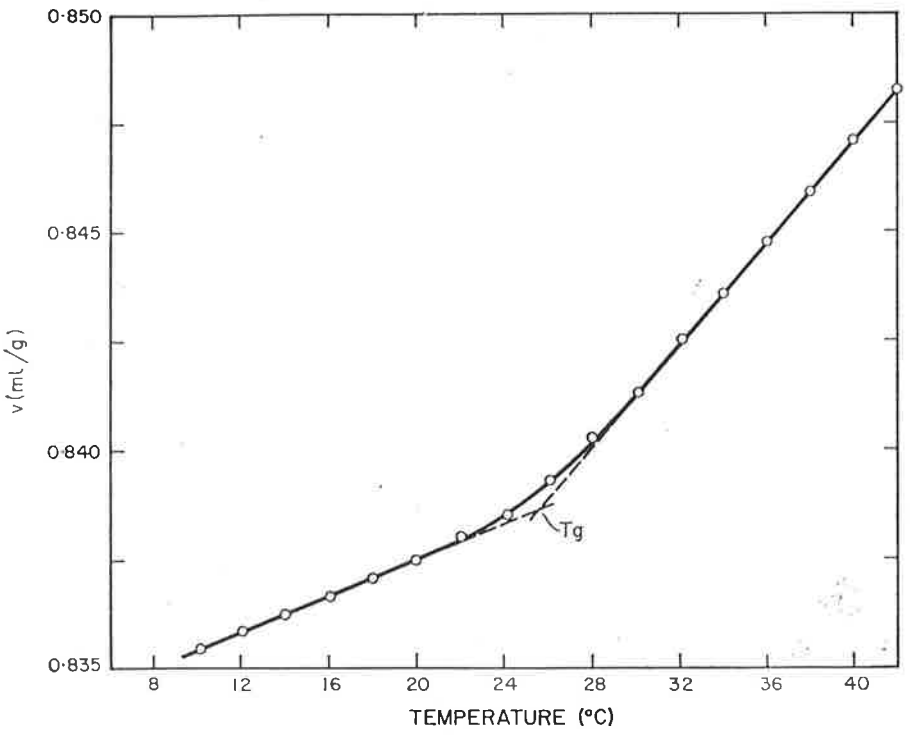

Figure 1.3 Specific volume of poly(vinyl acetate) as a function of temperature but with no evidence of physical ageing. The glass transition is taken as the intersection of the extrapolated glass and liquid lines (reproduced from [48]).

physical ageing. Figure 1.3 shows a typical volume-temperature (V-T) plot but in practise this curve is only produced on cooling from the rubbery state to the glass state. The hysteresis effect described by Rehage and Borchard [35] is observed when the polymer is heated to above T_g.

Simha and Boyer [51] (SB) have proposed that the glass and liquid expansion coefficients obtained from the slopes of V-T curves are related to the free volume fraction of the polymer. Along with the Williams-Landel-Ferry (WLF) equation [52], the SB equation predicts that the free volume fraction is constant at T_g, although conflicting evidence have been reported [53-59]. In addition, the thermal expansion coefficient is related to the empirical Gruneisen parameter [60-62], which describes the state of bonding and molecular motions in polymer solids. Another objective of this work is to examine the proposals of the SB and WLF theories by establishing a procedure in which the free volume fraction can be measured from dimensional changes associated with physical ageing.

The glass transition temperature is observed to be dependent on the timescale of the experiment [18-19], in which a rapid rate of cooling results in a higher T_g than for slow-cooled polymers (Fig. 2.3). Physical ageing is closely associated with the glass transition as both phenomena involves structural rearrangement upon a transition from an unstable glass to the equilibrium liquid state. It follows that the factors which affect the observation of the glass transition will also affect physical ageing in the same way. In order for any length-temperature curve to be meaningful, a prior knowledge of the polymer history and experimental details is essential. Because of the complexity involved in the interpretation and deconvolution of such curves, it is important that the specimen history is uncomplicated.

Linear and crosslinked acrylic polymers were chosen for study because of their availability and widespread use. Amorphous atactic PMMA exhibits a distinct glass-liquid transition which is accompanied by marked contraction in length. These observations make PMMA a suitable polymer for research, since its ageing behaviour and free volume fraction can be accurately characterised. The free volume fractions can be compared with the results of Simha and Boyer [51] to ascertain whether length contraction represents a direct measure of the free volume. The TMA was chosen because not only does it possess high sensitivity, but it also reveals other dimensional changes that can occur simultaneously with physical ageing. The high rate of data acquisition of the TMA allows rapid scanning of a wide range of samples with

different thermal histories. The more conventional technique for studying dimensional changes in polymers is volume dilatometry. Physical ageing is not manifest in volume dilatometry because of the lengthy periods (of the order of hours) [63-65] between measurements necessary for thermal equilibration. As the temperature approaches T_g, the timescale of relaxational processes which take place during ageing becomes shorter, hence these processes occur undetected during thermal equilibration.

A comprehensive review of the literature pertinent to physical ageing and topics relevant to ageing is presented in Chapter 2, which serves as a primary reference for the experimental chapters. The operations of the TMA are described in Chapter 3, along with the procedures for the preparation and casting of polymers. In addition, the validity of the TMA as a reliable technique for characterising dimensional changes in acrylate polymers is presented. The format of the experimental chapters (Chapters 3-11) is schematically represented by Figure 1.4, which indicates six different phenomena that result in dimensional instability: physical ageing, residual stresses, molecular orientation, the sorption and desorption of diluents and viscoelastic deformation. However, viscoelastic deformation occurs as a result of an applied stress at temperatures well above T_g, whereas dimensional changes arising from the other five processes take place as a result of structural rearrangement.

The effects of internal stresses generated during casting and rapid cooling from above to below T_g on the dimensional stability of PMMA are discussed in Chapter 3. Dimensional changes of PMMA arising from physical ageing are investigated as a function of thermal history and heating rate in Chapter 4. In this chapter, the observed dimensional changes are established as a quantitative measure of free volume. In addition, physical ageing may be characterised by thermal expansion coefficients and additional parameters such as the onset and endset temperatures of contraction. The ageing behaviour of PMMA under isothermal conditions is examined in Chapter 5 in which relaxation times and activation energies for ageing are obtained from the isothermal rates of contraction.

The dimensional instability of quenched oriented PMMA are presented in Chapter 6, in which dimensional changes associated with randomisation are measured parallel and perpendicular to the orientation axis. The activation energy of randomisation is also obtained from isothermal experiments and compared with the values obtained for physical ageing. The effect of varying the molecular weight on the ageing behaviour of PMMA is studied in Chapter

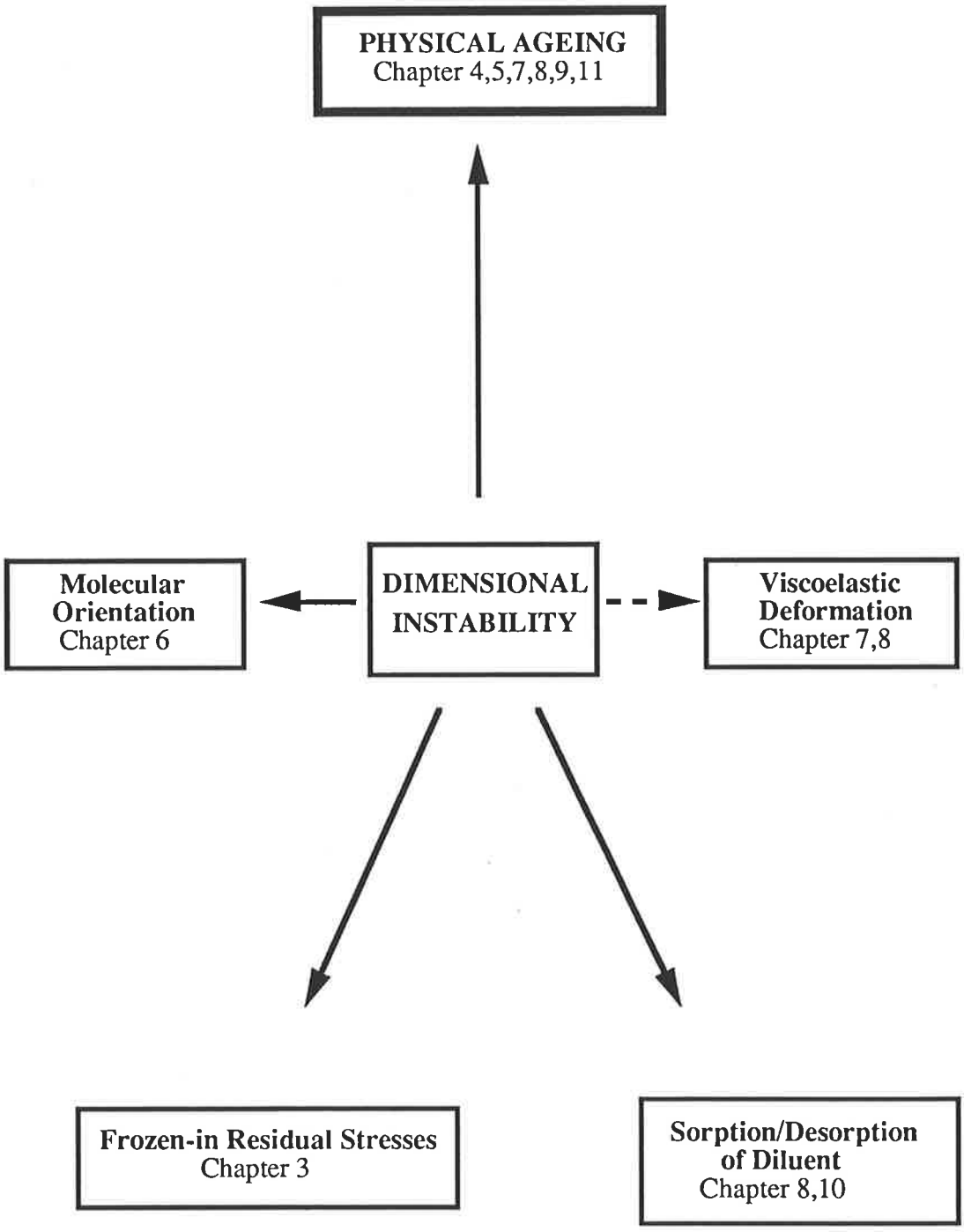

Figure 1.4 Dimensional instability of polymers arising from a number of different phenomena

7, in which three quenched PMMA specimens of varying molecular weights are investigated. The effect of plasticisation on the ageing behaviour of PMMA is studied in Chapter 8, where the dimensional changes of PMMA plasticised with three types of plasticiser are investigated. Chapter 9 presents the ageing behaviour of crosslinked PMMA, in which PMMA is copolymerised with a homologous series of [oligo(ethylene glycol) dimethacrylates]. An interesting study of the dimensional changes of dry and hydrated poly(2-hydroxyethyl methacrylate) is presented in Chapter 10. The effect of substituent groups on the α-position and the ester side group of poly(methyl acrylate) and a number of polymethacrylates is investigated in Chapter 11.

Chapter 1

1. S.S. Kim, H. Yavrouian and R.H. Liang, *Polym. Prepr.* **33(1)**, 1992.
2. K. Neki and P.H. Geil, *J. Macromol. Sci. Phys.* **B8**, 295 (1973).
3. L.J. Broutman and S.M. Krishnakumar, *Polym. Eng. Sci.* **16**, 74 (1976).
4. G. Levita and L.C.E. Struik, *Polymer* **24**, 1071 (1983).
5. T.D. Chang and J.O. Brittain, *Polym. Eng. Sci.* **22**, 1221, 1228 (1982).
6. E.S.W. Kong, *J. Appl. Phys.* **52**, 5921 (1981); *Composites Tech. Rev.* **4**, 97 (1982).
7. A.J. Hill, K.J. Heater and C.M. Agrawal, *J. Polym. Sci. Polym. Phys.* **28**, 387 (1990); *J. Mat. Sci. Lett.* **8**, 1414 (1989).
8. A.J. Hill and C.M. Agrawal, *J. Mat. Sci.* **25**, 5036 (1990).
9. E.S.W. Kong, *Adv. Polym. Sci.* **80**, 126 (1986).
10. N. Hill, W.E. Vaughn, A.H. Price and M. Davies, *Dielectric properties of Molecular Behaviour,* Van Nostrand Reinhold, London (1969).
11. M. Davies, ed., *Dielectric and Related Molecular Processes,* Volume **3**, The Chemical Society, London (1977).
12. P. Hedvig, *Dielectric Spectroscopy of Polymers,* Wiley, New York (1977).
13. C.R. Foltz and P.V. McKinney, *J. Appl. Polym. Sci.* **13**, 2235 (1969).
14. A. Gray and M. Gilbert, *Polymer* **17**, 44 (1976).
15. S.E.B. Petrie, *J. Polym. Sci. A2* **10**, 1255 (1972), *J. Macromol. Sci. Phys.* **B12(2)**, 225 (1976).

16. A.R. Berens and I.M. Hodge, *Macromolecules* **15**, 756, 762 (1982).

17. A.R. Berens and I.M. Hodge, *Macromolecules* **16**, 898 (1983).

18. A.J . Kovacs, *J. Polym. Sci.* **30**, 131 (1958).

19. A.J. Kovacs, *Fortschr Hochpolym. Forsch.* **3**, 394 (1963).

20. A.J. Kovacs, J.M. Hutchinson and J.J. Alkonis, *Proceedings of the Symposium on the Structure of Non-Crystalline Materials*, Cambridge, England (1976), P.H. Gaskell ed., Taylor and Francis (1977), p153.

21. L.C.E. Struik, *Polym. Eng. Sci.* **17(3)**, 165 (1977).

22. G. Goldbach and R. Rehage, *J. Polym. Sci.* **C16**, 2289 (1967); *Rheol. Acta* **6**, 30 (1967).

23. D.G. LeGrand, *J. Appl. Polym. Sci.* **13**, 2129 (1969).

24. L.C.E. Struik, *Rheol. Acta* **5**, 303 (1966); *Plast. Rubb. Process. Appl.* **2**, 41 (1982).

25. M.G. Wyzgoski, *Polym. Eng. Sci.* **16**, 265 (1976); *J. Appl. Polym. Sci.* **25**, 1443 (1980).

26. A.J. Kovacs, J.J. Aklonis, J.M. Hutchinson and A.R. Ramos, *J. Polym. Sci. Polym. Phys. Ed.* **17**, 1097 (1979).

27. R.E. Robertson, *J. Polym. Sci. Symp.* **63**, 173 (1978); *J. Polym. Sci. Phys.* **17**, 597 (1979).

28. G. Levita and T.L. Smith, *Polym. Eng. Sci.* **21**, 936 (1981).

29. M.R. Tant and G.L. Wilkes, *Polym. Eng. Sci.* **21**, 874 (1981).

30. C. Bauwens-Crowet and J.C. Bauwens, *Polymer* **23**, 1599 (1982).

31. H.H.D. Lee and F.J. McGarry, *J. Macromol. Sci. Phys.* **B29(1)**, 11-29 (1990); **B29(2&3)**, 185-202 (1990); **B29(2&3)**, 237-248 (1990).

32. L.C.E. Struik, *Physical Ageing in Amorphous Polymers and Other Materials*, Elsevier, Amsterdam (1978).

33. F. Simon, *Z. Anorg. Allgem. Chem.* **203**, 219 (1931).

34. G.O. Jones, *Glass*, Methuen (1956).

35. G. Rehage and W. Borchard, *The Physics of Glassy Polymers*, R.N. Haward ed., Applied Science (1973), Chapter One.

36. M.V. Volkenshtein and O.B. Ptitsyn, *Soviet Phys.-Tech. Phys.* **1**, 2138 (1957).

37. M.C. Shen and A. Eisenberg, *Progress in Solid State Chemistry* **3**, 407, Pergamon Press (1966).

38. P. Meares, *Trans. Faraday Soc.* **53**, 31 (1957).

39. T.G. Fox and P.J. Flory, *J. Appl. Phys.* **21**, 581 (1950); *J. Phys. Chem.* **55**, 221 (1951).

40. A.K. Doolittle, *J. Appl. Phys.* **22**, 1031, 1471 (1951); **23**, 236 (1952).

41. A. Bondi, *J. Phys. Chem.* **16**, 929 (1954).

42. F. Bueche, *J. Chem. Phys.* **21**, 1850 (1953); **24**, 418 (1956); **30**, 738 (1959); **36**, 2940 (1962).

43. J.D. Ferry and R.A. Stratton, *Kolloid Z.* **171**, 107 (1960).

44. F.E. Simon, *Ergeb. Exact Naturw.* **9**, 222 (1930).

45. W. Kauzmann, *Chem. Rev.* **43**, 219 (1948).

46. J.H. Gibbs, *J. Chem. Phys.* **25**, 185 (1956).

47. J.H. Gibbs and E.A. DiMarzio, *J. Chem. Phys.* **28**, 373, 807 (1958).

48. P. Meares, *Polymers: Structure and Bulk Properties*, Van Nostrand (1965).

49. J.M.G. Cowie, *Polymers: Chemistry and Physics of Modern Materials*, Intertext (1973).

50. J. Zarzycki ed., *Glasses and Amorphous Materials,* Volume **9**, *Materials Science and Technology, A Comprehensive Treatment,* R.W. Cahn, P. Haasen and E.J. Kramer eds., (1991).

51. R. Simha and R.F. Boyer, *J. Chem. Phys.* **37(5)**, 1003 (1962).

52. M.L. Williams, R.F. Landel and J.D. Ferry, *J. Am. Chem. Soc.* **77**, 3701 (1955).

53. R.A. Haldon and R. Simha, *J. Appl. Phys.* **39(3)**, 1890 (1968).

54. L.A. Wood, *J. Polym. Sci.* **28**, 319 (1958).

55. K.H. Illers, *Makromol. Chem.* **127**, 1 (1969).

56. J. Lal and G.S. Trick, *J. Polym. Sci.* **A2**, 4559 (1964).

57. M.L. Dannis, *J. Appl. Polym. Sci.* **1**, 121 (1959).

58. S. Krause, J.J Gormley, N. Roman, J.A. Shetter and W.H. Watanabe, *J. Polym. Sci.* **A3**, 3573-3586 (1965).

59. W.J. Schell, R. Simha and J.J. Aklonis, *J. Macromol. Sci. Chem.* **A3(7)**, 1297-1313 (1969).

60. E. Gruneisen, *Ann. Phys.* **10**, 211 (1908); **38**, 257 (1912).

61. O.L. Anderson, *Phys. Rev.* **144**, 553 (1966).

62. B. Hartmann, *Acustica* **36**, 24 (1976-1977).

63. N. Bekkedahl, Journal of Research of the National Bureau of Standards, Research Paper RP2016, **42**, 145 (1949).

64. O.S. Tyagi and D.D. Deshpande, *J. Appl. Polym. Sci.* **37**, 2041-2050 (1989).

65. H. Hocker, G.J. Blake, and P.J. Flory, *Trans. Faraday Soc.* **67**, 2251 (1971).

CHAPTER 2
LITERATURE REVIEW

2.1 PHYSICAL AGEING 9

2.2 FREE VOLUME MODELS

2.2.1 The Williams-Landel-Ferry (WLF) Model 11

2.2.2 The Simha-Boyer Model 15

2.2.3 The Struik Model 18

2.3 BASIC ASPECTS OF PHYSICAL AGEING

2.3.1 Physical Ageing Occurs Generally 21

2.3.2 The Timescale of Physical Ageing 22

2.3.3 The Thermoreversibility of Physical Ageing 24

2.3.4 The Temperature Range for Physical Ageing 24

2.3.5 The Non-Linearity and Asymmetry of Physical Ageing 27

2.3.6 The Single-Parameter Model for Volume Recovery 29

2.3.7 The Two-Parameter Model for Volume Recovery 31

2.3.8 The Multi-Parameter Model for Volume Recovery 33

2.3.9 Molecular Motions of Poly(Methyl Methacrylate) and Poly(*n*-Alkyl Methacrylates) 35

2.3.10 Mechanical Modelling of Molecular Behaviour 38

2.3.11 Physical Ageing and Residual Stresses 40

2.3.12 Physical Ageing and Annealing 45

2.3.13 Physical Ageing and The Glass Transition 47

2.3.14 Physical Ageing and The Thermal Expansion Coefficient 51

BIBLIOGRAPHY 58

GLOSSARY OF SYMBOLS 67

CHAPTER 2

2.1 PHYSICAL AGEING

Physical ageing has been known for many years as an inherent property of glassy materials [1-7]. Materials are said to age when their properties change with time; these changes occur because a non-equilibrium state is frozen-in during the cooling of the material from above to below T_g. Above T_g the relaxation times are short enough to enable material properties such as volume and entropy to follow the changes in temperature, but below T_g the retardation times become too long.

The consequence is a slow structural relaxation process that induces the following changes in material properties [8, 16, 19]: for example, isothermal contraction (densification) has been observed [5, 7] for amorphous polymers in their glassy state; creep-recovery tests for many glassy polymers have shown a horizontal shift towards increasing time with an increase in ageing time (Fig. 1.1); the direct-current conductivity of conducting polymers (e.g. polarised PVC) was found to be lowered by physical ageing, due to the reduction in the mobility of charge carriers (e.g. ions) by the decrease in vacant sites, thereby resulting in a loss in conductivity. The entropy and the internal energy of a polymer is reduced during physical ageing by continuously losing heat, although in exceedingly small amounts. When an aged sample is heated to above T_g, it reabsorbs the heat it lost during ageing and this is manifested as an endothermic peak in DSC measurements. The height of the peak increases with ageing time, and such peaks may be used as a convenient measure of the state of ageing in a sample.

Time-temperature superposition studies were developed in the 1950s [9-11] as a technique for studying the phenomenon of physical ageing. At that time it was established that for the temperature range just above T_g, a change in temperature caused a shift of the mechanical or dielectric relaxation curves along the logarithmic time scale. The shifting occured without appreciable change in shape, and this formed the basis for time-temperature superposition procedures. The whole effect of temperature upon relaxation can therefore be described by a shift function, log a(T), and this function applied to the mechanical relaxation of small strains, dielectric relaxations, as well to the mechanical behaviour at large strains, e.g. fracture behaviour of rubbery materials [12]. Since temperature only affected the position of the

response curve on the time scale, this implied that the mechanical response of a material can be characterised by a single time parameter, τ.

Experiments have shown a tremendous change of approximately 10 orders of magnitude in τ over the temperature range between T_g and 50-100 C above T_g. Williams, Landel and Ferry [9] have proposed that the variations in τ are primarily due to thermal expansion of free volume V_f with increasing temperature, and using an equation proposed by Doolittle [13] which connects viscosity with V_f, the famous WLF equation was derived. If the material was rapidly cooled through the glass transition range and subsequently kept at a constant temperature $T_a < T_g$, the retardation times below T_g become so long that the changes in V_f can no longer keep up with the cooling process. To a first approximation the value of V_f at T_g is frozen-in and V_f no longer decreases with temperature during further cooling from T_g to T_a (Fig. 2.1).

By applying the WLF equation to the temperature range below T_g a similar trend for τ can be expected, i.e. there is a sharp increase in τ during cooling from above T_g and a constant value of τ during further cooling from T_g to T_a (Fig. 2.1). Thus it was assumed that the constancy of V_f during cooling from T_g to T_a results in a similar constancy in τ [14]. However, several studies showed that at the isothermal temperature T_a the specific volume V slowly decreases with time [4-7]. This volume relaxation or ageing effect was explained by the gradual relaxation of the free volume V_f towards its equilibrium value, as indicated by the dashed line in Figure 2.1. According to the WLF treatment, a decrease in V_f will be accompanied by an increase in τ. Consequently, during isothermal ageing below T_g, the mechanical response curves will shift towards the right along the logarithmic time scale with no appreciable change in shape. An example of the superposition of creep curves of rigid PVC is shown in Figure 1.1.

In spite of its empirical success, the WLF equation had not proved the physical validity of the concept of free volume; this concept served only as an elegant means to interpret experimental facts [8]. Before further discussing the limitations of the WLF treatment, it is instructive to consider the general aspects of the WLF model and other free volume models.

2.2 FREE VOLUME MODELS

Central to physical ageing is the concept of free volume as a convenient way of

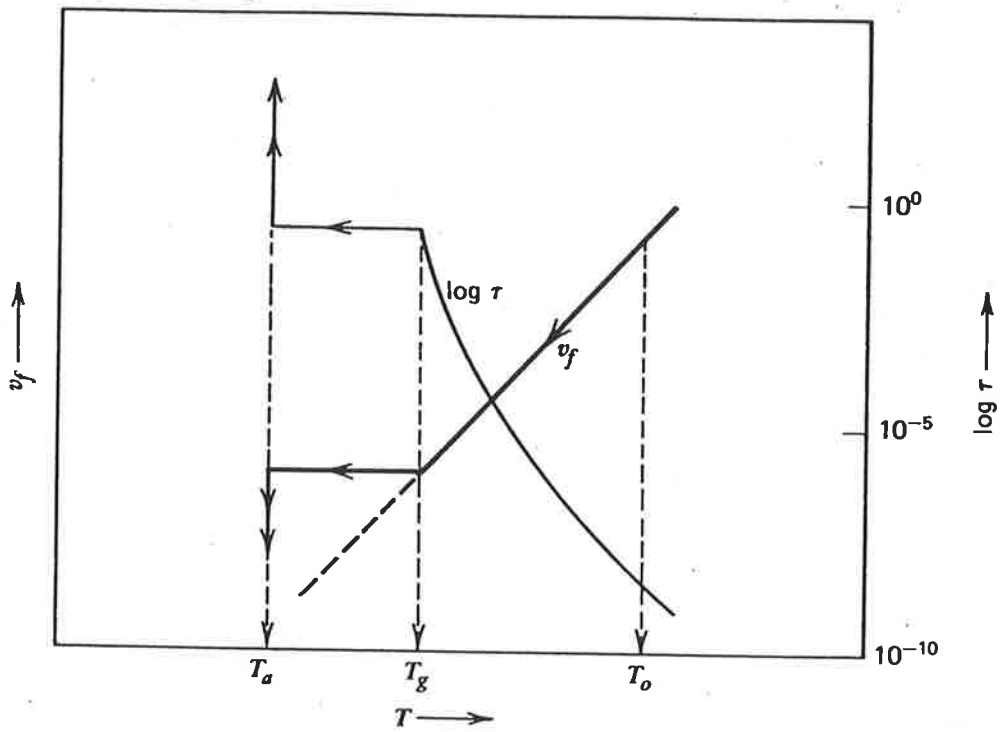

Figure 2.1 Changes in free volume V_f with relaxation time τ during rapid cooling from $T_0 > T_g$ to $T_a < T_g$ and subsequent isothermal ageing at T_a. The time units on the τ-scale are arbitrary; the dashed line is the supposed equilibrium line for V_f below T_g (reproduced from [14]).

interpretating molecular changes during structural rearrangement. Various authors have used differing definitions of the free volume and there is some confusion about its definition and measurement. Three free volume models will be reviewed: (1) the Williams-Landel-Ferry [9] model; (2) the Simha-Boyer [36] model; and (3) the semi-quantitative model proposed by Struik [16].

2.2.1 The Williams-Landel-Ferry (WLF) Model

This model relates mechanical and dielectric relaxation times at a temperature T to a standard reference temperature, usually T_g, for a series of polymers to enable empirical correlations to be obtained. It enables the rationalisation of viscoelastic and time-dependent mechanical behaviour of polymeric materials close to their glass transition temperature [17].

This model is based on the existence of a temperature-dependent occupied volume. Doolittle [13, 18] proposed that the specific volume, V, of a polymer was equal to the sum of the free volume, V_f, and the occupied volume, V_0. V_0 was taken to be the value of V extrapolated to 0 K and was regarded as a constant independent of temperature. The occupied volume included not only the volume of the molecules as represented by their van der Waals radii, but also by the volume associated with their molecular vibrations. This definition assumes that V_f must tend to zero as the temperature approaches absolute zero and that the increase of V with temperature, due to thermal expansion, is associated entirely with an increase in V_f. However, for a material in thermodynamic equilibrium above T_g, V and τ become unique functions of temperature and it is impossible to decide whether the temperature or specific volume is responsible for the variations in τ [8]. The relationship between V, V_f, V_0 and temperature is shown in Figure 2.2.

In a liquid-like system, the local free volume is continually being redistributed throughout the medium, occuring simultaneously with the random thermal motions of the molecules. The basic idea underlying the free volume approach to structural relaxation is that the molecular mobility at any temperature is dependent on the distribution of free volume at that temperature [19]. However, Hill *et al.* [20] found that the free volume concentration remained unchanged during ageing, but decreased after the polymer was cooled from the ageing temperature. It was suggested that the free volume decrease is the consequence of molecular changes which occur during ageing, that is, changes in the mobility resulted in the lowering of

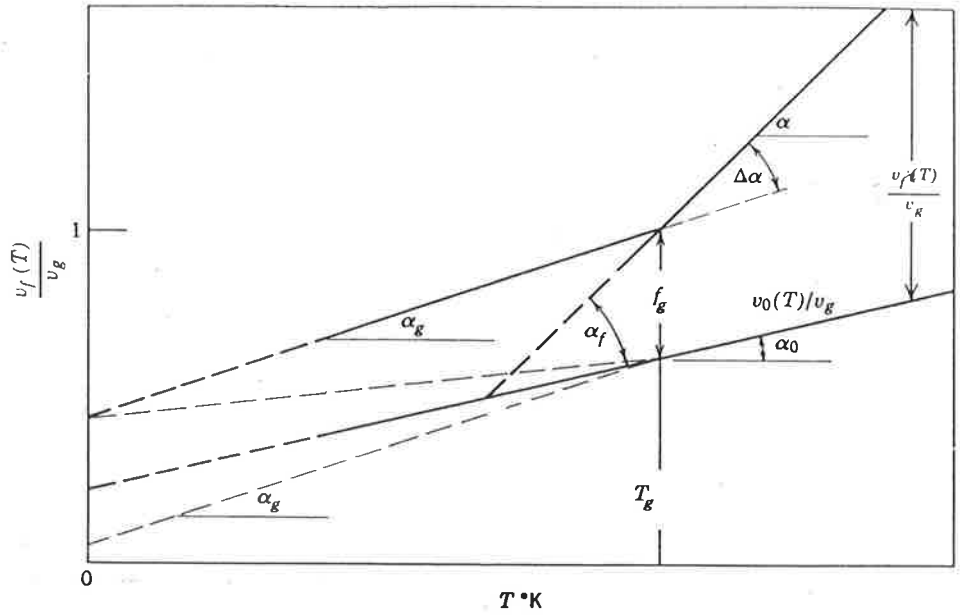

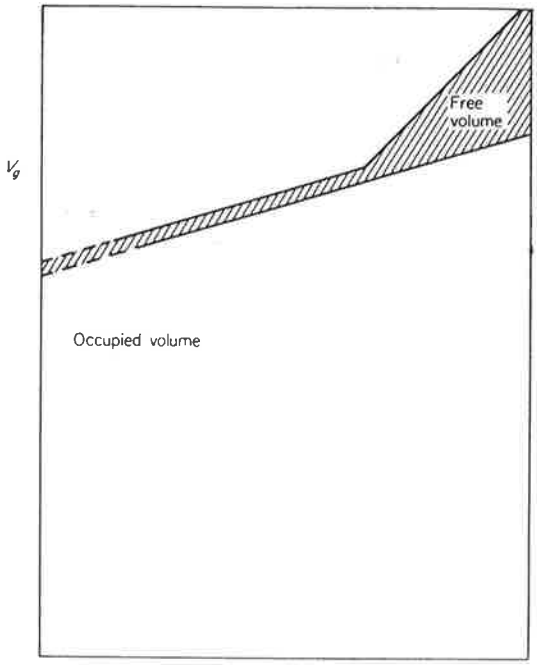

Figure 2.2 Schematic variation of the total specific volume, occupied volume, and free volume (relative to specific volume at T_g) with temperature. f_g is the free volume fraction at T_g, α is the liquid expansion coefficient, α_g is the glass expansion coefficient, and α_o is the thermal expansion coefficient of the occupied volume (reproduced from [9] and [10]).

the free volume.

The viscosity of a liquid η can be expressd by the Doolittle equation [13] as:

$$\eta = A \exp(B/f) \tag{2.1}$$

where A and B are constants and $f = (V_f/V)$ is the *free volume fraction.* The temperature dependence of relaxation times in the glass transition region is described by the WLF equation [9]:

$$\log a(T) = C_1(T - T_g)/(C_2 + T - T_g) \tag{2.2}$$

where the empirical constants C_1 and C_2 have approximate values of -17.44 and 51.6 respectively. Equation (2.2) was found to apply in the temperature range between T_g to T_g + 100 C [10]. The WLF equation can also be derived from on the basis of Doolittle's empirical free volume equation:

$$\ln a(T) = \ln [\eta/\eta_g] = B.(1/f - 1/f_g) \tag{2.3}$$

where f and f_g are the fractional free volumes at temperature T and T_g respectively. If the free volume fraction f was assumed to increase linearly with temperature according to

$$f = f_g + \Delta\alpha(T - T_g) \tag{2.4}$$

where $\Delta\alpha$ is the difference between the cubical liquid and glass thermal expansion coefficients, $\alpha_l - \alpha_g$, then it follows from (2.3) and (2.4) that the same form of the WLF equation can be obtained:

$$\ln a(T) = [B/f_g].(T - T_g)/[(f_g/\Delta\alpha) + (T - T_g)] \tag{2.5}$$

By assuming that B=1, as was the case with Doolittle's work [13] on simple liquids, f_g can be calculated. Comparing the coefficients with the WLF equation (Eq. 2.2) the fractional free

volume f_g was found to have the value of 0.025 and $\Delta\alpha = 4.8 \times 10^{-4}\ K^{-1}$.

The concept that the quantity f_g was approximately the same for all polymers and thus can be represented by a "universal value" was first proposed by Fox and Flory [15]. A closer examination of the experimental data by Ferry [10] has revealed variations in the values of the "universal" constants, particularly C_1, C_2, and $\Delta\alpha$ among different polymers. Examination of the $\Delta\alpha$ values for a range of polymers showed that this quantity is by no means constant, but varied between 2.9 and $7.0 \times 10^{-4}\ K^{-1}$ which would give values of f between 0.015 and 0.036 [21]. Williams [22] found that the constant B in the Doolittle equation (Eq. 2.1) should have a value of 0.91 and that its value is temperature and molecular weight independent. The constant A is, however, strongly molecular weight sensitive up to a molecular weight of about 35 000.

There is an uncertainty about the values of T_g, which is strongly dependent on the measurement technique employed and the experimental time scale. Different experimental methods do not always give values of T_g which agree exactly for each polymer (see Section 2.3.13). When comparing results from different workers, it is important that the method of determining the T_g is precisely defined, along with the experimental conditions, otherwise potentially misleading comparisons will be made [23]. Furthermore, there is no precise point at which a polymer changes from a glass to a liquid [24]. Inherent difficulties in defining and specifying the Tg is due to the fact that the glass transition occurs over a temperature range, although it is commonly and arbitrarily taken to be the intersection of the extrapolated glass and liquid lines of a volume-temperature curve (Fig. 1.2). The extrapolated T_g was shown by Kovacs [5] to be dependent on the cooling rate, where the T_g obtained by rapid cooling (0.02 hours) was found to be higher than the one obtained by slow cooling (100 hours) (Fig. 2.3). This observation suggests that theoretical models which relate the free volume with T_g are susceptible to errors arising from the ambiguity of the location of the T_g.

Another reason for scepticism about the WLF model is that the theoretical basis for the model was based on the proposals of Cohen and Turnbull [25-26] from considerations on the equilibrium size distribution of holes. In addition, the WLF model was developed entirely from measurements made in thermodynamic equilibrium. However, the material is not in equilibrium below T_g, thus the distribution of hole sizes in the glass state is not expected to be the same as the distribution above T_g. Therefore, the application of the WLF treatment to the

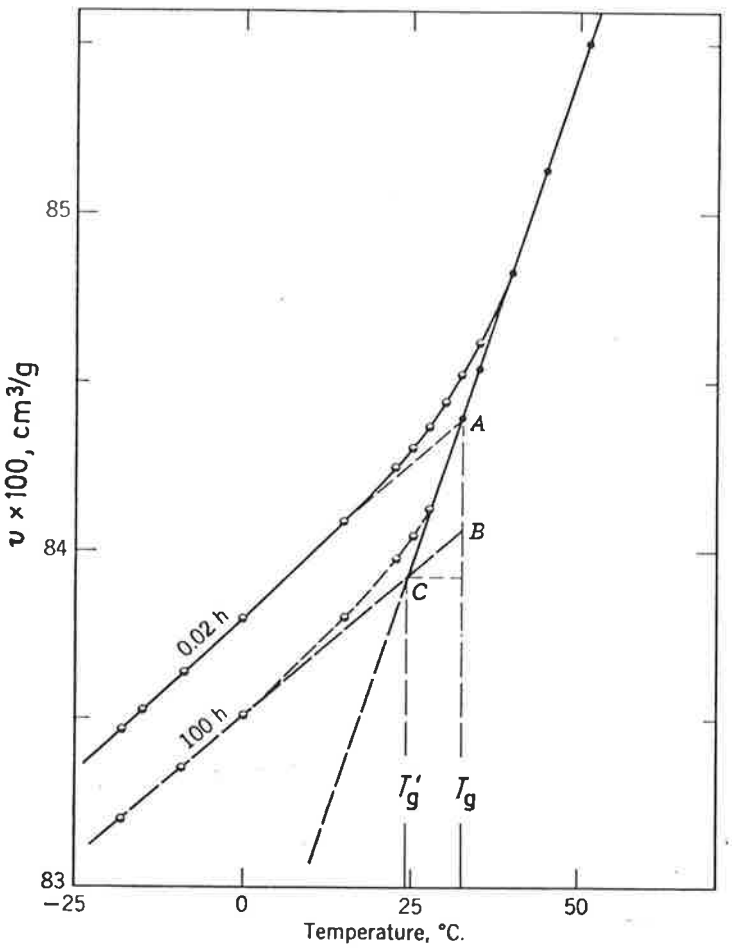

Figure 2.3 Specific volume versus temperature plot for poly(vinyl acetate), measured after cooling from above T_g. Plot shows the effect of the duration of experiment on the glass transition temperature, $T_g' = T_g$ (100 hours) $< T_g$ (0.02 hours) (reproduced from [5]).

free volume below T_g appears to be doubtful.

Various researchers [27-32] have performed pioneering experiments to test the hypotheses of the WLF model. Amorphous glassy materials were quenched from above to below T_g and aged at some temperature $T_a < T_g$. After various times t_e had elapsed at T_a the specimens were tested by creep [27, 32], dynamic-mechanical [28-30], and dielectric techniques [31]. All researchers found that the relaxation rate decreased with increasing t_e. Following these early studies, Struik [19] carried out a comprehensive investigation of the effect of ageing on the small-strain creep of approximately forty materials, the majority of which were synthetic amophous polymers. Other materials investigated were semicrystalline polymers, natural polymers, and low molecular weight glasses. In all cases the same ageing effect as in Figure 1.1 was observed. Similar effects for stress-relaxation were reported by Sternstein [33-34] and Cizmecioglu *et al.* [35]. These experimental observations strongly supported the the assumed applicability of the WLF free volume concept below T_g.

A critical check of the applicability of the WLF theory at temperatures below T_g was made by Struik [19]. As early as 1954, Kovacs [4, 7] recognised that the volume relaxation below T_g critically depended on the preceeding thermal history. If a material was quenched from an equilibrium state at T_0 to a temperature T_a and allowed to *partially* age at T_a, upon reheating to T_0 the volume of the specimen goes through a maximum before contracting towards equilibrium values (curves 3-7 in Fig. 2.4). The origin of this effect will be explained in Section 2.3.5, but here the stress will be on the application of the phenomenon.

If the WLF equation is applied below T_g, the following observations should be expected. (1) During ageing at T_a the monotonic volume contraction will be accompanied by a monotonic shifting of the creep curves to the right. This has been shown to be the case in Figure 1.1. Similarly, the quench from 100 C to 85 C (curve 7 in Fig. 2.4) resulted in a monotonic shift to the right. (2) After an upquench from a non-equilibrium state, the volume maximum will be accompanied by a shift to the left during the dilatation phase and by a shift to the right during the contraction phase. This behaviour is shown in Figure 2.5. It is obvious that the shifts log a(T) in the mechanical creep curves follow the changes in the specific volume. Similar results [19] were obtained for a number of temperatures below T_g for polystyrene (PS), PVC, and polycarbonate (PC). From these results, Struik [8] concluded that the WLF free volume concept can be applied in the temperature range below T_g.

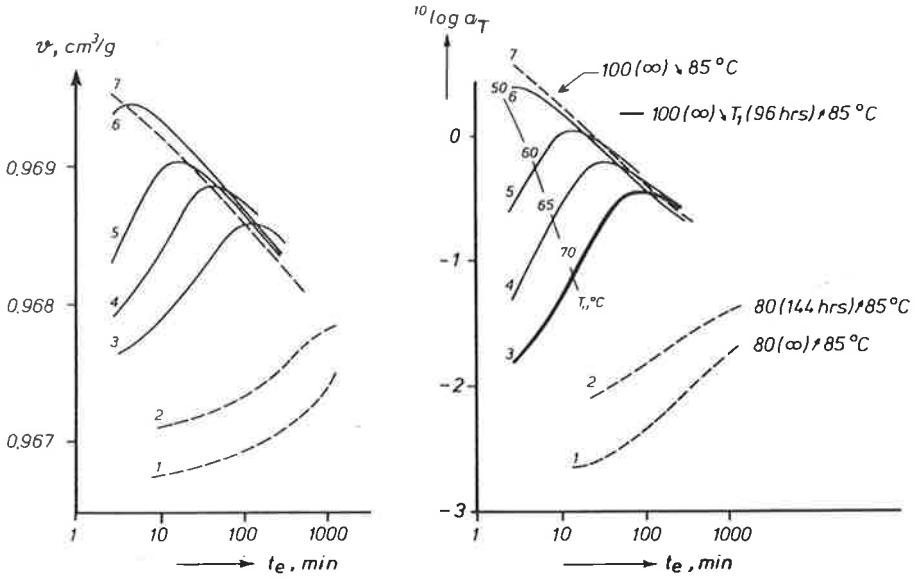

Figure 2.4 Isothermal volume relaxation (left) and simultaneous changes in the mechanical creep properties (right) of polystyrene heated or cooled to the final temperature T (∞) of 85 C. ^{10}log a(T) is the shift of the creep curve relative to the one measured 25 minutes after a simple quench from 100 C to 85 C. The notation 100 (∞) → T_1 (96 hours) → 85 C means a quench from thermodynamic equilibrium at 100 C to intermediate temperature T_1 (isothermal time 96 hours), followed by an upquench to 85 C. t_e denotes the time elapsed at the final temperature of 85 C (reproduced from [8]).

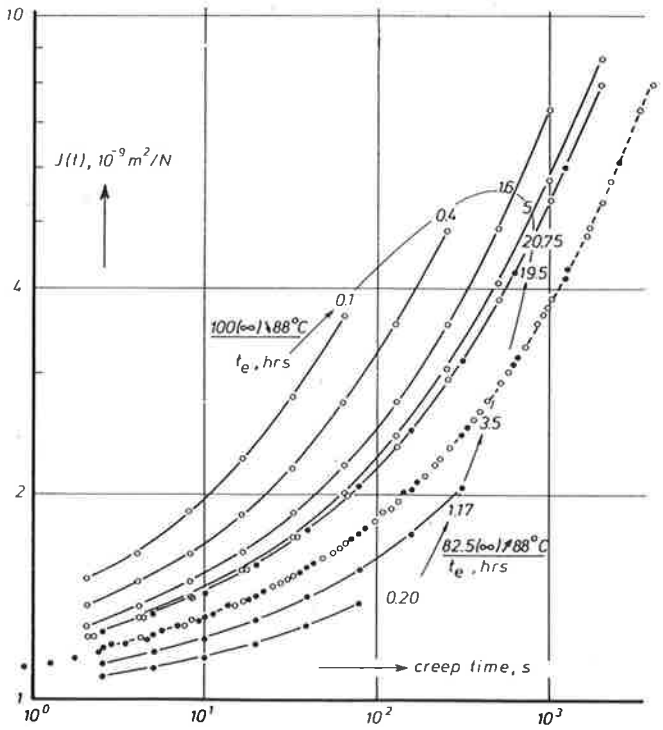

Figure 2.5 Small-strain torsional curves at 88 C for polystyrene at various times t_e elapsed after temperature jumps from equilibrium states at 100 C (open circles) and 82.5 C (filled circles). The master curve at 3.5 hours after the upquench was obtained by horizontal superposition of all data (reproduced from [19]).

However, there are some problems arising from the application of this concept at temperatures far below T_g. For temperatures close to T_g, the free volume of most polymers obtained from the WLF equation correspond to a value of approximately 0.02; at low temperatures (100-200 C below T_g), the free volume decreases to a value of 0.005-0.009. This decrease in free volume must produce a very large increase in the relaxation times, for example, the decrease from 0.02 to 0.006 will cause an increase of the relaxation times by 50 orders of magnitude (from Eq. 2.1, if B is taken to be unity). These large changes in relaxation times would be reflected in large shifts of the mechanical creep curves along the time scale; with decreasing temperature the creep curve would be shifted by 50 decades. However, no such large shifts were found experimentally [19]. This result shows that there are limitations in the applicability of the WLF-Doolittle model below T_g.

2.2.2 The Simha-Boyer Model

The free volume was regarded by Fox and Flory [15] as being essential for molecular motion by rotation or translation to occur. The specific volume of a material is only partly occupied by molecules which leads to the presence of unoccupied free volume, which is presumed to consist of "holes" of molecular sizes or imperfections in the packing order of molecules which arise from their random array. It is into this unoccupied volume that molecules must be able to move in order to adjust from one conformational state to another [21].

According to the Simha-Boyer model [37], the free volume will be frozen in and will remain at a constant value in the glass state. It follows that the hole size and distribution of free volume within the glass will also remain fixed below T_g. The glass transition temperature for any polymer will be that temperature at which the free volume reaches a critical value below which there is insufficient room for molecular motion. The glass will, however, contract or expand with decreasing or increasing temperature due to the normal expansion process of all molecules under thermal agitation. In addition to the molecular expansion process, there will be an expansion of the free volume above T_g which will result the larger expansion of the liquid state than of the glass [21]. It is proposed [37] that the difference between the glass and liquid expansion coefficients reflect the expansivity of the free volume fraction. This proposal is supported by Boyer [36] who observed a pronounced relationship between the volume

expansion $\Delta\alpha$ and the structure of the polymer, in which a free volume fraction of 0.113 was obtained from the slope of the plot of $\Delta\alpha$ vs. $(1/T_g)$ (Fig. 2.6).

The construction of the volume-temperature plot according to Simha and Boyer [37] is shown in Figure 2.7. The specific volume of an amorphous polymer is extrapolated to absolute zero to yield the intercepts $V_{0,g}$ and $V_{0,l}$, which represent the hypothetical occupied volume at absolute zero for the glass and the liquid states. The free volume fraction f at T = 0 K is defined as $(V_{0,g} - V_{0,l})/V_{0,g}$ [38], which leads to the Simha-Boyer equation for free volume fraction below T_g:

$$f = V_f/V = \Delta\alpha T_g \qquad (2.6)$$

This relationship was tested on a wide variety of polymers which differed in chain stiffness, geometry and molecular weight, and a "universal" value of 0.113 for f was obtained [37]. Thermal expansivity data by van Krevelen [39] for a range of polymers found the mean value for $\Delta\alpha T_g$ to be 0.11, with a mean deviation of 17%. This value for f is considerably higher than the value of 0.025 obtained by Williams, Landel and Ferry [9]. The different values obtained for the free volume fraction highlight the ambiguity and difficulty in reaching a common definition for the free volume.

Although there exists some experimental evidence (e.g. Fig. 2.6) to support the Simha-Boyer equation (Eq. 2.6), the assumption that the thermal expansion coefficient remains constant with temperature has to be questioned. The linear thermal expansivities of PMMA and other poly(*n*-alkyl methacrylates) were shown to have at least doubled its value in the temperature range -180 C to 100 C (Fig. 2.8) [40]. The ambiguity of the location of the T_g has already been mentioned, therefore, the expression $\Delta\alpha T_g$ is always susceptible to discrepancies which arise from different measurement techniques and experimental conditions [23]. It was pointed out by Sharma *et al.* [41] that the inclusion of the expansion coefficients of semi-crystalline polymers such as polyethylene (PE), poly(tetrafluoroethylene) and poly(vinylidene chloride) to obtain the "universal" free volume fraction of 0.113 is inappropriate, as only expansion coefficients of *completely amorphous polymers* should be used. It was assumed [37] that in the case of partially crystalline polymers, the T_g will not be affected appreciably by crystallinity and that the thermal expansivity for the completely amorphous polymer can be

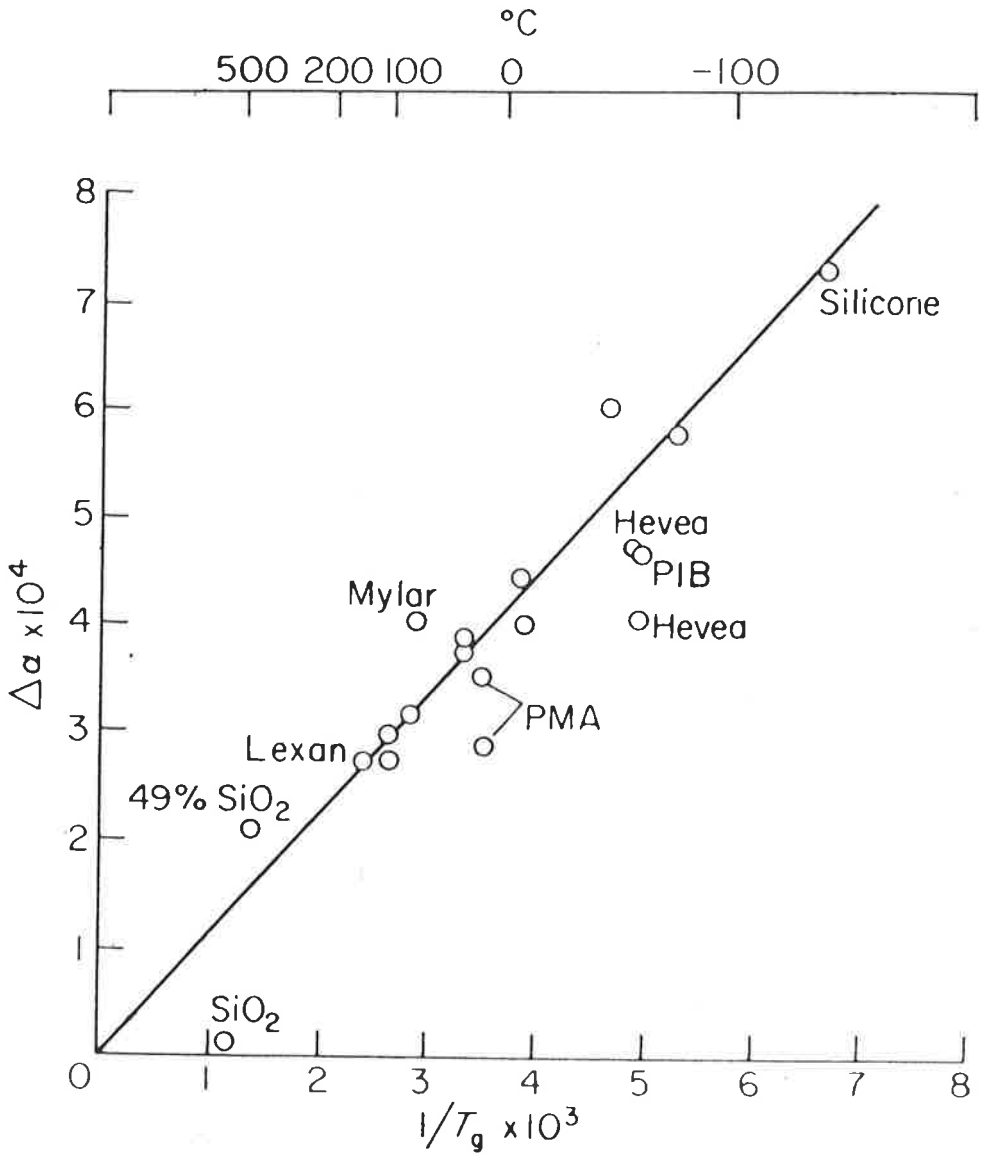

Figure 2.6 Differences in the expansion coefficients ($\Delta\alpha = \alpha_l - \alpha_g$) plotted against the reciprocal absolute temperature. The value of the fractional free volume obtained from the slope of this line is 0.113 (reproduced from [36]).

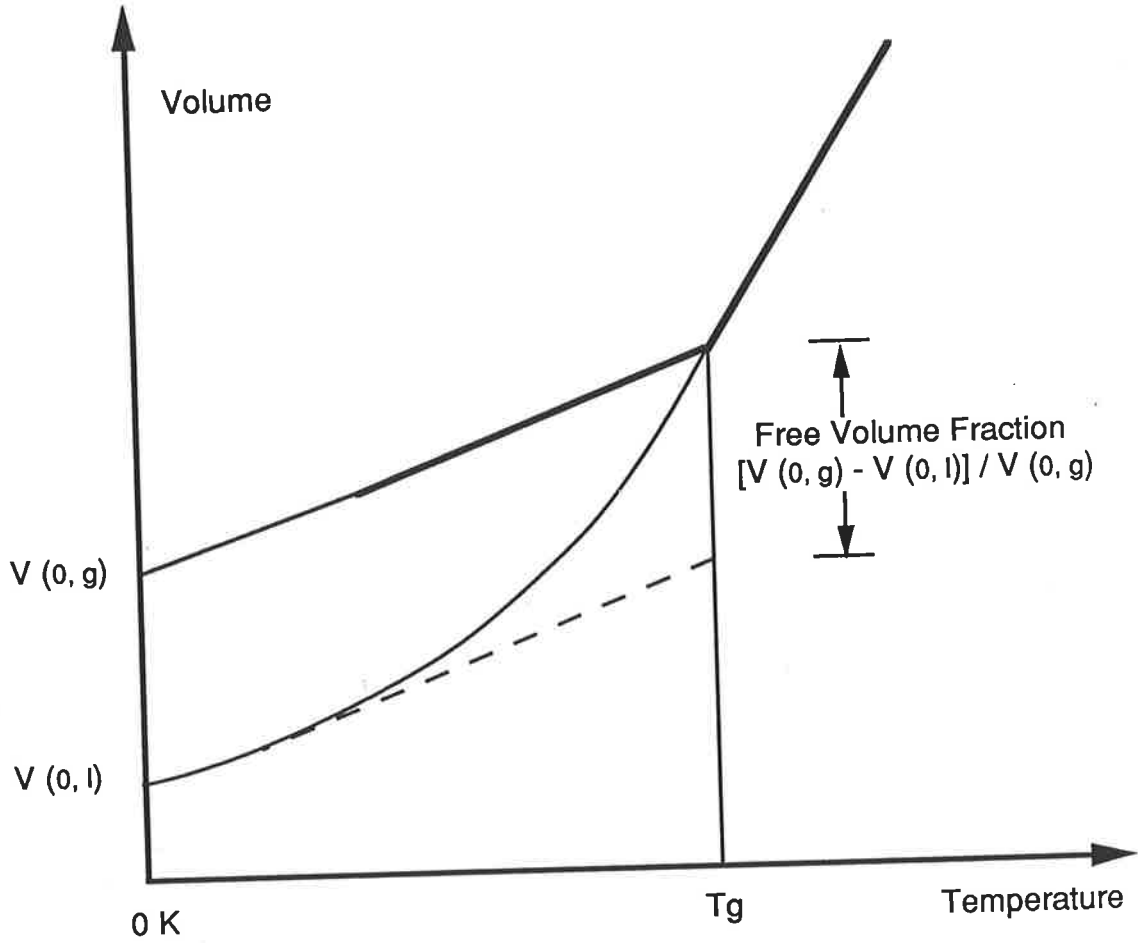

Figure 2.7 The free volume fraction according to Simha and Weil [38]. $V_{0,g}$ and $V_{0,l}$ are the specific volumes of the glass and liquid states extrapolated to zero Kelvin.

calculated if the percent crystallinity of the specimen is known. Linear PE of varying degrees of crystallinity had been studied by Stehling and Mandelkern [42], who obtained $\Delta\alpha T_g = 0.046$ from expansion coefficients extrapolated to the completely amorphous polymer.

Data for a series of poly(*n*-alkyl methacrylates) [43] showed a systematic decrease in $\Delta\alpha T_g$ on lengthening the side chain, up to *n*=12. $\Delta\alpha T_g$ for PMMA was 0.096, but this value decreased to 0.045 for poly(*n*-butyl methacrylate), n=4. Although the difference (α_l - α_g) remained approximately constant for the series, the decrease in T_g with increasing *n* resulted in the lowering of $\Delta\alpha T_g$ [37]. Simha and Boyer explained the discrepancies by considering low temperature glass-glass transitions found [44] below T_g for the poly(*n*-alkyl methacrylate) system where these sub-T_g transitions were presumed to arise from side-chain motions. Therefore, additional free volume was generated by the freezing of these motions at temperatures well below T_g [37], resulting in α'_g (the superscript ' indicate that this is a linear expansion coefficient) being larger for polymers with side groups (α'_g for PMMA was 0.75 x 10^4 K^{-1} and increased to 1.86 x 10^4 K^{-1} for poly(*n*-hexyl methacrylate) [40]). It was suggested [37] the appropriate quantity in Equation 2.6 should be α'_{gg}, the thermal expansion coefficient below the second transition temperature where $\alpha'_{gg} < \alpha'_g$ (the transition is indicated as 2 in Fig. 2.8). The use of α'_{gg} and α''_{gg} [40] (an even lower temperature glass-glass transition indicated as 3 in Fig. 2.8) succeeded in producing "reasonable" values (between 0.10-0.12) of $\Delta\alpha T_g$. Similar lowering of $\Delta\alpha T_g$ due to high values of α'_g with increasing side chain length was also noted for the poly(vinyl alkyl ethers) [45-46]. By taking into account all glass-glass transitions, the free volume fraction calculated for a range of poly(vinyl alkyl ethers) and poly(*n*-alkyl methacrylates) still showed a small decrease on increasing side chain length, ranging from 0.121 to 0.106 and 0.132 to 0.106 respectively [45].

The explanation of additional free volume created by cryogenic glass-glass transitions appears to be self-contradictory. If the free volume fraction f is given by $\Delta\alpha T_g$, then the additional free volume should result in an increase in f with increasing side chain length. The use of the glass-glass expansion coefficient, α'_{gg}, contradicts a reply [47] to Sharma *et al.* [41], in which it was explicitly stated that the cubical liquid and glass expansion coefficients, α_l and α_g, that are used in Equation 2.6 are measured *immediately* above and below T_g.

A review [41] of a variety of polymer systems, including linear and branched amorphous polymers, and polymers and organic glasses of high and low molecular weights,

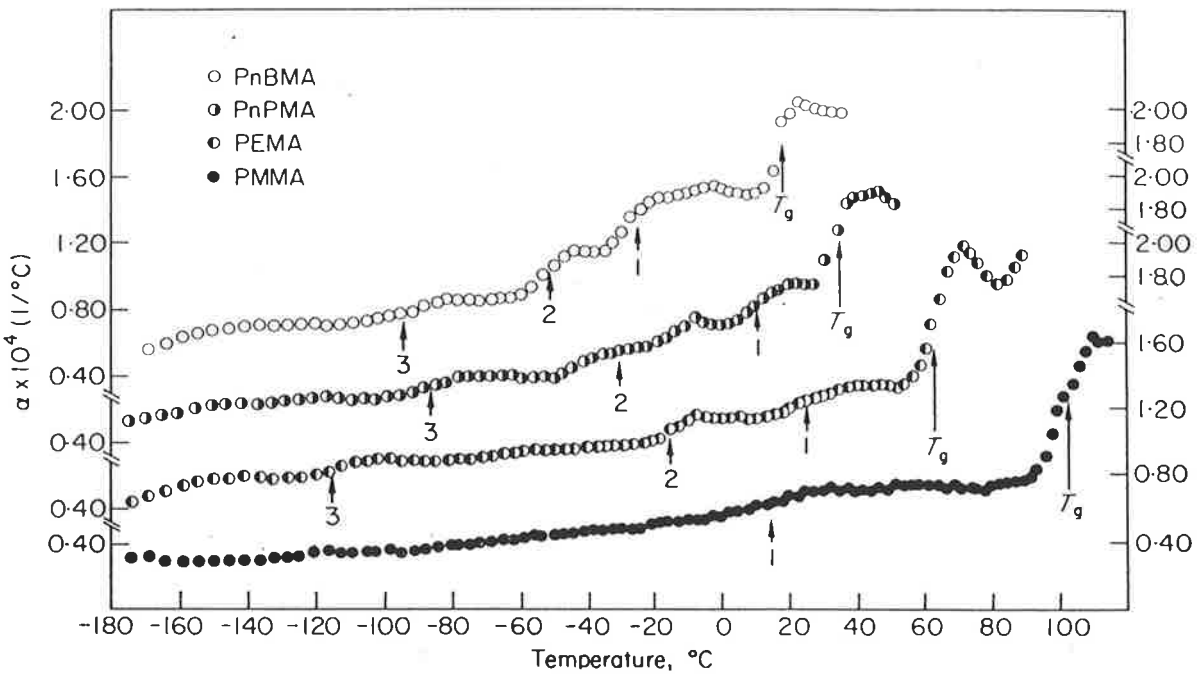

Figure 2.8 Linear expansion coefficients as a function of temperature for some poly(n-alkyl methacrylates): PMMA poly(methyl methacrylate), PEMA poly(ethyl methacrylate), PnPMA poly(*n*-propyl methacrylate), and PnBMA poly(*n*-butyl methacrylate). The various glass-glass transitions below T_g are indicated. α' is not constant but shows a small rise with increasing temperature (reproduced from [40]).

showed considerable scatter for the values of $\Delta\alpha T_g$ in the range 0.03-0.140. The free volume fractions of a number of polymers and organic substances from [41] are listed in Table 2.1 (a different notation, $\Delta\beta T_g$, is used in [41] instead of $\Delta\alpha T_g$)

TABLE 2.1

Free volume fractions of a number of polymers and organic substances calculated using the Simha-Boyer equation ($f = \Delta\alpha T_g$)

Polymer	$\Delta\alpha T_g$	Reference
Natural Rubber	0.0804	48
Polyethylene (PE)	0.0462	42
Poly(dimethyl siloxane)	0.140	49
Poly(isobutylene)	0.0830	41
	0.094	37
Poly(methyl acrylate) (PMA)	0.082	50
Poly(vinyl acetate) (PVAc)	0.1180	51
Poly(vinyl chloride) (PVC)	0.0763	52
Poly(methyl methacrylate) (PMMA)	0.0926	43
	0.1202	53
Glucose	0.0513	54
Glycerol	0.0289	55
	0.085	37

The results for branched poly(n-alkyl methacrylates) and poly(n-vinyl alkyl ethers) are listed in [40, 45-46]. Simha and Boyer [47] has admitted that Equation 2.6 is obeyed predominantly by high molecular weight polymers without long alkyl side chains, and $\Delta\alpha T_g$ drops from approximately 0.1 for high molecular weight polymers to around 0.08 for low molecular weight glasses [37].

2.2.3 The Struik Model

This model states that the segmental mobility, M, of any system of particles,

molecules, etc., primarily depends on the degree of packing, or in other terms on the free volume, V_f [16]. This concept is very general and much older than the suggestion that mobility is determined by temperature [56]. It is generally accepted that free volume is made up of holes [57], perhaps of the order of molecular or monomeric dimensions, or smaller voids associated with packing irregularities [10]. The free volume in a system is distributed over holes of various sizes [25-26]. Molecular transport in simple liquids can occur when a molecule moves into voids which have a size greater than some critical value v^*. These voids are created by the redistribution of free volume arising from the cooperative motion of neighbouring molecules, which, represents the molecular basis for free volume [25-26]. Because of the small size of most of these holes, only a few holes of molecular dimensions can contribute to the mobility, and hence the ageing process [57]. Therefore, the mobility is primarily determined by the distribution function of such holes [19], viz. by the number of holes larger that v^*. The average free volume will not be a good measure of mobility, particularly not for non-equilibrium states below the T_g.

The Struik model predicts that the segmental mobility and the free volume fraction of a polymer above T_g must be large, where the polymer behaves as a rubber or a fluid. On cooling there will a simultaneous decrease in M and V_f (Fig. 2.1). The changes in V_f are brought about by a redistribution of holes and the rate of this process, dV_f/dt, is determined by M. A closed loop scheme relating V_f, M and dV_f/dt is shown in Equation 2.7:

$$V_f \Rightarrow M \Rightarrow dV_f/dt \Rightarrow V_f \Rightarrow \text{etc.} \qquad (2.7)$$

The closed loop scheme is essential for an understanding of physical ageing and the glass transition [7, 27]. It suggests that during cooling the decrease in V_f cannot continue indefinitely; below a certain temperature M becomes so small that the changes in V_f fail to keep up with the changes in temperature. Upon further cooling below T_g, V_f remains constant to a first approximation. A second consequence of Equation 2.7 is that the mobility cannot simply become zero, even at temperatures below T_g. It has been observed [7] that below T_g glasses undergo a slow and spontaneous volume contraction, that is, physical ageing. For this to happen there must still be some mobility. Simultaneously, other properties of the glassy polymer which depend on the mobility will also undergo changes.

The free volume cavity size and free volume concentration of glassy polycarbonate has been monitored using Positron Annihilation Lifetime Spectroscopy (PALS) during and after ageing [20, 58-60]. The PALS technique is sensitive to the size and concentration of empty free volume sites, by measuring the annihilation of *orthopositronium* (oPs) in these sites below T_g [61-63]. The lifetime parameters associated with the annihilation of oPs can be interpreted as reflecting the average size of the cavity in which the oPs annihilates, and also the concentration of cavities in the material [20, 63]. It was found that the number of free volume cavities (or holes, in this context) were lowered after the polymer was cooled from the ageing temperature [20] (120 C for 240 hours, the T_g for polycarbonate is 150 C [59]). The radii of "open volume sites" for polycarbonate were measured to range from 2.86 to 3.09 Angstroms [59], which corresponded to "open volumes" ranging from 9.80×10^{-29} m^3 to 1.24×10^{-28} m^3. The open volume must be of the order of molecular dimensions in order to accommodate the polymer molecules which occupy it during structural rearrangement.

The validity of the PALS results [58-63] were investigated by considering the molar and specific volumes of PMMA, polystyrene (PS), and poly(ethylene terepthalate) (PET). The molar volumes of PMMA, PS, and PET are approximately 86×10^{-6}, 99×10^{-6}, and 144×10^{-6} m^3/mol respectively at 25 C [39]. The molar volumes were converted to specific volumes by dividing with Avogardo's Number, 6.02×10^{23}. The data are presented in Table 2.2.

TABLE 2.2

Molar and specific volumes of amorphous polymers

Polymer	Molar Volume (m^3/mol)	Specific Volume (m^3)
PMMA	86×10^{-6}	1.43×10^{-28}
PS	99×10^{-6}	1.64×10^{-28}
PET	144×10^{-6}	2.39×10^{-28}

The size of the "open volume sites" are of the same order as the specific volumes of PMMA, PS and PET, which suggests that the amount of unoccupied volume available is sufficient to accommodate molecular motion. Struik's model considers the free volume concept in a qualitative way, where free volume is regarded more as a qualitative measure of mobility rather than as a real and measurable volume [19]. The quantitative free volume models are regarded as

being self-inconsistent and inadequate to fully describe physical ageing and volume relaxation [19]. The success of the qualitative free volume model can be seen in the following sections in which it is used to explain the effects of physical ageing on a number of polymer properties.

2.3 BASIC ASPECTS OF PHYSICAL AGEING

The basic aspects of physical ageing are discussed systematically in the following sections, in which the claim [16] that nearly all aspects of physical ageing can be explained by the qualitative free volume concept is also examined. The molecular motions pertinent to the ageing behaviour of PMMA, which is primary polymer used in this work, and that of higher poly(*n*-alkyl methacrylates), are discussed in Section 2.3.9.

2.3.1 Physical Ageing Occurs Generally

Physical ageing appears to be a feature of the glassy state, that is, it can occur in a wide variety of glass-forming materials. It has been observed to occur in many types of polymer systems containing *glassy* regions, for example, totally glassy polymers, semi-crystalline polymers, and polymeric network glasses [5]. Creep compliance tests performed on a diverse variety of materials such as polystyrene (PS), epoxy resins, bitumen, shellac, amorphous sugar, organic and inorganic glasses [16], all show similar ageing effects, i.e. by a monotonic shift along the logarithmic time scale without changing the shape of the creep curves (e.g. Fig 1.1). Moreover, ageing is believed to possess a similar mechanism for all amorphous glassy materials. Kovacs [7] have shown that the general characteristics of isothermal structural recovery (see Section 2.3.5) of PVAc and glucose [5] appeared to be non-specific, suggesting that there must be a remarkable similarity in the molecular processes which control the conformational rearrangements, irrespective of chemical composition.

The effect of physical ageing on the creep behaviour of poly(vinyl acetate) is shown in Figure 1.1, in which a sequence of creep curves were obtained at equal increments of ageing times t_e which increased by a factor of three. As the polymer ages, a constant horizontal shift (log a(T)) along the time scale was observed, such that physical ageing may be characterised by the relationship between log a(T) and log t_e according to

$$\mu = -(d \log a(T)/d \log t_e) \qquad (2.8)$$

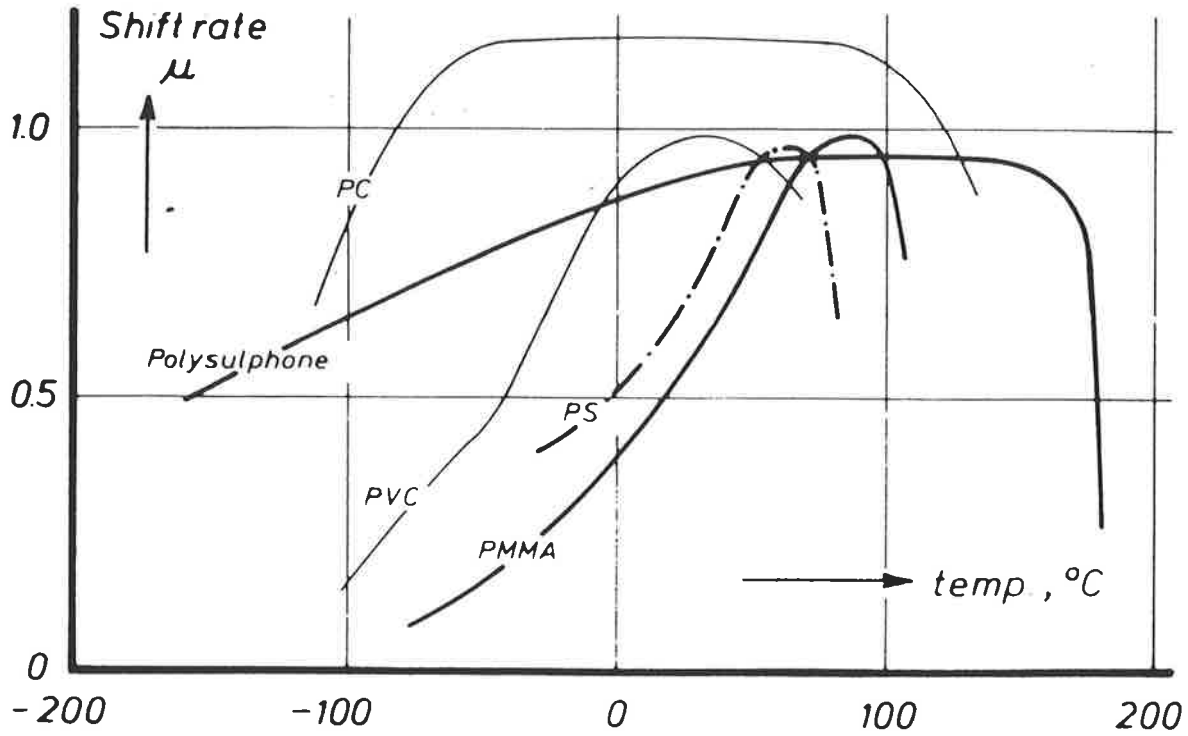

Figure 2.9 The shift rate, μ, versus temperature for various polymers. The ageing range is defined when μ is constant and approximately unity (reproduced from [16]).

where μ is the shift rate [19]. The shift rates measured at various temperatures for a number of polymers were claimed to be approximately constant at a value of about unity (Fig. 2.9) [16]. Thus for every tenfold increase in the ageing time t_e, the creep curves shifted by a factor of ten to the right, i.e. the relaxation times increased proportionally with t_e. Small values of μ above T_g and at temperatures well below T_g indicated that little or no ageing took place. However, a closer examination of Figure 2.9 has raised some doubts on Struik's conclusions.

If the same ageing mechanism was operating for all polymers, the relationship between μ and temperature must then be the same for the five polymers tested, but two types of μ-T curves were observed: (1) after an initial rise, the value of μ remained unchanged at a value of about unity over a wide temperature range (100-150 degrees), suggesting that ageing occurs at the same rate in this temperature range (a schematic curve is shown in [65]). This was observed for PC and polysulphone. (2) A steady rise in μ, briefly reaching a maximum value of approximately one, was observed for PMMA, PS and PVC. No constant value for μ was observed, thus the rate of ageing appeared to continue at an increasing rate for these polymers. For curves of type (2), the shift rate log a(T) can hardly be said to vary proportionally with ageing time.

Other experiments [19] found that some materials, for example, bitumen, shellac, and plasticised PVC, have maximum values of μ of only 0.65-0.80 instead of unity. In the case of bitumen and plasticised PVC, these deviations were interpreted as being related to the broad glass transitions of these materials. For creep experiments with large stresses (45-60 MPa), it was shown that μ was much less than unity [19, 28, 67-69]. Struik [8, 19] suggested that the large deformation process generated free volume and partially erased the previous ageing, thus reducing the ageing rate. These discrepancies [19, 28, 67-69] suggest that Struik's [19] proposal that the shift rate of all polymers should be unity appears to be an oversimplification.

2.3.2 The Timescale of Physical Ageing

Physical ageing in glassy polymers can be accelerated by heating to temperatures close to T_g [64]. However, the working temperatures of glassy polymers are usually below T_g, for example, a PMMA specimen at 25 C is approximately 80 C below its T_g of 105 C [43].

The question is raised as to how long physical ageing will continue in glassy polymers at temperatures below T_g. In Figure 1.1 the rate of ageing of PVC continues at an approximately constant double-logarithmic rate for at least three years (1000 days), i.e. the time needed to establish thermodynamic equilibrium, t_{eq}, changes by a factor of ten for each three degrees, and t_{eq} increases exponentially with (T_g - T). If t_{eq} at T_g was arbitrarily taken to be 100 seconds, then t_{eq} at temperatures below T_g can be expressd by an analogous equation to the WLF expression (Eq. 2.5) [14, 19]:

$$t_{eq} = 100 \times 10^{(T_g - T)/3} = 100.\exp[0.77(T_g - T)] \qquad (2.9)$$

with t_{eq} in seconds, and (T_g - T) in degrees C. Thus at about 25 degrees below T_g the equilibration time had already reached approximately 730 years, and at 40 degrees below T_g (which is the case for the PVC specimen in Fig. 1.1) t_{eq} attains a timescale of 75 million years. These rough estimates of t_{eq} indicate that *physical ageing persists for the entire lifetime of the polymer at temperatures below T_g*. However, the free volume concept [19] predicts that the mobility of the polymer decreases as more free volume is annihilated, hence physical ageing is a self-delaying process and equilibrium is approached asymptotically.

A method for predicting long term creep from short time tests, based on the kinetics of ageing, has been developed [19, 66] to determine the rate of ageing after long periods of time had elapsed after quenching. This method required the testing time to be small compared with the ageing time t_e to ensure that little ageing took place during the testing. The creep response of a glassy polymer stored over a long period (27.5 years) was measured at 20 C. The sample was then reheated to above T_g to completely erase its previous ageing; after subsequent requenching to 20 C the creep at various ageing times of, say, 0.1 to 100 days were measured. The shift rate log a(T) of these curves can be obtained, and if the constancy of μ holds, the position of the creep curve at 10^4 (27.5 years) days can be found by extrapolation. However, if the measurements were carried out at temperatures close to T_g the effect of ageing may be significant, even at relatively short testing times. Although this method has been claimed to be successful in predicting the long term creep behaviour of PVC [19] (a difference of 25% was found after extrapolation from 3 to 30 years), there is an uncertainty concerning μ remaining constant at unity (as observed for PMMA, PS and PVC, μ is not constant at all). Struik [16]

had expressed doubts on the extrapolation of creep curves with values of μ much less than unity, and admitted that μ may increase with time.

2.3.3 The Thermoreversibility of Physical Ageing

Any previous ageing undergone by a polymer can be completely erased by heating to above T_g. The thermoreversibility of physical ageing in rigid PVC is illustrated by an elegant experiment which is illustrated in Figure 1.1. The creep of the PVC specimen was measured at 40 C at various ageing times between 0.03-1000 days after quenching from 90 C. Following the measurements the sample was reheated to 90 C for twenty minutes (about 10 C above T_g) to erase the ageing, requenched to 40 C and the creep was measured again after one day (results indicated by crosses). The data for t_e = one day agree to within 2 % with the results obtained four years earlier [16]. This experiment conclusively shows that the ageing during the 1000-day period at 40 C was completely erased by reheating to 90 C for only twenty minutes, and following requenching to 40 C, ageing was observed to resume in PVC.

2.3.4 The Temperature Range for Physical Ageing

It has been mentioned that physical ageing is a common phenomenon and that it persists for long periods in the glass state. However, does a limiting temperature exists at which ageing becomes ineffective?

The "ageing range" proposed by Struik [16, 19] is determined by the temperature range in which the value of μ is equal to unity. The ageing range is very wide and differs from one polymer to another. In addition to the main glass-rubber transition, many amorphous polymers undergo secondary relaxation processes below T_g which makes the resolution of the α- and β- peaks difficult. Dynamic mechanical measurements of poly(ethyl methacrylate), poly(*n*-butyl methacrylate) and poly(*n*-hexyl methacrylate) showed that the α and β relaxation regions of the higher poly(*n*-alkyl methacrylates) merge into a single region [70-71]. It was concluded [17] that the β relaxation in these polymers was considerably influenced by the α process, which suggests that the β relaxation may be involved as a precursor to main-chain motions and contribute to physical ageing.

From the shift rate curves in Figure 2.9, it appears that physical ageing takes place between the temperature range which is bounded by T_g as the upper bound and by the highest

secondary transition temperature T_β as the lower bound [19]. The ageing range for PC lies between T_β = -100 C and T_g =130 C, but for PVC the ageing range is more difficult to determine and should fall between -50 C and 70 C. Struik [16, 19] proposed that the persistence of secondary motions below T_g implied that there is sufficient free volume to admit side-group motions which give rise to secondary transitions, but not enough to allow segmental main-chain motions to occur. Therefore, Struik is suggesting that the mechanism responsible for physical ageing is segmental motion of the main chain and such motion ceases at temperatures below T_β.

The insensitivity of secondary relaxations to physical ageing was studied by investigating the effect of thermal history on secondary relaxation processes in a number of amorphous polymers [72]. Four torsion pendulum runs at a frequency of 1 Hz were made on rigid PVC sheets between -170 C and T_g. The first run was carried out on a specimen as received, to allow the estimatation of T_g and to gain an impression on the trend of the modulus and damping in the glassy state. After this measurement, the PVC sheets were annealed overnight between glass sheets at 85 C to relax possible frozen-in stresses. The second run was performed after heating to 85 C for twenty minutes and quenching to -170 C. A third run was performed on a specimen slow cooled from 85 C to 25 C at a rate of 0.5 C per hour. The sample was cooled to -170 C after being kept at room temperature for several days. The fourth run involved repeating the heating and quenching procedures on the same sample used in the second run. The results of the four runs are shown in Figure 2.10 and clearly show the thermoreversibility of physical ageing, i.e. the effects of ageing can be totally erased by heating to above T_g at 85 C and reintroduced by quenching. An inspection of Figure 2.10 shows that changes in thermal history (quenching, slow cooling) did not give rise to new damping peaks, and the location and height of well-pronounced secondary loss peaks in Figure 2.9 were hardly influenced by thermal history [72]. The insensitivity of the secondary peaks to thermal history suggests that physical ageing is not likely to be affected by secondary relaxations. Recent short term creep experiments performed on amorphous PMMA at 23 C also found no apparent change in the retardation parameters for the β-relaxation [73].

However, the results of creep studies on some amorphous polymers do not fully support Struik's suggestions. Plazek *et al.* [74] found the torsional creep curves for PS at 90 C and 95 C shifted to longer times and also broadened with increasing ageing time. These effects

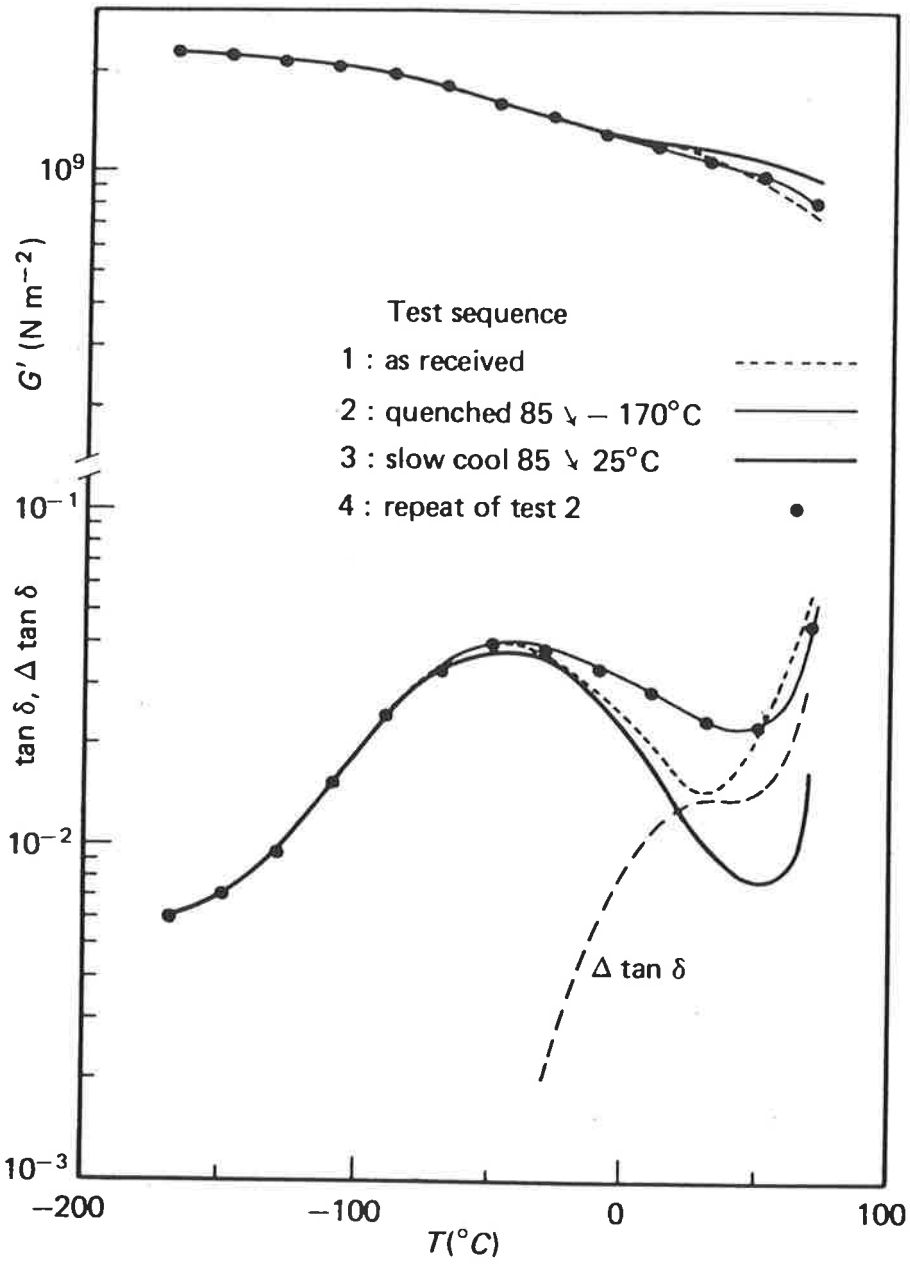

Figure 2.10 Modulus and damping at 1 Hz for rigid poly(vinyl chloride), as measured during heating from -170 C to 65 C at an average rate of 0.67 C min^{-1}. The thermal histories (quenching and slow cooling) and the four experiments are described in the text. $\Delta\tan\delta$ is the difference in tan δ between a quenched (test 4) and a slowly cooled sample (test 3) (reproduced from [72]).

were ascribed to an increase coupling of the relaxing molecules to their surroundings, decreasing the β-component. Johari [75-76] contends that by keeping a glass at an isothermal temperature below T_g for several hours the number of the configurational states, or the number of molecules participating in the β relaxation, are reduced. This contention was supported by results which showed a decrease in the height of the β relaxation peak in plots of dielectric loss at fixed frequency against temperature in glasses which were obtained by cooling from above to below T_g at progressively slower rates. Struik [19] inferred that the above mentioned effect was due entirely to changes in the low temperature tail of the main α relaxation peak which extends into the β relaxation region. He found the decrease in peak height to be maximum near T_g and negligible at temperatures in the β region.

In a later paper, Johari [77] studied the variation of tan δ with frequency and temperature in poly(propylene oxide) (PPO) and a toulene-pyridine mixture. Figures 2.11(a) and 2.11(b) show the decrease in tan δ peaks after progressively slower cooling from above T_g, in which T_g and T_β obtained from tan δ loss peaks were 198 K and 165 K for PPO and 127 K and 105 K for 43.3 mol percent toulene-pyridene.. Isothermal tan δ measurements of different frequencies were made at the annealing temperature after the specimens were kept at various temperatures between T_β and T_g for 1-5 hours. The results in Figure 2.12(a) and 2.12(b) clearly show a decrease in the height of the β peak with increasing ageing time, with the largest change in tan δ (Δtan δ) observed near the β peak. If the decrease in tan δ was due to the tail of the α relaxation peak [19], then Δtan δ should have been greatest at higher temperatures, as shown by Struik's data [72] for PVC (Fig. 2.10), in which the Δtan δ peak is located at a higher temperature than the β relaxation peak.

The decrease of the β relaxation peak of amorphous PMMA after ageing at 59.5 C has also been observed by dynamic mechanical measurements [78-79]. It was also observed that the relative position of the β peak was not affected by ageing, which supports Johari's [75-76] suggestion that the population of molecular groups which relax in the β region was decreased by physical ageing. It was also concluded [79] that the decrease of the β relaxation peaks with ageing was due to the concomitant shift of the α relaxation towards higher temperatures. In addition, a new peak was observed between the β and α peaks [79]. This peak was attributed to the fact that ageing produces a decrease of the loss tangent up to the ageing temperature, but leaves the loss tangent above this temperature unaltered. Experimental

Figure 2.11 (a) The variation of tan δ with temperature of 43.3 mol % toluene-pyridine glass (T_g = 127 K). Curve 1 is for a sample cooled at a rate of 0.3 Ks^{-1}, curve 2 is for a sample warmed up to 130 K and cooled at 10 mKs^{-1}, curve 3 is for a sample which was annealed at 116.5 K for 5 hours and then cooled from 116.5 K.

(b) The variation of tan δ with temperature of poly(propylene oxide) below T_g (T_g = 198 K). Curves 1 and 2 represent the same thermal history as in Fig. 2.11 (a), curve 3 is for a sample annealed at 178.4 K, warmed to 200 K and measured, and curve 4 is for a sample annealed at 192.7 K for 5 hours and then measured (reproduced from [77]).

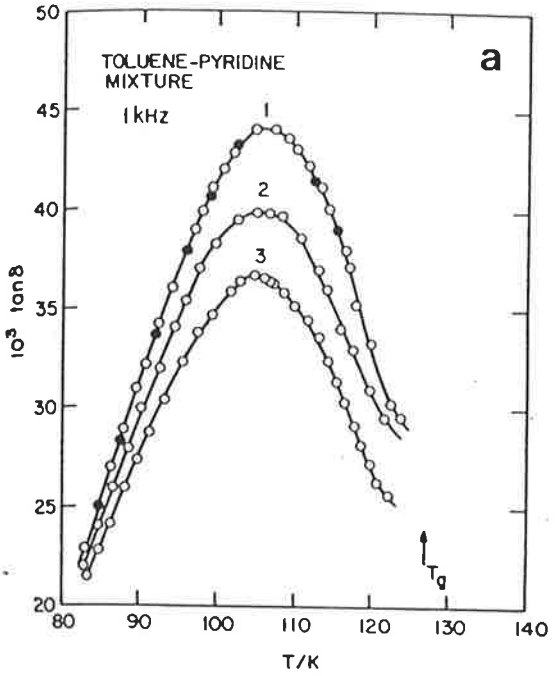

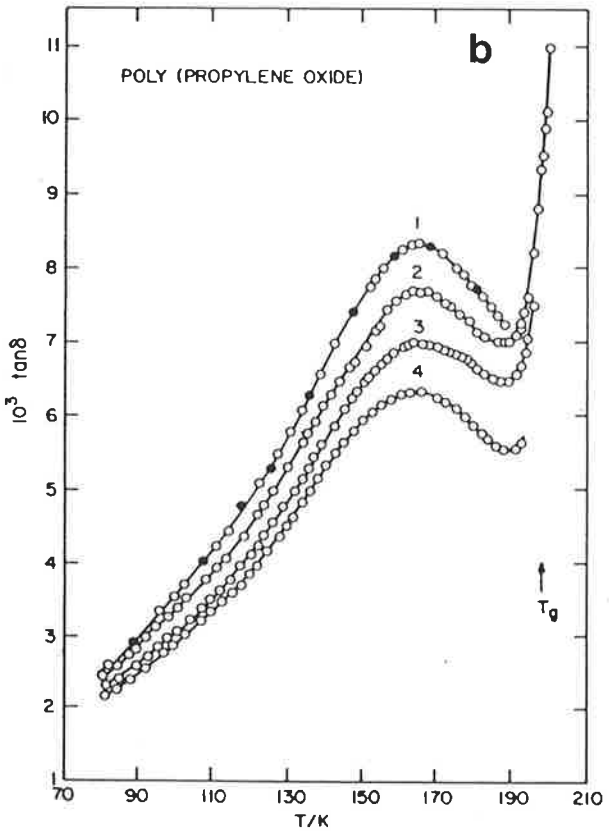

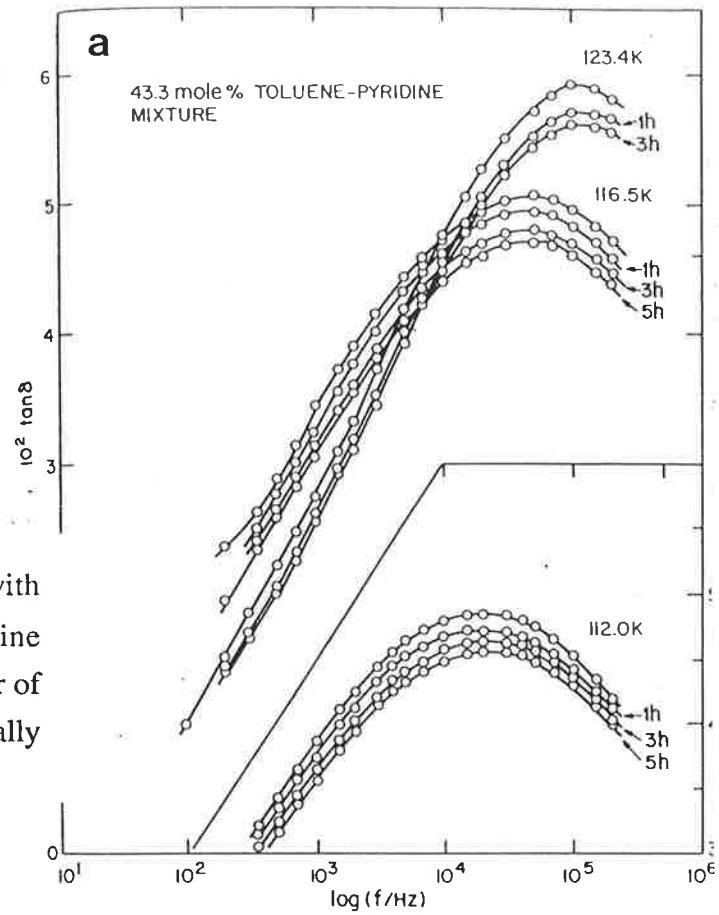

Figure 2.12 (a) The variation of tan δ with frequency for 43.3 mol% toluene-pyridine glass at different temperatures. The number of hours for which the glass was kept isothermally is indicated next to the curve.

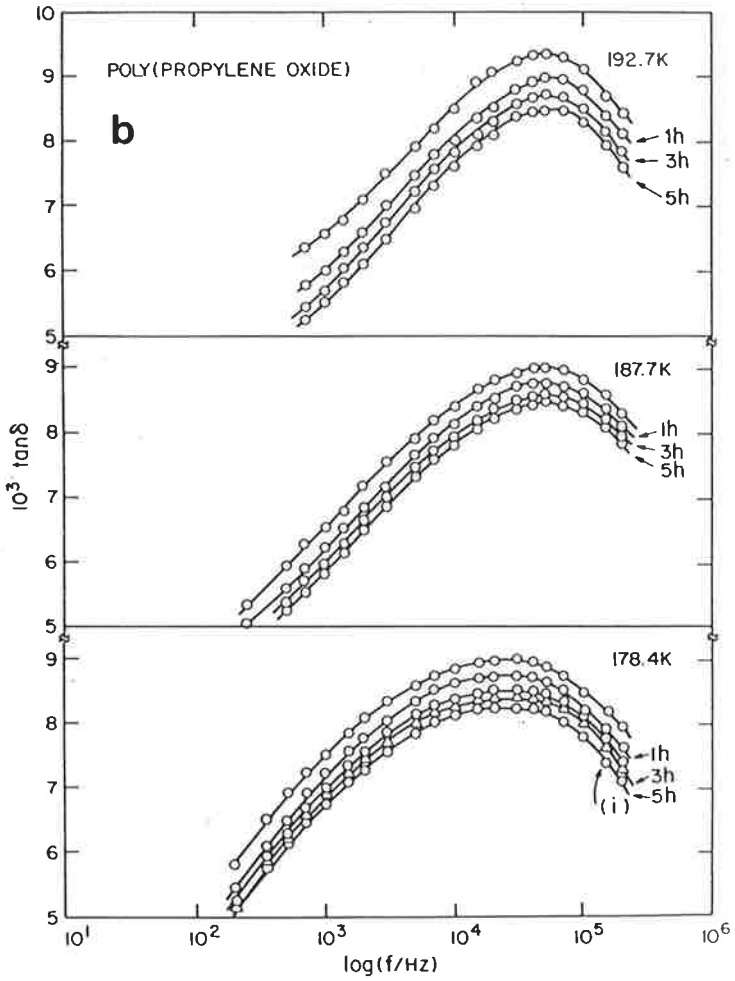

(b) The variation of tan δ with frequency for poly(propylene oxide) at different temperatures. The number of hours for which the glass was kept isothermally is indicated next to the curve. Curve (i) was obtained after heating the annealed glass to 182 K and cooled at 10 mKs^{-1} (reproduced from [77]).

results contrary to Struik's [19] claim that physical ageing does not occur below T_β include the differential thermal studies of Petrie [80], who observed that the enthalpy relaxation in atactic PS and amorphous poly(ethylene terepthalate) (PET) parallel the changes observed in dynamic mechanical measurements. Goldbach and Rehage [81] found that the weak secondary peaks for PS disappear after annealing, but Struik [72] found the opposite effect, i.e. the peaks become more distinct and separated from the glass transition peak.

These discrepancies indicate that presently, there is no conclusive evidence to suggest that physical ageing will totally disappear below . The main obstacle to reaching a conclusive solution is that physical ageing of a specimen to equilibrium below T_g requires an experimentally infeasible long timespan. It appears that Struik's method [19, 66] of predicting the long term creep behaviour of polymers from short time tests (Section 2.3.2) may be the most realistic way of looking at the ageing behaviour at long periods of time below T_β.

2.3.5 The Non-Linearity and Asymmetry of Physical Ageing

The volume relaxation (recovery) process is non-linear in principle [27]. This may be understood from Kovacs' [5, 7] observation of the contraction isotherms of PVAc, in which the variation in volume following quenching from equilibrium at 40 C to various temperatures T is plotted as a function of time (Figure 2.13). δ represents a dimensionless measure of the departure from equilibrium , and is defined as $\delta = (V - V_{eq})/V_{eq}$, where V is the actual specific volume and V_{eq} represents the specific volume at equilibrium; t_i is the time at which the sample is deemed to have reached thermal equilibrium at T. As the sample is quenched to lower temperatures, the initial departure $\delta(t_i)$ at t_i = 0.01 hours, increases. δ(0.01 h) at 35 C is approximately 0.3, but increased to a value of about 4.7 when quenched to 19.8 C. Simultaneously, the time required to reach volume equilibrium (i.e. $\delta = 0$) rapidly increases. But the most significant feature of the isotherms is their non-linearity with respect to the magnitude of the initial departure from equilibrium. If the data in Figure 2.13 were normalised by the factor δ(0.01 h), the resulting curves would not yield a single master curve, as in the case of a linear behaviour [82]. It was also pointed out that the shape of the isotherms is rather insensitive to the chemical composition of the material, as only small differences were observed for glucose [5], PVA and other vinyl polymers [5, 83], borosilicate crown glass [84] and amorphous selenium [85].

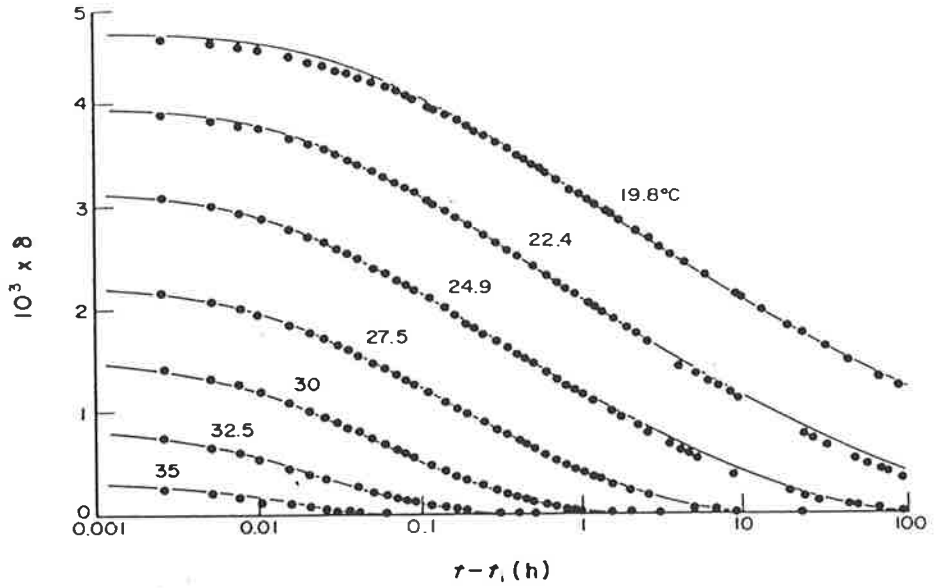

Figure 2.13 Non-linear isothermal contraction of glucose after quenching from 40 C to different temperatures as indicated (reproduced from [7]).

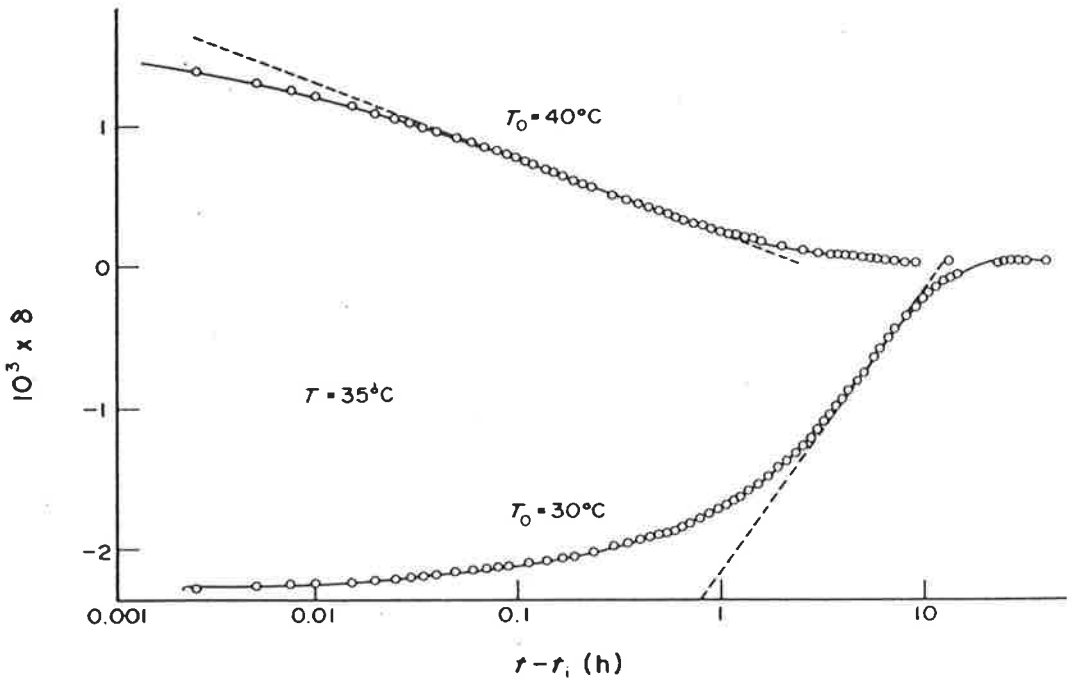

Figure 2.14 Asymmetry of structural recovery: the expansion and contraction isotherms for poly(vinyl acetate) glass at 35 C after heating or cooling from T = 35 +/- 5 C (reproduced from [7]).

The asymmetry of volume recovery is shown for PS [27] and PVAc [7] in Figure 2.14. If a glass was allowed to reach thermodynamic equilibrium at a temperature $T_0 = (T - \Delta T)$ or $T_0 = (T + \Delta T)$, then the volume recovery at the temperature T will differ depending upon whether the the glass is heated or cooled towards T, even at the same initial value of δ. If the specimen is approaching equilibrium from a higher temperature, the contraction is autoretarded, that is, the departure from equilibrium is increased by the lowering of temperature. Hence the mobility decreases with decreasing temperature and the contraction is self-delaying. Conversely, if the approach towards equilibrium is from a lower temperature, the expansion is autocatalytic, that is, the mobility increases as the material moves towards an equilibrium state of higher mobility. At the same values of time, the contracting curve is always closer to equilibrium than the expanding one, and it was concluded that the rate of contraction is always greater than that of expansion [82]. Clearly the character of the expansion isotherm is quite different from that of the contraction isotherm, although both are non-linear.

To recapitulate, volume recovery depends on: (1) the magnitude of the initial departure from the equilibrium state, the further a specimen is cooled from T_g, the larger is the departure; and (2) the sense of the departure, i.e. whether the sample is contracting or expanding towards equilibrium.

One of the more complicated features of non-linear structural recovery of glasses is the *memory effect* (Section 2.2.1), which arises when a material is first allowed to partially recover at a temperature T_1 below T_g, and then heated rapidly to a higher temperature and allowed to recover. Figure 2.15 illustrates the memory effect of PVAc, which was quenched from 40 C to various T_1s, followed by reheating to 30 C. The departure from equilibrium δ actually increases and passes through a maxima, before contracting towards equilibrium at a rate similar to that obtained after direct quenching from 40 C [7]. The height of the maxima decreases and the position of the maxima is shifted to the right as the difference $(T_g - T_1)$ decreases.

The non-linear effects of the first two examples can be attributed to the dependence of the retardation times, τ_i, upon the actual non-equilibrium state of the specimen, whereas the memory effect is accounted for by the multiplicity of retardation mechanisms controlling structural recovery [82]. If recovery involved a single mechanism, then the memory effect would not be apparent and the specimen merely reduce its initial value of δ. If volume

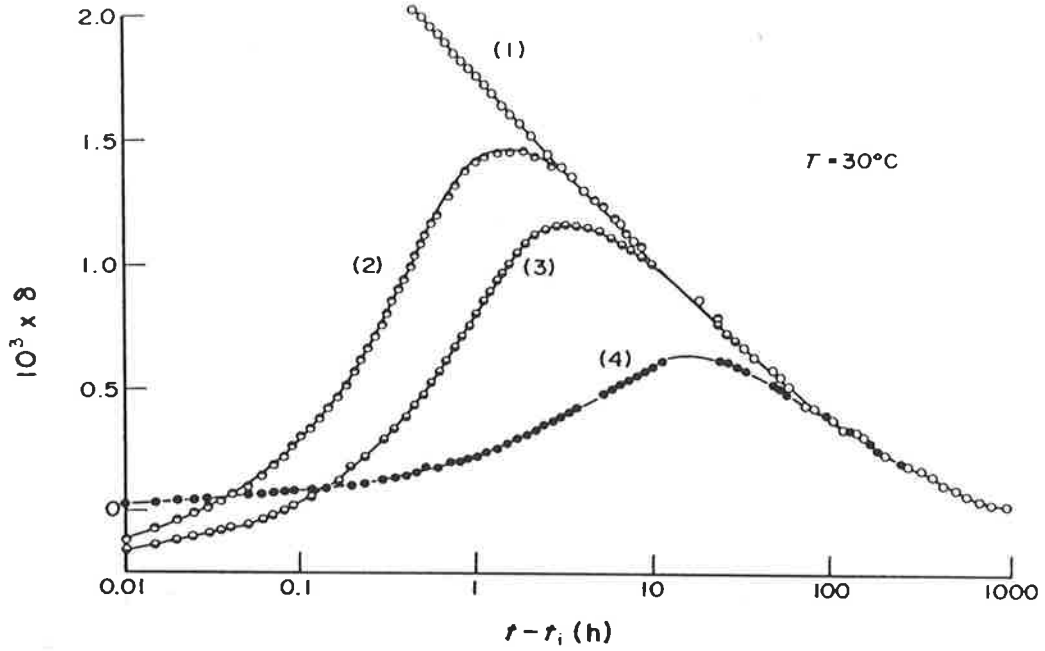

Figure 2.15 Isothermal evolution at T = 30 C for poly(vinyl acetate) showing the memory effect: (1) quench from 40 C to 30 C; (2) quench from 40 C to 10 C for 160 hours, followed by rapid heating to 30 C; (3) quench from 40 C to 15 C for 140 hours, followed by rapid heating to 30 C; (4) quench from 40 C to 25 C for 90 hours, followed by rapid heating to 30 C (reproduced from [7]).

equilibrium is reached at T_1 prior to heating to 30 C, a distribution of τ would give rise to a linear recovery over a wider range of δ. Under such circumstances, the departure from linearity (the second example) would occur symmetrically for contraction and expansion. As none of these consequences were fulfilled by experimental data, neither non-linearity nor asymmetry can be attributed to a distribution of τ [82]. Tool *et al.* [86-87] assigned these features to the variation of retardation times with the actual structure of the specimen. The description of single- and multi-parameter models for describing volume relaxation is considered in the following sections.

2.3.6 The Single-Parameter Model for Volume Recovery

Physical ageing has been shown [19] to be intimately related to volume recovery, in which the changes in polymer properties which occur during physical ageing and volume recovery are attributed to changes in segmental mobility M. Since the relaxation times of the glassy polymer are directly related to M, the mechanical and dielectric properties of the polymer will be influenced by ageing as a result of changes in relaxation times [16]. These hypotheses are supported by the changes observed in the creep properties of PVC at 40 C (Fig. 1.1). An increase in the ageing time t_e from 0.03-1000 days resulted in a curve shift of nearly five decades, that is, for a fixed creep time of say, 10^3 seconds, the creep compliance was reduced by about 40%. The individual creep curves could be superimposed by a horizontal shift to form a single master curve at t_e = 1000 days, which implies that the changes in creep properties are affected only by changes in the relaxation times. Since the shape of the creep curve was not altered by physical ageing, it was deduced that an increase in ageing time changes all relaxation times by exactly the same factor.

The one-parameter model, based on a single relaxation time τ [7, 88-89], assumes that molecular mobility is controlled essentially by the state of the glass characterised by its free volume [9, 13] or configurational entropy [90]. The foundation of the free volume theory is that the mobility of polymer segments primarily depends on the distribution of free volume in the polymer [25-26]. According to this model, the non-equilibrium state of a system can be fully specified by the temperature, pressure, and only one ordering parameter, which is the retardation time, τ.

The derivation of the basic one-parameter differential equation [7] will be presented

here in a general way. The rate of change of the specific volume V at constant atmospheric pressure can be expressed by [7, 82, 88]:

$$dV/dt = \alpha_g.V_{eq}.(dT/dt) - [(V - V_{eq})/\tau] \quad (2.10)$$

where α_g is the thermal expansion coefficient of the glass and dT/dt is the rate of cooling (negative sign) or heating (positive sign). Equation 2.10 should be applicable to any thermal history involving e.g. linear or exponential heating or cooling, and can be rewritten in terms of δ, the deviation of the free volume fraction from its value at equilibrium:

$$-d\delta/dt = \Delta\alpha.(dT/dt) + (\delta/\tau) \quad (2.11)$$

where $\Delta\alpha = \alpha_l - \alpha_g$. Using the free volume approach, the Doolittle equation [13] (Eq. 2.1) can be written as:

$$\tau = \tau_g.\exp(B/f) \quad (2.12)$$

where τ and τ_g are the relaxation times at temperatures T and at T_g and B is a constant of the order of unity. Equation 2.3 can therefore be written in the form

$$\tau = \tau_g.\exp(1/f - 1/f_g) \quad (2.13)$$

Substituting Equation 2.13 into Equation 2.11 the one-parameter equation based on the free volume can be obtained [88]:

$$-d\delta/dt = \Delta\alpha.(dT/dt) + [(\delta.\exp(b/f_g))/(\tau_g.\exp(b/f))] \quad (2.14)$$

Quantitative agreement between theoretical (Eq. 2.14) and experimental results can only be obtained for cooling experiments and for isothermal (dT/dt = 0) contraction following cooling from above T_g. Experiments involving volume expansion, either on heating or in isothermal conditions, show a significant departure from the theoretical predictions [88].

Greiner and Schwarzl [91-92] found that experimental contraction isotherms of PS could be fitted very well by a single relaxation time model, but the fit was shown to be very poor when expansion isotherms were considered and a six-parameter equation was required.

The failure of the single relaxation time equation to model volume expansion and the memory effect was attributed to the oversimplification introduced in the theory, that is, that the non-equilibrium glass state can be adequately characterised by a single relaxation time and hence a single retardation mechanism [7, 88]. This discrepancy is resolved by using a two-parameter model [96, 106-107], in which the free volume fraction is considered to consist of two independent parameters, that is the free volume and occupied volume, and when a distribution of retardation times was assumed [82, 93].

2.3.7 The Two-Parameter Model for Volume Recovery

According to Matsuoka [96], the free volume fraction f is not a directly measurable volume quantity, but is an empirical parameter evaluated from relaxation experiments. The free volume fraction, f, characterises the shift in relaxation times, and thus acts as a parameter for characterising physical ageing. Various models for free volume (e.g. Simha-Boyer [37], Cohen-Turnbull [26]) will give different values for the fractional free volume. One of the weaknesses of most free volume models is the oversimplified implicit assumptions of how the occupied portion of the total specific volume should behave. In most models, the occupied volume (that is, the total volume minus the free volume), is assumed to exhibit the same thermal expansion and compressibility as that of the glassy state. Matsuoka and Kwei [97] observed that the thermal expansion coefficient of the occupied volume was about the same as that of the glassy state, whereas the occupied volume was observed to exhibit a much higher compressibility than the glass.

However, there is much ambiguity in arriving at the value of the occupied volume on a purely theoretical basis. The occupied volume of polymers is expected to depend on the configurational characteristics, for example, isotactic polymers would have a smaller occupied volume than syndiotactic or even atactic polymers, although the specific volumes of these polymers in the rubbery states are the same. The net result is that atactic and syndiotactic polymers show a higher T_g than isotactic polymers [98], as was found for PMMA [99-100] and other polymethacrylates [101]. This was attributed to the possibility that the energy barriers to

rotation are lower in the isotactic form than in the less crowded syndiotactic form [24]. The T_g for atactic and syndiotactic polymers (e.g. polypropylene [102], PS [103], and PET [104]) were however, found to be approximately the same. The occupied volume was found to be considerably greater than the crystalline volume [105], therefore it was argued [96] that there is a significant amount of vacancies associated with the occupied volume.

The isothermal expansion curve has been shown to exhibit a different shape from the contraction curve (Section 2.3.5), because the rate of volume change is very small initially, but later is accelerated. Aklonis and Kovacs [106] have shown that the basic one-parameter equation (Eq. 2.14) is not precise enough to describe the observed behaviour, and more than one relaxation time is required. However, the essential aspect of the dependence of volume recovery on the free volume fraction is still considered to be valid [96]. The two-parameter model proposed by Aklonis and Kovacs [106] can be explained physically by considering the fractional free volume to consist of two independent parameters, namely, the free volume and the occupied volume. By considering the free volume and the occupied volume as two separate parameters, the asymmetric behaviour of Figure 2.14 and the memory effects of Figure 2.15 can be quantitatively modelled. During isothermal contraction of a glassy polymer, the volume decrease is accompanied by the decrease in free volume while the occupied volume supposedly remained constant. However, this is not always the case; the rate of decrease of the free volume is determined by rate constant $k = 1/\tau$, and if the rate of an imposed deformation (in this case the rate is zero) is equal or less than $1/\tau$, the fractional free volume will change in response to the deformation, by a slow and gradual densification. If the specimen was suddenly compressed at a rate greater than $1/\tau$, the specimen will be elastically compressed where, upon removal of the external force, will recover. This fast elastic response does not involve any changes in the free volume fraction, but involves a change (unrelaxed pertubation) in the occupied volume [96].

It was proposed that when a glass is suddenly heated, the occupied volume would not instantaneously expand to its equilibrium value; rather it expands in a delayed manner according to the prevailing relaxation time dictated by the *effective* free volume. The effective free volume is the amount estimated from the specific volume plus a contribution equal to the unrelaxed pertubation in the occupied volume. By considering the time-dependent expansion of the occupied volume, the asymmetric behaviour of volume expansion and memory effect can be described. In Figure 2.14, the rate of expansion is initially small, owing to the delayed

expansion of the occupied volume and thus the small value of the fractional free volume; the approach to equilibrium is later accelerated when the expansion of occupied volume becomes more significant. If the specimen was heated froma much lower initial temperature, the rate of expansion of occupied volume can exceed the rate of decrease of free volume, and the total volume can reach maximum values above the value at equilibrium [96, 107], giving rise to memory effects.

Using Kovacs' [7] data for PVAc, Matsuoka [96] and Bair *et al.* [108] have shown that the consideration of the occupied volume as a second parameter yields calculated results which compare favourably (Fig. 2.16a) with the experimental data shown in Figure 2.14. The memory effect in which the volume first deviates away from equilibrium was also successfully described by the two-parameter equation [96] (Fig. 2.16b). This model with the changeable occupied volume could well be defined in terms of the redistribution of free volume. The physical nature of the occupied volume is still speculative, but it is known to be less densely packed than the crystal lattice. The change in occupied volume may be considered in terms of the relative populations of various configurations that change as the system deviates further from the equilibrium state [96].

2.3.8 The Multi-Parameter Model for Volume Recovery

The introduction of a multi-parameter model involving more than one ordering parameter was performed and thermodynamically justified by Kovacs *et al.* [94]. A physical model is adopted in which a system in a non-equilibrium state is completely characterised by the temperature, pressure, and a series of ordering parameters, τ_i (i = 1,....N). Each ordering parameter is associated with a particular mode of molecular motion, which contributes a specific fraction δ_i to the total recoverable free volume δ. A basic assumption of this model is that δ_i remains unaffected by other retardation mechanisms, even if these occur at a shorter time scale. Equation 2.11 is obeyed by every recovery mechanism and involves a retardation time τ_i which is assumed to depend on the total free volume of the system at any time and temperature. This means that expressions developed for τ can be used for all τ_i without further modification. This is equivalent to assuming that the shape of the retardation spectrum, or the distribution function, remains invariant but can be shifted with respect to changes in temperature and δ [88, 94].

Assuming that the time dependence of each individual fraction δ_i can be expressed

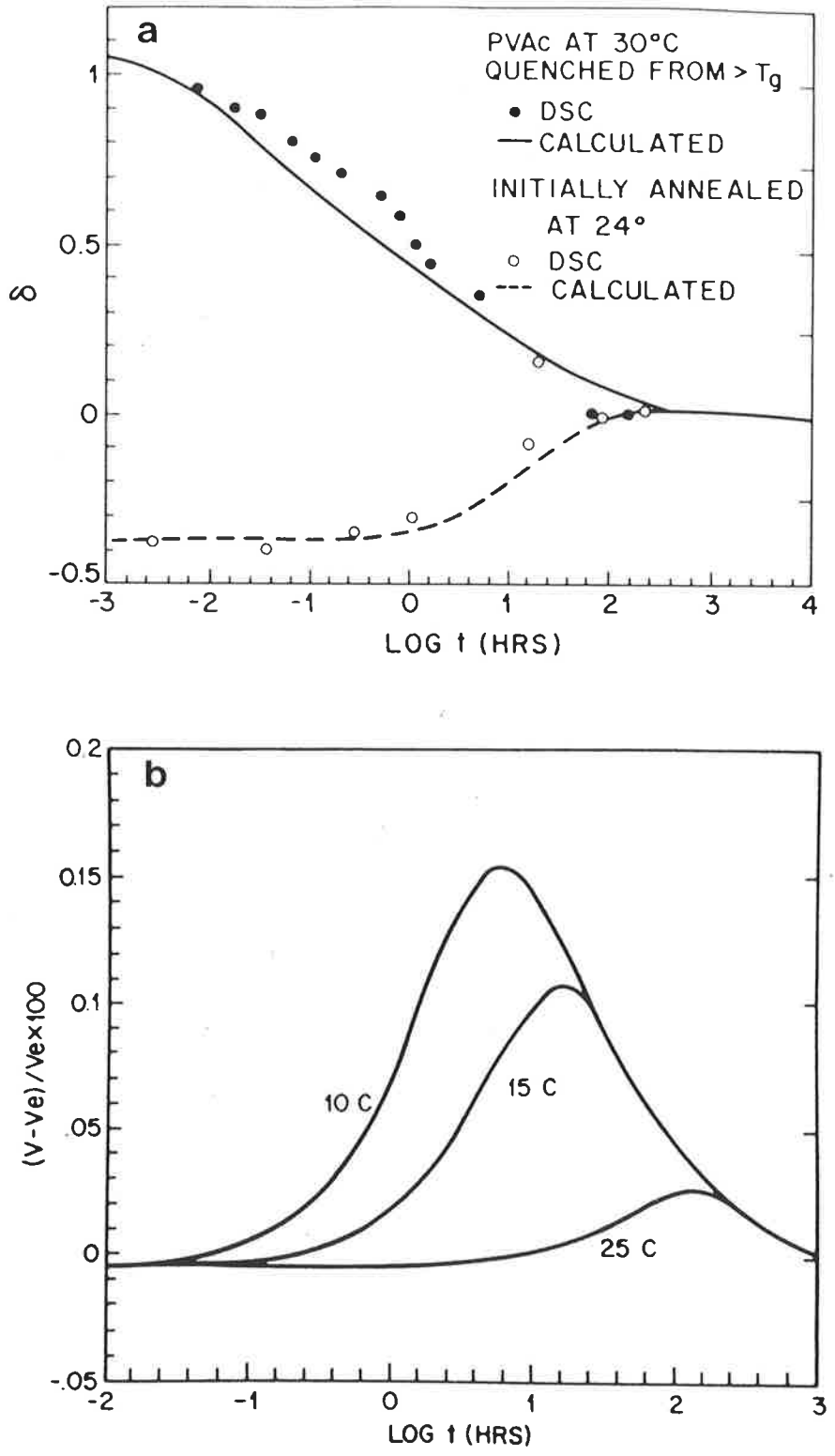

Figure 2.16 (a) Two-parameter modelling of the enthalpy recovery of poly(vinyl acetate) during cooling or heating to 30 C. δ represents the departure from equilibrium as in Figures 2.13 to 2.15 (reproduced from [108]). (b) Quantitative modelling of the memory effect using a two-parameter model (reproduced from [96]).

in the form of Equation (2.11), then each change of the system will be governed by N differential equations of the form [92]:

$$-d\delta_i/dt = \Delta\alpha_i.(dT/dt) + (\delta_i/\tau_i) \quad (i = 1,....N) \qquad (2.15)$$

where $\Sigma\ \delta_i = \delta$ and $\Sigma\ (d\delta_i/dt) = d\delta/dt$, (i = 1,....N). Non-linearity is attributed only to the variation of τ_i with δ, and the term (δ_i/τ_i) measures the effect of the distribution of τ_i on the overall shift rate. (δ_i/τ_i) depends on the temperature (through τ_i), time, and in general on the thermal history of the specimen [88]. For recovery experiments involving more than one temperature jump, the incomplete stabilisation at intermediate temperatures result in memory effects, because (δ_i/τ_i) will contain residual terms which have not vanished during the previous thermal history.

The iteractive calculation of retardation times has revealed [88] the theoretical distribution to be wide, extending to five decades of τ_i. Similar results were obtained by Goldbach and Rehage [93]. The asymmetric distribution consists of two parts: a short-time tail of three decades wide, was associated with about 10% of δ_0, the initial departure from equilibrium following the T-jump, and a long-time portion spanning two decades, was associated with the major portion of δ_0. Greiner and Schwarzl [92] showed that a multi-parameter equation involving six retardation times, ranging from 5×10^{-6} to 8s, was required to fit the expansion isotherms of PS. A smaller number of retardation times, even when extended over five orders of magnitude of the time scale, did not lead to a satisfactory agreement.

However, the application of this model revealed one serious discrepancy, arising from a common assumption that the equilibrium state is independent of any previous thermal history, and can be uniquely determined by temperature and pressure alone. Expansion isotherms for poly(vinyl acetate) [7] showed that for the same temperature as δ approached zero, the limiting τ_i values were not uniquely determined by temperature, but depended on the previous thermal history of the specimen [95]. Pertinent experiments revealed that structural rearrangements still occured in apparent voluminal equilibrium of the polymer and they affected the time scale of molecular motions in an appreciable manner. Accordingly, the distribution function for τ_i is not uniquely determined by temperature and the actual departure from equilibrium but also depends on some other structural changes which contributes to the volume

recovery. Despite its successes and improvements over the single parameter model, the multi-paramater model still cannot fully account for structural recovery [88].

2.3.9 Molecular Motions of Poly(Methyl Methacrylate) and Poly(n-Alkyl Methacrylates)

According to Struik's free volume model [16, 19] (Section 2.2.3) the mobility of a glass cannot become zero, even at temperatures below T_g. This hypothesis is supported by the experimental observation of spontaneous densification during physical ageing [5, 7]. Solid state NMR measurements of PMMA and a series of glassy, crosslinked poly[oligo(ethylene glycol) dimethacrylates] [109-110] have revealed that the backbone carbons (quartenary C and -CH_2-) and the side-group carbons (-CO-, -OCH_3, α-CH_3) of PMMA are very mobile at room temperature. Hence, local motion involving small molecular groups can take place at low temperatures with apparently negligible effect on the ageing process. A knowledge of the molecular motions which are responsible for the relaxational transitions is essential.

Transitions in polymers becomes observable when the time scale of the experiment becomes comparable with the relaxation times of the molecular processes responsible for the transitions. The early investigation of relaxational processes of PMMA in the glass transition (α-relaxation) region has been studied by mechanical [111-113] and dielectric [114-115] methods. Although various values of T_g for amorphous PMMA have been reported, these variations may be due to differences in stereoregularity between different samples or to the presence of absorbed moisture. The value of 105 C [43, 53, 117] is commonly accepted for the glass transition temperature of PMMA.

Generally, the glass transition of amorphous polymers has been attributed to freezing-in of the large scale rotational and translational motion of the backbone chain segments of the polymer. While similar notations (α, β, γ, etc.) [116] are used to designate the various transitions, it is unlikely that the resulting transitions will represent similar molecular motions with polymers of different structures and composition. Each polymer system needs to be investigated individually and assignment of molecular motion attached to each of the relaxation modes [21].

The T_g of poly(*n*-alkyl methacrylates) have been shown [43] to decrease when the number of carbon atoms in the ester side group is increased, from 105 C for PMMA to

approximately -65 C for semi-crystalline poly(*n*-dodecyl methacrylate). An explanation given for these observations is that as the length of the side chain increases, neighbouring chains are pushed further apart, thus decreasing the hindrance to the backbone chain motions. This effect is similar to that produced by the addition of plasticiser, and is usually known as *internal plasticisation* [17]. In support of this hypothesis is the observation that the specific volume shows a systematic decrease (hence a systematic decrease in density) with increasing length of the *n*-alkyl group [43]. Internal plasticisation is not observed if the *n*-alkyl group is replaced by the bulkier iso- or tertiary-alkyl group, for example, the respective T_gs of poly(*t*-butyl methacrylate) and poly(*i*-butyl methacrylate) are about 55 C and 40 C higher than that for poly(*n*-butyl methacrylate) [40]. Hence the shorter and more rigid iso- and tertiary-butyl groups are far less effective at internal plasticisation than the linear flexible *n*-butyl group, and the intramolecular rotations of these bulky groups increases the steric hindrance to the α-relaxation. The T_g is also appreciably increased when the *n*-propyl and *n*-hexyl groups are replaced by the isopropyl and cyclohexyl groups respectively.

Steric hindrance to main chain motion caused by the rotation of the α-methyl group of PMMA is believed to be responsible for the large difference in T_g between PMMA and poly(methyl acrylate) (PMA), which has no α-methyl group. The T_g of 9 C for PMA [39, 50] is 96 C lower than the T_g of PMMA. The rotation of the α-CH_3 in PMMA is consistent with a NMR line-width narrowing centred at about -110 C [118-120], which PMA does not exhibit in the same temperature region. Thus this relaxation region is probably due to the rotations of the α-methyl group and not the methyl groups in the ester side-chains.

The β-relaxation in PMMA has been observed from mechanical measurements by a number of workers [70, 121-123], and it is attributed to the hindered rotation of the ester -$COOCH_3$ group about the C-C bond which links it to the main chain. The steric hindrance to this rotation comes largely from the α-methyl substituents of the two *adjacent* repeating units [70]. Some experimental evidence [17, 124] seems to indicate that the rotational motion of the ester group requires a slight deformation of adjacent bond angles of the backbone. Therefore, this type of motions has been referred to as *a side group motion with some main chain cooperation* [125-126]. However, Johari [77] argues that the predominant mechanism for the β-relaxation is not from side group motion, but arises from the hindered motions of relatively loose molecules in the interstitial regions of well-packed clusters in a glass. While the

phenomenological aspects of this relaxation are well developed, its molecular basis and mechanism remains questionable [127].

The dynamic-mechanical results of Heijboer [70] (Fig. 2.17) show the β loss peak for PMMA at 10 C and the peak at 120 C is due to the α-relaxation discussed previously. Volume-temperature data of Heydeman and Guicking [128] for PMMA revealed the existence of two relaxations below T_g at 62 C and 7 C; volumetric transitions at 15 C and -30 C were reported by Martin *et al.* [129], while Haldon and Simha [40] indicated the presence of transitions at -130 C and at approximately -50 C in addition to the one at 15 C. Various transitions in the 20-70 C range have also been reported by various authors using dilatometric techniques [43, 128-131]. Whilst the reported transitions falling just below room temperature may be associated with the β-relaxation attributed to motions of the ester side group, the transitions between 20 C and 70 C are more difficult to reconcile. Furthermore, the β-relaxation peak has been shown to merge with the main α-relaxation peak on lengthening the ester side chain over a wide temperature range [40, 44], so that the resolution of α- and β-transitions would be impossible.

Literature values for the activation energies E_{act} of the α-transition of PMMA range from 80 kcal/mole [116] to 250 kcal/mole [113, 132]. E_{act} values quoted for the β–relaxation of PMMA obtained from dielectric and mechanical measurements ranged from 17-30 kcal/mol [17]. The temperature dependence of relaxation times of the α-relaxation was found to conform to the WLF equation [17] The dielectric retardation spectra of PMMA and other poly(*n*-alkyl methacrylates) [133] show the α–relaxation shift to shorter relaxation times (i.e. the main-chain mobility is increased) as the length of the alkyl group increases. This observation is consistent with the lowering of the T_g and the temperature of the mechanical α-peak.

For the β–relaxation the temperature dependence of the relaxation times was found to obey the Arrhenius equation, but there are conflicting views concerning the dependency of E_{act} for the relaxation in poly(*n*-alkyl methacrylates) on the length of the side group. It was concluded by McCrum *et al.* [17], that the relaxation times for the β–process is independent of the *n*-alkyl group length; for longer *n*-alkyl groups the situation is complicated by the merging of the α and β relaxations, thus the assignment of a single relaxation mechanism in the higher methacrylates to the β–relaxation is unlikely to be correct.

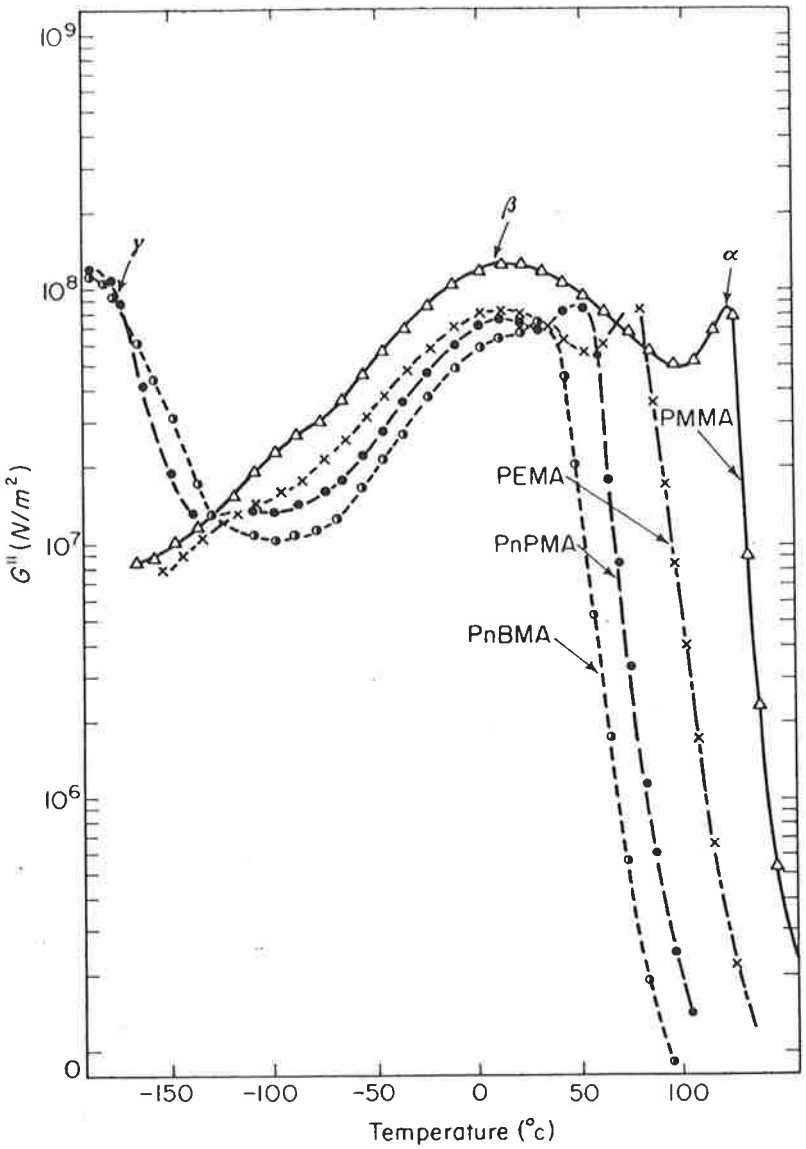

Figure 2.17 Temperature dependence of loss modulus G" at 1 Hz for poly(methyl methacrylate), poly(ethyl methacrylate), poly(*n*-propyl methacrylate) and poly(*n*-butyl methacrylate) (reproduced from [70]).

2.3.10 Mechanical Modelling of Molecular Behaviour

If an amorphous polymer was subjected to an external stress at temperatures above T_g, the chains can instantaneously rearrange into different configurations to accommodate the deformed structure, however, if the stress was applied at temperatures below T_g, the rearrangements take place over a longer period of time. This time-delayed molecular response to mechanical stresses and strains is known as the *viscoelastic* behaviour of the polymer.

A qualitative representation of all the phenomena generally observed with viscoelastic materials, viz. instantaneous and retarded elastic strain, equilibrium viscous flow, instantaneous and retarded elastic recovery, and permanent set, may be represented by a four-parameter mechanical model [134]. This mechanical model consists of a Hookean spring and a Newtonian dashpot arranged in series, coupled to a parallel spring-dashpot (Kelvin-Voigt) combination (Fig. 2.18). The model elements can be identified with the various molecular response mechanisms in polymers, and it can therefore be used to predict influences that changes in molecular structure will have on mechanical properties. The following paragraphs discuss three molecular responses in a general way.

(1) *Elastic and Instantaneous Response*: the spring in series represents the elastic and instantaneous (independent of time) response of a polymer. This could be applied to the elastic and reversible straining of bond angles and bond lengths. Since these deformations involve interatomic bonding, they occur essentially instantaneously from a macroscopic point of view. If plastics were perfectly elastic, the shape of, the molecular orientations, and internal stresses in the specimen would be determined only by the stresses acting upon the specimen; upon unloading, the dimensions and shape would be fixed and independent of time. In practise this is not so. Dimensional instabilities due to stresses in the past (e.g. processing history) only arise because the mechanical properties of plastics are time-dependent (viscoelastic) [135].

(2) *Viscoelastic Response*: the Kelvin-Voigt element represents the viscoelastic response of a solid; the spring represents the restoring force brought of the chain segments, which tends to return chains oriented by a stress to their most random or highest entropy configuration. The dashpot represents the resistance of the polymer chains to uncoiling and coiling, caused by temporary mechanical entanglements of the chains and molecular friction during these processes. Since coiling and uncoiling require cooperative motion of many chain segments, they cannot occur instantaneously and hence account for retarded elasticity. The

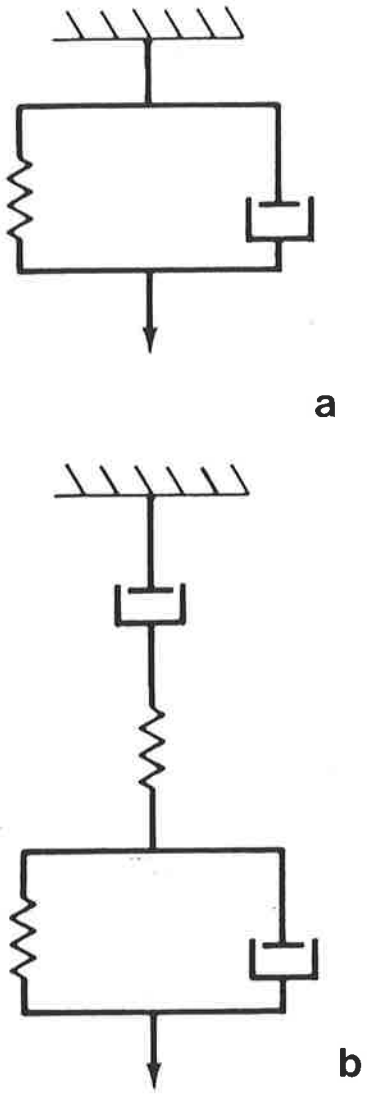

Figure 2.18 Linear viscoelastic models: (a) the Kelvin-Voigt element, with dashpot and spring in parallel; and (b) the four-parameter model.

viscoelastic response of a polymer to creep is dependent on the load applied and the temperature.

Examples of the viscoelastic nature of physical ageing include the shifting to longer creep times with increasing ageing time (Fig. 1.1), and non-linear isothermal volume recovery (Figs. 2.13-2.15). The creep recovery is slower at lower temperatures when the polymer is in its glassy state, but as the temperature is raised, the creep response correspondingly becomes quicker. The different responses observed when changing from a glass to a melt reflect the different rates of molecular motion present in the two states [136]. Volume relaxation which occurs during physical ageing may be qualitatively described by the viscoelastic elements. Above T_g, the rapid changes in molecular configuration can be represented by the unified response of all four mechanical analogues. At the glass transition, molecular mobility becomes increasingly slow such that they can no longer keep up with changes in temperature. The response of the springs become restricted, until at below T_g, their contribution to volume recovery becomes minimal. The long period of time required to reach equilibrium (e.g. at 25 C below T_g physical ageing is expected to continue for about 730 years [14, 19]) in the glass state indicates that an instantaneous recovery mechanism is unlikely, even though small scale intramolecular rotation and side-chain rotation may take place below T_g. The same effect is also expected of the dashpot in series (characterising molecular slippage), as main chain motion has ceased below T_g and viscous flow can no longer take place. The delayed response of the Kelvin-Voigt dashpot becomes important in determining the macroscopic viscoelastic behaviour of the polymer during physical ageing.

However, it was shown in Section 2.3.8 that a distribution of retardation times exists corresponding to the many relaxation modes which contribute to volume recovery [89]. Hence, the molecular basis of viscoelastic response of polymers lies in the multiplicity of retardation times, which suggests that it is likely that more than one Kelvin-Voigt elements are required to completely describe the process of ageing.

(3) *Permanent Deformation*: molecular slippage and irreversible deformation can be represented by the dashpot in series. The slip of polymer molecules past one another is responsible for *viscous flow* and permanent set. At high loads some irreversible deformation may occur, even at low temperatures. Although various aspects of molecular behaviour may be qualitatively represented by individual elements of the four-parameter model, the model must be

treated in its entirety in order to describe the molecular behaviour of amorphous polymers correctly.

2.3.11 Physical Ageing and Residual Stresses

In addition to physical ageing, another source of dimensional instability in polymers arises from frozen-in residual stresses. These stresses are known to affect a number of polymer properties, for example, frozen-in molecular orientation produces an entropic reaction stress [135, 137] which affects the glass thermal expansivity (see Section 2.3.14). However, residual stresses can also be beneficial by extending the fatigue life of polymers [140-141] and improving resistance to applied external stresses [138-139].

Residual stresses in a polymer may contain one or more of *thermal*, *curing* and *entropic* stresses. Thermal stresses, like physical ageing, are thermoreversible, since it can be completely removed by heating to above T_g and reintroduced by rapid cooling. Curing stresses can be completely removed by annealing (see Section 2.3.12) the polymer at temperatures near or above T_g, but the complete removal of entropic and shaping stresses is expected to require higher temperatures above T_g as large scale cooperative motion is required for randomisation and the resumption of an amorphous structure. On the other hand, physical ageing is not caused by shaping stresses or thermal stresses but occurs when the polymer is cooled into the unstable glass state [135]. The gradual increase in density with time [7, 19] cannot be avoided and it occurs in all glasses, even in the absence of residual stresses. The origins and nature of residual stresses in polymers and its effect on physical ageing are discussed in the following sections.

Thermal (Cooling) Stresses

If an amorphous material is cooled rapidly through T_g, the temperature in the material is non-uniform and a temperature gradient is formed. The inhomogeneity of the cooling is responsible for the generation of thermal stresses. Because the polymer changes from a soft melt into a stiff glass, part of these stresses are frozen-in. Such stresses are only due to the non-uniform (rapid) cooling and arise irrespective of whether shaping stresses are present or not [137].

A polymer may be rapidly quenched from above to below T_g by immersing in liquid

nitrogen. However, the use of liquid nitrogen for quenching has been rejected by Struik [72] for two reasons: firstly, quenched samples may absorb moisture during transfer from the liquid nitrogen bath to the measuring instrument, and secondly, the high cooling rates will produce cooling stresses in the specimen. On the other hand, dynamic-mechanical tests [79] of liquid nitrogen-quenched PMMA samples showed that poor data reproducibility was observed only during the first ten minutes of ageing, which suggested that the effect of thermal stresses on the ageing and mechanical loss behaviour of PMMA was not significant at long experimental times. It was concluded that the use of liquid nitrogen was necessary for good quenching [79]. Lee and McGarry [143] estimated the cooling rates during quenching in liquid nitrogen to be in the range of 500-700 C per second. However, the authors [143] did not report any problems with their liquid nitrogen-quenched PS samples arising from thermal stresses.

The following example describes the origin of thermal stresses resulting from differential dimensional changes, which serve to restrain the normal expansion or contraction of adjacent volume elements in a material. Toughened glass formed by *thermal tempering* [138] is first heated to above T_g but below the softening temperature. It is then quickly cooled to room temperature in a jet of air or in an oil bath. The thermal stresses arise from differences in cooling rates for the surface and interior regions; initially, the surface cools more rapidly and becomes rigid as the temperature drops to below T_g. The contraction of the surface is counteracted by the interior, which is at a higher temperature and thus is still liquid. With continued cooling the contraction by the interior is restricted by the rigid surface; the interior core tends to draw in the surface, thus imposing inwards radial stresses. As a consequence, thermally-tempered glass sustains compressive stresses on the surface and tensile stresses at interior regions. The stresses at the surface will be counterbalanced by stresses in the interior, resulting in a stress-free glass [137, 139]. Toughened glass is one example of deliberately inducing thermal stresses to enhance the strength of the glass.

The introduction of thermal stresses were found to result in an improvement in the mechanical properties of polymers. For example, PMMA and bisphenol-A polycarbonate (PC) sheets quenched from temperatures just above T_g to 0 C was shown [139] to contain surface compressive stresses in the order of 21 Mpa, and interior tensile stresses of at least 7 Mpa. The impact strength of some of the PC samples were doubled and crazing was suppressed. These observations were confirmed by Hornberger and Devries [140] for PC, where surface stresses

as high as 31 MPa were produced after quenching in liquid nitrogen. The residual stresses were not removed even after annealing for 40 000 hours at 65 C. The mean fatigue life of the treated samples were found to improve by a factor of ten over that of untreated samples. The presence of a compressive residual stress at the surface of polycarbonate specimens was also found to decrease the sensitivity of the polymer to surface scratches and flaws [142].

It has been suggested [19] that the mechanical deformation of polymers generate free volume, irrespective of the nature of the deformation. This hypothesis is supported by the results of Rabinowitz and Beardmore [141], who were able to change the fatigue behaviour of PMMA from a "brittle" type to a "ductile" type by thermal treatment. The observations of Rabinowitz and Beardmore [141] suggest that the introduction of cooling stresses resulted in the erasure of physical ageing by the loss of embrittlement. On the other hand, the effect of residual stresses on the ageing behaviour of polymers have been shown to be insignificant by a number of authors [19, 155]. The ageing of a PVC sample was tested directly by creep measurements at 40 C after injection moulding, and the creep curves were found to shift continuously to the right (bold curves, Fig. 2.19), thus confirming the expectation that processed plastics will show ageing effects [19]. To find out the effect of internal stresses, the sample was subjected to a second ageing test at 40 C in which it was annealed at 110 C for 24 hours and requenched to 40 C. Ageing was found to resume (thermoreversibility) but the internal stresses in the injection-moulded sample were shown to have only a small effect on the creep (fine curves, Fig. 2.19). It was concluded [19] that the creep was affected to a greater extent by physical ageing than by residual stresses. A similar conclusion was also reached by Sandilands and White [155] for poly(4-methyl 1-pentene) (P4MP1). The fatigue fracture behaviour of injection-moulded P4PM1 was found to show little sensitivity to the following post-moulding conditions: ageing for one month at room temperature, annealing at 24 hours at 175 C, aged at -18 C for fourteen months, and mechanically conditioned by stress cycling at 0-6.45 MPa at 25 C. Physical ageing had little effect on the residual stress and stress-relaxation behaviour of P4PM1, but cyclic loading increased the level of the residual stresses.

Curing Stresses

Curing stresses in polymers are generated at the onset of vitrification. Vitrification can be attributed to the growing polymer fraction as polymerisation continues within the already

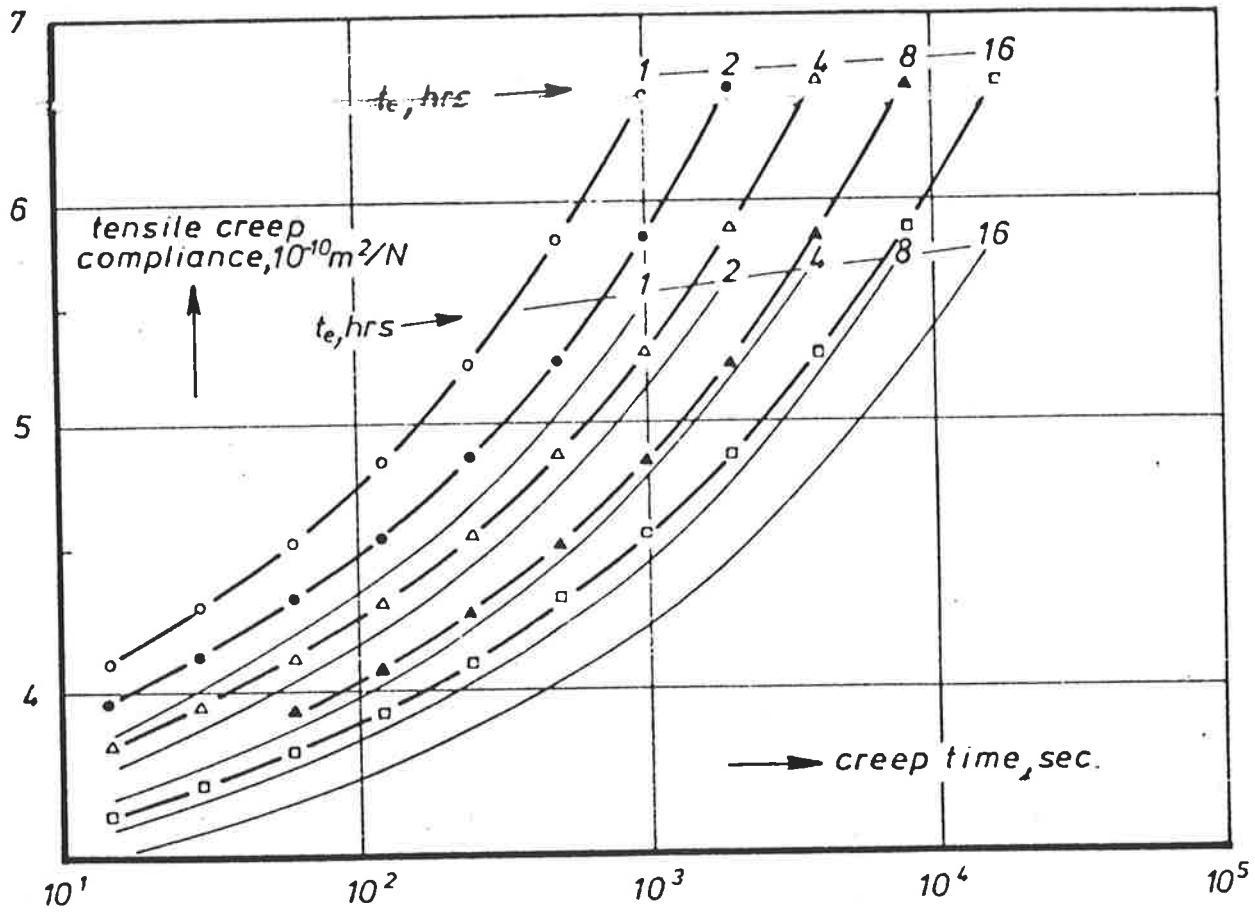

Figure 2.19 Small-strain tensile creep of an injection-moulded sample of rigid poly(vinyl chloride). Bold curves were obtained when, immediately after moulding, the sample was rapidly heated from 20 C to 40 C and tested at 40 C after t_e of 1, 2, 4, 8, and 16 hours. Fine curves were obtained for the same sample when, after the first set of tests, it was annealed at 110 C for one night, quenched to 40 C, and measured at 40 C as before (reproduced from [19]).

gelled resin, and the concomitant loss of the plasticiser action of the monomer [146]. The volume contraction of regions of high cure with dense clusters of macromolecular chains will be restrained by regions of low cure. However, the reverse happens when the regions of low cure polymerises, the contraction of these regions will be restricted by the vitrified clusters, thus tensile and compressive stresses can be generated in a similar way to thermal stresses at the surface and interior of a material.

A study of the isothermal curing of epoxide resins [144] revealed that volume contraction took place in three stages: (1) curing above T_g, (2) cooling from the temperature of cure to T_g, and (3) cooling to below T_g. The maximum contraction of the epoxide resins upon coversion from monomer to full cure was estimated at 10%. The fraction of the total contraction which occured during curing increased from 1% for poly(dodecamethylethyl-enediamine) to 44% for poly(ethylenediamine). This was reflected in the shrinkage stresses measured at 25 C (about 100 C below T_g), in which the magnitude of the stresses were found to increase with T_g and increasing crosslink density, ranging from approximately 3 MPa for poly(dodecamethylethylenediamine) to 6.5 MPa for poly(ethylenediamine). Shrinkage stresses were almost absent in the rubbery region, which was attributed to the high molecular mobility of the chains in this region. It was concluded [144] that the curing stresses were mainly induced by shrinkages during cooling in the glassy region.

Similar results were obtained by Plepys and Farris [145] for the cure of a three-dimensionally contrained commercial epoxy resin (T_g = 80 C) from 40 C to 90 C, in which the monomer was cured in a cylindrical stainless steel tubes. Gelation occured after seven hours during isothermal curing at 40 C. At this point the stress began increasing rapidly over the next five hours before slowly levelling out for the remainder of the cure. The shrinkage stress was measured to be 8 MPa at the end of the isothermal curing. Following isothermal curing at 40 C, the resin was heated to 90 C at a rate of 10 C per hour. The epoxy resin was under 15 MPa compression at the end of the temperature ramp. The resin was held at 90 C for two hours during which the compressive stress decreased to 10 MPa. Following cooling to 30 C, the magnitude of the stress in the epoxy resin reached a maximum value of 25 MPa. The largest increase in curing stresses was also observed after cooling to below T_g.

The considerable magnitude of curing stresses are evident in the curing of cast sheet samples of crosslinked poly(ethylene glycol dimethacrylate) (PEGDMA). Uncracked samples

of PEGDMA could not be cast due to the brittle nature of the polymer and the large contraction (15.7 volume percent [147]) on polymerisation [109-110, 148-150].

Entropic Stresses

Products of amorphous polymers are usually made by deformation of the material in the molten or rubbery state. The processing of plastics by extrusion, injection moulding, etc., may be regarded as a quench [19], where the subsequent shaping of the polymer by cooling to below T_g freezes-in the deformation and results in a state of molecular orientation. It has been claimed [137] that frozen-in entropic stresses and the subsequent contraction upon the heating of an oriented specimen are two expressions of the same phenomenon. As an example, the uniaxial compression or elongation of a specimen will result in entropic stresses which will act reversibly with temperature [135, 137]. If a polymer is stretched by an external stress σ_0 above T_g, the chains will be oriented to the extent that the entropic rubber-elastic reaction stress σ_r balances σ_0. When the material is rapidly cooled to below T_g, the cooling will freeze in the state of orientation and the entropic stress σ_r. Therefore, entropic stresses in amorphous polymers are generated by the anisotropy of the molecules [137]. The presence of such stresses causes the modification of mechanical properties and any change in the magnitude and orientation of these stresses during post-moulding may be important. Entropic stresses are known to supress crazing at the surface [139, 151-152] and promote ductile, shear yielding behaviour in glassy polymers [153].

The study of the effects of entropic and cooling stresses on the cyclic tensile fatigue behaviour of injection-moulded polysulfone by Mandell *et al.* [152] supported the suggestion that the effects of physical ageing are partially removed by residual stresses. The fatigue behaviour of annealed and quenched specimens with no entropic stresses were compared with the behaviour of as-moulded specimens which contained both cooling and entropic stresses. The tests were continued until the specimen either fractured or necked (shear yielding). It was observed that the yield stress increased with ageing, but decreased with increasing residual stress levels, that is, annealed specimens were found to have the highest yield stress followed by the as-moulded and quenched specimens.

Similar conclusions were derived from the work of Coxon and White [154], who reported that polypropylene specimens aged at higher temperatures lost much of their residual

stress. The relaxation of entropic stresses during physical ageing was also observed to be accompanied by dimensional changes. Stress relaxation tests of injection-moulded polypropylene bars at 22 C performed by the authors [154] found that the length of the bars became shorter on ageing. To relieve stress in the region of compression, flow must occur in the region of tension and vice-versa. It was suggested, from the observed shortening, that contractile flow in the surface is easier than extensional flow in the interior. Moulding stresses were found to relax even at -40 C, suggesting that γ- and β-relaxations [17] associated with physical ageing may be involved in the stress relaxation process.

Although the effects of residual stresses on mechanical properties have been extensively studied [137-145, 151-155], conflicting evidence concerning the effect of residual stresses on physical ageing indicate that the relationship between the two phenomena is not well understood. There appears to be some evidence [153-154] to suggest that the introduction of residual stresses causes a partial and gradual erasure of ageing, which supports the hypothesis [19] that additional free volume is generated by mechanical deformation or by cooling stresses. It may be inferred that the rate of ageing of a polymer should increase with increasing levels of residual stresses. This was recently confirmed by the work of Haidar and Smith [156] and Bartos *et al.* [157], who showed that the rate of ageing of stretched or drawn PC films increased with increasing temperature and static strain.

2.3.12 Physical Ageing and Annealing

The annealing of polymers is a poorly understood process in which it is usually defined as a process wherein the polymer is brought to a certain temperature, usually near or above the T_g, kept there for a time, and then cooled slowly and gradually to room temperature [158]. The primary reason for annealing include the reduction or removal of residual stresses and strains and an improvement in dimensional stability. However, the annealing of quenched samples of PS at 80 C resulted in density changes of up to 0.2% [27], while the intrinsic yield stress of PS specimens annealed at 110 C was found to be 12% higher than for quenched specimens [159-160]. Similarly, the yield stress for annealed and quenched PMMA samples tested at 80 C under constant load was found to be reduced by quenching [161]. Other property changes upon annealing include a decrease in enthalpy, which is manifested during heating to above T_g as an endothermic peak [80], and a shift in creep relaxation time [162], which

increases with increasing temperature.

In addition, property changes which are brought about by annealing are similar to the changes produced by physical ageing. This was implicitly acknowledged by Hodge *et al.* [163-164], where the parameter t_e is defined interchangeably as "ageing time" and "annealing time". In some references, for example in [19], [158] and [165], the term "annealing" has been used synonymously with physical ageing, although Struik [19, 135] uses the term "pre-annealing" to describe the method in which volume relaxation (i.e. physical ageing) is reduced after isothermal heating. These examples indicate the prevailing misconception and confusion that are associated with annealing.

At the present time there is no defined procedure for annealing, however, LeGrand [158] suggested that the most desirable annealing temperature for amorphous materials is above T_g, where the relaxation of stress and orientation is most rapid. On the other hand, thermal degradation (chemical ageing), distortion, and warping of the material may occur at these temperatures. It was suggested [158] that the polymer should be heated to the highest possible temperature where the maximum rate of strain release can take place without subjecting the material to thermal degradation, followed by very slow cooling to avoid the reintroduction of thermal stresses. The annealing time necessary depended on the thickness and geometry of the material, the annealing medium, and the degree of relief required [158].

However, such an annealing procedure was rejected by Struik [135], who stated that "the widespread opinion that the efficiency of annealing increases with annealing temperature is wrong", and suggested that the highest efficiency of annealing is achieved at some annealing temperature T_a which lies between the working temperature T_w and the T_g (Fig. 2.20). The efficiency of annealing, which refers to the reduction in the rate of volume relaxation at T_w after the annealing period, goes through a maximum and then drops to zero when T_a approaches T_g. In other words, Struik is suggesting that there is little advantage in annealing at temperatures very close to the T_g. However, the following example will show that Struik's suggestion for the optimum annealing temperature is incorrect and is self-contradictory.

The volume relaxation of PVC (T_g of PVC is 82 C [52]) was measured at 20 C after quenching from 85 C [19]. Three PVC samples were prepared, one from a direct quench from 85 C to 20 C, and the remaining samples were annealed at 50 C for 2 hours and 18 hours before cooling to 20 C. The rate of volume relaxation was lowest (that is, the greatest amount

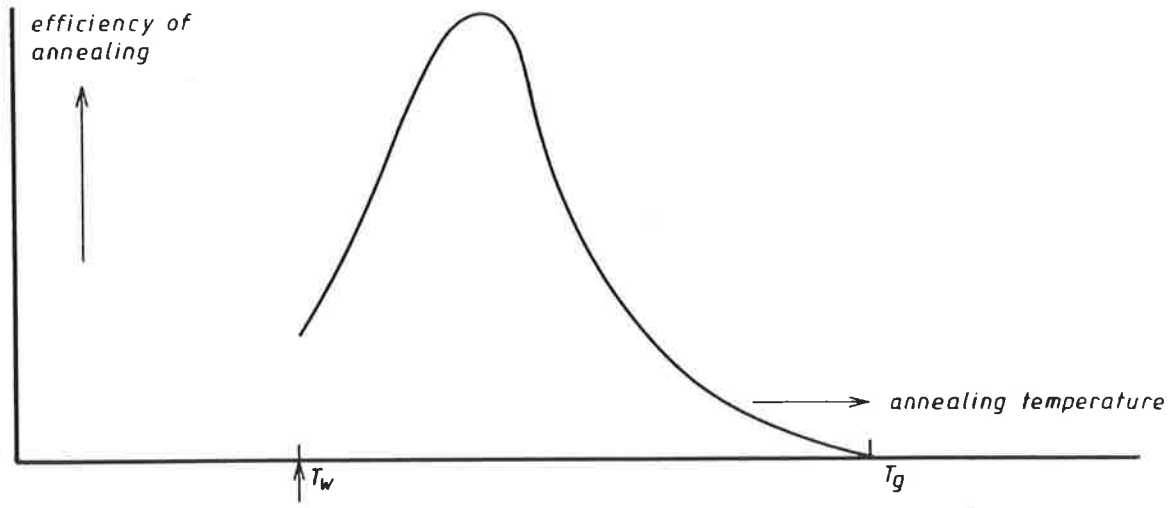

Figure 2.20 Schematic representation of the efficiency of annealing versus annealing temperature T_a; T_w is the working temperature of interest. The most efficient annealing temperature supposedly lies somewhere between T_w and T_g, according to Struik (reproduced from [135]).

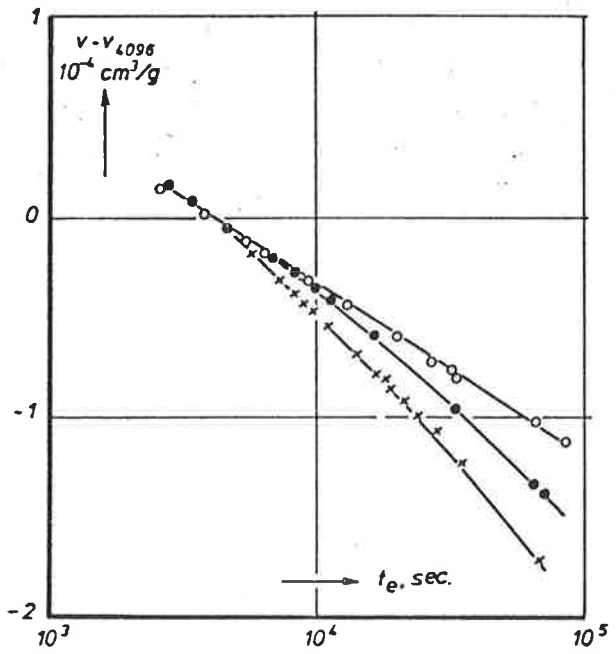

Figure 2.21 Volume relaxation of poly(vinyl chloride) at 20 C; v_{4096} denotes the specific volume at a t_e of 4096 seconds. Three samples were prepared: (1) after direct quenching from 85 C to 20 C (crosses), (2) after quenching from 85 C to 50 C, the sample was isothermally annealed at 50 C for 2 hours before cooling to 20 C (filled circles), (3) as with (2), but the isothermal period at 50 C was 18 hours (open circles).

of ageing had taken place) for the sample annealed at 50 C for 18 hours (Fig. 2.21). It was concluded [19] that the ageing at 20 C is only partially eliminated by annealing at a higher temperature (50 C) below T_g, and that ageing at 50 C had a greater effect on the relaxation times than at 20 C. It is obvious that the rate of volume relaxation and ageing increases with increasing annealing temperature. However, Struik's appraisal of the experimental evidence in Figure 2.21 [19] appear to contradict his suggestion [135] that the highest efficiency of annealing is achieved at some temperature T_a below T_g (Fig. 2.20). Furthermore, if annealing was carried out at 25 C below T_g, the complete erasure of physical ageing would take about 730 years (Section 2.3.2). It may be concluded that the annealing of a polymer at temperatures below T_g would only partially remove volume relaxation effects and that the polymer is unlikely to attain equilibrium within a feasible timescale.

On the other hand, if LeGrand's [158] suggestion was adopted and annealing was carried out above T_g, the effectiveness of the annealing procedure will largely depend on the cooling rate past the glass transition region. Although thermodynamic equilibrium and stress relaxation may be speedily achieved above T_g, the possible reintroduction of free volume and thermal stresses upon cooling will defeat the purpose of annealing. Because volume relaxation cannot be avoided in all glasses below T_g [16], it follows that on cooling to below T_g physical ageing will be regenerated.

In view the problems associated with annealing at above T_g and the slow rate of recovery at annealing temperatures too far below T_g, an optimum annealing temperature would be chosen near but below T_g. However, there is an uncertainty associated with the location of T_g as the glass transition has been shown [24] to occur over a temperature range, therefore the choice of a suitable annealing temperature remains difficult.

2.3.13 Physical Ageing and The Glass Transition

It has been shown [5, 7, 66, 183] that the rate of volume recovery increases with temperature, particularly when the temperature is near the glass transition region. These observations suggest that physical ageing and the glass transition are closely related as both processes are associated with changes in molecular mobility, which, in turn, will affect other properties.

The glass transition is a characteristic phenomenon not only of amorphous

polymers, but of any liquid which can be supercooled to a significantly low temperature without crystallising [10]. The transition from glass-like to liquid-like behaviour in amorphous materials has been observed to be a kinetic phenomenon [21, 82, 166], that is, the observation of the transition depends on the timescale of the experiment. In addition, the glass transition and volume relaxation do not occur instantaneously, but take place over a period of time, which suggests that the kinetics of both processes are governed by a distribution of relaxation times. Crowson and Arridge [167] observed a glass transition of at least 20 C wide for the diglycidyl ether of bisphenol A.

These observations can be explained by considering Struik's [19] free volume model, in which the mobility of a polymer is determined by the distribution of free volume having a critical volume [25-26] sufficient for molecular motion. It follows that there must be a distribution of relaxation times, where each relaxation time is responsible for a particular relaxational mode [82]. Thus the occurence of the glass-liquid transition over a temperature range is attributed to the distribution of relaxation times associated with the many relaxational modes in a polymer. The glass transition of a polymer is also recognised by large changes in many physical properties with respect to temperature, but in particular, the heat capacity C_p, compressibility κ, and thermal expansion coefficient α. Figure 2.22 illustrates a schematic volume-temperature curve with the corresponding discontinuity in α. Although the expansion coefficient changes very steeply in the glass transition, it is only partially discontinuous and Figure 2.23 is more likely to be observed. Consequently, there are doubts as to whether the glass transition is a true second-order thermodynamic transition.

A second-order transition is characterised by continuity in both the free energy and its first partial derivatives, i.e. $(\delta G/\delta T)_P = -S$, $(\delta G/\delta P)_T = V$, and $[\delta(G/T)/\delta(1/T)]_P = H$, and by a *discontinuity* in the second partial derivatives of the free energy function with respect to the relevant state variables, i.e. $(\delta S/\delta T)_P = C_p/T$, $(\delta H/\delta T)_P = C_p$, $(\delta V/\delta P)_T = \kappa$, and $(\delta V/\delta T)_P = \alpha V$ [168]. Thus, there is no discontinuity in entropy S, specific volume V, or enthalpy H at the glass transition, but there is discontinuity in C_p, κ, and α. By considering the pressure dependence of the transition temperature, the Ehrenfest [169] equations can be derived:

$$(dP/dT) = (\Delta\alpha/\Delta\kappa) \qquad (2.16a)$$

$$(dP/dT) = (\Delta C_p/T\Delta\alpha) \qquad (2.16b)$$

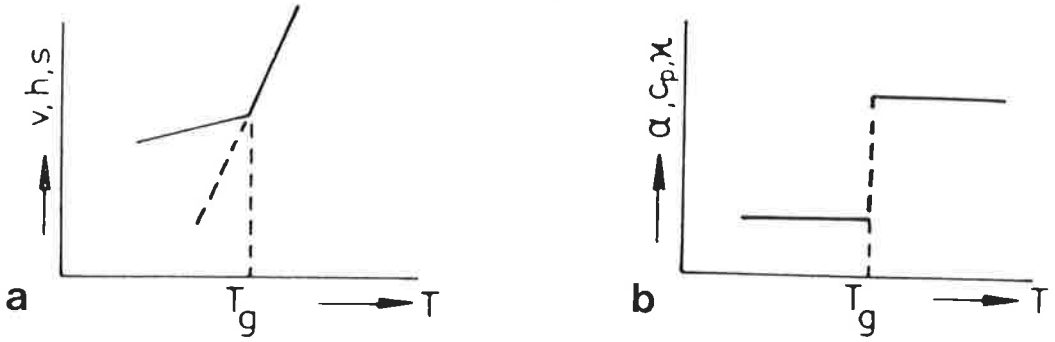

Figure 2.22 Schematic representation of changes in (a) specific volume V, enthalpy H, and entropy S, with temperature and in (b) the partial derivatives (expansion coefficient α, heat capacity C_p, and compressibility κ) with respect to the relevant state variables for the vitrification process.

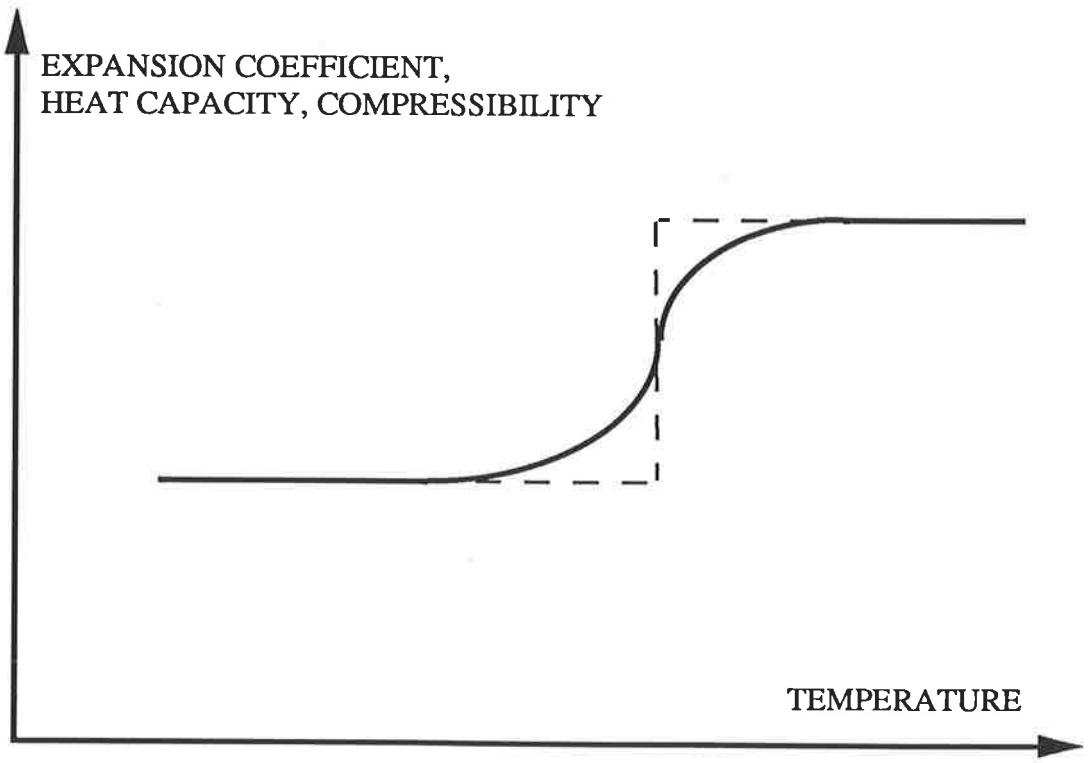

Figure 2.23 Schematic representation of the partial discontinuity of the expansion coefficient, heat capacity and compressibility with temperature.

By equating Equations 2.16a and 2.16b, the Prigogine-Defay [170] ratio, R, is obtained:

$$R = (\Delta\kappa.\Delta C_p)/T.V.(\Delta\alpha)^2 = 1 \qquad (2.17)$$

For a second-order transition, both Ehrenfest relationships must be fulfilled, as must Equation 2.17. Rehage and Borchard [171] showed that the Ehrenfest equations only hold when there is thermodynamic equilibrium on both sides of the transition, i.e. when the thermodynamic quantities of the substance can be described by two and only two variables, e.g. T and P (a phase with two degrees of freedom). Clearly, according to Rehage and Borchard, the Ehrenfest equations cannot describe the existing non-equilibria in the glass state.

However, conflicting results have arisen, where some authors [173] have claimed that Equations 2.16a-2.17 are obeyed in glasses while other authors report otherwise [172, 174-175]. The confusion is due to the interpretation of "mixed" PVT data [166] from glasses of different formation histories. Data from "variable-formation glasses" [172] were obtained from isobaric cooling of the polymer melt from above to below T_g at different pressures, and for "constant-formation glasses", after isobaric cooling to the appropriate temperatures, incremental pressure changes were applied. The PVT data for the two types of glasses are not the same: in the case of variable-formation glasses, Zoller [173] found that $(dP/dT) = (\Delta\alpha/\Delta\kappa)$ for four different polymers. On the other hand, McKinney and Golstein [172] and Oels and Rehage [174-175] show that Equation 2.16a was not obeyed for constant-formation glasses.

The introduction of an extra "ordering parameter" by Davies and Jones [176] to describe the non-equilibrium thermodynamic state of the glass appeared to be validated by the Ehrenfest equations (and the Prigogine-Defay ratio is unity), but upon defining a material with multiple ordering-parameters they [176] found that the Prigogine-Defay ratio to be greater than unity. This was contradicted by DiMarzio [177-178], who concluded that the Prigogine-Defay ratio is unity even for systems of more than one ordering parameter. Nevertheless, it was agreed [174, 176-178] that in order to correctly account for the glass transition behaviour, the *time-dependent behaviour* of the ordering parameters must be taken into account. In his review, McKenna [168] suggests that much of the discussion is unnecessary because the experiments measure a kinetic phenomenon, and therefore cannot test whether or not the glass transition is a

true second-order thermodynamic transition.

It has already been noted [23] that different experimental methods which are used to measure the glass transition do not always give values of T_g which agree exactly for each polymer. The following example lists the different values of T_g obtained by various methods for a chlorinated polyether, poly(3, 3-bischloromethyloxacyclobutane) (Table 2.3) [180].

TABLE 2.3

Effect of experimental timescale on the glass transition temperature of poly(3, 3-bischloromethyloxacyclobutane)

Method	Frequency (cycle/sec)	T_g, C
Electrical Tests	1000	32
Mechanical Vibration	89	25
Slow Tensile	3	15
Dilatometry	10^{-2}	7

Brydson [181] indicated that it was almost impossible to quote precisely a single figure for T_g of a given species of polymer, except to provide a list of "best" values for T_g. The definition of T_g taken from V-T curves was described by Meares [24] as "arbitrary", and Brydson [181] stated that "different workers using a variety of methods arrive at different numerical values (of T_g) for reasons that do not have an obvious explanation". These reasons, and the fact that the glass transition is strongly dependent on the timescale and frequency of the measuring technique, contribute to the spread of values of T_g for the same polymer in literature.

For volume-temperature work, the most common definition for the T_g is the intersection of the extrapolated glass and liquid lines (Fig. 2.24). Other definitions, for example, may be derived from heat capacity-temperature curves [23, 179] (Fig. 2.25): (1) the extrapolated onset T_g, T_{go}(DSC), (2) the T_g at half-height, $T_g(1/2\Delta C_p)$, and (3) the enthalpic T_g, T_gH, which is defined by the intersection of the liquid and glassy enthalpy curves [182]. Physical ageing, which is responsible for the volume hysteresis [171] observed on heating (Fig. 1.1), effectively distorts the idealised volume-temperature curve and an extrapolated T_g could not be obtained in such V-T curves.

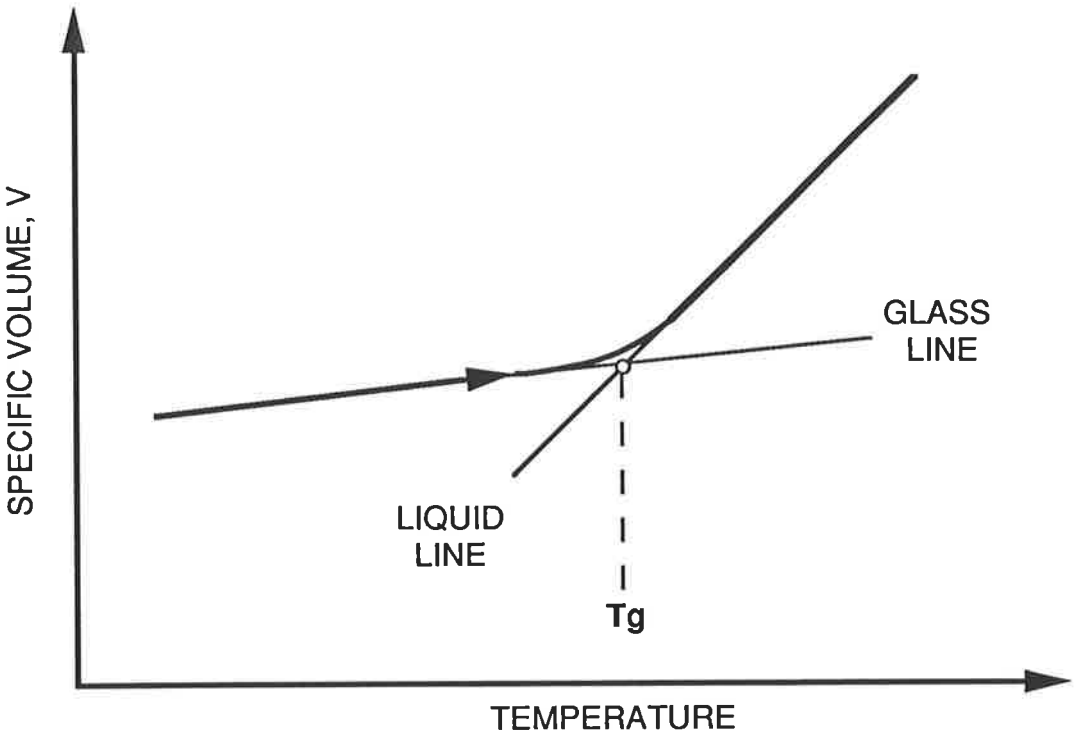

Figure 2.24 Definition of the glass transition temperature from a volume-temperature plot.

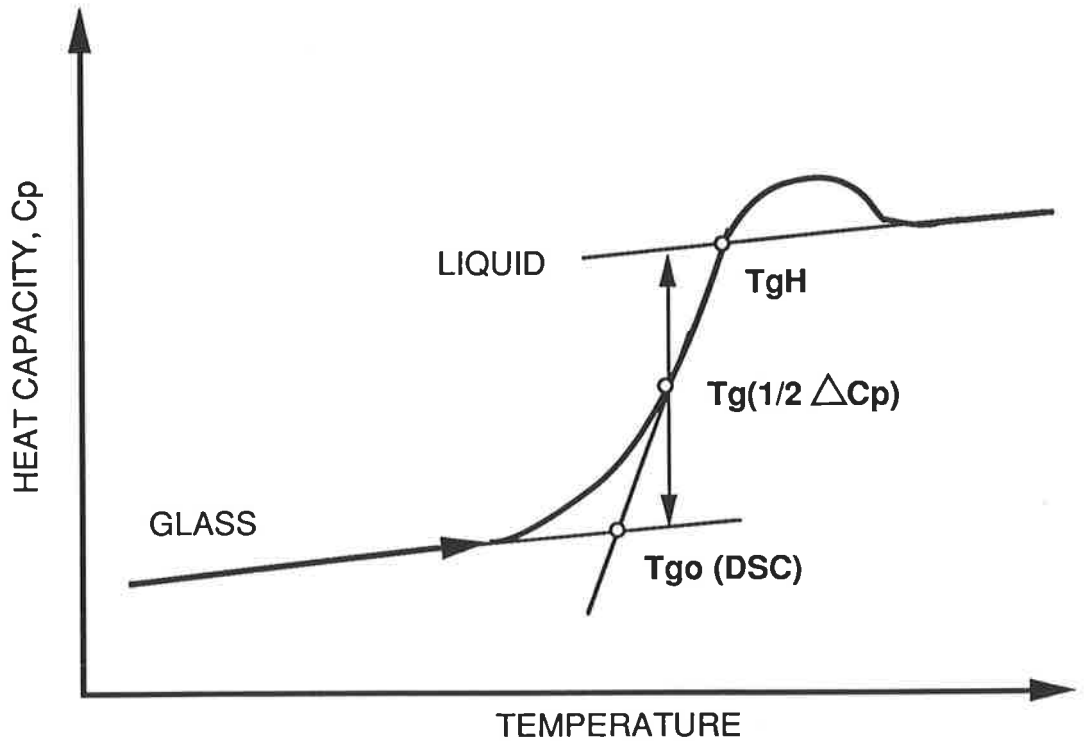

Figure 2.25 Definitions of the glass transition temperature from a heat capacity-temperature plot (after [177, 180]).

The glass transition occurs because the specific volume of the material can no longer contract and follow the so-called equilibrium liquid line below T_g. If an underlying equilibrium curve was assumed to exist, then at infinitely slow cooling the T_g should be lowered to the extent that it coincides with the equilibrium line [184]. However, for experimental and practical reasons, this cannot be proved and Rehage and Borchard [1671] concluded that such an event is very unlikely. If volume relaxation is considered as attempting to reach this hypothetical equilibrium line below T_g, then an aged polymer should be assume more liquid-like characterisitcs. However, aged polymers have been shown to be more glass-like, e.g. they become stiffer and more brittle [20], and the stress relaxation rates become longer [16]. In fact, physical ageing is said to be the continuation of the vitrification process around T_g [19]. Hence, the existence of an underlying equilibrium line in the glass state appears to be doubtful.

2.3.14 Physical Ageing and The Thermal Expansion Coefficient

The origin of a finite expansion coefficient lies in the asymmetry of the potential energy-distance curve and therefore in the anharmonic vibrations of atoms in a solid [187]. The thermal expansion of a polymer on heating is a phenomenon which depends mainly on internal, intermolecular forces, and is the result of a combination of vibrational modes consisting of (1) *interchain* vibrations which are essentially governed by van der Waals bonds between the chains, and (2) *intrachain* vibrations governed by covalent bonds along the chains [185]. Swan [186] has shown that the thermal expansivities of polymer crystals is much smaller along the chain axis rather than perpendicular to the chain axis. Hence, it is expected that interchain vibrations will have a larger contribution to the thermal expansion of a polymer.

When a material is heated, the vibration amplitudes of the atoms are increased and hence, the interatomic distances are increased. If the potential energy curve between a pair of atoms was exactly parabolic even for large amplitudes of vibration, then the mean separation of the two atoms would always be the same and thus the forces bonding one atom to another would be termed as "*harmonic*". A solid bound by purely harmonic interatomic forces would not expand with temperature. Thus the thermal expansion will depend on the strength of the bonds between the atoms: a tightly-bound covalent structure such as diamond or silicon carbide will have a small coefficient of expansion, whereas in a polymer with weak interchain forces the coefficient of expansion will be higher. Table 2.4 lists some values of the linear thermal

expansion coefficient, α', for a range of materials [188].

TABLE 2.4

Linear Thermal Expansion Coefficients ($\alpha' \times 10^6\ K^{-1}$)

Low (α' ~0-10)		Medium (α' ~10-50)		High (α' ~50-300)	
Borosilicate Glass	3	Concrete	12	Epoxy Resins	50-100
Fused Silica	0.5	Gold	14	PMMA	80
Diamond	1	Quartz	13	Paraffin	300
Porcelain	4	Silicon	24	Rubbers	200-250

The shape of a potential energy curve is largely determined by the strength of the bonding between atoms, that is, on the steepness and depth of the curve; the intrachain bond has a greater bond strength than the interchain bond, thus there is greater symmetry in the intrachain potential [189]. The bond dissociation energy for single carbon-carbon bonds is about 80-88 kcal/mol, but the van der Waals energy measured for the relative stabilities of the different conformations (*gauche*, *anti*) of *n*-butane range from only 0.8 kcal/mol to 6.1 kcal/mol [190]. Figure 2.26 illustrates two schematic potential energy-distance curves, one representing covalent bonding and the other van der Waals bonding. The horizontal lines across the curve represent different average energy levels, and hence different temperatures. With increasing vibrational energy, the mean distance between atoms increases towards greater separation. The thermal expansion is expressed by the relative change in length, $\Delta r/r_o$, where r_o is the mean interatomic distance. The higher asymmetry in the van der Waals curve results in a larger expansion.

Thermal Expansion Coefficient (Expansivities)

The linear thermal expansion coefficient of a polymer is taken as the slope of the glass and liquid lines from a length-temperature curve, giving the the linear glass and liquid expansion coefficients respectively, α'_g and α'_l. The expansion coefficients, α'_g and α'_l, of a polymer are not independent of temperature, but generally shows a gradual increase with temperature. Haldon and Simha [40, 191] measured the linear expansivities of a number of

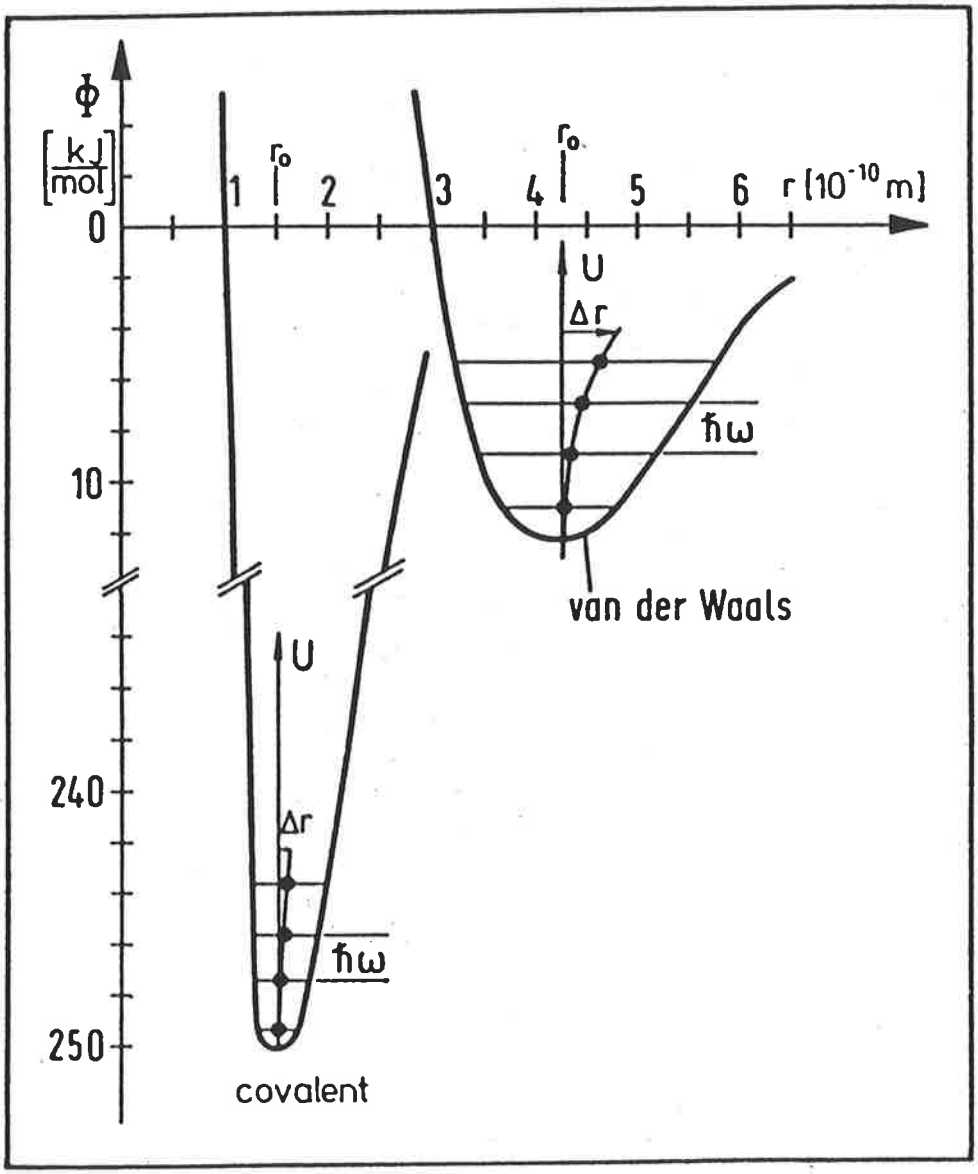

Figure 2.26 Schematic representation of potential energy-distance curves for intrachain (covalent) and interchain (van der Waals) bonding; the expansion Δr is greater for interchain bonding (reproduced from [185]).

polymers in the cryogenic temperature range from 20-200 K. Polymethacrylates showed an increasing α'_g up to ~40 K (with the exception of PMMA), followed a glass-glass transition located between 80 and 110 K. The magnitude of this transition (indicated by a step in the α'-temperature plot) increased with the flexibility of the alkyl side group and appeared to be consistent with dynamic-mechanical [44, 192] and proton spin lattice relaxation data [193] for the higher members of the series [191]. The molecular motion associated with the transition in PMMA is the rotation of the ester methyl group [193].

However, there is a large change in the expansion coefficient on passing through the glass transition, hence it is usually convenient to ignore the gradual increase in α'_g with increasing temperature [39]. The linear expansion coefficients are expressed as (unit K^{-1}):

$$\alpha' = l_0^{-1}.(dl/dT) = l_0^{-1}.(dl/dt).(dT/dt) \qquad (2.18)$$

where l_0 and l represent the initial and instantaneous sample lengths respectively, dT/dt is the heating rate, dl/dT and dl/dt represent the length changes with respect to temperature and time respectively. The linear expansion coefficient of an unoriented amorphous polymer is normally assumed to be isotropic, thus the volume or *cubical thermal expansion coefficient*, α, can be approximated as $\alpha = 3\alpha'$ [39, 135].

The value of the expansion coefficient is sensitive to structural changes in a polymer. In the case of oriented polymers, the linear expansivity will be dependent on the direction of the orientation. Struik [135] has derived the following relationship between the linear expansivities and the volume (cubical) expansivity α :

$$\alpha = \alpha'// + 2\alpha'_{\perp} \qquad (2.19)$$

where $\alpha'//$ and $\alpha'_{\perp}$ represent the linear expansivities parallel and perpendicular to the axis of orientation. The volume expansivity is independent of both the direction and the degree of orientation, while $\alpha'//$ decreases and $\alpha'_{\perp}$ increases with increasing orientation [135, 194-202]. This may be understood from Figure 2.27, in which the thermal vibrations in the tranverse direction of a perfectly oriented chain will lead to a shortening of the chain with increasing temperature, thus decreasing $\alpha'//$. The degree of orientation may be defined [135] as

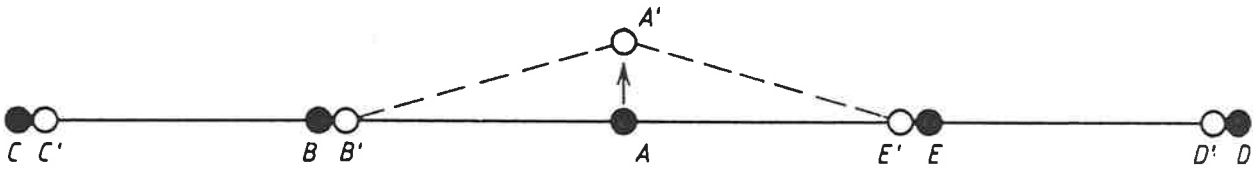

Figure 2.27 The negative thermal expansion of a perfectly orientated chain (ABCDE) arises from the transverse (perpendicular to the chain axis) vibration of the chain. The displacement of the central atom A to A' leads to inward shifts of atoms B, C, D and E to B', C', D' and E' (reproduced from [135]).

$$(\alpha'// - \alpha'//_\infty)/(\alpha' - \alpha'//_\infty) \qquad (2.20)$$

or assuming that $\alpha'//_\infty = 0$ [198-199],

$$1 - (\alpha'// \div \alpha') = (\alpha' - \alpha'//)/\alpha' \qquad (2.21)$$

where $\alpha'//_\infty$ is the thermal expansivity of a perfectly oriented polymer. However, the assumption that $\alpha'//_\infty = 0$ in Equation 2.21 is an oversimplification, since $\alpha'//_\infty$ will be negative in a perfectly oriented chain (Figure 2.27) [135]. Although reports of negative $\alpha'//$ values for amorphous polymers are not known, the stretching of rigid amorphous PVC near T_g results in an $\alpha'//$ value of almost zero [135]. On the other hand, negative thermal expansion coefficients are well-known [137, 194, 202-206] from X-ray measurements of highly oriented crystalline polymers. It was suggested [135] that negative $\alpha'//$ values are more easily observed in semi-crystalline polymers than in amorphous polymers because of the more regular chain structure (hence a higher degree of orientation) of crystallites.

α' has been shown [40] to increase with increasing side-chain length, as is the case with the homologous poly(*n*-alkyl methacrylates) series: α'_g for PMMA was 75 ppm/K, and increased to 186 ppm/K for poly(n-hexyl methacrylate). It was proposed by Haldon and Simha [40] that the side chains retained excess free volume upon quenching, which led to the high values of α'_g. It may be inferred that the longer side-chains act like a short polymer chain and contribute to the interchain vibration, thus increasing the thermal expansivity of the higher methacrylates. The value of α' was also found [40] to be affected by the rate of cooling from above to below T_g. Specimens of poly(*n*-butyl methacrylate) cooled from T_g to -190 C (T_g = 18 C) in one hour had the lowest expansion coefficient measured at -140 C (0.71×10^4 K^{-1}), and that specimens quenched from 100 C to -190 C had the highest (0.83×10^4 K^{-1}). This observation was consistent with the freezing in of excess free volume on quenching, in which the increase in α'_g arises from the expansion of excess free volume.

Haldon and Simha [40] reported that the use of a quartz rod for dilatation measurements resulted in a drop in α'_g in the vicinity of T_g. This was attributed to the weight of the rod on the sample, whose modulus is considerably reduced on heating from below to

above T_g. It was found that the reduction of the weight of the rod led to reproducible results. However, another possibility for the observation of the lowering of α'_g near T_g may arise as a result of physical ageing. This possibility is consistent with the fact that if α'_g increases with an increase in free volume, then the reduction of free volume upon ageing will result in a decrease in α'_g.

The Gruneisen Constant

The thermal expansion coefficient of a polymer has been shown to arise primarily from the anharmonicity of the interchain vibrations. The magnitude of the expansion coefficient is sensitive to variations in polymer structure and to thermal history, and is also related to a number of material properties, in particular, density, bulk modulus and heat capacity. This relationship is expressed by an empirical parameter, known as the *Gruneisen Constant*, γ [207]. The Gruneisen Constant thus expresses the relationship between the thermal and mechanical properties of solids, and it is recognised [37, 183, 208-210] as an important parameter in understanding the structure and properties of solid polymers.

The definition for the Gruneisen Constant γ, a dimensionless number, is [211]:

$$\gamma = (\alpha.B_T) / (\rho.C) \qquad (2.22)$$

where α = cubical coefficient of thermal expansion, (ppm/K)
B_T = the isothermal bulk modulus, (N/m^2)
ρ = specific density, (g/cm^3)
C_v = specific heat capacity at constant volume (J.K/g)

Attempts to relate γ to intermolecular potential functions have been met so far with semi-quantitative success [211]; the magnitude of γ is a measure of the asymmetry, or the anharmonicity, of a polymer system [187]. If $\gamma = 0$ the system would be totally harmonic, and would exhibit no thermal expansion and no thermal conductivity, but this is not usually encountered in practice. Metals and ionic crystals, which are predominantly harmonic, have low γ values, ca. 1-2, while polymers, especially those with weak interchain forces and higher anharmonicities, have relatively high γ values, ca. 4-10 [185]. For polymers, the situation is more complicated because of the anisotropy of the molecular vibrations; along the polymer

chain the strong covalent bonds have a low Gruneisen number, while in between chains the weak van der Waals bonds have a high Gruneisen number [211].

Several problems arise when this definition is applied to polymers: (1) firstly, to obtain values of the different parameters from different experiments and sources, there exists an uncertainty whether the physical properties (e.g. molecular weight) of the polymer used was the same in all cases [185]; (2) secondly, while data for α and ρ are usually available, B_T and C_v are frequently estimated; (3) thirdly, as pointed out by Wada *et al.* [210] and subsequently confirmed by others [211], only that portion of the heat capacity due to interchain vibrations, $C_{v,i}$, should be used in Equation 2.22 to calculate γ. If the measured or calorimetric heat capacity is used, γ will be lower by a factor of five to twenty. Since values for the interchain heat capacity are difficult to obtain, this imposes a further limitation of the usefulness of Equation 2.22; (4) furthermore, it has already been shown that the value of α show a small dependence on temperature [39, 191]; (5) similarly, ultrasonic measurements of the bulk modulus of PMMA show that B_T is not linear with pressure or with temperature [212]. With these difficulties in mind, γ should be considered as a general indication of the degree of anharmonicity of a polymer structure.

There are two different types of γ which must be distinguished: (1) the *Lattice Gruneisen Constant* γ_L is obtained using the pressure dependence of the bulk modulus (dB_T/dP) [185]. γ_L relates the movement of polymer chains in relation to one another and is determined primarily by interchain vibrations [213]. (2) On the other hand, the *Thermodynamic Gruneisen Constant* γ_T is obtained when various dynamic techniques are used, e.g ultrasonic absorption [211-212]. γ_T is an average over all interchain and intrachain vibrational modes, employing parameters such as the specific heat and thermal conductivity [213]. The ratio γ_L/γ_T for polymers is between 4-30, while for metals and ionic crystals γ_L/γ_T is approximately one [214-216]. The Gruneisen Constants, γ_T, γ_L, for PMMA are listed in Table 2.5.

An inspection of Table 2.5 reveals that the interchain vibrations increases the Gruneisen Constant by about 16-22 % [219]. Physical ageing accompanied by a decrease in volume, thermal expansion coefficient and internal energy [19], and is expected to lower the value of γ (even though there will be an increase in the bulk modulus); this expectation is justified as the calculated value of γ_L for PMMA in the liquid state (3.86) is lower than for the glass state (4.91). Moreover, γ_L had a value of about 3.8-4.2 for most amorphous polymers in

the liquid state [218], which suggests that the liquid state can be described by a single value of γ_L. It was proposed [220] that the Lattice Gruneisen Constant is related to the fractional free volume by:

$$f = (\gamma_L + 1)^{-1} \qquad (2.23)$$

If an approximate value of $\gamma_L = 4.96$ was taken for PMMA in the glass state, then according to Equation 2.23 the fractional free volume is 0.17. The approximate values for the free volume fraction estimated by Simha and Boyer [37] were $\alpha_l T_g = 0.164$ and $\Delta\alpha T_g = 0.113$, hence there appears to be some justification in associating γ_L with the free volume. A qualitative relationship between γ_L and the fractional free volume suggests that the Gruneisen Constant can be used as an indicator of structural changes and thermal history, that is, the freezing-in of free volume is likely to be reflected in a higher value of γ, as a result of an increase in the interchain contributions to the thermal expansivity. Conversely, physical ageing will result in a lowering of γ as a consequent of decreases in bulk polymer properties.

TABLE 2.5

Gruneisen constants for poly(methyl methacrylate) at 25 C

Polymer	γ_T	γ_L
Poly(methyl methacrylate)	0.82 [185]	5.2, 6.8 [212]
		4.1 [210]
		4.0, 4.8 [185]
	1.12 [216]	4.94 [217]
		4.911 [218]

Chapter 2

1. F. Simon, *Z. Anorg. Allgem. Chem.* **203**, 219 (1931).
2. H.R. Lillee, *J. Am. Ceram. Soc.* **16**, 619 (1933).
3. E. Jenckel, *Z. Electrochem.* **43**, 769 (1937); **45**, 202 (1939).

4. A.J. Kovacs, *Thesis, Fac. Sci., Paris* (1954).

5. A.J . Kovacs, *J. Polym. Sci.* **30**, 131 (1958).

6. A.J. Kovacs, *Trans. Soc. Rheol.* **5**, 285 (1961).

7. A.J. Kovacs, *Fortschr Hochpolym. Forsch.* **3**, 394 (1964).

8. L.C.E. Struik, *Failure of Plastics*, W, Brostow and R.D. Cornelius eds., Hanser (1986), Chapter 11.

9. M.L. Williams, R.F. Landel and J.D. Ferry, *J. Am. Chem. Soc.* **77**, 4701 (1955).

10. J.D. Ferry, *Viscoelastic Properties of Polymers*, Wiley (1970), 2nd Edition.

11. F.R. Schwarzl and A.J. Staverman, *J. Appl. Phys.* **23**, 838 (1952).

12. F.R. Eirich and T.L. Smith, *Fracture: An Advanced Treatise*, Vol(**VII**), Academic Press, New York (1972), Chapter 7.

13. A.K. Doolittle, *J. Appl. Phys.* **22**, 1471 (1951).

14. L.C.E. Struik, *Encyclopedia of Polym. Sci. Eng.* Vol(**1**), 2nd Edition, Wiley, New York (1989), p595 ff.

15. T.G. Fox and P.J. Flory, *J. Am. Chem. Soc.* **70**, 2384 (1948); *J. Appl. Phys.* **21**, 581 (1950).

16. L.C.E. Struik, *Polym. Eng. Sci.* **17(3)**, 165 (1977).

17. N.G. McCrum, B.E. Read and G. Williams, *Anelastic and Dielectric Effects in Polymeric Solids*, Wiley and Sons (1967).

18. A.K. Doolittle, *J. Appl. Phys.* **23**, 236 (1952).

19. L.C.E. Struik, *Physical Ageing in Amorphous Polymers and Other Materials*, Elsevier, Amsterdam (1978).

20. A.J. Hill, K.J. Heater and C.M. Agrawal, *J. Polym. Sci. Polym. Phys.* **28**, 387-405 (1990).

21. G.E. Roberts and E.F.T. White, *The Physics of Polymer Glasses*, R.N. Haward ed., Applied Science Publishers (1973), Chapter 3.

22. M.L. Williams, *J. Appl. Phys.* **29**, 1396 (1958).

23. J.M.G. Cowie and R. Ferguson, *Macromolecules* **22**, 2307 (1989).

24. P. Meares, *Polymers: Sturcture and Bulk Properties*, Van Nostrand (1965).

25. M.H. Cohen and D. Turnbull, *J. Chem. Phys.* **31**, 1164 (1959).

26. D. Turnbull and M.H. Cohen, *J. Chem. Phys.* **34**, 120 (1961).

27. L.C.E. Struik, *Rheol. Acta* **5**, 303 (1966).

28. A.J. Kovacs, R.A. Stratton and J.D. Ferry, *J. Phys. Chem.* **67**, 152 (1963).

29. H.H. Meyer and J.D. Ferry, *Trans. Soc. Rheol.* **9(2)**, 343 (1965).

30. H.H. Meyer, P.M.F Mangin and J.D. Ferry, *J. Polym. Sci.* **A3**, 1785 (1965).

31. S. Kastner, *J. Polym. Sci.* **16**, 4121 (1968).

32. D. Plazek and J.H. Magill, *J. Chem. Phys.* **45**, 3038 (1966).

33. S.S. Sternstein and T.C. Ho, *J. Appl. Phys.* **43**, 4370 (1972).

34. S.S. Sternstein, *Am. Chem. Soc. Polym. Prepr.* **17**, 136 (1976).

35. M. Cizmecioglu, R.F. Fedors, S.D. Hong and J. Moacanin, *Polym. Eng. Sci.* **21**, 940 (1981), *Am. Chem. Soc. Polym. Prepr.* **24**, 31 (1983).

36. R.F. Boyer, *Rubb. Chem. Tech.* **36**, 1303 (1963).

37. R. Simha and R.F. Boyer, *J. Chem. Phys.* **37(5)**, 1003 (1962).

38. R. Simha and C.E.Weil, *J. Macromol. Sci. Phys.* **B4(1)**, 215-226 (1970).

39. D.W. Van Krevelen, *Properties of Polymers: Their Estimation and Correlation with Chemical Structure*, Elsevier (1976), 2nd Edition.

40. R.A. Haldon and R. Simha, *J. Appl. Phys.* **39(3)**, 1890 (1968).

41. S.C. Sharma, L. Mandelkern and F.C. Stehling, *J. Polym. Sci. Polym. Letters* **B10**, 345 (1972).

42. F.C. Stehling and L. Mandelkern, *Macromolecules* **3(2)**, 242 (1970).

43. S.S. Rogers and L. Mandelkern, *J. Phys. Chem.* **61**, 985 (1957).

44. E.A.W. Hoff, D.W. Robinson and A.H. Willbourn, *J. Polym. Sci.* **18**, 161 (1955).

45. W.J. Schell, R. Simha and J.J. Aklonis, *J. Macromol. Sci. Chem.* **A3(7)**, 1297 (1969).

46. J. Lal and G.S. Trick, *J. Polym. Sci.* **A2**, 4559 (1964).

47. R.F. Boyer and R. Simha, *J. Polym. Sci.* **B(11)**, 33-44 (1973).

48. N. Bekkedahl, *J. Res. Nat. Bur. Std.* **13**, 411 (1934).

49. C.F. Weir, W.H. Lesser and L.A. Wood, *J. Res. Nat. Bur. Std.* **44**, 367 (1950).

50. H. Fujita and E. Maekawa, *J. Phys. Chem.* **66**, 1053 (1966).

51. R.H. Wiley and G.M. Brauer, *J. Polym. Sci.* **4**, 351 (1949).

52. K.H. Hellwege, W. Knappe and P. Lehmann, *Kolloid-Z. Z. Polym.* **183**, 110 (1962).

53. S. Loshaek, *J. Polym. Sci.* **15**, 391 (1955).

54. G.S. Parks, H.M. Huffmann and F.R. Catton, *J. Phys. Chem.* **32**, 1366 (1928).

55. M. Samsoen, *Ann. Phys.* **9**, 35 (1928).

56. R.E. Robertson, *J. Chem. Phys.* **44**, 3950 (1966).

57. M.J. Richardson and N.G. Savill, *Polymer* **18**, 3 (1977).

58. A.J. Hill, I.M. Katz and P.L. Jones, *Polym. Eng. Sci.* **30**, 762 (1990).

59. A.J. HIll, *Materials Forum* **14**, 174-182 (1990).

60. A.J. Hill and C.M. Agrawal, *J. Mat. Sci.* **25**, 5036-5042 (1990).

61. H. Nakamishi and Y.C. Jean, *Positron and Positronium Chemistry: Studies in Physical and Theoretical Chemistry,* D.M. Schraeder and Y.C. Jean eds., Elsevier, New York, **57**, 159 (1988).

62. Y.Y. Wang and Y.C. Jean, *Positron Annihilation*, L. Dorikens-Vanpraet, M. Dorikens and D. Segers eds., World Scientific, New Jersey (1989), p787.

63. A.J. Hill, P.L. Jones, J.H. Lind and G.W. Pearsall, *J. Polym. Sci. Polym. Chem. Ed.* **26**, 1541 (1988).

64. L.C.E. Struik, *Ann. N. Y. Acad. Sci.* **279**, 78 (1976).

65. L.C.E. Struik, *Polymer* **28**, 1521 (1987).

66. L.C.E. Struik, *Polymer* **30**, 799 (1989).

67. J.M. Crissman and G.B. McKenna, *J. Polym. Sci. Polym. Phys.* **28**, 1463 (1990).

68. G.M. McKenna and A.J. Kovacs, *Polym. Eng. Sci.* **24**, 1131 (1984).

69. L.C.E. Struik, *Polymer* **30**, 815 (1989).

70. J. Heijboer, *Physics of Non-Crystalline Solids*, North-Holland, Amsterdam (1965).

71. J. Heijboer, *Makromol. Chem.* **35A**, 86 (1960).

72. L.C.E. Struik, *Polymer* **28**, 57 (1987).

73. B.E. Read, P.E. Tomlins and G.D. Dean, *Polymer* **31**, 1204 (1990).

74. D.J. Plazek, K.L. Ngai and R.W. Rendell, *Polym. Eng. Sci.* **24**, 1111 (1984).

75. G.P. Johari and M. Goldstein, *J. Chem. Phys.* **53**, 2372 (1970).

76. G.P. Johari, *J. Chem. Phys.* **58**, 1766 (1973); *Ann. N.Y. Acad. Sci.* **279**, 117 (1976).

77. G.P. Johari, *J. Chem. Phys.* **77(9)**, 4619 (1982).

78. L. Guerdox and E. Marchal, *Polymer* **22**, 1199 (1981).

79. R. Diaz-Calleja, A. Ribes-Greus and J.L. Gomes-Ribelles, *Polymer* **30**, 1433 (1989).

80. S.E.B. Petrie, *J. Macromol. Sci. Phys.* **B12**, 225 (1976).

81. G. Goldbach and G. Rehage, *Kolloid Z.* **216**, 56 (1967).

82. A.J. Kovacs, J.M. Hutchinson and J.J. Aklonis, *Proceedings of the Symposium on the Structure of Non-Crystalline Materials*, Cambridge, England (1976), P.H. Gaskell ed., Taylor and Francis (1977), p153.

83. H. Endo, T. Fujimoto and M. Nagasawa, *J. Polym. Sci. Part A-2* **7**, 1669 (1970).

84. H.N. Ritland, *J. Am. Ceram. Soc.* **37**, 370 (1954).

85. T. Sekiguti, *Sci. Papers, Inst. Phys. Chem. Res.* **54**, 281 (1960).

86. A.Q. Tool and C.G. Eichlin, *J. Am. Ceram. Soc.* **14**, 276 (1931).

87. A.Q. Tool, *J. Am. Ceram. Soc.* **29**, 240 (1946).

88. J.M. Hutchinson and A.J. Kovacs, *J. Polym. Sci. Polym. Phys. Ed.* **14**, 1575 (1976).

89. J.M. Hutchinson and A.J. Kovacs, *Proceedings of the Symposium on the Structure of Non-Crystalline Materials*, Cambridge, England (1976), P.H. Gaskell ed., Taylor and Francis (1977), p167.

90. G. Adam and J.H. Gibbs, *J. Chem. Phys.* **28**, 373 (1958).

91. R. Greiner, *Thesis*, Enlargen (1987).

92. R. Greiner and F.R. Schwarzl, *Colloid Polym. Sci.* **267**, 39-47 (1989).

93. G. Goldbach and G. Rehage, *Rheol. Acta* **6**, 30 (1967).

94. A.J. Kovacs, J.J. Aklonis, J.M. Hutchinson and A.R. Ramos, *J. Polym. Sci. Polym. Phys. Ed.* **117**, 1097 (1979).

95. G. Goldstein and M. Nakonecznyi, *Phys. Chem. Glasses* **6**, 126 (1965).

96. S. Matsuoka, *Polym. Eng. Sci.* **21(14)**, 907 (1981).

97. S. Matsuoka and T.K. Kwei, *Macromolecules, An Introduction to Polymer Science,* F.A. Bovey and F.H. Winslow eds., Academic Press (1979), Chapter 6.

98. Y. Ishida, S. Togami and K. Yamafuji, *Kolloid-Z Z. Polym.* **221**, 1, 16 (1967).

99. W.E. Goode, F.H. Owens, R.P. Fellman, W.H. Snyder and J.E Moore, *J. Polym. Sci.* **46**, 317 (1960).

100. W.G. Gall and N.G. McCrum, *J. Polym. Sci.* **50**, 489 (1961).

101. J.A. Shetter, *J. Polym. Sci.* **B1**, 209 (1963).

102. G. Natta, F. Danusso and G. Moraglio, *J. Polym. Sci.* **25**, 119 (1957).

103. S. Newman and W.P. Cox, *J. Polym. Sci.* **46**, 29 (1960).

104. A.B. Thompson and D.W. Woods, *Trans. Faraday Soc.* **52**, 1383 (1956).

105. S. Matsuoka and Y. Ishida, *J. Polym. Sci. Part C* **14**, 247 (1966).

106. J.J. Aklonis and A.J. Kovacs, *Contemporary Topics in Polymer Science*, M. Shen ed., Vol(3) (1979), p267.

107. S. Matsuoka and H.E. Bair, *J. Appl. Phys.* **48**, 4058 (1977).

108. H.E. Bair, G.E. Johnson, E.W. Anderson and S. Matsuoka, *Polym. Eng. Sci.* **21(14)**, 930 (1981).

109. P.E.M. Allen, G.P. Simon, D.R.G Williams and E.H.Williams, *Polymer Bulletin* **11**, 593-600 (1984).

110. P.E.M. Allen, G.P. Simon, D.R.G Williams and E.H.Williams, *Macromolecules* **22**, 809-816 (1989).

111. A.P. Alexandrov and J.S. Lazurkin, *Acta. Phys. Chem. USSR* **12**, 647 (1940).

112. J.R. McLoughlin and A.V. Tobolsky, *J. Colloid Sci.* **7**, 555 (1952).

113. F. Bueche, *J. Appl. Phys.* **26**, 738 (1955).

114. G.P. Mikhailov and others, *J. Tech. Phys. USSR* **26**, 1924 (1956); *Sov. Phys. Tech. Phys.* **1**, 1857 (1956).

115. G.P. Mikhailov, T.I. Borisova and D.A. Dmitrochenko, *J. Tech. Phys. USSR*, **26**, 1924 (1956).

116. K. Deutsch, E.A.W. Hoff and W. Reddish, *J. Polym. Sci.* **13**, 565 (1954).

117. J. Heijboer, *Chem. Weekblad.* **48**, 264 (1952).

118. J.G. Powles, *J. Polym. Sci.* **22**, 19 (1956).

119. W.P. Slichter and E.R. Mandell, *J. Appl. Phys.* **30**, 1473 (1959).

120. K.M. Sinnott, *J. Polym. Sci.* **42**, 3 (1960).

121. J. Heijboer, *Kolloid Z.* **134**, 149 (1956); **148**, 36 (1956).

122. K. Schmeider and K. Wolf, *Kolloid Z.* **127**, 65 (1952); **134**, 149 (1953).

123. J. Koppelmann, *Physics of Non-Crystalline Solids*, North Holland, Amsterdam (1965) p255.

124. G.A. Russell *et al.*, *J. Polym. Sci. Polym. Phys. Ed.* **18**, 1271 (1980).

125. J. Heijboer, *Ann. N.Y. Acad. Sci.* **279**, 104 (1976).

126. J. Heijboer, *Int. J. Polym. Mat.* **6**, 11 (1977).

127. J. Kolarik, *Adv. Polym. Sci.* **46**, 120 (1982).

128. P. Heydeman and H.D. Guicking, *Kolloid Z.* **193**, 16 (1963).

129. G.M. Martin, S.S. Rogers and L. Mandelkern, *J. Polym. Sci.* **20**, 579 (1956).

130. T. Holt and D. Edwards, *J. Appl. Chem.* **15**, 223 (1965).

131. H.F. Atkinson and A.A. Grant, *Nature* **211**, 627 (1966).

132. H. Sasabe and S. Saito, *J. Polym. Sci. A2* **6**, 1401 (1968).

133. J.D. Ferry and S. Strella, *J. Colloid Sci.* **12**, 53 (1958).

134. S.L. Roshen, *Fundamentals Principles of Polymeric Materials for Practicing Engineers,* Barnes and Noble, New York (1971), Chapter 18.

135. L.C.E. Struik, *Internal Stresses, Dimensional Instabilities and Molecular Orientations in Plastics*, Wiley (1990).

136. F. Bueche, *Physical Properties of Polymers*, Interscience (1962).

137. L.C.E. Struik, *Polym. Eng. Sci.* **18(10)**, 799 (1978).

138. W.D. Callister Jr., *Materials Science and Engineering, An Introduction*, Wiley (1991).

139. P. So and L.J. Broutman, *Polym. Eng. Sci.* **16(12)**, 785 (1976).

140. L.E. Hornberger and K.L. Davies, *Polym. Eng. Sci.* **27(19)**, 1473 (1987).

141. S. Raboniwitz and P. Beardmore, *J. Mater. Sci.* **9**, 81 (1974).

142. M.T. Takemori, *Fatigue Fracture of Polycarbonate*, General Electric Report No. 81CRD289 (1981).

143. H.H.D. Lee and F.J. McGarry, *J. Macromol. Sci. Phys.* **B29(1)**, 11-29 (1990).

144. M. Shimbo, M. Ochi and Y. Shigeta, *J. Appl. Polym. Sci.* **26**, 2265-2277 (1981).

145. A.R. Plepys and R.J. Farris, *Polymer* **31**, 1932 (1990).

146. P.E.M. Allen, G.P. Simon, D.R.G. Williams and E.H. Williams, *Eur. Polym. J.* **22(7)**, 549-557 (1989).

147. V. McGinniss and R.M. Holsworth, *J. Appl. Polym. Sci.* **19**, 2243 (1975).

148. M. Atsuta and D.T. Turner, *Polym. Eng. Sci.* **22(7)**, 438 (1982).

149. J.P. Berry, *J. Polm. Sci. Polym. Phys. Ed.* **A1**, 993 (1963).

150. S. Loshaek and T.G. Fox, *J. Polym. Sci.* **15**, 371 (1955).

151. L.J. Broutman and S.M. Krishnakumar, *Polym. Eng. Sci.* **16(2)**, 74 (1976).

152. J.F. Mandell, K.L. Smith and D.D. Huang, *Polym. Eng. Sci.* **21(17)**, 1173 (1981).

153. S. Rabinowitz and P. Beardmore, *CRC Crit. Rev. Macromol. Sci.* **1**, 1 (1972).

154. L.D. Coxon and J.R. White, *Polym. Eng. Sci.* **20(3)**, 230 (1980).

155. G.J. Sandilands and J.R. White, *J. Appl. Sci.* **30**, 4771-4792 (1985).

156. B. Haidar and T.L. Smith, *Polymer* **31**, 1904 (1990).

157. J. Bartos, J. Muller and J.H. Wendorff, *Polymer* **31**, 1678 (1990).

158. D.G. LeGrand, *Encyclopedia of Polym. Sci. Eng.* Vol(2), 2nd Edition, Wiley, New York (1989), p43 ff.

159. D.H. Ender, *J. Macromol. Sci. Phys.* **B4**, 635 (1970).

160. S. Matsuoka, H.E. Bair, S.S. Bearder, H.E. Kern and J.T. Ryan, *Polym. Eng. Sci.* **18**, 1073 (1978).

161. I.M. Hodge and A.R. Berens, *Macromolecules* **15**, 762-770 (1982).

162. I.M. Hodge and G.S. Hurvard, *Macromolecules* **16**, 371-375 (1983).

163. *Proceedings of the 12th North American Thermal Analysis Society,* Williamsburg, Va. September (1983).

164. M.R. Tant and G.L. Wilkes, *Polym. Eng. Sci.* **21**, 874 (1981).

165. R.J. Crowson and R.C.G. Arridge, *Polymer* **20**, 747 (1979).

166. G.B. McKenna, *Comprehensive Polymer Science*, C. Booth and C. Price, eds., Pergamon Press (1989), Volume **2**, Chapter 10.

167. P. Ehrenfest, *Proc. Kon. Akad. Wetensch. Amsterdam* **36**, 153 (1933).

168. I. Prigogine and R. Defay, *Thermodynamic Chimique*, Edition Desoer, Liege, Belgium (1950).

169. G. Rehage and W. Borchard, *The Physics of Polymer Glasses*, R.N. Haward ed., Applied Science Publishers (1973), Chapter 1.

170. J.E. McKinney and M. Goldstein, *J. Res. Natl. Bur. Std. Sect. A* **78A**, 331 (1974).

171. P. Zoeller, *J. Polym. Sci. Polym. Phys. Ed.* **20**, 1453, (1982).

172. H.-J. Oels and G. Rehage, *Macromolecules* **10**, 1036 (1977).

173. G. Rehage and H.-J. Oels, *High Temp.-High Pressures* **9**, 545 (1977).

174. R.O. Davies and G.O. Jones, *Adv. Phys.* **2**, 370 (1953).

175. E.A. DiMarzio, *J. Appl. Phys.* **45**, 4143 (1974).

176. E.A. DiMarzio, *Macromolecules* **10**, 1407 (1977).

177. M.J. Richardson, *Comprehensive Polymer Science*, C. Booth and C. Price, eds., Pergamon Press (1989), Volume **1**, Chapter 36.

178. D.J.H. Sandiford, *J. Appl. Chem.* **8**, 786 (1958).

179. J.A. Brydson, *Polymer Science*, A.D. Jenkins ed., Vol. **1**, North-Holland, Amsterdam (1972), Chapter 3.

180. M.J. Richardson and N.G. Savill, *Polymer* **16**, 753 (1975).

181. G.O. Jones, *Glass*, Methuen (1956).

182. J.H. Gibbs and E.A. DiMarzio, *J. Chem. Phys.* **28**, 373 (1958).

183. R.W. Warfield, *Die Makromolekulare Chemie* **175**, 3285-3297 (1974).

184. P.R. Swan, *J. Polym. Sci.* **56**, 403 (1962).

185. G. Schwarz, *Cryogenics* **28**, 248 (1988).

186. L. Holliday and J.D. Robinson, *Polymer Engineering Composites*, M.O.W. Richardson ed., Applied Science (1977), Chapter 6.

187. R.E. Barker Jr., *J. Appl. Phys.* **38(11)**, 4234 (1967).

188. R.T. Morrison and R.N. Boyd, *Organic Chemistry*, 4th Edition, Alyn and Bacon (1983).

189. R.A. Haldon and R. Simha, *Macromolecules* **1(4)**, 340 (1968).

190. M.C. Shen, J.D. Strong and F.J. Matusik, *J. Macromol. Sci. Phys.* **B1**, 15 (1967).

191. W.P. Slichter, *J. Polym. Sci. Part C* **14**, 89 (1966).

192. C.L. Choy, *Developments in Oriented Polymers,* I.M. Ward ed., Applied Science Publishers, London (1975), Chapter 4.

193. W. Retting, *Coll. Polym. Sci.* **259**, 52 (1981).

194. J. Hennig, *Kolloid Z.* **202**, 167 (1965).

195. J. Hennig, *J. Polym. Sci.* **C16**, 2751 (1967).

196. W. Retting, *Coll. Polym. Sci.* **257**, 689 (1979).

197. W. Retting, *Pure Appl. Chem.* **50**, 1725 (1978).

198. L.H. Wang, C.L. Choy and R.S. Porter, *J. Polym. Sci. Phys.* **20**, 633 (1982): **21**, 657 (1983).

199. C.L. Choy, W.P. Leung and E.L. Ong, *Polymer* **26**, 884 (1985).

200. J.R.C. Pereira and R.S. Porter, *Polymer* **25**, 869 (1984).

201. C.L. Choy, S.P. Wong and K. Young, *J. Polym. Sci. Phys.* **22**, 979 (1984).

202. C.L. Choy, M. Ito and R.S. Porter, *J. Polym. Sci. Phys.* **21**, 1427 (1983).

203. G.A.J. Orchard, G.R. Davies and I.M. Ward, *Polymer* **25**, 1203 (1984).

204. S.A. Jawad, G.A.J. Orchard and I.M. Ward, *Polymer* **27**, 1201 (1985).

205. E. Gruneisen, *Ann. Phys.* **10**, 211 (1908); 38, 257 (1912).

206. J.R. Asay, S.R. Urzendorski and A.H. Guenther, *Report AFWL-TR 67-91 (Air Force Weapons Lab)*, July 1968.

207. C.K. Wu, G. Jura and M. Shen, *J. Appl. Phys.* **43**, 4348 (1972).

208. Y. Wada, A. Itani, T. Nishi and S. Nagai, *J. Polym. Sci. Part A-2*: **7**, 201-208 (1969).

209. B. Hartmann, *Acustica* **36**, 24 (1976-1977).

210. J.R. Asay, D.L. Lamberson and A.H. Guenther, *J. Appl. Phys.* **40(4)**, 1768 (1969).

211. B.K. Sharma, *J. Phys. D: Appl. Phys.* **15**, 1273-1277 (1982).

212. J.C. Slater, *Introduction to Chemical Physics*, McGraw-Hill, New York (1939), p238.

213. I. Gilmour, A. Trainor and R.N. Haward, *J. Polym. Sci. Polym. Phys. Ed.* **16**, 1277, 1291 (1978).

214. B.K. Sharma, *Acustica* **48**, 118, 121, 193 (1981).

215. B.K. Sharma, *J. Phys. D. Appl. Phys.* **16**, 1959-1965 (1983).

216. B.K. Sharma, *Polym. Comm.* **30**, 346 (1989).

217. B.K. Sharma, *J. Phys. D. Appl. Phys.* **15**, 1735-1740 (1982).

218. B.K. Sharma and R.R. Reddy, *Pramana J. Phys.* **28**, 195 (1987).

GLOSSARY OF SYMBOLS

$\alpha_{(g, l)}$	Cubical Thermal Expansion Coefficient (Glass or Liquid)
$\alpha'_{(g, l)}$	Linear Thermal Expansion Coefficient (Glass or Liquid)
α'_{gg}	Linear Expansion Coefficient of a Second Glass-Glass Transition
α''_{gg}	Linear Expansion Coefficient of a Third Glass-Glass Transition
$\alpha'//$	Linear Thermal Expansion Coefficient Parallel to the Axis of Orientation.
$\alpha'\perp$	Linear Thermal Expansion Coefficient Perpendicular to the Axis of Orientation.
$\alpha'//_\infty$	Linear Thermal Expansion Coefficient of a Perfectly Oriented Polymer Parallel to the Axis of Orientation
B_T	Isothermal Bulk Modulus (or reciprocal compressibility)
C_p	Heat Capacity at Constant Pressure
C_v	Heat Capacity at Constant Volume
$C_{v, i}$	Interchain Heat Capacity at Constant Volume
δ	Departure from Equilibrium
δ_0	Initial Departure from Equilibrium
E_{act}	Energy of Activation
f	Fractional Free Volume
f_g	Fractional Free Volume at T_g
G	Free Energy of System
γ	Gruneisen Constant
γ_L	Lattice (Interchain) Gruneisen Constant
γ_T	Thermodynamic Gruneisen Constant
H	Specific Enthalpy
η	Viscosity
η_g	Viscosity at T_g
κ	Bulk Compressibility (reciprocal bulk modulus)
l	Instantaneous Sample Length
l_0	Initial Sample Length
log a(T)	Creep Curve Shift Function

M	Segmental Mobility
μ	Ageing Shift Rate
P	Pressure
R	Prigogine-Defay Ratio
r_o	Mean Interatomic Distance
ρ	Density
S	Entropy
σ_o	External Applied Stress
σ_r	Rubber-Elastic Reaction Stress
T_g (or T_α)	Glass Transition Temperature
T_β	Secondary (β) Transition Temperature
T_a	Annealing Temperature
T_0	Initial Temperature
T_w	Working Temperature
t_e	Equilibration or Ageing Time
t_{eq}	Time Required to Attain Thermodynamic Equilibrium
τ	Relaxation Time
τ_g	Relaxation Time at T_g
V	Specific Volume
V_{eq}	Specific Volume at Equilibrium
V_f	Free Volume
V_0	Occupied Volume
$V_{0,g}$	Extrapolated Occupied Volume of Glass at 0 K
$V_{0,l}$	Extrapolated Occupied Volume of Liquid at 0 K
v^*	Critical Volume for Molecular Transport

CHAPTER 3
EXPERIMENTAL AND VALIDITY OF MEASURING TECHNIQUE

3.1 MATERIALS: DESCRIPTION 69

3.2 POLYMER CURING AND CASTING 70

3.3 THERMOMECHANICAL ANALYSER (TMA) 71

3.4 VALIDITY OF MEASURING TECHNIQUE

3.4.1 Dimensional Changes Arising From Residual Stresses and Physical Ageing 73

3.4.2 Dimensional Changes Arising From the Sorption and Desorption of Diluents 77

3.4.3 Dimensional Changes Arising From Viscoelastic Deformation 77

3.4.4 Dimensional Changes Arising From Molecular Orientation 77

SUMMARY 78

BIBLIOGRAPHY 79

CHAPTER 3

3.1 MATERIALS: DESCRIPTION

The abbreviations, industrial source, molecular weights and structural formulae of the materials used in this work are listed in the following section.

MONOMER	ABBREVIATION	MOL. WEIGHT
Methyl Acrylate	MA	86
Methyl Methacrylate	MMA	100
Ethyl Methacrylate	EMA	114
IsoButyl Methacrylate	IBMA	142
Benzyl Methacrylate	BzylMA	162
2-Hydroxyehtyl Methacrylate	HEMA	130
(Ethylene Glycol) DiMethacrylate	EGDMA	198
Di (Ethylene Glycol) DiMethacrylate	DiEGDMA	242
Tri (Ethylene Glycol) DiMethacrylate	TriEGDMA	286
Tetra (Ethylene Glycol) DiMethacrylate	TetEGDMA	330
Poly-400-(Ethylene Glycol) DiMethacrylate	P400EGDMA	536
Poly-1000-(Ethylene Glycol) DiMethacrylate	P1000EGDMA	1136
PLASTICISER		
DiButyl Pthalate	DBP	278
DiOctyl Pthalate	DOP	391
TriCresyl Phosphate	TCP	368

Molecular Formulae and Source

MONOMER	MOLECULAR FORMULA	SOURCE
MA	$H_2C=CH.COO.CH_3$	Fluka
MMA	$H_2C=C(CH_3).COO.CH_3$	Fluka
EMA	$H_2C=C(CH_3).COO.(CH_2CH_3)$	Fluka
IBMA	$H_2C=C(CH_3).COO.(CH_2CH(CH_3)CH_3)$	Aldrich
BzylMA	$H_2C=C(CH_3).COO.(C_6H_5)$	Aldrich
HEMA	$H_2C=C(CH_3).COO.(CH_2CH_2OH)$	Mitsubishi
EGDMA	$H_2C=C(CH_3).COO.(CH_2CH_2O)_n.CO.C(CH_3)=CH_2$	Fluka
DiEGDMA	as for EGDMA, n = 2	PolySciences

TriEGDMA	as for EGDMA n = 3	Aldrich
TetEGDMA	as for EGDMA, n = 4	Fluka
P400EGDMA	as for EGDMA, n = 9	PolySciences
P1000EGDMA	as for EGDMA, n = 22	PolySciences

PLASTICISER

DBP	$C_6H_4.(COO.C_4H_9)_2$	May and Baker
DOP	$C_6H_4.(COO.C_8H_{17})_2$	Aldrich
TCP	$OP.(OC_6H_4.CH_3)_3$	Fluka

Most monomers were used with inhibitor as supplied, since the attempted removal of the inhibitor resulted in a number of problems, e.g. removal of inhibitor by the NaOH wash method [1] caused precipitation. The precipitation was prevented by diluting the monomer with dichloromethane prior to the 10% NaOH wash, but the removal of the solvent by vacuum distillation resulted in spontaneous gelling of the monomer at low temperatures [2]. Similar difficulties were encountered by Gordon and Roe [3] with uninhibited EGDMA. Atsuta and Turner [4] concluded that low levels of inhibitor would have little effect on the polymerisation process and final polymer properties, hence the monomers were used without further purification. The monomer MMA were stored over anhydrous calcium hydride, while all other monomers and plasticisers were dried over molecular sieves. All monomers were kept refrigerated.

3.2 POLYMER CURING AND CASTING

All monomers were polymerised by radical polymerisation. The peroxide initiator was recrystallised benzoyl peroxide (bpo, molecular weight 242.23) at a concentration of 0.2 mole percent. To prevent the formation of low molecular weight (approximately 7×10^3), "β-polymer" [5], oxygen was removed from the samples by bubbling high-purity, oxygen-free nitrogen gas through the reaction mixtures. The characteristics of the β-polymer in diallyl systems have been examined by Ito *et al.* [6]. The β-polymer is believed to occur early in the cure [7] and is the result of incomplete polymerisation of a number of monomer units at only one end.

The method of casting was similar to Cowperthwaite's [8], where 1.6 mm-thick polymer sheets were cast between glass sheets using Silastic tubing (Dow Corning) as a gasket

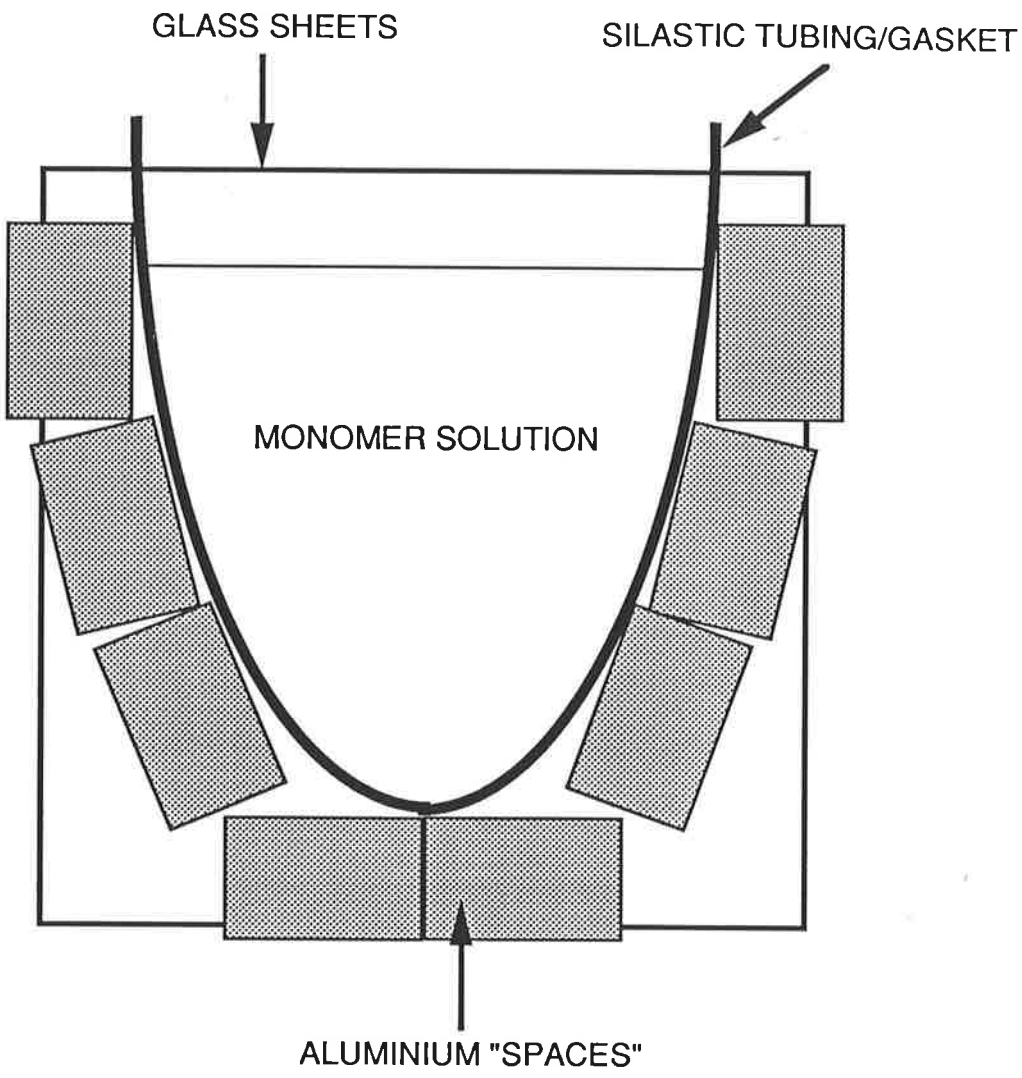

Figure 3.1 Sample casting between glass plates and using Silastic tubing as a gasket. "Bulldog" clips were used to clamp the cast assembly.

(Fig. 3.1). A two-stage curing process was employed, in which the first stage involved isothermal curing of the monomer until vitrification, followed by postcure at above T_g to drive the polymerisation to completion. The temperature of cure required depended on the particular monomer. Polymers that were glassy at room temperature were cured at the initial temperature of 60 C, followed by postcure at 125 C for 2-3 hours. Similarly, polymers that were rubbery at room temperature and plasticised PMMA samples were cured initially at 70 C, then postcured at 100 C for 2-3 hours. After postcuring, the samples were allowed to cool in the atmosphere to room temperature. The polymer samples were stored in sealed polyethylene bags and placed in a dessicator.

3.3 THERMOMECHANICAL ANALYSER (TMA)

Thermal analysis is defined [9-10] by ICTA (the International Confederation for Thermal Analysis) as a "term covering a group of techniques in which a physical property of a substance and/or its reaction product(s) is measured as a function of temperature". Thermomechanical analysis is a technique in which the deformation of a substance is measured under a non-oscillatory load as a function of temperature; *thermodilatometry*, on the other hand, is a technique in which the dimensions of a substance are measured as a function of temperature as the substance is subjected to a controlled temperature program [11].

A *Mettler TMA40* thermomechanical analyser (Fig. 3.2) was used to perform the thermal analysis. The specifications of the thermal experiment are entered via a keyboard into an external processor which is connected to the TMA40. Cut samples (5 x 5 x 1.6 mm^3) were placed on the support and a constant and static load (usually 0.1 N) was applied on the sample via a silica quartz probe (3 mm diameter). This assembly was enclosed in a heating/cooling chamber which was purged with nitrogen gas to maintain an inert atmosphere throughout the experiment. For subambient work, liquid nitrogen was used as coolant and was transferred into a dewar placed inside the chamber. The base of the probe was connected to a linear variable differential transformer (LVDT), and any change in the sample dimension resulted in a voltage output from the transformer. The voltage output from the TMA is simultaneously recorded by the external processor and is converted into numerical data, which is then transfered to a NEC PowerMate 1 personal computer. A software package written specifically for the Mettler thermoanalysis system, Graphware, allowed access to the data and display the

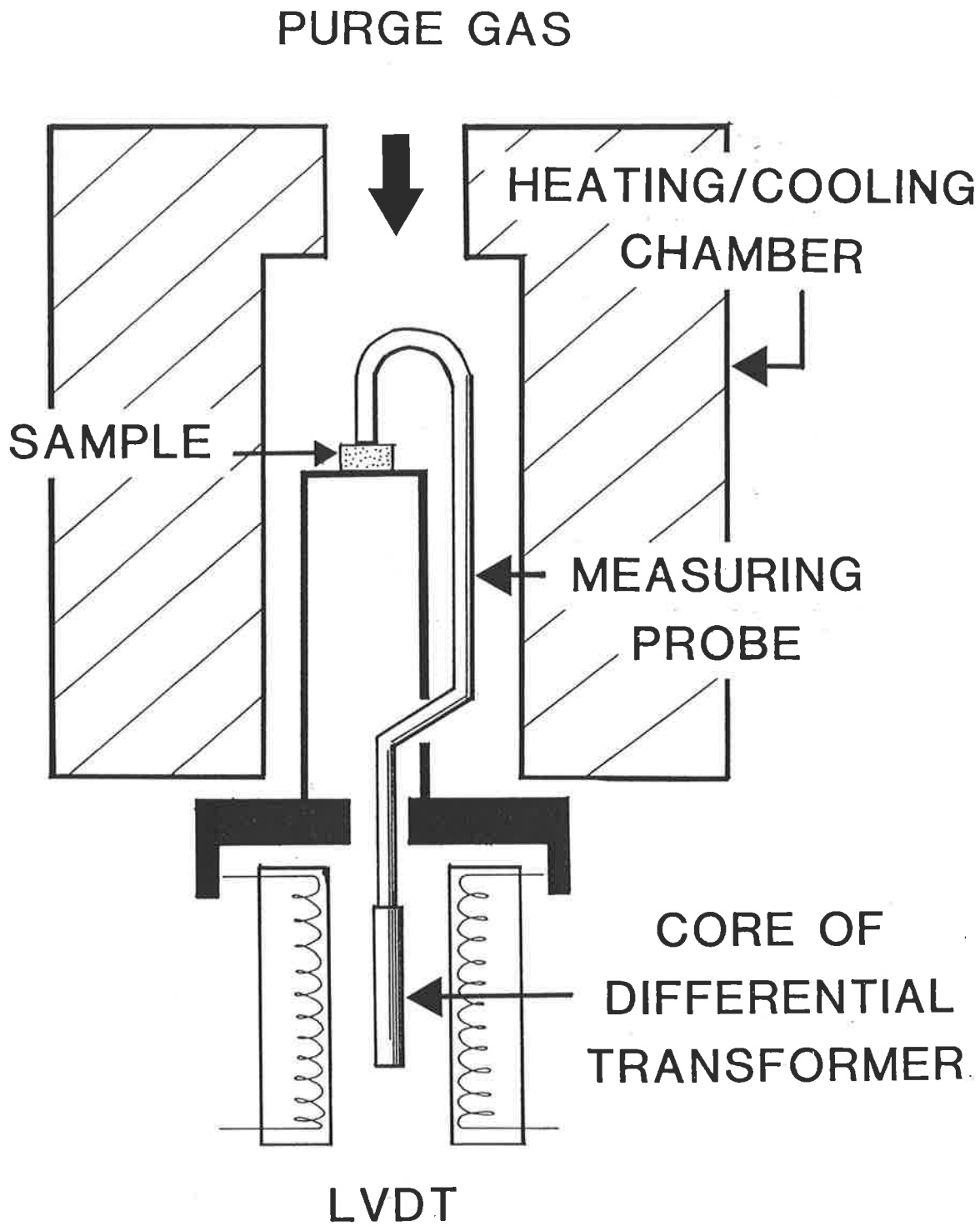

Figure 3.2 Schematic illustration of the sample and probe inside a thermomechanical analyser.

experimental curves. Graphware files can then be converted into ASCII-format files to be used on MS-DOS spreadsheet programs like Microsoft Excel. The TMA40 is capable of detecting dimensional changes of 1 μm and has a temperature range between -100 C to +300 C.

The main advantages of the Mettler TMA40 analyser are its high rate of data acquisition and its sensitivity to very small length changes. The high sensitivity of the TMA allows one to measure dimensional changes which would not be possible with volume dilatometry. Complicated thermal experiments with multiple temperature steps, different heating rates, kinetic and isothermal sections, etc., can also be readily programmed. Repeated runs can be easily carried out, if required, to check the reproducibility and reliability of the results. Volume dilatometry [12], on the other hand, is often a tedious and laborious technique. The calibration of the volume dilatometer requires considerable time, a procedure which involves degassing for twenty four hours followed by measuring the volume changes of pure mercury over the temperature range of interest. It has been suggested [13] that at least 5 hours was required for the system to attain thermal equilibrium, and five consecutive readings that were reproducible should be taken over a period of 2 hours to provide a reliable value. Although mercury is considered to be the best confining liquid because of the availability of accurate density data for this substance over a wide temperature range and its inertness to most polymers [13-14], the handling of poisonous mercury represents a serious health hazard.

More importantly, the long intervals between measurements mean that volume changes during physical ageing is unlikely to be observed since the polymer may have aged inside the dilatometer. This is especially true near the glass transition, where the rate of the molecular mobility becomes comparable with the timescale of the measurement. The small specimen required for thermal analysis facilitates rapid thermal equilibration, thus enabling measurement of rapid length changes in the glass transition region to be taken at short time intervals (of the order of seconds).

3.4 VALIDITY OF MEASURING TECHNIQUE

One of the objectives of this work is to establish that the measurement of linear dimensional changes represents a novel technique in which the structural and conformational rearrangement of polymers associated with dimensional instability may be characterised. In order to verify that the experimental information provided by length measurements are reliable,

the effects of the five different sources of dimensional instability (as shown in Fig. 1.4) on the dimensional changes of polymers have to be separately identified and distinguished.

3.4.1 Dimensional Changes Arising From Residual Stresses and Physical Ageing

The presence of residual stresses in polymers have been shown to influence the rate of ageing [19] and may complicate the interpretation of length-temperature curves, since the magnitude of thermal stresses in quenched polymers is known [15, 17-18, 23] to be quite considerable at room temperature, in the order of 10-20 MPa. Residual stresses may be introduced into polymers during the curing and manufacturing stages, in which curing stresses [15] and entropic stresses [18] are frozen-in by rapid cooling from above to below T_g. Cooling or thermal stresses [16-18, 22] are also generated by rapid and non-uniform cooling to below T_g as a result of differential shrinkage experienced by the polymer (Section 2.3.11). On the other hand, rapid cooling from above to below T_g also freezes in excess free volume which lead to physical ageing, irrespective of whether residual stresses are present or not [31]. Therefore, an as-received polymer sheet which has been cast between glass sheets is likely to exhibit dimensional instability arising from physical ageing and residual stresses.

The length change-temperature (ΔL-T) plots of several as-received cast PMMA specimens obtained from different locations on a sheet (Fig. 3.3) (thereby creating a "thermal atlas") are shown in Figures 3.4 and 3.5. These specimens were heated in the TMA at a constant rate of 2 C/min from 25 C to 165 C under a static load of 0.1 N. The thickness of the postcured sheet ranged from 1.536 mm for specimen E1 to 1.728 mm for specimen C5.

Anomalously low glass expansivities (α'_g) (as low as -85 x 10^{-6} K^{-1}) are observed at temperatures well below the T_g of PMMA of 105 C [29, 30]. It is known that the frozen-in curing stresses [15] and surface thermal stresses [16-18] are compressive in nature, and that the presence of these stresses result in abnormally small or negative expansion. On the other hand, these observations are also consistent with the hypothesis [31] that the transverse vibrations of oriented polymer chains will result in negative expansion (Fig. 2.27). The variation in the magnitude of thermal stresses in quenched polycarbonate (PC) (T_g = 150 C) was measured by Saffell and Windle [24] as a function of annealing time. The compressive surface stresses were found to have relaxed from 14 MPa to 2 MPa after annealing times of less than 10 hours at 120

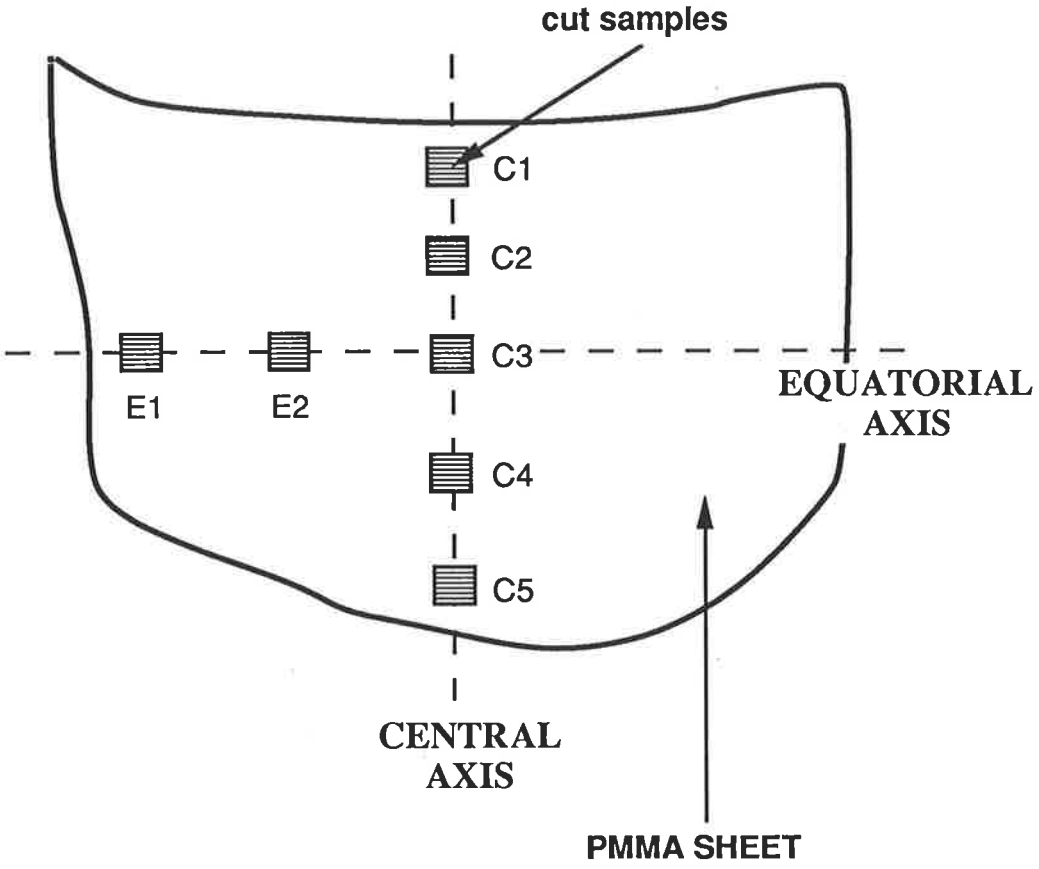

Figure 3.3 Thermal atlas of a cast poly(methyl methacrylate) sheet

FIGURE 3.4 FIRST HEATING RUN FOR AS-CAST EQUATORIAL PMMA SAMPLES

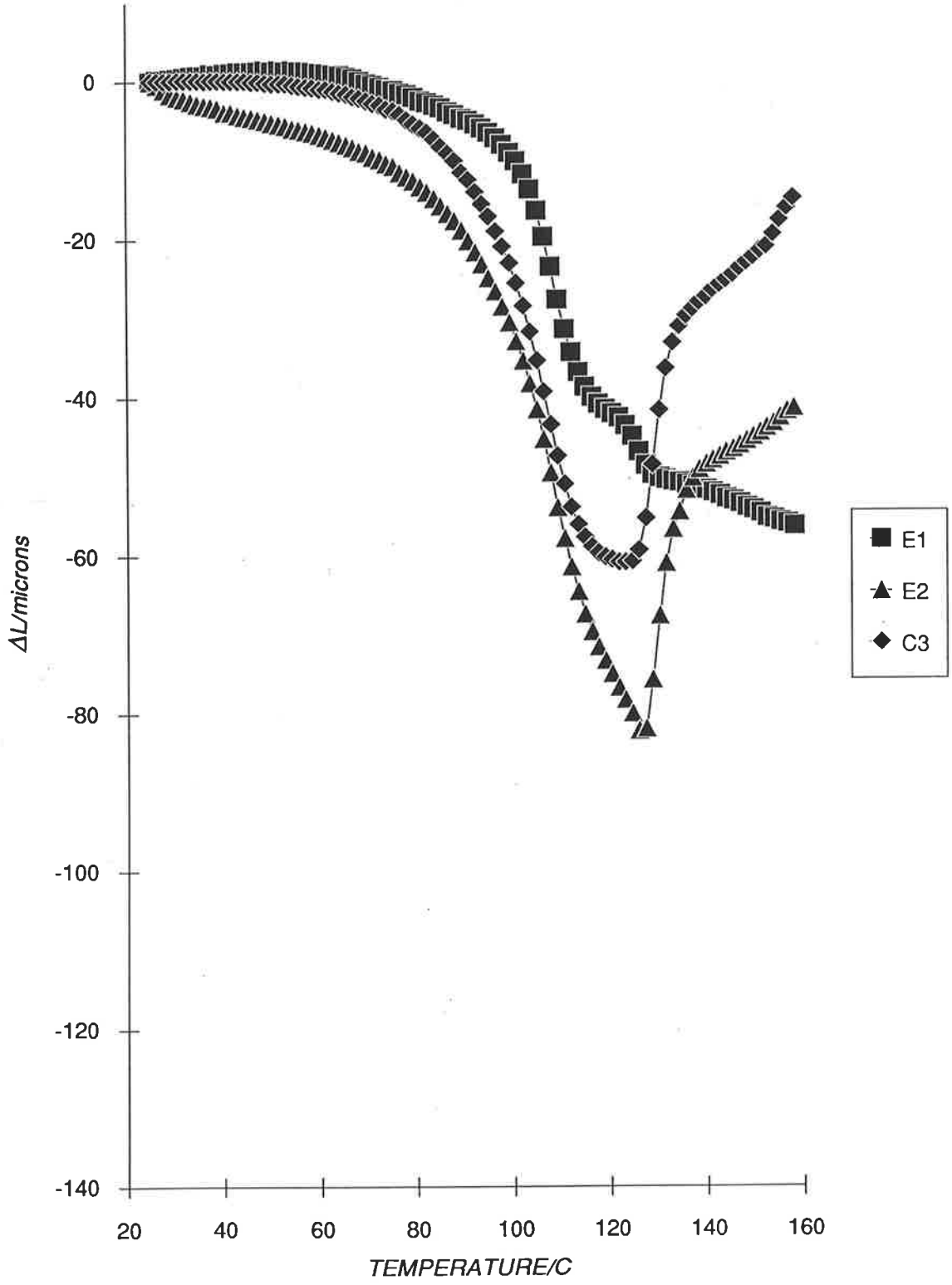

FIGURE 3.5 FIRST HEATING RUN FOR AS-CAST AXIAL PMMA SAMPLES

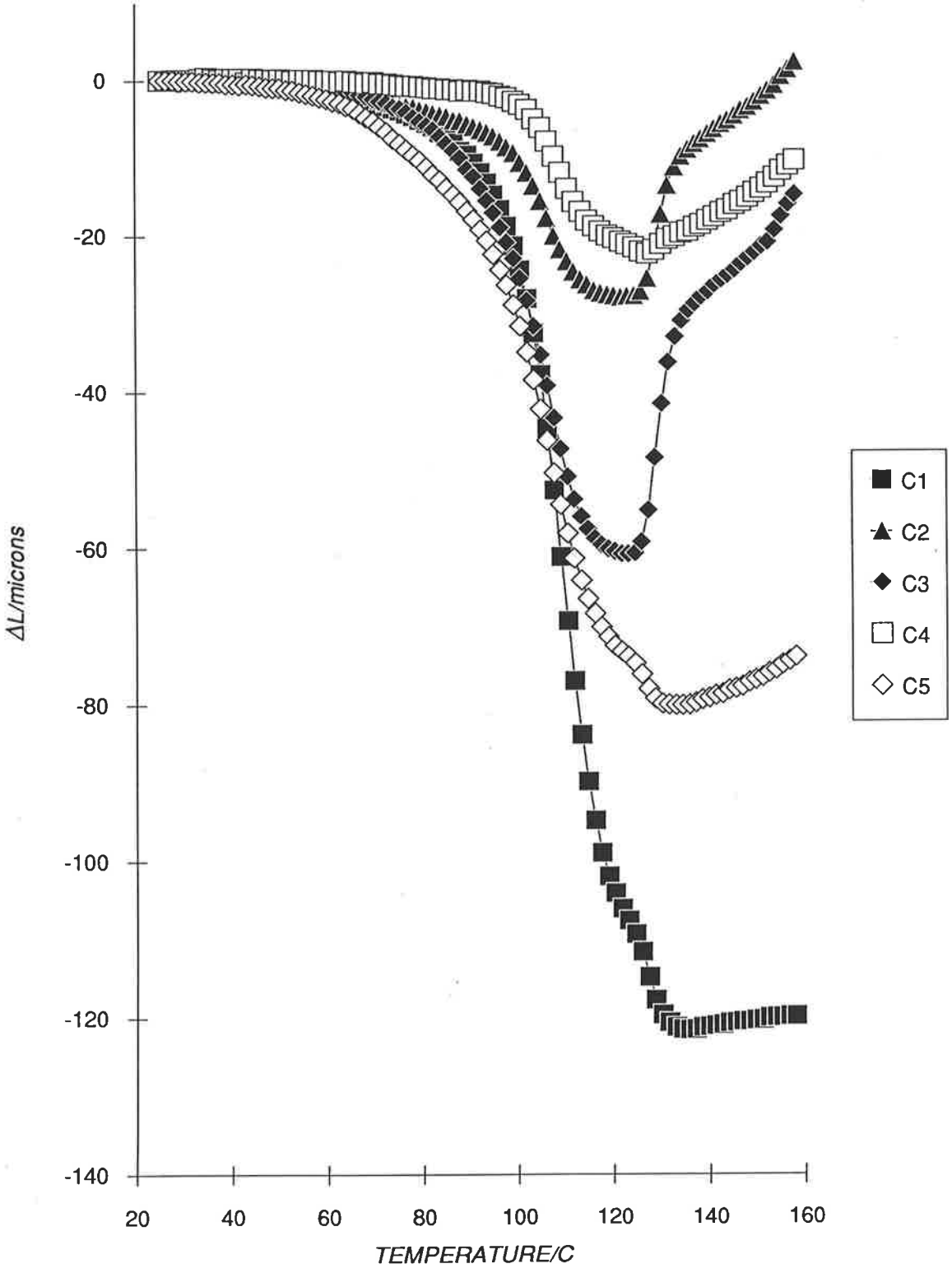

C. The hypothesis that low or negative values of α'_g are caused by frozen-in residual stresses was tested by subjecting as-received cast PMMA specimens to annealing experiments in which the specimens were isothermally annealed at a temperature T_a between 80 C to 150 C for 60 minutes, followed by slow cooling to 25 C in an air-oven at a rate less than 1 C/min. After annealing, the specimens were heated in the TMA from 25 C to 165 C at a constant rate of 2 C/min and a static load of 0.1 N. For these experiments, a separate PMMA sheet was used and the specimens were cut near the centre of the sheet. The annealing of as-received cast PMMA below T_g is expected to result in the removal of residual stresses. The ΔL-T curves of annealed PMMA are presented as a function of annealing temperature in Figure 3.6 while the linear glass and liquid expansivities, α'_g and α'_l, are shown in Table 3.1.

TABLE 3.1

Glass and liquid expansion coefficients (10^{-6} K^{-1}) of annealed poly(methyl methacrylate) as a function of annealing temperature

Annealing Temperature (C)	α'_g	α'_l
80	34	326
90	35	292
110	40	288
130	44	320
150	62	155

Figure 3.6 shows that the marked contraction observed at 90-130 C decreases with increasing annealing temperature. This contraction is observed even after annealing at 45 C above T_g and could not be erased by slow cooling. It may be concluded that this contraction is always present, regardless of the annealing temperature and the rate of cooling from above to below T_g. In addition, the contraction is found to be thermoreversible, where a sequence of experiments in which a single annealed specimen was repeatedly heated to above T_g (160 C) and subsequently cooled to below T_g at the same rate produced ΔL-T curves which were nearly superimposible (Fig. 3.7).

It is proposed that the contraction observed between 90-130 C characterises the

FIGURE 3.6 REMOVAL OF INTERNAL STRESSES IN CAST PMMA BY ANNEALING

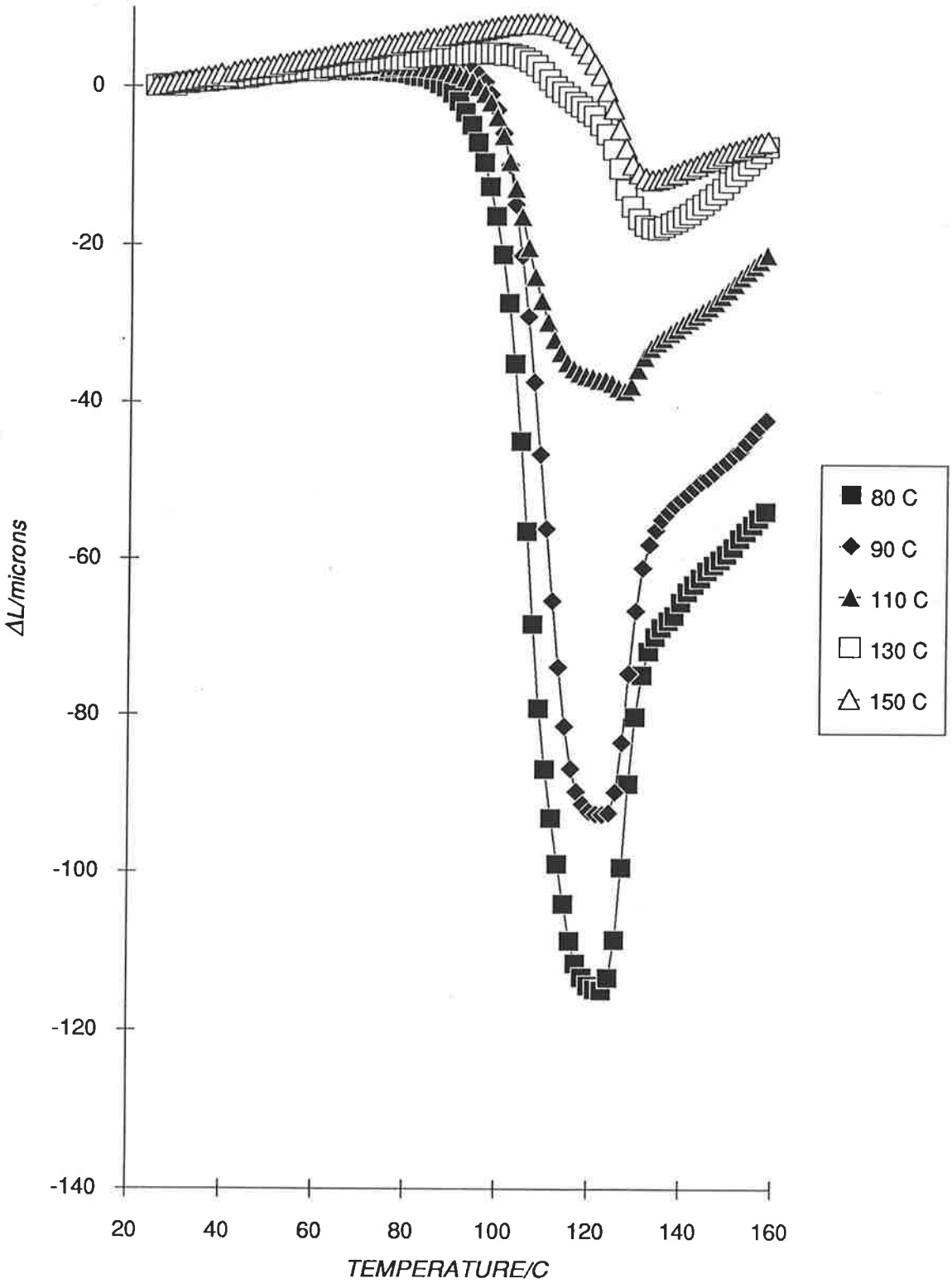

FIGURE 3.7 THE THERMOREVERSIBILITY OF CONTRACTION NEAR THE GLASS TRANSITION IN PMMA

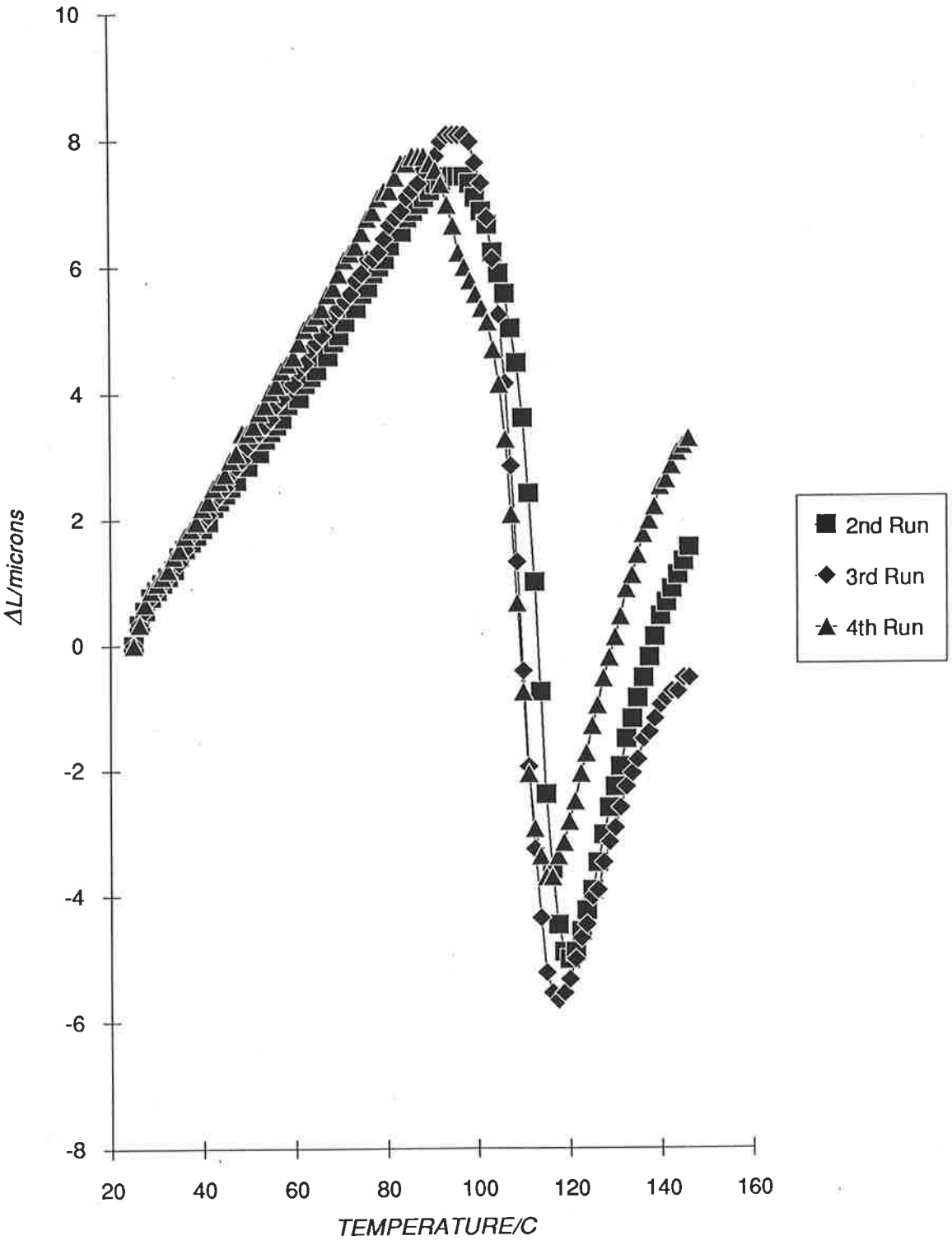

collapse of frozen-in free volume [20-21], in accordance with the reports of a number of authors [25, 38-43]. Lee and McGarry [40-41] have shown that the quenching of polystyrene from various initial temperatures above T_g to lower ageing temperatures (below T_g) results in the freezing-in of different amounts of excess free volume. The collapse of free volume was manifested by spontaneous decrease in specific volume during isothermal ageing below T_g [40-41]. Schematically, the collapse of free volume during length contraction may be represented by Figure 3.8, where it is assumed that a constant amount of free volume remains frozen-in after quenching (hatched area) and that the free volume fraction is zero (i.e. the attainment of equilibrium) at T_{end}. However, the validity of the assumption of a constant free volume below T_g will be discussed in greater detail in Chapter 4. Although Table 3.2 shows that the length contraction ΔL, which is defined as the difference between the maximum and the minimum sample lengths, decreases slightly with increasing number of runs, it is likely that the amount of frozen-in free volume is gradually reduced by repeated heating and cooling cycles. Therefore, these observations show that length contraction in the glass transition region of PMMA is associated with the process of physical ageing. The magnitude of ΔL as a quantitative measure of free volume fraction will be established in Chapter 4.

Table 3.2 shows that the thermal expansion coefficients obtained from repeated runs remained relatively unchanged. On the other hand, it is observed from Table 3.1 that α'_g increases with an increase in T_a, rising from 34 x 10^{-6} K^{-1} after annealing at 80 C to 62 x 10^{-6} K^{-1} after one hour at 150 C. The final value obtained at 150 C correlates with the value of 75 x 10^{-6} K^{-1} obtained by Haldon and Simha [29] for PMMA. Although positive values of α'_g were attained by annealing, α'_g obtained between 80-130 C were still lower than the value of Haldon and Simha [29]. These observations appear to correlate with the results of Saffell and Windle [24], who observed that subsequent annealing up to 100 hours at 120 C did not result in further stress relaxation in PC. The perseverance of low values of α'_g after annealing at T_a below 130 C suggests that the complete removal of frozen-in residual stresses is only achieved by annealing at above 130 C.

With the exception of the specimen annealed at 150 C, the values of α'_l are much higher than literature values for PMMA which are approximately 160 x 10^{-6} K^{-1} [30, 32-33]. It will be shown in Section 4.4.3 that large α'_l values are a consequence of endothermic peaks which are characteristic of annealed or slow-cooled polymers when heated to above T_g [34-37].

The absorption of heat energy at T_g causes an increase in thermal vibrations which corresponds to larger liquid expansion coefficients.

TABLE 3.2

Thermal expansivities (10^{-6} K^{-1}) and length contraction of poly(methyl methacrylate) subjected to repeated heating runs (specimen C3 in Figure 3.4-3.5)

Run No.	α'_g	α'_l	ΔL (10^{-6} m)
1	-10.9	309.3	60.9
2	74.5	242.5	7.6
3	75.4	254.1	6.3
4	75.7	250.5	5.6

However, the nature of the sudden and rapid expansion occuring over a narrow temperature range 125-135 C (Fig. 3.6) has yet to be established. Figure 3.6 shows that this expansion is observed for specimens which were annealed between 80-110 C, and that the expansion progressively decreases with increasing annealing temperature until it disappears completely at 130 C and 150 C. It is also noted that this sudden expansion could not be observed in Figure 3.7 when the specimen was repeatedly heated to 160 C. The observation that the sudden expansion is removed by annealing or heating to elevated temperatures above 130 C suggests that it is not associated with physical ageing.

It is proposed that the sudden and rapid expansion is due to the release of entropic stresses [18, 20] which arise from frozen-in molecular orientation. It is believed that molecular orientation in PMMA was generated during postcuring above T_g at 125 C when the polymer sheet was subjected to a constant compressive stress when it remained clamped between two glass sheets during postcure. These proposals are consistent with the observation that the stresses were completely erased only when the specimen was heated to above the postcure temperature of 125 C, and is suppported by reports [24-28] which indicate that the removal of entropic stresses was achieved at longer annealing times or by increasing the annealing temperature. The presence of entropic stresses may also be related to low α'_g values of as-received cast PMMA which are believed to arise from tranverse vibrations of oriented chains.

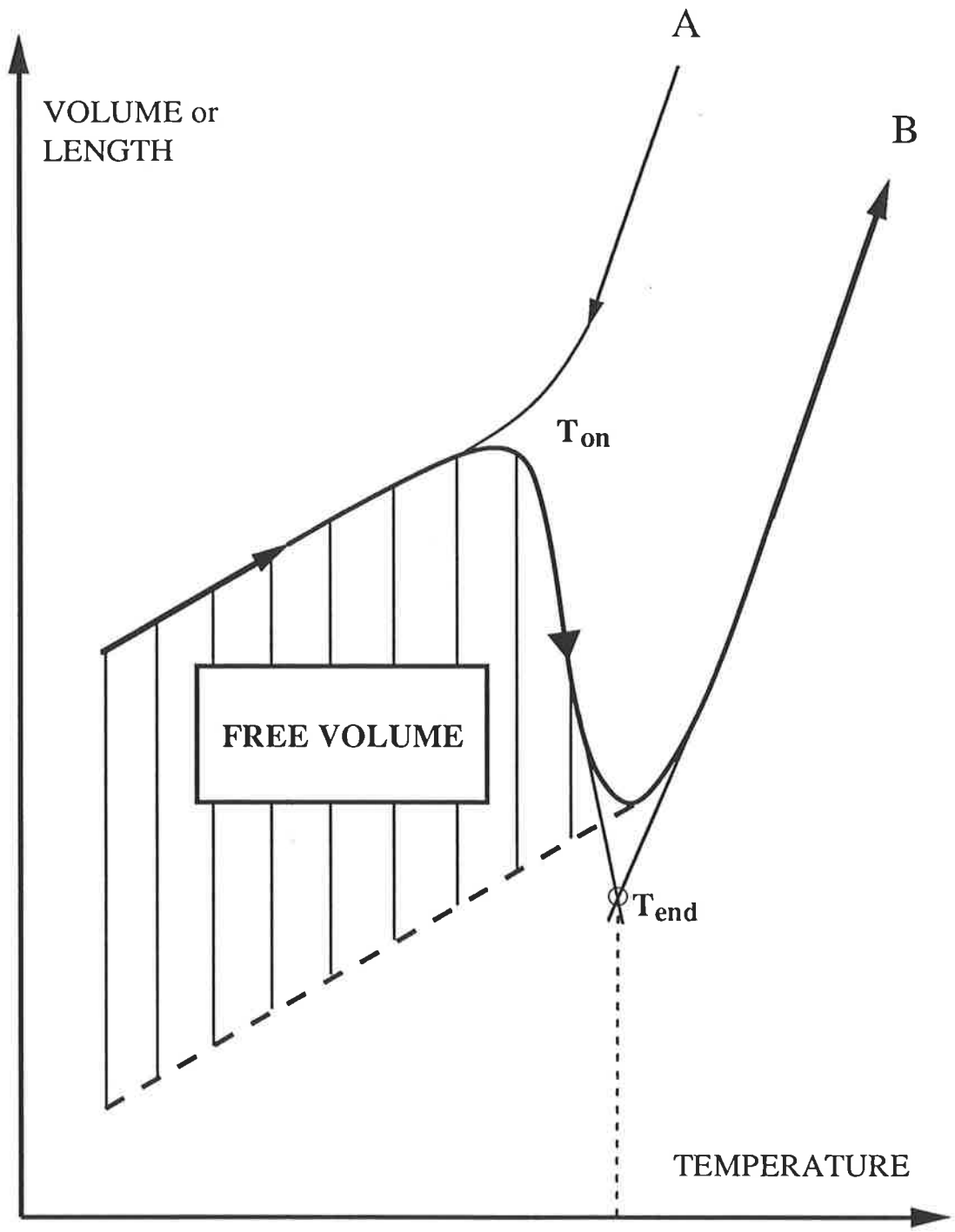

Figure 3.8 The observation of length contraction is associated with the collapse of free volume (hatched area). Rapid cooling from above to below T_g freezes-in free volume (Curve **A**). Upon reheating, the length-temperature curve does not follow the cooling curve but instead display a contraction in the vicinity of the glass transition region (Curve **B**; compare Fig. 1.2). The onset and endset temperatures of contraction are determined by the extrapolated glass, contraction and liquid lines (as shown for T_{end}).

Hence, the effects of residual stresses and physical ageing on dimensional changes of PMMA have been successfully identified and distinguished. These effects are summarised in Figure 3.9.

3.4.2 Dimensional Changes Arising From Sorption and Desorption of Diluents

The sorption of moisture by poly(2-hydroxyethyl dimethacrylate) (PHEMA) is known [44] to occur in two stages, in which water molecule occupy voids during the early stages of sorption, while the uptake of water at prolonged periods of hydration result in the swelling of PHEMA which is accompanied by expansion. Preliminary experiments in Chapter 10 indicate that the loss of water from hydrated PHEMA results in length contraction. In addition, these experiments suggest that dimensional changes of wet PHEMA may provide information concerning the nature of water molecules that reside in PHEMA.

3.4.3 Dimensional Changes Arising From Viscoelastic Deformation

Polymeric specimens which undergo viscoelastic deformation at temperatures above T_g are low-molecular weight PMMA (Chapter 7), highly-plasticised PMMA (Chapter 8), and poly(*iso*-butyl methacrylate) (PIBMA) and poly(benzyl methacrylate) (PBzylMA) (Chapter 11) which exhibit large decreases in modulus upon changing from glass to liquid. Viscoelastic deformation is recognised by the persistence of contraction at temperatures well above T_g and by a permanent indentation on the specimen.

3.4.4 Dimensional Changes Arising From Molecular Orientation

Chapter 6 shows that oriented PMMA exhibit large and rapid dimensional changes in the range 125-135 C. These changes are associated with the erasure of molecular orientation (randomisation) as the specimen regains a random and amorphous structure. In addition, it was found that the dimensional changes may result in length expansion or contraction, according to the relative directions of measurement and orientation. The temperature range at which randomisation of PMMA occurs overlaps the high temperature side of the ageing range, hence the deconvolution of the effects of randomisation and ageing may be complicated if both processes result in contraction. On the other hand, the task of dintinguishing the effects of

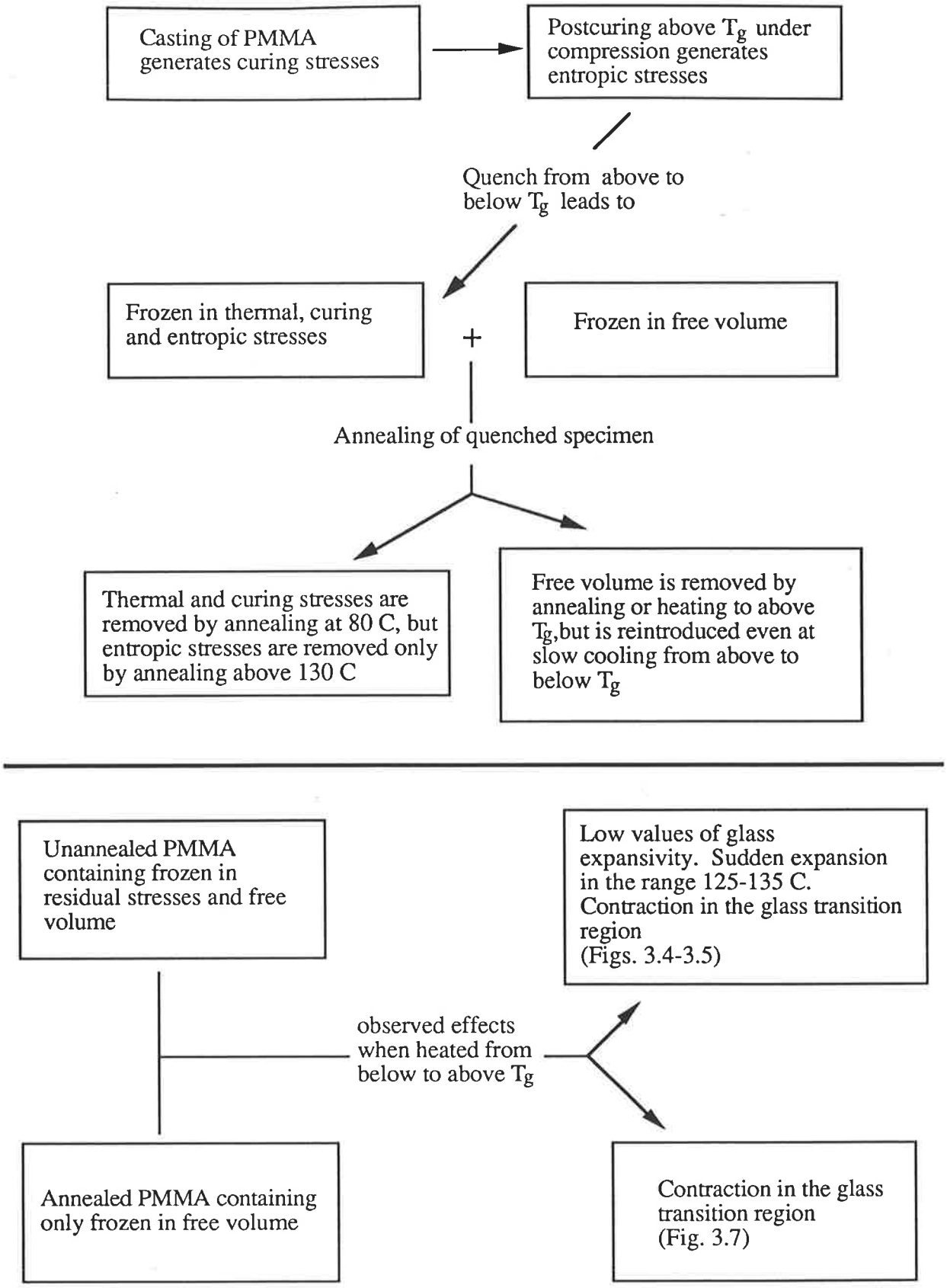

Figure 3.9 Schematic representation of the observed effects of residual stresses and physical ageing on dimensional changes of PMMA.

ageing and randomisation is made easier if both processes result in opposing effects, viz. contraction and expansion.

The effects of the various phenomena on the dimensional instability of polymers are summarised in Table 3.3.

TABLE 3.3

Summary of dimensional changes in polymers

Phenomenon	Observed Effects
Physical Ageing	Contraction in glass transition region; length contraction at temperatures below T_g may be observed in isothermal experiments.
Residual Stresses	Low values of α'_g; small expansion in the glass state below T_g; sudden expansion between 120-130 C if entropic stresses are present.
Sorption/Desorption of Diluents	Expansion observed during swelling of polymer; contraction observed during desorption of diluent.
Viscoelastic Deformation	Persistent contraction at temperatures well above T_g; permanent indentation on specimen.
Molecular Orientation (PMMA)	Sudden and rapid dimensional changes between 125-135 C. Expansion or contraction may be observed depending on whether measurement is parallel or perpendicular to the orientation axis.

3.5 SUMMARY

(1) A description of the materials used and the thermomechanical analyser have been provided along with details of the polymer casting procedure. Dimensional instabilities arising from the release of frozen-in residual stresses were successfully identified and distinguished from changes arising from physical ageing. An overview of the effects of a number of related phenomena on dimensional changes of polymers was provided.

(2) The observation of length contraction in the glass transition region of PMMA

was attributed to physical ageing, in which the contraction indicated the collapse of free volume frozen in during cooling from above to below T_g. The contraction was found to decrease upon an increase in annealing temperature and was observed to be thermoreversible.

Chapter 3

1. M. Fisher, *PhD. Thesis*, University of Adelaide (1983).
2. G.P. Simon, *PhD. Thesis*, University of Adelaide (1986).
3. M. Gordon and R.J. Roe, *J. Polym. Sci.* **21**, 39 (1956).
4. M. Atsuta, D.T. Turner, *Polym. Eng. Sci.*, **22(7)**, 438 (1982).
5. M.M. Mogilevich, N.A. Sukhanova, G.V. Korolev, *Vysokmol. Soyed*, **A15(7)**, 1478 (1973).
6. K. Ito, Y. Murase and Y. Yamashita, *J. Polym. Sci. Polym. Chem. Ed.* **13**, 87 (1975).
7. G.V. Korolev, L.I. Makhonia and A.A. Berlin, *Vysokomol. Soyed*, **A3(2)**, 198 (1961).
8. G.F. Cowperthwaite, J.J. Foy, M.A. Malloy, *Biomedical and Dental Applications of Polymers*, C.G. Geblen and F.F. Koblitz eds., Plenum Press, New York (1981), p397.
9. R.C. MacKenzie, *Pure Appl. Chem.* **57**, 1737 (1985).
10. M.J. Richardson, *Comprehensive Polymer Science*, C. Booth and C. Price, eds., Pergamon Press (1989), Vol(**1**), Chapter 36.
11. G. Lombardi, *For Better Thermal Analysis*, ICTA, Rome (1980), p18-19.
12. N. Bekkedahl, *J. Res. Nat. Bur. Std.* **42**, 145 (1949).
13. O.S. Tyagi and D.D. Deshpande, *J. Appl. Polym. Sci.* **37**, 2041-2050 (1989).
14. H. Hocker, G.J. Blake and P.J. Flory, *Trans. Faraday Soc.* **67**, 2251 (1971).
15. M. Shimbo, M. Ochi and Y. Shigeta, *J. Appl. Polym. Sci.* **26**, 2265-2277 (1981).
16. P. So and L. Broutman, *Polym. Eng. Sci.* **16(12)**, 785 (1976).
17. L.E. Hornberger and K.L. Davies, *Polym. Eng. Sci.* **27(19)**, 1473 (1987).
18. L.C.E. Struik, *Polym. Eng. Sci.* **18**, 799 (1978).
19. J. Bartos, J. Muller and J.H. Wendorff, *Polymer* **31**, 1678 (1990).
20. L.C.E. Struik, *Physical Ageing in Amorphous Polymers and Other Materials*, Elsevier, Amsterdam (1978).
21. S. Matsuoka, *Polym. Eng. Sci.* **21(14)**, 930 (1981).

22. W.D. Callister Jr., *Materials Science and Engineering, An Introduction,* Wiley (1991).

23. A. Siegmann, A. Buchman and S. Kenig, *Polym. Eng. Sci.* **22(1)**, 40 (1982).

24. J.R. Saffell and A.H. Windle, *J. Appl. Polym. Sci.* **25**, 1117-1129 (1980).

25. L.C.E. Struik, *Ann. N.Y. Acad. Sci.* **279**, 78 (1976).

26. K.C. Rusch, *Polym. Eng. Sci.* **12(4)**, 288 (1972).

27. M. Trzandel and M. Kryszewski, *Polymer* **29**, 418 (1988).

28. M. Trzandel and M. Kryskewski, *Polymer* **29**, 619 (1988).

29. R.A. Haldon and R. Simha, *J. Appl. Phys.* **39(3)**, 1890 (1968).

30. S. Loshaek, *J. Polym. Sci.* **15**, 391 (1955).

31. L.C.E. Struik, *Internal Stresses, Dimensional Instabilities and Molecular Orientations in Plastics,* Wiley, Chichester (1990).

32. S.S. Rogers and L. Mandelkern, *J. Phys. Chem.* **61**, 985 (1957).

33. J.C. Whitman and A.J. Kovacs, *J. Polym. Sci.* **C16**, 4443 (1969).

34. A.R. Berens and I.M. Hodge, *Macromolecules* **15**, 756-761 (1982).

35. C.R. Foltz and P.V. McKinney, *J. Appl. Polym. Sci.* **13**, 2235 (1969).

36. S.E.B. Petrie, *J. Polym. Sci. Part A-2* **10**, 1255 (1972).

37. A. Gray and M. Gilbert, *Polymer* **17**, 44 (1976).

38. A.J. Kovacs, *J. Polym. Sci.* **30**, 131 (1958).

39. A.J. Kovacs, *Fortschr Hochpolym. Forsch.* **3**, 394 (1963).

40. H.H.D. Lee and F.J. McGarry, *J. Macromol. Sci. Phys.* **B29(1)**, 11-29 (1990).

41. H.H.D. Lee and F.J. McGarry, *J. Macromol. Sci. Phys.* **B29(2&3)**, 237-248 (1990).

42. L.C.E. Struik, *Polymer* **28**, 1869 (1987).

43. D.G. LeGrand, *J. Appl. Polym. Sci.* **13**, 2129 (1969).

44. D.T. Turner, *Polymer* **23**, 197 (1982).

CHAPTER 4
PHYSICAL AGEING IN PMMA

4.1 INTRODUCTION 81

4.2 SAMPLE PREPARATION AND EXPERIMENTAL 82

4.3 LENGTH CONTRACTION AS A QUANTITATIVE MEASURE OF FREE VOLUME 83

4.4 RESULTS AND DISCUSSION

4.4.1 Free Volume Fraction 84

4.4.2 Temperature Range for Length Contraction 88

4.4.3 Thermal Expansion Coefficient 91

4.4.4 Relaxation Times for Length Contraction 96

4.4.5 Gruneisen Constant of Poly(Methyl Methacrylate) 97

4.5 SUMMARY 99

BIBLIOGRAPHY 100

GLOSSARY OF SYMBOLS 104

CHAPTER 4

4.1 INTRODUCTION

It has been established in Chapter 3 that the observation of length contraction in the vicinity of the glass transition region of PMMA is associated with the collapse of free volume [35-38]. Enthalpy and density measurements as a function of physical ageing have shown that the ageing process results in a denser molecular packing of polymer chains [1-4], hence the effect of physical ageing has been inferred to reduce the free volume content [5-10]. Therefore, the free volume fraction of a polymer is considered to be a sensitive indicator of the state of physical ageing.

The main objective of this chapter is to establish length contraction as an alternative and quantitative measure of free volume. The renowned Williams-Landell-Ferry (WLF) [11] and Simha-Boyer (SB) [12] free volume theories both proposed that the free volume fraction frozen-in at T_g may be taken to be constant for all polymers, but due to the different interpretations of free volume the SB theory suggests a value of 0.113 while a lower value of 0.025 is proposed by the WLF theory. However, volumetric [13-16] and differential scanning calorimetric (DSC) [17-20] studies show that thermal history has a pronounced effect on the ageing behaviour of the polymer. In view of such experimental evidence, it is of interest to determine whether the free volume fraction of PMMA specimens with different thermal histories can be described by a single universal constant.

The thermal expansion coefficient is also an important variable in elucidating the nature of polymer structures. For example, it is also known to be susceptible to changes in free volume [30], and that the incorporation of expansion coefficients in the Gruneisen equation (Eq. 2.20) provides a semi-quantitative description of the degree of anharmonicity in a polymer. Haldon and Simha [30] observed that the glass expansivities of different specimens of poly(*n*-butyl methacrylate) varied according to the thermal history of the specimen. Specimens that were quenched from above to below T_g generally had larger glass expansivities than annealed specimens, where the larger expansivity was interpreted as reflecting the expansion of frozen-in free volume. Unfortunately, the effect of thermal history on liquid expansivity was not reported. In spite of the close relationship between the thermal expansivity and the structural

state of a polymer, the effect of physical ageing on the expansivity has rarely been investigated. This chapter presents a detailed study of the glass and liquid expansivities of PMMA as a function of physical ageing and thermal history is presented. The results indicate that the expansivities are sensitive to the thermal history of a polymer and closely reflect the changes in free volume.

The glass transition temperature has been criticised as being incapable of reflecting the true physical meaning of the glass-rubber transition [16, 34]. As observed in Figure 3.7, the idealised volume/length-temperature (V-T and L-T) plots in Figures 2.2 and 2.7 could not be obtained for PMMA by slow and careful cooling to below T_g or by increasing the annealing temperature to 150 C. Consequently, the T_g, which is usually defined as the intersection of the extrapolated glass and liquid lines, could not be measured from the L-T plots produced in this work. A new method of characterising the glass transition of PMMA is proposed, in which the boundaries of the glass transition region may be defined by additional parameters which characterise the length contraction.

4.2 SAMPLE PREPARATION AND EXPERIMENTAL

Two types of PMMA specimens of different thermal histories were prepared:

(1) *quenched* specimens were prepared by initially equilibrating the sample on a hotplate at about 150 C for 10-15 minutes to completely remove the presence of internal stresses. Following equilibration, the specimen was quenched in liquid nitrogen for ten minutes. The cooling rate of the quenching process was estimated by Lee and McGarry [16] to be in the range of 500-700 C/sec, but Hill and Agrawal [21-22] predicted a cooling rate of only 27 C/min. Although it is recognised that rapid quenching produces thermal stresses [23], Struik [10] found that that the shift rate of creep curves was affected only to a small degree by internal stresses formed during quenching. After quenching the specimens were removed from the liquid nitrogen bath and stored immediately in a dessicator to prevent uptake of moisture. Diaz-Calleja *et al.* [24] have shown that poor reproducibility in dynamic mechanical data due to thermal stresses is only significant within the first ten minutes after quenching. Hence a period of approximately 20 minutes was allowed to elapse before the specimen was placed in the thermomechanical analyser to minimise any poor reproducibility which may arise from thermal stresses.

(2) *Slow-cooled* specimens were prepared by equilibrating at 130-135 C for a period of about 75 minutes, followed by slow cooling at a rate of less than 1 C/min to ambient temperature. The specimens were kept dry in a dessicator for 20 minutes prior to experimentation.

Thermal analysis was performed by a Mettler TMA 40 thermomechanical analyser under a range of heating rates from 0.05 C/min to 20 C/min. The length changes were measured under a constant static load of 0.1 N applied by a flat-based quartz probe with a base diameter of 3 mm and dry nitrogen gas was continually purged through the specimen chamber.

4.3 LENGTH CONTRACTION AS A QUANTITATIVE MEASURE OF FREE VOLUME

According to Kovacs [14, 25], $\delta = (V - V_{eq})/V_{eq}$ represents a dimensionless measure of the departure from thermodynamic equilibrium, where V_{eq} is the specific volume at equilibrium. Let the initial volume of a quenched specimen be defined by $V_0 = L_x . L_y . L_z$, and the volume at equilibrium by $V_{eq} = (L_x - \Delta L_x).(L_y - \Delta L_y).(L_z - \Delta L_z)$ where $L_{x,y,z}$ and $\Delta L_{x,y,z}$ represent the initial specimen length and the length contraction respectively. The thickness of the specimen has been arbitrarily designated as the z-axis, while the width and length are collectively designated as the (x, y)-axis (Fig. 4.1). The shaded area represents the face that is in contact with the probe during measurement. The contraction ΔL is taken as the difference between the maximum and minimum sample lengths, L_{max} and L_{min}, as illustrated in Figure 4.2. The free volume V_f is defined by the difference between the initial and equilibrium volumes by (refer Fig. 3.8):

$$V_f = (V_0 - V_{eq}) = L_z.[2L_{x,y}.\Delta L_{x,y} - (\Delta L_{x,y})^2] + \Delta L_z.(L_{x,y} - \Delta L_{x,y})^2 \qquad (4.1)$$

Measurements of the lengths L_x and L_y of slow-cooled and quenched specimens indicate that L_x and L_y are similar and that a common symbol $L_{x,y}$ may be used to denote L_x and L_y. It is also assumed that ΔL_x and ΔL_y are the same for the two types of PMMA and the symbol $\Delta L_{x,y}$ is used. Length measurements along the (x, y)-axis found that both quenched and slow-cooled PMMA displayed a similar contraction $\Delta L_{x,y}$ of approximately 100 μm (Fig. 4.3).

In the case of slow-cooled PMMA, $(\Delta L_z/L_z)$ and $(\Delta L_{x,y}/L_{x,y})$ were found to have

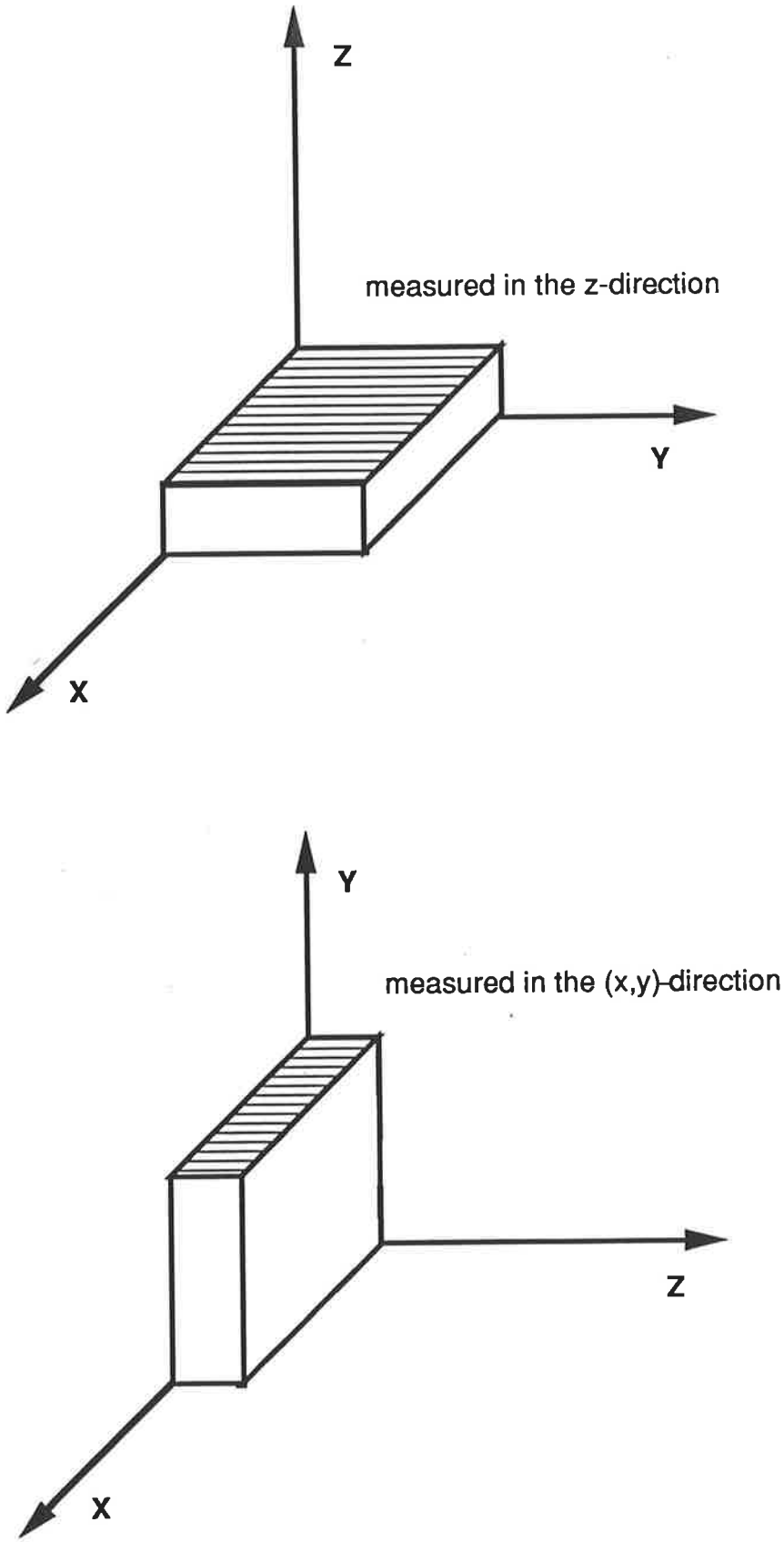

Figure 4.1 Cartesian Axes For Sample Measurement

FIGURE 4.2 MEASUREMENT OF LENGTH CONTRACTION IN PMMA

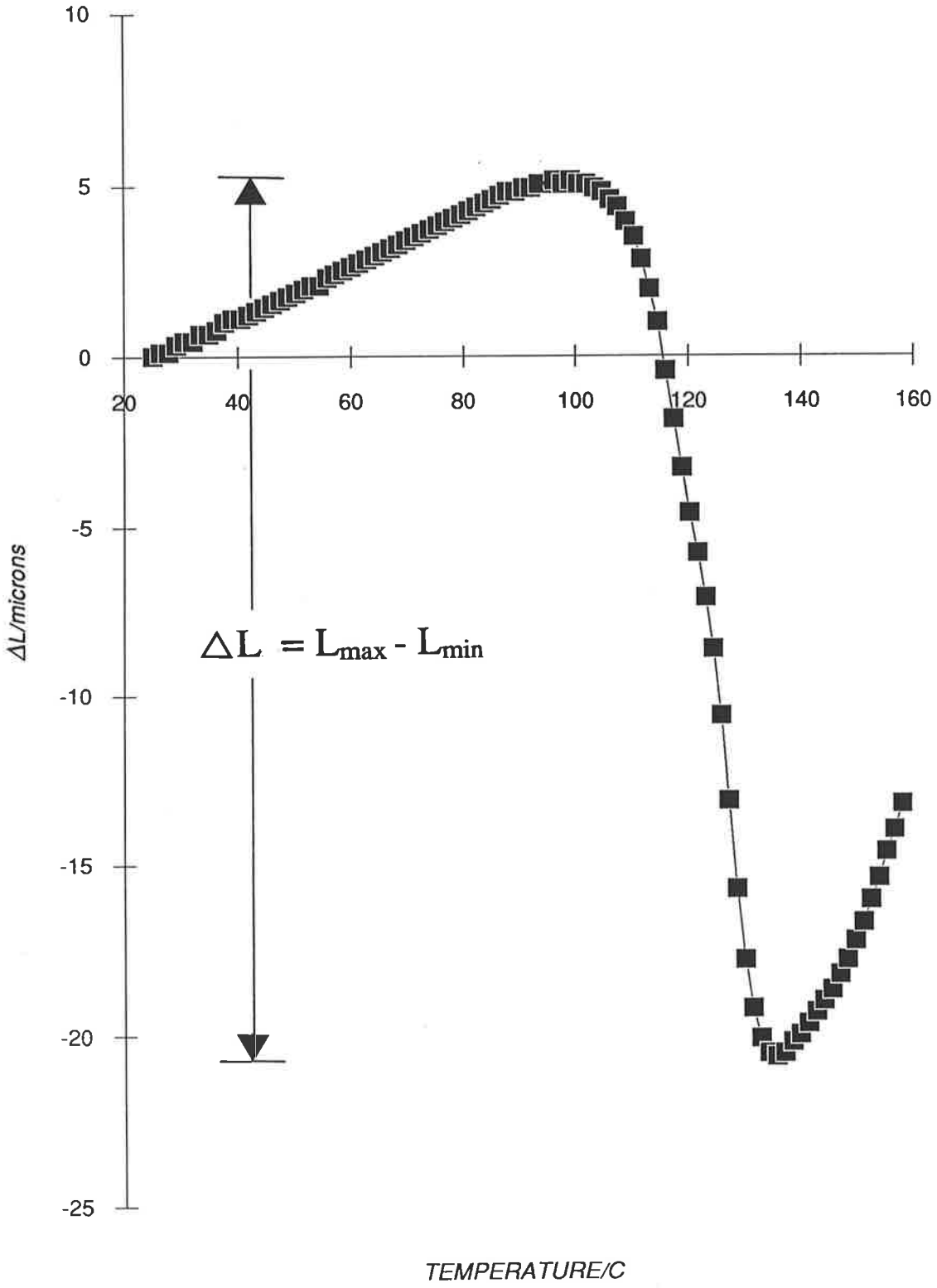

FIGURE 4.3 LENGTH CONTRACTION IN QUENCHED AND SLOW-COOLED PMMA MEASURED ALONG THE (X, Y) AXIS AT 2 C/min

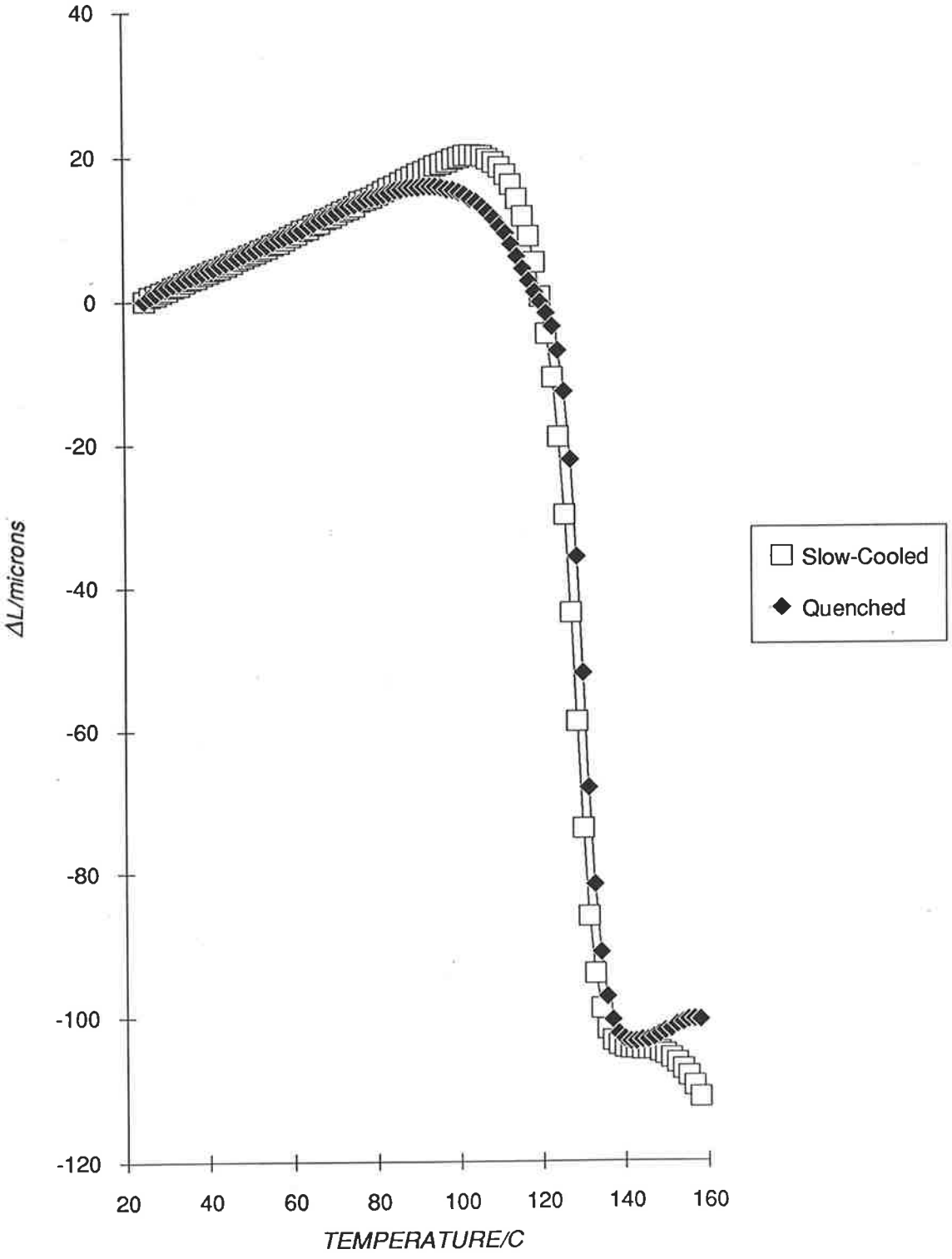

respective values of approximately 0.02, thus the contraction of slow-cooled PMMA is considered to be isotropic as the condition $(\Delta L_z/L_z) = (\Delta L_{x,y}/L_{x,y})$ is fulfilled. On the other hand, $(\Delta L_z/L_z)$ and $(\Delta L_{x,y}/L_{x,y})$ of quenched PMMA have values of 0.06 and 0.02 respectively, which indicates that the contraction is not isotropic. No explanation could be offered at the present time for the non-isotropic nature of the contraction. Repeated thermal runs on quenched PMMA have confirmed that the contractions ΔL_z and $\Delta L_{x,y}$ are similar, therefore by imposing the assumption $\Delta L_z = \Delta L_{x,y}$ Equation 4.1 simpifies to

$$V_f = L_z.[2L_{x,y}.\Delta L_z - (\Delta L_z)^2] + \Delta L_z.(L_{x,y} - \Delta L_z)^2 \qquad (4.2)$$

for quenched specimens. In the case of slow-cooled PMMA, $\Delta L_{x,y}$ can be replaced by the corresponding ΔL_z of the quenched specimen provided that the measurements were determined at the same heating rate. The free volume fraction, f, is defined as

$$f = (V_0 - V_{eq})/V_{eq} = V_f/V_{eq} \qquad (4.3)$$

where $V_{eq} = (L_z - \Delta L_z).(L_{x,y} - \Delta L_{x,y})^2$.

4.4 RESULTS AND DISCUSSION

4.4.1 Free Volume Fraction

The ΔL-T plots of quenched and slow-cooled PMMA are presented in Figures 4.4-4.6, and the values of ΔL_z and V_f are listed in Tables 4.1-4.2. The free volume V_f is calculated from Equation 4.2 where $L_{x,y}$ is assumed to be equal to 4.798×10^{-3} m. The magnitude of length contraction and free volume fraction are based on the concept that volume relaxation (physical ageing) in amorphous polymers is attributed to the collapse of free volume [35-38]. Using this concept, Chow [35-37] and Perez [38] were able to fit Kovacs' [15] contraction isotherms and memory effect curves for poly(vinyl acetate) (PVA). Volume relaxation is also associated with a continual decrease in mobility [32], hence a consequence of the lowering of free volume is a concomitant reduction in segmental mobility.

Literature values [26-31] of free volume fraction of PMMA calculated from the Simha-Boyer relationship [13] (Equation 2.6) range from 0.093-0.1450 (Table 4.1). The free

FIGURE 4.4 PHYSICAL AGEING IN QUENCHED PMMA: 0.05 C/min TO 1 C/min

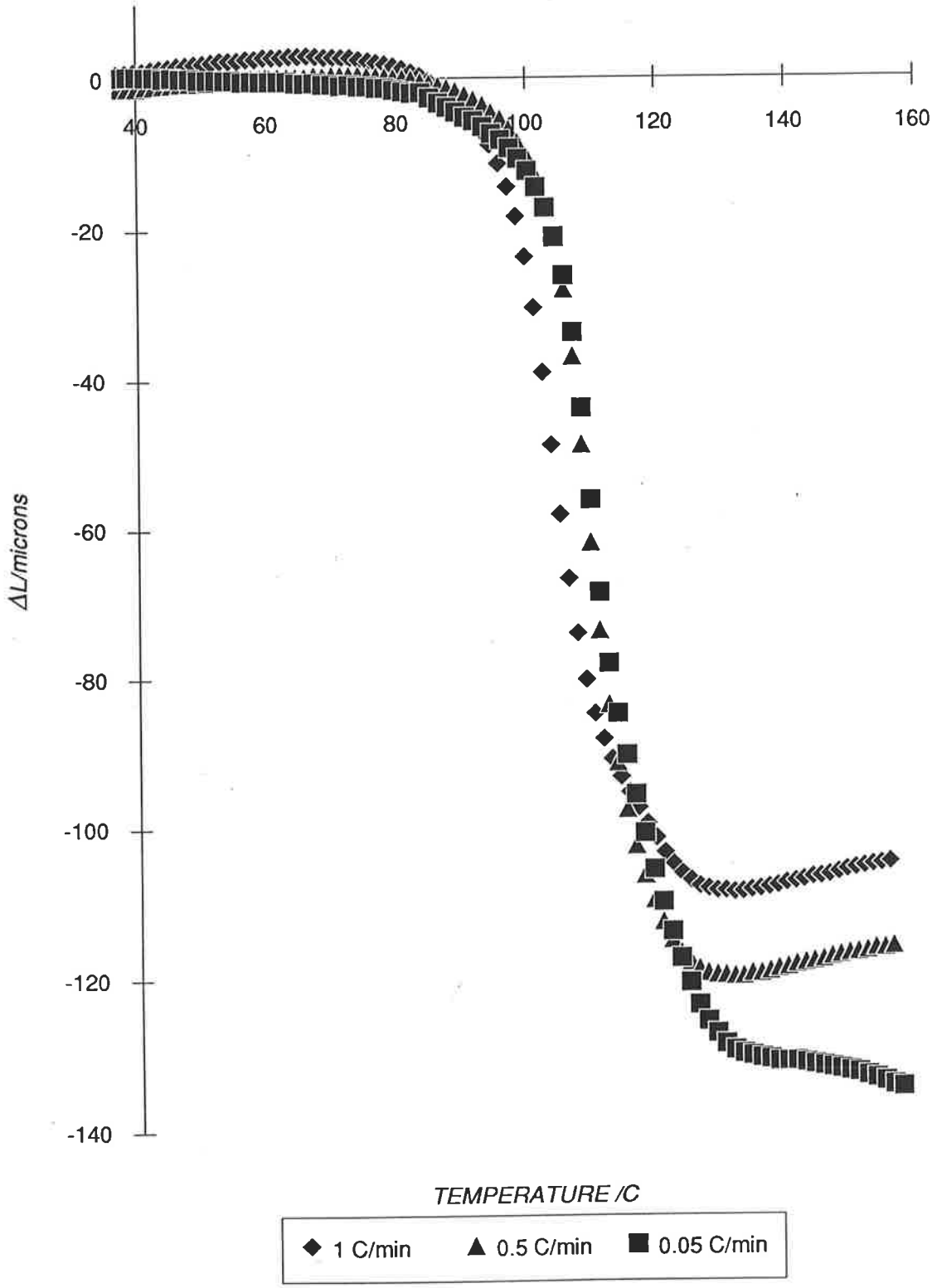

FIGURE 4.5 PHYSICAL AGEING IN QUENCHED PMMA: 2 C/min TO 20 C/min

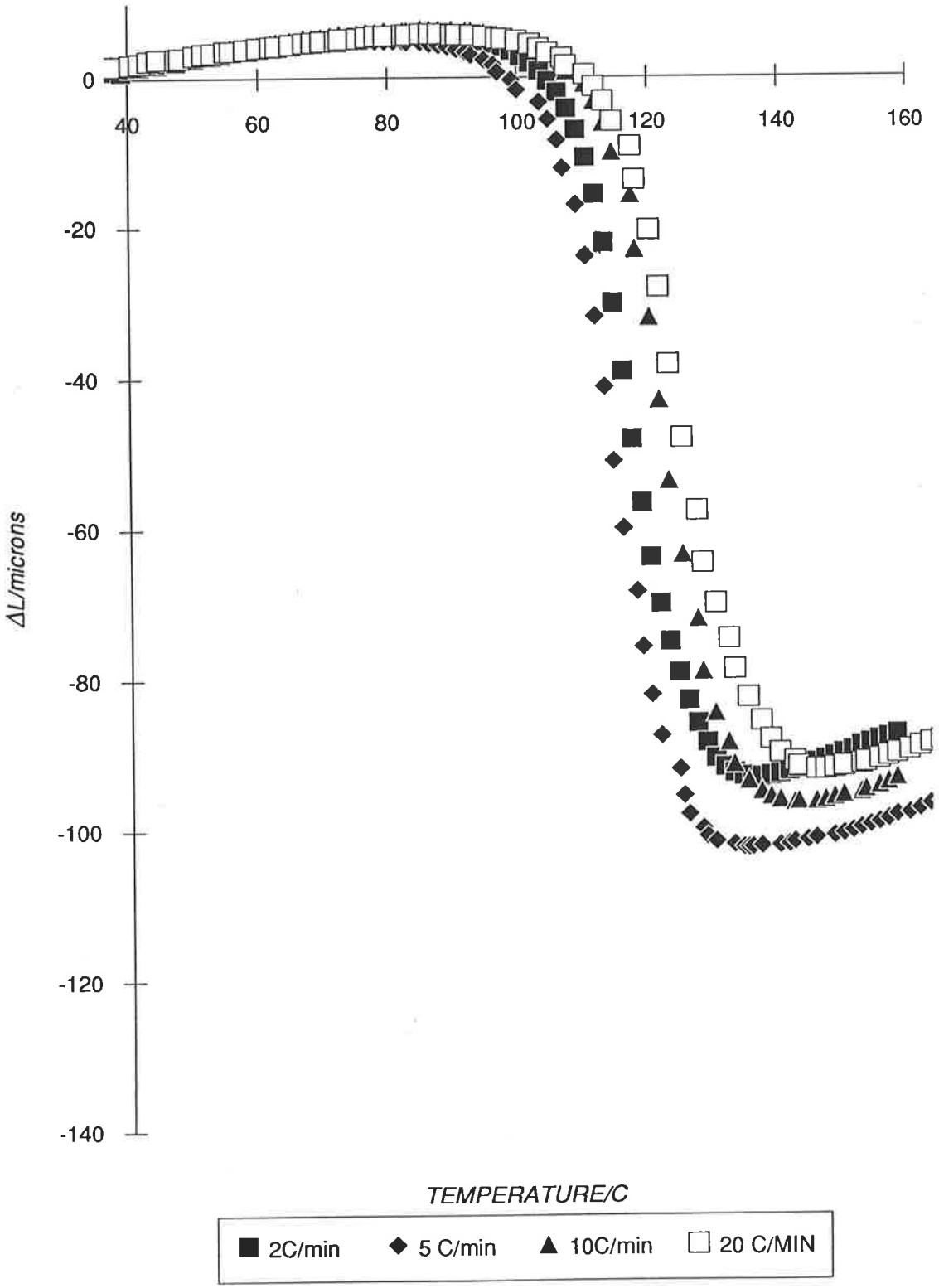

FIGURE 4.6 PHYSICAL AGEING IN ANNEALED PMMA: 0.5 C/min TO 10 C/min

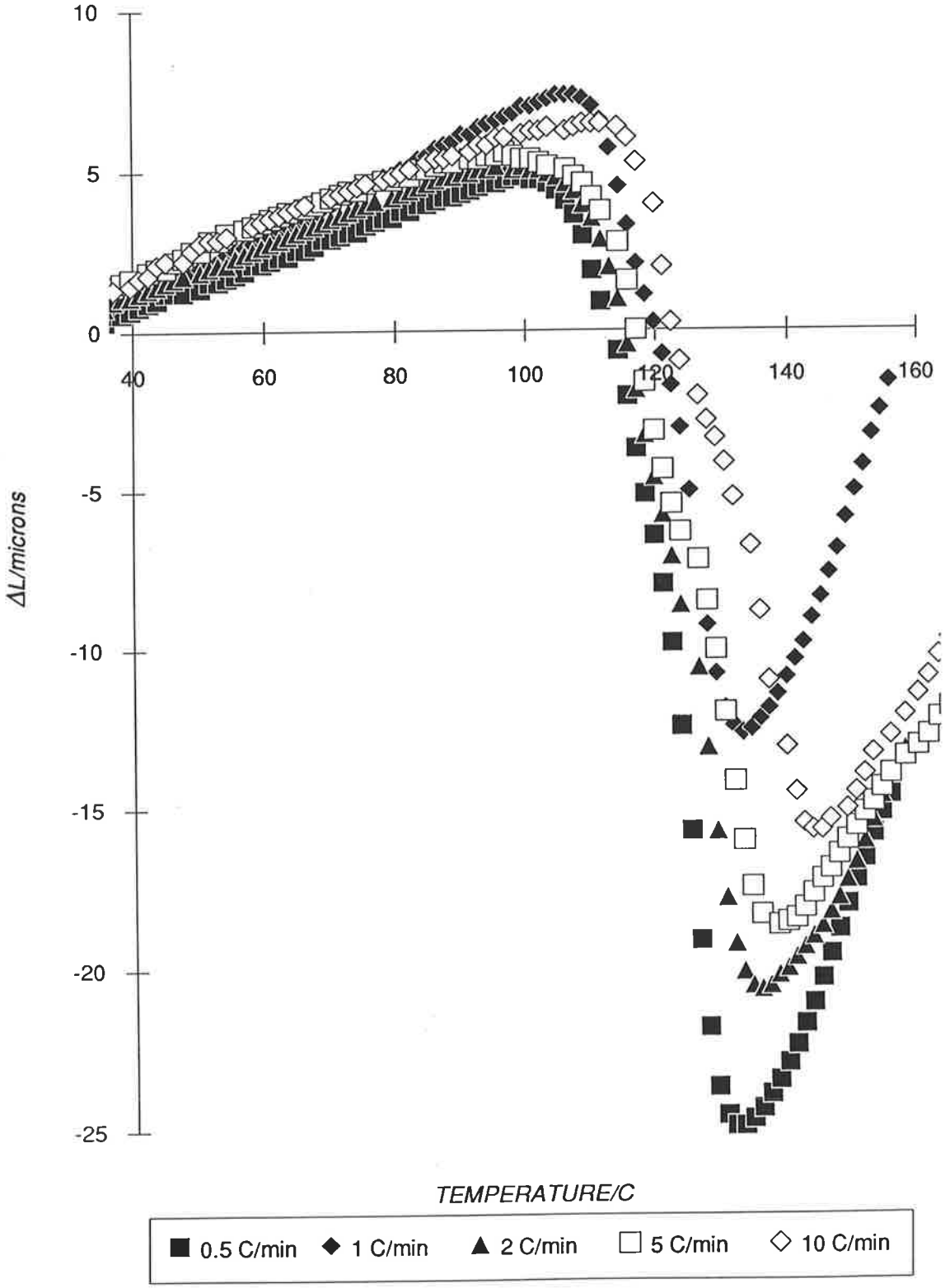

volume fraction of 0.102-0.130 of quenched PMMA correlates with the universal value of 0.113 proposed by Simha and Boyer, and supports their definition of free volume (Fig. 2.7). However, the fractional free volumes of slow-cooled PMMA is reduced by about 50 % to 0.0561-0.0672 (Table 4.2). The observations indicate that for PMMA, 0.130 represents the maximum free volume fraction which may be frozen-in by quenching whereas a limiting free volume fraction of 0.056 cannot be removed by slow cooling at a rate less than 1 C/min. This indicates that up to half the free volume fraction of quenched PMMA may be recovered by slow cooling.

TABLE 4.1

Length contraction and free volume fraction of quenched PMMA

Heating Rate (C/min)	ΔL_z (m)	V_f (m^3)	f
0.05	1.25×10^{-4}	4.53×10^{-9}	0.130
0.5	1.20×10^{-4}	4.47×10^{-9}	0.120
1	1.15×10^{-4}	4.38×10^{-9}	0.112
2	1.11×10^{-4}	4.13×10^{-9}	0.109
5	1.07×10^{-4}	4.02×10^{-9}	0.107
10	1.06×10^{-4}	3.95×10^{-9}	0.107
20	9.80×10^{-5}	3.59×10^{-9}	0.102

TABLE 4.2

Length contraction and free volume fraction of slow-cooled PMMA

Heating Rate (C/min)	ΔL_z (m)	V_f (m^3)	f
0.5	2.9×10^{-5}	2.39×10^{-9}	0.0672
1	2.0×10^{-5}	2.13×10^{-9}	0.0596
2	2.8×10^{-5}	2.10×10^{-9}	0.0574
5	2.4×10^{-4}	2.09×10^{-9}	0.0575
10	2.2×10^{-4}	2.00×10^{-9}	0.0561

The observation of two values for the free volume fraction of PMMA suggests that the effect of physical ageing on free volume were not taken into account by the SB and WLF theories. The free volume fraction cannot remain constant below T_g due to the occurence of physical ageing. Although Simha and Boyer [12] reported a "small linear decrease in volume with temperature associated with the contraction of the lattice", they nevertheless assumed the local polymer configuration below T_g to be unchanged due to negligible molecular mobility. This assumption was supported by the results of Lee and McGarry [34], who showed the amount of trapped free volume in quenched polystyrene could not be increased by increasing the temperature of equilibration above 110 C (about 13 C above T_g). However, the rate of ageing has been shown to increase at temperatures near T_g [39] and vary exponentially with temperature after quenching [34]. The observation of isothermal volume contraction below T_g [13-14, 16] indicates that the polymer structure and free volume fraction are not totally frozen-in and some mobility still exists below T_g.

The experimental fractional free volume values of ~0.13 and ~0.06 for quenched and slow-cooled PMMA specimens are considerably higher than the universal WLF value of 0.025. The free volume fraction is considered by the WLF-Doolittle [40-41] theory to be the fractional increase in volume resulting from thermal expansion [11], whereas according to the SB treatment, the free volume represents the difference between the liquid and glass specific volumes extrapolated to absolute zero [12, 42] (Fig. 4.7). One major criticism of the WLF theory is that their ideas were applied to the temperature range below T_g based entirely on measurements made at thermodynamic equilibrium. But the assumption that changes in free volume below T_g will be the same as above T_g was found to fail at 100-200 C below T_g [43]. The empirical constants used in the WLF equation (Equations 2.2-2.5) have been shown not to be independent of temperature and molecular weight [44], therefore there is a limit to the application of the WLF-Doolittle model at temperatures below T_g. While the search for a molecular interpretation of physical ageing and the glass transition has been considerably advanced by the SB and WLF free-volume theories, the experimental data of Tables 4.1-4.2 show that both theories have significant limitations.

The free volume fraction decreases non-linearly with increasing heating rate (Figs. 4.8-4.9). This is attributed to collapse of free volume holes [25, 37], in which a relaxation time τ_i is attributed to the collapse of each individual hole such that the collapse of the smaller holes

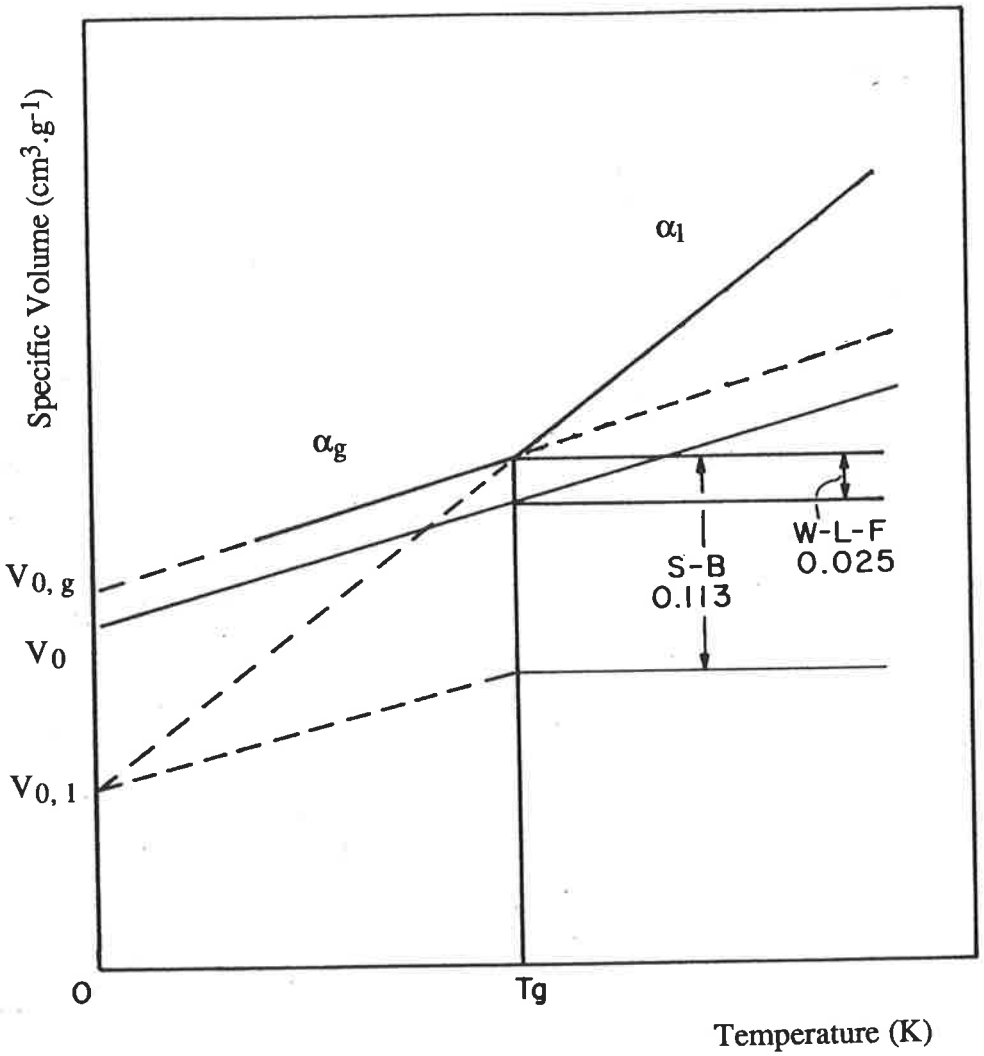

Figure 4.7 Schematic diagram of free volume as defined by Williams, Landell and Ferry (W-L-F), and Simha and Boyer (S-B). V_0 is the occupied volume, $V_{0,g}$ and $V_{0,l}$ are the occupied glass and liquid volumes extrapolated to absolute zero (reproduced from M.C. Shen and A. Eisenberg, *Progress in Solid State Chemistry* **3**, 407 Pergamon Press, (1966)).

FIGURE 4.8 FRACTIONAL FREE VOLUME OF QUENCHED PMMA WITH HEATING RATE

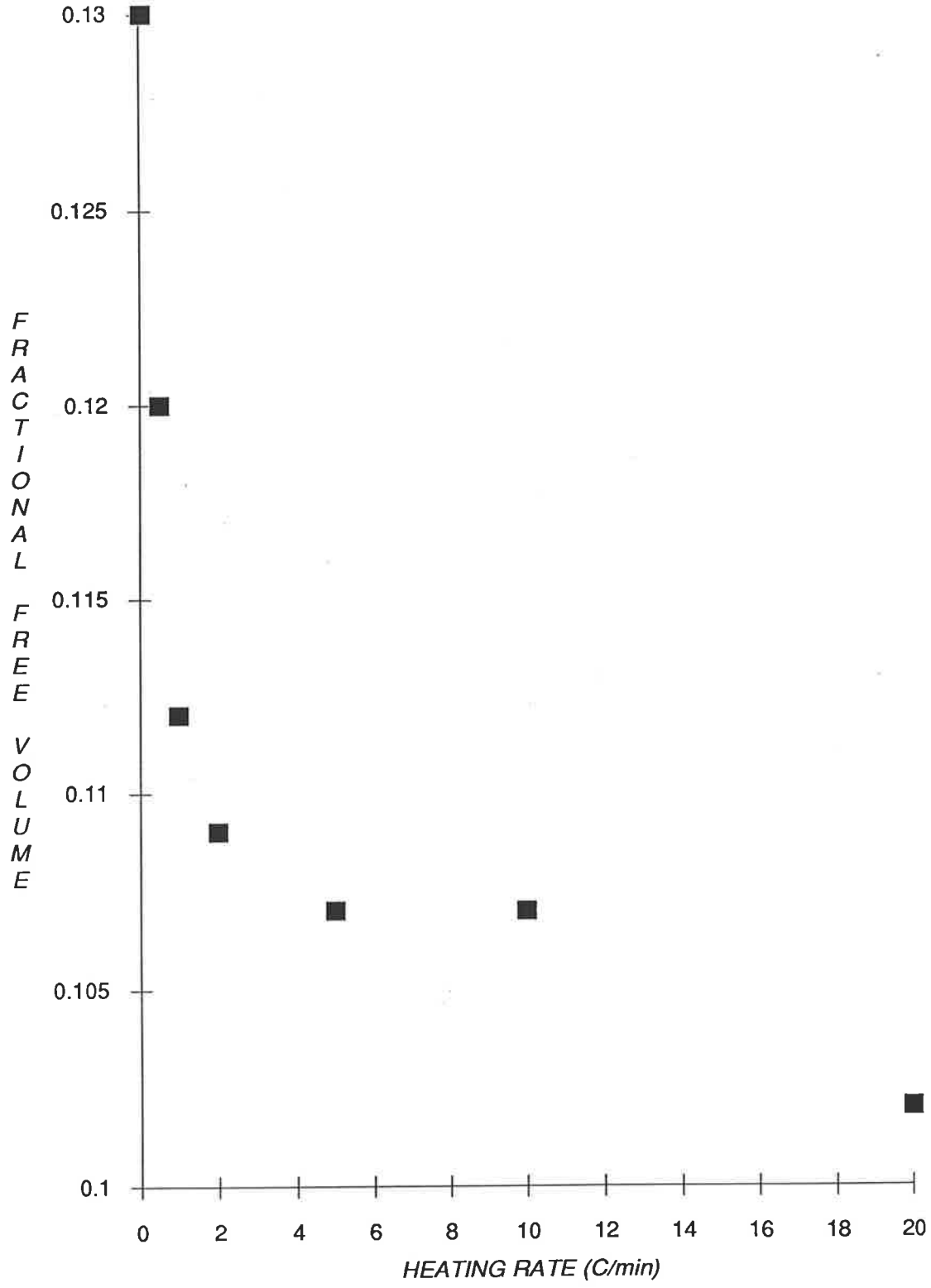

FIGURE 4.9 FRACTIONAL FREE VOLUME OF SLOW-COOLED PMMA WITH HEATING RATE

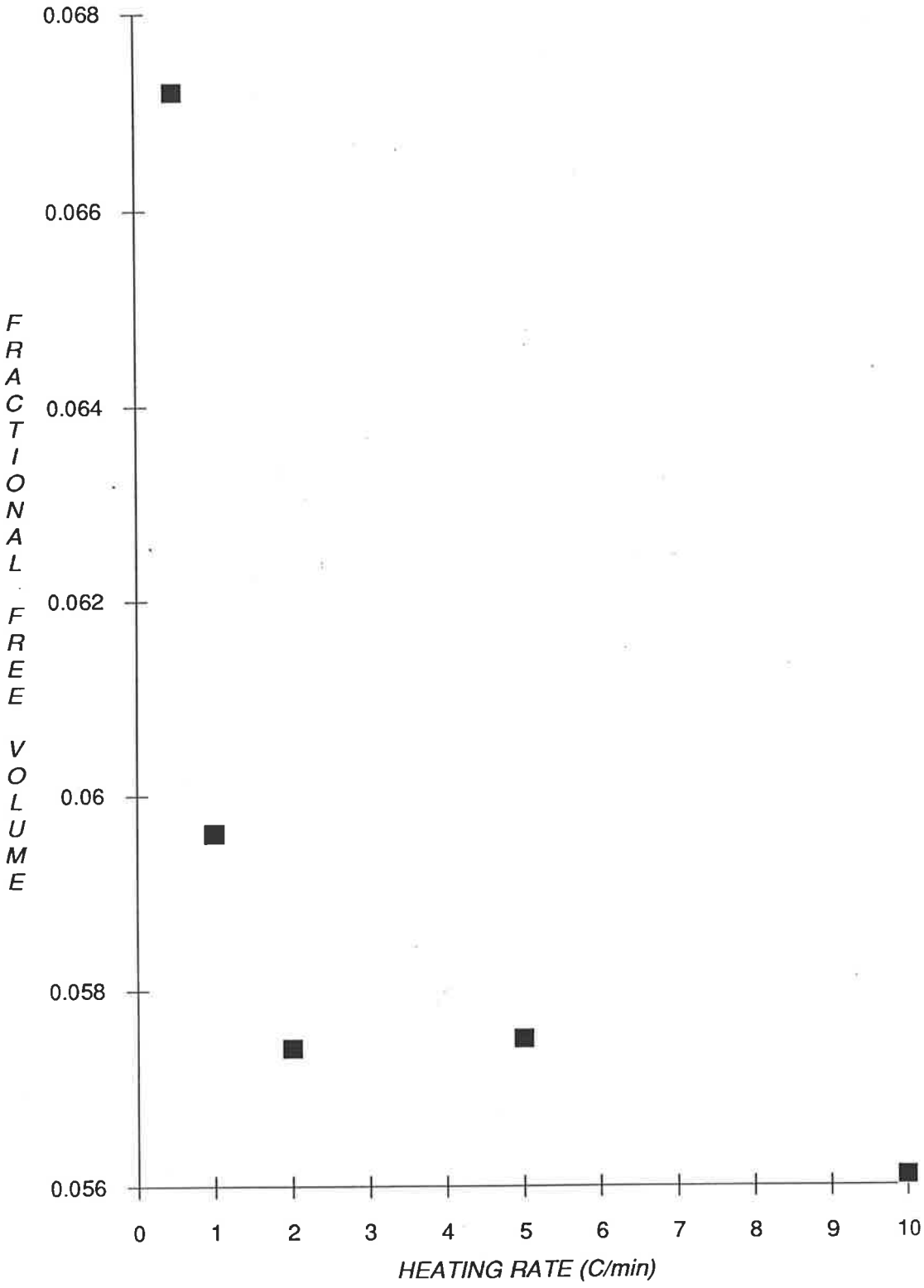

(shorter relaxation times) occurs first [45]. If the experimental timescale is long, the specimen is at thermal equilibrium and the collapse of holes associated with short and long relaxation times have sufficient time to take place. On the other hand, a short experimental timescale may not allow enough time for the measurement of the collapse of large holes such that a greater contraction is generally observed for experiments with slower heating rates. Equation 2.10 describes the relationship between the free volume fraction and heating rate under isobaric conditions. Substitution of $f = (V_0 - V_{eq})/V_{eq}$ into Equation 2.10 gives [25, 46]

$$dV/dt = \alpha_g.V_{eq}.dT/dt - (f.V_{eq})/\tau \tag{4.4a}$$

Alternatively, Equation 4.4a can also be written in this form [46]:

$$dV/dt = \alpha_g.V_{eq} - (V_0 - V_{eq})/(\tau.dT/dt) \tag{4.4b}$$

Assuming that length contraction measured under a constant rate of heating can be described by a single relaxation time τ, the incorporation of Equation 4.4b into Equation 4.4a produces the following expression:

$$\tau = f.(\alpha_g.dT/dt)^{-1} \tag{4.5}$$

The macroscopic relaxation time τ is directly related to the free volume fraction and is inversely proportional to the heating rate. It is infered from Equation 4.5 that the observed length contraction contains contributions only from the collapse of holes associated with relaxation times which are smaller, or of the order of the average relaxation time τ. The calculation of τ according to Equation 4.5 is presented in Section 4.4.4.

In addition, the number of free volume holes in a quenched polymer may be estimated from the contraction in length. Although the complicated nature of polymeric systems does not allow an exact computation of the population of free volume holes, nevertheless a physical model incorporating a number of oversimplifications has been proposed by Bueche [52] for qualitative analysis of segmental motion near T_g. It assumed that the free volume V_f to consist of n_f holes of similar size V_h, such that $n_f = V_f/V_h$. The correct treatment does not

assume these holes to be of equal size, but the computation of the range of hole sizes which can exist in a polymer is physically impossible. Each hole containing a free volume V_h was also assumed to be spherical in shape, and that each hole acted independently of every other hole. This constituted a serious error, as two adjacent holes may actually coalesce to comprise a hole large enough for molecular motion to occur. The average volume of an individual hole of amorphous PMMA has been measured using positron annihilation spectroscopy (PALS) [50-51] to be 1.84×10^{-28} m^3, and if V_f for quenched and annealed PMMA is taken to be 4×10^{-9} and 2×10^{-9} m^3, the number of unoccupied holes which collapsed during ageing is 2.2×10^{19} and 1.1×10^{19} respectively. Although the incorporation of PALS data allows a numerical evaluation of the hole population in a polymer, the quantitative validity of the values obtained has to be treated with caution due to the oversimplifications used in the model to evaluate n_f.

4.4.2 Temperature Range for Length Contraction

Length contraction was observed in Figures 4.4-4.6 over a temperature range of 20-30 C (Tables 4.3-4.4), in agreement with Crowson and Arridge's [48] observation of a glass transition range of at least 20 C. The transition takes place over a temperature range as a consequence of the range of relaxation times associated with the multiplicity of relaxation mechanisms operating near the glass transition region.

To characterise the temperature range for length contraction, the temperature of the onset of contraction, T_{on}, is defined as the intersection between the extrapolated glass line and contraction line, while the temperature of the endset of contraction, T_{end}, is defined by the intersection of the extrapolation of the contraction line and liquid line. The contraction range is thus bounded by T_{on} and T_{end}. The values of T_{on} and T_{end} for quenched and slow-cooled PMMA are presented in Tables 4.3 and 4.4.

Experimental reports [10, 39, 45] show that the rate of ageing is not contant over the entire temperature range below T_g, which suggests that the size of free volume holes of glassy polymers are not constant. Since length contraction is attributed with the collapse of free volume, it is proposed that the onset of contraction is associated with the annihilation of small free volume holes with short relaxation times. Bartos *et al.* [45] suggested that upon slow cooling to below T_g, the lowering of the macroscopic free volume is predominantly due to the reduction in the population of small free volume holes, such that physical ageing leads to the

narrowing of the free volume distribution arising from the relaxation of smaller holes.

A mathematical model utilising a dual distribution function of relaxation times to characterise isothermal volume recovery has been developed by Kovacs *et al.* [25, 49]. The distribution consists of a short time portion of $-2 \leq \log(\tau/\text{hr}) \leq -0.125$, which contributes 15% to the recovery, with the remainder of the distribution coming from a long time portion of $0 \leq \log(\tau/\text{hr}) \leq 2$. If a quenched specimen is assumed to contain the complete distribution of relaxation times, the observation of a 50 % reduction in free volume fraction upon slow cooling is expected to result in a greater decrease of relaxation times in the short time portion. This expectation is supported by the large value of $\tau/\tau_g = \exp(1/f) = 17 \times 10^6$ for slow-cooled PMMA, which suggests that the process of ageing in slow-cooled specimens is associated mainly with the collapse of larger holes.

Equation 4.5 infers that T_{on} will shift to a lower temperature upon an increase in the timescale of measurement. Table 4.3 shows that for a slow heating rate of 0.05 C/min T_{on} is 104 C, but increases to 113 C when the heating rate was increased to 20 C/min. The longer relaxation times accompanying the higher proportion of large holes also shifts T_{on} to a higher temperature, for example, at the heating rate of 1 C/min T_{on} of quenched PMMA is 104 C, whereas the corresponding T_{on} of slow-cooled PMMA has increased to 110 C (Table 4.4). On the other hand, T_{end} of quenched PMMA remained unchanged at 132 C (Table 4.3) even when the heating rate was raised from 2 C/min to 20 C/min, which suggests that there is a fairly constant distribution of holes such that the contraction terminated at the same temperature.

However, T_{end} of slow-cooled PMMA is not constant but increases with heating rate (Table 4.4). It has been suggested that the annihilation of free volume in slow-cooled PMMA is caused predominantly by the collapse of large holes, and that the observed contraction contains contributions only from the collapse of holes associated with relaxation times which are of the order of the average relaxation time τ as determined in Equation 4.5. Therefore, it is likely that the non-constancy of T_{end} may be due to the fact that the long relaxation times associated with the collapse of large holes become increasingly dependent on the rate of measurement and require a higher endset temperature at fast rates of heating.

It is interesting to note that the attainment of equilibrium, as characterised by the termination of contraction at T_{end}, is only reached at temperatures approximately 20-27 C above the conventional T_g for PMMA of 105 C (Table 4.3). This means that some volume relaxation

continue to take place at temperatures just above T_g and equilibrium is only readily attained in PMMA when the specimen is heated to above 132 C. This hypothesis is strongly supported by experimental evidence provided by Lee and McGarry [34], who observed that the amount of free volume trapped in atactic polystyrene by quenching from above to below T_g (97 C) was dependent on the initial temperature of equilibration, even at temperatures above "T_g". A constant free volume was frozen-in only when the equilibration temperature was at least 13 C above T_g at 110 C. Kovacs *et al.* [25] also reported that structural rearrangements still occured in *apparent* voluminal equilibrium of the glass which affected the timescale of molecular motions in an appreciable manner.

TABLE 4.3

Onset and endset temperatures for contraction and contraction range for quenched PMMA

Heating Rate (C/min)	T_{on} (C)	T_{end} (C)	$T_{on} - T_{end}$ (C)
0.05	104	124	20
0.5	104	127	23
1	104	127	23
2	104	132	28
5	105	132	28
10	110	132	22
20	113	132	19

The temperature shift of T_{on} from a quenched to a slow-cooled specimen, ΔT_{on}, may be related to the reduction in the free volume fraction according to the expression:

$$\Delta T_{on} = -\theta^{-1}.\ln [\tau \text{ (quenched)}/\tau \text{ (slow-cooled)}] = -\theta^{-1}.[f \text{ (quenched)}^{-1} - f \text{ (slow-cooled)}^{-1}] \quad (4.6)$$

where θ is a function of the activation energy E_{act} and temperature [49]. The characteristic value of θ for polymer glasses is unity and using values of f from Tables 4.1-4.2 the calculated temperature shift ΔT_{on} is approximately 6-8 C. An inspection of Tables 4.3-4.4 show that experimental shifts of T_{on} range from 4-7 C. The agreement between experiment and theory

indicates that T_{on} of PMMA is determined by the size of the free volume holes. However, there was poor agreement between values of T_{end} and ΔT_{end}. As the specimen approaches thermodynamic equilibrium, τ no longer depends on temperature alone, but also on other variables such as $\Delta\alpha$, δ and a partition function (1-x), which determines the relative contributions of temperature and structure (δ) to τ ($0 \leq x \leq 1$) [49].

TABLE 4.4

Onset and endset temperatures for contraction and contraction range for slow-cooled PMMA

Heating Rate (C/min)	T_{on} (C)	T_{end} (C)	T_{on} - T_{end} (C)
0.5	110	131	21
1	110	132	22
2	109	133	24
5	109	137	26
10	117	145	28

It is proposed that the parameters T_{on} and T_{end} provide an alternative assignment of the glass transition. It has been shown that the contraction range is similar to the glass transition range observed by Crowson and Arridge [48] and that equilibrium is attained above T_{end}. If the annihilation of free volume holes is considered to be accomplished mainly by cooperative motions it follows that T_{on} is also associated with the onset of cooperative main-chain motion and hence the onset of glass transition. This proposal raises the following issues: can physical ageing continue at temperatures below the secondary transition range, and whether polymer glasses can be aged to equilibrium below T_g without the need for cooperative motion. These issues are discussed in greater detail in Chapter 5.

4.4.3 Thermal Expansion Coefficient

The linear thermal expansion coefficient α' was obtained from the slopes of the glass (α'_g) and liquid (α'_l) lines of L-T plots. Linear expansion coefficients obtained from measurements along the (x, y) axis were found to be similar to those that were measured along the z-axis. The cubical or volume expansion coefficient α may be assumed as isotropic, i.e. α

$= 3\alpha'$, therefore one can write:

$$\alpha = V_0^{-1}.(dV/dt).(dt/dT) \qquad (4.7)$$

where V_0 is the initial volume. The linear and cubical expansion coefficients of quenched and slow-cooled PMMA are presented in Tables 4.5-4.6.

Experimental reports in which volume dilatometry is used to observe dimensional changes of polymers normally present a single value each for α_g and α_l. However, Haldon and Simha [30] observed that α'_g is not constant but is influenced by the temperature and by the free volume fraction frozen-in below T_g. It has been observed that α'_g obtained from L-T plots produced in this work initially show a slight increase with temperature but later decreases as the specimen begins to contract near T_{on}. The glass expansivities of PMMA were thus obtained in the range 40-50 C where it was assumed that the effect of contraction on the magnitude of α'_g is negligible. On the other hand, α'_l was obtained between 140-150 C at which the specimen was at equilibrium.

TABLE 4.5

Linear and cubical thermal expansion coefficients (10^{-6} K^{-1}) for quenched PMMA

Heating Rate (C/min)	α'_g	α_g	α'_l	α_l	$\alpha_l - \alpha_g$
0.05	42.6	127.8	-151.5	-454.5	-582.3
0.5	48.7	146.1	130.4	391.2	245.1
1	53.5	160.5	132.0	396.0	235.5
2	56.4	169.2	142.8	428.4	259.2
5	66.9	200.7	155.7	467.1	266.4
10	72.4	217.2	160.4	481.2	264.0
20	79.2	237.6	161.5	484.5	246.9

Table 4.5 shows a general increase in α'_g and α'_l of quenched PMMA with heating rate. The measured thermal expansivities at heating rates above 5 C/min are in agreement with literature values [26-27, 30, 53-54] which range from 182-293 x 10^{-6} K^{-1} for α_g and 460-591

x 10^{-6} K^{-1} for α_l. The low values of α_g at slower heating rates support the hypothesis that α_g is reduced by physical ageing. It has been observed [30] that while α'_g of quenched poly(*n*-butyl methacrylate) was larger than those of annealed specimens, the variation in α_g between the two types of poly(*n*-butyl methacrylate) became smaller as the temperature was increased. The increase in α_g was attributed to the freezing-in of excess free volume upon quenching, and the subsequent reduction in discrepancy was due to the gradual diffusion of free volume with increasing molecular mobility upon heating [30]. The expansion coefficient of the free volume α_f may be approximated by the difference $\Delta\alpha$ [11], i.e. $\alpha_f \approx (\alpha_l - \alpha_g)$. The WLF treatment leads to an average value of $\Delta\alpha = 4.8 \times 10^{-4}$, but Simha and Boyer [12] found this to be far from the actual case, and reported values of $\Delta\alpha$ ranging from 2.45×10^{-4} for PMMA to 9.30×10^{-4} for poly(dimethyl siloxane). The experimental values of $\Delta\alpha$ of 2.45×10^{-4} to 2.66×10^{-4} for quenched PMMA agree with the results of Simha and Boyer, and suggests that the SB definition of free volume is more appropriate than the WLF definition.

A comparison of the expansivities of slow-cooled PMMA specimens in Table 4.6 show that α_g is independent of the heating rate and is lower than those of quenched specimens. This constancy of α_g is attributed to the smaller variation (that is, a narrower distribution of free volume hole sizes as suggested by Bartos *et al.* [45]) in the free volume fraction of slow-cooled specimens. However, the value of the liquid expansivity is considerably higher in slow-cooled specimens than in quenched specimens. This is surprising, since the expansivity should be independent of thermal history at thermodynamic equilibrium.

TABLE 4.6

Linear and cubical thermal expansion coefficients (10^{-6} K^{-1}) for slow-cooled PMMA

Heating Rate (C/min)	α'_g	α_g	α'_l	α_l	$\alpha_l - \alpha_g$
0.5	51.7	155.1	355.6	1066.8	911.7
1	57.3	171.9	356.4	1069.2	898.0
2	52.4	157.2	334.2	1002.6	845.4
5	51.2	153.6	265.0	795.0	641.4
10	56.4	169.2	238.9	716.7	547.5

It is proposed that the abnormally large α_l values are a consequence of the endothermic peaks which are characteristic of annealed specimens during physical ageing. This hypothesis can be verified by relating the amount of excess thermal energy absorbed by the specimen with the increase in the liquid expansivity. The thermal energy Q absorbed at constant pressure may be represented by the following equation [55]:

$$Q = \Delta C_p.(T_g - T_r) \tag{4.8}$$

where Q has units of $J.g^{-1}$ and $\Delta C_p = (C_{p,l} - C_{p,g})$ is the difference between the specific heat capacity at constant pressure in the glass and liquid states, and T_r is a reference temperature. The difference between thermal energies absorbed by slow-cooled and quenched PMMA, ΔQ = Q (slow-cooled) - Q (quenched), represents the excess thermal energy absorbed by slow-cooled specimens, hence

$$\Delta Q = \Delta C_p.[T_g \text{ (slow-cooled)} - T_g \text{ (quenched)}] \tag{4.9}$$

Substitution of the Simha-Boyer equation (Equation 2.6) into Equation 4.8 yields

$$\Delta Q = \Delta C_p.[f/\Delta\alpha \text{ (slow-cooled)} - f/\Delta\alpha \text{ (quenched)}] \tag{4.10}$$

The value of ΔC_p for PMMA [56-57] is obtained from specific heat capacity values near T_{on} ~104 C ($C_{p,g}$), and above T_{end} ~130 C ($C_{p,l}$). From the data of O'Reilly [58] $C_{p,g}$ (378 K) = 1.876 $J.K^{-1}.g^{-1}$, $C_{p,l}$ (411 K) = 2.143 $J.K^{-1}.g^{-1}$, thus ΔC_p = 0.267 $J.K^{-1}.g^{-1}$. The free volume fraction and $\Delta\alpha$ are obtained from Tables 4.1-4.2 and Tables 4.5-4.6. Table 4.7 lists ΔQ values along with the increase in α_l of slow-cooled specimens, $\Delta\alpha_l = [\alpha_l \text{ (slow-cooled)} - \alpha_l \text{ (quenched)}]$. The thermal energy absorbed by the slow-cooled specimens was found to increase with heating rate as predicted by Petrie [55] and by Hodge and Berens [59]. The data of Table 4.7 indicates that the increase in the liquid expansivity of a slow-cooled specimen is proportional to the excess thermal energy absorbed by the specimen, that is, the large volume expansion in the liquid state is a result of an increase in thermal activation.

TABLE 4.7

Values of ΔQ and $\Delta\alpha_l$ obtained from quenched and slow-cooled PMMA specimens

Heating Rate (C/min)	ΔQ (J.g^{-1})	$\Delta\alpha_l$ (10^{-6} K^{-1})
0.5	-111.1	675.6
1	-109.3	673.2
2	-94.2	574.2
5	-83.3	327.9
10	-80.9	235.5

The product $(\alpha_l - \alpha_g).T_g$ was proposed by Simha and Boyer [12] as a measure of free volume fraction, in which $(\alpha_l - \alpha_g)$ represents the expansion of free volume. According to Fox and Flory [33], the glass transition occurs when the free volume reaches a constant value which does not change upon further decreases in temperature. The conventional T_g defined by extrapolation of the glass and liquid lines in a L-T or a V-T plot could not be obtained from Figures 4.4-4.6. It has been suggested that the glass transition may be more appropriately represented by a temperature range which encompasses the contraction region rather than by the assignment of a single T_g (Section 4.4.2).

In addition, the incorporation of experimental values of f and $\Delta\alpha$ into the Simha-Boyer equation produced unacceptable values of T_g (105 C for PMMA [26]). Substituting f = 0.11 and $\Delta\alpha$ = 260 x 10^{-6} K^{-1} into Equation 2.6 results in a calculated T_g of 150 C for quenched PMMA, whereas substituting f = 0.06 and $\Delta\alpha \approx$ 700 x 10^{-6} K^{-1} yields a T_g of 86 C for slow-cooled PMMA. The reason for these substantial deviations in T_g using the SB equation lies primarily in the fact that the parameters T_g, α'_g and α'_l all show significant variations with temperature and thermal history. Fractional free volumes derived from the SB and WLF empirical equations suffer from oversimplifications which fail to recognise that the thermophysical properties of polymers are influenced by a number of factors, such as the physical state (e.g. whether amorphous or crystalline), chemical structure (e.g. increasing side-chain lengths, tacticity), and thermal history (e.g. residual stresses, physical ageing).

In view of the sensitivity of α'_g and α'_l to physical ageing, it appears that the assignment of a single expansivity value for any particular polymer would be incorrect. It is

suggested that accurate measurements of glass expansivity may be made in regions where low temperature glass-glass transitions are absent, or such that the influence of these transitions on α'_g are minimal. For example, the sub-T_g glass-glass transitions of a series of poly(*n*-alkyl methacrylates) are shown in Figure 2.8. In the case of poly(*n*-butyl methacrylate) (PnBMA), three sub-T_g transitions are located at -20 C, -50 C and -90 C. It is observed that α'_g of PnBMA increases rapidly between -60 C and -10 C, followed by a plateau before rising sharply again from 20 C onwards. Thus, a reasonably constant value of α'_g between the first sub-T_g transition and T_g of PnBMA may be obtained in the region -10 C to 10 C. A slight decrease in α'_g between 0 and 15 C was also observed for PnBMA, which may be an indication of ageing.

4.4.4 Relaxation Times for Length Contraction

The macroscopic relaxation time τ has been shown to be proportional to the free volume fraction and inversely related to the heating rate and the glass expansion coefficient (Section 4.4.2). Tables 4.8-4.9 presents the relaxation times calculated according to Equation 4.5, using the glass expansivities in Tables 4.5-4.6.

TABLE 4.8

The effect of heating rate on the macroscopic relaxation time of quenched PMMA

Heating Rate (C/min)	f	α_g (10^{-6} K^{-1})	τ (s)
0.05	0.130	128	1.22×10^6
0.5	0.120	146	9.86×10^5
1	0.112	161	4.17×10^5
2	0.109	169	1.93×10^5
5	0.107	201	6.39×10^3
10	0.107	217	2.30×10^3
20	0.102	238	1.29×10^3

The relaxation time τ represents the average of the individual relaxation times τ_i associated with the *i*th relaxation mechanism, and has values $7 \leq \text{Ln}(\tau/s) \leq 14$. The value of τ thus provides a qualitative picture of the ageing process, in which long-time relaxation

mechanisms dominate when Ln τ = 12-14, and conversely, at the other end of the time spectrum, short-time relaxation mechanisms dominate when Ln τ = 7-8.

TABLE 4.9

The effect of heating rate on the macroscopic relaxation time of slow-cooled PMMA

Heating Rate (C/min)	f	α_g (10^{-6} K^{-1})	τ (s)
0.5	0.0672	155	5.20×10^4
1	0.0596	172	2.08×10^4
2	0.0574	157	1.10×10^4
5	0.0575	154	4.48×10^3
10	0.0561	169	1.99×10^3

Figure 4.10 shows the plot of τ against the heating rate for quenched and slow-cooled PMMA. At the rate of 0.5 C/min, the relaxation time of slow-cooled PMMA is about half the corresponding relaxation time of quenched PMMA. This result correlates with the lowering of the free volume fraction by about 45% after slow cooling. On the other hand, the discrepancy in relaxation times between the two types of PMMA specimens becomes smaller at increasing heating rates, which indicates that the length contraction at high rates of heating contains contributions mainly from short-time relaxations of the order of ~10^3 seconds. The relaxation time at thermodynamic equilibrium, τ_g, is obtained by extrapolating to f = 0 from the plot of Ln τ against f (Fig. 4.11). The value of τ_g of 5.8×10^{-8} to 3.9×10^{-3} seconds is comparable with the postulated relaxation times (ranging from 10^{-6} to 10^1 seconds) of Greiner and Schwarzl [47] for polystyrene.

4.4.5 Gruneisen Constant of Poly(Methyl Methacrylate)

The Gruneisen constant γ [60] provides a quantitative description of the structure of solid polymers by relating the thermal expansion coefficient with other thermal and mechanical properties (Equation 2.20). The magnitude of γ is a measure of the asymmetry of bond energies which become more pronounced from covalent bonds to van der Waal bonds. Wada *et al.* [61] and Warfield [62] have pointed out that since the anharmonicity of a system arises

FIGURE 4.10 PLOT OF RELAXATION TIME OF QUENCHED AND SLOW-COOLED PMMA AGAINST HEATING RATE

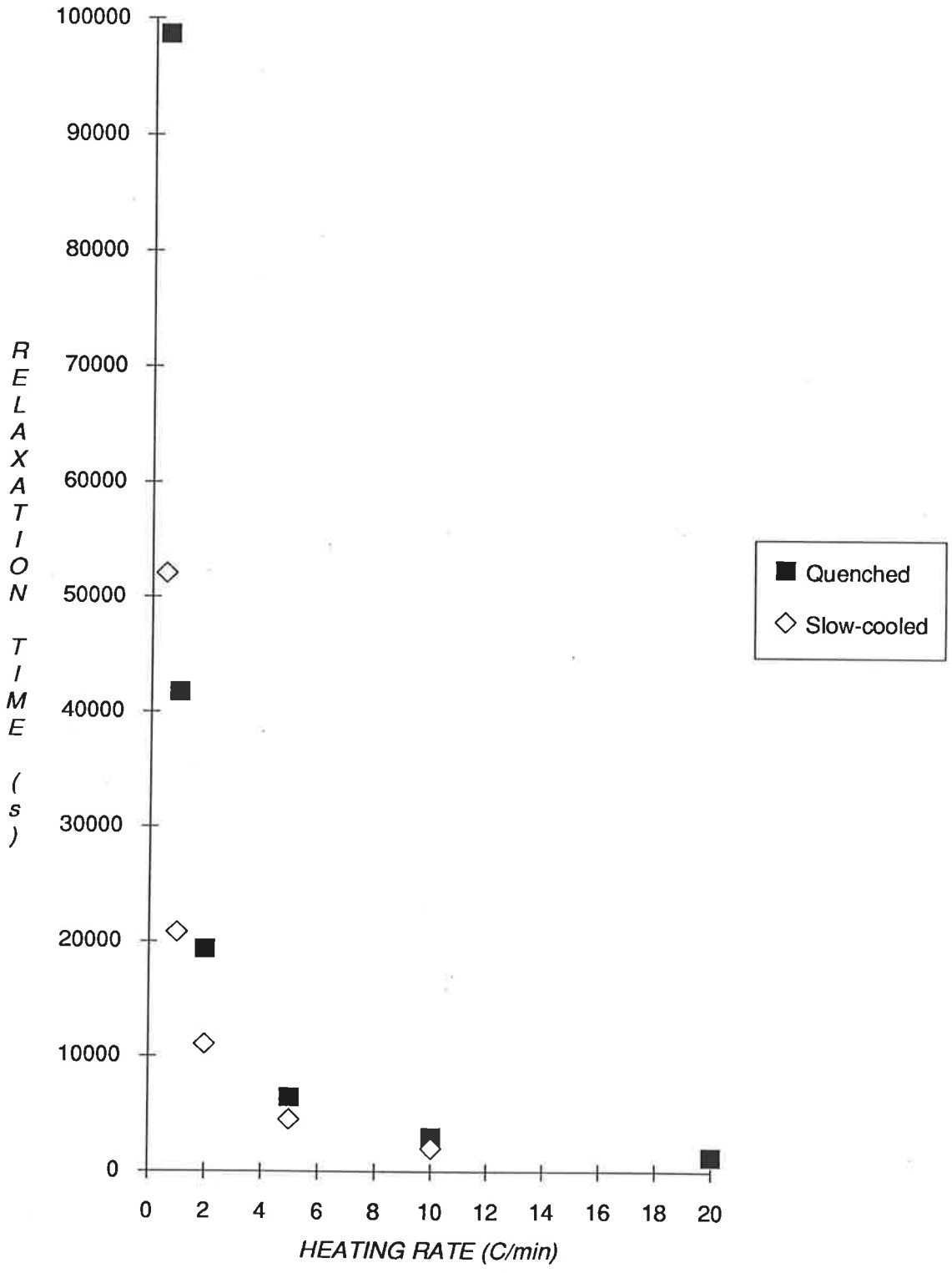

FIGURE 4.11 PLOT OF LN(RELAXATION TIME) AGAINST FREE VOLUME FRACTION OF QUENCHED AND SLOW-COOLED PMMA

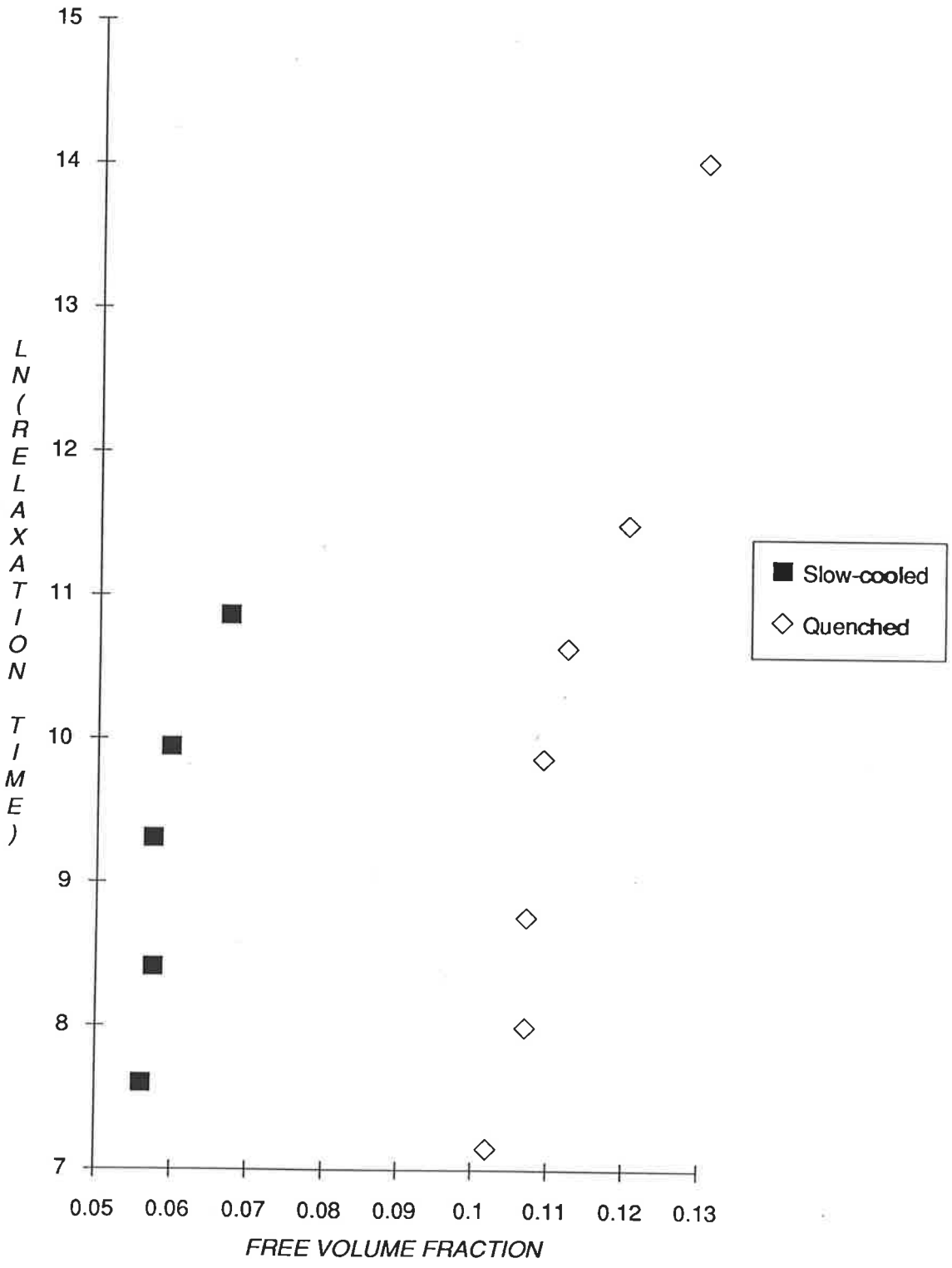

predominantly from interchain vibrations, only the portion of heat capacity due to interchain vibrations, $C_{v,\,i}$, should be used in Equation 2.20, otherwise γ will be low by a factor of five to twenty.

The following parameters were used to calculate the lattice Gruneisen parameter γ_L of PMMA: isothermal bulk modulus determined at 25 C and at atmospheric pressure, $B_T = 5.9 \times 10^9$ N/m^2 [63], density $\rho = 1.17 \times 10^6$ g/m^3 [28], $C_{v,\,i} = 0.23$ J.K.g^{-1}, as calculated by Wada *et al.* [61], and $\alpha_g = 210 \times 10^{-6}$ K^{-1} and 165×10^{-6} K^{-1} for quenched and annealed PMMA respectively. The substitution of these variables into Equation 2.20 yields $\gamma_L = (\alpha_g.B_T)/(\rho.C_{v,\,i}) = 4.6$ for quenched PMMA and 3.6 for slow-cooled PMMA. The experimental γ_L values are in good agreement with literature values [61-65] listed in Table 2.5 ($\gamma_L = 4.0$–6.8). The lower value of γ_L for slow-cooled PMMA is directly related to the smaller free volume fraction in these specimens. Sharma and Reddy [66-67] claimed that the free volume fraction is related to γ_L according to $f = (\gamma_L + 1)^{-1}$ (Equation 2.21), but substitution of the experimental γ_L values into this equation produced rather large free volume fractions of 0.22 and 0.28. The results of Sharma and Reddy appear to be incorrect as they suggest that slow-cooled specimens contained more free volume than the quenched specimens.

So far, the calculation of γ_L of PMMA is restricted only to the glass state below T_g. From a detailed mathematical description given by Barker [68], it was indicated that γ should increase with temperature as a result of an increase in equilibrium interchain spacing. If the density and the interchain heat capacity are assumed to remain the same above T_g, and the bulk modulus [63] at 140 C is 4.2×10^9 N/m^2, the substitution of $\alpha_l = 480 \times 10^{-6}$ K^{-1} (quenched) and 800×10^{-6} K^{-1} (slow-cooled) into Equation 2.20 results in $\gamma_L = 7.5$ for quenched PMMA and 12.5 for slow-cooled PMMA. However, Sharma [67] reported that the value of γ_L is lower in the liquid state above T_g. The reason for this discrepancy is unclear, since it was mentioned [67] that the larger volume expansion above T_g introduces a greater degree of disorder (and hence greater anharmonicity) into the polymer structure. The ratio γ_L (liquid)/γ_L (glass) is 3.5 for slow-cooled PMMA and 1.6 for quenched PMMA, where the smaller ratio for quenched PMMA suggests that it contains more frozen-in "liquid-like" character.

The interpretation of the magnitude of γ_L has been largely substantiated by experimental observation, however, the evaluation of γ_L suffers from the fact that the measurement of different variables may have been performed on polymer samples of varying

composition and history. Although the lattice Gruneisen parameter shows promise as a sensitive indicator of structural changes, the incorporation of thermal expansivity, density and heat capacity into the Gruneisen equation leads to some uncertainty about the reliability of γ_L as the magnitude of these parameters are known to be affected by physical ageing.

4.5 SUMMARY

(1) The free volume fraction of amorphous PMMA was determined from length contraction in the vicinity of the glass transition region. Length contraction was attributed to the collapse of free volume holes of different sizes, such that the collapse of small holes with short relaxation times occured first. The free volume fraction was observed to vary with heating rate, in which a smaller free volume fraction was obtained upon an increase in heating rate. This was attributed to the insufficient time available for the measurement of relaxation processes with long relaxation times.

(2) The free volume fraction of quenched PMMA of about 0.11 suggested that the SB definition of the free volume is more appropriate than the WLF definition. However, the free volume fraction was lowered by about 45% to approximately 0.06 upon slow cooling at 1 C/min. The variance in free volume fraction of PMMA indicated that the universal free volume fraction proposed by the two empirical free volume models did not take into account the effects of thermal history and physical ageing.

(3) Length contraction was observed to occur over a temperature range of 20-28 C in the vicinity of the glass transition, which supported the hypothesis that the glass transition cannot be described by a single temperature. This was attributed to the distribution of relaxation times accompanying the annihilation of free volume holes of various sizes. The termination of contraction at about 132 C suggested that true thermodynamic equilibrium is only attained when a specimen is heated to about 20-27 C above "T_g". The Simha-Boyer equation $f = \Delta\alpha.T_g$ produced unacceptable values of T_g for PMMA, which supported the contention that the conventional definition of T_g from V-T and L-T curves may not have any physical meaning in describing the glass transition process.

(4) The primary effect in the lowering of free volume by slow cooling was the reduction in the population of small free volume holes associated with short relaxation times. This resulted in an increase in the onset temperature for contraction by 4-7 C, and an increase in

relaxation time at slower heating rates to 10^5-10^6 seconds. The decreasing discrepancy in relaxation times between quenched and slow-cooled specimens at high heating rates indicated that the contraction at fast heating rates contains mainly contributions from relaxation processes with short relaxation times of the order of 10^3 seconds.

(5) The glass thermal expansion coefficient was observed to be a sensitive indicator of changes in free volume fraction. The larger value of α_g for quenched specimens was attributed to the higher free volume fraction. Abnormally large values of liquid expansivities in slow-cooled specimens were found to be directly related to the excess thermal energy absorbed by the specimen when heated through the glass transition.

(6) The lattice Gruneisen constant was calculated for PMMA by incorporating the experimental thermal expansivity values and other thermomechanical properties from a number of sources. The calculated γ_L values were found to closely follow the degree of anharmonicity in the specimens studied, in which the value of γ_L was larger for quenched specimens than for slow-cooled specimens. In addition, γ_L was found to be larger for the liquid state than for the glass state, in accordance with the greater anharmonicity in the polymer structure above T_g.

Chapter 4

1. D.G. LeGrand, *J. Appl. Polym. Sci.* **13**, 2129 (1969).
2. S.E.B. Petrie, *J. Polym. Sci. Polym. Phys. Ed.* **10**, 1255 (1975).
3. J.R. Flick and S.E.B. Petrie, *Structure and Properties of Amorphous Polymers: Studies in Physical and Theoretical Chemistry,* A.G. Walton ed., Elsevier, Amsterdam, **10**, 145 (1978).
4. M. Washer, *Polymer* **26**, 1545 (1985).
5. A.J. Kovacs, R.A. Stratton and J.D. Ferry, *J. Phys. Chem.* **67**, 152 (1963).
6. S.E.B. Petrie, *J. Macromol. Sci. Phys.* **B12**, 225 (1976).
7. D.H. Ender, *J. Macromol. Sci. Phys.* **B4**, 635 (1970).
8. R.E. Robertson and C.W. Joynson, *J. Appl. Polym. Sci.* **16**, 733 (1972).
9. L.C.E. Struik, *Polym. Eng. Sci.* **17(3)**, 165 (1977).
10. L.C.E. Struik, *Physical Ageing in Amorphous Polymers and Other Materials*, Elsevier, Amsterdam (1978).
11. M.L. Williams, R.F. Landell and J.D. Ferry, *J. Am. Chem. Soc.* **77**, 4701 (1955).

12. R. Simha and R.F. Boyer, *J. Chem. Phys.* **37(5)**, 1003 (1962).

13. A.J. Kovacs, *J. Polym. Sci.* **30**, 131 (1958).

14. A.J. Kovacs, *Fortschr Hochpolym. Forsch.* **3**, 394 (1963).

15. L.C.E. Struik, *Ann. N. Y. Acad. Sci.* **279**, 78 (1976).

16. H.H.D. Lee and F.J. McGarry, *J. Macromol. Sci.-Phys.* **B29(1)**, 11-29 (1990).

17. K.-H. Illers, *Makromol. Chem.* **127**, 1 (1969).

18. A. Gray and M. Gilbert, *Polymer* **17**, 44 (1976).

19. M.G. Wysgoski, *J. Appl. Polym. Sci.* **25**, 1455 (1980).

20. A.R. Berens and I.M. Hodge, *Macromolecules* **15**, 756 (1982).

21. A.J. Hill, K.J. Heater and C.M. Agrawal, *J. Polym. Sci. Polym. Phys.* **28**, 387 (1990).

22. C.M. Agrawal, K.J. Heater and A.J. Hill, *J. Mat. Sci. Lett.* **8**, 1414-1415 (1989).

23. L.C.E. Struik, *Polymer* **28**, 57 (1987).

24. R. Diaz-Calleja, A. Ribes-Grues and J.L. Gomes-Ribelles, *Polymer* **30**, 1433 (1989).

25. A.J. Kovacs, J.M. Hutchinson and J.J. Aklonis, *Proceedings of the Symposium on the Structure of Non-Crystalline Materials,* Cambridge, p153 (1976).

26. S. Loshaek, *J. Polym. Sci.* **15**, 391-404 (1955).

27. S.S. Rogers and L. Mandelkern, *J. Phys. Chem.* **61**, 985 (1957).

28. D.W. van Krevelen, *Properties of Polymers: Their Estimation and Correlation With Chemical Structure*, Elsevier, Amsterdam (1976).

29. L.A. Wood, *J. Polym. Sci.* **28**, 319 (1958).

30. R.A. Haldon and R. Simha, *J. Appl. Phys.* **39(3)**, 1890 (1968).

31. J.C. Wittman and A.J. Kovacs, *J. Polym. Sci.* **C16**, 4443 (1969).

32. L.C.E. Struik, *Polymer* **29**, 1347 (1988).

33. T.G. Fox Jr., and P.J. Flory, *J. Appl. Phys.* **21**, 581 (1950).

34. H.H.D. Lee and F.J. McGarry, *J. Macromol. Sci. Phys.* **B29(2&3)**, 237-248 (1990).

35. T.S. Chow, *J. Chem. Phys.* **79**, 4602 (1983).

36. T.S. Chow, *Polym. Eng. Sci.* **24**, 915 (1984).

37. T.S. Chow, *Macromolecules* **17**, 2336-2340 (1984).

38. J. Perez, *Polymer* **29**, 483 (1988).

39. L.C.E. Struik, *Polymer* **28**, 1869 (1987).

40. A.K. Doolittle, *J. Appl. Phys.* **22**, 1031 (1951).

41. A.K. Doolittle, *J. Appl. Phys.* **22**, 1471 (1951).

42. R. Simha and C.E. Weil, *J. Macromol. Sci.-Phys.* **B4(1)**, 215-26 (1970).

43. L.C.E. Struik, *Failure of Plastics,* W. Brostow and R.D. Corneliussen eds., Hanser (1986), Chapter 11.

44. G.E. Roberts and E.F.T. White, *The Physics of Polymer Glasses*, R.N. Haward, ed., Applied Science (1973), Chapter 3.

45. J. Bartos, J. Muller and J.H. Wendorff, *Polymer* **31**, 1678 (1990).

46. J.J. Hutchinson and A.J. Kovacs, J. Polym. Sci. Polym. Phys. Ed. **14**, 1575 (1976).

47. R. Greiner and F.R. Schwarzl, *Colloid Polym. Sci.* **267**, 39-47 (1989).

48. R.J. Crowson and R.C.G. Arridge, *Polymer* **20**, 747 (1979).

49. A.J. Kovacs, J.J. Aklonis, J.M. Hutchinson and A.R. Ramos, *J. Polym. Sci. Polym. Phys. Ed.* **17**, 1097-1162 (1979).

50. Y.C. Jean, H. Nakanishi, LY Hao and T.C. Sandreczki, *Phys. Rev. B* **42(15)**, 9705 (1990).

51. For example, see *Positron Solid-state Physics*, W. Brandt and A. Dupasquier, North-Holland, Amsterdam (1983).

52. F. Bueche, *Physical Properties of Polymers*, Interscience (1962).

53. S.C. Sharma, L. Mandelkern and F.C. Stehling, *J. Polym. Sci. Polym. Lett.* **10**, 345-356 (1972).

54. P.S. Wilson and R. Simha, *Macromolecules* **6(6)**, 902 (1973).

55. S.E.B. Petrie, *J. Polym. Sci. A-2* **10**, 1255-1272 (1972).

56. J. Biros, T. Larina, J. Trekoval and J. Pouchly, *Colloid Polym. Sci.* **260**, 27-30 (1982).

57. H. Yoshida and Y. Kobayashi, *Polym. Eng. Sci.* **23(16)**, 907 (1983).

58. J.M. O'Reilly, H.E. Bair and F.E. Karasz, *Macromolecules* **15**, 1083-1088 (1982).

59. I.M. Hodge and A.R. Berens, *Macromolecules* **15**, 762-770 (1982).

60. E. Gruneisen, *Ann. Phys.* **10**, 211 (1908).

61. Y. Wada, A. Itani, T. Nishi and S. Nagai, *J. Polym. Sci. A-2* **7**, 201 (1969).

62. R.W. Warfield, *Die Makromolekulare Chemie* **175**, 3285-3297 (1974).

63. J.R. Asay, D.L. Lamberson and A.H. Guenther, *J. Appl. Phys.* **40(4)**, 1768 (1969).

64. B. Hartmann, *Acustica* **36**, 24 (1976-1977).

65. B.K. Sharma, *J. Phys. D: Appl. Phys.* **15**, 1273, 1735 (1982); **16**, 1959 (1983).

66. B.K. Sharma and R.R. Reddy, *Pramana J. Phys.* **28**, 195 (1987).

67. B.K. Sharma, *Polym. Comm.* **30**, 346 (1989).

68. R.E. Barker Jr., *J. Appl. Phys.* **38(11)**, 4243 (1967).

GLOSSARY OF SYMBOLS

$\alpha'_{g,\,l}$	Linear Thermal Expansion Coefficient in the Glass and Liquid State
$\alpha_{g,\,l}$	Cubical Thermal Expansion Coefficient in the Glass and Liquid State
α_f	Cubical Thermal Expansion Coefficient of Free Volume
B_T	Isothermal Bulk Modulus
$C_{p,\,g,\,l}$	Specific Heat Capacity at Constant Pressure in the Glass and Liquid State
$C_{v,\,i}$	Specific Interchain Heat Capacity at Constant Volume
δ	Measure of the Departure From Equilibrium
E_{act}	Energy of Activation
f	Free Volume Fraction
γ	Gruneisen Constant
γ_T	Lattice (Interchain) Gruneisen Constant
$L_{x,\,y,\,z}$	Sample Length Measured Along the x, y, or z Axis
$\Delta L_{x,\,y,\,z}$	Length Contraction Measured Along the x, y, or z Axis
$L_{max,\,min}$	Maximum and Minimum Sample Length
dL/dt	Rate of Change in Sample Length with Time
n_f	Number of free Volume Holes
Q	Thermal Energy Absorbed
θ	Material Constant of the Order of Unity
ρ	Specific Density
T_g	Glass Transition Temperature
T_r	Reference Temperature
T_{on}	Temperature for the Onset of Contraction
T_{end}	Temperature for the Endset of Contraction
ΔT	Temperature Shift Between Specimens of Different Thermal Histories
dT/dt	Experimental Heating Rate
τ_i	Relaxation Time Associated with the *i*th Relaxation Process
τ_g	Relaxation Time at T_g
V_0	Initial Specific Volume
V_{eq}	Specific Volume at Thermodynamic Equilibrium

V_f	Free Volume
V_h	Average Hole Volume
dV/dt	Rate of Volume Change With Respect to Time
x	Relative Contribution of Temperature and Structure to τ

CHAPTER 5
ISOTHERMAL PHYSICAL AGEING OF PMMA

5.1 INTRODUCTION 106

5.2 EXPERIMENTAL 107

5.3 RESULTS AND DISCUSSION

5.3.1 Isothermal Ageing

Length Contraction 108

Relaxation Rates and Relaxation Times 111

Activation Energy for Physical Ageing 116

5.3.2 Sequential Ageing

Length Contraction 119

Relaxation Rates 120

5.4 SUMMARY 122

BIBLIOGRAPHY 123

GLOSSARY OF SYMBOLS 126

CHAPTER 5

5.1 INTRODUCTION

The rapid measurement of dimensional changes in a heating experiment may not necessarily allow the specimen to first attain thermal equilibrium due to the short period of time spent at a particular temperature. Therefore, the macroscopic free volume obtained from heating experiments is the average of separate contributions from the collapse of individual holes of different sizes, and hence dimensional changes at individual temperatures cannot be determined from these results. The rate of heating was observed to influence the magnitude of length contraction, in which experiments with slower heating rates produced larger contractions while smaller contractions were observed at faster heating rates. These observations were due to the insufficient time allowed for the collapse of larger holes which require longer relaxation times.

The major proportion of length contraction of PMMA was observed to occur in the near vicinity of the glass transition (104-135 C). However, a number of authors [1-6] have shown from isothermal measurements the existence of volume relaxation at temperatures below T_g. Isothermal experiments of specimens at thermal equilibrium allow the study of structural relaxation at temperatures below T_g. Isothermal rates of contraction have been used by Struik [9] and Bartos *et al.* [5] to evaluate relaxation times associated with the mechanism(s) that are involved with the contraction. These relaxation times, in turn, may be incorporated into phenomenological equations such as the Narayanaswamy equation [32] to evaluate the activation energy of physical ageing.

The aim of this chapter is to measure the contraction of quenched PMMA over the temperature range 40-140 C under isothermal conditions and compare these results with those that were obtained from heating experiments in Chapter 4. A modified isothermal experiment in which the specimen is aged isothermally over a period of 60 minutes at regular temperature increments of 10 C was also carried out (Fig. 5.1). The major difference between the two types of isothermal experiments is that the thermal history of the specimen in the modified isothermal experiment is continually changing, whereas the initial histories of specimens in the unmodified experiment are the same. The results of these isothermal experiments suggest that cooperative motion is a prerequisite for the attainment of thermodynamic equilibrium and raises if a

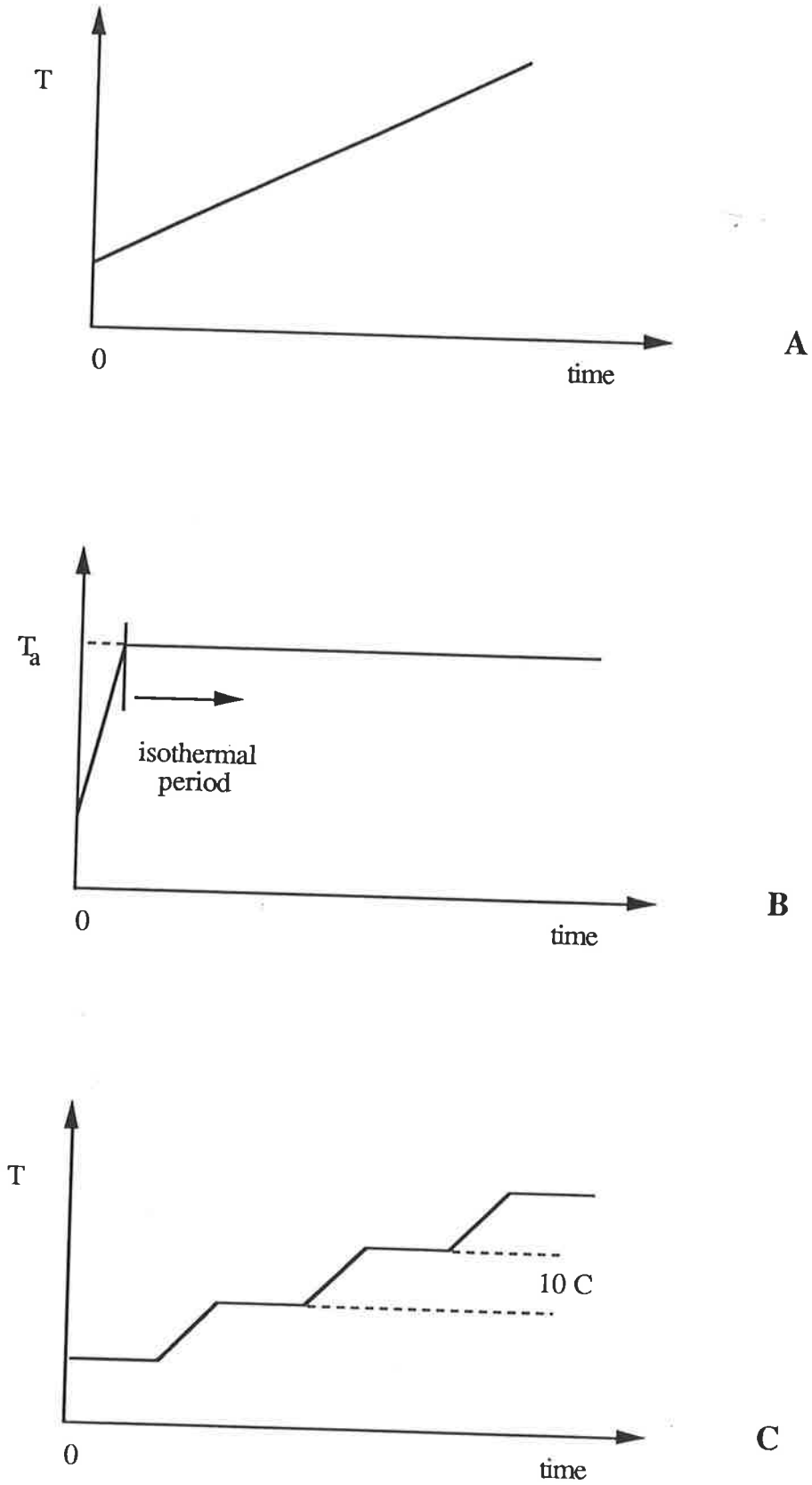

Figure 5.1 Temperature profile for (**A**) constant heating; (**B**) isothermal heating; and (**C**) sequential heating.

specimen can be completely aged by secondary relaxations alone.

5.2 EXPERIMENTAL

PMMA specimens were thermally equilibrated in the thermomechanical analyser at 140 C for 15 minutes and cooled rapidly at a rate of 20 C/min to 25 C under dry nitrogen. The specimens were immediately reheated at 20 C/min to the isothermal ageing temperature, T_a (which range from 40-140 C), and aged for a period (t_a) of 60 minutes under a constant load of 0.1 N. The rapid cooling and reheating was necessary to minimise any ageing which may occur before the commencement of the isothermal experiment. A different specimen was used for each run.

Length contraction below T_g can also be obtained by sequentially ageing a specimen in "steps" of increasing temperature, in which the isothermal period (t_a) for each step is of three hours duration. Three hours was considered to be a sufficient period for the observation of length contraction, especially in the glass transition region. The specimen was equilibrated at 140 C for 15 minutes, and was quenched in liquid nitrogen for 10 minutes. Following quenching, the specimen was allowed to thermally equilibrate at 25 C under dry nitrogen for 20 minutes to minimise any irreproducibility in results which may be caused by thermal stresses. The specimen was then sequentially aged from 60 C to 140 C according to the thermal profile in Table 5.1. A constant load of 0.1 N was applied on the specimen throughout the experiment.

TABLE 5.1

Thermal profile for sequential ageing (*ageing temperature)

Heating Step (C)	Heating Rate (C/min)	t_a (mins)
25 - 60*	0.5	180
60 - 70*	0.5	180
70 - 80*	0.5	180
80 - 90*	0.5	180
90 - 100*	0.5	180
100 - 110*	0.5	180
110 - 120*	0.5	180
120 - 130*	0.5	180
130 - 140*	0.5	180

5.3 RESULTS AND DISCUSSION

5.3.1 Isothermal Ageing

Length Contraction

The contraction isotherms of PMMA are plotted as a function of temperature and time in Figures 5.2 and 5.3. The magnitude of the contraction, ΔL_z, is observed to increase with temperature in accordance with the expectation that the rate of physical ageing increases with temperature [7-8]. The slow rates of relaxation in the glass state measured below T_g (105 C for PMMA [14, 45]) are reflected by the small ΔL_z ($\leq 1 \times 10^{-5}$ m) after 60 minutes. Contraction was still observed in specimens that were aged below T_g which indicates that the ageing process is still proceeding after a period of 60 minutes.

The initial large and rapid contractions observed above T_g, i.e. at T_a = 130 C and 140 C, are attributed to the high segmental mobility at these temperatures at which equilibrium is achieved rapidly. These observations are consistent with the proposal (Section 4.4.2) that the attainment of equilibrium is achieved rapidly above T_{eq} (132 C for quenched PMMA). The contraction ΔL_z has been associated with the collapse of free volume holes and a procedure in which the free volume V_f is evaluated from ΔL_z has been established (Section 4.4.1). The free volume measured after an isothermal period of 60 minutes is calculated from Equation 4.2 and the free volume fraction recovered after ageing at T_a, $f(T_a)$, is calculated in the same way for f from Equation 4.3. The average values of L_z and $L_{x,y}$ are taken to be 1.623×10^{-3} m and 4.798×10^{-3} m respectively. The values of T_a, ΔL_z, V_f and $f(T_a)$ are presented in Table 5.2.

The final value of $f(T_a) = 0.129$ at equilibrium (140 C) is approximately the same as the fractional free volume obtained for quenched PMMA (0.130) in Chapter 4. Therefore, f = 0.13 is taken to represent the maximum possible free volume fraction trapped in PMMA upon quenching. Within the experimental timescale, physical ageing of PMMA takes place as a linear function of logarithmic ageing time at temperatures below T_g [4] (Figs. 5.4-5.5). After an initial curvature, the curve of ΔL versus ln (time) becomes a straight line such that the rate of relaxation can be characterised by the slope of the straight lines [9]. On the other hand, as the specimen approaches thermodynamic equilibrium the isothermal contraction becomes non-linear [4] as observed at T_a = 130 C and 140 C. The free volume fractions measured after 60 minutes at various isothermal temperatures are plotted against ageing temperature in Figure 5.6.

FIGURE 5.2 ISOTHERMAL AGEING IN QUENCHED PMMA(numbers adjacent to curves indicate the isothermal ageing temperature)

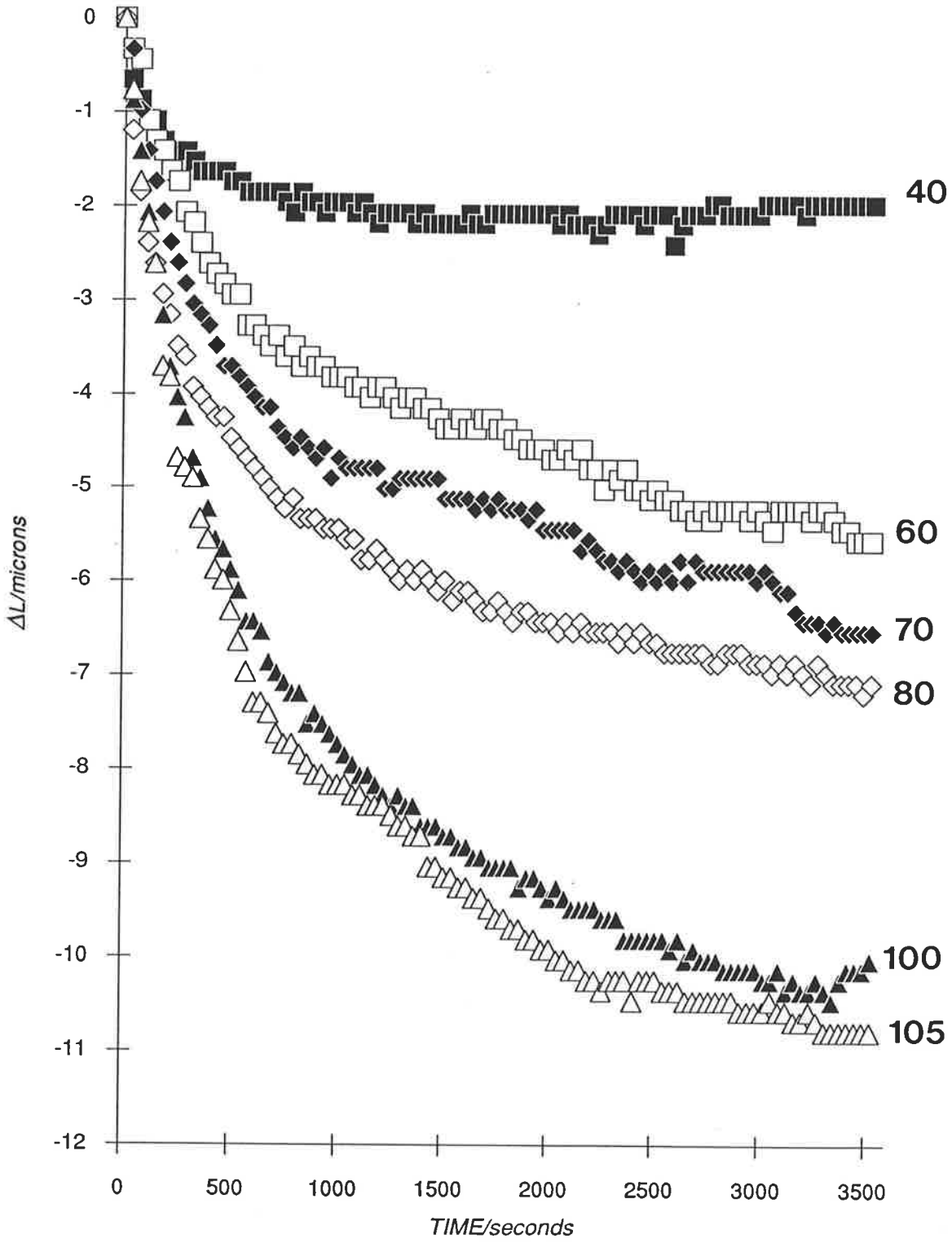

FIGURE 5.3 ISOTHERMAL AGEING IN QUENCHED PMMA (numbers adjacent to curves indicate the isothermal ageing temperature)

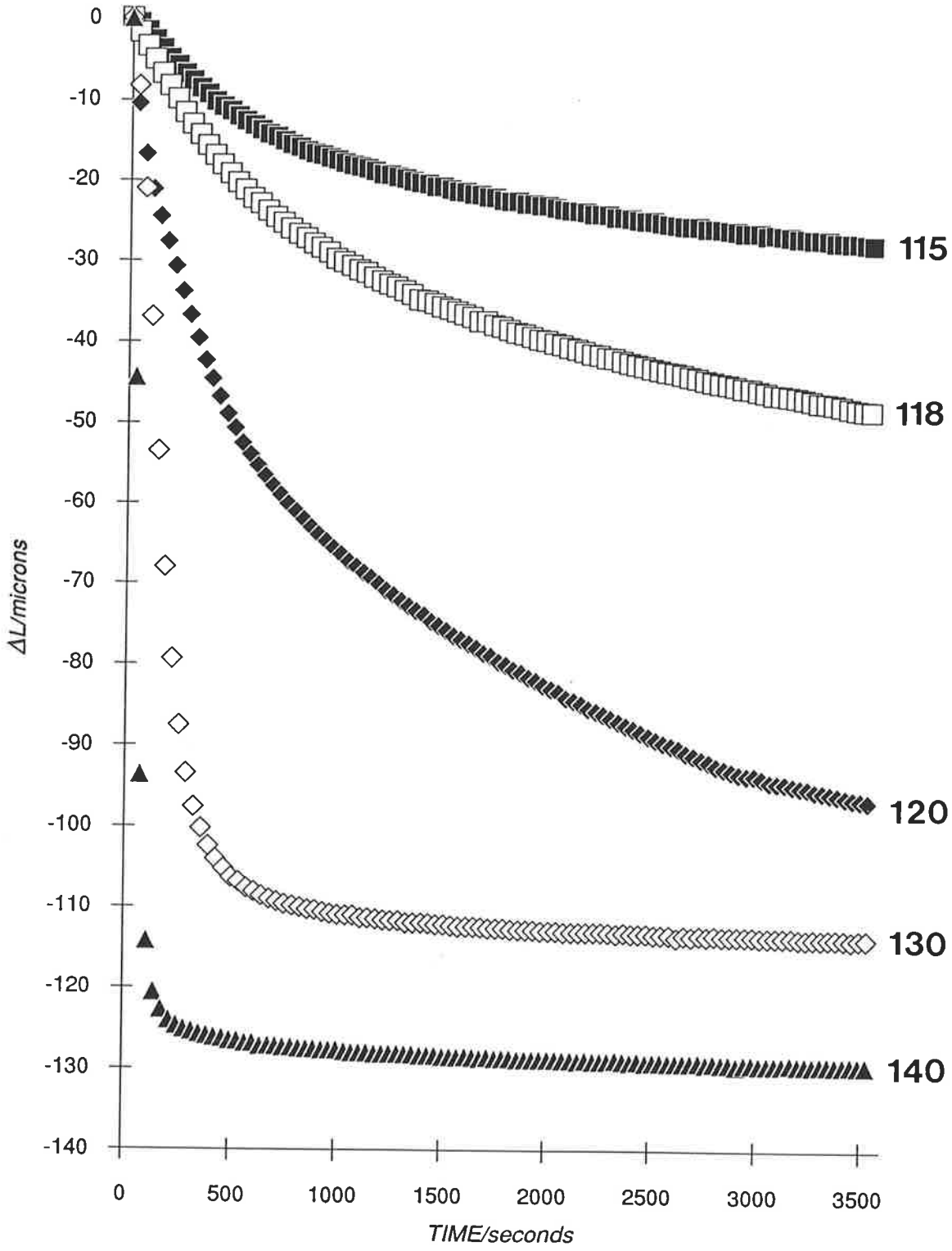

FIGURE 5.4 ISOTHERMAL LENGTH CONTRACTION AS A FUNCTION OF LN (TIME) (numbers adjacent to curves indicate the isothermal ageing temperature)

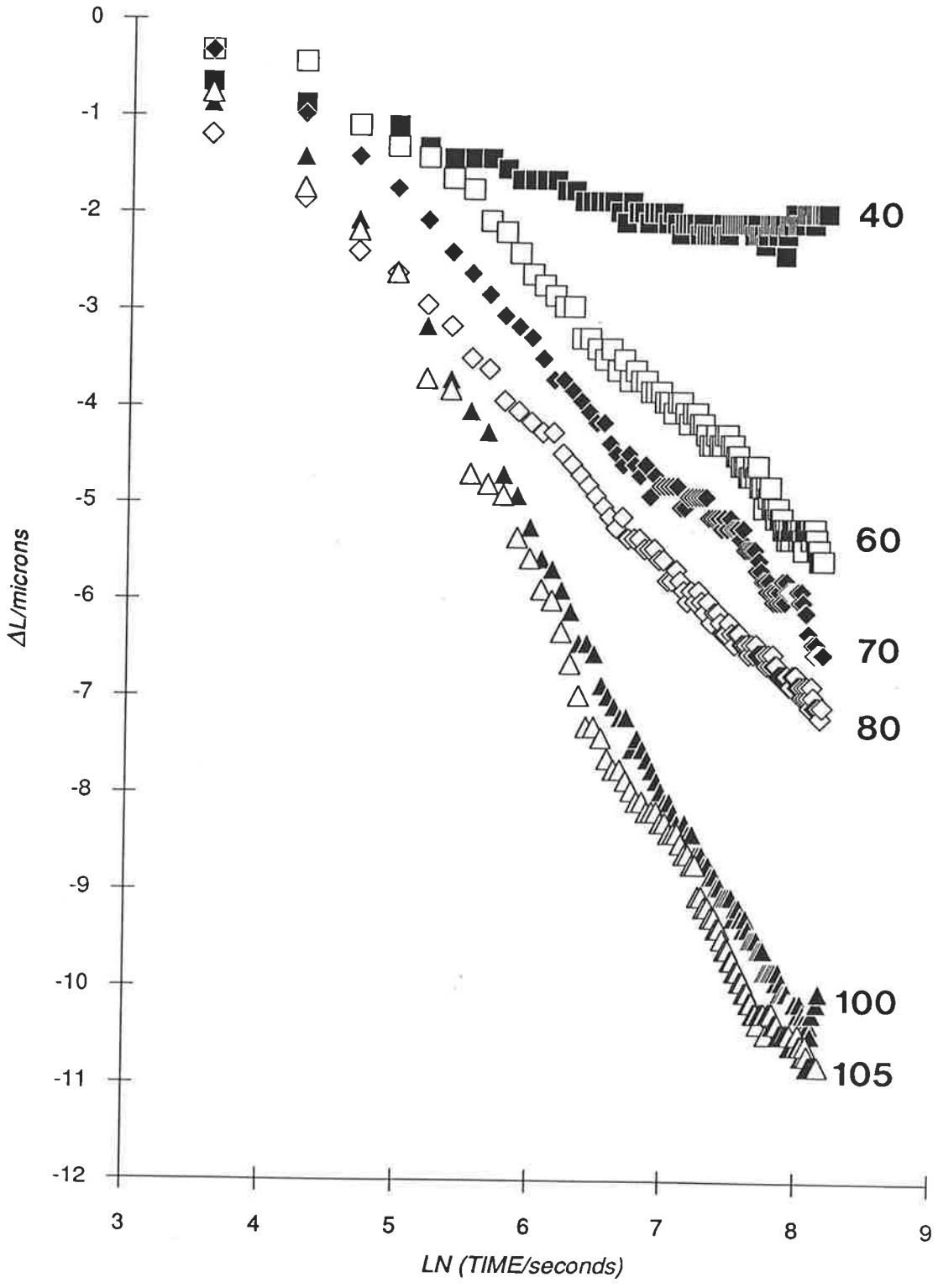

FIGURE 5.5 ISOTHERMAL LENGTH CONTRACTION AS A FUNCTION OF LN (TIME) (numbers adjacent to curves indicate the isothermal ageing temperature)

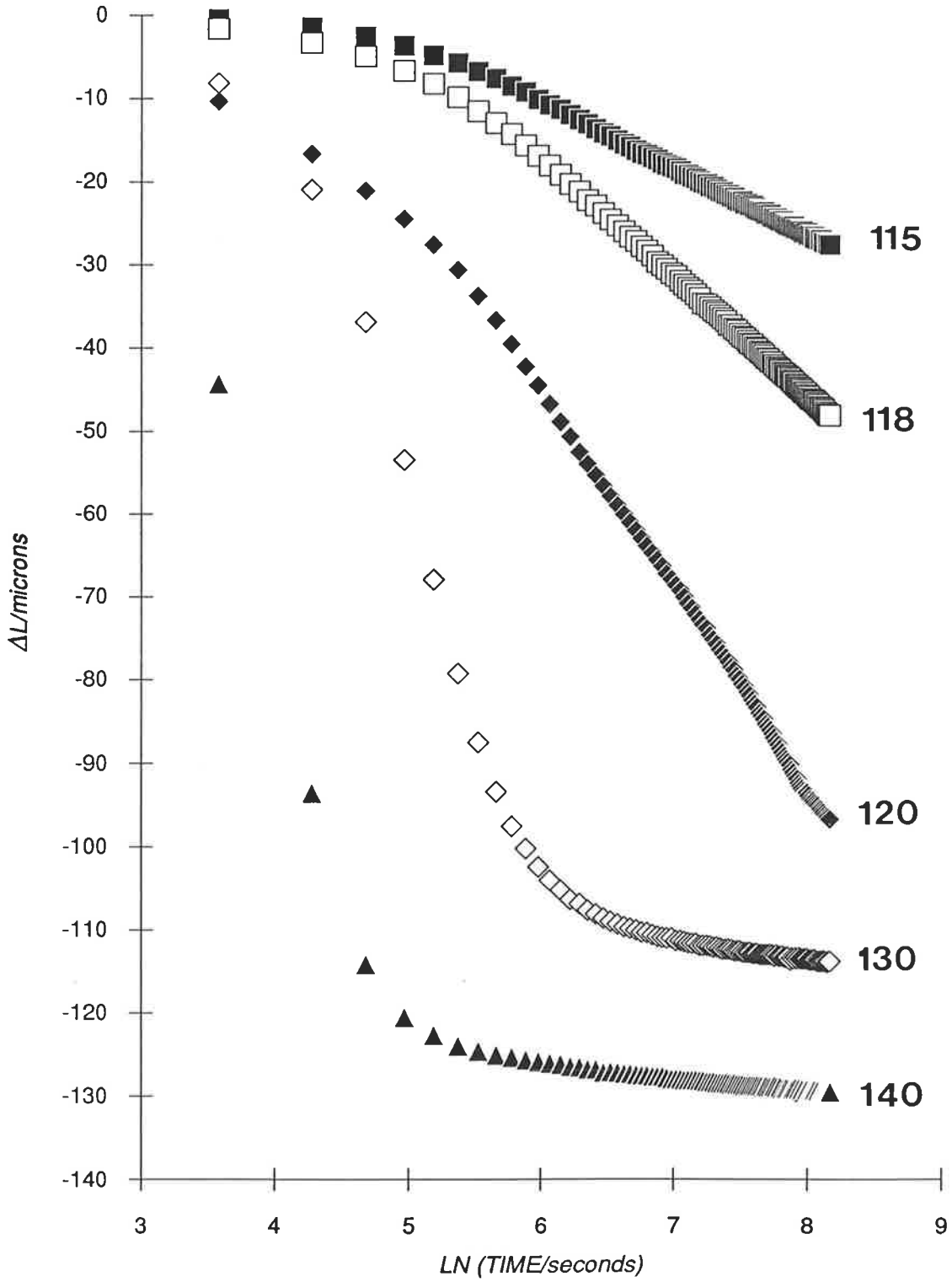

FIGURE 5.6 FREE VOLUME FRACTION MEASURED AFTER ISOTHERMAL AGEING FOR 60 MINUTES

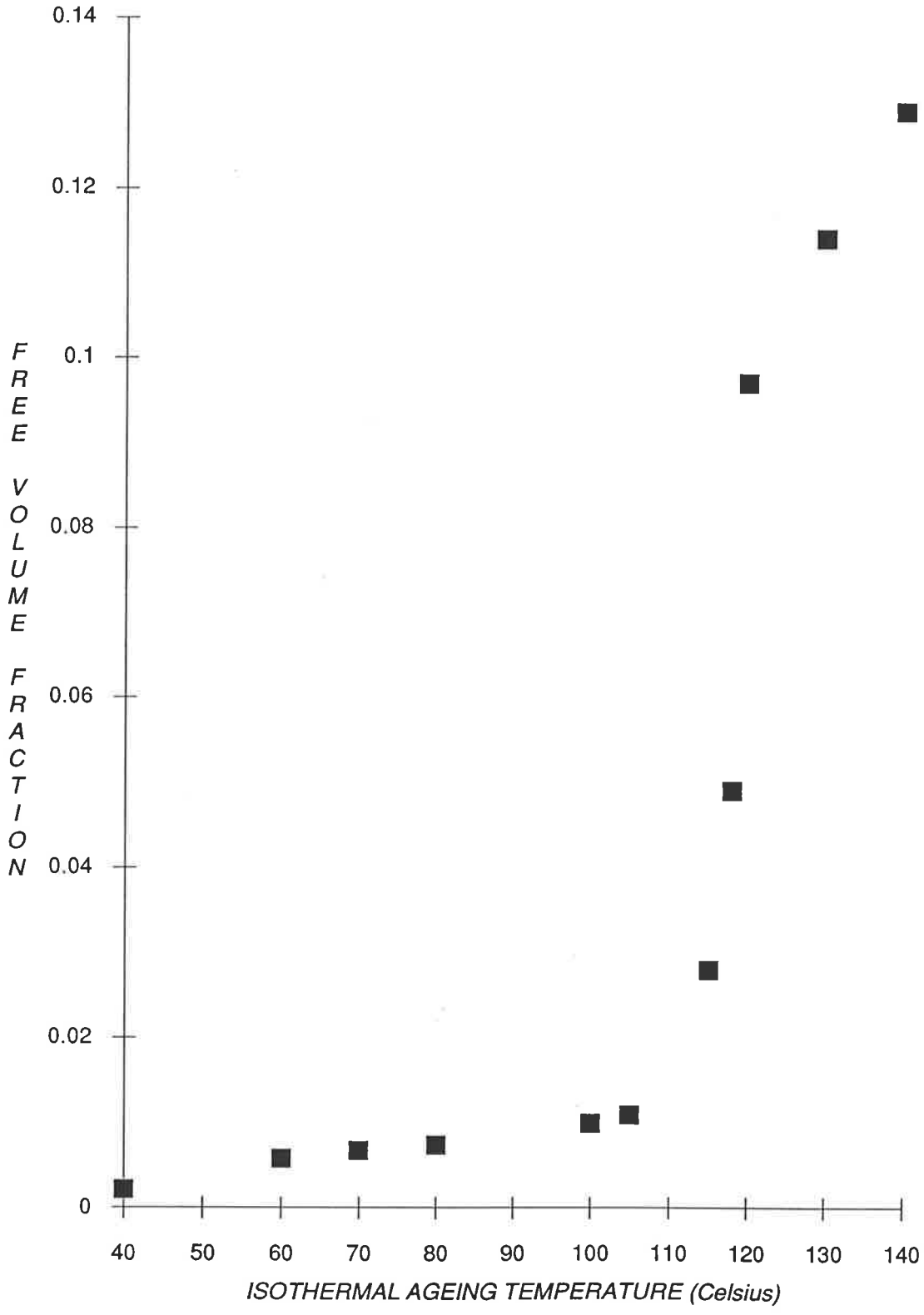

TABLE 5.2

Isothermal free volume and free volume fraction of quenched PMMA measured after 60 minutes

T_a (C)	ΔL_z (m)	V_f (m^3)	$f(T_a)$
40	2.07×10^{-6}	7.99×10^{-11}	0.0021
60	5.56×10^{-6}	2.14×10^{-10}	0.0057
70	6.54×10^{-6}	2.52×10^{-10}	0.0067
80	7.09×10^{-6}	2.73×10^{-10}	0.0073
100	1.01×10^{-5}	3.89×10^{-10}	0.010
105	1.08×10^{-5}	4.16×10^{-10}	0.011
115	2.73×10^{-5}	1.05×10^{-9}	0.028
118	4.82×10^{-5}	1.83×10^{-9}	0.049
120	9.68×10^{-5}	3.63×10^{-9}	0.097
130	1.14×10^{-4}	4.26×10^{-9}	0.114
140	1.30×10^{-4}	4.83×10^{-9}	0.129

The free volume fraction still frozen-in after ageing for 60 minutes at T_a, Δf, is defined as the difference between the maximum free volume recovered at 140 C and the free volume fraction recovered at T_a such that $\Delta f = 0$ at 140 C:

$$\Delta f = f(140) - f(T_a) = 0.13 - f(T_a) \qquad (5.1)$$

Δf is plotted against isothermal ageing temperature in Figure 5.7. The observation of a marked increase in the collapse of free volume above 105 C indicates an increasingly significant contribution by segmental motion towards the annihilation of free volume. It is suggested that the temperature at which an increase in the collapse of free volume is observed may provide a useful measure of T_g as a function of changes in free volume fraction. The T_g of 105 C for PMMA obtained from Figure 5.7 agrees very well with the results of Simha *et al.* [14-15] and other authors [10, 43-45]. The advantages of this technique are that the state of ageing in the specimen is taken into account and discrepancies which may arise as a result of variations in

FIGURE 5.7 UNAGED FREE VOLUME FRACTION AFTER ISOTHERMAL AGEING FOR 60 MINUTES

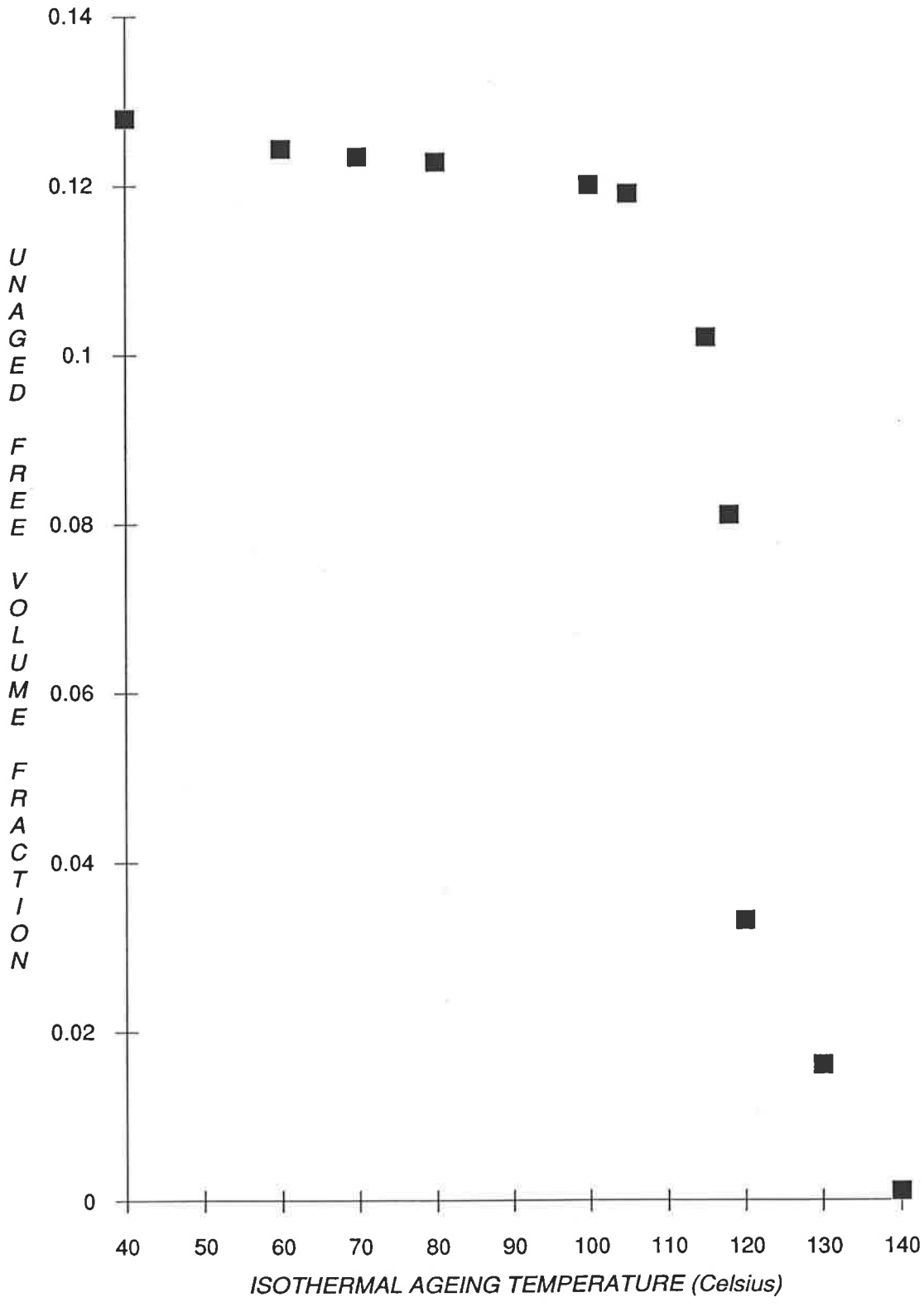

rates of measurement are avoided. However, in order to establish that Δf-T plots provide a reliable measure of T_g, further work is required where the measurement of Δf have to be obtained for different polymers and compared with T_g's obtained by other techniques.

Δf is observed to decrease essentially linearly with T_a between 40 C and 105 C. The relationship between Δf and T_a for 40 C ≤ T_a ≤ 105 C at t_a = 60 minutes is described by the following equation

$$\Delta f = -1.3 \times 10^{-4}.T_a + 0.1326 \qquad (5.2)$$

where $f(T_a) > 0$. If Equation 5.2 is assumed to hold for all temperatures below 40 C, the recovery of free volume ceases (i.e. $f(T_a) = 0$, $\Delta f = 0.13$) when T_a = 20 C. This is significant because the limiting temperature of 20 C is located within the β-relaxation region for PMMA. The dynamic-mechanical results of Diaz-Calleja *et al.* [10] show the β-relaxation of PMMA measured at 1 Hz occurs over a wide temperature range between -20 C to +80 C, although a narrower range of -23 C to +27 C was reported by Kolarik [11]. Torsion pendulum measurements of as-cast PMMA specimens indicate that the β-transition lies between -40 C to +50 C (Figure 5.8). Because of the width of the β-relaxation, T_β, which is often taken to be the temperature at the maximum height of the mechanical or dielectric β-relaxation peak, has literature values which range from 10 C to 30 C [11-14].

In addition, Equation 5.2 predicts a slight increase in free volume fraction when T_a lies below 20 C ($\Delta f > 0.13$), reaching a maximum value of 0.1326 at 0 K. The hypothesis that excess free volume is frozen in at T_β was first proposed by Simha *et al.* [14-15] to account for the observation of unusually large values of α_g in poly(*n*-alkyl methacrylates) with long flexible side-chains. It was proposed [14-15] that large α_g values between T_g and T_β were due to the presence of additional free volume created by the rotation of the ester side-groups, and that the "true" glass expansivity for these polymers should be measured below their respective T_β. The result $\Delta f \geq 0.13$ such that $f(T_a) \leq 0$ indicates that free volume recovery in PMMA will not be affected by physical ageing below the temperature range for β-relaxation. This appears to support Struik's [16-17] controversial hypothesis in which physical ageing is said to occur only between T_g and T_β. In view of conflicting experimental evidence [18-23] which suggests that relaxational processes which occur below T_β continue to be affected by physical ageing, it is

FIGURE 5.8 DYNAMIC - MECHANICAL RELAXATION OF QUENCHED PMMA (1Hz)

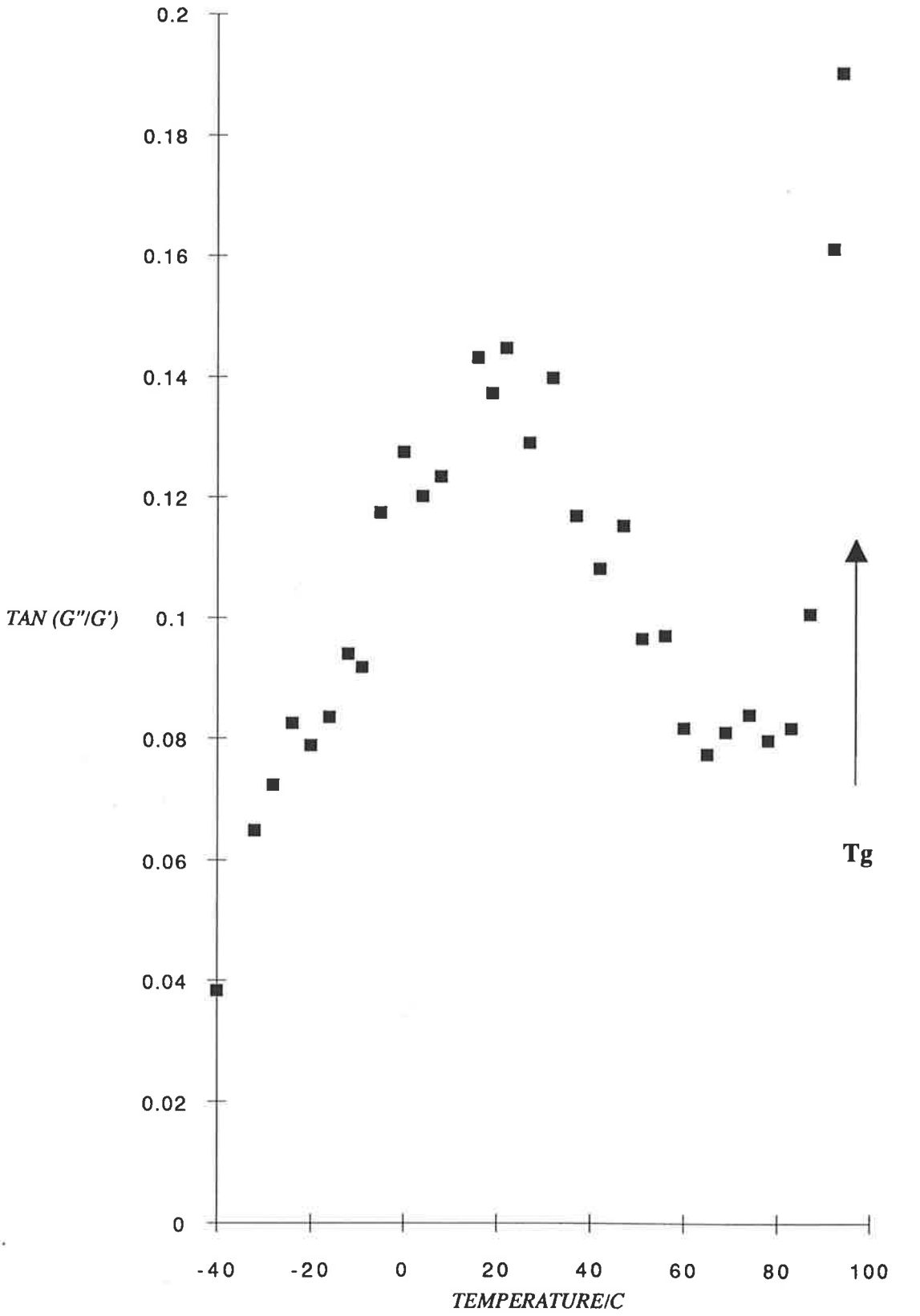

proposed that: (1) assuming that the recovery of free volume of PMMA varies linearly with T_a for all temperatures below T_g, the freezing of secondary relaxation at 20 C generates additional free volume as schematically shown in Figure 5.9; and (2) physical ageing is ineffective in bringing about complete structural recovery to equilibrium within an ageing period of one hour at temperatures below 20 C.

Proposal (2) was confirmed by the following test. The free volume recovered, $f(T_a)$, between 40 C and 105 C was calculated using Equation 5.2 at various ageing times of 900, 1800, 2700 and 3000 seconds from the curves in Figure 5.2. The limiting temperature at which physical ageing becomes ineffectual, i.e. when $\Delta f = 0$, was found to range from 19-23 C. It follows that at thermal equilibrium below T_β, structural recovery would not observed in PMMA in isothermal experiments within an ageing period of the order of hours.

An examination of Johari's [19] paper shows that the ageing temperatures of toluene-pyridine mixture and poly(propylene oxide) specimens lie on the high temperature side of the β-transition. The thermally-stimulated depolarisation results of Guerdoux and Marchal [21] were obtained for PMMA specimens quenched by dipping in water; the mechanical damping peaks of polysulfone and polycarbonate have been shown by Struik [17] to be lowered by the presence of moisture. Although some of the PMMA specimens of Guerdox and Marchal [21] were aged at 20 C, their results have to be treated with some doubt due to the effects of moisture. The dynamic-mechanical curves of quenched and slow-cooled specimens of PMMA, rigid PVC, amorphous PET and poly(*tert*-butyl methacrylate) from Struik's [17] paper (Fig. 5.10) all show deviations on the high temperature side of the β-relaxation peak. These curves further strengthen the hypothesis that physical ageing should become negligible on the low temperature side of the β-transition.

Relaxation Rates and Relaxation Times

The relaxation process of quenched PMMA can be characterised by plotting the change in length ΔL as a function of the isothermal temperature T_a. The rate of relaxation, r, is defined by the slopes of the curves in Figures 5.4-5.5 according to the expression [9]:

$$-r = (3/L_z)[(dL_z/d\ln t_a)/2.303] \qquad (5.3)$$

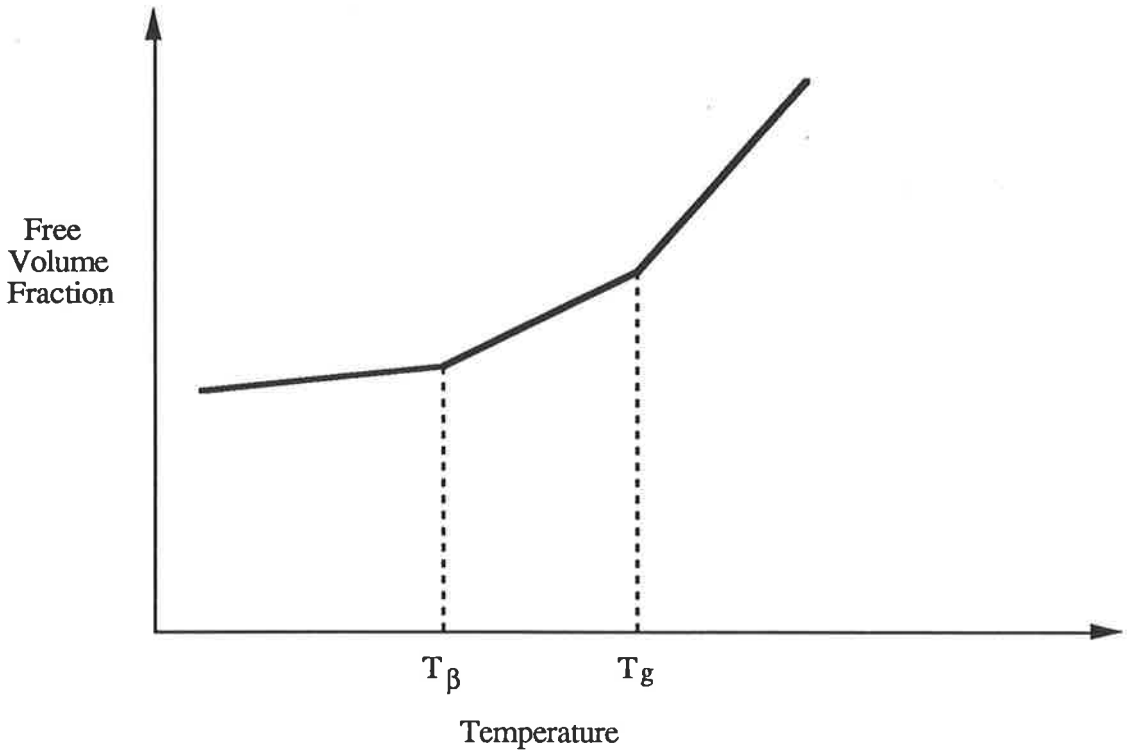

Figure 5.9 Schematic diagram (not drawn to scale) of increase in free volume fraction at T_β and T_g.

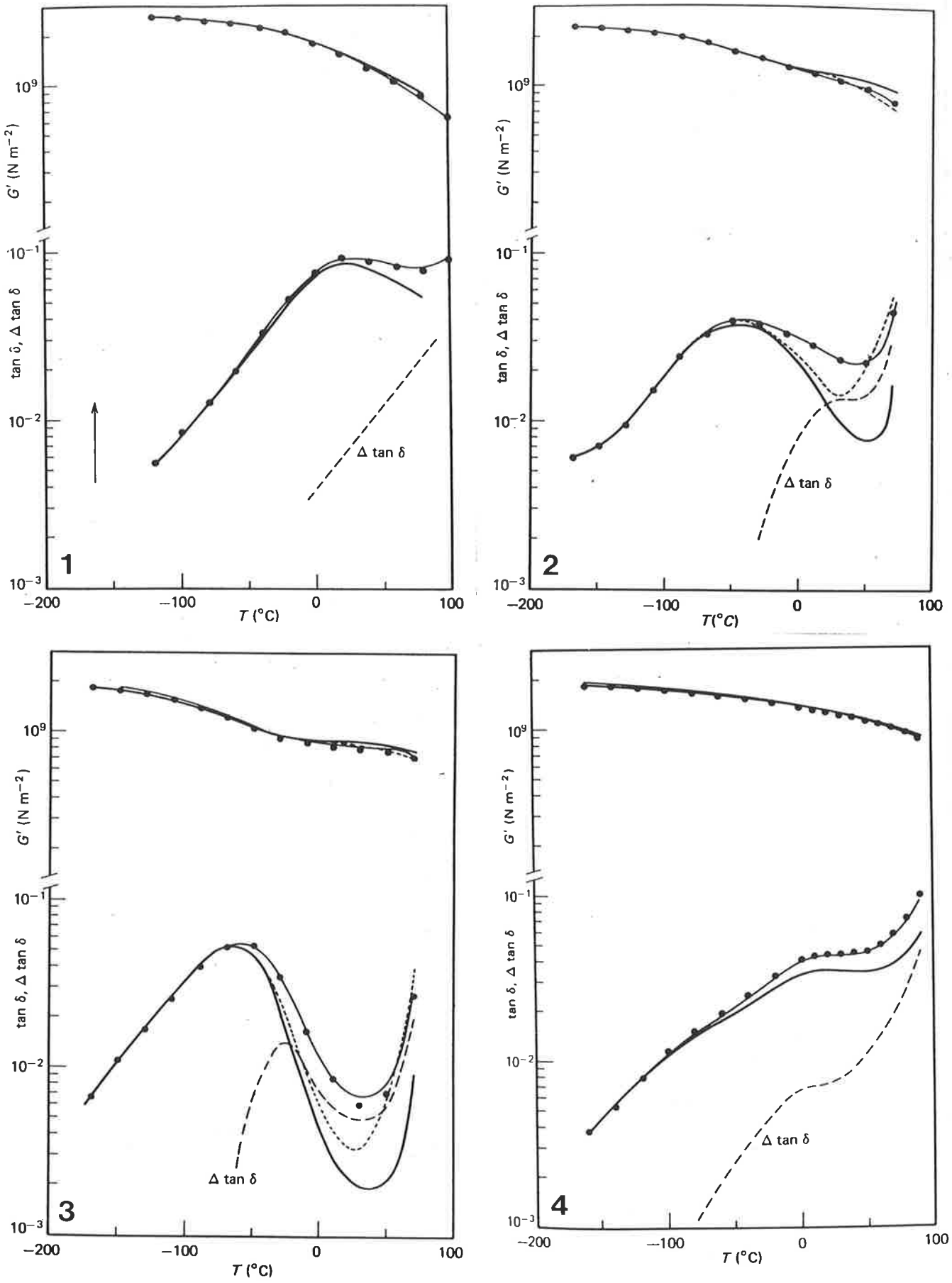

Figure 5.10 Modulus and damping curves at 1 Hz in the β-relaxation range for 1. poly(methyl methacrylate) **2.** poly(vinyl chloride) **3.** amorphous poly(ethylene terepthalate) **4.** poly(*tert*-butyl methacrylate). The solid line is obtained for a slow-cooled specimen and the solid line with dots is for a quenched specimen. The additional dashed line in **2** and **3** are for an as-received specimen (reproduced from [17]).

where the initial length $L_z = 1.623 \times 10^{-3}$ m is the average specimen thickness for quenched PMMA (Table 5.3). The values of -r are plotted as a function of T_a in Figure 5.11, where the rates of relaxation are similar to the results of Struik [9]. It is observed that the relaxation rate is not constant but increases with increasing temperature, in accordance with the results of Struik [9] and Bartos *et al.* [5]. This observation is accompanied by a concomitant increase in the rate of free volume collapse with increasing temperature (Fig. 5.6). The striking similarity between Figure 5.11 and Figure 5.6 indicates that the changes in free volume with ageing temperature are intimately related with the relaxation rate at that particular temperature.

TABLE 5.3

Isothermal rates of relaxation measured between 40 C to 140 C

T_a (C)	$-dL_z/d\ln(t_a)$ (10^{-6} m.sec^{-1})	$-r$ (10^{-4} s^{-1})
40	0.414	3.32
60	1.044	8.38
70	1.494	11.99
80	1.580	12.68
100	1.777	14.26
105	2.696	21.64
115	7.966	63.93
118	15.045	120.8
120	18.435	148.0
130	60.511*	485.7
140	71.084*	570.5

*measured between ln (time) = 4.0-5.5

The isothermal relaxation times at the ageing temperature T_a, $\tau(T_a)$, were calculated from Equations 2.13 and 2.14 [24-25] where f_g has a constant value of 0.13 and represents the maximum free volume fraction frozen-in during quenching, $f(T_a)$ is the free volume fraction recovered at T_a, and the departure from equilibrium $\delta(T_a)$ is the free volume fraction which has not been recovered after ageing at T_a, i.e. $\delta(T_a) = \Delta f = f_g - f(T_a)$.

FIGURE 5.11 RELAXATION RATE OF QUENCHED PMMA AS A FUNCTION OF ISOTHERMAL AGEING TEMPERATURE

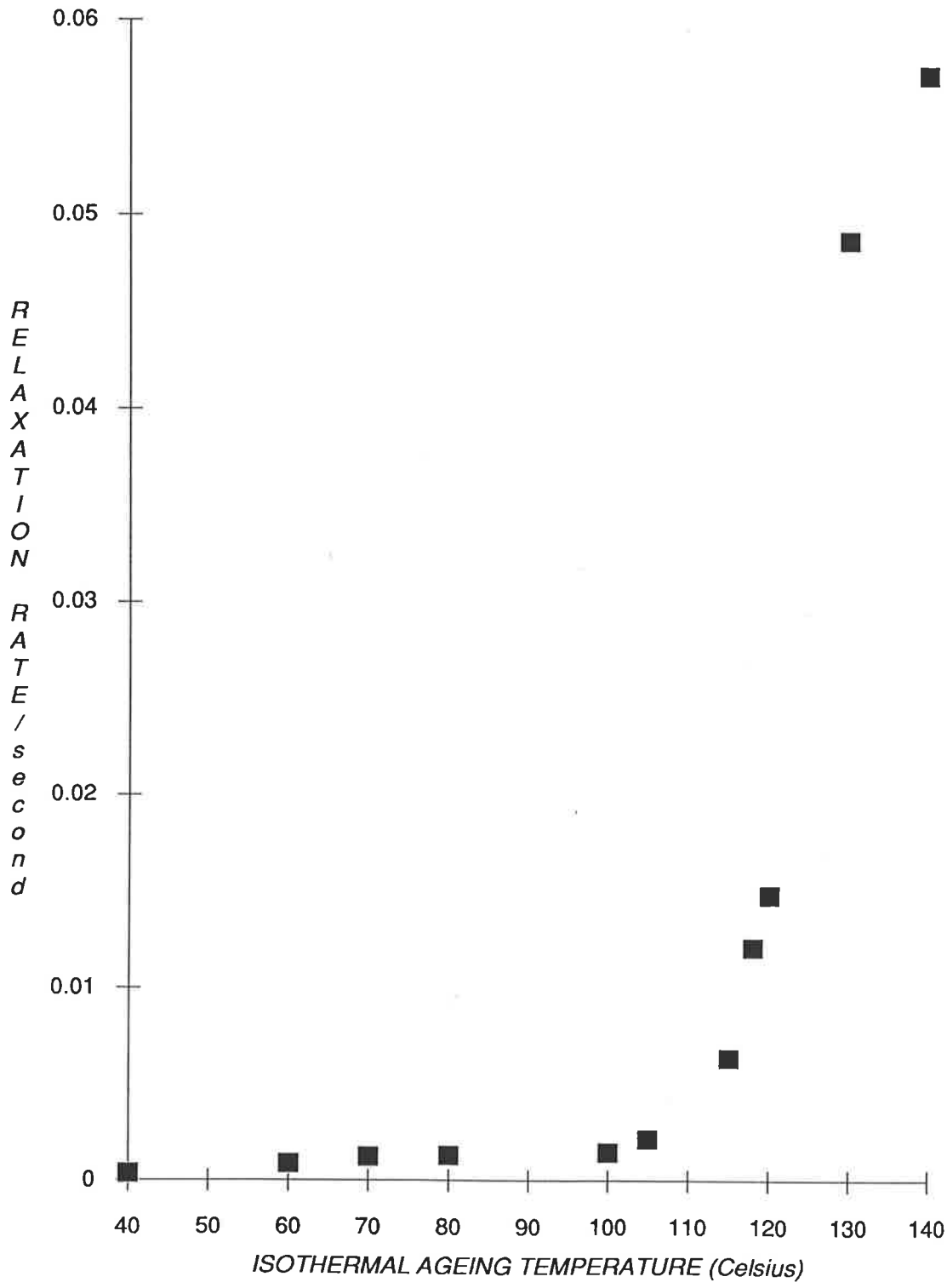

Firstly, the relaxation time at equilibrium, τ_g, at T_a = 140 C is determined from Equation 2.14. For isothermal measurements, dT/dt = 0 which reduces Equation 2.14 to

$$-d\delta(T_a)/dt = (\delta/\tau_g).\exp(1/f_g - 1/f)$$

or, replacing with the notations used in this work,

$$-r = (\Delta f/\tau_g).\exp(7.6923 - 1/f) \qquad (5.4)$$

Substituting the following values $-r = 5.70 \times 10^{-2}$ s^{-1}, f = 0.129, and Δf = 0.001, τ_g was calculated to be 1.65×10^{-2} s. The relaxation times $\tau(T_a)$ were calculated from Equation 2.13 assuming that the ageing process at any T_a can be described by a single time parameter. It is also assumed that the specimen will continue to age indefinitely at the same rate measured after one hour of ageing. This does not take into account that physical ageing is a self-delaying process [3], in which the process naturally slows down as more and more free volume is recovered. However, the calculated relaxation times $\tau(T_a)$ will be shown to provide a good indication of the timespans required to achieve equilibrium at various ageing temperatures. $\tau(T_a)$ is calculated according to Equation 5.5:

$$\tau(T_a) = (1.65 \times 10^{-2}).\exp(1/f - 7.6923) \qquad (5.5)$$

The time required for the establishment of equilibrium, t_{eq}, is a function of the relaxation time and free volume and may be estimated by:

$$t_{eq} \approx 140.\exp(1/f - 1/f_g) \qquad (5.6)$$

where 140 seconds is the time required to attain equilibrium at 140 C (100 seconds has been recommended as a reasonable time for τ_g [3], [25]). A similar equation had been proposed by Struik [3], in which the changes in t_{eq} were calculated with respect to the difference between the ageing temperature and the glass transition ($T_g - T_a$). Struik's equation was not used because the location of T_g extrapolated from the glass and liquid lines of L-T plots could not be

determined, and it was considered that t_{eq} is better estimated from calculations involving changes in free volume. The data obtained from Equations 5.4-5.6 are presented in Table 5.4.

TABLE 5.4

Isothermal relaxation times as a function of ageing temperature and free volume fraction

T_a (C)	$f_g - f$	$\tau(T_a)$ (s)	$\tau(T_a)/\tau_g$	t_{eq} (s)
40	0.128	4.80×10^{201}	2.90×10^{203}	4.10×10^{205}
60	0.124	1.17×10^{71}	7.10×10^{72}	9.94×10^{74}
70	0.123	4.98×10^{59}	3.02×10^{61}	4.22×10^{63}
80	0.123	2.34×10^{54}	1.42×10^{56}	1.99×10^{58}
100	0.120	2.02×10^{38}	1.23×10^{40}	1.72×10^{42}
105	0.119	2.28×10^{34}	1.38×10^{36}	1.94×10^{38}
115	0.102	2.44×10^{10}	1.48×10^{12}	2.07×10^{14}
118	0.081	5.49×10^{3}	3.33×10^{5}	4.66×10^{7}
120	0.033	2.26×10^{-1}	1.37×10^{1}	1.92×10^{3}
130	0.016	4.86×10^{-2}	2.94	4.12×10^{2}
140	0.001	1.75×10^{-2}	1.06	1.49×10^{2}

The first point of interest concerns the data at the ageing temperature of 120 C. An inspection of the contraction isotherm at 120 C (Fig. 5.3) shows that equilibrium is not attained within one hour despite the relatively rapid relaxation time of 2.26×10^{-1} s. On the other hand, it was estimated from Equation 5.6 that equilibrium would be attained within 2000 seconds at 120 C. The discrepancy between t_{eq} and $\tau(T_a)$ is attributed to the inherent self-retarding nature of physical ageing, in which the rate of structural relaxation progressively becomes slower as less free volume is available for molecular motion. The large values of $\tau(T_a)$ below T_{eq} (40-115 C) correlate with Struik's [3] estimates of equilibration times, in which 100 million years (3×10^{15} s) are required to age a specimen to equilibrium at 40 C below T_g. These values of $\tau(T_a)$ between 40-115 C suggests that it is unlikely that a specimen can be aged to equilibrium in this temperature range within a feasible experimental timescale.

The validity of the the calculated values of $\tau(T_a)$ in Table 5.4 are compared with the

work of Hutchinson and Kovacs [25], who showed that the relaxation time on reaching $\delta = 0$ isothermally at 15 C below T_g ("T_g" was taken to be the temperature at which equilibrium is instantaneously attained) is ~2.94 x 10^5 hours (1.1 x 10^9 seconds). The result of Hutchinson and Kovacs [25] correlates with a $\tau(T_a)$ value near 115 C which is approximately 15-25 C below the equilibrium temperature range at 130-140 C. The relaxation times in Table 5.4 are also consistent with the proposal of a distribution of relaxation times spanning the range $10^{-4.5}$-10^2 hours (10^{-1}-10^5 s) in the glass transition region [26-28]. The isothermal contraction of polystyrene at various ageing temperatures was successfully modelled by Greiner and Schwarzl [29] using a six-parameter equation with relaxation times ranging from 5 x 10^{-6} to 8 seconds. In addition, Gomez-Ribelles *et al.* [36] predicted that $\tau(T_a)$ of PMMA is equal to one second in the temperature range 123-129 C. The data of Table 5.4 indicates that $\tau(T_a)$ is approximately equal to one second in the range 118-120 C, which provides a good correlation with the results predicted by Gomez-Ribelles *et al.* [36].

Relaxations at and below the glass transition region are both non-exponential and non-linear [30]. The non-linear character is usually treated by the Narayanaswamy [31] equation (described as the N equation), in which $\tau(T_a)$ is made a function of the departure from equilibrium. The most commonly used functional form of the Narayanaswamy expression is [32]:

$$\tau(T_a) = A.\exp[x\Delta h^*/(RT_a) + (1-x)\Delta h^*/(RT_f)] \qquad (5.7)$$

where R is the gas constant and x is a measure of non-linearity ($1 \geq x > 0$; $x = 1$ for linear relaxation).

Although relaxations in the glass state below T_g are satisfactorily described by the N expression, it has several shortcomings. Firstly, the use of the fictive temperature T_f as the "equilibrium temperature" [33] such that the departure from equilibrium is measured by $T_f - T$, has a serious limitation in that it assumes that every nonequilibrium state can be associated with a single equilibrium state. This is only true for exponential relaxations that exhibit no memory effect [34]. Secondly, the non-linearity parameter x and the pre-exponential factor A have no clear physical meaning [30, 35], however, Gomes-Ribelles *et al.* [36] has calculated A using Ln $A = -\Delta h^*/(RT_r)$, where T_r is defined as the temperature at which the relaxation time is one

second. Thirdly, the physical significance of the inverse relationship between x and the activation enthalpy Δh^* is unknown [30] although Δh^* is usually taken to be equal to the activation energy E_{act} [37]. Finally, the N expression predicts an Arrhenius temperature dependence for the equilibrium state (i.e. $T = T_f$), which is in conflict with the established WLF expression [38]. Associated with this are unusually large values of $\Delta h^*/R$, as values as high as 225×10^3 K have been reported [35, 39].

Figure 5.12 shows the equilibrium relaxation times for PMMA obtained from the Narayanaswamy [31] (chain line) and Adam-Gibbs (AG) [40] (full lines and shaded area) models, and from dielectric measurements (open circles) [41] as reported by Gomes Ribelles *et al.* [36] (the notation for τ_g in [36] is τ^{eq}). The equilibrium relaxation times were obtained by a least-squares fit of four adjustable parameters in which a single parameter (E_{act}, or D, a function of temperature, heat capacity, free energy barrier and configurational entropy [34]) was kept fixed at a certain value. In the N model, E_{act} was fixed at 838 kJ mol^{-1}, while in the AG model D was varied between 17-63 kJ mol^{-1} [36]. It was found [36] that some of the adjustable parameters (x, T_r) were affected by the choice of the constant value for E_{act} and D, even though the overall fit of the heat capacity curves appeared to be unaffected. It is observed that the dielectric results in Figure 5.12 gave the best agreement with the data of Table 5.4. The coorelation between the experimental data of Table 5.4 and the results of [25-29] and [36] indicates that isothermal measurements of length contraction may be used to provide a reliable measure of relaxation times.

Activation Energy for Physical Ageing

The activation energy for structural relaxation in PMMA is calculated by plotting the $\mathrm{Ln}(\tau(T_a)/\tau_g)$ as a function of $(1/T_a.1/f)$ according to the following expression:

$$\mathrm{Ln}(\tau(T_a)/\tau_g) = -(E_{act}/R).(1 - 1/f)^{-1}.(1/T_a.1/f) + (1 - 1/f)^{-1}.E_{act}/(RT_{eq}) \qquad (5.8)$$

where the pre-exponential factor A, T_f and Δh^* are replaced by τ_g, T_{eq} and E_{act} respectively such that $T_{eq} = 413$ K is the temperature at which equilibrium is readily attained in PMMA. It was observed that reasonable agreement between E_{act} values calculated from the slope and from the intercept was obtained when the parameter x was substituted by the term $-(f - 1)^{-1}$. In

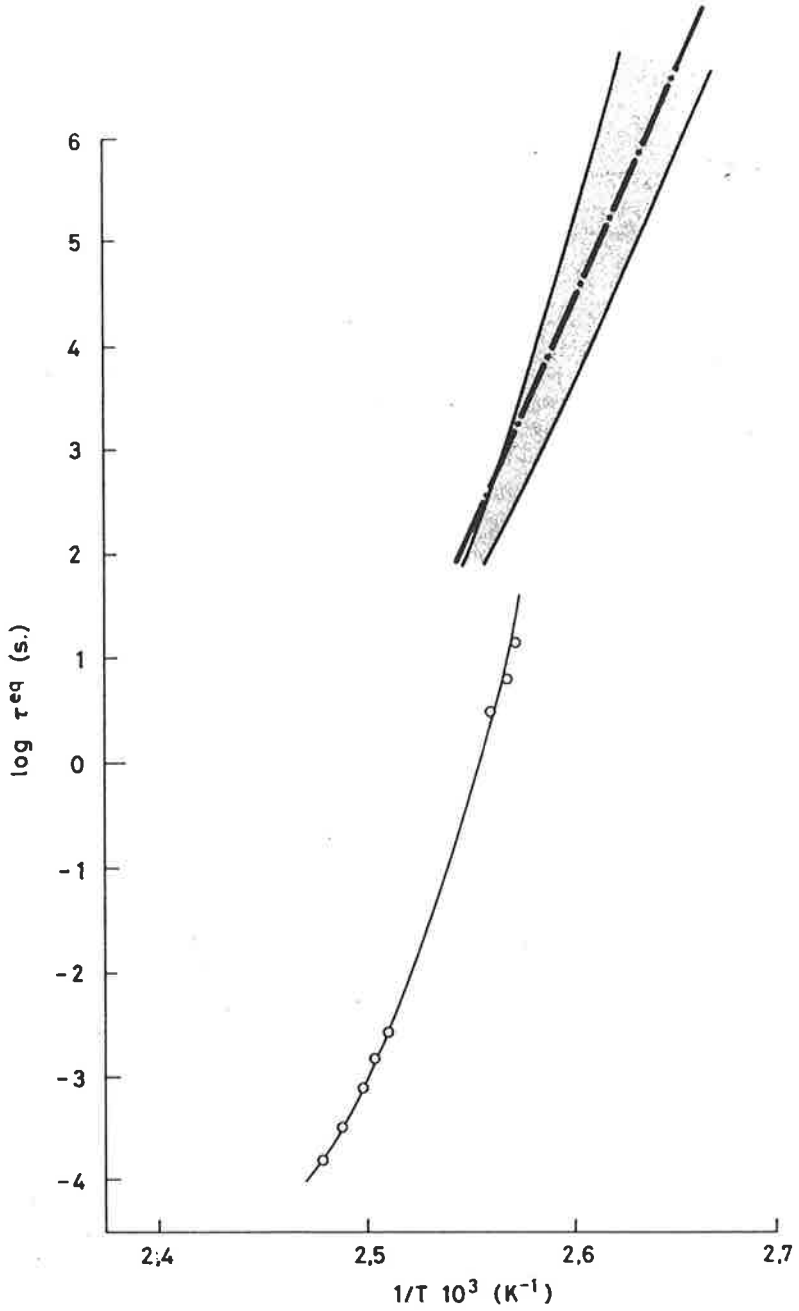

Figure 5.12 Equilibrium relaxation times τ^{eq} (τ_g) of PMMA predicted from the Adam-Gibbs model for specimens of different thermal histories (shaded area), and from the Narayanaswamy model (chain line). The equilibrium relaxation times obtained from dielectric results are denoted by the open circles (reproduced from [36]).

addition, these activation energies are found to be comparable to literature values for the α and β transitions for PMMA. Figure 5.13 shows that $Ln(\tau(T_a)/\tau_g)$ varies as a linear function of $(1/T_a.1/f)$, yielding a slope of 312 K^{-1} and an intercept of -0.69. The activation energies are thus obtained by the following expressions and are presented in Table 5.5:

$$E_{act} = -312 \times 8.314 \times (1 - 1/f) \quad (5.9a)$$

$$E_{act} = -0.69 \times 8.314 \times 413 \times (1 - 1/f) \quad (5.9b)$$

TABLE 5.5

Activation energies (kJ mol^{-1}) of quenched poly(methyl methacrylate) as a function of isothermal ageing temperature and free volume fraction

T_a (C)	f	E_{act} (Eq. 5.9a)	E_{act} (Eq. 5.9b)
40	0.0021	1233	1126
60	0.0051	506	462
70	0.0067	385	351
80	0.0073	353	322
100	0.010	257	235
105	0.011	233	213
115	0.028	90	82
118	0.049	50	46
120	0.097	24	22
130	0.114	20	18
140	0.129	18	16

Literature values of E_{act} for the glass (α) transition of PMMA range from 330 kJ mol^{-1} [42] to 462 kJ mol^{-1} [43-44], while activation energies of 70-126 kJ mol^{-1} have been reported for the the β-transition [45-47]. The high activation energies in the region 40-105 C (213-1233 kJ mol^{-1}) suggest that the process of physical ageing is associated with cooperative main-chain motions that are responsible for the glass transition.

FIGURE 5.13 PLOT OF MODIFIED NARAYANASWAMY EQUATION (EQUATION 5.8) FOR QUENCHED PMMA

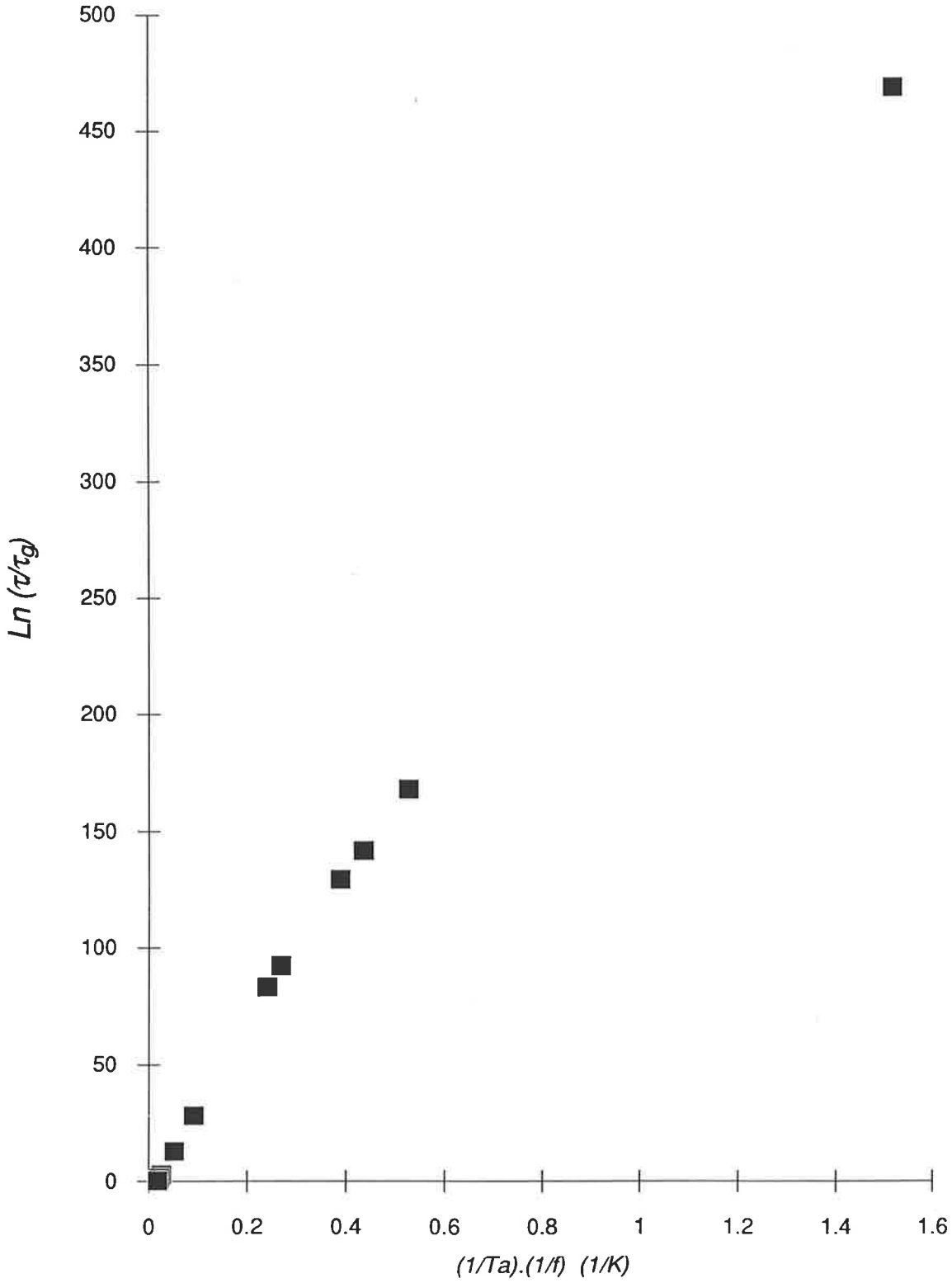

Lee and McGarry [48] have shown that true equilibrium is achieved only at temperatures considerably higher than T_g (this "equilibrium" temperature was suggested in Section 4.4.2 as T_{end}). The question remains as to whether quenched polymer specimens can be fully aged at temperatures well below T_g without the participation of cooperative main-chain motion. Although it is accepted that the relaxation of side-groups will lead to some volume recovery, the attainment of "equilibrium" in the β-relaxation range may actually represent the limit at which structural recovery can take place, that is, the disappearance of volume contraction after ageing below T_g does not conclusively prove that the specimen has reached equilibrium. The observations of Lee and McGarry [48] and those of this work suggest that isothermal ageing of polymers is unlikely to result in complete structural recovery below T_g nor by secondary relaxations alone. These observations are also consistent with earlier predictions (Equation 5.2) that physical ageing of PMMA becomes ineffective below 20 C.

It is known [11, 45] that the activation energy of the α-relaxation of poly(*n*-alkyl methacrylates) decreases on lengthening the side-chain and it was proposed by Simha and Boyer [15] that the side-chains retained excess free volume on cooling. However, as the glass transition temperature also decreases with side-chain length, the product $3(\alpha'_l - \alpha'_g).T_g$ will decrease down the series and is not a reliable measure of free volume fraction [14]. It is suggested that the glass expansivity may provide an indication of free volume changes, where increases in free volume fraction are accompanied by increases in α_g. An inspection of the glass expansivities and activation energies of poly(*n*-alkyl methacrylates) in references [14] and [45] indicates an inverse relationship between the activation energy and free volume in which α_g increases more sharply than the corresponding decrease in activation energy. For example, the increase in α'_g (10^{-6} K^{-1}) progressing from PMMA to PEMA is (114 - 75)/75 = 0.52 [14], while E_{act} decreases by (210 - 460)/460 = -0.54 (although E_{act} for PEMA is listed as high as 385 kJ mol^{-1}) [45]. Similarly, the changes in f and E_{act} are 0.83 and -0.55 for P(*n*-propyl MA), 0.97 and -0.78 for P(*n*-butyl MA), and 1.48 and -0.81 for P(*n*-hexyl MA). The observation that an increase in free volume is accompanied by a lowering of activation energy at the glass transition supports the hypothesis [3, 16] that the molecular mobility of a polymer is determined by the distribution of local free volume fraction.

5.3.2 SEQUENTIAL AGEING

Length Contraction

The length contraction measured between 60-140 C is plotted as a function of temperature and isothermal period t_a in Figures 5.14-5.15. Length contraction is observed to increase with temperature between 60-110 C, but between 120-140 C the contraction becomes smaller as the specimen approaches thermodynamic equilibrium. To calculate the free volume fraction recovered after ageing for 180 minutes, the sum of the contraction $\Sigma\Delta L$ and the free volume fraction $\Sigma f(T_a)$ from previous temperatures should be included as the specimen is continuously aged stepwise at increasing temperatures. The relevant data is presented in Table 5.6, in which V_f and f are calculated from Equations 4.2-4.3.

The final value of the free volume fraction $\Sigma f(T_a) = 0.136$ correlates with the fractional free volumes obtained from isothermal ageing (0.129) and by heating at 0.05 C/min (0.13) (Chapter 4). Hence the macroscopic free volume fraction of quenched PMMA can be measured by ageing the specimen isothermally or sequentially, or by heating slowly at a constant rate. The plot of $\Sigma f(T_a)$ vs. T_a in Figure 5.16 shows that the collapse of free volume is greatest between 90-120 C, which correlates with the contraction range of 104-132 C for quenched PMMA (Chapter 4).

TABLE 5.6

Length contraction and free volume fraction of PMMA measured after 180 minutes at each T_a

T_a (C)	ΔL (m)	$\Sigma\Delta L$ (m)	ΣV_f (m^3)	$\Sigma f(T_a)$
60	1.64×10^{-6}	1.64×10^{-6}	6.31×10^{-11}	0.00169
70	2.07×10^{-6}	3.71×10^{-6}	1.43×10^{-10}	0.00383
80	2.84×10^{-6}	6.54×10^{-6}	2.52×10^{-10}	0.00676
90	6.21×10^{-6}	1.23×10^{-5}	4.91×10^{-10}	0.0132
100	4.02×10^{-5}	5.23×10^{-5}	2.01×10^{-9}	0.0540
110	5.78×10^{-5}	1.11×10^{-4}	4.14×10^{-9}	0.111
120	1.81×10^{-5}	1.29×10^{-4}	4.79×10^{-9}	0.128
130	4.47×10^{-6}	1.33×10^{-4}	4.95×10^{-9}	0.133
140	3.16×10^{-6}	1.36×10^{-4}	5.06×10^{-9}	0.136

FIGURE 5.14 SEQUENTIAL AGEING IN QUENCHED PMMA (numbers adjacent to curves indicate the ageing temperature)

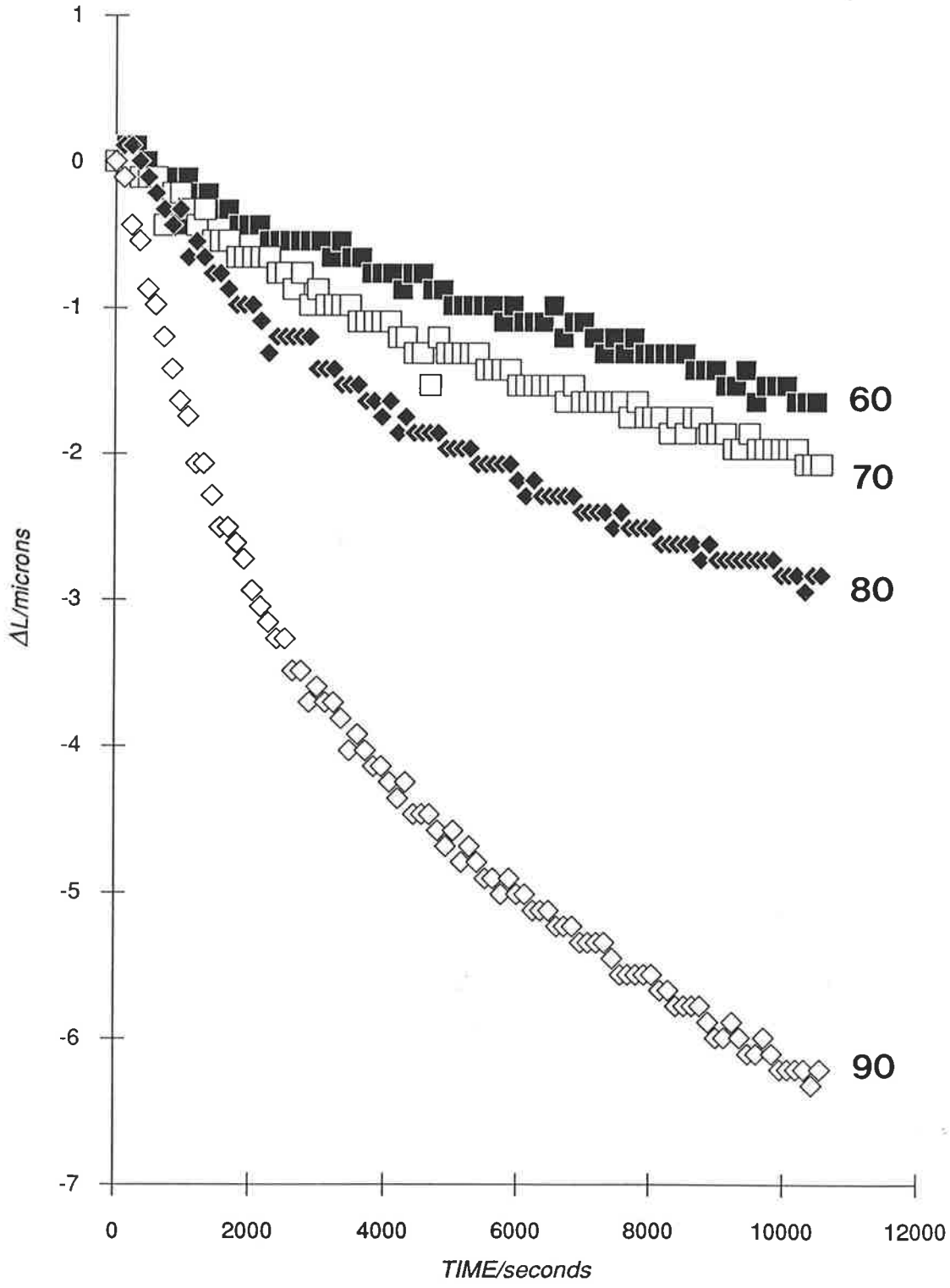

FIGURE 5.15 SEQUENTIAL AGEING IN QUENCHED PMMA (numbers adjacent to curves indicate the ageing temperature)

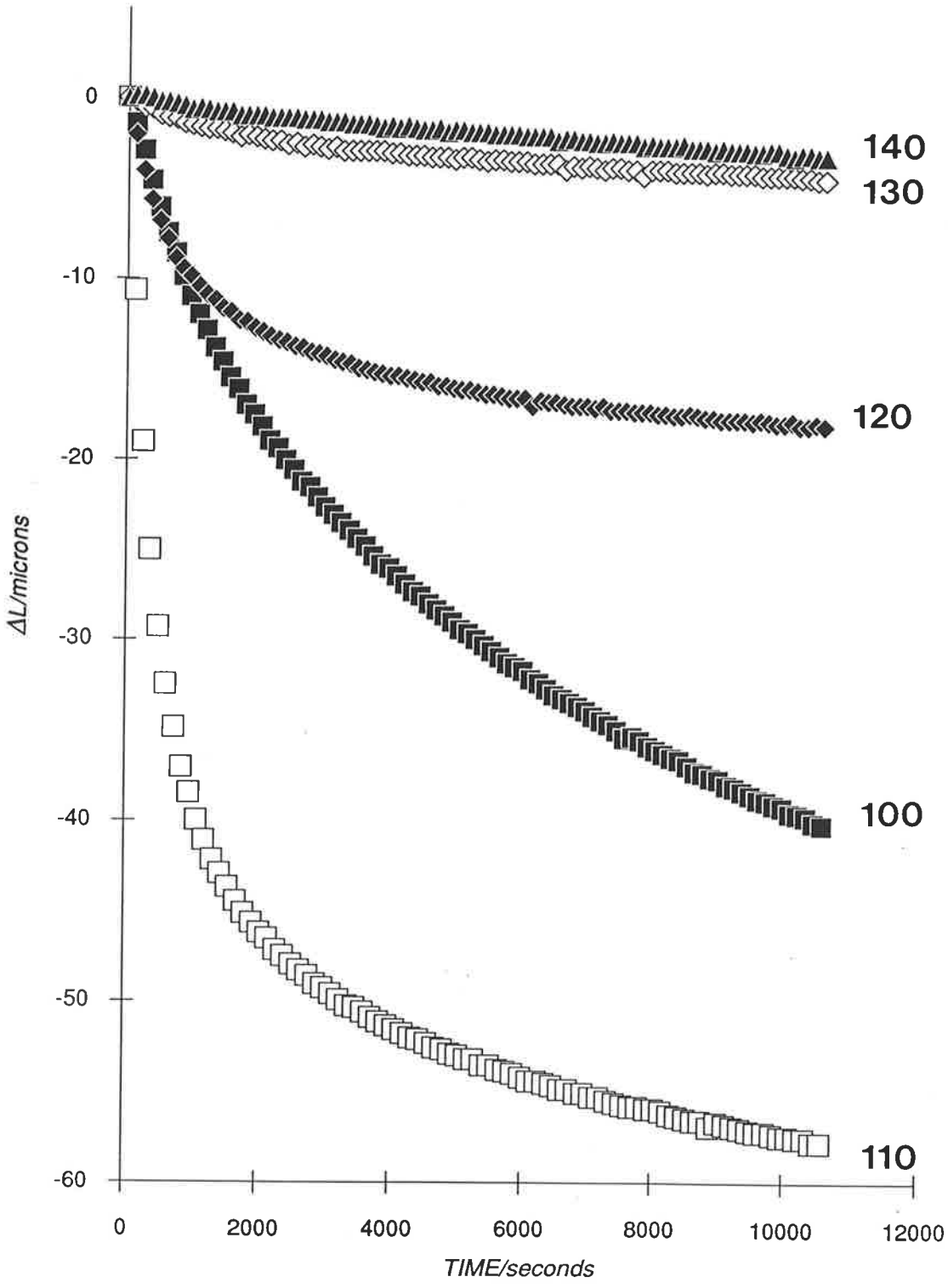

FIGURE 5.16 SUM OF FREE VOLUME FRACTION AS A FUNCTION OF ISOTHERMAL AGEING TEMPERATURE OVER 3 HOURS

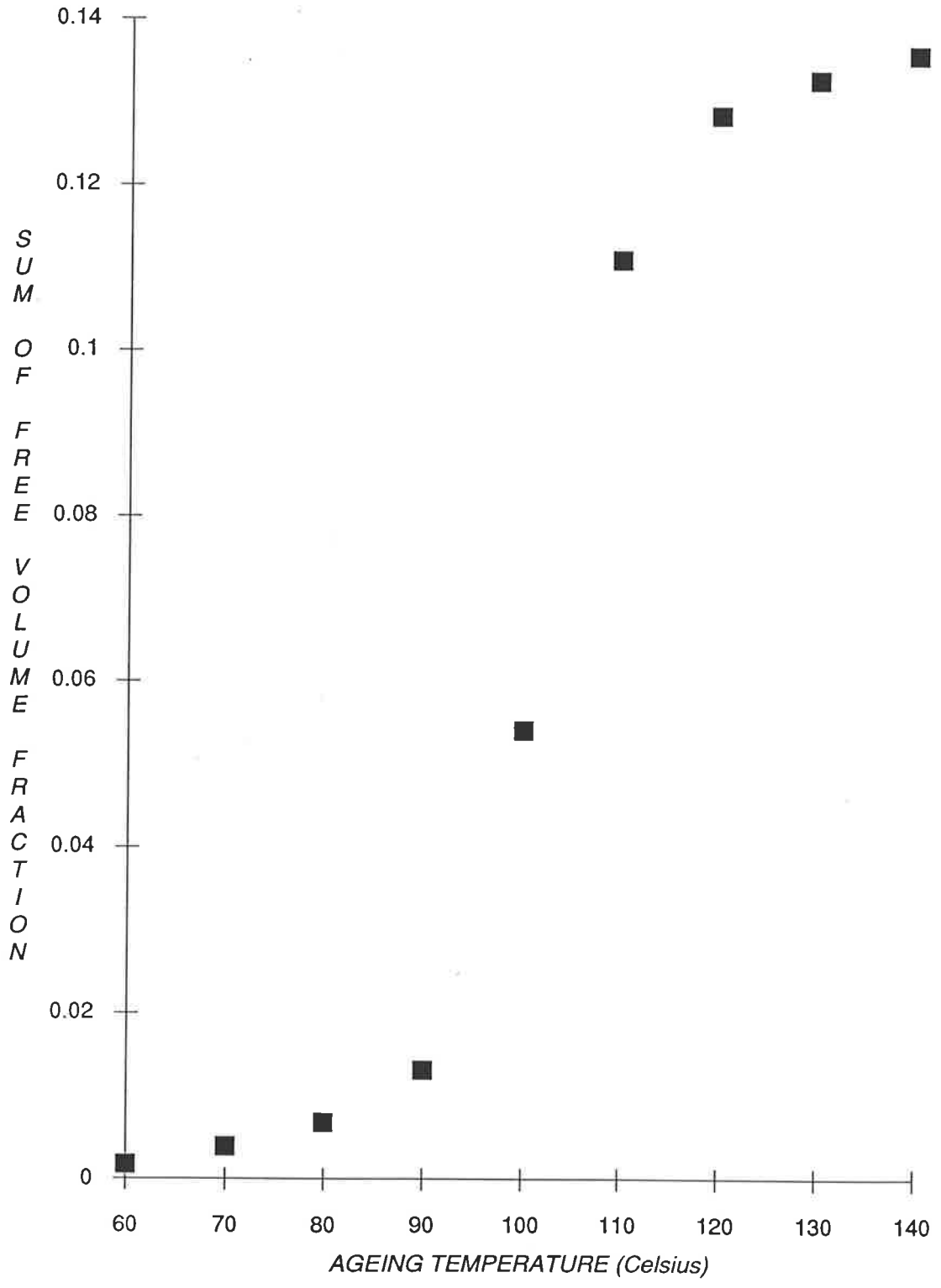

Relaxation Rates and Relaxation Times

The relaxation rate, -r, is calculated in the same way as for isothermal ageing. It is suggested that the rates of relaxation obtained by sequential ageing cannot be compared directly with the rates obtained isothermally because the specimens in the isothermal experiment have the same free volume fraction prior to ageing, whereas the specimen in the sequential ageing experiment has a lower free volume fraction at each succeeding step. However, the rates in Table 5.7 are comparable to the values in Table 5.3 in the region 60-90 C, where free volume changes are not significant. The rate of relaxation is greatest between 100-110 C indicating an increase in the rate of ageing in the glass transition region.

TABLE 5.7

Isothermal rates of relaxation measured between 60 C to 140 C

T_a (C)	$-dL_z/d\ln(t_a)$ (10^{-6} m.sec^{-1})	$-r$ (10^{-4} s^{-1})
60	1.348	10.82
70	1.179	9.46
80	1.125	9.03
90	2.496	20.03
100	15.194	122.0
110	13.736	110.3
120	2.479	19.90
130	1.780	14.29
140	2.131	17.10

To calculate the relaxation time $\tau(T_a)$, τ_g is assumed to remain unchanged at 1.65 x 10^{-2} s at 140 C. $\tau(T_a)$ was calculated as a function of $\exp(1/f_g - 1/\Sigma f(T_a))$ according to Equation 2.13 and the results are presented in Table 5.8. The relaxation times of sequentially aged PMMA are of the same order as those in Table 5.4, however, good agreement between the two sets of data is observed only at equilibrium. The large $\tau(T_a)$ values at 60-70 C may be attributed to the large initial free volume fraction during the early stages of sequential ageing, as

was observed for $\tau(T_a)$ at 40 C in Table 5.4. On the other hand, $\tau(T_a)$ decreases rapidly in the glass transition region between 100-120 C, where relaxation times of sequentially aged PMMA are lower than those obtained for isothermally aged PMMA. It is suggested that the differences in $\tau(T_a)$ in this temperature range are due to the fact that the free volume fraction of sequentially aged PMMA is progressively reduced at the end of each temperature step, such that ~10% of the total free volume fraction (0.136) has been removed prior to ageing at 100 C. Since $\tau(T_a)$ is a function of $1/\Sigma f(T_a)$, the recovery of free volume thus results in a decrease in $\tau(T_a)$.

TABLE 5.8

Isothermal relaxation times as a function of ageing temperature and free volume fraction determined after an isothermal period of 180 minutes

T_a (C)	$f_g - \Sigma f(T_a)$	$\tau(T_a)$ (s)	$\tau(T_a)/\tau_g$	t_{eq} (s)
60	0.134	6.4×10^{251}	3.9×10^{253}	5.4×10^{255}
70	0.132	2.2×10^{108}	1.4×10^{110}	1.9×10^{112}
80	0.129	1.96×10^{59}	1.19×10^{61}	1.66×10^{63}
90	0.123	1.08×10^{28}	6.55×10^{29}	9.17×10^{31}
100	0.082	1.17×10^{3}	7.07×10^{4}	9.89×10^{6}
110	0.025	8.66×10^{-2}	5.25	7.35×10^{2}
120	0.0076	2.55×10^{-2}	1.54	2.16×10^{2}
130	0.0033	1.98×10^{-2}	1.20	1.68×10^{2}
140	0.0003	1.68×10^{-2}	1.02	1.42×10^{2}

The plot of $\ln(\tau(T_a)/\tau_g)$ against $(1/T_a).1/\Sigma f(T_a)$ according to the modified N-equation (Equation 5.8) yields a slope of 333 K^{-1} and an intercept of -4.10 (Fig. 5.17). The activation energies obtained from the slope are in agreement with the values presented in Table 5.5, however, E_{act} obtained from the intercept are higher by a factor of 5 (Table 5.9). The large activation energies in the region 60-90 C support the hypothesis that a polymer is unlikely to attain equilibrium by isothermal ageing below T_g.

FIGURE 5.17 PLOT OF MODIFIED NARAYASWAMY EQUATION FOR QUENCHED PMMA AGED SEQUENTIALLY

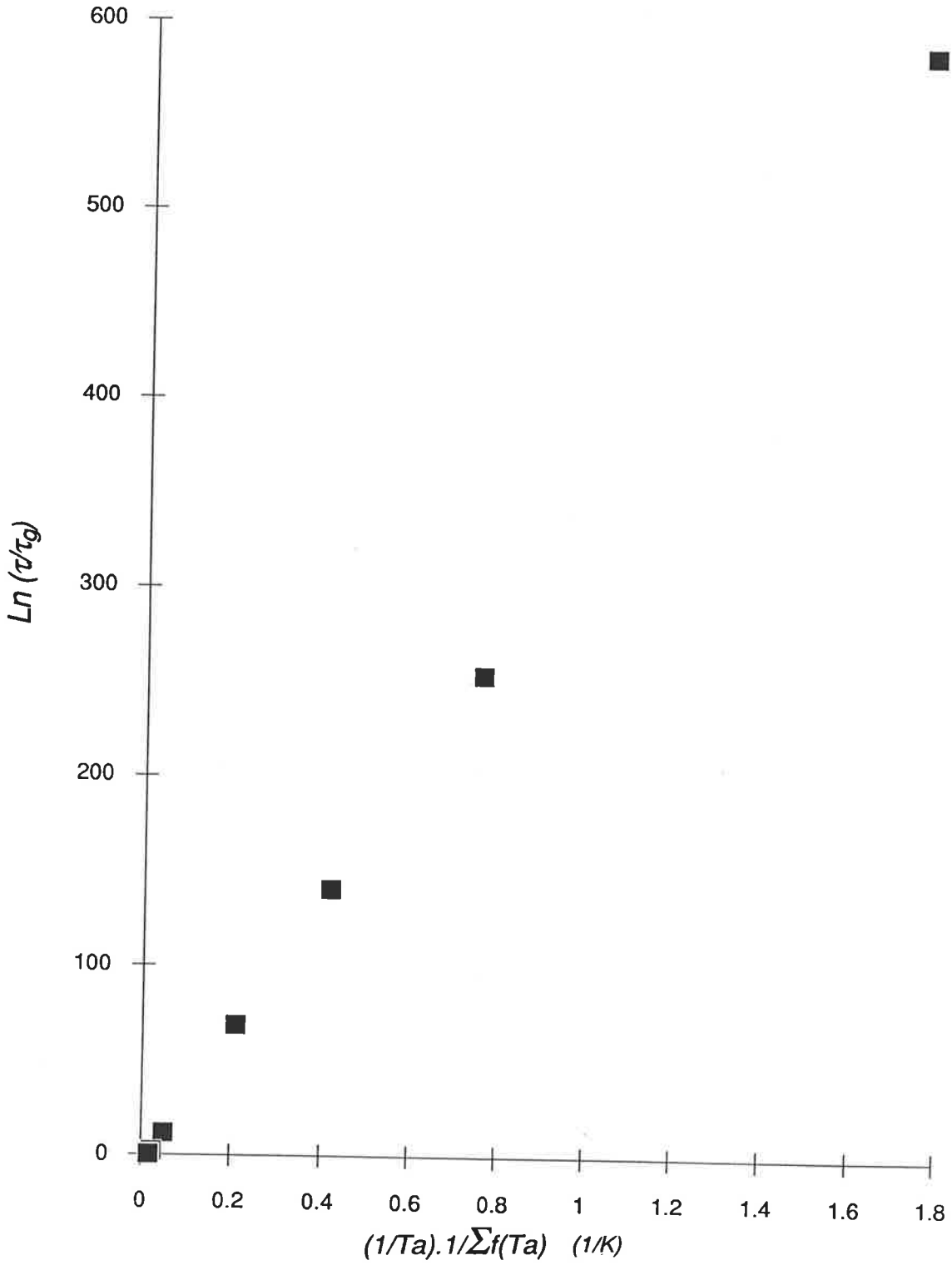

5.5 SUMMARY

(1) Length measurements during isothermal and sequential ageing of quenched PMMA has been measured. The contraction at equilibrium above T_g was found to correspond with the results obtained at a constant heating rate, in which the maximum free volume fraction frozen in quenched PMMA was approximately 0.13.

TABLE 5.9

Activation energies (kJ mol^{-1}) of sequentially aged poly(methyl methacrylate) as a function of isothermal ageing temperature and free volume fraction

T_a (C)	$\Sigma f(T_a)$	E_{act} (Eq. 5.9a)	E_{act} (Eq. 5.9b)
60	0.00169	1635	8113
70	0.0038	720	3572
80	0.00676	407	2018
90	0.0132	207	1027
100	0.0540	49	240
110	0.111	22	110
120	0.128	19	94
130	0.133	18	90
140	0.136	18	87

(2) In the temperature range 40-105 C, the collapse of free volume occured as a linear function of ageing temperature. This linear relationship suggested that the effectiveness of physical ageing in bringing about volume contraction within a period of 60 minutes ceases at about 20 C, and supported the hypothesis that additional free volume will be created by the freezing-in of secondary motions. One problem with the experimental reports from opponents of this hypothesis was that their polymer specimens were aged in temperature regions where secondary motions are still active, and hence their arguments are inconclusive.

(3) A modified form of the Narayaswamy expression was employed to calculate the activation energy barrier to structural relaxation at each isothermal temperature. Large activation energies were obtained for the temperature range below T_g suggested that physical ageing

involved relaxation mechanisms that are associated with cooperative main-chain motion. On the basis of the available experimental evidence, it appeared doubtful that a specimen can be aged to equilibrium without the participation of main-chain relaxation.

(4) Sequential ageing of PMMA showed that the rate of ageing is dependent on the ageing temperature and the free volume fraction. A general trend was observed, in which the initial rate of ageing was slow but steadily increased to a maximum in the glass transition region before decreasing again as the specimen approached equilibrium.

Chapter 5

1. A.J. Kovacs, *J. Polym. Sci.* **30**, 131 (1958).
2. A.J. Kovacs, *Fortschr. Hochpolym. Forsch.* **3**, 394 (1963).
3. L.C.E. Struik, *Physical Ageing in Amorphous Polymers and Other Materials*, Elsevier, Amsterdam (1978).
4. H.D. Lee and F.J. McGarry, *J. Macromol. Sci.-Phys.* **B29(1)**, 11-29 (1990).
5. J. Bartos, J. Muller and J.H. Wendorff, *Polymer* **31**, 1678 (1990).
6. R.E. Robertson, *J. Polym. Sci. Polym. Symp.* **63**, 173 (1978).
7. L.C.E. Struik, *Ann. N. Y. Acad. Sci.* **279**, 78 (1978).
8. A.J. Hill, K.J. Heater and C.M. Agrawal, *J. Polym. Sci. Polym. Phys.* **28**, 387 (1990).
9. L.C.E. Struik, *Polymer* **28**, 1869 (1987).
10. R.Diaz-Calleja, A. Ribes-Grues and J.L. Gomez-Ribelles, *Polymer* **30**, 1433 (1989).
11. J. Kolarik, *Adv. Polym. Sci.* **46**, 120 (1982).
12. J. Heijboer, *Physics of Non-Crystalline Solids*, North Holland, Amsterdam (1965).
13. D.J. Meier, *Molecular Basis of Transitions and Relaxations*, Gordon and Breach, New York (1978).
14. R.A. Haldon and R. Simha, *J. Appl. Phys.* **39(3)**, 1890 (1968).
15. R. Simha and R.F. Boyer, *J. Chem. Phys.* **37(5)**, 1003 (1962).
16. L.C.E. Struik, *Polym. Eng. Sci.* **17(3)**, 165 (1977).
17. L.C.E. Struik, *Polymer* **28**, 57 (1987).
18. G.P. Johari, *Ann. N. Y. Acad. Sci.* **279**, 117 (1976).
19. G.P. Johari, *J. Chem. Phys.* **77**, 4619 (1982).

20. V.E. Malpass, *Appl. Polym. Symp.* **12**, 267 (1969).

21. L. Guerdoux and E. Marchal, *Polymer* **22**, 1199 (1981).

22. E. Ito, K. Tajima and Y. Kobayashi, *Polymer* **24**, 877 (1983).

23. E.J. Roche, *Polym. Eng. Sci.* **23**, 390 (1983).

24. A.K. Doolittle, *J. Appl. Phys.* **22**, 1471 (1951).

25. J.M. Hutchinson and A.J. Kovacs, *J. Polym. Sci. Polym. Phys. Ed.* **14**, 1575 (1976).

26. A.J. Kovacs, J.M. Hutchinson and J.J. Alkonis, *Proceedings of the Symposium on the Structure of Non-Crystalline Materials*, Cambridge, England (1976), P.H. Gaskell ed., Taylor and Francis (1977), p153.

27. A.J. Kovacs, J.J. Aklonis, J.M. Hutchinson and A.R. Ramos, *J. Polym. Sci. Polym. Phys.* Ed. **17**, 1097 (1979).

28. J. Perez, *Polymer* **29**, 483 (1988).

29. R. Greiner and F.R. Schwarzl, *Rheol. Acta.* **23**, 378 (1984).

30. I.M. Hodge, *Macromolecules* **19**, 936-938 (1986).

31. O.S. Narayanaswamy, *J. Am. Ceram. Soc.* **54**, 491 (1971).

32. C.T. Moynihan, A.J. Easteal, M.A. DeBolt and J. Tucker, *J. Am. Ceram. Soc.* **59**, 12 (1976).

33. A.Q. Tool and C.G. Eichlin, *J. Am. Ceram. Soc.* **14**, 276 (1931).

34. I.M. Hodge, *Macromolecules* **20**, 2897 (1987).

35. I.M. Hodge and A.R. Berens, *Macromolecules* **15**, 762-770 (1982).

36. J.L. Gomez-Ribelles, A. Ribes-Greus and R. Diaz-Calleja, *Polymer* **31**, 223 (1990).

37. I.M. Hodge and A.R. Berens, *Macromolecules* **18**, 1980-1984 (1985).

38. M.L. Williams, R.F. Landell and J.D. Ferry, *J. Am. Chem. Soc.* **77**, 3701 (1955).

39. I.M. Hodge, *Macromolecules* **16**, 898 (1983).

40. G. Adams and J.H. Gibbs, *J. Chem. Phys.* **43**, 139 (1965).

41. J.L. Gomez-Ribelles, *Eng. Sci. D. Thesis*, Universidad Politecnica de Valencia (1983).

42. K. Deutsch, E.A.W. Hoff and W. Reddish, *J. Polym. Sci.* **13**. 565 (1954).

43. S. Saito and T. Nakajima, *J. Appl. Polym. Sci.* **2**, 93 (1959).

44. G.P. Mikhailov, *J. Polym. Sci.* **30**, 605 (1958).

45. N.G. McCrum, B.E. Read and G. Williams, *Anelastic and Dielectric Effects in Polymeric Solids*, Wiley (1967).

46. J. Heijboer, J.M.A. Bass, B. van de Graaf and M.A. Hoefnagel, *Polymer* **28**, 509 (1987).

47. J.M.G. Cowie and R. Ferguson, *Polymer* **28**, 503 (1987).

48. H.H.D. Lee and F.J. McGarry, *J. Macromol. Sci. Phys.* **B29(2&3)**, 237-248 (1990).

GLOSSARY OF SYMBOLS

A	Pre-Exponential Factor
$\alpha'_{g,\,l}$	Linear Thermal Expansion Coefficient of the Glass and Liquid State
$\delta(T_a)$	Departure From Equilibrium at T_a
dT/dt	Experimental Heating Rate
E_{act}	Energy of Activation
f	Free Volume Fraction
$f(T_a)$	Fractional Free Volume Recovered After Isothermal Ageing at T_a
Δf	Unrecovered (Unaged) Fractional Free Volume in Polymer Specimen
f_g	Free Volume Fraction at Thermodynamic Equilibrium
Δh^*	Enthalpy of Activation
L_z	Sample Length Measured Along the Z-Axis (Thickness)
$L_{x,y}$	Sample Length Measured Along the (X, Y) Axis
ΔL_z, ΔL	Length Contraction
N	Narayanaswamy
R	Universal Gas Constant
r	Isothermal Rate of Relaxation
T_g	Glass Transition Temperature
T_a	Isothermal Ageing Temperature
T_{eq}	Temperature at Which Thermodynamic Equilibrium is Readily Attained
T_f	Fictive Temperature
T_r	Temperature at Which the Relaxation Time is One Second
T_β	Temperature Denoting the Maximum of the Secondary Relaxation Peak
t_a	Isothermal Ageing Period
t_{eq}	Time Required for the Establishment of Thermodynamic Equilibrium
$\tau(T_a)$	Retardation Time at T_a
τ_g	Retardation Time at Thermodynamic Equilibrium
V_f	Macroscopic Free Volume
WLF	Williams-Landell-Ferry
x	Empirical Measure of Non-Linearity

CHAPTER 6
RANDOMISATION AND PHYSICAL AGEING IN ORIENTED PMMA

6.1 INTRODUCTION 127

6.2 EXPERIMENTAL 129

6.3 RESULTS AND DISCUSSION

6.3.1 Quenched Oriented PMMA

Dimensional Changes 129

Thermal Expansion Coefficient 132

6.3.2 Slow-Cooled Oriented PMMA

Length Changes Under Constant Rate of Heating 133

Length Changes During Sequential Ageing 134

Relaxation Times and Free Volume Fraction 135

Activation Energy of Randomisation 135

6.4 SUMMARY 137

BIBLIOGRAPHY 138

GLOSSARY OF SYMBOLS 140

CHAPTER 6

6.1 INTRODUCTION

When a polymer is subjected to rapid cooling from above to below T_g, three types of dimensional instability are generally observed.

(1) The spontaneous volume relaxation of the polymer leads to a gradual increase in density with time [1-2]. The glass state below T_g is a thermodynamically unstable state hence the approach towards attaining an equilibrium structure becomes a driving force for molecular rearrangement and volume relaxation [3]. This type of dimensional instability is known as physical ageing and occurs in most amorphous polymers below T_g.

(2) The second type of dimensional instability arises as a result of non-uniform temperature distribution in the polymer. As the surface of a polymer cools more rapidly than the interior, the initial contraction at the surface can be accommodated by the core which is still in the melt state. On the other hand, when the core cools down and hardens, the contraction in the interior is not easily accommodated by the surface which had already become glassy. Thermal stresses are thus built up in the polymer, in which surface stresses are generally compressive and interior stresses are tensile in nature [4-5].

(3) The third type of dimensional instability arises when amorphous plastic products are manufactured by the deformation of the material in the molten or rubbery state and subsequently cooled rapidly to below T_g. This deformation produces molecular orientation which is frozen-in upon cooling [6]. An amorphous polymer is said to be oriented when the direction of the main-chain segments are not distributed randomly in space [7-8]. Although molecular orientation in polymers is generally accompanied by frozen-in strains, it should not be confused with mechanical strains or frozen-in deformations. It has been shown [9-10] that the extent of orientation cannot be determined directly from the degree of deformation, nor from dimensional changes accompanying the release of stresses when the polymer is heated to above T_g.

Mechanical deformation associated with segmental motion (e.g. molecular orientation) is said to generate free volume, irrespective of the nature of the deformation (e.g. tensile, uniaxial compression, shear) [2]. The origin of this hypothesis was based on the free

volume concept [11] which implies that the segmental mobility is determined by the free volume. Mechanical tests at low strains show that the free volume of a glassy polymer is too small to allow large scale segmental motion, yet such large scale motion appears to be possible at sufficiently high stress levels. It follows that the requisite free volume must have been generated during the deformation of the polymer. But what causes the increase in free volume during mechanical deformation? Matsuoka and Bair [12] performed an experiment involving pure shear of polycarbonate (PC) and found that there was an enthalpy increase with shear deformation. According to their model, this suggested an increase in free volume with shear. If a polymer is mechanically dilated, the relaxation time will become decrease rapidly since the relaxation time is an exponential function of (1/f) (see Equations 2.12-2.13). The volume increase may be considered as the mixing of additional vacant sites, with the final result being a net increase in fractional free volume. However, if a polymer is subjected to a quick compression, the imposed rate of deformation is greater than $1/\tau$ and the material will simply respond elastically by reducing its occupied volume. The specific volume of the polymer would be reduced but not the free volume fraction, thus the net effect of uniaxial compression is an increase in free volume fraction and a reduction in relaxation time [13].

The *randomisation* of an oriented amorphous polymer is defined as a process in which the polymer loses its imposed molecular orientation to obtain a random, amorphous structure. As the amount and distribution of free volume of an amorphous polymer is expected to change upon deformation, it is of interest to consider the effects of molecular orientation on physical ageing. Bartos *et al.* [14] reported that the rate of ageing of polycarbonate was increased by cold-drawing, presumably from an increase in the width of the free volume distribution. However, dimensional changes attributed to randomisation have been shown to be anisotropic and is dependent on the direction of the imposed deformation [1]. So far, there is little indication if the effects of molecular orientation on physical ageing are uniform and independent of direction.

The main objective of this chapter is to study the dimensional changes of uniaxially-compressed amorphous PMMA and to separate and distinguish the changes that are associated with randomisation from those caused by physical ageing. The hypothesis [2] that free volume is generated by mechanical deformation was also examined by comparing free volume fractions of oriented PMMA with values obtained for unoriented PMMA in Chapters 4 and 5.

6.2 EXPERIMENTAL

Cast PMMA specimens have been uniaxially compressed to two different thicknesses from an initial thickness of ~1624 μm, according to the following thermal histories.

(1) Quenched specimens were compressed between copper blocks in a specially-constructed compression apparatus at 150 C for 10 minutes, followed by quenching in liquid nitrogen for 10 minutes. The specimen was then allowed to warm to 25 C over a period of 20 minutes under dry nitrogen inside the TMA. Specimens were heated in the TMA from 25 C to 165 C at a constant rate of 2 C/min under a static load of 0.1 N. Separate measurements were carried out to measure the dimensional changes perpendicular (z-axis) and parallel ((x, y)-axis) to the orientation axis. The sample lengths along the z- and (x,y)-axes were *ca* 1100 and 5800 μm respectively. Specimens prepared by this method have been designated as "quenched oriented PMMA",

(2) Slow-cooled specimens were prepared by compressed between steel blocks in a hydraulic press at 140 C for 5 minutes, followed by stepwise cooling in which the temperature of the specimen was lowered to 25 C in decrements of 10 C after an isothermal period of one hour at each temperature. Thermal analysis involved heating the specimen from 60 C to 130 C in increments of 10 C (except between 110 C and 120 C, where the temperature was first raised to 115 C from 100 C) where the specimen was isothermally aged for different periods from 10,000 to 21,000 seconds at each temperature step (see Table 5.1 and Figure 5.1 for thermal profile). Specimens prepared according to this method are designated as "slow-cooled oriented PMMA", in which the average sample length was about 300 μm.

6.3 RESULTS AND DISCUSSION

6.3.1 Quenched Oriented PMMA

Dimensional Changes

Figure 6.1 shows the ΔL-T plots of quenched oriented PMMA measured parallel and perpendicular to the axis of orientation. The ΔL-T plot of quenched unoriented PMMA is also included for comparison. At the completion of each experiment and after the specimens had cooled, it was observed that the oriented specimens always regained its initial dimensions in

FIGURE 6.1 LENGTH CHANGES IN QUENCHED ORIENTED AND UNORIENTED PMMA

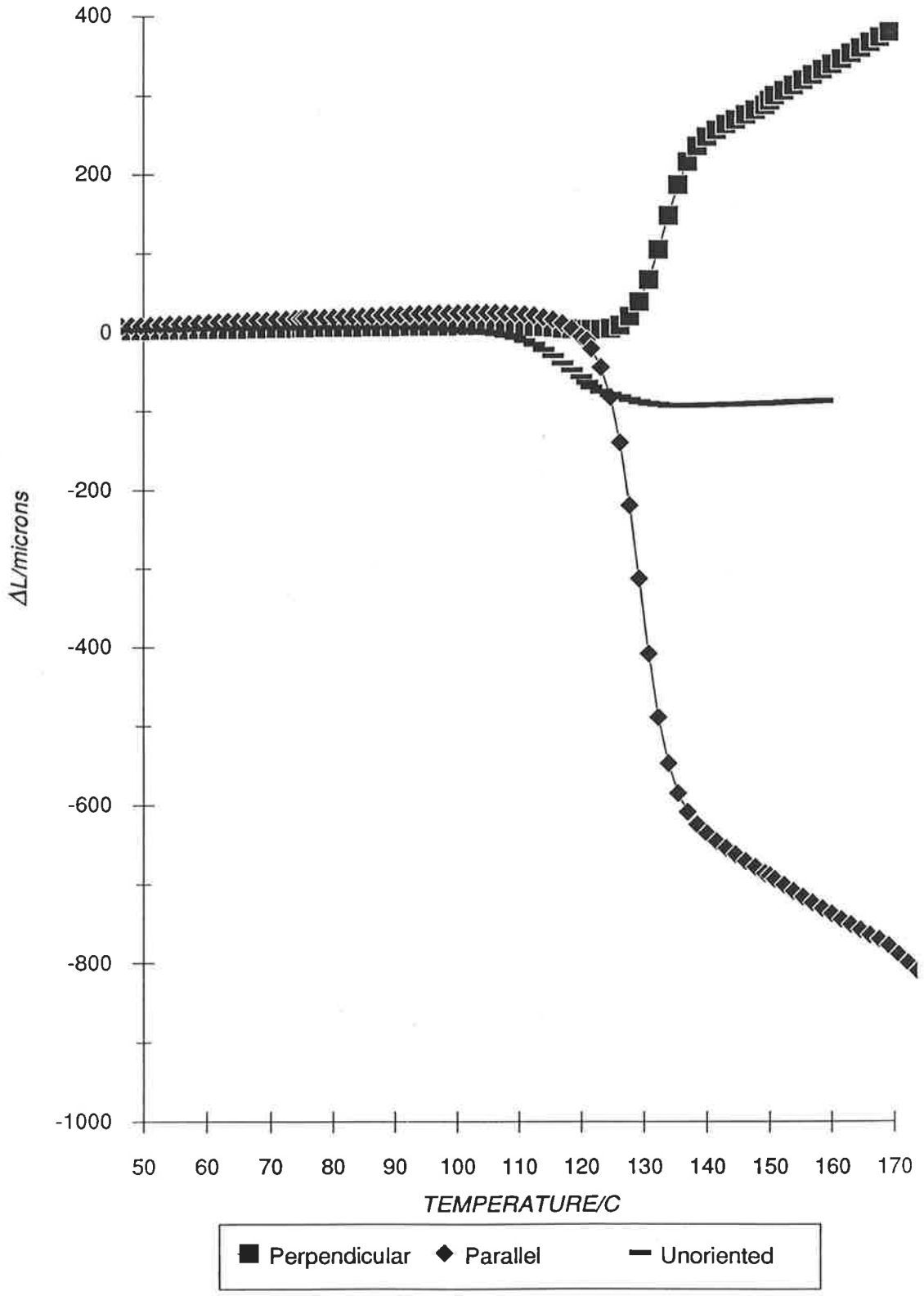

the unoriented state, which served as tangible proof that the orientation in the specimen had been completely removed.

Significant length changes (250-600 μm) were displayed by the oriented specimens above T_g in the temperature range 125-140 C. These large length changes are attributed to randomisation in which oriented specimens lose their molecular orientation in the process of attaining a random structure. Randomisation of an oriented polymer is attributed to the release of frozen-in entropic stresses which act in the opposite direction to the imposed deformation [15]. These stresses may be understood by considering an unoriented polymer which is compressed by an external stress σ. If the compression was carried out at equilibrium the polymer chains will be oriented to the extent that the rubber-elastic reaction stress σ_r balances σ. If the compressed specimen is suddenly cooled to below T_g and the applied deformation is then removed, the molecular orientation and the entropic stress σ_r will be frozen-in [6]. The entropic stresses of oriented glassy polymers is quite considerable, and had been measured to be 20-25 MPa for drawn polycarbonate [16] and 18-31 MPa for drawn poly(ethylene) [17]. The frozen-in entropic stresses are only manifested when the oriented polymer is heated, in which the changes in dimension accompanying the release of stresses will depend on the direction of orientation. This is supported by the observation that dimensional changes associated with randomisation depended on the direction of measurement relative to the orientation axis. Expansion is observed when the measurement is perpendicular to the orientation axis, whereas contraction is observed when the measurement is parallel to the orientation. These observations indicate that the polymer chains are aligned along the (x, y) axis (Fig. 6.2). No explanation could be offered at the present time regarding the gradual contraction observed above 140 C in the parallel direction, even though there is no indication of permanent indentation on the specimen as proof of viscous flow (Section 7.3.4).

Physical ageing always results in length contraction. The temperature range of physical ageing in quenched unoriented PMMA lies between 104-132 C (Section 4.4.2), which indicates that randomisation is preceded by ageing and that the removal of molecular orientation requires a greater degree of segmental motion and a larger free volume fraction. A trace of contraction was observed for oriented PMMA measured perpendicular to the axis of orientation whereas a length change of about 650 μm in the range 120-135 C was observed in the parallel direction. Since length changes associated with physical ageing and randomisation parallel to

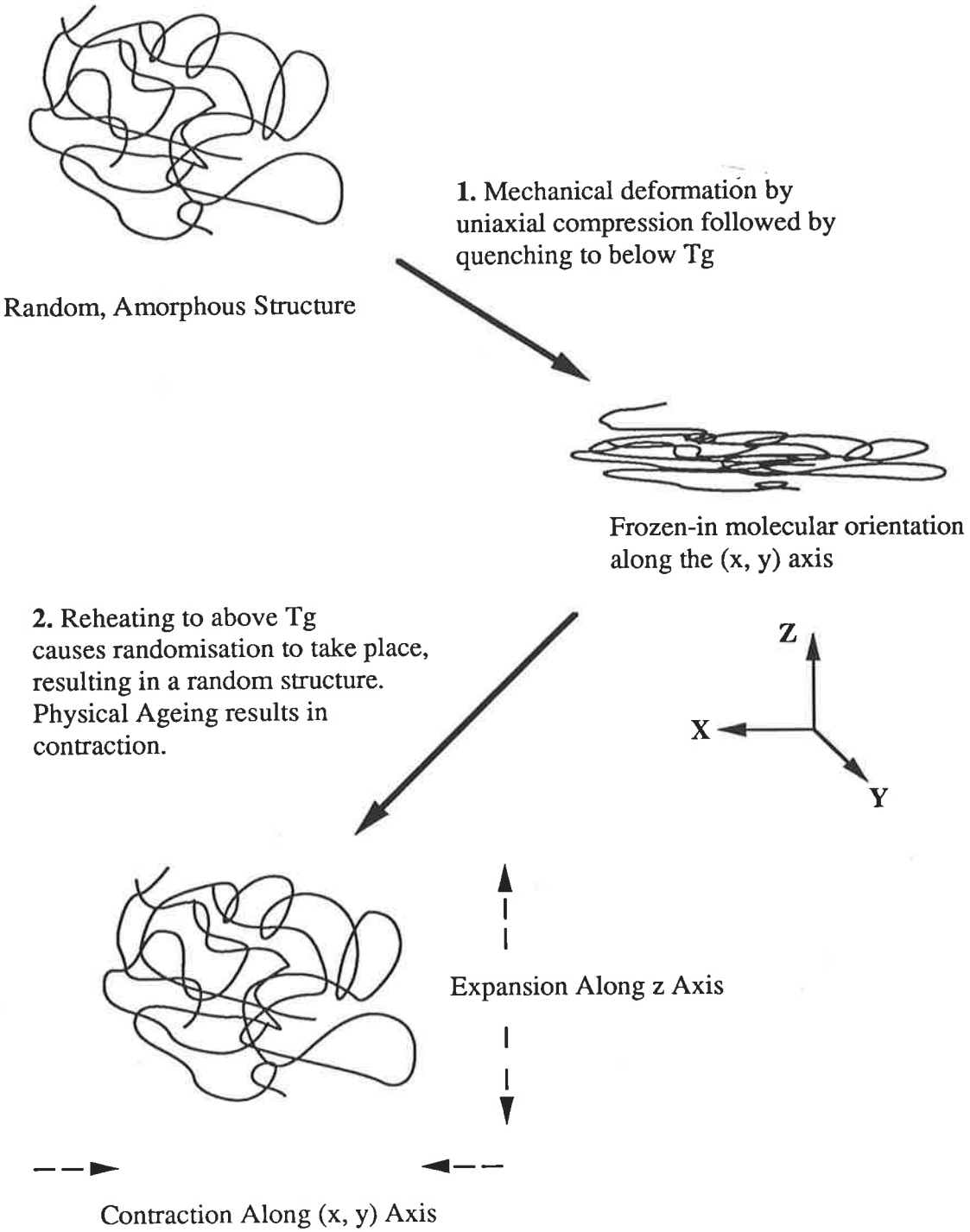

Figure 6.2 The introduction of molecular orientation by uniaxial deformation and length changes accompanying randomisation, which reverts the oriented polymer back to its original random structure.

the orientation result in contraction, it is difficult to distinguish the two processes from the parallel curve. In addition, there is an overlap in the temperature range of ageing and randomisation at about 130 C, which suggests that the same molecular mechanisms may be operating for both ageing and randomisation above T_g. However, randomisation in the perpendicular direction results in length expansion which is opposite in direction to the contraction ascribed to physical ageing. Therefore, the study of length changes of oriented PMMA in the perpendicular direction is more suitable for distinguishing the effects of ageing and randomisation. Although the perpendicular curve in Figure 6.1 clearly shows the expansion ascribed to randomisation between 125-140 C, the effects of physical ageing are not noticeable. On the other hand, dimensional changes associated with both processes are observed in sequentially aged oriented PMMA which will be discussed in Section 6.3.2.

Struik [2] found little difference in the shift rates of creep curves of stretched and amorphous poly(vinyl chloride) (PVC), and suggested that oriented polymers will age in the same way as unoriented ones. Contrary to Struik's claim, dimensional changes of oriented PMMA measured perpendicular to the orientation displayed only a trace of contraction, but when the measurement was made parallel to the orientation the magnitude of contraction was at least six times greater than that usually observed for unoriented PMMA. The different dimensional behaviour exhibited by the oriented and unoriented specimens suggests that the free volume fraction is not the same for the two types of polymer.

The free volume fraction of quenched unoriented PMMA has been shown in Chapters 4 and 5 to reach a maximum value of about 0.13. If the hypothesis [2, 12] that extra free volume is generated by mechanical deformation or by molecular orientation is correct, then the free volume fraction of the oriented specimens must be greater than 0.13. The free volume fraction of oriented PMMA is calculated from length changes ascribed to physical ageing and randomisation between 105-137 C, and it is assumed that dimensional changes associated with both processes contribute to the annihilation of free volume. The length contraction in the parallel direction is $\Delta L_{x,y}$ = 24.0908 - (-609.476) = 633.567 x 10^{-6} m. But length changes in the perpendicular direction contain an expansion portion as well as a contraction portion, thus ΔL_z = (7.3030 - 3.1610) + (215.949 - 3.1610) = 216.93 x 10^{-6} m. The free volume V_f and fractional free volume f are calculated in the same way using Equations 4.1 and 4.3, where L_z and $L_{x,y}$ are 1.150 x 10^{-3} m and 5.830 x 10^{-3} m respectively. The calculations yield V_f = 8.06

x 10^{-9} m^3 and assuming an equilibrium volume of 3.80 x 10^{-8} m^3, f = 0.212, which indicates that the free volume fraction of quenched oriented PMMA has been increased by uniaxial compression.

Thermal Expansion Coefficient

It is well-established that the thermal expansion of oriented polymers is anisotropic and that this behaviour arises from the anisotropy of molecular chains [18-23]. The thermal expansion of polymers is related to the asymmetry and the depth of the binding potentials, in particular, the interchain potential [24-26]. It is assumed that the covalent bonds between the stiff C-C backbone chains have a lower expansivity than the Van der Waals bonds perpendicular to the chains [27]. This assumption is verified by the glass expansivities ($\alpha_g = 3\alpha'_g$) in Table 6.1, in which the axis of molecular orientation is along the (x, y)-axis and perpendicular to the z-axis. The data of Table 6.1 shows that $\alpha_g\perp > \alpha_g > \alpha_g//$, where the glass expansivities measured parallel and perpendicular to the axis of orientation are designated as $\alpha_g//$ and $\alpha_g\perp$ respectively, and α_g is the glass expansion coefficient of the amorphous polymer. This order of magnitude indicates that thermal expansion along the axis of orientation arises from intrachain vibrations of stiff carbon-carbon backbone chains, whereas the expansion perpendicular to the orientation is dominated by interchain vibrations of weak van der Waal bonds which results in a larger value for $\alpha_g\perp$.

TABLE 6.1

Linear and cubical glass thermal expansion coefficients (10^{-6} K^{-1}) of quenched unoriented and oriented poly(methy methacrylate)

Thermal History	α'_g	α_g
Quenched, Unoriented	67.1	201.3
Quenched, Oriented along (x, y)-axis ($\alpha_g//$)	57.8	173.4
Quenched, Oriented along z-axis ($\alpha_g\perp$)	104.2	312.6

The following relationship is found to hold for quenched oriented PMMA:

$$2.\alpha_g'\perp + \alpha_g'// = \alpha_g \qquad (6.1)$$

Using $\alpha'_g\perp = 104 \times 10^{-6}\ K^{-1}$ and $\alpha'_g// = 58 \times 10^{-6}\ K^{-1}$, the glass expansivity calculated from Equation 6.1 is $266 \times 10^{-6}\ K^{-1}$, which correlates with the value of $201.3 \times 10^{-6}\ K^{-1}$ obtained for unoriented PMMA. This result indicates that the volume expansivity of the glass state is not influenced by the degree of orientation, in agreement with the results of Struik [15].

6.4.1 Slow-Cooled Oriented PMMA

Length Changes Under Constant Rate of Heating

A slow-cooled oriented PMMA specimen was heated from 25 C to 160 C at a constant heating rate of 2 C/min under a load of 0.1 N. At the completion of the experiment, the sample recovered its original dimensions of $L_z \approx 1.6 \times 10^{-3}$ m and $L_{x,y} \approx 5.0 \times 10^{-3}$ m. Randomisation is evident by the large and sudden expansion of $\Delta L_z = 1.490 \times 10^{-3}$ m at 125 C (Fig. 6.3). The expansion ceased at approximately 140 C, in accordance with the expectation that equilibrium is readily attained at 140 C. As observed in Table 6.1, the thermal expansivity $\alpha'_g\perp$ is higher than the glass expansivity α'_g of unoriented PMMA, gradually increasing from $106.4 \times 10^{-6}\ K^{-1}$ at 40-70 C, to $170.8 \times 10^{-6}\ K^{-1}$ at 90 C and $308.3 \times 10^{-6}\ K^{-1}$ at 110 C. The large values of $\alpha'_g\perp$ are attributed to the increasing contribution of the anharmonic interchain vibrations with temperature [18].

Unfortunately, length changes could not be determined along the (x, y) axis because the final specimen thickness of 300 μm made measurements in the (x, y) direction impractical. Therefore, the free volume V_f cannot be calculated from Equation 4.1 without the knowledge of $\Delta L_{x,y}$. However, the free volume fraction can be estimated from $f = (V_0 - V_{eq})/V_{eq}$, where V_0 and V_{eq} are the initial and equilibrium volumes of the oriented polymer. The initial dimensions of the oriented specimen are $L_z = 3.00 \times 10^{-4}$ m and $L_{x,y} = 1.4 \times 10^{-2}$ m, thus $V_0 = 5.88 \times 10^{-8}$ m^3. It is assumed that the specimen will attain an equilibrium volume of 3.80×10^{-8} m^3, so $V_f = V_0 - V_{eq} = 2.08 \times 10^{-8}$ m^3 and $f = 0.55$. Uniaxial compression of amorphous PMMA has been shown again to result in an increase in free volume fraction.

FIGURE 6.3 RANDOMISATION IN HIGHLY ORIENTED POLY(METHYL METHACRYLATE)

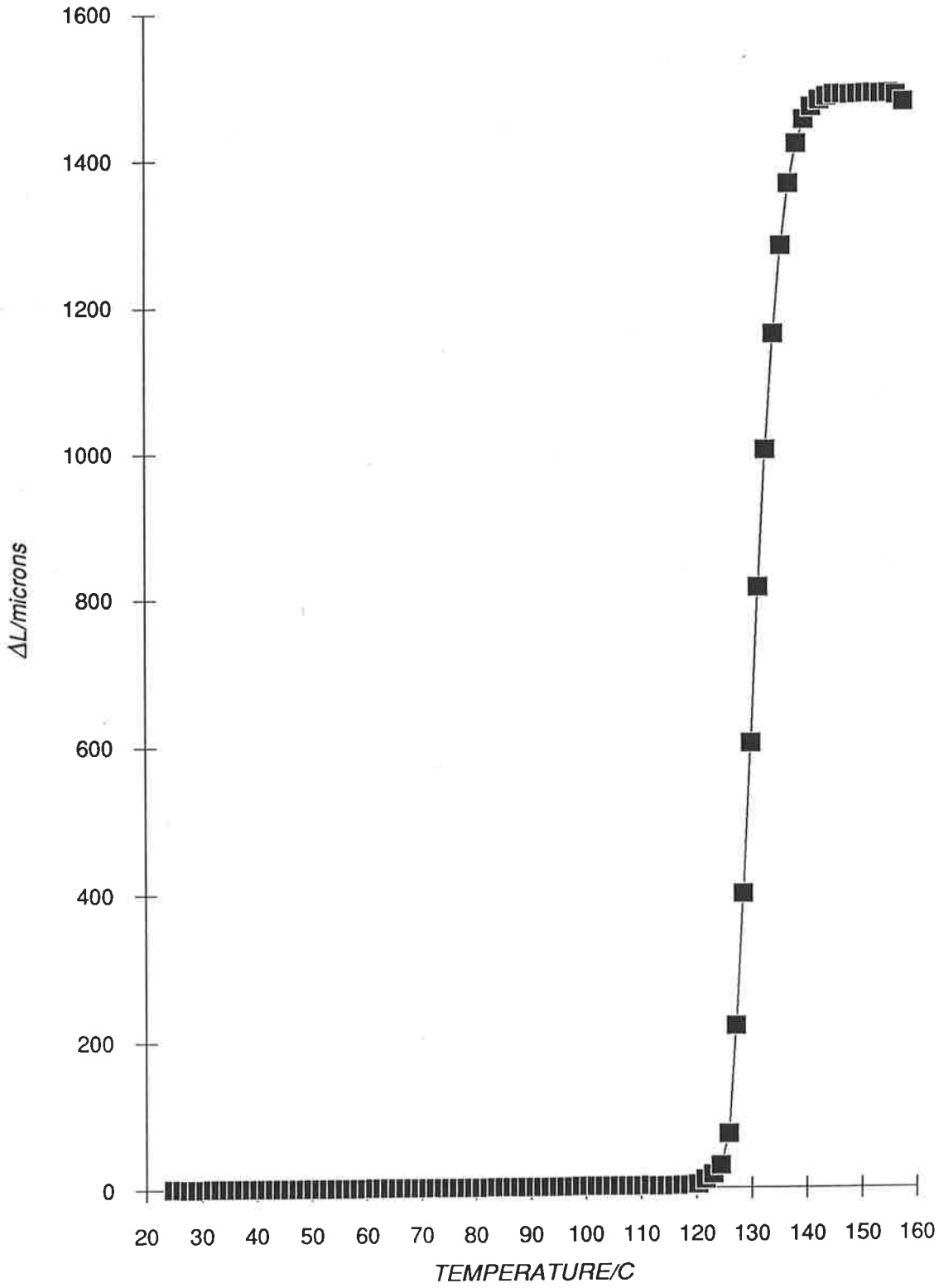

Length Changes During Sequential Ageing

Sequential ageing of slow-cooled oriented PMMA was carried out in the temperature range 60-130 C. The length change along the z-axis, ΔL_z, is plotted as a function of isothermal period t_a in Figures 6.4-6.5. Length changes measured at the end of the isothermal period (10,000-21,000 seconds) are plotted as a function of ageing temperature in Figure 6.6.

Length contraction associated with physical ageing is observed between 80-90 C (Fig. 6.4). However, the magnitude of ΔL_z of slow-cooled oriented PMMA is lower than the contraction observed for quenched unoriented PMMA (Fig. 5.14). For example, ΔL_z of the oriented specimen is approximately 0.7×10^{-6} m at 90 C after a period of 2×10^4 seconds, whereas the corresponding contraction after 1×10^4 seconds at 90 C is about 6.5×10^{-6} m for unoriented PMMA. It appears that the alignment of polymer chains tend to restrict the motions of molecular segments in the direction perpendicular to the orientation. Cooperative motion of main-chain segments have been shown in Chapter 5 to be a primary mechanism in the ageing process, hence it is suggested that the small values of ΔL_z are due to frozen-in orientation which is not erased below T_g (105 C). Similarly, the anomalous expansion observed at 60-70 C (Fig. 6.4) may be caused by the restricted motions of side-groups and main-chain segments such that physical ageing cannot take place at these temperatures.

An inspection of Figure 6.5 indicate a large and rapid expansion in the range 110-130 C. The greatest increase in length is observed at 120 C which is followed by a decrease in expansion at 130 C as the specimen approaches its random and unoriented dimensions. The expansion cannot be due to ageing, as sequential ageing of quenched unoriented PMMA resulted in length contraction (Figs. 5.14-5.15), hence the expansion must arise from randomisation. The observation of expansion in the glass transition region of PMMA indicates that randomisation is associated with cooperative motion in the main chain and suggests that randomisation cannot take place below T_g where cooperative motion is not possible. This suggestion is consistent with Figure 6.6, where there is relatively little change in length between 60-100 C followed by large increases in length from 110 C onwards. The effects of ageing and randomisation may be distinguished from Figures 6.5 and 6.6, in which dimensional changes below 110 C are affected by physical ageing and length changes ascribed to randomisation are observed between 110-130 C.

FIGURE 6.4 SEQUENTIAL AGEING OF HIGHLY ORIENTED POLY(METHYL METHACRYLATE)

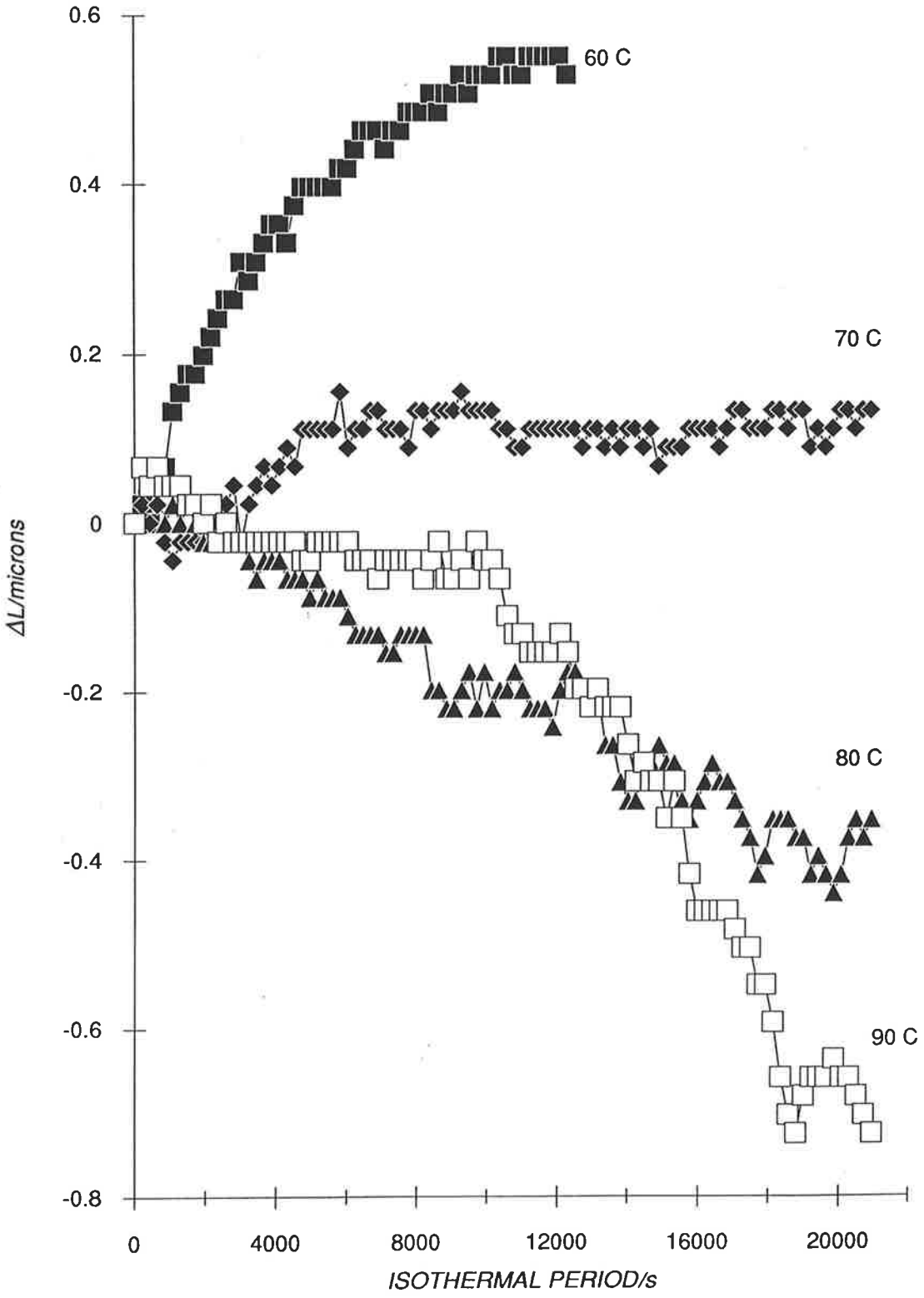

FIGURE 6.5 SEQUENTIAL AGEING OF HIGHLY ORIENTED POLY(METHYL METHACRYLATE)

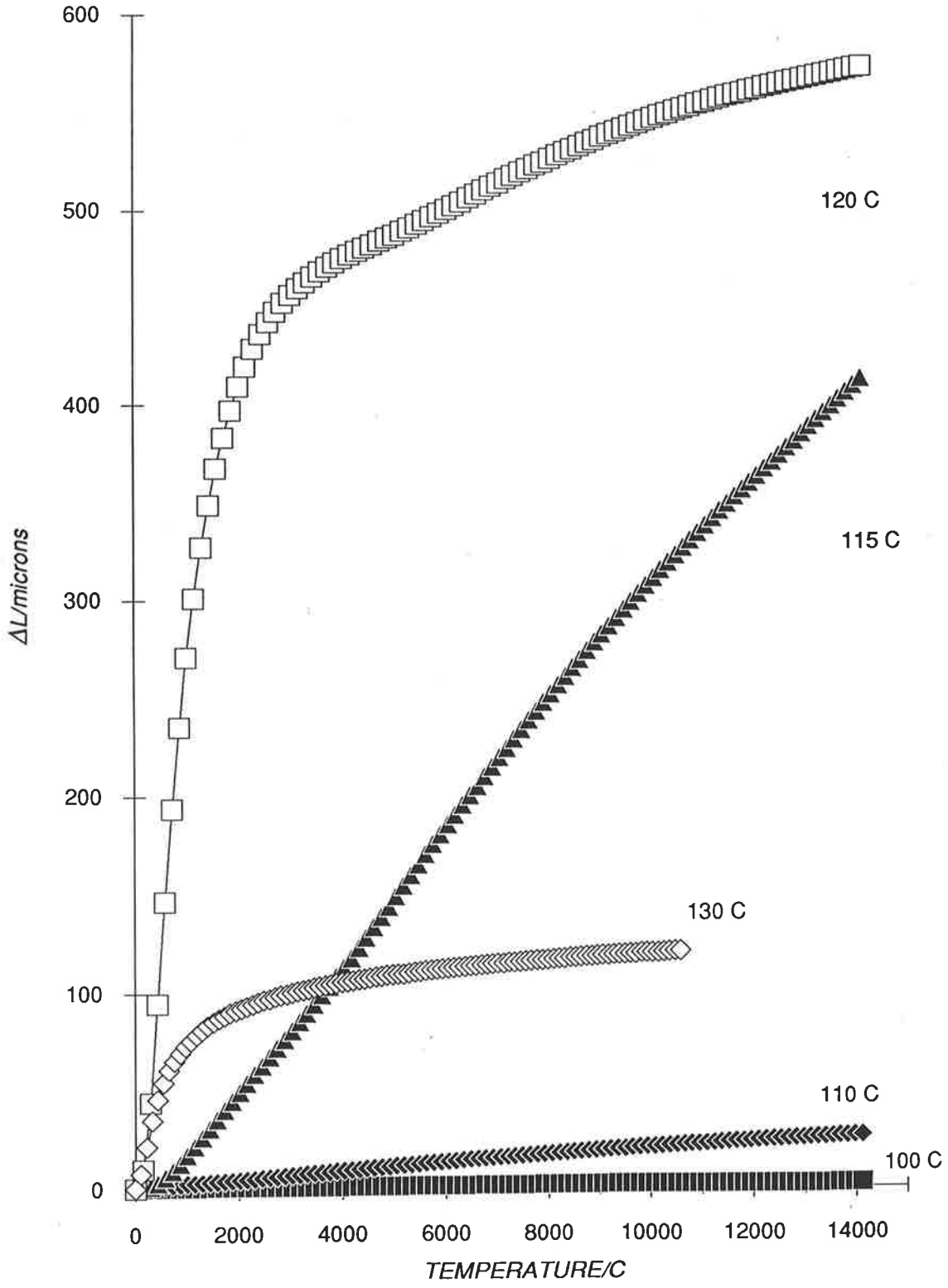

FIGURE 6.6 LENGTH CHANGE OF ORIENTED PMMA MEASURED PERPENDICULAR TO MOLECULAR ORIENTATION

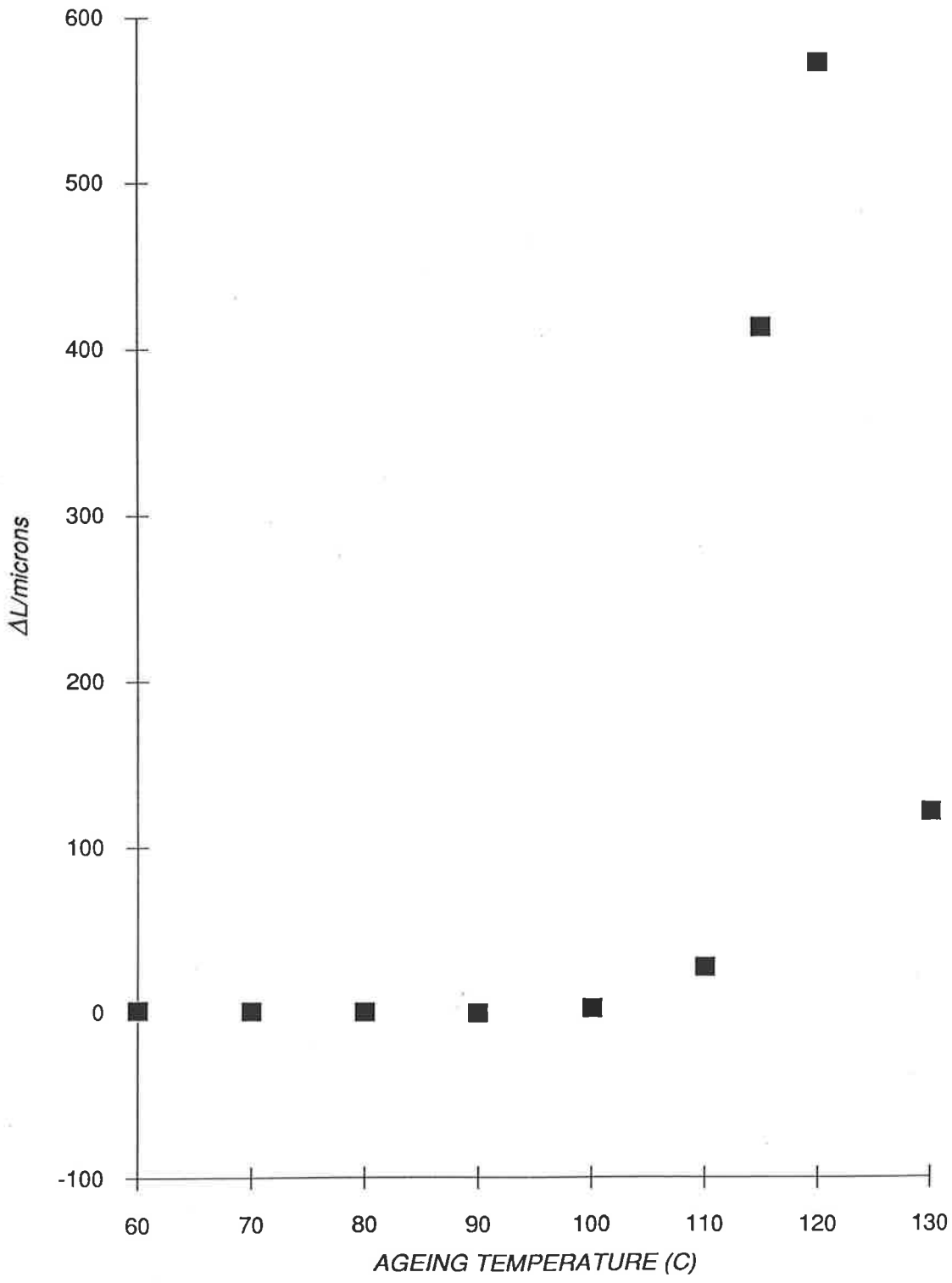

Relaxation Times and Free Volume Fraction

The anisotropy of length changes in an oriented specimen is clearly shown in Figure 6.1, and the ambiguity in the determination of $\Delta L_{x,y}$ means that the relaxation time and the fractional free volume cannot be calculated in a straightforward way using Equation 4.1 or 4.2. To obtain the free volume fraction recovered at each T_a, the following assumptions are made: (1) both length contraction and expansion contribute to the collapse of free volume, (2) the total sum of length change, $\Sigma\Delta L_z$, from 60-130 C represents the recovery of a free volume fraction f_g of 0.55, (3) the free volume fraction recovered at individual temperatures, $\Sigma f(T_a)$, is proportional to the final length change at 130 C, e.g. if total length change at 130 C is 1.00 x 10^{-3} m, the free volume fraction recovered when $\Sigma\Delta L_z = 0.50 \times 10^{-3}$ m will be 0.275, (4) the relaxation time at thermodynamic equilibrium (140 C), τ_g, is the same as determined for amorphous PMMA at 7.18 x 10^{-3} seconds, while the relaxation time at the ageing temperature T_a, $\tau(T_a)$, is estimated from $\tau_g.\exp(1/\Sigma f(T_a) - 1/f_g)$, and (5) as the data for 140 C is not available, the relaxation time at 130 C is taken to be 1.65 x 10^{-2} seconds.

Assumption (3) suggests that the free volume fraction can be characterised from ΔL_z alone, which constitutes an error as ΔL_z and $\Delta L_{x,y}$ are not of equal magnitude. However, it is impossible to estimate $\Delta L_{x,y}$ at different ageing temperatures, therefore the values of $\tau(T_a)$ and f have to be approximated from ΔL_z. The ensuing discussion will nevertheless show that the values of the parameters in Table 6.2 do not contradict the hypothesis that molecular rearrangement during randomisation is a result of main-chain relaxation. The asterisk (*) indicates that the values of $\tau(T_a)$ are too large for evaluation between 60-90 C, which indicates that the fractional free volume recovered at these temperatures is very small in comparison with the total free volume fraction of 0.55.

Activation Energy of Randomisation

It has been shown in Section 5.3.2 that a modified Narayanaswamy equation [28-29] (Eq. 5.8) adequately describes the temperature dependence of free volume fraction and $\tau(T_a)$ for sequentially-aged unoriented PMMA. Figure 6.7 shows the plot of $\mathrm{Ln}(\tau(T_a)/\tau_g)$ against $(1/\Sigma f(T_a)).(1/T_a)$, where T_{eq} is 413 K and 373 K $\leq T_a \leq$ 403 K. The equation of the line is:

FIGURE 6.7 PLOT OF MODIFIED NARAYANASWAMY EQUATION USING SEQUENTIAL AGEING DATA OF SLOW-COOLED ORIENTED PMMA

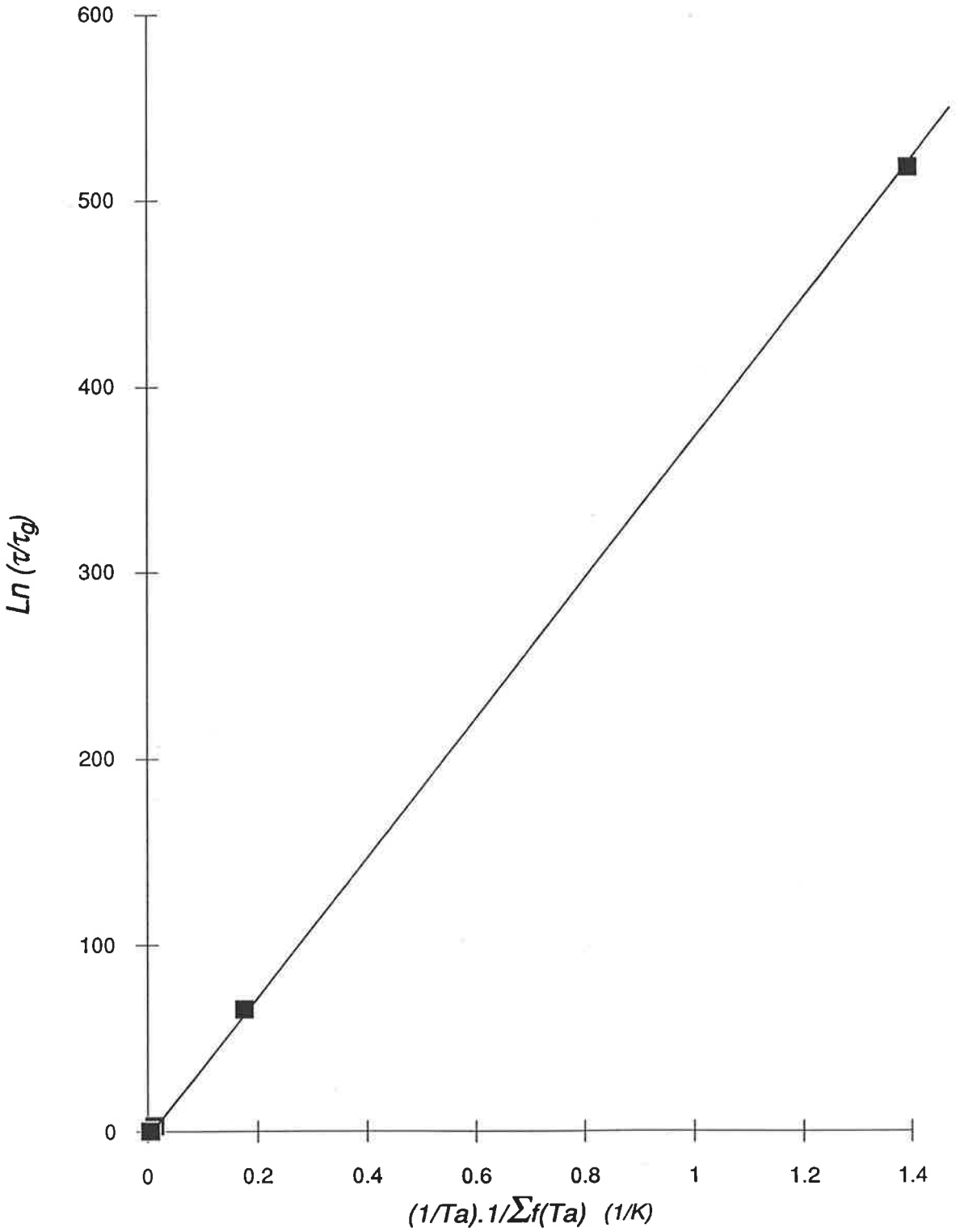

$$\mathrm{Ln}(\tau(T_a)/\tau_g) = 373.(1/\Sigma f(T_a)).(1/T_a) - 1.301 \qquad (6.2)$$

where R is the universal gas constant and the slope is equal to $-E_{act}.(1 - 1/f)^{-1}/R$. The activation energies calculated from the slope of Equation 6.2 are compared with values of E_{act} obtained for sequentially aged unoriented PMMA (Table 5.9) in Table 6.3.

TABLE 6.2

Estimated free volume fractions and isothermal relaxation times determined for slow-cooled oriented poly(methyl methacrylate)

T_a (C)	$\Sigma\Delta L_z$ (m)	$\Sigma f(T_a)$	$\tau(T_a)$ (s)	$\tau(T_a)/\tau_g$
60	5.280×10^{-7}	2.55×10^{-4}	*	*
70	6.600×10^{-7}	3.19×10^{-4}	*	*
80	1.078×10^{-6}	5.21×10^{-4}	*	*
90	1.803×10^{-6}	8.72×10^{-4}	*	*
100	3.979×10^{-6}	1.93×10^{-3}	1.2×10^{233}	7.0×10^{225}
110	3.078×10^{-5}	1.49×10^{-2}	3.95×10^{26}	2.39×10^{28}
115	4.435×10^{-4}	2.15×10^{-1}	2.83×10^{-1}	1.72×10^{2}
120	1.016×10^{-3}	4.91×10^{-1}	2.05×10^{-2}	1.24
130	1.137×10^{-3}	5.50×10^{-1}	1.65×10^{-2}	1.00

One consequence of a larger free volume fraction is that the availability of extra room for molecular manoeuvre results in a lowering of activation energy. This can be seen for temperatures above 115 C, in which E_{act} of oriented PMMA (f = 0.55) is lower than those of unoriented PMMA (f = 0.136). On the other hand, the activation energy of 1608 kJ mol^{-1} at 100 C is much higher than the activation energy observed [30-33] for the glass transition of unoriented PMMA (335-460 kJ mol^{-1}), which conclusively shows that randomisation does not occur below T_g (105 C). However, E_{act} becomes comparable to literature values observed [30-33] for the glass transition of unoriented PMMA at 110 C which suggests that randomisation proceeds with cooperative motions of main-chain segments above T_g.

TABLE 6.3

Activation energies at various isothermal temperatures obtained for randomisation of slow-cooled oriented poly(methyl methacrylate)

T_a (C)	$\Sigma f(T_a)$	E_{act} (kJ mol^{-1})	E_{act} (Table 5.9)
100	1.93×10^{-3}	1608	47
110	1.49×10^{-2}	205	22
115	2.15×10^{-1}	11	not available
120	4.91×10^{-1}	3.2	19
130	5.50×10^{-1}	2.5	18

6.4 SUMMARY

(1) Large and rapid length changes were observed between 125-140 C when uniaxially-compressed PMMA specimens were heated to above T_g. These length changes were attributed to randomisation, which results in the removal of molecular orientation such that the specimen reverts to its original unoriented state. The separate effects of physical ageing and randomisation were distinguished from the sequential ageing of oriented PMMA. Dimensional changes below 110 C were affected by physical ageing while changes ascribed to randomisation were observed between 110-130 C.

(2) The observation of randomisation in the temperature range above T_g suggested that the removal of molecular orientation could only proceed by cooperative motion of main-chain segments. This suggestion was subsequently confirmed by calculations of activation energies which revealed large activation energy barriers below T_g.

(3) Uniaxial compression of PMMA was found to affect the free volume fraction, increasing from 0.13 for the unoriented polymer to 0.21-0.55 for oriented specimens. This observation is in agreement with the hypothesis that imposed mechanical deformation resulted in the generaion of free volume.

(4) The linear glass expansivity of oriented PMMA was found to reflect the relative contributions of intrachain and interchain vibrations. Intrachain vibrations of stiff backbone

chains along the direction of orientation contributed mainly to $\alpha_g//$, whereas interchain vibrations of greater anharmonicity contributed to $\alpha_g\perp$ such that $\alpha_g\perp > \alpha_g//$. However, the volume expansivity was not affected by orientation.

Chapter 6

1. F. Simon, *Z. Anorg. Allgem. Chem.* **203**, 219 (1931).

2. L.C.E. Struik, *Physical Ageing in Amorphous Polymers and Other Materials*, Elsiever, Amsterdam (1978).

3. A.J. Hill, K.J. Heater, C.M. Agrawal, *J. Polym. Sci. B: Polym. Phys.* **28**, 387 (1990).

4. P. So and L. Broutman, *Polym. Eng. Sci.* **16(12)**, 785 (1976).

5. L.E. Hornberger and K.L. Davies, *Polym. Eng. Sci.* **27(19)**, 1473 (1987).

6. L.C.E. Struik, *Polym. Eng. Sci.* **18(10)**, 799 (1978).

7. E. Wohlisch, *Kolloid-Z.* **89**, 239 (1939).

8. F.H. Muller, *Kolloid-Z.* **95**, 138, 306 (1941).

9. G. Menges and G. Wubken, *Plastverarbeiter* **23**, 318 (1972).

10. T.T. Jones, *Pure Appl. Chem.* **45**, 41 (1976).

11. L.C.E. Struik, *Polym. Eng. Sci.* **17(3)**, 165 (1977).

12. S. Matsuoka and H.E. Bair, *J. Appl. Phys.* **48**, 4058 (1977).

13. S. Matsuoka, *Polym. Eng. Sci.* **21(14)**, 907 (1981).

14. J. Bartos, J. Muller and J.H. Wendorff, *Polymer* **31**, 1678 (1990).

15. L.C.E. Struik, *Internal Stresses, Dimensional Instabilities and Molecular Orientations in Plastics*, Wiley (1990).

16. M. Trznadel and M. Kryszewski, *Polymer* **29**, 418 (1988).

17. G.A.J. Orchard, G.R. Davies and I.M.Ward, *Polymer* **25**, 1203 (1984).

18. L.H. Wang, C.L. Choy and R.S. Porter, *J. Polym. Sci. Polym. Phys. Ed.* **20**, 633-640 (1982).

19. K.H. Hellwage, J. Henig and W. Knappe, *Kolloid Z. Z. Polym.* **188**, 121 (1963).

20. C.P. Buckley and N.G. McCrum, *J. Mater. Sci.* **8**, 1123 (1973).

21. C.L. Choy, *Developments in Oriented Polymers,* I.M. Ward ed., Applied Science, London, (1982).

22. C.L. Choy, F.C. Chen and K. Young, *J. Polym. Sci. Polym. Phys. Ed.* **19**, 335 (1981).

23. C.L. Choy, F.C. Chen and E.L. Ong, *Polymer* **20**, 1191 (1979).

24. R.E. Barker Jr., *J. Appl. Phys.* **38(11)**, 4234 (1967).

25. R.W. Warfield, *Die Makromol. Chem.* **175**, 3285-3297 (1974).

26. G. Schwarz, *Cryogenics* **28**, 248 (1988).

27. P.R. Swan, *J. Polym. Sci.* **56**, 403 (1962).

28. O.S. Narayanaswamy, *J. Am. Ceram. Soc.* **54**, 491 (1971).

29. C.T. Moynihan, A.J. Easteal, M.A. DeBolt and J. Tucker, *J. Am. Ceram. Soc.* **59**, 12 (1976).

30. K. Deutsch, E.A.W. Hoff and W. Reddish, *J. Polym. Sci.* **13**, 565 (1954).

31. J.M.G. Cowie and R. Ferguson, *Polymer* **28**, 503 (1987).

32. J. Heijboer, J.M.A. Bass, B. van de Graaf and M.A. Hoefnagel, *Polymer* **28**, 509-513 (1987).

33. N.G. McCrum, B.E. Read and G. Williams, *Anelastic and Dielectric Effects in Polymeric Solids*, Wiley and Sons, London (1967).

GLOSSARY OF SYMBOLS

α'_g	Linear Glass Expansion Coefficient
$\alpha'_g//$	Linear Glass Expansivity Parallel to the Axis of Orientation
$\alpha_g \perp$	Linear Glass Expansivity Perpendicular to the Axis of Orientation
α_g	Cubical Glass Expansion Coefficient
$\alpha_g//$	Cubical Glass Expansivity Parallel to the Axis of Orientation
$\alpha_g \perp$	Cubical Glass Expansivity Perpendicular to the Axis of Orientation
E_{act}	Energy of Activation
f	Free Volume Fraction
$\Sigma f(T_a)$	Sum of Free Volume Fraction Recovered After Ageing at T_a
$L_{x,y}$	Specimen Length Measured Along the (x, y) Axis
L_z	Specimen Length Measured Along the z Axis
$\Delta L_{x,y}$	Length Change Along the (x, y) Axis
ΔL_z	Length Change Along the z Axis
$\Sigma \Delta L_z$	Sum of Length Change Along the z Axis
R	Universal Gas Constant
σ	Applied Stress Imposed by Mechanical Deformation
σ_r	Rubber-Elastic Reaction Stress to Applied Stress σ
T_g	Glass Transition Temperature
T_a	Isothermal Ageing Temperature
T_{eq}	Temperature at Which Thermodynamic Equilibrium is Attained Readily
t_a	Isothermal Ageing Period
τ_g	Relaxation Time at Thermodynamic Equilibrium
$\tau(T_a)$	Relaxation Time at Ageing Temperature T_a
TMA	Thermal Mechanical Analyser
V_f	Free Volume
V_0	Initial Volume
V_{eq}	Specific Volume at Thermodynamic Equilibrium

CHAPTER 7
PHYSICAL AGEING AND MOLECULAR WEIGHT

7.1 INTRODUCTION 141

7.2 EXPERIMENTAL 143

7.3 RESULTS AND DISCUSSION

7.3.1 Viscosity-Molecular Weight Relationship 144

7.3.2 Free Volume Fraction 146

7.3.3 Length Contraction At a Constant Rate of Heating 149

7.3.4 Dimensional Changes of Low Molecular Weight PMMA 149

Free Volume Fraction 151

Relaxation Times and Activation Energy 152

7.4 SUMMARY 153

APPENDIX

Measurement of Viscosity 154

Determination of Molecular Weight 154

BIBLIOGRAPHY 156

GLOSSARY OF SYMBOLS 158

CHAPTER 7

7.1 INTRODUCTION

The first extensive study of the variation of the glass transition temperature with molecular weight (MW) was performed on polystyrene (PS) by Fox and Flory [1-2]. The specific volumes of PS fractions were found to increase linearly with $1/M_n$ (number-average molecular weight) at temperatures well above T_g and was relatively constant for molecular weights above 25,000. The T_g was found to be almost independent of molecular weight above 25,000 but decreased rapidly with decreasing molecular weight below this value, where T_g for high and low molecular weight PS (MW = 8.5×10^4 and 2970) were 100 C and 40 C respectively. Fox and Flory also observed that the specific volumes of PS fractions below the glass transition were independent of molecular weight and concluded that the same internal configuration had been frozen-in below T_g, i.e. the free volume frozen-in at T_g is the constant and is independent of molecular weight.

Since many physical properties of amorphous polymers are closely related to the local configurational arrangement of the polymer segments, it was suggested that the specific volume act as a simple index of configurational structure [1-2]. The dependence of the specific volume on molecular weight was attributed to the influence of end groups, in which the end groups were seen to disrupt the local configurational order of the styrene units. It was observed [1-2] that an increase in the concentration of end groups resulted in an increase in specific volume. An alternative description of the effect of end groups is to regard them as "diluents" in the molecular structure [3-4]. The mobility of a chain end is considered to be greater than the middle segment of a polymer chain, as the middle segment is restricted at both ends by other repeating units whereas the chain end is restrained only at one end. Consequently, a higher free volume associated with each chain end than the middle segment of a chain. Therefore, a sample containing more chain ends (i.e. lower molecular weight) will have to be cooled further to reach the point at which the relaxation time is the same as that of a sample containing fewer chain ends, resulting in a decrease in glass transition temperature with decreasing molecular weight.

However, the T_g is only a vague indicator of network mobilities at ambient temperature [11] and very often the reason for the choice of a T_g is simply one of convenience

[12]. An alternative approach was adopted by Doolittle [5-6], who showed that at high temperatures the viscosities η of *n*-paraffins of different molecular weights could be expressed in terms of the fractional free volume f (Equations 2.1 and 2.3), leading to the derivation of the Williams-Landell-Ferry (WLF) equation [7] (Equations 2.2 and 2.5). Kovacs *et al.* [8-10] extended the Doolittle equation to include a relaxation time parameter τ associated with the free volume fraction (Equations 2.12-2.13), such that

$$\text{Ln}\ (\eta/\eta_g) = \text{Ln}\ (\tau/\tau_g) = \text{Ln}\ a(T) = (1/f - 1/f_g) \tag{7.1}$$

where η_g, τ_g and f_g refer to the values at T_g and a(T) is the shift function used in the WLF equation. The ambiguities associated with the use of T_g are avoided in Equation 7.1, whereas experimental data which attempt to correlate T_g with MW seem to suffer from scatter, especially when the results are based on a variety of experimental techniques.

The volume-temperature-molecular weight studies of a number of polymers by Fox and Loshaek [13] led to the following empirical relationships describing the free volume V_f of a polymer of molecular weight M:

$$V_f = 0.205(M + 117)/(M + 322) \tag{7.2}$$

$$V_f = 0.116(M + 208)/(M + 322) \tag{7.3}$$

It was assumed that the rate of increase of free volume with temperature was equal to the expansivity, $dV_f/dT = \alpha_f$, and that the increase in free volume corresponded to the difference between the liquid and glass expansion coefficients, $dV_f/dT = \alpha_f = (\alpha_l - \alpha_g)$. Examination of these equations indicated that for $M > 3000$ the variation of V_f with M is so small that experimental detection would be difficult, which led to the earlier erroneous conclusion [1-2] that the T_g represented a state of iso-free volume which is independent of molecular weight. Equations 7.2-7.3 suggested that the free volume will decrease with decreasing M, in accordance with the predictions of Bueche [14]. At T_g, the internal segmental jump frequency is the same for all polymers, while the number of segments which must cooperate to produce a single segmental jump decreases as the value of M decreases. The resulting effect is a decrease in the magnitude of free volume needed to yield the critical jumping frequency [14-15].

Although the conclusions of Fox and Loshaek are supported by Miller [26], it contradicts the experimental results of Doolittle [5] and Beevers and White [21], who showed that the lowering of molecular weight increases the free volume fraction. On the other hand, Williams *et al.* [16] reported that the addition of methanol resulted in the lowering of the free volume of PMMA in the range $35{,}000 \leq MW \leq 550{,}000$. Turner [17] proposed that the effect of reducing the MW is to increase the free volume both by the formation of chain ends and by the release of entanglements. The introduction of a low-molecular weight diluent such as methanol into PMMA may be considered to have the same effect on the free volume as the formation of chain ends. However, it was assumed [16] that the release of entanglements was primarily responsible for the overall changes in free volume and that the increase in free volume upon the addition of methanol was not significant. The conclusion of Williams *et al.* [16] was based on calculations which showed that the free volume generated by the release of entanglements was lower in methanol-equilibrated PMMA than in dry PMMA. This conclusion is in conflict with the free volume concept [18] which predicts that an increase in free volume would shift the T_g to lower temperatures as the motions of molecular segments become less hindered. This prediction is supported by stress-relaxation studies [16] which showed that T_g's of PMMA-methanol systems were lower than those of PMMA.

In this chapter, the free volume fraction-MW relationship has been investigated using two different techniques. The first technique involves the measurement of intrinsic viscosities of PMMA solutions of different MW, while the second technique involves the measurement length contraction under a constant load using a thermomechanical analyser (TMA). The results of both techniques suggest that the concept of chain ends as diluents in a polymer structure is more appropriate and that the free volume fraction of a polymer increases with decreasing molecular weight.

7.2 EXPERIMENTAL

The casting of PMMA sheets from liquid monomer has been described in detail in Section 3.2. High molecular weight and low molecular weight PMMA (PMMA (HMW), PMMA(LMW)) were compression moulded into flat sheets from polymer beads (Polysciences, Pennsylvania) at 210 C and 180 C respectively.

The experimental procedures describing the measurement of viscosity and the determination of molecular weight are included in the Appendix at the end of the chapter. The viscosity-average molecular weights $[M]_\eta$ of the three PMMA specimens are presented in Table7.1.

TABLE 7.1

Viscosity-average molecular weights of poly(methyl methacrylate)

Polymer	Molecular Weight, $[M]_\eta$
Cast PMMA	1.24×10^6
PMMA (HMW)	3.20×10^5
PMMA (LMW)	9.80×10^4

Cast PMMA and PMMA (HMW) were thermally equilibrated at 140 C for 15 minutes. PMMA (LMW) was equilibrated at the lower temperature of 110 C as the polymer was found to depolymerise at 140 C. After the specimens had been equilibrated, they were quenched in liquid nitrogen for 10 minutes and subsequently allowed to warm to 25 C under dry nitrogen inside the TMA. A period of 20 minutes was allowed to elapse in order to minimise any poor reproducibility which may occur as a result of cooling stresses [19-20]. The specimen was heated in the TMA from 25 C to 165 C at a constant rate of 2 C/min under a static applied load of 0.1 N.

7.3 RESULTS AND DISCUSSION

7.3.1 Viscosity-Molecular Weight Relationship

The intrinsic viscosities $[\eta]$ of the PMMA solutions are shown in Table 7.2 with the Huggins-Kraemer constants k' and k". The data of Table 7.2 leads to a double logarithmic relationship between $[\eta]$ and $[M]_\eta$

$$\text{Ln } [M]_\eta = (0.580)\text{Ln } [\eta] - 8.298 \qquad (7.4)$$

which has the same form as the empirical relationship obtained for polystyrene by Fox and Flory [1]

$$\text{Ln } [M]_\eta = 2.303.(\text{Ln } [\eta] + 4.013)/0.74 \qquad (7.5)$$

TABLE 7.2

Intrinsic viscosities (g/100 cm^3) and Huggins-Kraemer constants of poly(methyl methacrylate)

	[η] (Eq. 7.14)	[η] (Eq. 7.15)	k'	k"	k' - k"
Cast PMMA	0.8520	0.8580	0.7796	0.1730	0.61
PMMA (HMW)	0.3893	0.3906	1.0434	0.4497	0.59
PMMA (LMW)	0.1960	0.1961	0.6310	0.1116	0.52

The relationship between Ln [η] and Ln $[M]_\eta$ is shown in Figure 7.1. A similar relationship for PMMA was obtained from the data of Beevers and White [21], who studied of the variation of T_g as a function of $[M]_n$. PMMA specimens of a range of molecular weights from 3000 to 76,000 were dissolved in a variety of solvents and the viscosities of the polymer solutions were measured between 60-110 C. The plot of Ln [η] against Ln $[M]_n$ (Fig. 7.2) leads to the following relationship:

$$\text{Ln } [M]_n = (0.757)\text{Ln } [\eta] + 9.406 \qquad (7.6)$$

The slope of the line corresponds to the Mark-Houwink constant of 0.76 used by the authors [21]. The same result is also observed in Equation 7.4, in which the slope of 0.580 is the same as the Mark-Houwink constant for the *n*-butyl acetate/PMMA system at 25 C [22]. Equations 7.4 and 7.6 suggests that the intrinsic viscosity of a polymer is related to its molecular weight according to the general expression:

$$\text{Ln } [M]_n = a.\text{Ln } [\eta] + C \qquad (7.7)$$

FIGURE 7.1 RELATIONSHIP BETWEEN INTRINSIC VISCOSITY AND MOLECULAR WEIGHT OF PMMA

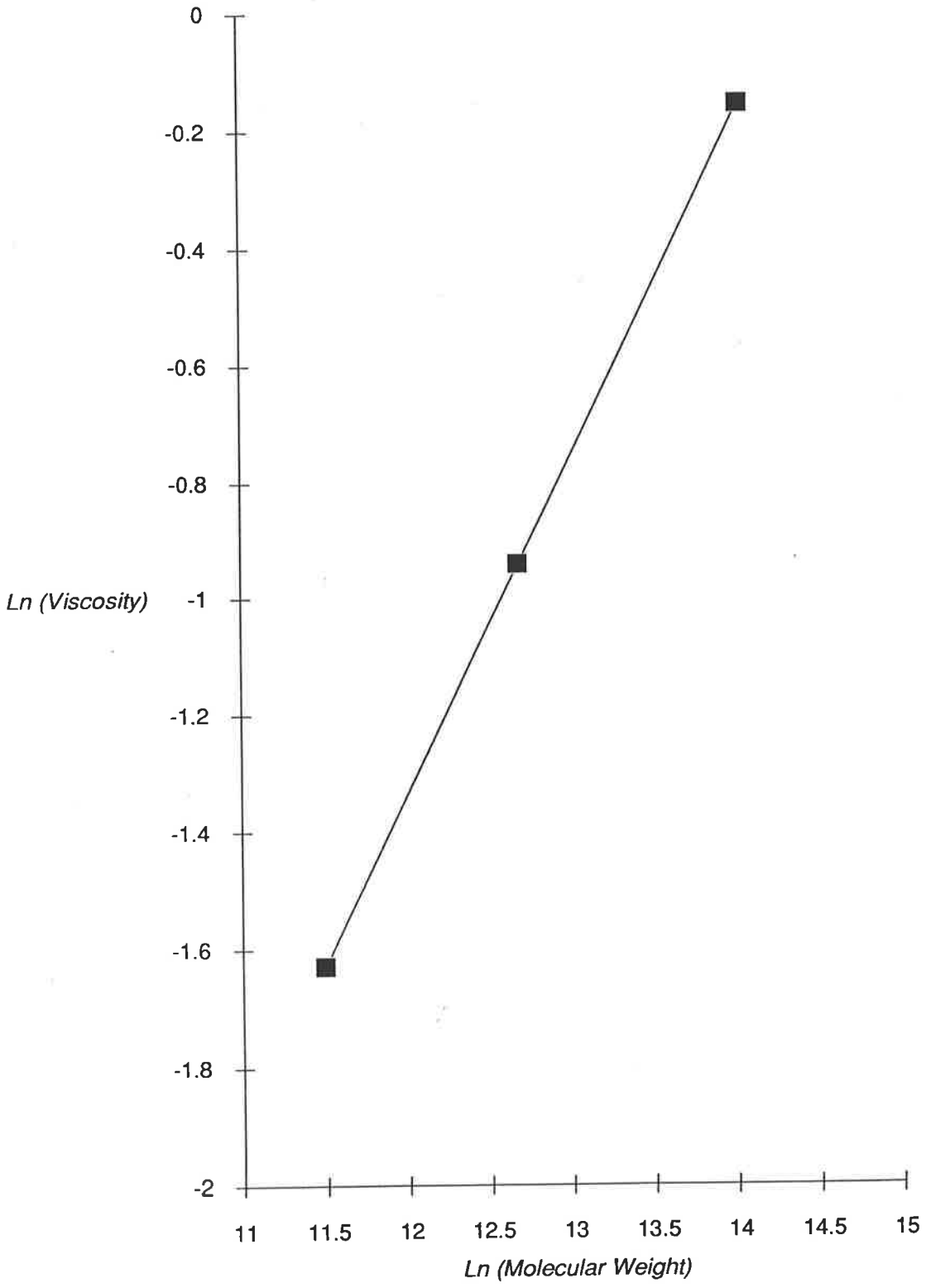

FIGURE 7.2 RELATIONSHIP BETWEEN INTRINSIC VISCOSITY AND MOLECULAR WEIGHT, data from Beevers and White [17]

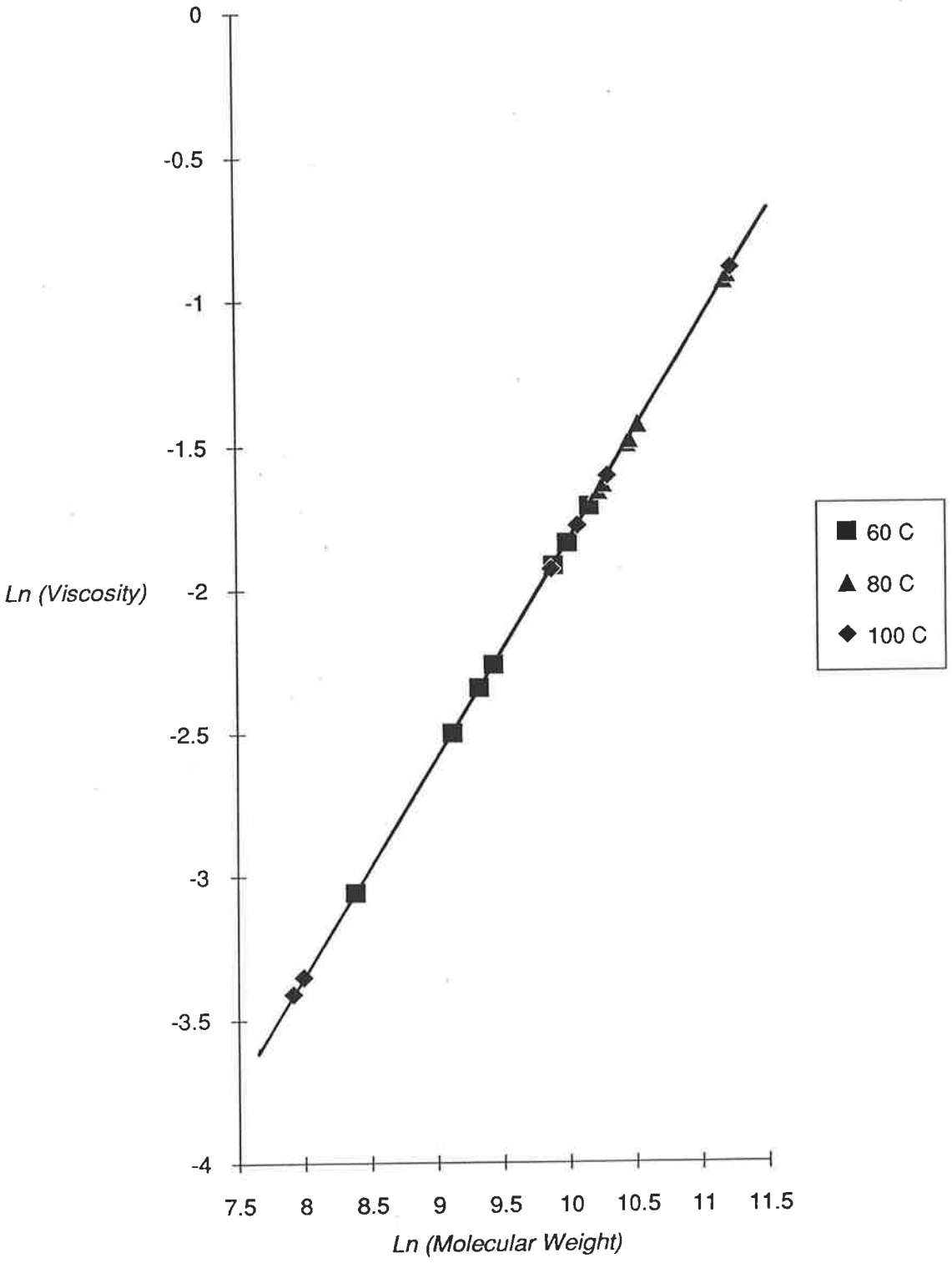

where a is the Mark-Houwink constant and C is the intercept. In addition, Figure 7.2 suggests that this general relationship is independent of solvent type and the temperature of measurement.

7.3.2 Free Volume Fraction

The relationship between the intrinsic viscosity and free volume fraction (f) of a polymer is expressed by the Doolittle [5] equation:

$$\ln [\eta] = B/f + \text{Ln } A \qquad (2.1)$$

where Ln A and B are empirical constants determined for a series of *n*-alkane hydrocarbons, and have values of -7.6505 and 0.9995 respectively. The free volume fractions of the PMMA specimens were determined from Doolittle's equation and are presented in Table 7.3. The determination of free volume fraction from viscosity measurements poses an interesting question, that is, whether the thermal history of a polymer is erased when it is dissolved in an organic solvent. The lowering of the glass transition by plasticisation [23-24] has been attributed to the increase in free volume contributed by the plasticiser, in which the increase in the concentration of diethyl phthalate (DEP) from 0 to 0.5 vol./vol. % resulted in the lowering of T_g of PMMA from 104 C to -4 C [25]. If a dissolved polymer is considered to be equivalent to a highly-plasticised polymer, then the determination of free volume fraction at 25 C (above T_g) suggests that the previous history of the polymer had been erased.

TABLE 7.3

Free volume fractions of as-received poly(methyl methacrylate) specimens determined from viscosity measurements at 25 C

Specimen	$[M]_\eta$	$[\eta]$ (g/dl)	f
Cast PMMA	1.24×10^6	0.8550	0.133
PMMA (HMW)	3.20×10^5	0.3900	0.149
PMMA (LMW)	9.80×10^4	0.19605	0.166

The free volume fraction of 0.133 of Cast PMMA correlates with the limiting fractional free volume of 0.13 of quenched PMMA, as determined in Chapters 4 and 5. This result suggests that the free volume fraction of a polymer solution corresponds to the maximum free volume fraction which can be accommodated by the polymer at T_g. The dissolution of a polymer may be pictured as a conversion of a rigid glass to a flexible and mobile liquid [25], which has a sufficiently loose structure to accommodate a larger free volume fraction.

From Table 7.3 the free volume fractions of the PMMA specimens are observed to increase with decreasing molecular weight, and supports the hypothesis that a low molecular weight polymer with a higher concentration of chain ends will result in an increase in free volume [3-4]. However, conflicting results by Miller [26] show that the free volume fraction of polystyrene at T_g increases with molecular weight. The free volume fraction was determined from a similar expression to Equation 7.8, with the exception that the pre-exponential term log A was allowed to vary with molecular weight. Log A was defined by Williams [27] as the viscosity at infinite temperature and infinite free volume, and increased linearly with log M_n. Miller's data showed little change in Ln [η] when the molecular weight was increased from 1675 to 1.34×10^5, therefore the increase in free volume fraction was attributed to the attendant increase in log A. This led to the conclusion that the glass transition was more accurately described as an "iso-viscous" state rather than an "iso-free volume" state [26], i.e. the viscosity at T_g may be assumed to be constant but not the free volume fraction.

An alternative definition of the pre-exponential term by O'Connor and Scholsky [28] suggests that Miller's conclusions are incorrect. The fractional free volume of a polymer of molecular weight M_n, f_m, is related to the limiting free volume fraction f_∞ of a high molecular weight polymer by

$$f_m = f_\infty + A/M_n \tag{7.9}$$

where A is a constant. Equation 7.9 indicates that the increase in the free volume fraction f_m upon a decrease in molecular weight is attributed to the free volume contribution of end groups, which is in agreement with the theory of Shen *et al.* [3-4]. A similar conclusion is also inferred from Simha and Boyer [29], who suggested that side-groups (which are approximated as chain

ends) retained excess free volume which are frozen-in below the temperature range for secondary relaxation.

The incorporation of Equation 2.1 into Equation 7.4 suggests that Ln $[M]_\eta$ will vary linearly with 1/f. Figure 7.3 shows the plot of Ln $[M]_\eta$ against 1/f in which the free volume fraction-molecular weight relationship for PMMA is described by

$$\text{Ln } [M]_\eta = (1.724)/f + 1.107 \qquad (7.8)$$

and the slope is equal to B/a. Equation 7.8 predicts an increase in free volume fraction upon a decrease in molecular weight. The free volume fractions of the homologous *n*-alkanes in Doolittle's paper [5] were calculated using Equation 7.8 and compared with his results. The free volume fraction was defined by Doolittle [5] as v_f/v_0, where v_0 is the volume occupied by 1 gram of liquid extrapolated to absolute zero without change of phase and v_f is the volume of free space per gram of liquid at any temperature. The free volume fractions were measured over a range of temperatures in which the best agreement between the calculated and experimental values was at 150 C. The results are presented in Table 7.4.

TABLE 7.4

Free volume fractions of *n*-alkanes measured at 150 C from Equation 7.8.

Molecular Weight	Doolittle [5]	Equation 7.8
128.25	0.520	0.460
156.30	0.467	0.437
184.35	0.434	0.419
240.46	0.394	0.394
394.74	0.348	0.354
506.95	0.333	0.337
899.68	0.305	0.303

FIGURE 7.3 RELATIONSHIP BETWEEN FREE VOLUME FRACTION AND MOLECULAR WEIGHT OF PMMA

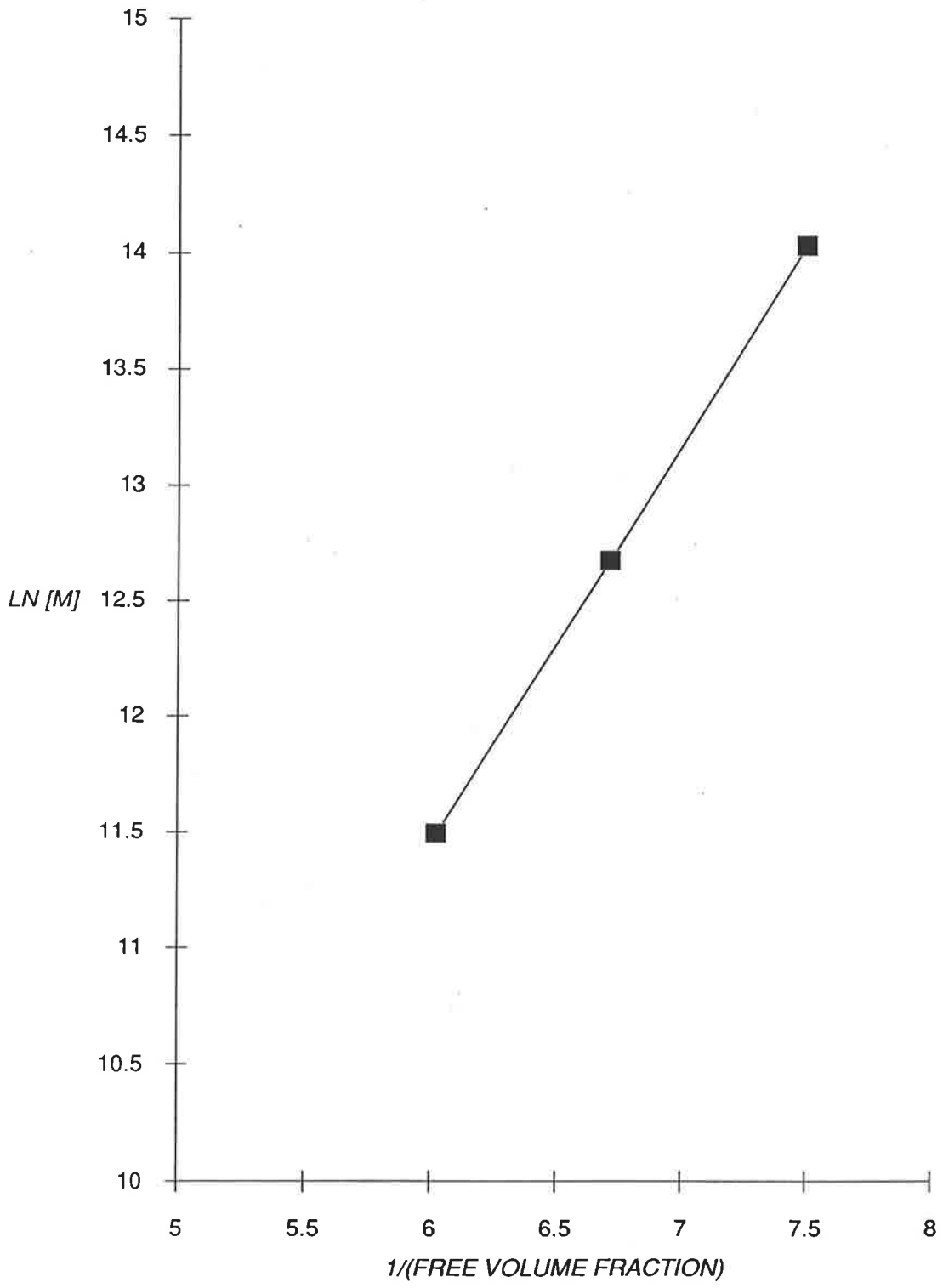

7.3.3 Length Contraction At a Constant Rate of Heating

Figure 7.4 shows the length-temperature curves of the three quenched PMMA specimens measured at a heating rate of 2 C/min. PMMA (HMW) is observed to have a larger length contraction than Cast PMMA which indicates that a higher free volume fraction exists in PMMA (HMW). The sharp expansion observed at 150 C for PMMA (HMW) is attributed to the release of frozen-in orientation which had not been erased during thermal equilibration at 140 C. The orientation was generated during compression moulding at 210 C and was frozen in as the polymer was cooled to below T_g. On the other hand, frozen-in orientation in Cast PMMA may be erased by heating to above 130 C (Chapter 6). Length contraction of PMMA (LMW) is observed to occur in two stages. The first stage at 100 C is attributed to the collapse of free volume holes [30], and is followed by further contraction at 130 C which is associated with permanent and non-reversible viscous flow. At the completion of the experiment when the specimen had cooled to 25 C, it was found that the probe had indented the specimen during the experiment. The indentation on the specimen could not be erased by heating to above T_g which suggests that the deformation could be ascribed to irreversible viscoelastic deformation.

7.3.4 Dimensional Changes of Low Molecular Weight Poly(Methyl Methacrylate)

A two-stage contraction process in PMMA (LMW) was observed in which the first stage between 100-130 C has been attributed to physical ageing whereas the second stage at T > 130 C is ascribed to viscoelastic deformation. In order to confirm that the observed changes in length above 130 C is caused by viscoelastic deformation, dimensional changes in PMMA (LMW) were studied under isothermal conditions in the range 80-150 C. To ensure the removal of all internal stresses the specimens were heated in an air-oven at 110 C for 2 hours and allowed to cool slowly to 25 C. The specimens were placed inside the preheated TMA in which a period of 7-9 minutes was allowed to elapse for the specimen to reach thermal equilibrium. The preheating of the specimen is necessary, especially at high temperatures, to ensure that the specimen is completely aged at the start of the experiment. This eliminates physical ageing as being a possible cause of length contraction at these temperatures. The glass probe was then lowered on the specimen at a constant load of 0.1 C and length changes were measured over a period of 60 minutes between 80-150 C (Figs. 7.5-7.6).

FIGURE 7.4 EFFECT OF MOLECULAR WEIGHT ON PHYSICAL AGEING OF PMMA

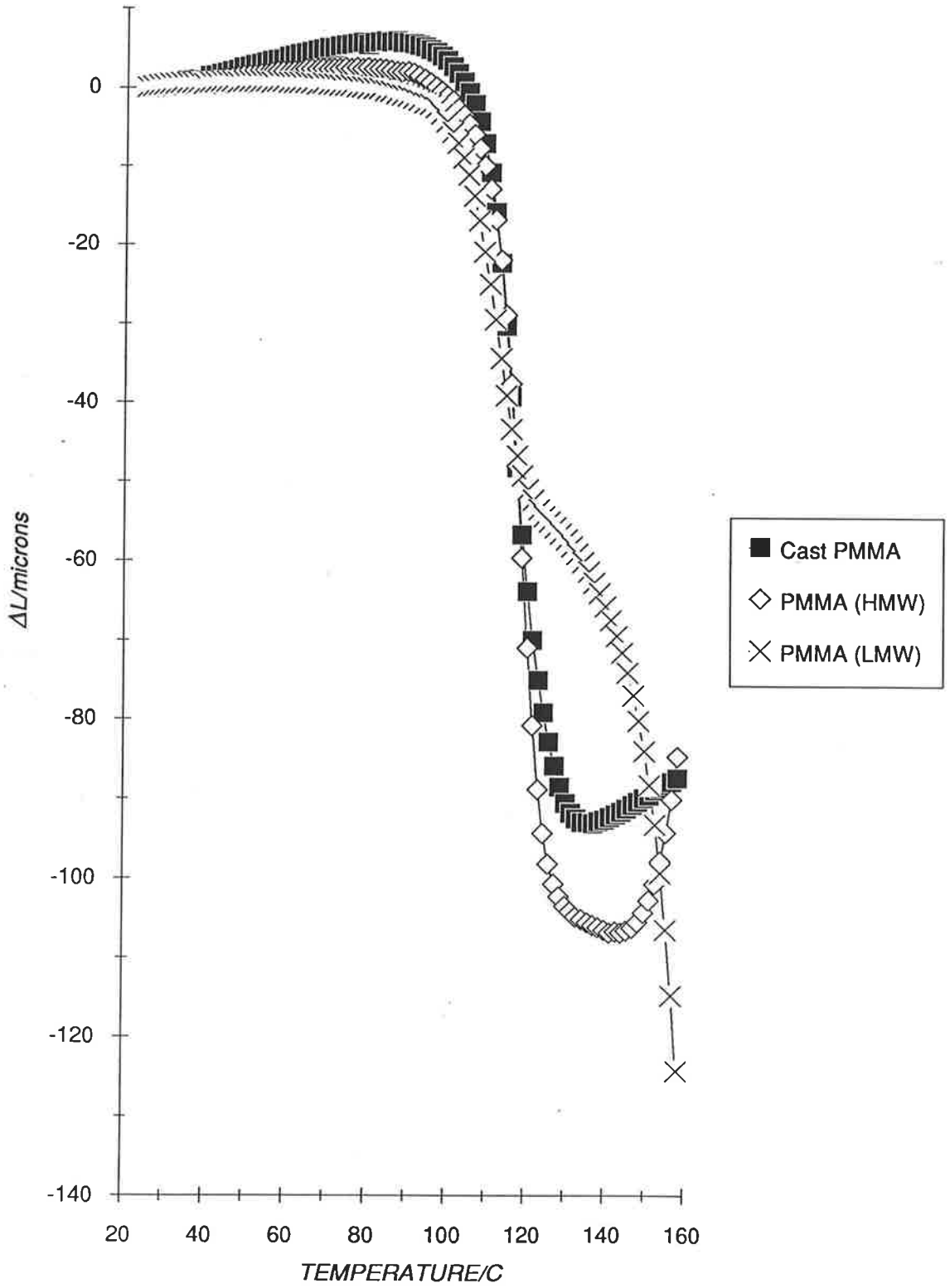

FIGURE 7.5 ISOTHERMAL LENGTH CONTRACTION OF PMMA (LMW) (numbers adjacent to curves indicate the isothermal ageing temperature)

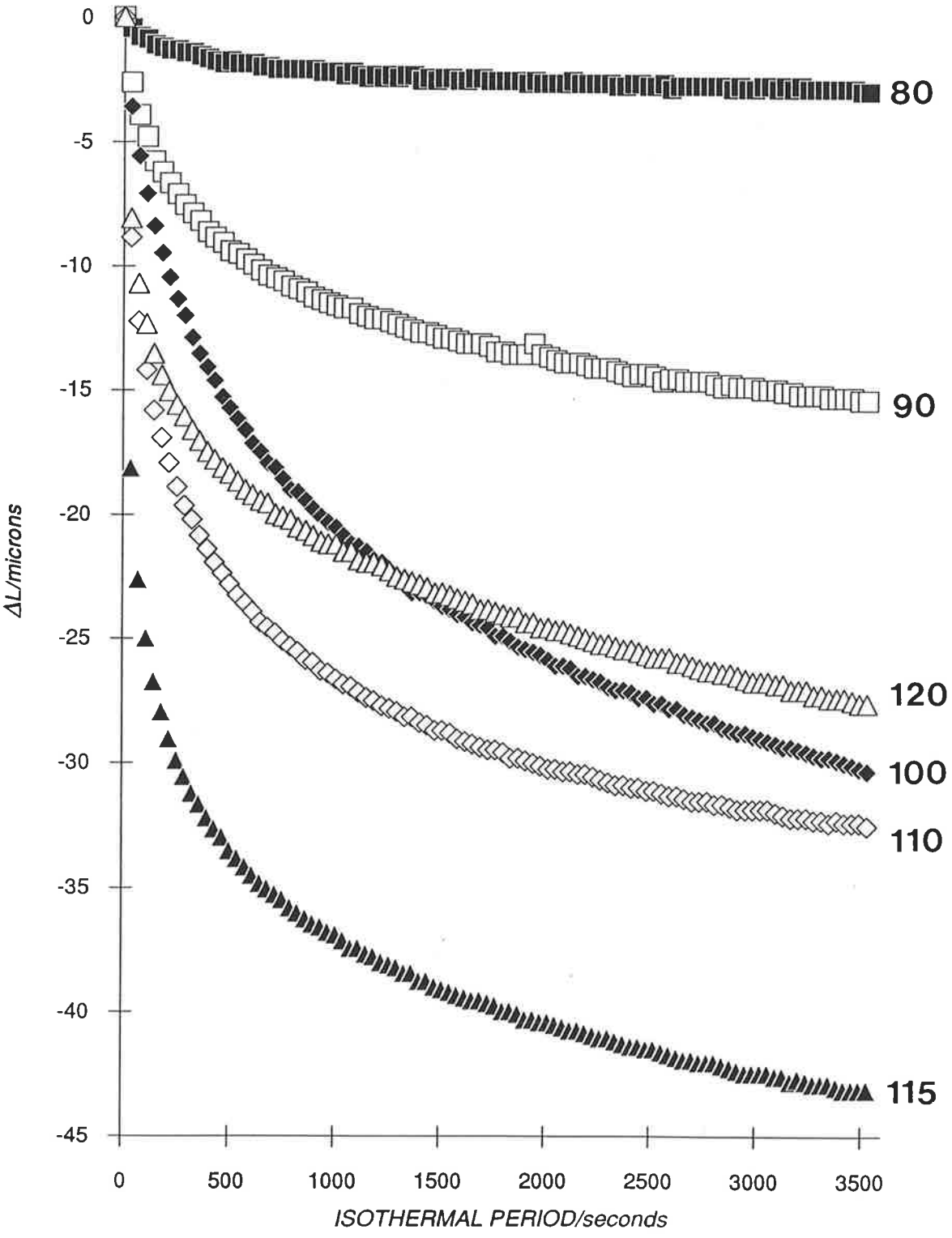

FIGURE 7.6 ISOTHERMAL LENGTH CONTRACTION OF PMMA (LMW) (numbers adjacent to curves indicate the isothermal ageing temperature)

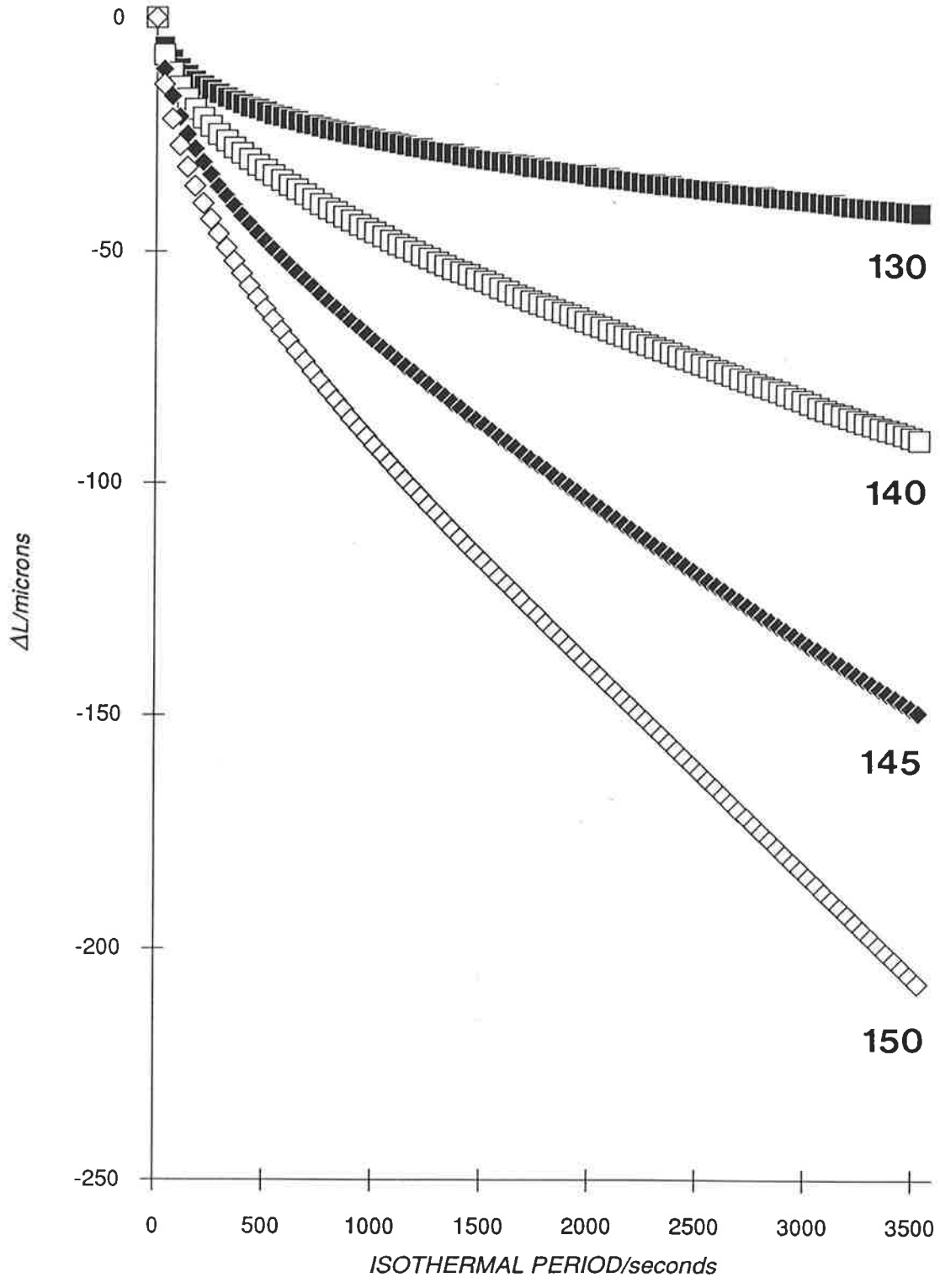

An inspection of Figure 7.5 indicates that length contraction between 80-120 C increases with an increase in ageing temperature, in accordance with the well-established fact that the rate of ageing increases with temperature [31-35]. Hence the curve at 120 C appears to be out of sequence with the other curves. It is suggested that the smaller contraction is a result of pre-ageing during thermal equilibration at 120 C, in which some ageing had already taken place in the specimen before the commencement of the experiment. The order of the three curves between 100-115 C indicate that these specimens were pre-aged to a smaller extent such that they undergo larger contractions during isothermal measurement. The continuation of length contraction after 60 minutes indicates that the specimens had not attained equilibrium after 60 minutes.

At the completion of the experiment the specimens were inspected for indentation. No indentation could be found on the specimens aged between 80-110 C, although a shallow indentation was observed for the specimen aged at 120 C. The absence of indentation indicates that the contraction curves in Figure 7.5 are associated with physical ageing. On the other hand, all of the specimens aged between 130-150 C were indented by the probe, which conclusively shows that PMMA (LMW) specimens undergo viscoelastic deformation under a light load when heated to above 130 C. Figure 7.6 also shows that the extent of deformation of PMMA (LMW) increases with temperature.

The rate of physical ageing is characterised by the relaxation rate r according to [36]:

$$-r = (3/L_z)[dL_z/dLn(t_a)/2.303] \qquad (5.3)$$

where t_a is the isothermal period in seconds and the average specimen thickness L_z is 1.1242 x 10^{-3} m. The isothermal relaxation rates for PMMA (LMW) within a period of 60 minutes are presented as a function of the ageing temperature in Table 7.5 and in Figure 7.7. The relaxation rates of quenched Cast PMMA from Table 5.3 are included for comparison.

The steady rise in relaxation rate from 130 C onwards indicates the presence of viscoelastic deformation, and is consistent with the observation of permanent indentation in the specimens at 130 C. Thus the temperature range of physical ageing in PMMA (LMW) appears to be restricted to below 130 C. Columns 3 and 4 of Table 7.5 show that the relaxation rates of PMMA (LMW) between 90-110 C are higher than the corresponding rates of quenched Cast

FIGURE 7.7 RELAXATION RATES OF SLOW-COOLED LOW MOLECULAR WEIGHT POLY(METHYL METHACRYLATE)

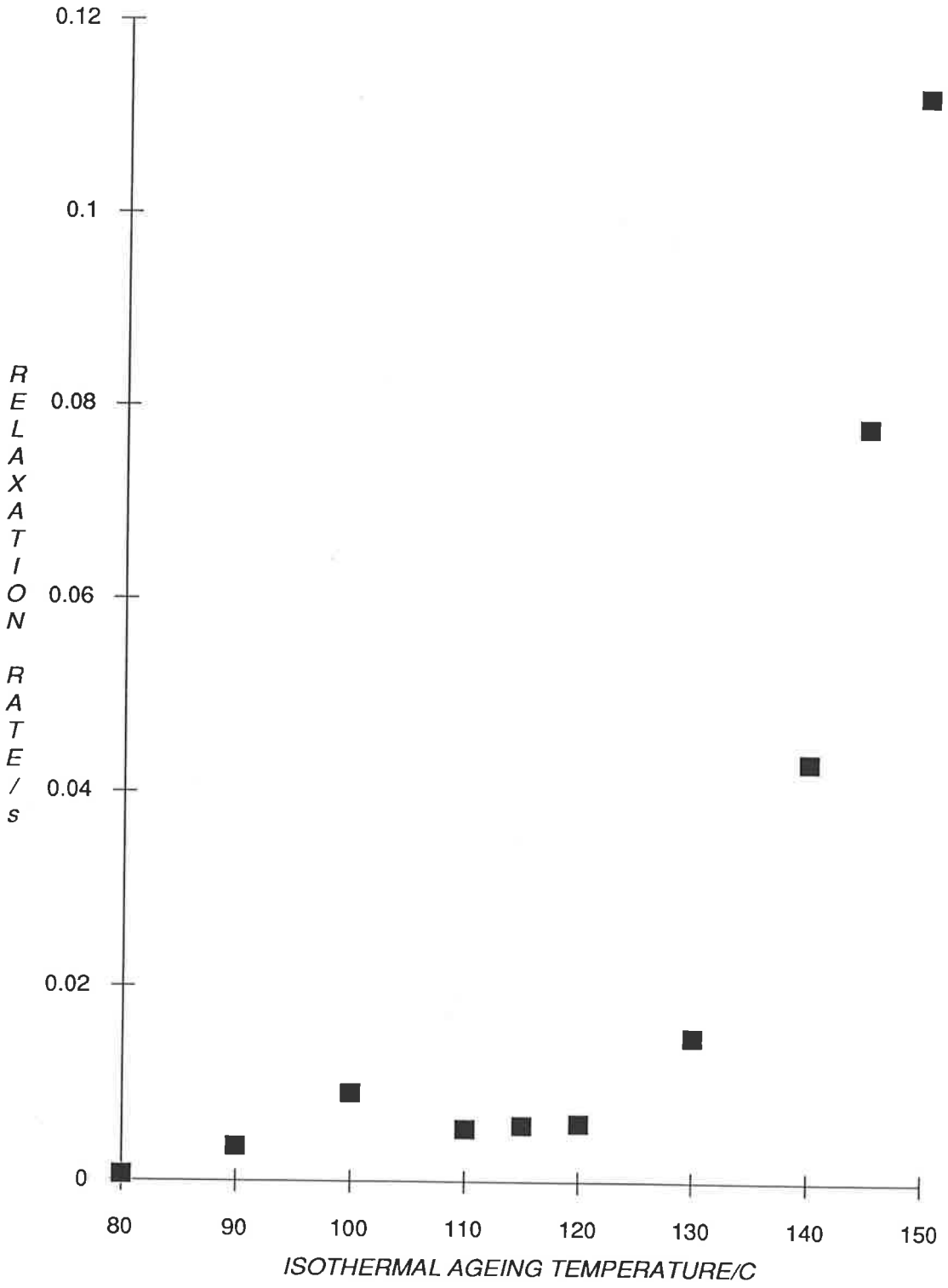

PMMA. This is attributed to the larger free volume fraction of PMMA (LMW) which is associated with greater segmental mobility and allows molecular motion to take place more easily.

TABLE 7.5

Isothermal rates of relaxation of slow-cooled low molecular weight poly(methyl methacrylate)

T_a (C)	$dL_z/dLn(t_a)$ (10^{-6} m.s^{-1})	-r (s^{-1})	-r (s^{-1}) (Table 5.3)
80	-0.507	0.00059	0.00127
90	-3.052	0.00354	
100	-7.790	0.00903	0.00143
110	-4.607	0.00534	0.00216 *
115	-4.965	0.00575	0.00639
120	-5.138	0.00595	0.0148
130	-12.812	0.0149	
140	-37.216	0.0431	0.0570
145	-67.214	0.0779	
150	-96.804	0.1122	

* measured at 105 C

Free Volume Fraction

The free volume fraction of PMMA (LMW) is not easily obtained from length contraction measurements because the polymer undergoes viscoelastic deformation in the temperature range above the glass transition. As the free volume is defined as the difference between the maximum and the minimum sample lengths (Fig. 4.2), the continual collapse of the specimen under load makes the determination of the minimum length difficult (Fig. 7.4). Furthermore, the pre-ageing of specimens during thermal equilibration means that the specimens would have different free volume fractions prior to measurement. In view of the ambiguities that are associated with length contraction, the fractional free volume at equilibrium f_g of PMMA (LMW) is assumed to have the same value as determined from viscosity measurements, i.e. $f_g = 0.166$ (Table 7.3).

The length contraction of slow-cooled Cast PMMA has been shown to be isotropic in Section 4.3, in which the length contractions are related to the initial sample lengths by

$$(\Delta L_{x,y}/L_{x,y}) = (\Delta L_z/L_z) \qquad (7.11)$$

In order to calculate $\Delta L_{x,y}$ from Equation 7.11 and the free volume fraction from Equations 4.1 and 4.3, the contraction in slow-cooled PMMA (LMW) is also assumed to be isotropic. The the specific volume at equilibrium V_{eq} is $(V - \Delta L_z).(V - \Delta L_{x,y})^2$ where the initial lengths L_z and $L_{x,y}$ are taken to be 1.1242×10^{-3} m and 5.02×10^{-3} m respectively. The free volume fractions recovered after 60 minutes, $f(T_a)$, between 80-120 C are presented in Table 7.6. Table 7.6 shows that the free volume fraction recovered in the temperature range 90-120 C in PMMA (LMW) is higher than Cast PMMA, in accordance with the free volume fractions obtained from viscosity measurements (Table 7.3).

TABLE 7.6

Free volume fractions of slow-cooled low molecular weight poly(methyl methacrylate) obtained after isothermal ageing for 60 minutes

T_a	ΔL_z (m)	V_f (m^3)	$f(T_a)$
80	2.948×10^{-6}	2.22×10^{-10}	0.008
90	1.540×10^{-5}	8.64×10^{-10}	0.031
100	3.036×10^{-5}	2.23×10^{-9}	0.086
110	3.254×10^{-5}	2.39×10^{-9}	0.092
115	4.313×10^{-5}	3.14×10^{-9}	0.125
120	2.763×10^{-5}	2.04×10^{-9}	0.078

Relaxation Times and Activation Energy

The relaxation time of PMMA (LMW) at the ageing temperature T_a, $\tau(T_a)$, is obtained with the assumption that the equilibrium relaxation time τ_g is independent of molecular weight and thermal history, i.e. $\tau_g = 1.65 \times 10^{-2}$ s. It is also assumed that PMMA (LMW) readily attains thermodynamic equilibrium at 130 C (T_{eq}). The free volume fraction at 120 C is

corrected from 0.078 to 0.166 (f_g) due to pre-ageing of the specimen, in which the assignment of f_g at 120 C will be shown to have no effect on the value of the activation energy. $\tau(T_a)$ is calculated according to Equation 7.12 and the values are presented in Table 7.7.

$$\tau(T_a) = 1.65 \times 10^{-3}.\exp(1/f - 6.024) \qquad (7.12)$$

For isothermal measurements, the activation energy of physical ageing is calculated from a modified Narayanaswamy expression (Equation 5.8) [35, 37-38] in which the slope of the plot of Ln $(\tau(T_a)/\tau_g)$ versus $(1/T_a).(1/f)$ is equal to $-(E_{act}/R).(1 - 1/f)^{-1}$ (Equation 5.9a). An empirical slope of 351 K^{-1} was obtained from the plot in Figure 7.8 and the respective energies of activation are tabulated in Table 7.7. An inspection of the data of Table 7.7 indicate that E_{act} of PMMA (LMW) in the glass transition region and at equilibrium are similar to those of Cast PMMA (Table 5.5), which clearly shows that the process of physical ageing in both types of PMMA are facilitated by cooperative main-chain motion.

TABLE 7.7

Isothermal relaxation times of slow-cooled low molecular weight poly(methyl methacrylate)

T_a (C)	$\tau(T_a)$ (s)	Ln $(\tau(T_a)/\tau_g)$	$(1/T_a).(1/f)$ (K^{-1})	E_{act} (kJ mol^{-1})
80	3.29×10^{50}	1.20×10^{2}	0.3582	366
90	7.60×10^{5}	1.77×10^{1}	0.0652	66
100	4.73×10^{0}	5.66×10^{0}	0.0313	31
110	2.07×10^{0}	4.83×10^{0}	0.0283	29
115	1.23×10^{-1}	2.01×10^{0}	0.0207	21
120	1.65×10^{-2}	3.46×10^{-3}	0.0153	15

7.4 SUMMARY

(1) The free volume fractions of PMMA specimens of different molecular weights have been shown by viscosity and length measurements to increase with decreasing molecular weight. A decrease in molecular weight is accompanied by an increase in the concentration of

FIGURE 7.8 PLOT OF MODIFIED NARAYANASWAMY EQUATION FOR LOW MOLECULAR WEIGHT PMMA

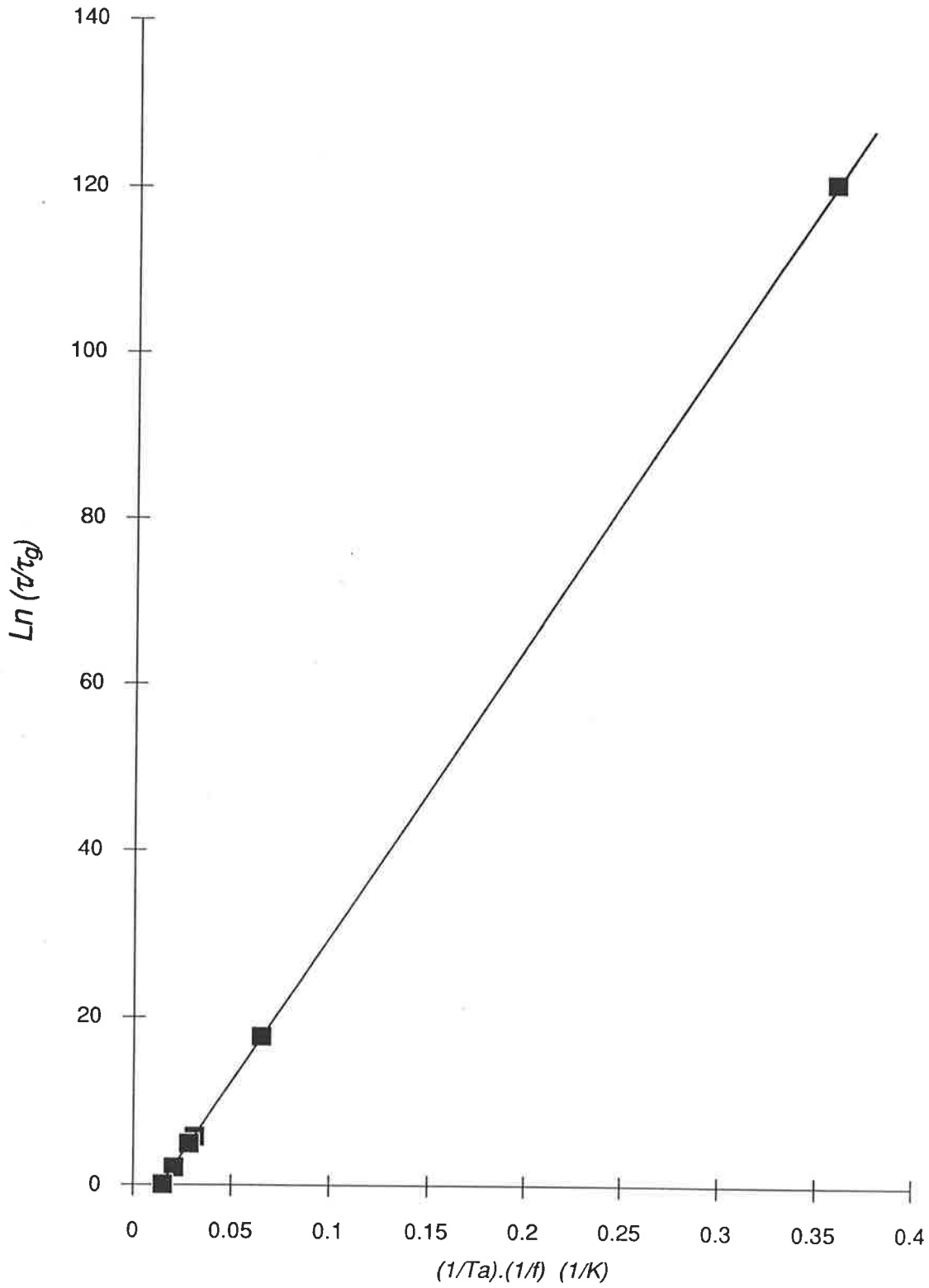

chain ends, in which the increase in free volume fraction is attributed to the higher free volume associated with chain ends.

(2) Length contraction measurements of low molecular weight PMMA showed that specimens which were aged from 130 C onwards were indented by the probe. The indentation was found to be permanent and irreversible, and was attributed to viscoelastic deformation.

(3) The rate of ageing in the glass transition region was found to be higher in low molecular weight PMMA than for Cast PMMA. This was consistent with the prediction of the free volume concept that an increase in free volume fraction resulted in an increase in segmental mobility.

(4) The activation energy for physical ageing in low molecular weight PMMA was found to be similar to those of Cast PMMA in the glass transition region. This observation indicated that physical ageing in Cast and low molecular weight PMMA is facilitated by cooperative motions of main-chain segments.

APPENDIX

Measurement of Viscosity

The viscosities of PMMA solutions were measured in an Ubbelohde capillary viscometer which has the advantage of being independent of the amount of solution in the viscometer [39]. Measurements at a series of concentrations are easily carried out by successive dilutions in the viscometer. The flow times of the solutions were measured electronically and is accurate to +/- 0.01 seconds. The measurements were carried out at a constant temperature of 25.0 C +/- 0.02 C. The flow times of four successive 5 cm^3 dilutions were measured in which an average value for each dilution was obtained after the flow times were reproducible to within +/- 0.03 seconds. The concentrations of the polymer solutions were diluted from an initial value of approximately 2.0 g/100 cm^3 to about 0.12 g/100 cm^3 at the highest dilution.

Determination of Molecular Weight

The specific viscosity, η_{sp}, is related to the relative viscosity, η_r, by

$$\eta_{sp} = \eta_r - 1 = (t/t_0) - 1 \qquad (7.13)$$

where t is the solution flow time and t_0 is the flow time of the pure solvent (seconds). The intrinsic viscosity $[\eta]$ can be determined by extrapolation of the data to zero concentration. Two methods of extrapolation were used, namely, the Huggins equation (Equation 7.14) and (2) the Kraemer equation (Equation 7.15):

$$(\eta_{sp})/C = [\eta] + k'.[\eta]^2.C \tag{7.14}$$

$$\text{Ln } (\eta_r)/C = [\eta] + k''.[\eta]^2.C \tag{7.15}$$

in which the Huggins and Kraemer constants are both dependent on the molecular shape of the solute [40] and they are related by [39]:

$$k' - k'' = 0.5 \tag{7.16}$$

The data for $(\eta_{sp})/C$ vs. C and $[\text{Ln } (\eta_r)]/C$ vs. C are presented in Figs. 7.9 and 7.10. The values for $[\eta]$, k' and k'' are tabulated in Table 7.2. The viscosity average molecular weight of a polymer, $[M]_\eta$, is obtained from the empirical Mark-Houwink equation [39-40]:

$$[\eta] = K.[M]_\eta^a \tag{7.17}$$

where the parameters K and a are constants for a given polymer in a given solvent at a given temperature. The Mark-Houwink constants for PMMA solutions in *n*-butyl acetate are $K = 25 \times 10^{-3}$ and $a = 0.58$ at 25 C [22].

FIGURE 7.9 SPECIFIC VISCOSITIES OF PMMA SOLUTIONS: THE HUGGINS EQUATION

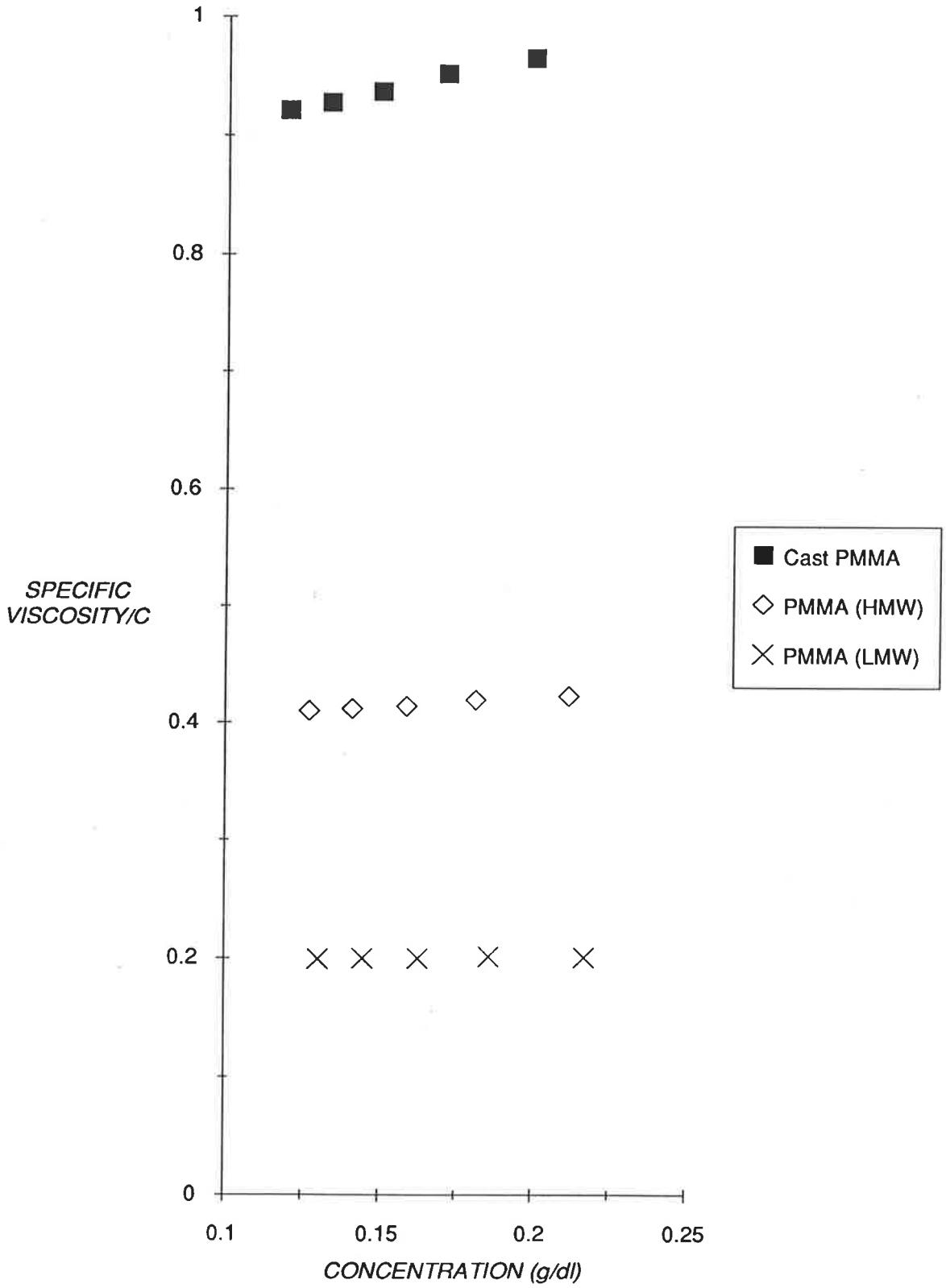

FIGURE 7.10 SPECIFIC VISCOSITIES OF PMMA SOLUTIONS: THE KRAEMER EQUATION

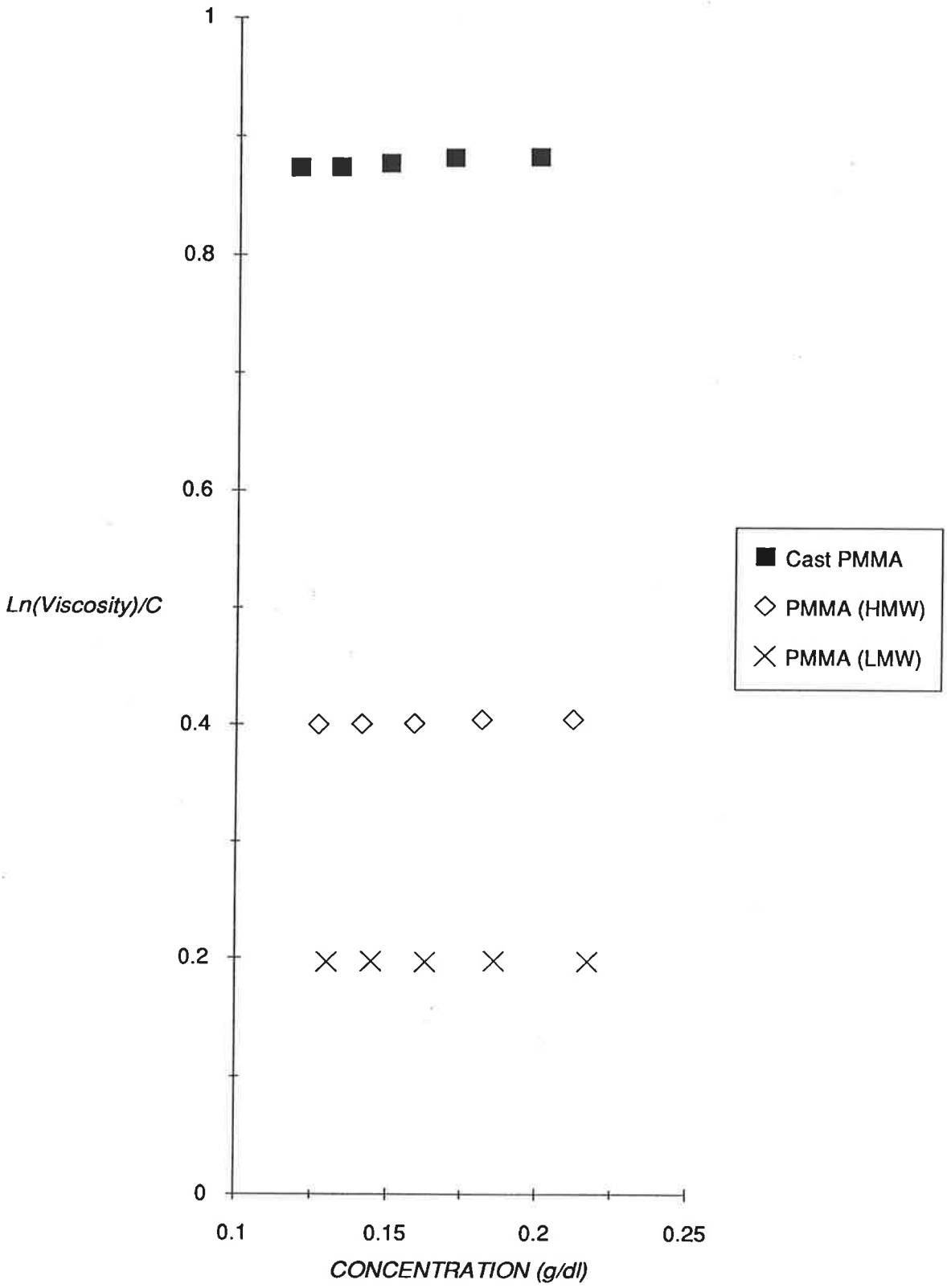

Chapter 7

1. T.G. Fox and P.J. Flory, *J. Appl. Phys.* **21**, 581 (1950).

2. T.G. Fox and P.J. Flory, *J. Polym. Sci.* **14**, 315 (1954).

3. M.C. Shen and A.V. Tobolsky, *Adv. Chem. Series* **48**, 27 (1965).

4. M.C. Shen and A. Eisenberg, *Progress in Solid State Chemistry* **3**, Pergamon Press, (1966) p407.

5. A.K. Doolittle, *J. Appl. Phys.* **22**, 471 (1951).

6. R.N. Haward, *The Physics of Glassy Polymers,* R.N. Haward ed., Aplied Science, London (1973), p1.

7. M.L. Williams, R.F. Landell and J.D. Ferry, *J. Am. Chem. Soc.* **77**, 3701 (1955).

8. A.J. Kovacs, *Fortschr Hochpolym. Forsch.* **3**, 394 (1963).

9. A.J. Kovacs, J.M. Hutchinson and J.J. Aklonis, *Proceedings of the Symposium on the Structure of Non-Crystalline Materials,* P.H. Gaskel ed., Cambridge, England, Taylor and Francs (1977), p153.

10. J.M. Hutchinson and A.J. Kovacs, *J. Polym. Sci. Polym. Phys. Ed.* **14**, 1575 (1976).

11. P.E.M. Allen, G.P. Simon, D.R.G. Williams and E.H. Williams, *Macromolecules* **22**, 809-816 (1989).

12. M.J. Richardson, *Comprehensive Polymer Science* **1**, C. Booth and C. Price eds., Pergamon Press (1989), Chapter 36.

13. T.G. Fox and S. Loshaek, *J. Polym. Sci.* **15**, 371-390 (1955).

14. F. Bueche, *Physical Properties of Polymers*, Interscience Publishers (1962).

15. S. Loshaek and T.G. Fox, *J. Am. Chem. Soc.* **75**, 3544 (1953).

16. D.R.G. Williams, P.E.M. Allen and V.T. Truong, *Eur. Polym. J.* **22(11)**, 911 (1986).

17. D.T. Turner, *Polymer* **19**, 789 (1978).

18. L.C.E. Struik, *Physical Ageing in Amorphous Polymers and Other Materials,* Elsevier, Amsterdam (1978).

19. R. Diaz-Calleja, A. Ribes-Grues and J.L. Gomes-Ribelles, *Polymer* **30**, 1433 (1989).

20. L.C.E. Struik, *Polymer* **28**, 57 (1987).

21. R.B. Beevers and E.F.T. White, *Trans. Faraday Soc.* **56**, 744 (1960).

22. G.V. Schultz and R.G. Kirste, *Z-Physik. Chem.* (Frankfurt) *30*, 171 (1961).

23. E.A. DiMarzio and J.H. Gibbs, *J. Polym. Sci.* **A1**, 1417-1428 (1963).

24. E.W. Fischer, G.P. Hellman, H.W. Spiess, F.J. Horth, U. Ecarius and M. Wehrle, *Makromol. Chem. Suppl.* **12**, 189-214 (1985).

25. F.N. Kelley and F. Bueche, *J. Polym. Sci.* **50**, 549-556 (1961).

26. A.A. Miller, *J. Appl. Sci.* **A2**, 1095-1103 (1964).

27. M.L. Williams, *J. Appl. Phys.* **29**, 1395 (1958).

28. K.M. O'Connor and K.M. Scholsky, *Polymer* **30**, 461 (1989).

29. R. Simha and R.F. Boyer, J. Chem. Phys. 37, 1003 (1962).

30. T.S. Chow, *Macromolecules* **17**, 2336-2340 (1984).

31. L.C.E. Struik, *Ann. N. Y. Acad. Sci.* **279**, 78 (1976).

32. L.C.E. Struik, *Physical Ageing in Amorphous Polymers and Other Materials,* Elsevier, Amsterdam (1978).

33. A.J. Hill, *Materials Forum* **14**, 174-182 (1990).

34. A.J. Hill, K.J. Heater and C.M. Agrawal, *J. Polym. Sci. B: Polym. Phys.* **28**, 387-405 (1990).

35. A.R. Berens and I.M. Hodge, *Macromolecules* **15**, 756-761 (1982).

36. L.C.E. Struik, Polymer **28**, 1869 (1987).

37. O.S. Narayanaswamy, *J. Am. Ceram. Soc.* **54**, 491 (1971).

38. C.T. Moynihan, A.J. Easteal, M.A. DeBolt and J. Tucker, *J. Am. Ceram. Soc.* **59**, 12 (1976).

39. F.W. Billmeyer, Jr., *Textbook of Polymer Science*, 3rd Edition, Wiley-Interscience (1984).

40. J.M.G. Cowie, *Polymers: Chemistry and Physics of Modern Materials*, Intertext (1973).

GLOSSARY OF SYMBOLS

A	Pre-Exponential Factor
a	Mark-Houwink Constant
a(T)	WLF Shift Constant
α_g	Cubical Expansion Coefficient of the Glass State
α_l	Cubical Expansion Coefficient of the Liquid State
α_f	Cubical Expansion Coefficient of Free Volume Fraction
C	Concentration of Polymer Solution
E_{act}	Energy of Activation
f	Free Volume Fraction
f_g	Free Volume Fraction at Thermodynamic Equilibrium
$f(T_a)$	Free Volume Fraction Recovered After Ageing at T_a
f_m	Free Volume Fraction of Polymer of Finite Molecular Weight
f_∞	Free Volume Fraction of Polymer of High Molecular Weight
η	Viscosity
η_{sp}	Specific Viscosity
η_r	Relative Viscosity
$[\eta]$	Intrinsic Viscosity
η_g	Viscosity at Equilibrium
K	Mark Houwink Constant
k', k"	Huggins and Kraemer Constants
L_z, $L_{x,y}$	Initial Sample Lengths
ΔL_z, $\Delta L_{x,y}$	Uniaxial Length Contraction
M, MW	Molecular Weight
$[M]_\eta$	Viscosity-Average Molecular Weight
$[M]_n$	Number-Average Molecular Weight
PMMA (HMW)	High Molecular Weight Poly(Methyl Methacrylate)
PMMA (LMW)	Low Molecular Weight Poly(Methyl Methacrylate)
R	Universal Gas Constant
-r	Rate of Relaxation

T_g	Glass Transition Temperature
T_a	Isothermal Ageing Temperature
T_{eq}	Temperature at Which Thermodynamic Equilibrium is Attained Readily
t_a	Isotehrmal Ageing Period
TMA	Thermomechanical Analyser
τ	Relaxation Time
τ_g	Relaxation Time at Equilibrium
$\tau(T_a)$	Relaxation Time at T_a
V_f	Free Volume
WLF	Williams-Landell-Ferry

CHAPTER 8
PHYSICAL AGEING AND PLASTICISATION

8.1 INTRODUCTION 160

8.2 EXPERIMENTAL 161

8.3 RESULTS AND DISCUSSION

8.3.1 Length Contraction At a Constant Heating Rate 163

8.3.2 Glass Transition Temperature of PMMA Plasticised With DBP 164

8.3.3 Free Volume Fraction of Plasticised PMMA 167

8.3.4 Thermal Expansion Coefficient of Plasticised PMMA 170

8.3.5 Isothermal Ageing of Quenched PMMA Plasticsed With DBP 172

Length Contraction and Free Volume Fraction 172

Rates of Relaxation and Activation Energies 173

8.4 SUMMARY 176

BIBLIOGRAPHY 177

GLOSSARY OF SYMBOLS 180

CHAPTER 8

8.1 INTRODUCTION

A *plasticiser* may be defined as a relatively low molecular weight substance of low volatility which, when added to another material, changes the physical and chemical properties of that material [1]. The plasticiser usually behaves like a solvent when mixed into a polymer and results in the lowering of the melt viscosity, the tensile modulus and the glass transition temperature [2-3]. It is believed [2] that about 80 % of all plasticiser production is consumed by the manufacture of poly(vinyl chloride) (PVC) formulations, where typical commercial PVC products contain from 20-50 wt % plasticiser.

The primary result of plasticisation is the lowering of the glass transition temperature [3-11]. The addition of a plasticiser shifts the relaxation time to shorter times [12], and in the framework of conventional free volume theory, this effect has been explained as due to an increase in free volume with the addition of plasticiser [5, 13-14, 33]. If the T_g represents an iso-free volume state for a polymer [15-16], then the T_g can be changed by altering its free volume at a given temperature [17-18]. A polymer can be mixed with a miscible liquid that contains more free volume than the pure polymer. If one assumes addivity of free volume [19], the diluent-polymer solution will contain more free volume at any given temperature than would the polymer alone. Consequently, the plasticised polymer must be cooled to a lower temperature in order to reduce its free volume to the amount always present at T_g [6]. The T_g may also be altered by the action of chain ends [20-21]. Since each chain end will necessarily possess more free volume than if it were chemically bound within a continuous chain, the presence of chain ends will increase the amount of free volume in the polymer at any given temperature. Hence, polymers incorporated with diluents or other polymers of very low molecular weights will have a lower value for T_g than for the pure homopolymer. The glass transition of the plasticised polymer is related to the weight fractions and glass transition temperatures of the plasticiser and polymer by [22]

$$T_g^{-1} = (w_1/T_{g1}) + (w_2/T_{g2}) \qquad (8.1)$$

where the subscript 1 and 2 refer to the plasticiser and polymer components respectively. Equation 8.1 has been evaluated experimentally [9-10] and has been successful in predicting the glass transition for both polymer-polymer and polymer-plasticiser blends. However, it will be shown that this equation fails when the T_g's between the two components are very different.

Although Equation 8.1 predicts a continuous decrease in T_g with increasing plasticiser concentration, there are some exceptions to this pattern [23-28]. Deutron NMR measurements of phenyl motion in polycarbonate found that the mean value of the activation energy and the average relaxation time was increased by plasticisation [28-30]. The plasticiser hinders the phenylene ring mobility, while on the other hand they facilitate segmental mobility. These opposite effects that the plasticisers have on the primary and secondary relaxations justify the use of the term *antiplasticisation* to describe the effects on the secondary relaxation [12]. Antiplasticisation was originally used to describe the property of a plasticised polymer in the glassy state below T_g as being harder and more brittle than the unplasticised polymer [3, 24].

Despite the fact that the effects of plasticisation on T_g has been well researched, little is known about the effects of plasticisation on the ageing process of PMMA. Gomez-Ribelles *et al.* [31] showed that physical ageing in poly(vinyl chloride) (PVC) was accelerated by plasticisation with dioctyl phthalate. It was proposed that the presence of a plasticiser increases the mobility of the backbone chains, which was thought to be responsible for ageing [32]. The purpose of this chapter is to investigate the nature of physical ageing in plasticised PMMA in which three plasticsers were used, namely, dibutyl phthalate (DBP), dioctyl phthalate (DOP) and tricresyl phosphate (TCP). The results indicate that the introduction of plasticisers have a significant effect on the rate of ageing and free volume fraction of PMMA.

8.2 EXPERIMENTAL

The casting procedure for plasticised PMMA depended on the plasticiser concentration and on the final state of the plasticised polymer. The plasticiser was added to the monomer solution prior to curing and the plasticiser-monomer mixture was then cured between glass sheets according to the method of Cowperthwaite [34]. Glassy plasticised PMMA specimens with low plasticiser concentrations were isothermally cured at 60 C. To minimise the loss of monomer and plasticiser during cure, the top edge of the mould was sealed with a commercial sealing film. When PMMA was plasticised with highly-toxic plasticisers like

tricresyl phosphate, the entire casting assembly was carefully placed inside a sealed polythene bag to prevent the evaporation of toxic fumes in the oven. After the plasticised sheet had vitrified, it was further postcured at 125 C for 2 hours. Plasticised PMMA with high plasticiser concentrations leading to soft or leathery specimens were initially cured at 60 C, followed by a gradual increase in temperature to 80 C. The sheets were postcured isothermally at 80 C until no further shrinkage could be observed. Specimens used in thermal analysis were taken from the centre of the sheet since oxygen is known to inhibit the polymerisation process [35-39]. Recrystallised dibenzoyl peroxide was used as the radical initiator, at a concentration of approximately 0.2 mole %.

The plasticiser concentration was calculated in terms of the mole percentage of methyl methacrylate monomer, thus the number of moles of plasticiser to be added to a *y*% MMA-plasticiser mixture is:

$$n_1 = (y/100).n_{MMA} \tag{8.2}$$

where n_{MMA} refers to the number of moles of MMA monomer. The plasticiser concentration can also be expressed as a weight fraction of the total mass of MMA-plasticiser mixture, viz.

$$w_1 = m_1/(m_1 + m_{MMA}) \tag{8.3}$$

where m_1 refers to the mass of the plasticiser. The weight fractions of the plasticisers in the MMA:DBP, MMA:DOP and MMA:TCP mixtures are presented in Table 8.1.

The plasticised PMMA specimens were thermally equilibrated for 15 minutes by heating to 140 C for glassy specimens or to 100-120 C for leathery specimens. This was followed by quenching in liquid nitrogen for 10 minutes. The specimen was immediately transferred to the TMA and was allowed to thermally equilibrate under dry nitrogen for 20 minutes. The sample chamber of the TMA had been programmed at the starting temperature which was determined by the glass transition region of the specimen. The starting temperature was selected such that it was at least 40 C below the onset temperature of contraction, whereas the final temperature was about 20 C above the endset temperature of contraction. The length

contraction of the specimen was measured at a constant rate of 2 C/min under a constant load of 0.1 N.

TABLE 8.1

Weight fractions of monomer-plasticiser mixtures

Mole Percent	w_{DBP}	w_{DOP}	w_{TCP}
5		0.16	
10	0.22	0.28	0.27
15	0.29	0.37	
20	0.36	0.44	0.43
30	0.46	0.54	0.53
40	0.53		0.60

8.3 RESULTS AND DISCUSSION

8.3.1 Length Contraction At a Constant Heating Rate

The ΔL-T plots of PMMA:DBP, PMMA:DOP and PMMA:TCP are shown in Figures 8.1-8.3. It is observed that an increase in plasticiser concentration generally resulted in an increase in length contraction and a lowering of the onset temperature of contraction (T_{on}). The lowering of T_{on} is consistent with observations [3-11] that T_g is lowered by the addition of plasticiser.

However, there is a very large decrease in contraction from 15 mol % to 20 mol % DOP (Fig. 8.2). This observation correlates with a change in texture from a soft, flexible sheet at 15 mol % DOP to a brittle and "crumbly" sheet at 20 and 30 mol % DOP. The appearance of small, white clusters at 20 and 30 mol % DOP indicates the existence of a two-phase system which suggests that phase separation had occured. At the present time, it is suggested that the separation of the polymer-plasticiser mixture into a miscible and non-miscible phase effectively reduces the amount of plasticised polymer and results in a smaller length contraction. The possibility of antiplasticisation has been discounted because antiplasticisation is usually observed when small amounts of plasticiser are added [3].

FIGURE 8.1 LENGTH CONTRACTION OF PMMA PLASTICISED WITH DBP (numbers adjacent to curves indicate the mole percentage of DBP)

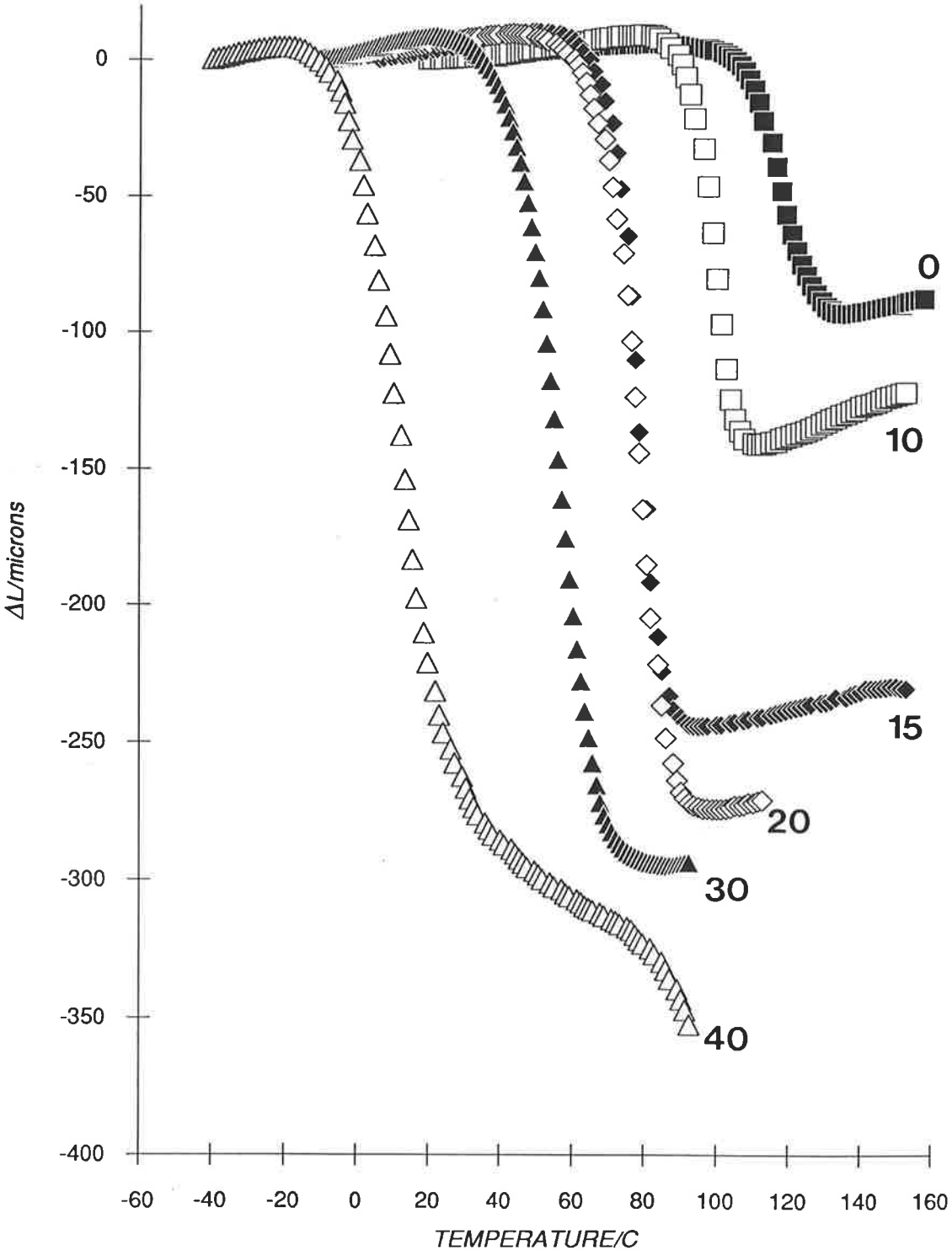

FIGURE 8.2 LENGTH CONTRACTION OF PMMA PLASTICISED WITH DOP (numbers adjacent to curves indicate the mole percentage of DOP)

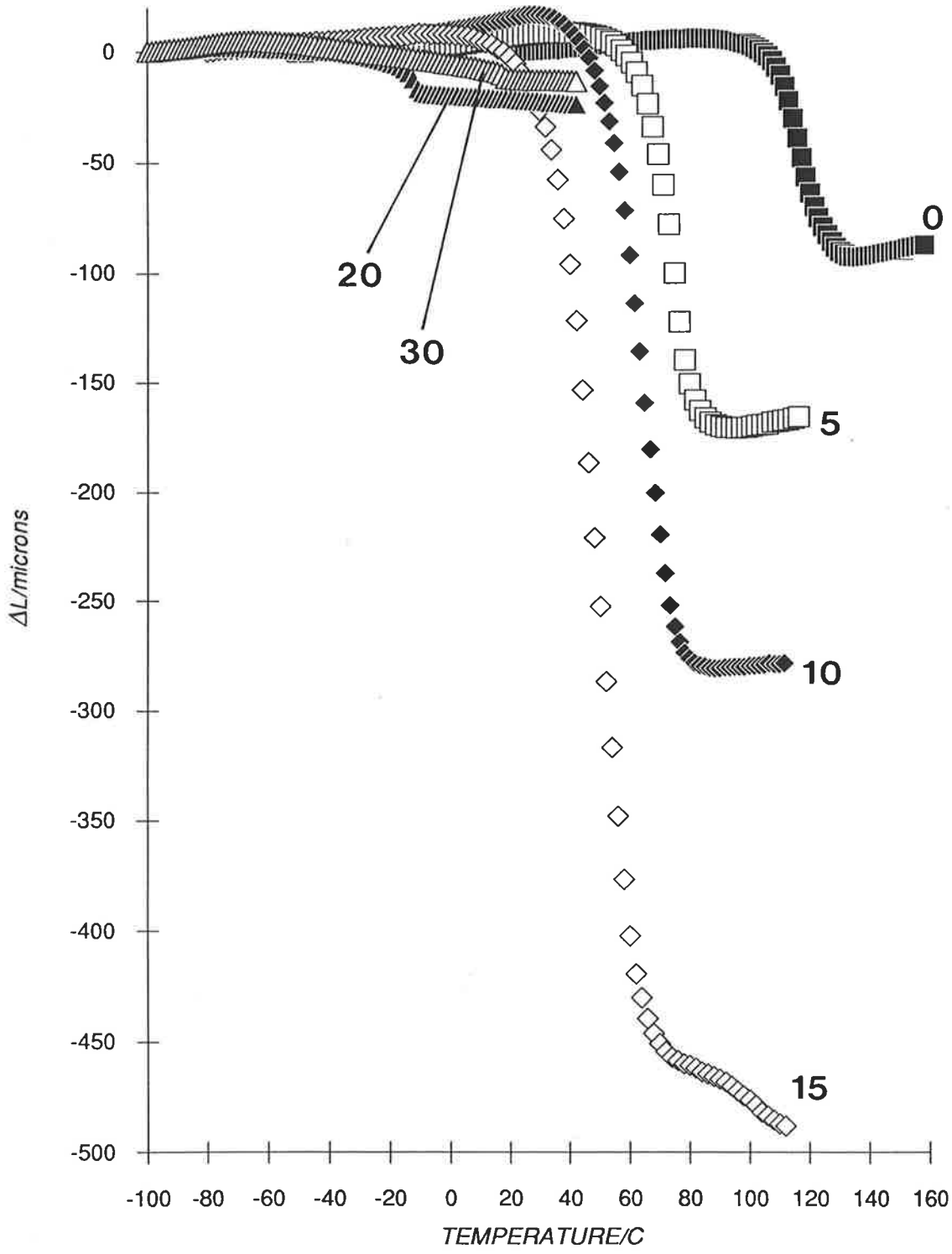

FIGURE 8.3 LENGTH CONTRACTION OF PMMA PLASTICISED WITH TCP (numbers adjacent to curves indicate the mole percentage of TCP)

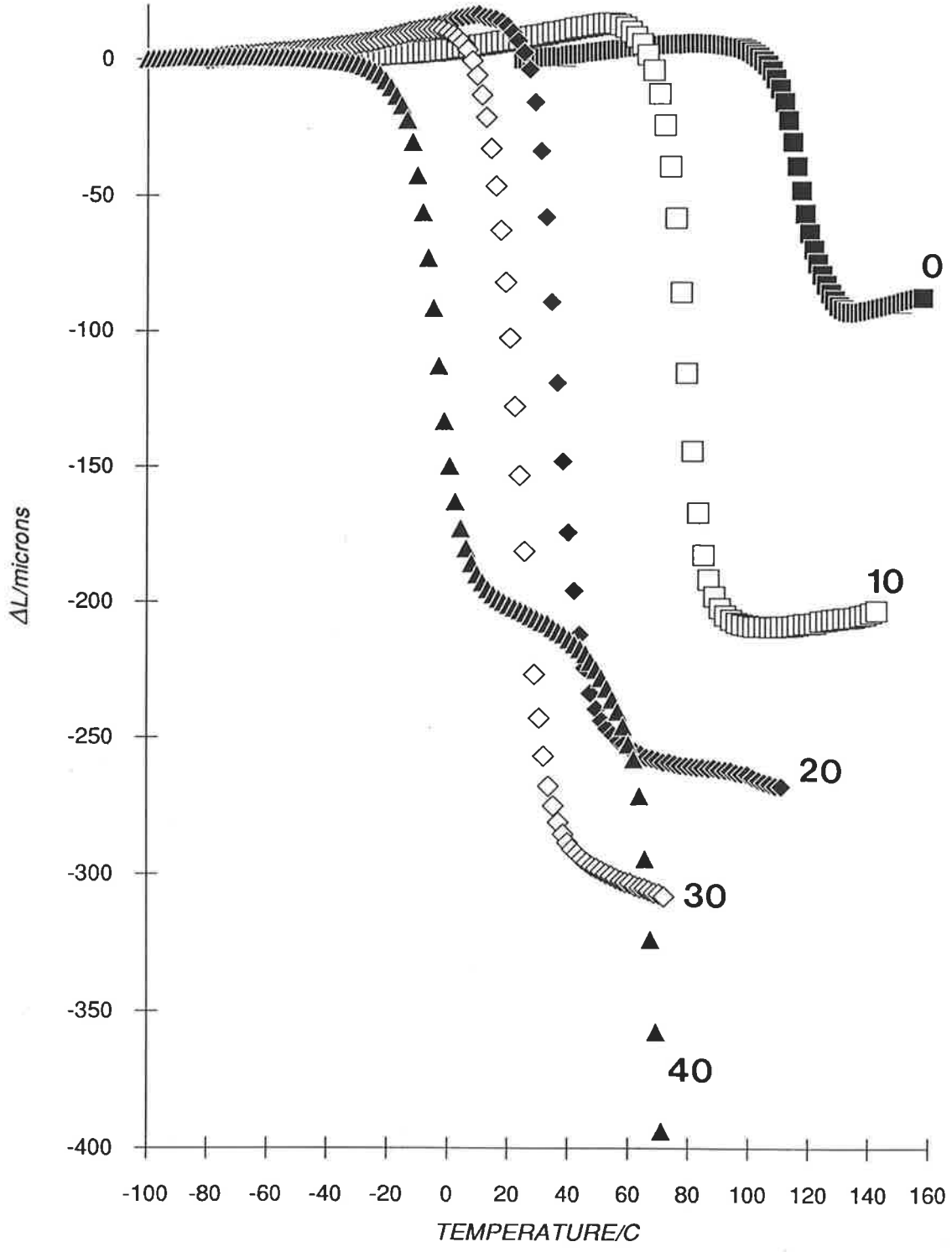

On the other hand, a number of authors [31, 40-41] have reported the occurence of two glass transitions in plasticised PVC systems. It was suggested that two separate glassy phases have been formed, in which the higher T_g was assigned to a non-crystalline syndiotactic phase whereas the lower T_g was assigned to atactic chain segments which were more miscible with the plasticiser [40-41]. A similar explanation was offered by Gomez-Ribelles *et al.* [31], who suggested the existence of two amorphous phases in unplasticised PVC, both with the same T_g but one of which does not absorb plasticiser. This conclusion was supported by the results of Foldes *et al.* [42], who found that the characteristic peak of the α dielectric relaxation of unplasticised PVC was split into two peaks in plasticised PVC, in which one of the peaks was located at the same temperature as that of the unplasticised PVC but the other peak was located at a lower temperature.

The perseverance of length contraction above T_g for polymers containing 40 mol % DBP, 15 mol % DOP and 30 mol % and 40 mol % TCP is similar to that observed for low molecular weight PMMA (Fig. 7.4), suggesting that viscoelastic deformation of these plasticised PMMA specimens is occuring by a similar viscous flow mechanism.

8.3.2 Glass Transition Temperature of PMMA Plasticised With DBP

In this section, the relationship between T_g and weight fraction of plasticiser is examined for the PMMA:DBP system. Fox [22] proposed that T_g of a plasticised polymer may be related to the respective weight fraction and T_g of the pure plasticiser and polymer according to Equation 8.1. An alternative relationship describing the composition dependence of T_g was developed by Pochan *et al.* [44] assuming that $\Delta C_{p1} = \Delta C_{p2}$:

$$\text{Ln } T_g = w_1.\text{Ln } T_{g1} + w_2.\text{Ln } T_{g2} \qquad (8.4)$$

A third version of Equation 8.1 is obtained if the heat capacity increments of the pure components have the same value and the logarithmic functions are suitable expanded [19]:

$$T_g = w_1.T_{g1} + w_2.T_{g2} \qquad (8.5)$$

The thermal expansion of pure DBP has been measured from -100 C to 0 C. Figure 8.4 shows a T_g for DBP at -81 C and a melting temperature T_m at *ca* -67 C. Literature values of T_g and T_m for DBP are -95 C [57] and -40 C [54] respectively. It is interesting to note that there is no evidence of physical ageing in pure DBP, which suggests that physical ageing may not be observed in low molecular weight solids. This may be due to the fact that low molecular weight solids contain larger free volume fractions which permit a rapid rate of ageing.

Using a value of 105 C for T_g of unplasticised PMMA, the T_g's of PMMA:DBP polymers were calculated according to Equations 8.1, 8.4 and 8.5. These values were then compared with the onset temperature of contraction, T_{on}, which has been considered to provide an alternative indicator of the glass transition (Section 4.4.2). The calculated glass transition temperatures and onset temperatures of contraction of PMMA:DBP are presented as a function of the weight fraction of DBP in Figure 8.5 and Table 8.2.

TABLE 8.2

Calculated glass transition temperatures and onset temperature for contraction of poly(methyl methacrylate) plasticised with dibutyl phthalate

Weight Fraction		*Glass Transition Temperature*			
w_{DBP}	w_{MMA}	Eq. 8.1 (C)	Eq. 8.4 (C)	Eq. 8.5 (C)	T_{on} (C)
0.22	0.78	39	53	64	82
0.29	0.71	22	38	51	54
0.36	0.64	7	23	38	51
0.46	0.54	-12	4	19	35
0.53	0.47	-23	-10	6	-8

Table 8.2 shows that plasticisisation of PMMA results in the lowering of T_g with increasing plasticiser concentration. The calculated T_g's are consistently lower than T_{on} in agreement with the data of Beirnes *et al.* [40] for PVC plasticised with DOP. The reason for the deviation from the empirical equations is that they assume that $T_{g1}/T_{g2} \approx 1$ whereas T_g of the two pure components differ by about 185 C [40]. It is also observed that T_{on} decreases with increasing DBP concentration. This observation supports the claim that the onset of the glass-rubber

FIGURE 8.4 THERMAL EXPANSION OF DIBUTYL PHTHALATE

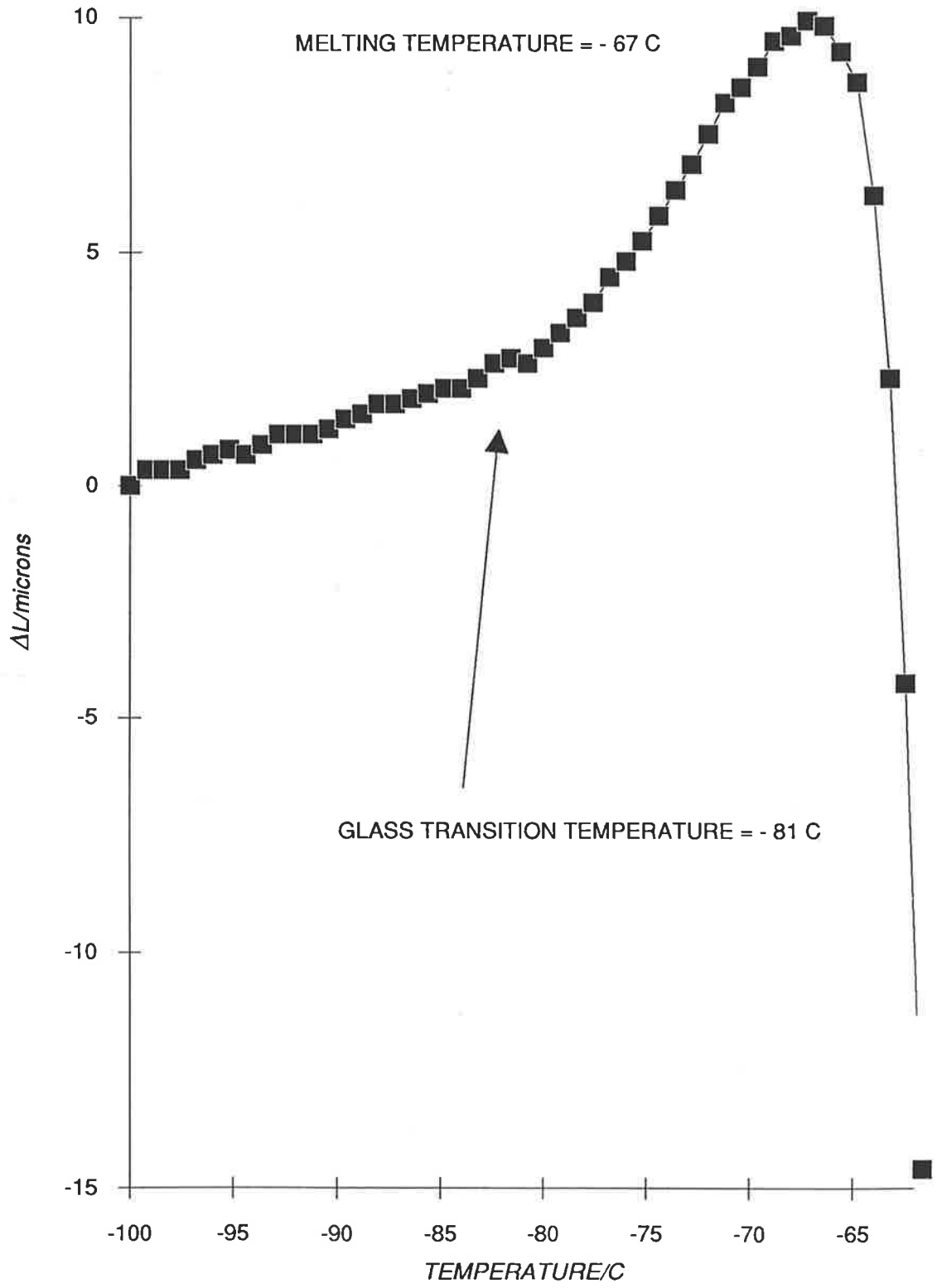

FIGURE 8.5 GLASS TRANSITION TEMPERATURES OF PMMA PLASTICISED WITH DBP

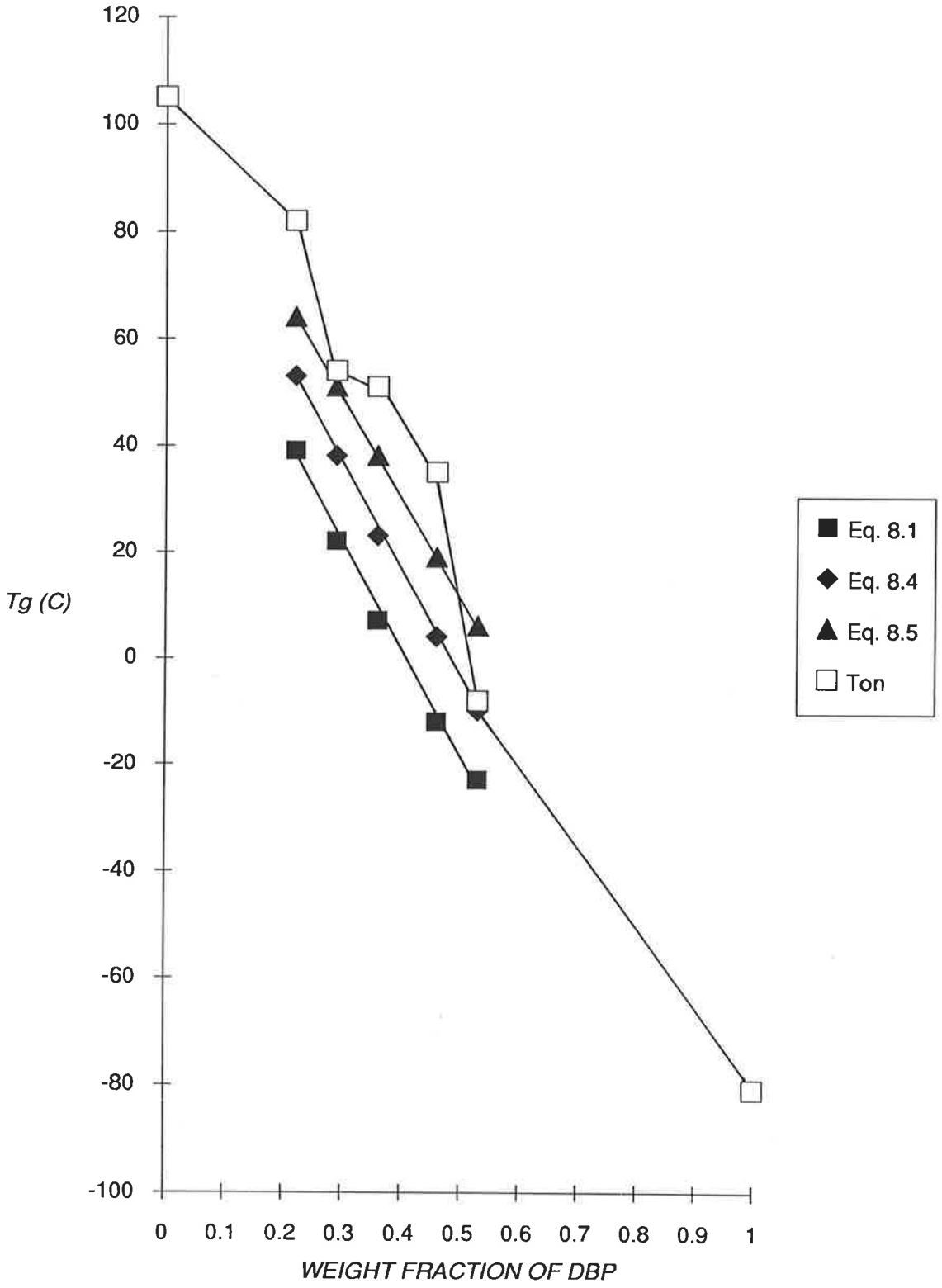

transition may be characterised by the onset of length contraction at T_{on}. In addition, the shift of T_{on} to lower temperatures (as characterised by $\Delta T_{on} = T_{on}(PMMA) - T_{on}(PMMA + plasticiser)$) increases with increasing plasticiser concentration. The values of T_{on} and ΔT_{on} of the three plasticised PMMA systems are presented in Table 8.3 and Figure 8.6.

TABLE 8.3

T_{on} (C) and ΔT_{on} (C) of plasticised PMMA as a function of weight fraction of plasticiser (w_1)

w_{DBP}	T_{on} (PMMA:DBP)	ΔT_{on} (PMMA:DBP)
0	104	0
0.22	82	22
0.29	54	50
0.36	51	53
0.46	35	69
0.53	-8	112

w_{DOP}	T_{on} (PMMA:DOP)	ΔT_{on} (PMMA:DOP)
0	104	0
0.16	57	47
0.28	44	60
0.37	30	74
0.44	-39	143
0.54	-64	168

w_{TCP}	T_{on} (PMMA:TCP)	ΔT_{on} (PMMA:TCP)
0	104	0
0.27	66	38
0.43	26	78
0.53	9	95
0.60	-13	117

An inspection of Table 8.3 and Figure 8.6 indicates that T_{on} is lowered to the greatest extent in PMMA:DOP while similar changes in T_{on} are observed for PMMA:DBP and PMMA:TCP (Table 8.3 and Figure 8.6). These observations suggest that the alkyl chains of DOP has a larger effect on lowering T_{on} than the bulky tri-phenyl groups of TCP. Therefore, the free volume fractions of PMMA:DOP are expected to be larger than those of PMMA:DBP and PMMA:TCP.

8.3.3 Free Volume Fraction of Plasticised PMMA

The free volume approach to understanding the complex behaviour of polymer-plasticiser systems was developed by Kelley and Bueche [5] in which the free volume of the plasticised polymer may be assumed as the sum of the free volume fractions contributed by the plasticiser, f_1, and by the polymer, f_2. The empirical equation for free volume of a polymer is

$$V_f = f_2.[0.025 + \Delta\alpha.(T - T_g)] + (1 - f_2).[0.025 + \alpha_p.(T - T_{g1})] \qquad (8.6)$$

where α_p and T_{g1} are the thermal expansion and glass transition temperature of the plasticiser. The shortcomings of Equation 8.6 are that it is derived from the WLF equation [15] which predicts a free volume fraction of only 0.025. In addition, T_g's of plasticised polymers have been shown to deviate from values calculated from phenomenological equations.

The free volume V_f of quenched plasticised PMMA is calculated from the length contraction ΔL_z using Equation 4.2 where the initial sample lengths L_z and $L_{x,y}$ are 1.75×10^{-3} m and 4.80×10^{-3} m. The free volume fraction f is defined as V_f/V_{eq}, in which the equilibrium volume is $(L_z - \Delta L_z).(L_{x,y} - \Delta L_{x,y})^2$. The free volume fractions of plasticised PMMA are presented in Table 8.4 and Figure 8.7. Figure 8.7 shows that the free volume fraction of plasticised PMMA increases with increasing plasticiser concentration, with the exception at 20% and 30% DOP. The largest increment is observed for PMMA:DOP in which the free volume fraction at 37 wt.% is about three times that of the unplasticised PMMA. These observations are consistent with the result that the largest decrease in T_{on} was observed for PMMA:DOP.

The variance of the free volume fraction with plasticiser concentration displayed by the three plasticised PMMA specimens indicates that the nature of polymer-plasticiser system is extremely complicated. The relationship between free volume fraction and plasticiser

FIGURE 8.6 ONSET TEMPERATURE OF CONTRACTION OF PLASTICISED PMMA

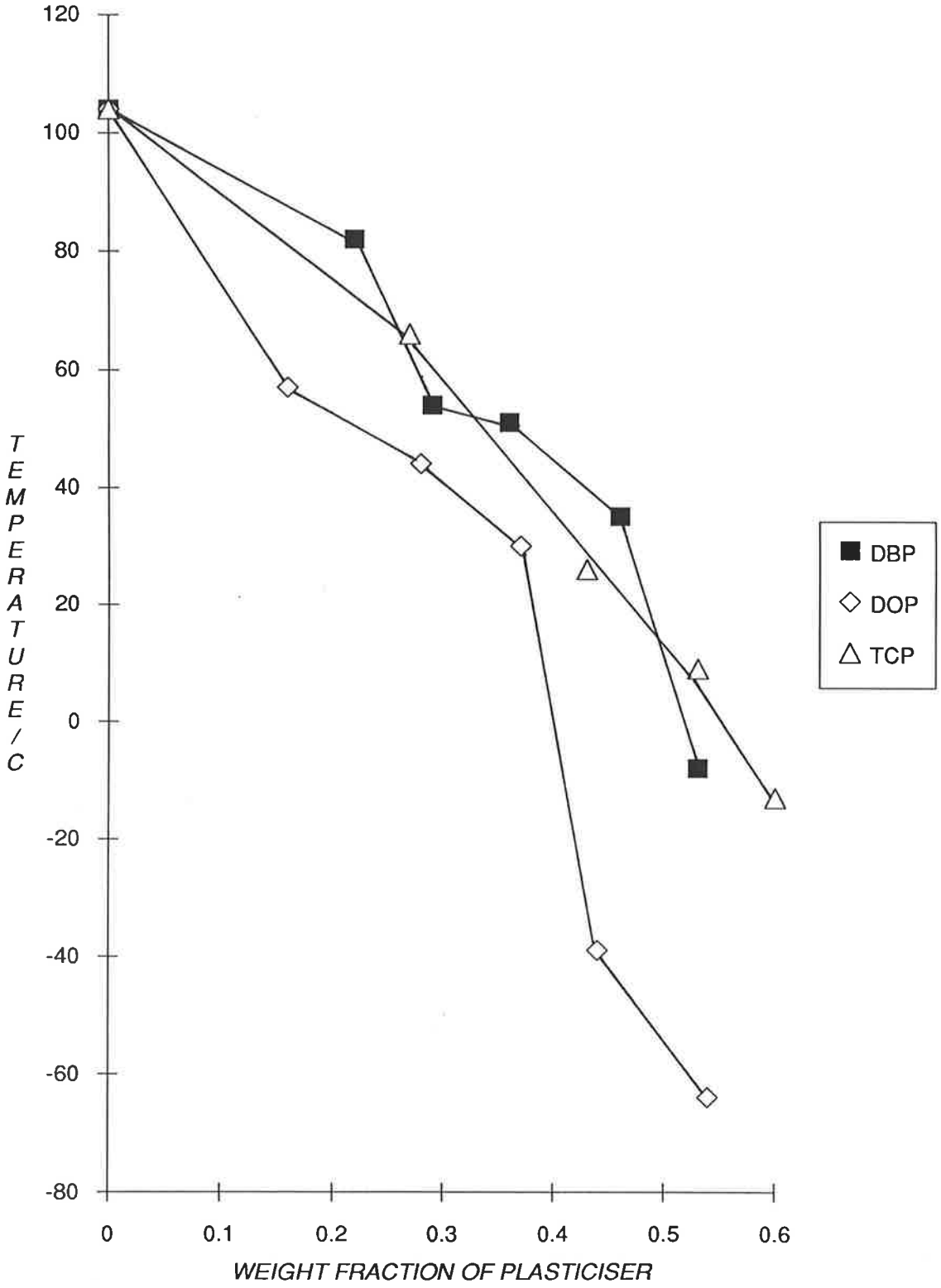

FIGURE 8.7 FREE VOLUME FRACTIONS OF PLASTICISED PMMA

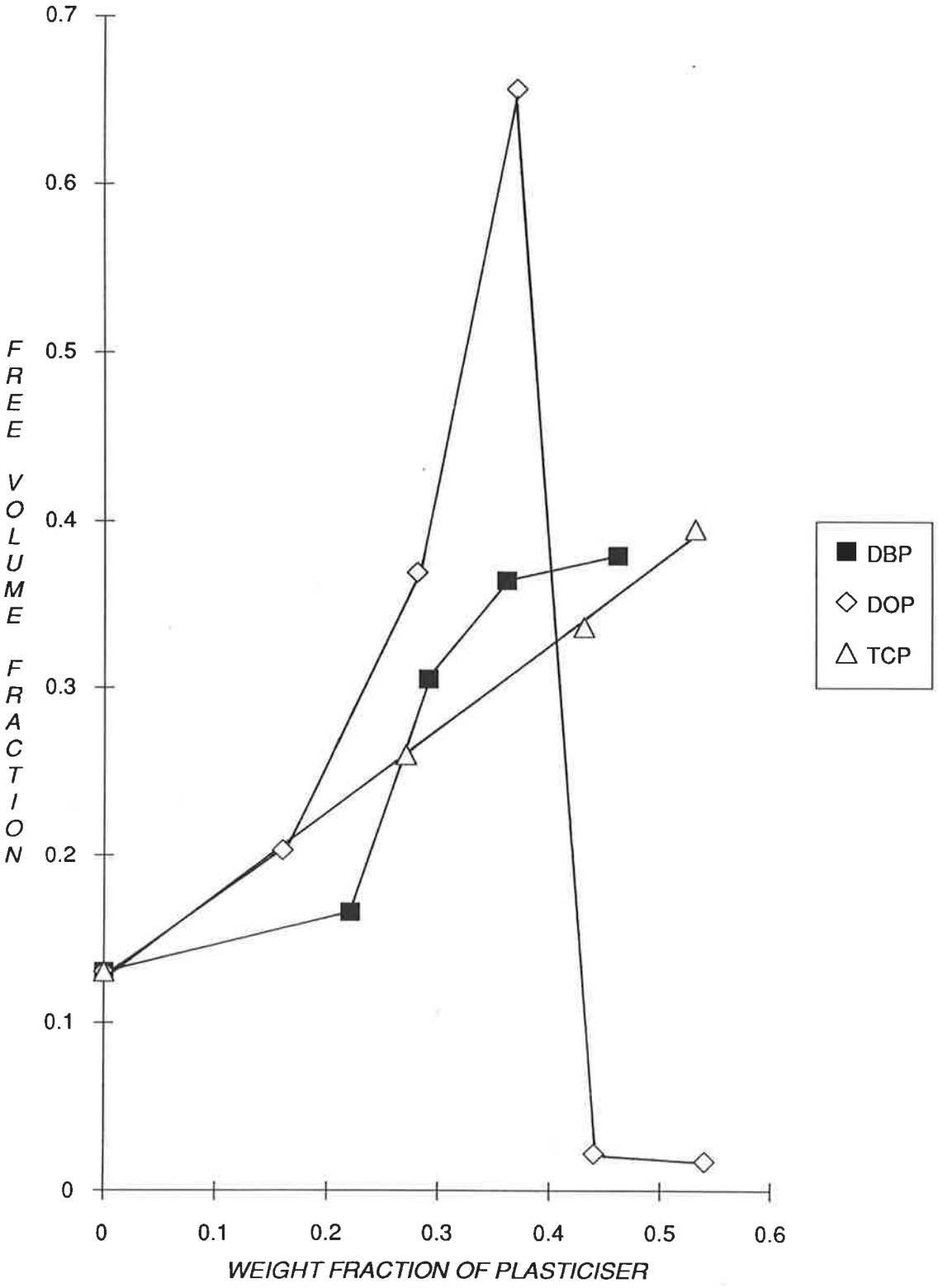

concentration of PMMA:TCP is approximately a straight line, whereas a sigmodial curve is observed for PMMA:DBP. On the other hand, the free volume fraction of PMMA:DOP rapidly increases with DOP concentration up to a weight fraction of about 0.40.

TABLE 8.4

Free volume fractions of plasticised PMMA as a function of weight fraction of plasticiser

w_1	f_{DBP}	f_{DOP}	f_{TCP}
0	0.13	0.13	0.13
0.16		0.203	
0.22	0.166		
0.27			0.260
0.28		0.369	
0.29	0.305		
0.36	0.364		
0.37		0.656	
0.43			0.336
0.44		0.0217	
0.46	0.379		
0.53			0.395
0.54		0.0168	

However, Williams *et al.* [43] and Elwell and Pehtrick [44] found that the free volume of polymer chains was lowered by the introduction of diluent. The reduction in free volume was attributed to the occupation of free volume sites by plasticiser molecules. NMR studies [45] of PVC plasticised with DBP indicated that the plasticised polymer contained no free DBP molecules up to a concentration as high as 52 wt.%, but that all of the DBP were at least partially restricted or bound. The study of water sorption in plasticised PMMA by Turner *et al.* [46-47] showed that the rate of water uptake was lowered in PMMA when plasticised with DOP. This was attributed to the filling of "microvoids" [48-49] in PMMA by DOP molecules, which otherwise would have been able to accommodate water. The average size of free volume

holes in PMMA is 1.84 x 10^{-28} m^3 [50], whereas the volume occupied by a plasticiser molecule is between 4.3-5.2 x 10^{-28} m^3. The volumes are estimated from the densities and molecular weights of DBP, DOP and TCP [51], in which the order of occupied volumes is DBP < TCP < DOP. It is suggested that adjacent holes may coalesce to comprise a hole large enough to accommodate a plasticiser molecule. The coalescence of holes into larger vacancies has been suggested by Bueche [6] as a possible mechanism to enable molecular motion to occur. Such plasticiser action is consistent with the *mechanistic theory* [52-54], which assumes that plasticisers are attracted to the polymer chains by forces of different magnitudes and that none of the plasticiser molecules are permanently bound. Instead, there is a continuous exchange whereby one plasticiser molecule becomes attached at a given point only to be dislodged by another molecule. Hence, a dynamic equilibrium exists between the "solvation" and "desolvation" of polymer chains and results in a decrease in rigidity of the polymer structure [44].

Nevertheless, the mechanistic theory does not account for the increase in free volume fraction observed in Figure 8.7 and Table 8.4. In view of the strong evidence which supports the concept of plasticiser molecules occupying free volume holes, a simple calculation shows that the available free volume in PMMA cannot accommodate every plasticiser molecule even at a concentration of 10 mole %. The molar volume of DBP is approximately 2.67 x 10^{-4} m^3, therefore a DBP concentration of 0.012 moles (the usual MMA concentration is about 0.12 moles) will occupy a volume of 3.2 x 10^{-6} m^3. Assuming that every available space is filled, the free volume of PMMA of 4.5 x 10^{-9} m^3 can only accommodate up to 0.15% of DBP molecules, which means that the vast majority of DBP molecules do not occupy free volume holes.

An alternative hypothesis is that the increase in free volume in plasticised PMMA is caused by the swelling of polymer by plasticiser molecules. A number of authors [48, 55-56] have reported a dual mechanism for the absorption of water in PMMA. The initial and faster process is associated with the filling of microvoids, which results in an increase in density and little change in dimensions. The second process is associated with the swelling of the polymer with little change in density [48]. ^{13}C NMR studies [56] showed that during the early stages of absorption, water molecules were found to be in contact with the backbone CH_2 and quaternary C. As the points of contact of initial water uptake were not the sites where water-polymer

interactions would be strongest, it was claimed that the coiled chains of amorphous PMMA form channels containing quartenary C and backbone CH_2 groups which allow the percolation of water during the initial uptake. It is suggested that the occupancy and transport of plasticiser molecules through these channels causes the polymer to swell. Consequently, physical ageing in a swollen plasticised polymer is enhanced by cooperative motion of main-chains.

The "effectiveness" of a plasticisicer may be characterised by the magnitude of the shift of T_{on} to lower temperatures, in which a more effective plasticser would result in a larger decrease in T_{on}. Therefore, the effectiveness of the three plasticisers studied may be ranked in the following order: DOP > DOP ≈ TCP. The relationship between the effectiveness of a plasticiser and the free volume fraction of the plasticised polymer is shown in Figure 8.8 where the free volume fraction is plotted as a function of ΔT_{on}. The similarity of Figure 8.8 with Figure 8.7 indicates that the the lowering of T_{on} by plasticisation is also accompanied by an increase in free volume fraction, which is in accordance with the predictions of the free volume theory [5, 13-14].

8.3.4 Thermal Expansion Coefficient of Plasticised PMMA

The linear glass and liquid thermal expansivities for PMMA:DBP, PMMA:DOP and PMMA:TCP are presented in Table 8.5. Negative values of α'_l indicate that the specimen had undergone viscous flow. The thermal expansivities of unplasticised PMMA determined at a heating rate of 2 C/min are $\alpha'_g = 56.4 \times 10^{-6}\ K^{-1}$ and $\alpha'_l = 142.8 \times 10^{-6}\ K^{-1}$.

The glass expansivity is plotted as a function of the plasticiser weight fraction in Figure 8.9. In general, α'_g of plasticised PMMA is larger than the value obtained for unplasticised PMMA with the exception of containing 0.60 weight fraction TCP. These observations are consistent with the hypothesis [58-59] that the freezing-in of excess free volume leads to an increase in α'_g. Figure 8.9 shows that α'_g of PMMA:DBP increases monotonically with increasing DBP concentration above 0.2 weight fraction of DBP. On the other hand, α'_g of PMMA:DOP and PMMA:TCP both show a large initial increase, but subsequent increases in plasticiser concentration result in a decrease in α'_g. This is surprising, since the data of Table 8.4 indicated that an increase in plasticiser concentration would result in an increase in free volume fraction and hence α'_g (except at 0.44 and 0.54 weight fraction DOP). It is possible that the bulky molecular groups of DOP and TCP undergo transitions at

FIGURE 8.8 RELATIONSHIP BETWEEN FREE VOLUME FRACTION AND THE SHIFT IN THE ONSET TEMPERATURE OF CONTRACTION

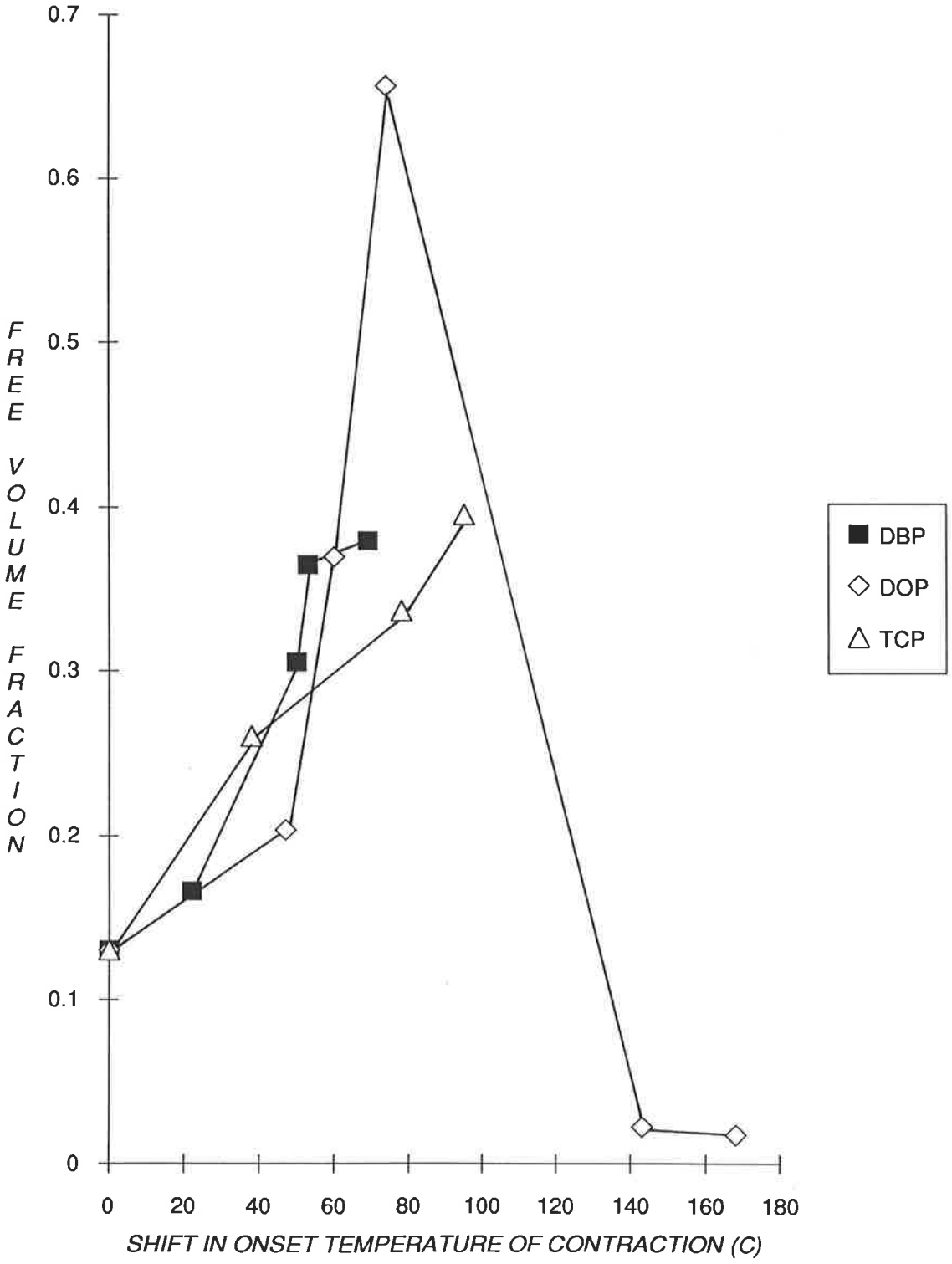

FIGURE 8.9 GLASS EXPANSION COEFFICIENTS OF PLASTICISED PMMA

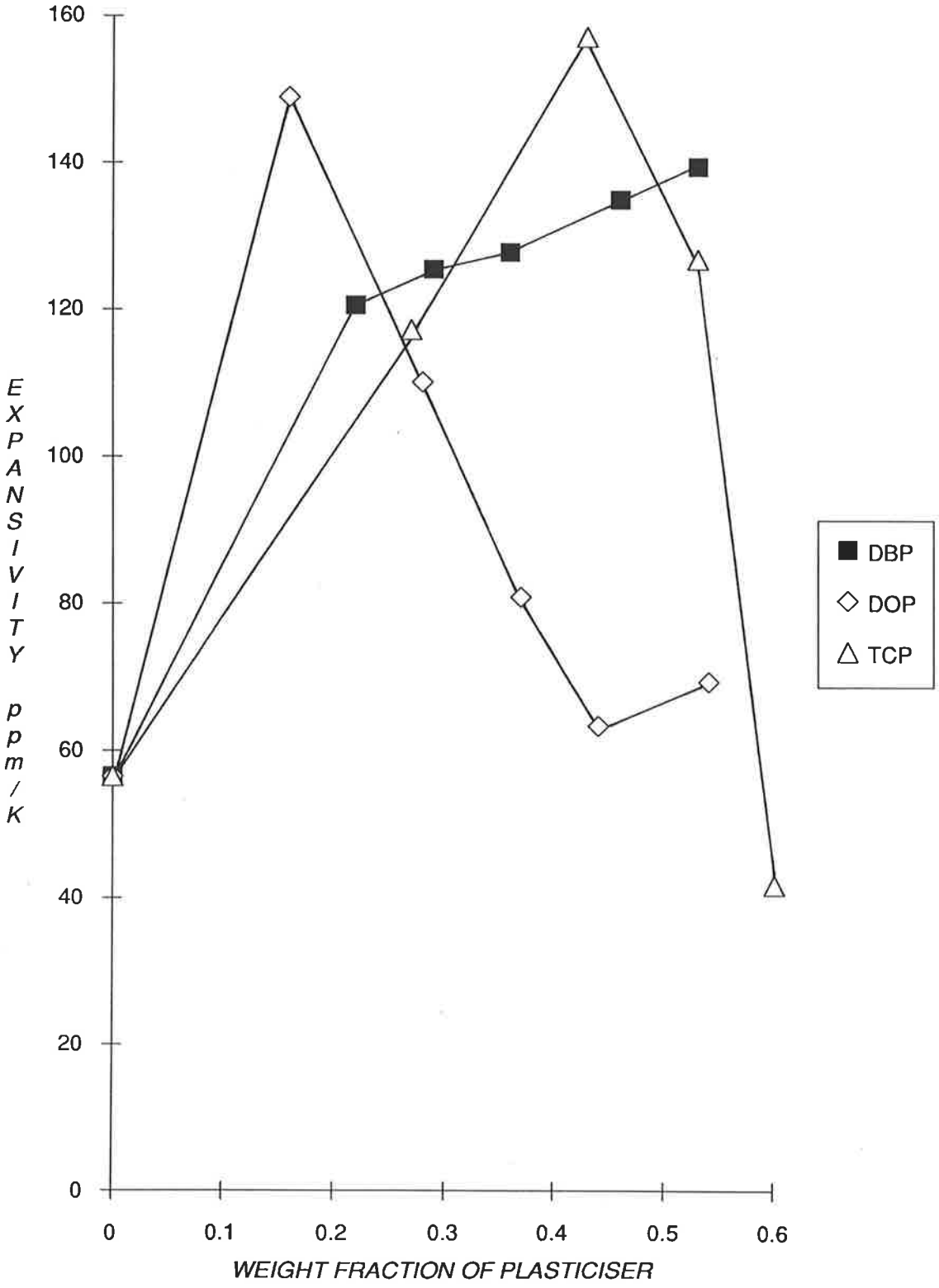

temperatures well below T_{on} which lead to the diffusion of "local free volume" and a decrease in α'_g [58-59]. The term local free volume is used to indicate that the transitions only annihilate free volume that is diffused by the rotation of the molecular moeity. These cryogenic transitions have little effect on the total free volume fraction (as indicated by Table 8.4) and have a significant effect on α'_g only at high plasticiser concentrations.

TABLE 8.5

Linear glass and liquid expansion coefficients (10^{-6} K^{-1}) of plasticised poly(methyl methacrylate) as a function of weight function of plasticiser

w_1	α'_g (DBP)	α'_l (DBP)	α'_g (DOP)	α'_l (DOP)	α'_g (TCP)	α'_l (TCP)
0.16			148.9	181.4		
0.22	120.5	329.3				
0.27					117.1	194.3
0.28			110.0	104.2		
0.29	125.4	211.1				
0.36	127.7	190.6				
0.37			80.9	-288.5		
0.43					157.1	-67.0
0.44			63.3	-56.3		
0.46	134.9	166.8				
0.53	139.4	-487.1			126.7	-226.8
0.54			69.3	-107.1		
0.60					41.7	-333.4

It is observed that α'_l initially increases to a value higher than unplasticised PMMA at low plasticiser concentration. Unfortunately, plasticised PMMA tend to have negative α'_l values at high plasticiser concentration as a result of viscous flow, which effectively limits the number of reliable data. This is clearly observed in Figures 8.1-8.3, in which the slopes of the liquid lines becomes progressively lower as more plasticiser is added. Therefore, the effect of

viscous flow on the dimensional changes of highly-plasticised specimens above the glass transition must be taken into account in the interpretation of α'_l values.

8.3.5 Isothermal Ageing of Quenched PMMA Plasticised With DBP

Plasticised PMMA specimens containing 10 mole % DBP (0.22 wt.%, PMMA:10 DBP) and 20 mole % DBP (0.36 wt.%, PMMA:20 DBP) were isothermally aged in the glass transition region. PMMA:10 DBP was aged in the temperature range 40-80 C, whereas PMMA:20 DBP was aged between 15-45 C. The specimens were thermally equilibrated at 110 C for 4 minutes followed by quenching in liquid nitrogen for 4 minutes. After quenching the specimens were allowed to warm to ambient temperature in a dessicator for 5 minutes, with the exception of the PMMA:20 DBP specimen aged at 15 C, which was warmed for one minute. The specimens were placed inside the preheated TMA approximately one minute before the start of the experiment and aged over a period of 60 minutes under a load of 0.1 N.

Length Contraction and Free Volume Fraction

Figures 8.10-8.11 show that the isothermal length contraction of the plasticised PMMA specimens increases with temperature. The curve at 80 C in Figure 8.10 indicates that the specimen had aged substantially as soon as the specimen was placed in the TMA. The free volume and free volume fraction of the plasticised specimens are calculated from Equations 4.2-4.3 in which the initial sample lengths L_z and $L_{x,y}$ have respective values of 1.75×10^{-3} m and 4.80×10^{-3} m. A value of 0.250 is assumed for the free volume fraction at 80 C. The results are presented in Table 8.6 and Figure 8.12.

A comparison of Figure 8.12 with Figure 5.6 suggests that although the free volume fraction of PMMA has been increased by plasticisation, the free volume fraction-temperature relationship of plasticised PMMA is similar to that of unplasticised PMMA in the glass transition region. This observation suggests that the mechanism responsible for the collapse of free volume, that is, the cooperative motion of main-chain segments, has not been affected by plasticisation.

FIGURE 8.10 ISOTHERMAL AGEING OF PMMA PLASTICISED WITH 10 MOLE % DBP (numbers adjacent to curves indicate the isothermal ageing temperature)

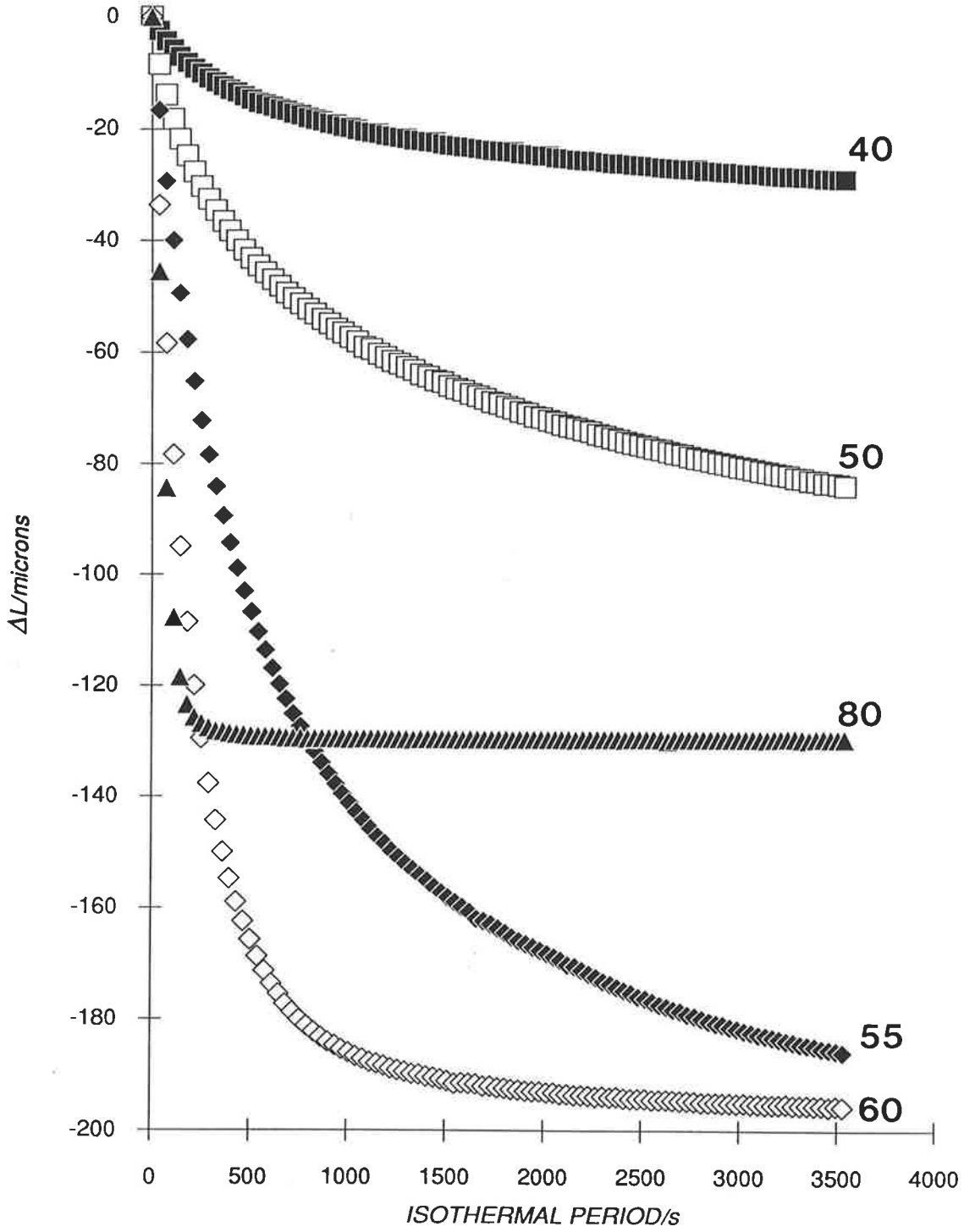

FIGURE 8.11 ISOTHERMAL AGEING OF PMMA PLASTICISED WITH 20 MOLE % DBP (numbers adjacent to curves indicate the isothermal ageing temperature)

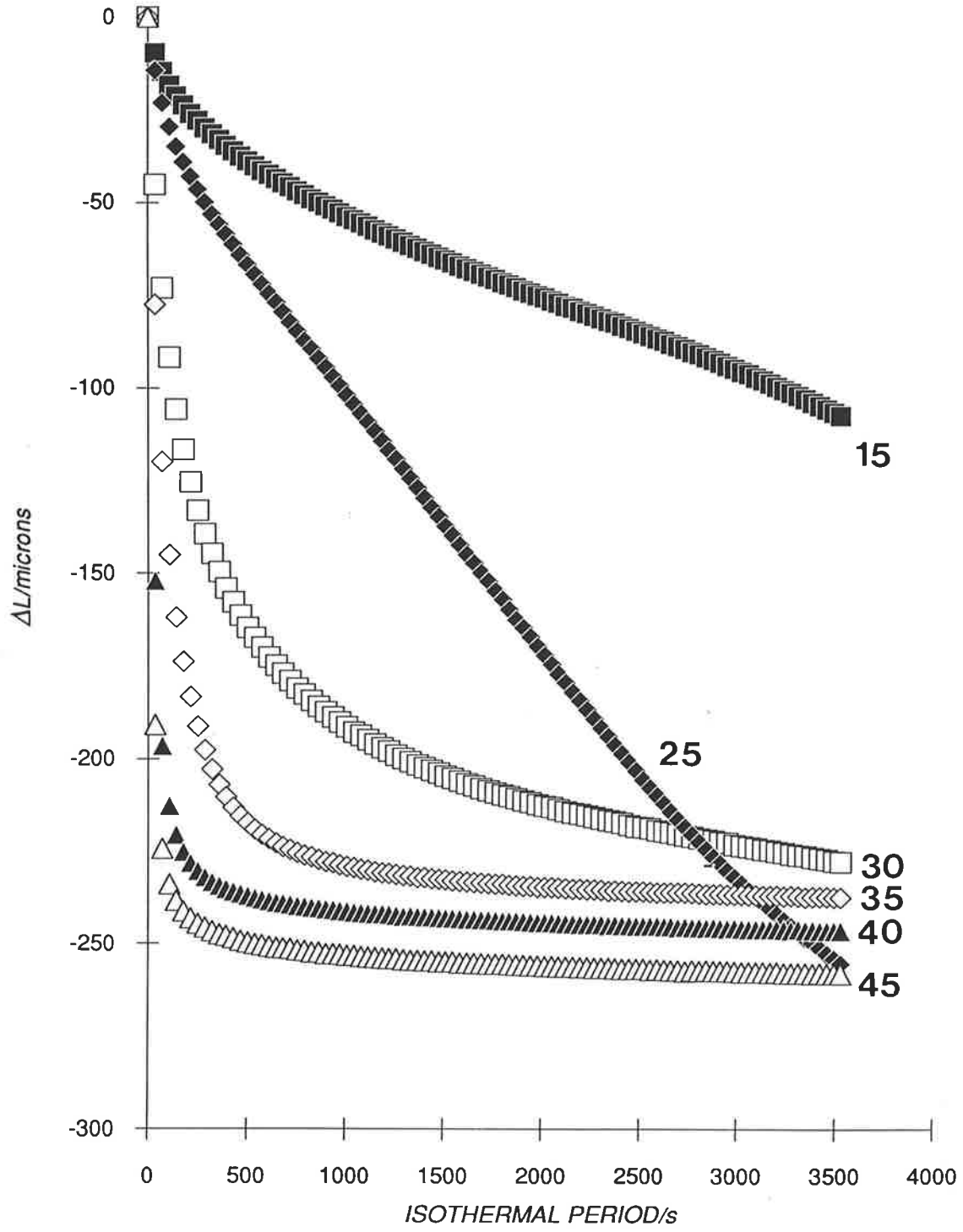

FIGURE 8.12 FREE VOLUME FRACTION OF PMMA PLASTICISED WITH DBP

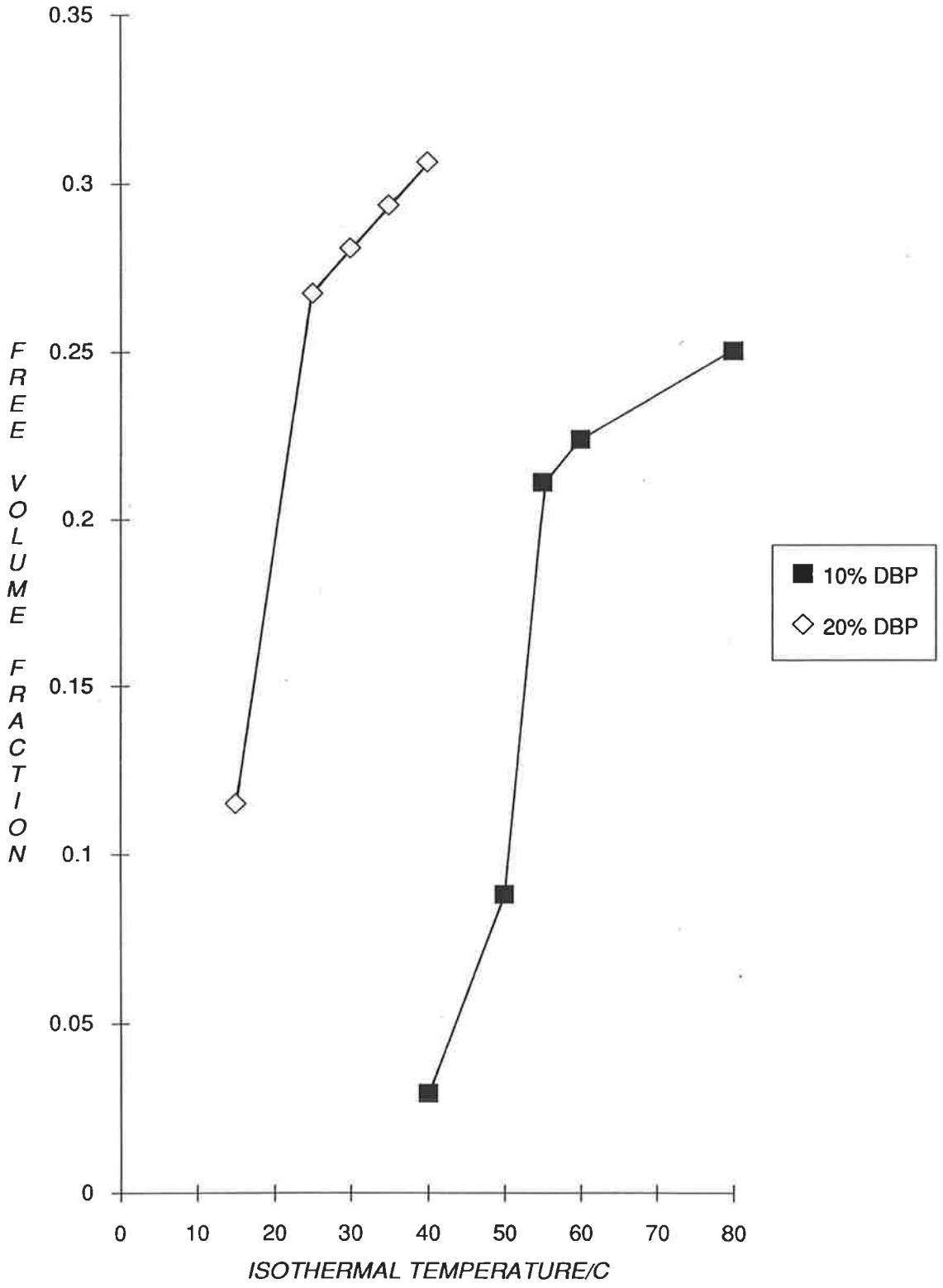

TABLE 8.6

Isothermal free volume fractions of quenched poly(methyl methacrylate) plasticised with dibutyl phthalate; the free volume fractions were measured after 60 minutes

T_a (C)	f (PMMA:10 DBP)	T_a (C)	f (PMMA:20 DBP)
40	0.029	15	0.115
50	0.088	25	0.267
55	0.211	30	0.281
60	0.224	35	0.294
80	0.250	40	0.306
		45	0.310

Rates of Relaxation and Activation Energies

The isothermal rates of relaxation, -r, are calculated from Equation 5.3 and are presented as a function of ageing temperature in Table 8.7 and Figure 8.13. The data of Table 8.7 suggests that the rate of ageing of PMMA at the glass transition region is increased by plasticisation.

A number of authors [12, 28, 31] have indicated that plasticisation accelerates the ageing process by shifting the relaxation times to lower times. This effect is confirmed by the data of Table 8.8, in which the following parameters are used: f_g = 0.130 for unplasticised PMMA, 0.251 for PMMA:10 DBP and 0.311 for PMMA:20 DBP; T_{eq} = 140 C for unplasticised PMMA, 80 C for PMMA:10 DBP and 45 C for PMMA:20 DBP. $Ln(\tau/\tau_g)$ was calculated from $\exp(1/f - 1/f_g)$ (Eq. 2.13).

The activation energy of physical ageing for plasticised PMMA was calculated according to the modified Narayanaswamy equation (Eq. 5.8) [60-61], in which the plot of Ln (τ/τ_g) vs. $(1/f).(1/T_a)$ yields a slope equal to $-E_{act}/R.(1 - 1/f)^{-1}$ (Eq. 5.9a). The data of PMMA:10 DBP and PMMA:20 DBP yielded respective slopes of 310 K^{-1} and 224 K^{-1} and the activation energies obtained from these slopes are presented in Table 8.9.

FIGURE 8.13 ISOTHERMAL RELAXATION RATES OF PLASTICISED PMMA

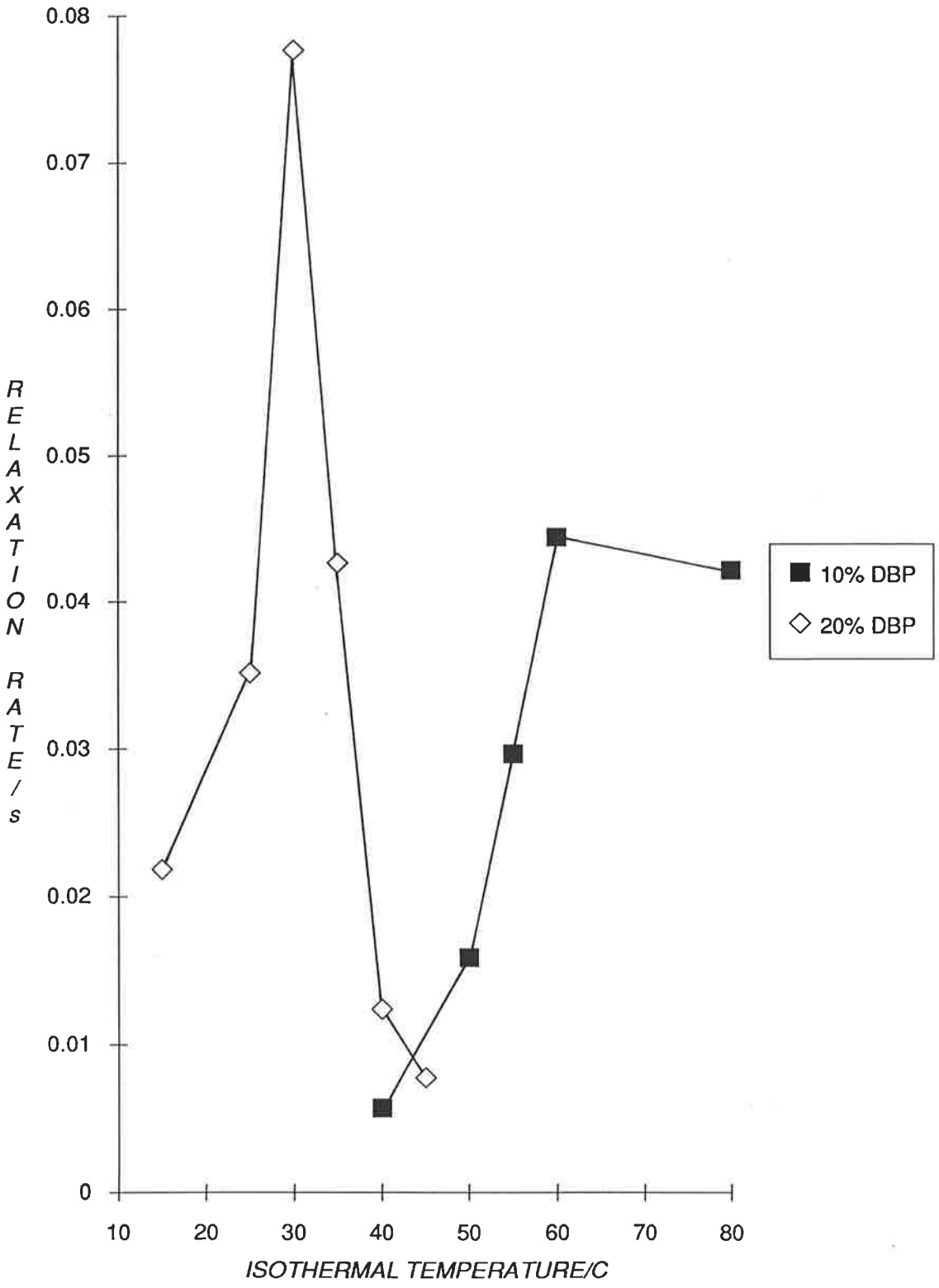

TABLE 8.7

Isothermal rates of relaxation (10^{-4} s^{-1}) for poly(methyl methacrylate) plasticised with dibutyl phthalate

T_a (C)	-r (PMMA:10 DBP)	T_a (C)	-r (PMMA:20 DBP)
40	5.64	15	218.0
50	158.1	25	351.3
55	296.1	30	776.4
60	444.2	35	426.4
80	421.2	40	123.3
		45	76.86

TABLE 8.8

Comparison of isothermal relaxation times, $Ln(\tau/\tau_g)$, of plasticised and unplasticised poly(methyl methacrylate) in the glass transition region

$T_{eq} - T_a$ (C)	PMMA	PMMA:10 DBP	PMMA:20 DBP
40	92.31	30.21	
30	83.22	7.37	5.49
25	28.02	0.75	
20	2.62	0.48	0.52
15			0.35
10	1.08		0.19
5			0.05
0	0.06	0.02	0.01

Table 8.10 presents a comparison of the activation energies of plasticised and unplasticised PMMA in terms of $T_{eq} - T_a$. It is clear that the plasticisation of PMMA results in lowering the activation energy, e.g. E_{act} is reduced by a factor of three by the addition of 10 mol % DBP at 40 C below T_{eq}. It is noted that E_{act} at equilibrium ($T_{eq} - T_a = 0$ C) is

progressively lowered from 18 kJ mol^{-1} for unplasticised PMMA to 7.7 kJ mol^{-1} at 10 mol % DBP and 4.1 kJ mol^{-1} at 20 mol % DBP.

TABLE 8.9

Isothermal activation energies (kJ mol^{-1}) of plasticised poly(methyl methacrylate)

T_a (C)	PMMA:10 DBP	PMMA:20 DBP
15		14
25		5.1
30		4.8
35		4.5
40	86	4.2
45		4.1
50	27	
55	9.6	
60	8.9	
80	7.7	

TABLE 8.10

Comparison of activation energies (kJ mol^{-1}) of plasticised and unplasticised poly(methyl methacrylate) in the glass transition region as a function of $T_{eq} - T_a$

$T_{eq} - T_a$ (C)	PMMA:10DBP	PMMA:20DBP	PMMA
40	86		257
30	27	14	233
25	9.6		90
20	8.9	5.1	24
15		4.8	
10		4.5	20
5		4.2	
0	7.7	4.1	18

These observations are consistent with the results of Gomez-Ribelles *et al.* [31] who found that enthalpy loss due to ageing increased with increasing plasticiser concentration. The increase in enthalpy loss was interpreted as indicative of the increased rate of ageing in plasticised PMMA. The reduction of the activation energy suggests that physical ageing takes place more easily in plasticised PMMA, which is consistent with the observation of higher free volume fraction and lower relaxation times.

8.4 SUMMARY

(1) Length contractions of PMMA plasticised with different concentrations of DBP, DOP and TCP were found to increase with increasing plasticiser concentration. However, phase separation at high concentrations of DOP resulted in a smaller contraction. The increase in length contraction was accompanied by the shifting of the onset temperature of contraction to lower temperatures.

(2) As a result of larger length contraction the free volume fraction of PMMA was increased by plasticisation. However, the increase in free volume fraction with plasticiser concentration was not uniform for each plasticiser. This observation indicated that the ageing behaviour of plasticised PMMA was extremely complex.

(3) An alternative theory suggested that plasticisation resulted in a decrease in free volume fraction. The reduction in free volume was caused by the filling of free volume holes by plasticiser molecules which was responsible for the effect of antiplasticisation. The available free volume in unplasticised PMMA was found to be insufficient in accommodating all of the plasticiser molecules, therefore the increase in free volume was attributed to the swelling of the polymer by plasticiser molecules. It was suggested that the plasticiser molecules which did not occupy free volume holes were located in hydrophobic channels formed by the coiling of backbone chains.

(4) Isothermal ageing of PMMA plasticised with DBP indicated that physical ageing was facilitated by cooperative motions of main chain segments. The activation energies of PMMA in the glass transition region were found to be lowered by plasticisation. The lowering of E_{act} indicated that physical ageing was energetically less demanding in plasticised PMMA

and was consistent with observations that the free volume fraction and the rate of ageing was increased by plasticisation.

Chapter 8

1. J.J. Bernando and H. Burrell, *Polymer Science*, Volume **1**, A.D. Jenkins, ed., North-Holland (1972) p538.

2. H.E. Bair, *Thermal Characterisation of Polymeric Materials*, E.A. Turi ed., Academic Press (New York), Chapter 9, p878 (1981).

3. J.R. Darby and J.K. Sears, *Plasticisers, Encyclopedia of Polymer Science and Technology,* Interscience, New York (1969), Volume **10**, p297.

4. E.A. DiMarzio and J.H. Gibbs, *J. Polym. Sci. Part A* **1**, 1417-1428 (1963).

5. F.N. Kelly and F. Bueche, J. Polym. Sci. 50, 549-556 (1961).

6. F. Bueche, *Physical Properties of Polymers*, Wiley, New York (1962).

7. J.D. Ferry, *Viscoelastic Properties of Polymers*, 2nd Edition, Wiley, New York (1970), Chapter 17.

8. M. Scandola, G. Ceccorulli, M. Pizzoli and G. Pezzin, *Polym. Bull.* **6**, 653 (1982).

9. T.S. Chow, *Macromolecules* **13**, 362 (1980).

10. D.M. Leisz, L.W. Kleiner and P.G. Gertenbach, *Thermochim. Acta* **35**, 51 (1980).

11. P.R. Couchman, *Polym. Eng. Sci.* **24**, 135 (1984).

12. K.L. Ngai, R.W. Rendell, A.F. Yee and D.J. Plazek, *Macromolecules* **24**, 61-67 (1991).

13. B.D. Malhorta and R.A. Pehtrick, *Eur. Polym. J.* **19**, 457 (1983).

14. B.D. Malhorta and R.A. Pehtrick, *Polym. Comm.* **24**, 165 (1983).

15. M.L. Williams, R.F. Landel and J.D. Ferry, *J. Am. Chem. Soc.* **77**, 3701 (1955).

16. T.G. Fox and P.J. Flory, *J. Appl. Phys.* **21**, 581 (1950).

17. M.H. Cohen and D. Turnbull, *J. Chem. Phys.* **31**, 1164 (1959).

18. T.G. Fox and S. Loshaek, *J. Polym. Sci.* **15**, 371, 391 (1955).

19. P.R. Couchman, *Macromolecules* **11**, 1156 (1978).

20. M.C. Shen and A. Eisenberg, *Progress in Solid State Chemistry*, Volume **3**, Pergamon Press, New York, (1966), p407.

21. M.C. Shen and A.V. Tobolsky, *Adv. Chem. Series* **48**, 27 (1965).

22. T.G. Fox, *Bull. Am. Phys. Soc.* **1**, 123 (1956).

23. W.J. Jackson Jr. and J.R. Caldwell, *Adv. Chem. Ser.* **48**, 185 (1965).

24. W.J. Jackson Jr. and J.R. Caldwell, *J. Appl. Polym. Sci.* **11**, 211, 227 (1965).

25. L.M. Robeson and J.A. Fauchner, *J. Polym. Sci. Part B* **7**, 59 (1969).

26. L.M. Robeson, *Polym. Eng. Sci.* **9(4)**, 277 (1969).

27. J.Y. Olayemi and N.A. Oniyangi, *J. Appl. Polym. Sci.* **26**, 4059-4067 (1981).

28. E.W. Fisher, G.P. Hellmann, H.W. Spiess, F.J. Horth, U. Ecarius and M. Wehrle, *Makromol. Chem. Suppl.* **12**, 189-214 (1985).

29. C. Schmidt, K.J. Kuhn and H.W. Spiess, *Prog. Colloid Polym. Sci.* **71**, 71 (1985).

30. H.W. Spiess, *Adv. Polym. Sci.* **66**, H.H. Kausch and H.G. Zachman eds., Springer-Verlag, Berlin (1984), p23.

31. J.L. Gomez-Ribelles, R. Diaz-Calleja, R. Ferguson and J.M.G. Cowie, *Polymer* **28**, 2262 (1987).

32. R.W. Robertson, *Ann. N. Y. Acad. Sci.* **371**, 21 (1981).

33. L.C.E. Struik, *Physical Ageing in Amorphous Polymers and Other Materials,* Elsevier, Amsterdam (1978).

34. G.F. Cowperthwaite, J.J. Foy, and M.A. Malloy, *Biomedical and Dental Applications of Polymers,* C.G. Geblen and F.F. Koblitz eds., Plenum Press, New York (1981), p397.

35. M.M. Mogilevich, N.A. Sukhanova and G.V. Korolev, *Vysokomol. Soyed* **A15(7)**, 1478 (1973).

36. G.V. Korolev, L.I. Makhonia and A.A. Berlin, *Vysokomol. Soyed* **A3(2)**, 198 (1961).

37. G.P. Simon, *Ph.D. Thesis,* University of Adelaide, South Australia (1986).

38. P.E.M. Allen, G.P. Simon, D.R.G. Williams and E.H. Williams, *Macromolecules* **22**, 809-816 (1989).

39. K. Ito, Y. Murase and Y. Yamashita, *J. Polym. Sci. Polym. Chem. Ed.* **13**, 87 (1975).

40. K.J. Beirnes and C.M. Burns, *J. Appl. Polym. Sci.* **31**, 2561-2567 (1986).

41. H.E. Bair and P.C. Warren, *J. Macromol. Sci. Phys.* **B20**, 381 (1981).

42. E. Foldes, T. Pazonyi and P. Hedvig, *J. Macromol. Sci. Phys.* **B15**, 527 (1978).

43. D.R.G. Williams, P.E.M. Allen and V.T. Troung, *Eur. Polym. J.* **22(11)**, 911 (1986).

44. R.J. Elwell and R.A. Pehtrick, *Eur. Polym. J.* **26(8)**, 853-856 (1990).

45. A.I. Maklahov, A.A. Maklahov, A.N. Temnikov and B.F. Teplov, *Polym. Sci. USSR* **20**, 1492 (1979).

46. S. Kalachandra and D.T. Turner, *J. Polym. Sci. Polym. Phys. Ed.* **25**, 697 (1987).

47. S. Kalachandra and D.T. Turner, *Polymer* **28**, 1749 (1987).

48. D.T. Turner, *Polymer* **23**, 197 (1982).

49. D.T. Turner, *Polymer* **28**, 293 (1987).

50. Y.C. Jean, H. Nakanishi, L.Y. Hao and T.C. Sandreczki, *Phys. Rev. B* **42(15)**, 9705 (1990).

51. *Catalogue Handbook of Fine Chemicals,* Aldrich Chemical Company Inc., Milwaukee (1990-1991).

52. A.K. Doolittle, *The Technology of Solvents and Plasticisers,* Wiley, New York (1954).

53. A.K. Doolittle, *J. Polym. Sci.* **2**, 121 (1947).

54. J.K. Sears and N.W. Touchette, *Encyclopedia of Polymer Science and Engineering, Supplement Volume,* Wiley (1989), p574 ff.

55. G.H. Fredickson and E. Helfand, *Macromolecules* **18**, 2201 (1985).

56. P.E.M. Allen, S. Hagias, G.P. Simon, E.H. Williams and D.R.G. Williams, *Polym. Bull.* **15**, 359-362 (1986).

57. G. Ceccorulli, M. Pizzoli and M. Scandola, *Polymer* **28**, 2077 (1987).

58. R. Simha and R.F. Boyer, *J. Chem. Phys.* **37(5)**, 1003 (1962).

59. R.A. Haldon and R. Simha, *J. Appl. Phys.* **39(4)**, 1890 (1968).

60. O.S. Narayaswamy, *J. Am. Ceram. Soc.* **54**, 491 (1971).

61. C.T. Moynihan, A.J. Easteal, M.A. DeBolt and J. Tucker, *J. Am. Ceram. Soc.* **59**, 12 (1976).

GLOSSARY OF SYMBOLS

α_p	Thermal Expansion of Plasticiser
ΔC_{p1}	Heat Capacity Change of Pure Plasticiser
ΔC_{p2}	Heat Capacity Change of Unplasticised Polymer
E_{act}	Energy of Activation
f	Free Volume Fraction
f_2	Free Volume Fraction of Unplasticised Polymer
$f(T_a)$	Free Volume Fraction Recovered After Isothermal Ageing at T_a
L_z, $L_{x,y}$	Initial Specimen Lengths
ΔL_z, $\Delta L_{x,y}$	Length Contraction
n_1	Moles of Plasticiser
n_{MMA}	Moles of Methyl Methacrylate Monomer
m_1	Mass of Plasticiser
m_{MMA}	Mass of Methyl Methacrylate Monomer
-r	Isothermal Rate of Relaxation
R	Universal Gas Constant
T_g	Glass Transition Temperature
T_{g1}	Glass Transition Temperature of Plasticiser
T_{g2}	Glass Transition Temperature of Unplasticed Polymer
T_a	Isothermal Ageing Temperature
T_{eq}	Temperature at Which Thermodynamic Equilbrium is Attained Readily
T_{on}	Onset Temperature of Length Contraction
T_{end}	Endset Temperature of Length Contraction
t_a	Isothermal Period
τ	Relaxation Time
τ_g	Relaxation Time at Equilibrium
V_f	Free Volume
V_{eq}	Specific Volume at Equilibrium
w_1, w_2	Respective Weight Fractions of Plasticer and Methyl Methacrylate Monomer

CHAPTER 9
PHYSICAL AGEING IN CROSSLINKED POLYMERS

9.1 INTRODUCTION 181

9.2 EXPERIMENTAL 184

9.3 RESULTS AND DISCUSSION

9.3.1 Length Contraction 186

9.3.2 Thermal Expansion Coefficient 188

9.4 SUMMARY 192

BIBLIOGRAPHY 193

GLOSSARY OF SYMBOLS 197

CHAPTER 9

9.1 INTRODUCTION

In many applications involving crosslinked polymers, the properties of the crosslinked network strongly influences the behaviour of the polymer. Thermoplastics undergo physical ageing to a greater extent than thermosets, as thermoplastics can undergo molecular rearrangement via cooperative motions whereas a tightly-crosslinked network will restrict such motions, i.e. crosslinking reactions are accompanied by a decrease in the segmental mobility of the polymer chains [1]. Ellis *et al.* [2] showed that increased crosslinking of polystyrene decreases the mobility of the polymer chains in the liquid state, such that the mobility of the liquid structure becomes similar to that of the glassy structure. Other property changes usually observed with an increase in crosslink density are increases in T_g [3-9], viscosity [10], impact strength [6, 11-12], tensile strength [9] and moisture uptake [13-17], whereas decreases in specific volume [8], thermal expansion coefficient [8, 18] and changes in heat capacity at T_g [2, 18-20] are observed.

It should be pointed out that the increase in tensile strength with crosslink density was observed only above T_g [9], whereas at temperatures far below T_g the tensile strength was found to be unaffected by crosslink density nor by the chemical composition of the crosslinking agent [6, 9]. It was proposed [6] that the tensile strength above T_g was mainly affected by the bulk density, which was observed to increase with increasing crosslink density at elevated temperatures [21]. On the other hand, at room temperature, a higher crosslink density was found to be accompanied by a lower bulk density which indicates the presence of a larger free volume than in loosely crosslinked networks. This lower packing efficiency is attributed to the geometric constraints imposed on the segmental packing by the crosslinked network [13, 21]. However, this view is not generally accepted [22]. The findings of Gupta *et al.* [21] that highly crosslinked polymers have the highest bulk densities at 100 C suggests that the geometric constraints are not too severe. In addition, the observations of Gupta *et al.* contradicts the results of Nielsen [8], who found that the densities of rigid crosslinked polymers generally increased linearly with increasing crosslink density.

Conflicting reports also exist concerning the effects of crosslink density on heat capacity changes ΔC_p. Contrary to reports [2, 18-20] which clearly show a decrease in ΔC_p (0.283 to 0.095 $J.g^{-1}K^{-1}$, [2]) with increasing crosslink density, a number of authors [23-25] found only small changes in ΔC_p (0.434 to 0.405 $J.g^{-1}K^{-1}$, [24]) of crosslinked epoxies upon decreasing the molecular weights between crosslinks. Findley *et al.* [26-27] observed that the thermal expansivities and dimensions of crosslinked epoxies and polyurethanes were not constant at constant temperature after heating and cooling. After the material had expanded upon heating, a gradual decrease in expansivity was observed with time. On the other hand, upon cooling the specimen to the starting temperature it initially contracted to below its original length but later gradually returned to its original length with time. It was suggested [26] that the expansion associated with an increase in thermal oscillations during heating is not resisted by the molecular segments between crosslinks, but by the three-dimensional network at the points of crosslinking which are joined by strong primary bonds. Thus an internal volumetric stress is built up in the network. At a constant temperature, molecular rearrangements by the segments between crosslinks gradually relieve the stress and cause a reduction in volume. A similar explanation was offered for the instabilities observed during susbsequent cooling. In a later paper [27], however, it was concluded that the major cause of observed changes in thermal expansivity was due to changes in the moisture content of the polymers.

A study of physical ageing in epoxy matrices and composites by Kong [28] revealed that a number of properties of crosslinked polymers are affected by physical ageing. As physical ageing proceeds, the following changes have been observed:

(1) decrease in mechanical damping [29] and impact strength [30];

(2) decrease in stress relaxation [31] and creep rates [1];

(3) decrease in moisture sorption and moisture diffusivity [28];

(4) increase in density [28];

(5) increase in hardness [30] and modulus [32];

(6) increase in the glass and liquid thermal expansivities [28].

These observations indicate that the effects of physical ageing associated with linear polymers [1, 33-40] are also observed with crosslinked polymers. The relaxation times of the crosslinked polymer have been observed to decrease with increasing ageing temperature, and the stress relaxation curves are shifted to longer times when the crosslink density is increased

[24]. For example, the creep compliance during the conversion of a 90/10 copolymer of MMA crosslinked with allyl methacrylate was measured at 80 C after various times had elapsed (Fig. 9.1). The curves show the same horizontal shifting as in physical ageing, but the compliance becomes increasingly smaller at longer times. The creep curves show a gradual progression from a lightly crosslinked material to a hard, insoluble network [1]. Hence the crosslinking of a linear polymer is expected to result in an increase in the rate of ageing. This was also implicitly suggested by Lee and McKenna [24], who found that an increase in T_g of crosslinked epoxies resulted in a slight increase in the rate of ageing.

This chapter investigates the ageing behaviour of an important class of crosslinked polymers, namely, poly[oligo(ethylene glycol) dimethacrylates]. Dimethacrylate networks are used extensively in dentistry as crown and bridge protheses [41], dental bonding agents [42] and tooth restorative composites [43-44]. In view of the important applications of dimethacrylate networks in the dental and engineering industries, it is surprising that the relationship between physical ageing and the molecular structure of these crosslinked networks has not been fully investigated. The first study of copolymers of PMMA and poly(glycol dimethacrylates) was carried out by Loshaek [3] in 1955, in which the effect of crosslinking on T_g was reported. More recently, the dynamic-mechanical and solid state NMR properties of a homologous series of poly[oligo(ethylene glycol) dimethacrylates] have been extensively studied by Allen *et al.* [45-47]. In the series, the flexible oxyethylene chains were crosslinked by stiff methacrylate links, in which the increasing length of the oxyethylene link, x, is a measure of the molecular weight between crosslinks, M_c. The approximate value of M_c is calculated from Equation 9.1 in which it is assumed that only a fraction, ε, of the number of moles of crosslinker per gram provides crosslinks on polymerisation [50]:

$$(0.5).M_c^{-1} = \text{moles of crosslinks/g} = (m_x/M_x).\varepsilon/(m_{MMA} + m_x) \qquad (9.1)$$

where m_x and M_x are the mass and molecular weight of the crosslinker respectively and m_{MMA} is the mass of MMA monomer. A value of 0.5 for ε was assumed by Lee and Turner [50] for the MMA-co-EGDMA system, thus this value of ε will be adopted in this work. However, it is known [46-47, 56, 59-61] that PEGDMA, PTriEGDMA and PTetEGDMA do not go to full cure even after postcuring at 150 C. DSC scans of the postcured specimens did not produce

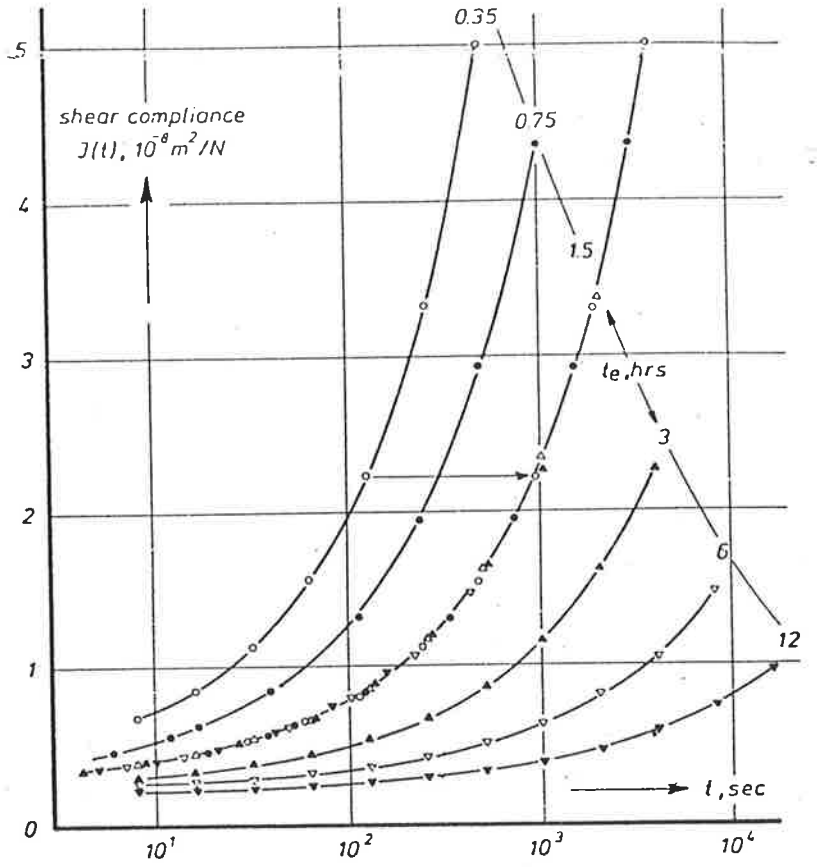

FIGURE 9.1 Isothermal changes in the small-strain torsional creep properties of a 90/10 copolymer of methyl methacrylate and allyl methacrylate. The sample was prepolymerized at 50 C during 42 hrs, next heated to 80 C, and tested at various times t_e elapsed at 80 C. The master curve for 1.5 hrs was obtained by almost horizontal shifts (see the arrow) (reproduced from [1]).

any residual exotherm even though residual unsaturation in the range 2-18 % could be detected by solid state NMR [46-47, 59]. Therefore, the interpretation of values of M_c have to take into account that M_c may be lowered by the presence of residual unsaturation.

The main objective of this work, therefore, is to characterise the ageing behaviour of crosslinked dimethacrylate polymers by linear dimension measurements and to correlate dimensional changes with the molecular structure of the network. Length measurements are also used to determine the minimum value of M_c necessary for the observation of physical ageing.

9.2 EXPERIMENTAL

Ethylene glycol dimethacrylate (EGDMA), tris- and tetrakis-(ethylene glycol dimethacrylates) (TriEGDMA and TetEGDMA), and poly(400 ethylene glycol dimethacrylate) (P400EGDMA) were copolymerised with methyl methacrylate (MMA) monomer according to Cowperthwaite's method [48], in which 1.6 mm thick sheets were cast between glass sheets using Silastic tubing as a gasket. The polymerisations were initiated by recrystallised dibenzoyl peroxide usually at 0.2 mol/mol %.

The crosslinker concentrations were determined in terms of the mole fraction percentage of crosslinker, viz.

$$\text{Mole Fraction \% of Crosslinker} = n_x/(n_x + n_{MMA}).100 \qquad (9.2)$$

where n_x and n_{MMA} are the number of moles of crosslinker and MMA respectively. The percentage mole fraction of the dimethacrylate-co-MMA copolymers are presented in Table 9.1 along with their respective values of M_c. Monomer mixtures which yielded polymers that were glassy at room temperature were isothermally cured until vitrification at an initial temperature of 60 C followed by postcuring at 125 C for three hours. P400EGDMA-MMA mixtures which resulted in rubbery polymers were cured at a higher initial temperature of 70 C and postcured at 110 C. It has been reported [48-49] that thermal and chemical degradation of dimethacrylate polymers occur above 200 C. Owing to the brittle nature of PEGDMA and the large contraction on polymerisation (15.7 vol % [51]), uncracked specimens of PEGDMA could not be cast. Similar difficulties had been reported by other authors [17, 47, 52-55], although the fortuitous

polymerisation of a bottle of EGDMA at room temperature [56] yielded a large uncracked specimen which was cut into smaller specimens suitable for fractography studies [57].

TABLE 9.1

Percentage mole fraction of poly(MMA-co-[oligo(ethylene glycol) dimethacrylate] copolymers and molecular weight between crosslinks

Copolymer	Percentage Mole Fraction	M_c
Poly(MMA-co-EGDMA) (M_x = 198)	9	1,200
	23	532
	50	298
	100	198
Poly(MMA-co-TriEGDMA) (M_x = 286)	50	386
	100	286
Poly(MMA-co-TetEGDMA) (M_x = 330)	14	918
	26	616
	47	430
	50	430
	100	330
Poly(MMA-co-P400EGDMA) (M_x = 536)	2	5,545
	9	1,536
	23	869
	41	679
	50	636
	100	536

Glassy specimens were thermally equilibrated above T_g at 150 C for 15-20 minutes to remove internal stresses, whereas rubbery P(400EGDMA-co-MMA) copolymers were

equilibrated at 100 C. The specimens were then quenched from above to below T_g in liquid nitrogen for 10 minutes and allowed to warm to room temperature inside a dessicator. Rubbery specimens which required sub-ambient starting temperatures were warmed under dry nitrogen inside the thermomechanical analyser. The specimens were heated at a constant heating rate of 2 C/min from below to above T_g under a constant load of 0.1 N.

9.3 RESULTS AND DISCUSSION

9.3.1 Length Contraction

The ΔL-T plots of P(MMA-co-EGDMA), P(MMA-co-TriEGDMA), P(MMA-co-TetEGDMA) and P(MMA-co-400EGDMA) copolymers are presented in Figures 9.2-9.6. It is observed that the magnitude of length contraction decreases with increasing dimethacrylate concentration, which indicates that segmental mobility is progressively reduced by an increase in crosslink density. Figures 9.2-9.6 show that the onset and endset temperature of length contraction are generally shifted to higher temperatures for all crosslinked PMMA copolymers with the exception of the P400EGDMA series. The ΔL-T curves of each of the dimethacrylate series are plotted with the ageing curve of PMMA in Figure 9.7.

The shift to higher temperatures is consistent with the well-known fact that the glass transition is increased by crosslinking [3-9]. However, T_g of P400EGDMA at -5 C [47, 59] is about 110 C lower than the T_g of PMMA, hence the T_g's of the P(MMA-co-400EGDMA) copolymers will lie at some temperature between those of the pure polymers.

Figure 9.2 shows the magnitude of the contraction ΔL of P(MMA-co-EGDMA) decreases from approximately 90-130 μm for quenched uncrosslinked PMMA (Figs. 4.4-4.5) to *ca* 27 μm at 9 % EGDMA. Physical ageing could not be observed from the ΔL-T plots at higher EGDMA concentrations of 23 % and 50 %, which suggests that M_c = 530 may represent the limiting value of the observation of contraction in P(MMA-co-EGDMA). Similar trends are also observed for P(HEMA-co-EGDMA) copolymers (Section 10.3.2). The ΔL-T plots of P(MMA-co-TriEGDMA) (Fig. 9.3) indicate that physical ageing is observed at 50 % TriEGDMA, which corresponds to a value of M_c of 386. However, the limiting value of M_c for P(MMA-co-TriEGDMA) could not be determined due to the lack of data. On the other hand, as was observed for PEGDMA, the TMA scan of PTriEGDMA resulted in a featureless plot. These observations are supported by dynamic-mechanical studies of PTriEGDMA [58],

FIGURE 9.2 PHYSICAL AGEING IN P(MMA-co-EGDMA) COPOLYMERS (numbers adjacent to curves indicate the percentage mole fraction of EGDMA)

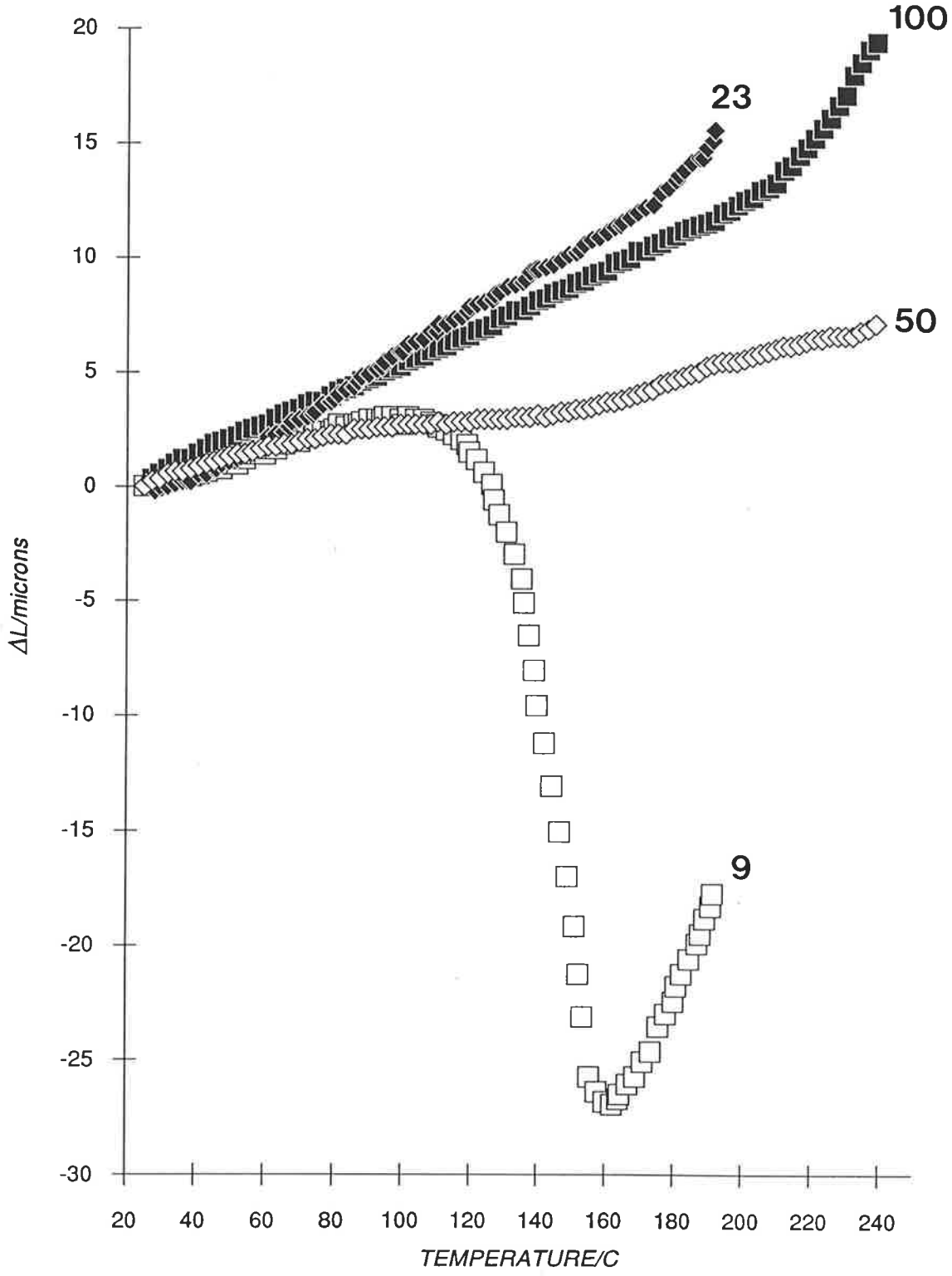

FIGURE 9.3 PHYSICAL AGEING IN P(MMA-co-TriEGDMA) COPOLYMERS (numbers adjacent to curves indicate the percentage mole fraction of TriEGDMA)

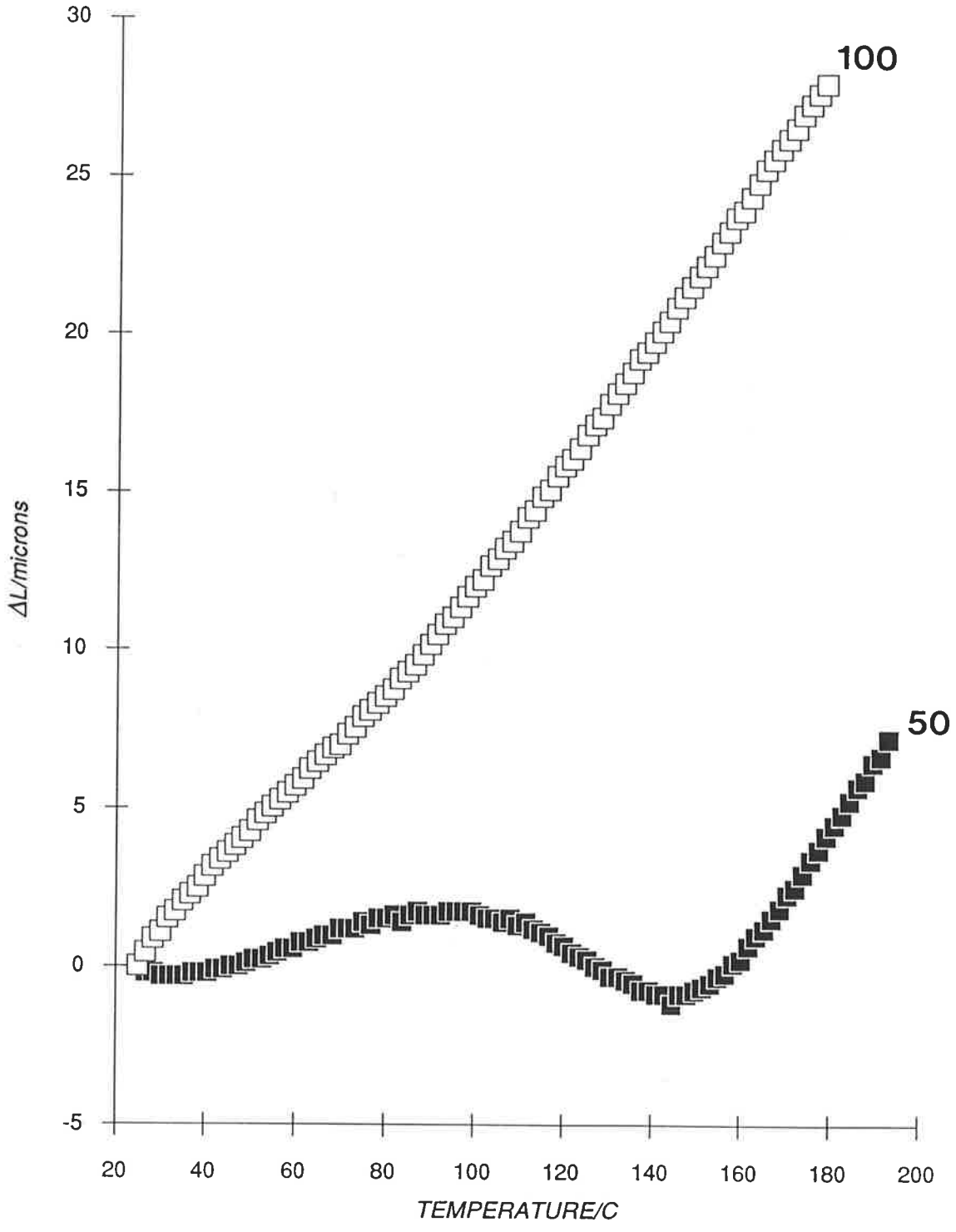

FIGURE 9.4 PHYSICAL AGEING IN P(MMA-co-TetGDMA) COPOLYMERS (numbers adjacent to curves indicate the percentage mole fraction of TetEGDMA)

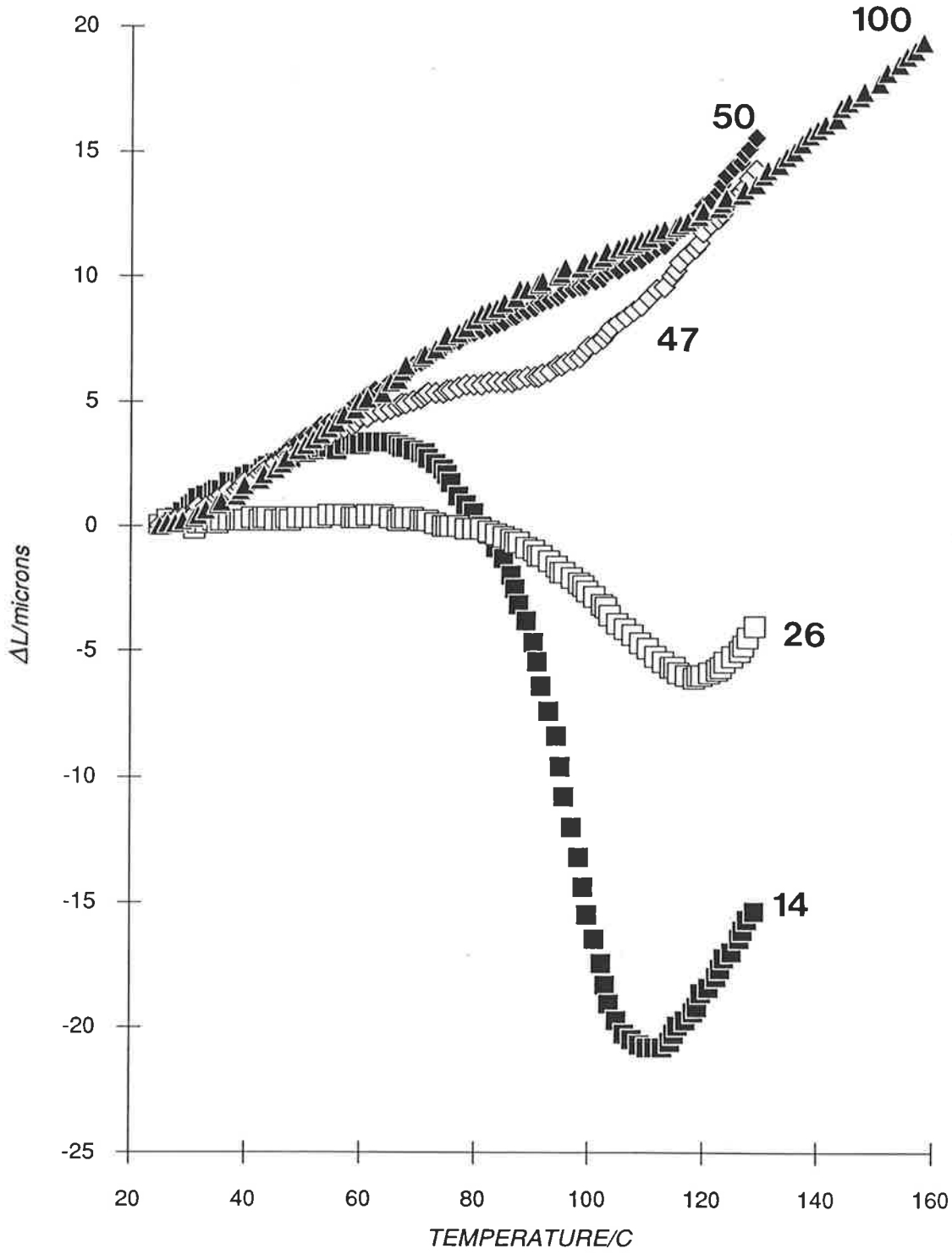

FIGURE 9.5 PHYSICAL AGEING IN P(MMA-co-400EGDMA) COPOLYMERS (numbers adjacent to curves indicate the percentage mole fraction of P400EGDMA)

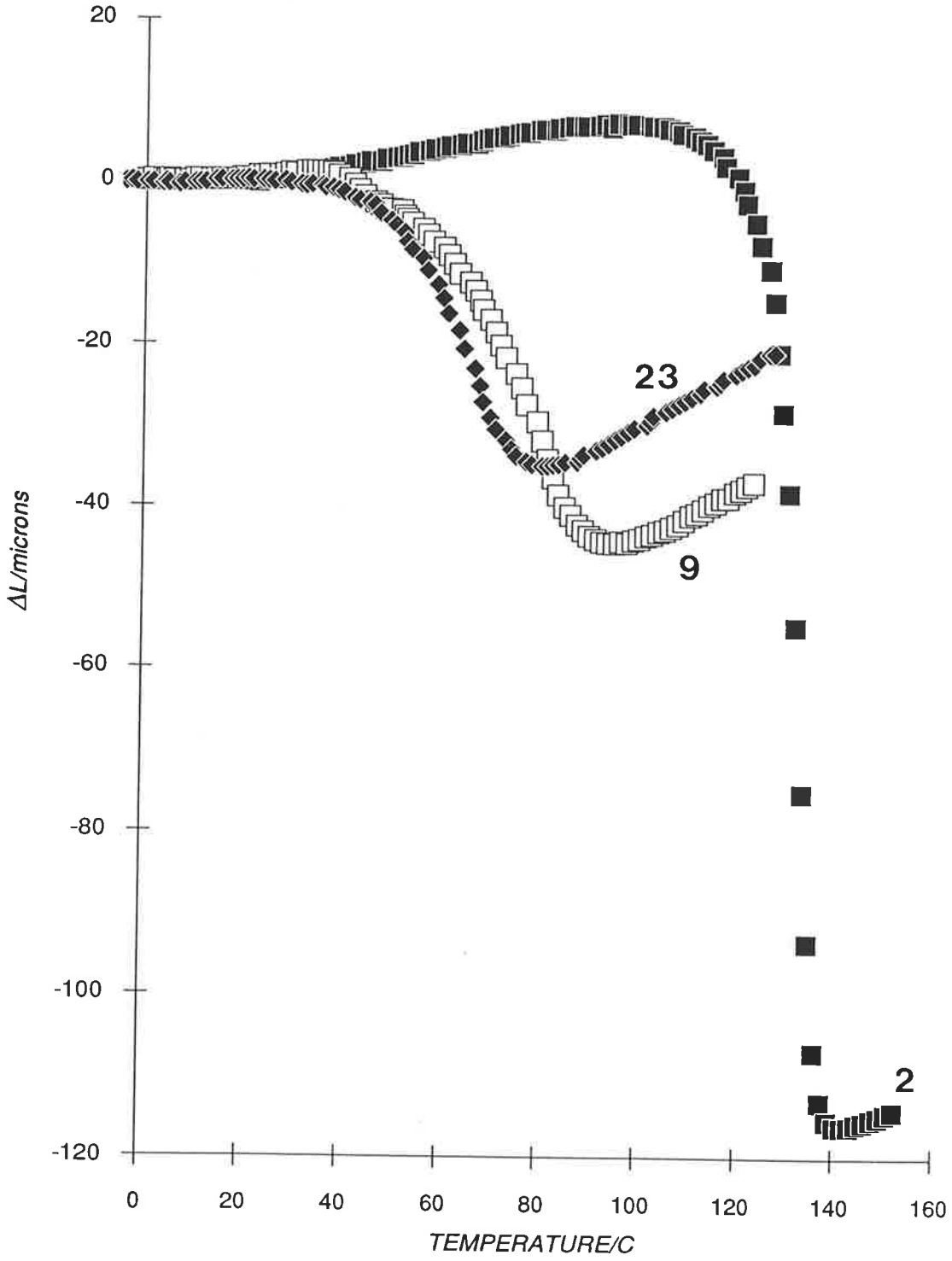

FIGURE 9.6 PHYSICAL AGEING IN P(MMA-co-P400EGDMA) COPOLYMERS AT HIGHER CONCENTRATIONS OF P400EGDMA (numbers adjacent to curves indicate the percentage mole fraction of P400EGDMA)

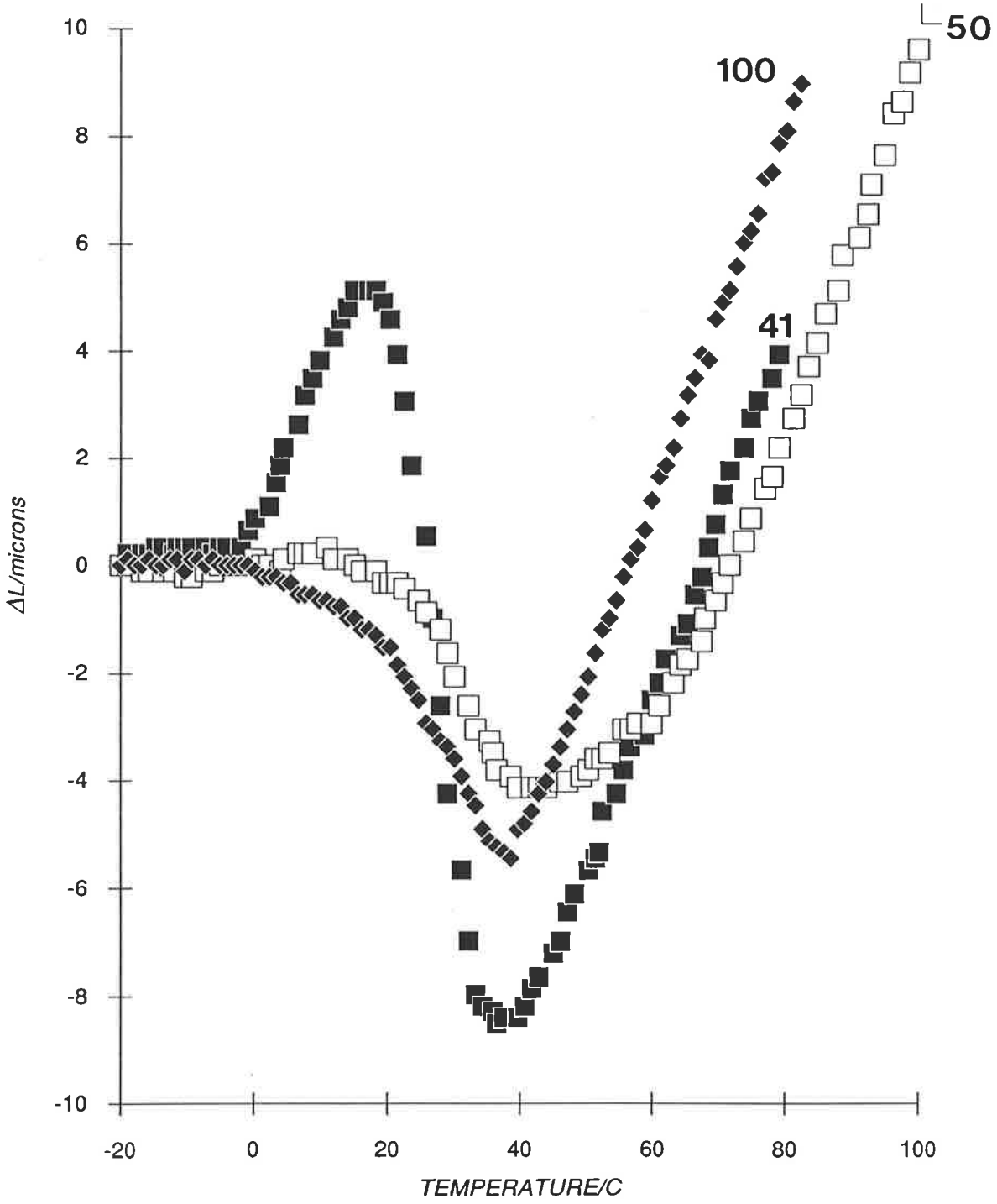

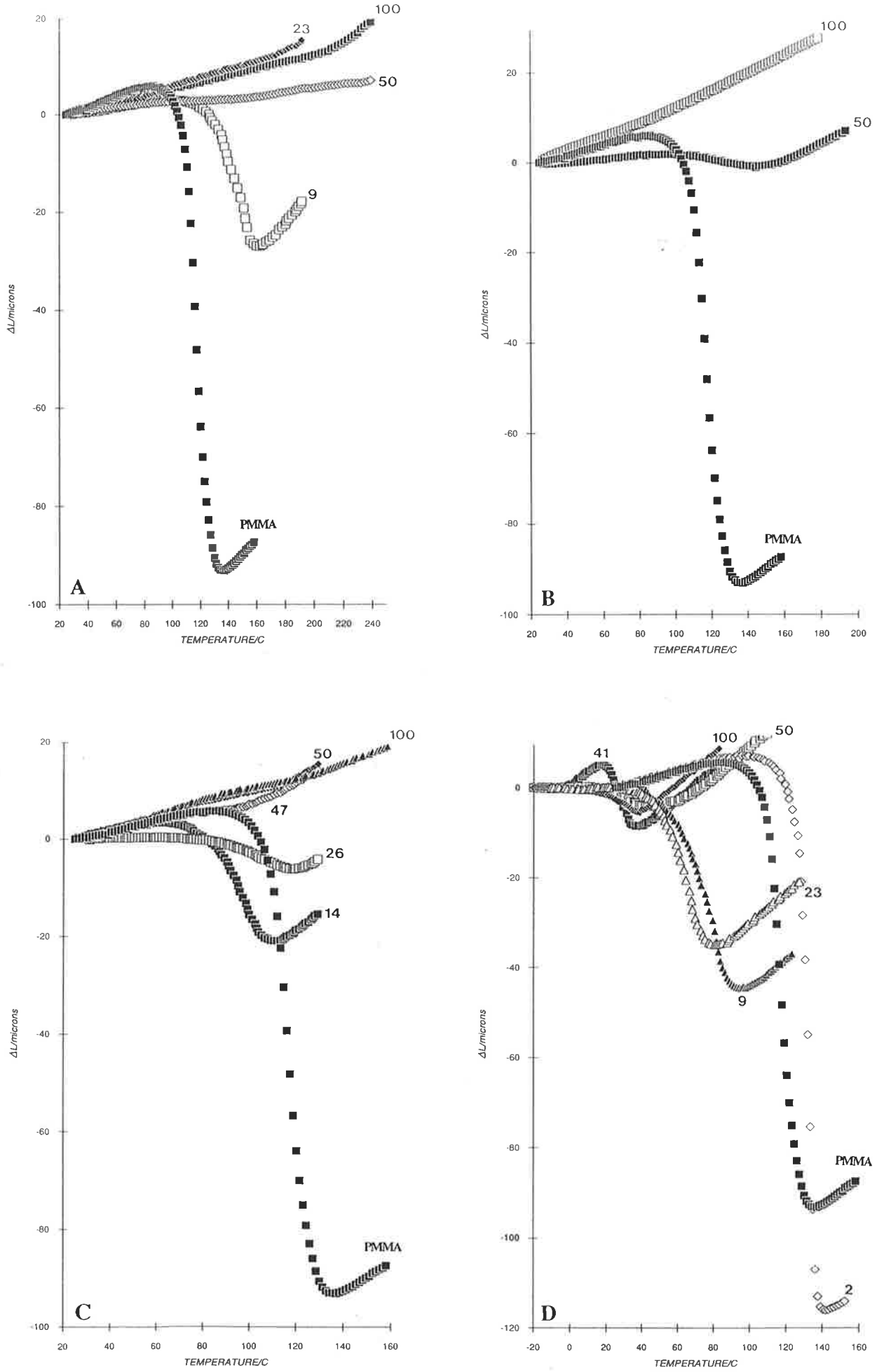

Figure 9.7 Comparison of physical ageing plot of PMMA with **A**. P(MMA-co-EGDMA) **B**. P(MMA-co-TriEGDMA) **C**. P(MMA-co-TetEGDMA) **D**. P(MMA-co-P400EGDMA) copolymers.

in which a featureless scan was observed in the range 120-200 C apart from the glass transition at 130 C (assigned by reference to the storage modulus).

A distinct glass transition at 216 C is observed as a sharp inflection in the curve for PEGDMA, which is higher than the T_g of 132 C quoted by Fox and Loshaek [53]. One advantage of the TMA is that only a small specimen is required for testing, whereas dynamic-mechanical measurements of T_g of PEGDMA have always been difficult due to the brittle nature of PEGDMA which does not allow the casting of a specimen of suitable size. Simon *et al.* [47, 59] have shown that T_g of poly(diethyleneglycol dimethacrylate) (PDEGDMA) is 160 C, which suggests that the T_g of PEGDMA at 132 C is incorrect since it is lower than the T_g of PDEGDMA.

Physical ageing of P(MMA-co-TetEGDMA) copolymers may be observed up to a concentration of 47 % (Fig. 9.4). It is noted in Figure 9.4 that anomalously low expansion between 25-80 C is observed at 26 % TetEGDMA, resulting in small values of α'_g (Table 9.5). At higher TetEGDMA concentrations, ageing is observed only by an inflection in ΔL in the glass transition region, for example, an inflection is observed at about 100 C for PTetEGDMA, which is consistent with the T_g of PTetEGDMA of 105-115 C [47]. These observations suggest that the limiting value of M_c for the observation of length contraction in P(MMA-co-TetEGDMA) is about 445, which is lower than the value obtained for P(MMA-co-EGDMA). The lower limiting value of M_c for P(MMA-co-TetEGDMA) is consistent with that the expectation that an increase in the length of the oxyethylene link will be accompanied by a concomitant increase in segmental mobility.

The increasing flexibility of the network as the oxyethylene chain length is increased from PEGDMA to P400EGDMA corresponds with the observation that physical ageing is observed for all P(MMA-co-400EGDMA) specimens (Figs. 9.5-9.6). This observation suggests that a value of M_c between 450-530 may represent the limit for the observation of ageing in poly(MMA-co-[oligo(ethylene glycol) dimethacrylate) copolymers (M_c of P400EGDMA is 536). It appears then, that the plot at 50 % TriEGDMA (M_c = 386) represent an anomaly to this conclusion.

It is observed that the magnitudes of ΔL of P(MMA-co-400EGDMA) are lower than that of uncrosslinked PMMA, with the exception at 2 % P400EGDMA. For example, the addition of 9 % P400EGDMA resulted in a contraction of *ca* 45 μm, whereas ΔL of pure

P400EGDMA only reached a value of *ca* 5.8 μm. These observations confirm that the segmental mobility of PMMA is restricted by crosslinking even in the presence of P400EGDMA which contain flexible crosslinks. No explanation could be offered at the present time for the observation of an anomalous expansion between 0-20 C at 41 % P400EGDMA.

9.3.2 Thermal Expansion Coefficient

It is known [8, 53, 62-63] that crosslinking has a pronounced effect on the thermal expansion coefficient, in which the thermal expansivity generally decreases with increasing crosslink density [8]. However, the present experimental data suggests that crosslinking affects the thermal expansivity in a more complex manner. The thermal expansivities of quenched P(MMA-co-EGDMA) copolymers are presented in Table 9.2 along with Loshaek's [3] values in Table 9.3.

TABLE 9.2

Thermal expansion coefficients (10^{-6} K^{-1}) of quenched P(MMA-co-EGDMA) copolymers

% Mole Fraction EGDMA	α'_g	α'_l	$3(\alpha'_g - \alpha'_l)$
0	56.4	142.8	259.2
9	48.5	237.0	565.5
23	45.1	171.7	379.8
50	43.0	52.0	27.0
100	42.6	152.6	330.0

It is observed from Tables 9.2 and 9.3 that the thermal expansivities of P(MMA-co-EGDMA) copolymers become smaller with increasing EGDMA concentration. However, some discrepancies exist between the experimental liquid expansivities and the values obtained by Loshaek. The first discrepancy concerns the experimental values of α'_l in Table 9.2 which are larger than Loshaek's values. Kong [28] has shown that the liquid expansion coefficient of a quenched epoxy composite increases with ageing, hence quenched P(MMA-co-EGDMA) specimens would be expected to have lower values of α'_l. However, it was admitted by Loshaek [3] that the uncertainty in the expansivities of P(MMA-co-EGDMA) copolymers may

be considerably greater than +/- 10%. It was observed by Loshaek [3] that both α'_g and α'_l of P(MMA-co-EGDMA) were smaller than the corresponding values for uncrosslinked PMMA, whereas α'_l obtained in this work are higher than those of uncrosslinked PMMA. However, the experimental value of 52.0 x 10^{-6} K^{-1} at 50 % PEGDMA is apparently in error, resulting in a low value of $3(\alpha'_g - \alpha'_l)$.

TABLE 9.3

Thermal expansion coefficients (10^{-6} K^{-1}) of P(MMA-co-EGDMA) copolymers by Loshaek [3]

Mole % PEGDMA	α'_g	α'_l	$3(\alpha'_g - \alpha'_l)$
0	62.2	168.3	318.3
13	68.0	109.0	123.0
23	59.3	99.0	119.1
35	58.0	91.7	101.1
55	47.3	78.3	93.0
85	42.0	70.0	84.0
100	39.3	51.7	37.2

The origin of a finite thermal expansion coefficient of a polymer is associated largely with anharmonic interchain vibrations [64-66]. Although it has been shown [64] that the introduction of crosslinks lowers the expansivity by decreasing the contribution of inter-chain vibrations, the higher values of α'_l and $(\alpha_g - \alpha_l)$ suggests that a higher free volume is trapped in P(MMA-co-EGDMA). It is suggested that the larger free volume is due to the lower efficiency in molecular packing in crosslinked polymers than in linear polymers. In addition, it is suggested that P(MMA-co-EGDMA) copolymers may not age to equilibrium at high EGDMA concentrations since segmental mobility is restricted in a tightly-crosslinked network. These suggestions thus lead to the proposal that P(MMA-co-EGDMA) copolymers may still retain unaged free volume even at temperatures above T_{end}.

Figure 9.8 indicates that the variation of α'_g of crosslinked PMMA with dimethacrylate concentration is extremely complex. It is observed that α'_g of P(MMA-co-EGDMA) gradually decreases with increasing EGDMA concentration, whereas α'_g of P(MMA-

FIGURE 9.8 GLASS EXPANSION COEFFICIENTS OF poly(MMA-oligo(ethylene glycol dimethacrylate) COPOLYMERS

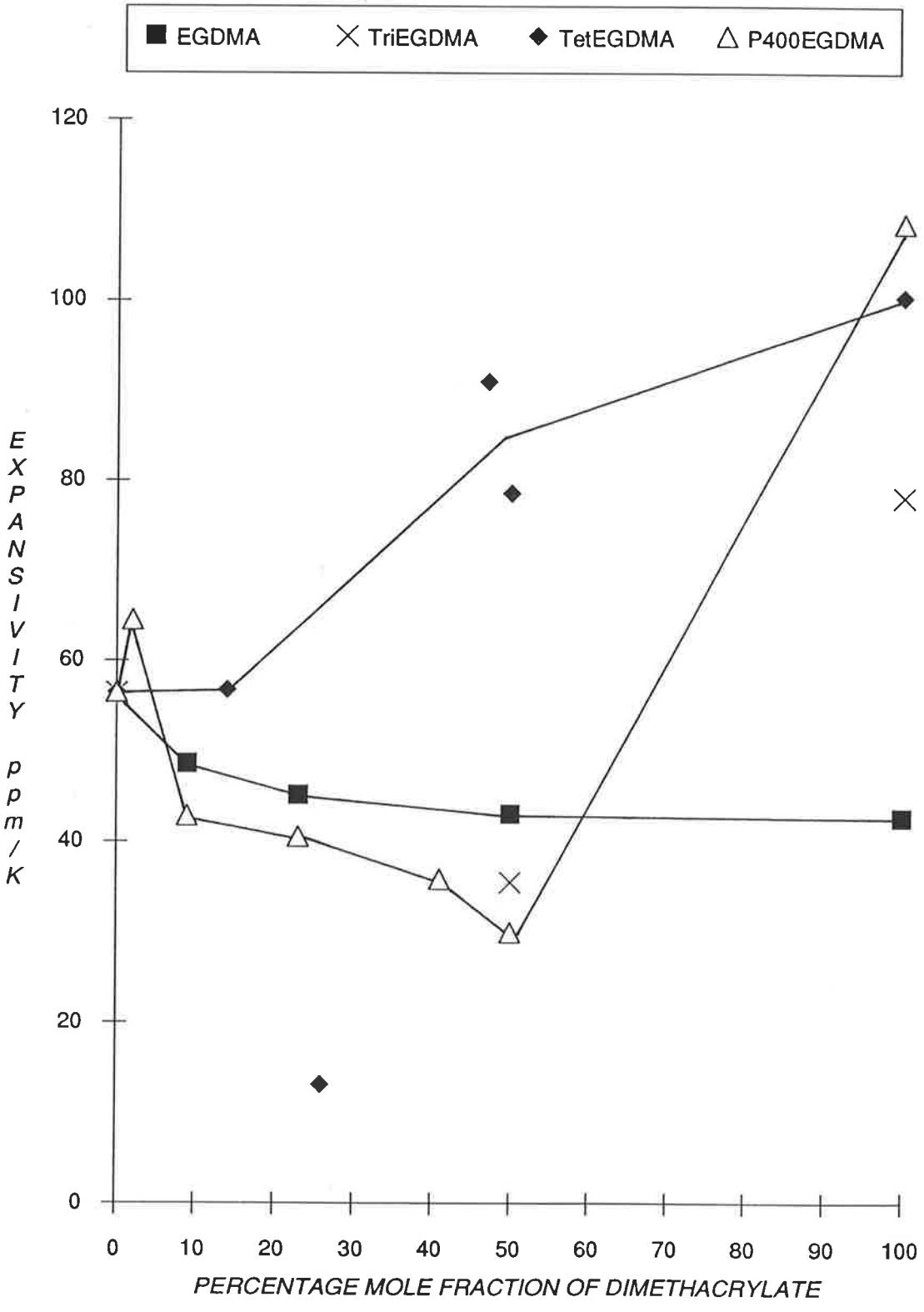

co-TetEGDMA) increases as the concentration of TetEGDMA increases (it has been noted in Section 9.3.1 that the value of α'_g of 13.2 x 10^{-6} K^{-1} at 26 % TetEGDMA is anomalously low). On the other hand, α'_g of P(MMA-co-P400EGDMA) copolymers initially decreases with P400EGDMA concentration, but later increases at higher crosslinker concentrations. Similarly, P(MMA-co-TriEGDMA) exhibited a decrease in α'_g at 50 % TriEGDMA but increases to 78.1 x 10^{-6} K^{-1} for the pure crosslinked polymer.

With the exception of P(MMA-co-EGDMA), the increase in α'_g at high crosslinker concentrations suggests that more free volume is trapped by highly-crosslinked PMMA copolymers when quenched from above to below T_g. It is observed (Tables 9.4-9.6) that α'_g of the pure crosslinked polymers are higher than that of uncrosslinked PMMA, and that α'_g increases on lengthening the oxyethylene chain, in the order: PEGDMA < PTriEGDMA < PTetEGDMA < P400EGDMA. The observation of larger values of α'_g for the pure crosslinked polymers supports the proposal that the efficiency of molecular packing is lowered by crosslinking. However, this proposal predicts that PEGDMA would have the lowest efficiency of molecular packing and thus the highest value of α'_g. It is possible that the larger α'_g of P400EGDMA arises from free volume being generated by the motion within the -$COO(CH_2CH_2O)_xCO$- links.

TABLE 9.4

Thermal expansion coefficients (10^{-6} K^{-1}) of quenched P(MMA-co-TriEGDMA) copolymers

% Mole Fraction TriEGDMA	α'_g	α'_l	$3(\alpha'_g - \alpha'_l)$
0	56.4	142.8	259.2
50	35.5	142.9	322.2
100	78.1	139.6	184.5

However, Allen *et al.* [47] suggested that the increasing flexibility of the oxyethylene chains led to an increase in activation energies associated with localised motion of these chains. On the other hand, dynamic-mechanical tests of crosslinked polymers [67-68] show that the height of the glass transition peak increased as the molecular weight between crosslinks increased. The same behaviour was observed in the dimethacrylate series [47]. It

has been suggested [69] that the height of the glass transition peak gives a measure of the number of mobile molecular units which contribute to the transition. Hence the contribution of the flexible oxyethylene link to the glass transition is reflected in the larger tan δ peak of P400EGDMA. This observation supports the proposal that free volume may be generated by the freezing of motion in the oxyethylene chain. Similarly, large values of α'_g observed for linear poly(alkyl methacrylates) with long side-chains has been attributed to extra free volume generated by the freezing of side-chain motions [70-71].

TABLE 9.5

Thermal expansion coefficients (10^{-6} K^{-1}) of quenched P(MMA-co-TetEGDMA) copolymers

% Mole Fraction TetEGDMA	α'_g	α'_l	$3(\alpha'_g - \alpha'_l)$
0	56.4	142.8	259.2
14	56.7	170.7	342.0
26	13.2	163.7	451.5
47	90.9	145.7	164.4
50	78.6	153.4	224.4
100	100.3	129.5	87.6

TABLE 9.6

Thermal expansion coefficients (10^{-6} K^{-1}) of quenched P(MMA-400EGDMA) copolymers

% Mole Fraction P400EGDMA	α'_g	α'_l	$3(\alpha'_g - \alpha'_l)$
0	56.4	142.8	259.2
2	64.5	155.6	273.3
9	42.8	203.1	480.9
23	40.5	220.0	538.5
41	35.8	228.7	578.7
50	30.0	226.7	590.1
100	108.5	235.9	382.2

The liquid expansivities of the four dimethacrylate copolymers are plotted as a function of dimethacrylate concentration in Figure 9.9. It is observed that α'_l initially increases at about 10 % dimethacrylate concentration, but decreases at higher concentrations. However, this trend was not observed for P400EGDMA in which α'_l becomes progressively larger with increasing dimethacrylate concentrations. The value of α'_l of P(MMA-co-TriEGDMA) appears to remain relatively unchanged, but this observation remains inconclusive as the values of α'_l between 0-50 % TriEGDMA are not known. The magnitude of α'_l of the glassy dimethacrylates (129.5-152.6 x 10^{-6} K^{-1}) are found to be similar to that of PMMA (142.8 x 10^{-6} K^{-1}), whereas α'_l of P400EGDMA is higher (235.9 x 10^{-6} K^{-1}). The larger value of α'_l for P400EGDMA is consistent with the hypothesis that free volume is generated by the freezing of the motion of oxyethylene chains.

The expansivity of the free volume α_f may be represented by the difference of the glass and liquid expansivities, $\alpha_f \approx 3(\alpha'_l - \alpha'_g)$ [69]. The plot of α_f vs. dimethacrylate concentration in Figure 9.10 clearly shows the presence of a maximum which is observed at approximately 9 % EGDMA, 26 % TetEGDMA and 50 % P400EGDMA. It is noted that the dimethacrylate concentration at which α_f is maximum increases on lengthening the oxyethylene chain, which suggests that a higher free volume fraction is more likely to be trapped in a flexible crosslinked network than a rigid one.

The observation of a maximum for α_f indicates that free volume is increased by crosslinking at low to intermediate dimethacrylate concentrations. On the other hand, the lowering of α_f at high concentrations of dimethacrylate indicates that the value of α'_l gradually approaches that of α'_g, suggesting that segmental mobility becomes increasingly restricted at high crosslink densities such that the mobility above T_g becomes similar to the mobility of the glass state below T_g. This suggestion is consistent with the observation of featureless ΔL-T plots of PTetEGDMA and PTriEGDMA and supports the hypothesis that highly crosslinked glassy polymers would retain unaged free volume even at above T_g.

9.4 SUMMARY

(1) Length contraction measurements of quenched specimens of PMMA crosslinked with a series of poly[oligo(ethylene glycol) dimethacrylates] indicated that the ageing behaviour of crosslinked PMMA is very dependent on the structure of the crosslinker. It was observed

FIGURE 9.9 LIQUID EXPANSION COEFFICIENTS OF poly(MMA-oligo(ethylene glycol) dimethacrylate) COPOLYMERS

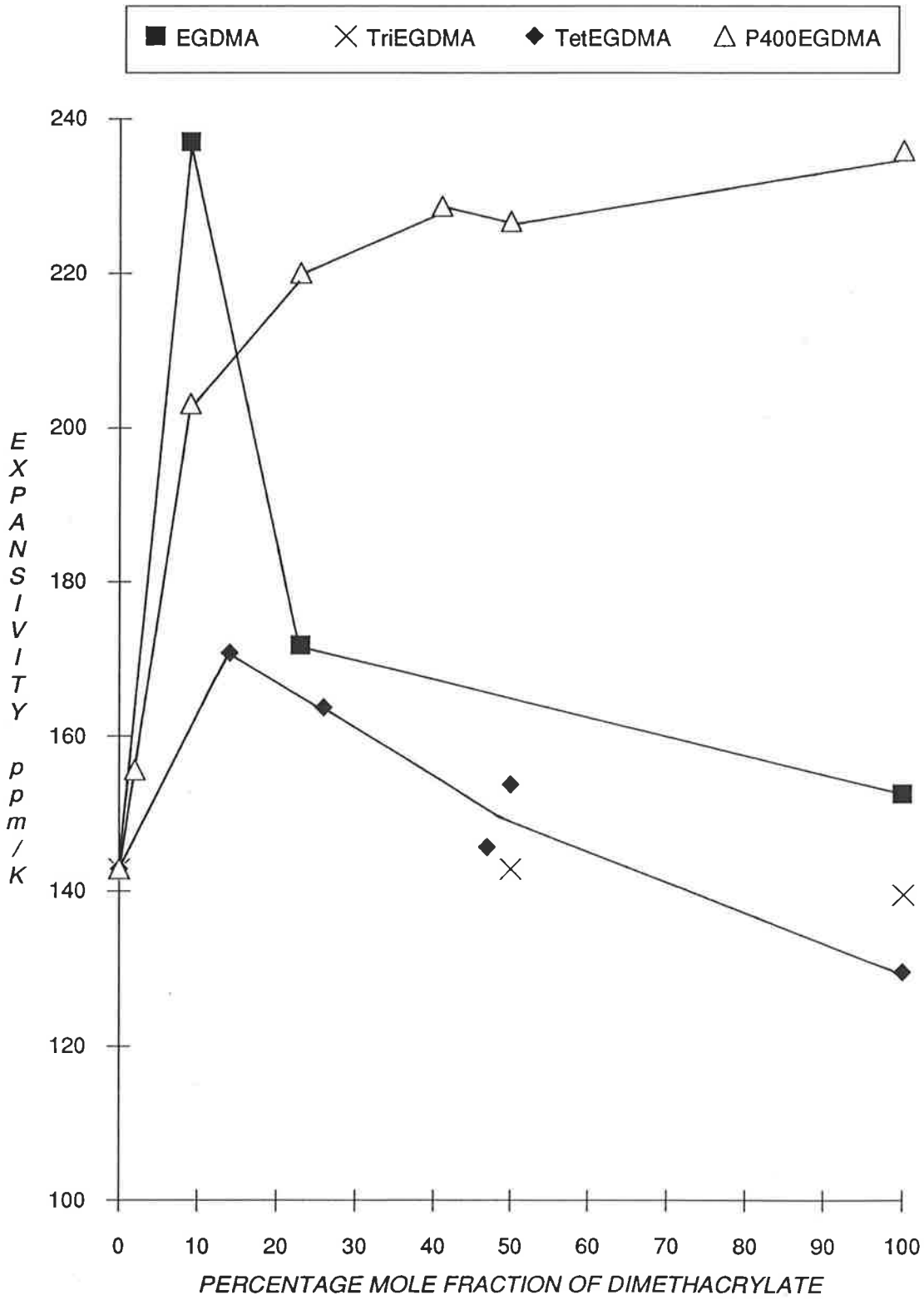

FIGURE 9.10 FREE VOLUME EXPANSIVITY OF poly(MMA-oligo(ethylene glycol) dimethacrylate) COPOLYMERS

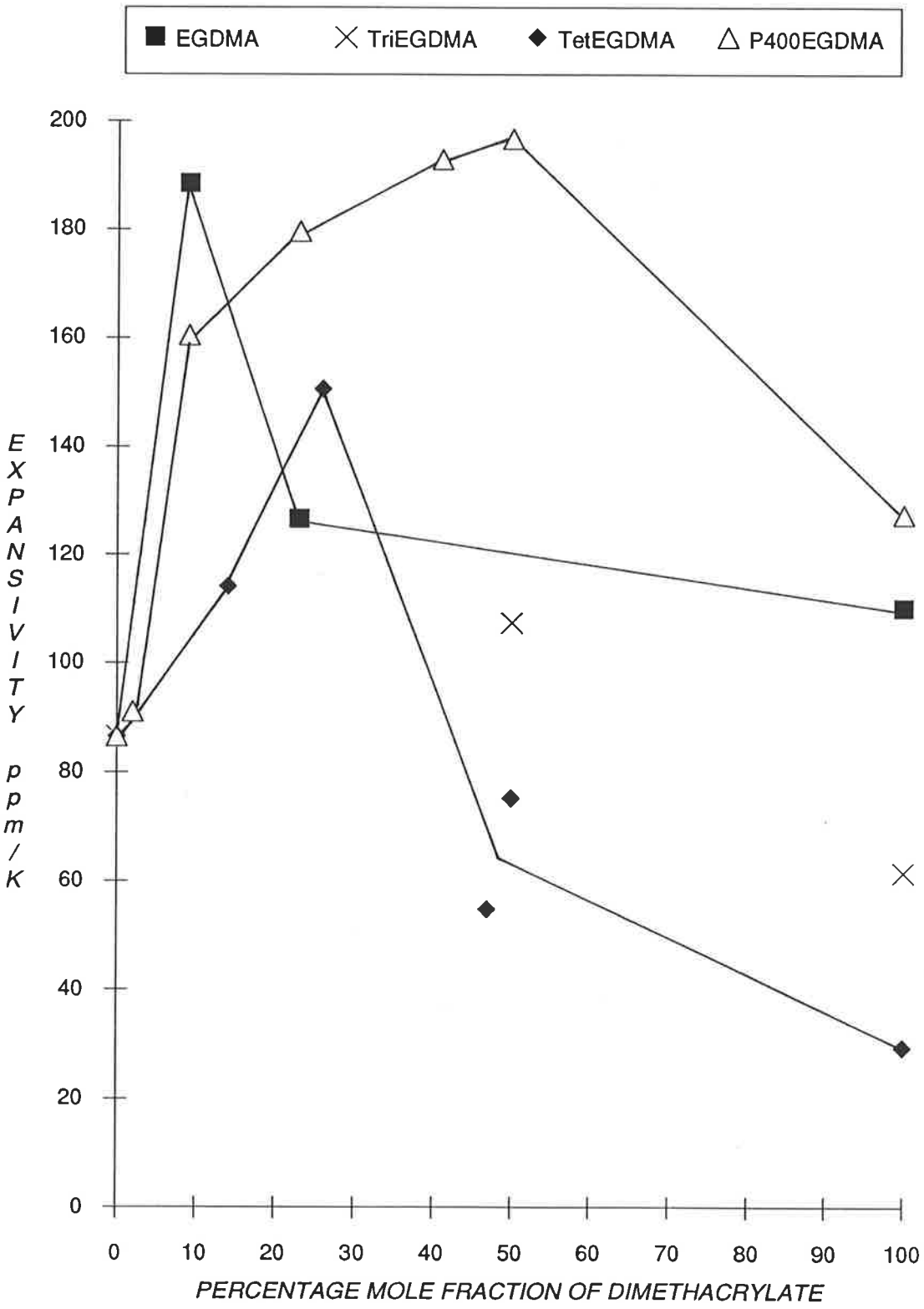

that physical ageing was increasingly restricted as the dimethacrylate concentration was increased. This observation suggested that ageing is restricted by low segmental mobility at high crosslink densities. On the other hand, the lengthening of the oxyethylene crosslink from EGDMA to P400EGDMA was accompanied by a gradual increase in length contraction which indicated that ageing is facilitated by greater segmental mobility inherent in a flexible network.

(2) Length measurements suggested that the limiting molecular weight between crosslinks for the observation of length contraction may lie in the range 450-530. In the case of PEGDMA, PTriEGDMA and PTetEGDMA, length contraction was not observed as M_c for these polymers were below 400. However, contraction was observed for P400EGDMA and all P(MMA-co-EGDMA) copolymers as M_c of P400EGDMA is approximately 536. It was proposed that the lower efficiency in molecular packing and the reduction of segmental mobility both result in free volume which remain unaged even at temperatures above T_g.

(3) The variation of thermal expansion coefficients with crosslinker concentration was found to be complex, where α'_g of P(MMA-co-EGDMA) copolymers was observed to decrease with increasing EGDMA concentration, whereas P(MMA-co-TetEGDMA) exhibited an increase in α'_g with increasing TetEGDMA concentration. On the other hand, an initial decrease in α'_g of P(MMA-co-P400EGDMA) was observed at low concentrations of P400EGDMA followed by an increase at high crosslink densities. With the exception of PEGDMA, α'_g of the pure crosslinked dimethacrylate polymers were found to be greater than that of PMMA, suggesting that the poor molecular packing of highly crosslinked polymers may result in the presence of unaged free volume even at above T_g.

(4) The liquid expansivities of crosslinked PMMA were observed to increase at low to intermediate dimethacrylate concentrations followed by a decrease at high crosslinker concentrations, suggesting that at high crosslinker concentrations, the mobility above T_g becomes progressively restricted where it gradually approaches the mobility below T_g.

Chapter 9

1. L.C.E. Struik, *Physical Ageing in Amorphous Polymers and Other Materials*, Elsevier, Amsterdam (1978).

2. T.S. Ellis, F.E. Karasz and G. Ten Brinke, *J. Appl. Polym. Sci.* **28**, 23 (1983).

3. S. Loshaek, *J. Polym. Sci.* **15**, 391-404 (1955).

4. J.D. LeMay and F.N. Kelley, *Adv. Polym. Sci.* **78**, 115-148 (1986).

5. C.H. Lau, K.A. Hodd and W.W. Wright, *Br. Polym. J.* **18**, 316-322 (1986).

6. J. Schroeder, P.A. Madsen and R.T. Foister, *Polymer* **28**, 929-940 (1987).

7. J.P. Bell, *J. Polym. Sci. A-2* **6**, 417-436 (1970).

8. L.E. Nielsen, *J. Macromol. Sci. Macromol. Chem.* **C3**, 69-103 (1969).

9. M. Shimbo and N. Nishitami, *J. Appl. Polym. Sci.* **29**, 1709-1721 (1984).

10. D.T. Landin and C.W. Macosko, *Characterisation of Highly Crosslinked Polymers,* S.S Labana and L.A. Dickie eds., *American Chemical Society Symposium Series* **243**, 33 (1984).

11. J.P. Bell, *J. Appl. Polym. Sci.* **14**, 1901-1906 (1970).

12. T. Kamon and H. Furukawa, *Adv. Polym. Sci.* **80**, 174-202 (1982).

13. R.J. Morgan, *Adv. Polym. Sci.* **72**, 1-43 (1985).

14. A. Apicella, L. Nicolais and C. de Cataldis, *Adv. Polym. Sci.* **66**, 189-207 (1985).

15. A. Apicella and L. Nicolais, *Adv. Polym. Sci.* **71**, 69-77 (1985).

16. M.T. Arouhime, J.K. Gillham and R.D. Small, *ACS Org. Coat. Plas. Chem. Prepr.* **49**, 576-582 (1983).

17. D.T. Turner and A.K. Abell, *Polymer* **28**, 297-302 (1987).

18. E.F. Oleinik, *Adv. Polym. Sci.* **80**, 49-99 (1986).

19. W. Wu and B.J. Bauer, *Polymer* **27**, 169 (1989).

20. W. Wu and B.J. Bauer, *Macromolecules* **19**, 1613 (1986).

21. V.B. Gupta, L.T. Drzal, W.W. Adams and C.Y.C. Lee, *Structure-Property Relationships in a Cured Epoxy Resin System,* 29th Natl. SAMPE Symp., April 3-5 (1983).

22. T. Kaiser, *Prog. Polym. Sci,* **14**, 373-450 (1989).

23. I.C. Choy, *Ph.D. Thesis,* University of Pittsburgh, Pennsylvania (1987).

24. A. Lee and G.B. McKenna, Polymer 29, 1812 (1988).

25. J.M. Barton, *Polymer* **20**, 1018 (1979).

26. W.N. Findley and R.M. Reed, *Polym. Eng. Sci.* **14(10)**, 724 (1974).

27. R. Mark and W.N. Findley, *Polym. Eng. Sci.* **18(1)**, 6 (1978).

28. E.S.W. Kong, *Adv. Polym. Sci.* **80**, 126 (1986).

29. E.S.W. Kong, *Composites Rev.* **4**, 97 (1982).

30. T.D. Chang and J.O. Brittain, *Polym. Eng. Sci.* **22**, 1221 (1982).

31. E.S.W. Kong, *Epoxy Resin Chemistry II,* R.S. Bauer ed., *Am. Chem. Soc. Symp. Series No. 221,* Chapter 9, Washington D.C. (1983), p171-191.

32. E.S.W. Kong, G.L. Wilkes, J.E. McGarth, A.K. Banthia, Y. Mohajer and M.R. Tant, *Polym. Eng. Sci.* **21(14)**, 943 (1981).

33. A.J. Kovacs, *J. Polym. Sci.* **30**, 131 (1958).

34. A.J. Kovacs, *Fortschr Hochpolym. Forsch.* **3**, 394 (1963).

35. L.C.E. Struik, *Rheol. Acta* **5**, 131 (1958).

36. L.C.E. Struik, *Polym. Eng. Sci.* **17(3)**, 165 (1977).

37. M.R. Tant and G.L. Wilkes, *Polym. Eng. Sci.* **21**, 874 (1981).

38. S.E.P. Petrie, *J. Macromol. Sci. Phys.* **B12(2)**, 225 (1976).

39. J.C. Bauwens, *Plast. Rubb. Process. Appl.* **7(3)**, 153-147 (1987).

40. J.C. Bauwens, *Failure of Plastics,* W. Brostow and R.D. Corneliussen eds., Hanser (New York) (1986), p235.

41. M. Atsuta, N. Nakabayashi and E. Masuhara, *J. Biomed. Mater. Res.* **5**, 183-195 (1971).

42. C.C. Eliades, A.A. Caputo and G.J. Vougioklalis, *IADR, 1st Joint Meeting of Continental European and Israeli Divisions,* Brussels, Sept. 15 (1984).

43. E. Asmussen, *Acta Odont. Scand.* **33**, 129-134 (1975).

44. I.E. Ruyter and I.J. Sjovik, *Acta Odont. Scand.* **39**, 133-146 (1981).

45. P.E.M. Allen, G.P. Simon, D.R.G. Williams and E.H. Williams, *Polym. Bull.* **11**, 593-600 (1984).

46. P.E.M. Allen, G.P. Simon, D.R.G. Williams and E.H. Williams, *Eur. Polym. J.* **22(7)**, 549-557 (1986).

47. P.E.M. Allen, G.P. Simon, D.R.G. Williams and E.H. Williams, *Macromolecules* **22**, 809-816 (1989).

48. G.F. Cowperthwaite, J.J. Foy and M.A. Malloy, *Biomedical and Dental Applications of Polymers,* C.G. Geblen and F. Koblitz eds., Plenum Press, New York (1981), p397.

49. T.R. Manley, *Chem. Ind. (London)* **22**, 1797 (1966).

50. H.B. Lee and D.T. Turner, *Polym. Eng. Sci.* **19(2)**, 95 (1979).

51. V. McGinnis, R.M. Holsworth, *J. Appl. Polym. Sci.* **19**, 2243 (1975).

52. S. Loshaek and T.G. Fox, *J. Am. Chem. Soc.* **75**, 3544 (1953).

53. T.G. Fox and S. Loshaek, *J. Polym. Sci.* **15**, 371 (1955).

54. J.P. Berry, *J. Polym. Sci. Polym. Chem. Ed.* **A1**, 993 (1963).

55. M. Atsuta and D.T. Turner, *Polym. Eng. Sci.* **22**, 438 (1982).

56. M. Atsuta and D.T. Turner, *J. Polym. Sci. Polym. Phys. Ed.* **20**, 1609 (1982).

57. D.T. Turner, *Characterisation of Highly Crosslinked Polymers,* S.S. Labana and R.A. Dickie eds., *American Chemical Society Symposium Series* **243**, 185 (1984).

58. T.W. Wilson and D.T. Turner, *Polym. Mater. Sci. Eng.* **59**, 413-417 (1988).

59. G.P. Simon, *Ph.D. Thesis,* University of Adelaide, South Australia (1986).

60. G.V. Korolev, B.R. Smirnov, L.A. Zhil'tsova, L.I. Makhonina, N.V. Tvogorov and A.A. Berlin, *Vysokomol. Soedin. Ser. A* **19**, 9 (1967).

61. B.Z. Ozerkovski and V.P. Roschupkin, *Dokl. Akad. Nauk. USSR* **248**, 657 (1979).

62. P. Mason, *Polymer* **5**, 625 (1964).

63. K. Shibayama and Y. Suzuki, *J. Polym. Sci.* **3A**, 2637 (1965).

64. L. Holliday and J.D. Robinson, *Polymer Engineering Composites,* M.O.W. Richardson ed., Applied Science, London (1977), Chapter 6, p263.

65. R.E. Barker Jr., *J. Appl. Phys.* **38(11)**, 4234 (1967).

66. G. Schawrz, *Cryogenics* **28**, 248 (1988).

67. T. Muryama and J.P. Bell, *J. Polym. Sci. Polym. Phys. Ed.* **A2**, 437 (1970).

68. A.L. Andrady and M.D. Sefcik, *J. Polym. Sci. Polym. Phys. Ed.* **21**, 2453 (1983).

69. G.E. Roberts and E.F.T. White, *The Physics of Polymer Glasses,* R.N. Haward ed., Wiley, New York (1973), Chapter 3, p153.

70. R. Simha and R.F. Boyer, *J. Chem. Phys.* **37(5)**, 1003 (1962).

71. R.A. Haldon and R. Simha, *J. Appl. Phys.* **39(3)**, 1890 (1968).

GLOSSARY OF SYMBOLS

α'_g	Linear Glass Expansion Coefficient
α'_l	Linear Liquid Expansion Coefficient
α_f	Expansion Coefficient of Free Volume
ΔC_p	Changes in Specific Heat Capacity
ε	Fraction of Crosslinker Which Reacts to Form Crosslinks
ΔL	Magnitude of Length Contraction
m_x	Mass of Crosslinker Monomer
m_{MMA}	Mass of Methyl Methacrylate Monomer
M_x	Molecular Weight of Crosslinker Monomer
M_{MMA}	Molecular Weight of Molecular Weight Monomer
n_x	Number of Moles of Crosslinker Monomer
n_{MMA}	Number of Moles of Methyl Methacrylate Monomer
T_g	Glass Transition Temperature
T_{on}	Onset Temperature of Length Contraction
T_{end}	Endset Temperature of Length Contraction

CHAPTER 10
PHYSICAL AGEING IN POLY(2-HYDROXYETHYL METHACRYLATE)

10.1 INTRODUCTION 198

10.2 EXPERIMENTAL

10.2.1 Preparation of PHEMA Specimens 202

10.2.2 Hydration of PHEMA Specimens 202

10.2.3 Preparation of PHEMA-KBr Specimens 203

10.2.4 Preparation of Poly(HEMA-co-EGDMA) Specimens 204

10.3 RESULTS AND DISCUSSION

10.3.1 Physical Ageing of Dry and Partially-Hydrated PHEMA 204

10.3.2 Effect of Crosslinking on Physical Ageing of Dry PHEMA 207

10.3.3. Physical Ageing of Dry PHEMA-KBr Polymers 208

10.4 SUMMARY 210

BIBLIOGRAPHY 210

GLOSSARY OF SYMBOLS 215

CHAPTER 10

10.1 INTRODUCTION

Polymeric hydrogels may be conveniently described as consisting of hydrophilic polymers that are swollen by water [1-2]. Hydrogels are capable of absorbing substantial amounts of solvent while still retaining essential properties of solids such as finite shear and compression moduli. Hydrogels are commonly lightly crosslinked so that they do not dissolve in water, which means that hydrogels are effectively water-swollen polymer networks.

Commercial and scientific interest in hydrogels were aroused in the early 1960s when Wichterle and Lim [3-4] demonstrated that hydrogels based on poly(2-hydroxy ethyl methacrylate) (PHEMA) could be used for the fabrication of soft contact lenses. The biological compatibility of PHEMA [5-15] makes it an ideal and important polymer for modelling water-polymer interactions in natural polymers such as proteins and polypeptides. The resultant interest in the biomedical applications of hydrogels is reflected by specific studies on, for example, artificial liver support systems [18-22] thromboresistance [23-24], reverse osmosis membranes [25-27], kidney dialysis membranes [11, 28-29], drug delivery systems [30-34], and in the increasing number of reviews of these applications [16, 35-36]. In addition, PHEMA exhibits a high degree of chemical stability and mechanical integrity, where it has been shown to be resistant to acid hydrolysis and reactions with amines [16], and incur alkaline hydrolysis only at high temperature and pH [17].

The polar hydroxy groups of PHEMA enable it to absorb large amounts of water up to 40-45 % of the total weight of the polymer [37-44]. At higher levels of hydration, PHEMA becomes heterogeneous and visually turbid [7-10, 12] as a result of phase separation. The uptake of water is also accompanied by the lowering of the glass transition [45-46], such that at high levels of hydration T_g drops to below room temperature [61]. Experimental evidence [1, 47-52] suggests that water in polymers can exist in more than one state and that these states of water in the hydrogel will affect its properties. Several useful bi- and tri-partite classification systems have been proposed but they are not readily interconvertible as these classifications are technique-dependent [61, 63]. It has been proposed [1] that the water present in a polymer network exists in a continuum of states between the two extremes, namely, water strongly

bound to the polymer network through hydrogen bonding, and water with a much greater degree of mobility which are unaffected by the polymer environment. The nomenclature used to describe the first type of water includes bound [48-49, 53-55] or non-freezing [44, 53, 55] water, whereas the second type of water is referred to as free [41, 53-55, 56-57] or freezing [44, 53, 55] water. Smyth *et al.* [58] suggested that the composition of water present in hydrated PHEMA comprised of bound water (less than 20 %), interfacial water (about 15 %) and freely diffusable water. Bound water corresponded to an average of two water molecules hydrogen-bonded to each polymer repeating unit [12-13], while interfacial water was attributed to dipole-dipole interactions with hydroxy groups [15] or hydrophobic interactions with polymer segments [59]. The fraction of each type of water is influenced by the degree of crosslinking [15], although the water uptake of PHEMA has been observed to be relatively insensitive to low degrees of crosslinking [5, 60], even when the crosslinks are as hydrophilic as P400EGDMA [61]. On the other hand, the percentage of absorbed water in PHEMA has been shown to increase with crosslinking [1, 61]. The increase in the amount of water uptake was attributed to the increase in the size and number of voids due to increased stresses during cure of the more densely crosslinked glasses [61]. However, the opposite effect was observed for the uptake of water. The networks absorb less water because they have become more dense and less flexible due to tighter crosslinking [61].

In the case of PHEMA, it has been observed [61] that the percentage of water accommodated in voids [65] rise to a maximum of 7.2 % 30 minutes after immersion when the water content (WC) was 14 %. When the equilibrium water content (EWC) [1] was reached, the percentage of water in voids dropped to about 3 % (corresponding to approximately 1.2 % of the total weight of the hydrogel). It is suggested that the voids arise from the inhomogeneous packing of polymer chains which are frozen in below T_g [65-67]. The conclusion that the sorption of small amounts of diluents are absorbed into voids is supported by reports [68-69] which show that the properties of some polymers were unaffected by the presence of diluent at low concentrations. The percentage of absorbed water in voids was also found to vary according to the relative humidities in which the specimens were conditioned. For specimens conditioned at 33 % RH, 35 % of water absorbed were present in voids; this value decreased to 4.3 % at 100 % RH. However, the percentage of the water in voids as a fraction of the total weight of the PHEMA hydrogel was fairly constant, at 1.4-1.6 % [61].

Hence it may be concluded that the majority of water molecules at the attainment of EWC do not reside in voids.

The distribution of water molecules in a polymer is also dependent on the period of time spent by the water molecules in the polymer network. Solid state NMR studies of the distribution of water in PMMA [70] indicate that in the early stages of water uptake, water molecules were located mainly in the hydrophobic regions, in contact with the backbone and quartenary carbons. The water molecules eventually make contact with the more polar side-groups later. These observations were consistent with Turner's [65] concept of a dual sorption mode, in which the initial and faster mode was associated with the filling of voids. The filling of voids is accompanied by an increase in density and without any change in dimensions, whereas the slower mode is accompanied by swelling and causes relatively little change in density.

The effect of hydrogen bonds between water molecules and hydrophilic hydroxy groups on the distribution of water in PHEMA must also be considered. In his review, Kong [64] showed that the deuterium NMR spectrum of heavy water (D_2O) absorbed by a quenched epoxy fibre over 3 months consisted of a sharp peak with some broadening on either side of the peak (Fig. 10.1). The single peak has been associated with freely-tumbling or less bound D_2O molecules (the deuterium NMR spectrum of D_2O is shown in Fig. 10.2), whereas the broadening indicated that the mobility of some of the D_2O molecules were restricted by hydrogen bonding. He proposed a model in which water absorbed by an epoxy essentially existed in two states, namely, bound water formed hydrogen bonds with polar epoxy groups, and less bound water residing in voids (Fig. 10.3). According to the sorption studies of Allen *et al.* [61, 70], the distribution of water in PHEMA after long periods of time is expected to be in regions where water-polymer interactions are strongest. Therefore, one can expect a high degree of hydrogen bonding in fully hydrated PHEMA or in specimens which has been stored in humid atmospheres for a long time.

The interaction between water and epoxy glasses has been studied as a function of ageing time by Kong [64]. Highly crosslinked epoxy resins were aged for various times at 140 C and were then subjected to 98 % relatively humidity at 40 C. The initial rate of sorption and the equilibrium sorption level were observed to decrease with increasing ageing time (Fig. 10.4). The diffusivity of water in epoxy resins was also observed to decrease with ageing time.

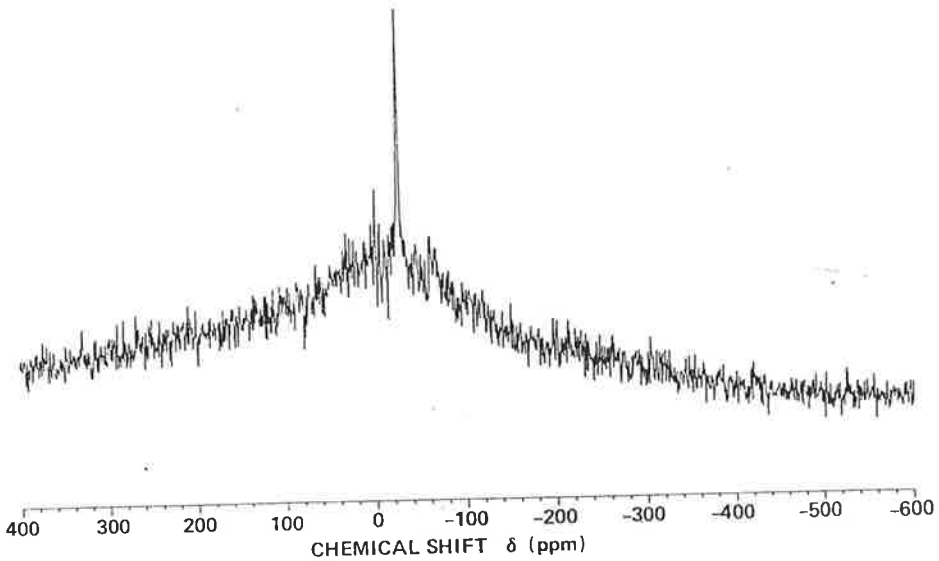

Figure 10.1 Deuterium NMR spectrum of heavy water absorbed by a quenched Fiberite 934 epoxy. The epoxy resin was immersed for 2 months at 23 C and 1 month at 40 C (reprinted from [64]).

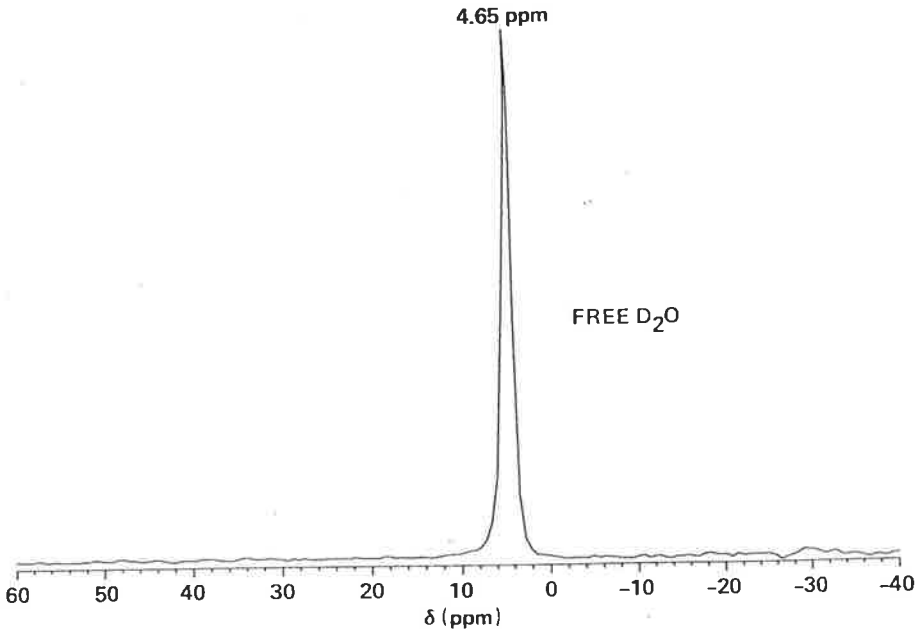

Figure 10.2 Deuterium NMR spectrum of free heavy water molecules (reprinted from [64]).

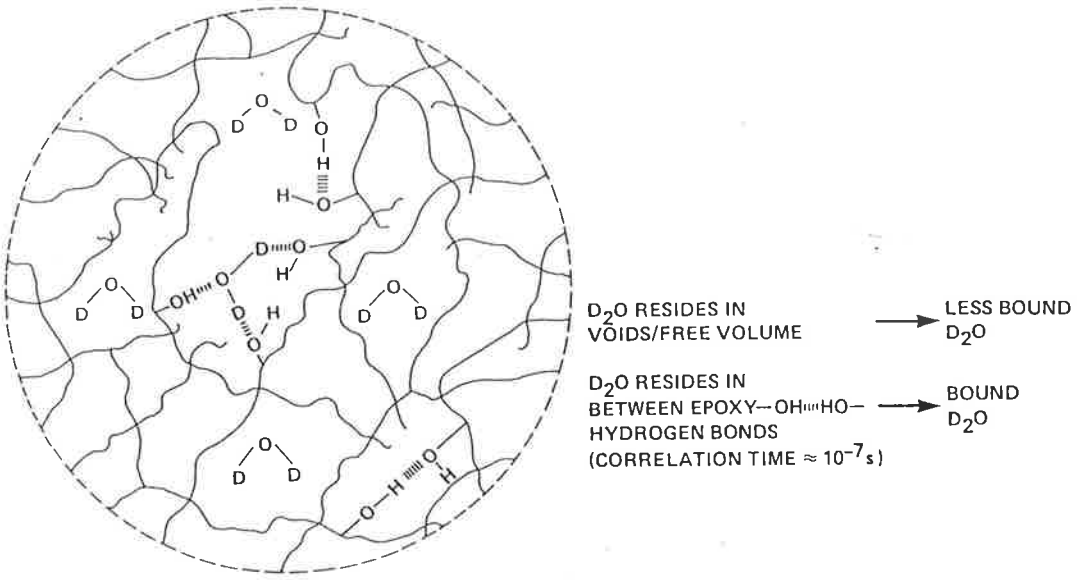

Figure 10.3 Model proposed by Kong [64] for "heavy water-epoxy interactions". Heavy water molecules may form aggregates in polymer voids or disrupt the hydrogen bonds in the resin.

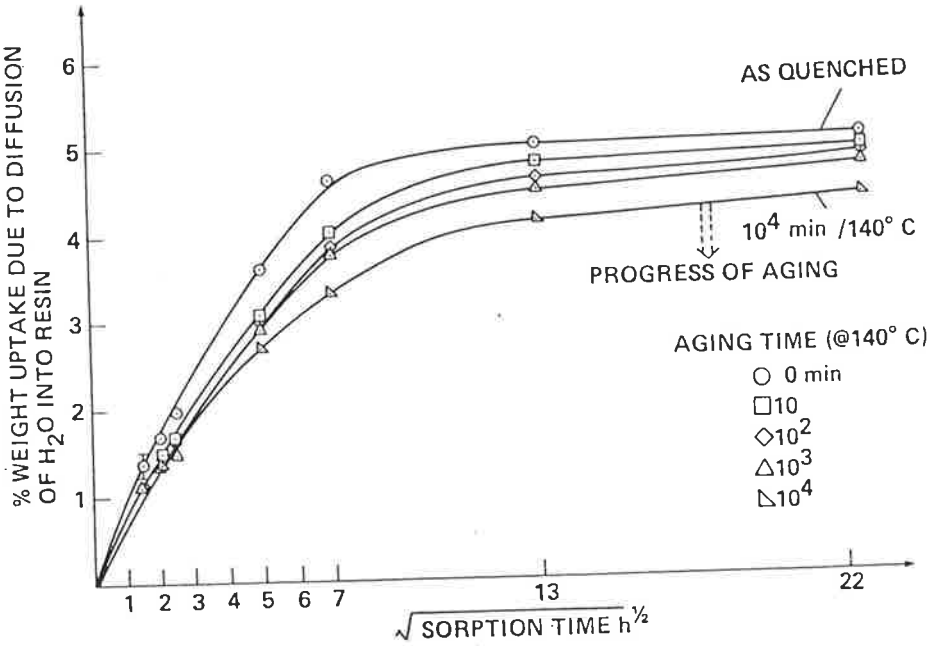

Figure 10.4 Moisture absorption behaviour of fully crosslinked Fiberite 934 resin as influenced by physical ageing (reprinted from [64]).

These observation supported the idea that the resin contracts and densifies during ageing below T_g, resulting in a decreased free volume [64]. In addition, it was found that swelling occurs to a greater degree in an aged specimen than a quenched specimen. It was suggested that water tends to swell the aged polymer as there are less free volume and vacant sites for diffusion. Therefore, polymer-solvent interactions are expected to increase as water diffuses into an aged epoxy network [64].

However, in spite of the substantial literature on hydrogels, relatively little work has been carried out on the effects of ageing on the sorption properties of network hydrogels. Results from another contemporary project in the same department looking at ion diffusion in PHEMA indicated that the ageing behaviour of PHEMA could be modified by the presence of fillers. It has been shown by Shanks and Howard [71-74] that the introduction of fillers into poly(vinyl chloride) (PVC) increases the T_g and retard the rate of ageing [75] of the filled polymer. These observations were attributed to the restriction of the mobility of polymer molecules by the adsorption of the polymer onto filler molecules. In addition, Trostyanskaya *et al.* [76] have shown for epoxy resins filled with quartz or glass powder that an increase in filler concentration was accompanied by an increase in the modulus of elasticity, free volume fraction at T_g and volume expansivity. However, in the case of polystyrene (PS) and PMMA, the presence of carbon fillers has been shown [71, 77] to decrease the T_g. It was proposed [71] that the lowering of T_g upon the addition of fillers was restricted only to brittle polymers. When these polymers were cooled from above to below T_g, the generation of thermal stresses (caused by non-uniform polymer shrinkage) result in the formation of cracks around the filler particles. The cracks not only lower the surface adhesion of the polymer to the filler but also create voids (i.e. free volume) which will cause a lowering of T_g. In this work, a study of physical ageing of PHEMA containing small amounts of potassium bromide (KBr) ions are presented.

This chapter presents a preliminary study of physical ageing of dry and hydrated PHEMA, in which dimensional changes of hydrated PHEMA were characterised as a function of water content and the period of hydration. Physical ageing of dry crosslinked poly(HEMA-co-EGDMA) was also studied and the results were compared with those obtained for poly-(MMA-co-[oligo(ethylene glycol) dimethacrylates] in Chapter 9.

10.2 EXPERIMENTAL

*10.2.1 Preparation of PHEMA Specimens**

HEMA was obtained from Mitsubishi Chemicals, by courtesy of SOLA Optical. It contained 50 ppm methyl hydroquinone as stabiliser and 0.3 % EGDMA as impurities left over from the production process [61, 78]. The monomer was dried over anhydrous magnesium sulphate and then stored over activated molecular sieves at -15 C. The peroxide initiator, *tert*-butyl per-2-ethyl hexanoate (Interox, Australia), was used as supplied at a concentration of 0.2% v/v. To prevent inhibition of the polymerisation by oxygen, high-purity nitrogen gas was bubbled through the monomer for 15-20 minutes prior to casting. The reaction mixture was cast between two glass sheets according to the procedure described by Cowperthwaite [79].

Due to the strong adhesion of PHEMA to glass, it was necessary to treat the surface of the glass sheets with trimethylchlorosilane (TMCS) prior to casting any monomer mixtures containing HEMA [80]. TMCS reacts with the silanol groups on the glass surface and prevents the bonding of the hydroxy group of HEMA to the surface of the glass. This facilitated the easy removal of the polymer from the mould. HEMA was cured isothermally at 60 C for approximately 2 hours until gelation had occured. The curing temperature was then raised in 10 C steps every hour up to 110 C. Following postcuring at 110 C for 12 hours, the temperature was slowly reduced over a period of 4-5 hours to ambient temperature. The resulting casts were clear and transparent.

10.2.2 Hydration of PHEMA Specimens

Partially hydrated specimens were obtained by placing as-cast PHEMA specimens either in deionised water or stored over saturated salt solutions at different relative humidities (RH) at constant temperatures of 20 C and 25 C [81-82]. A constant temperature water bath was used to maintain the desired temperature to +/- 1 C, and the specimens were stored in sealed containers over several months. It has been shown [83] that humidities obtained this way are within +/- 3% of the published values in [81-82]. The water content absorbed by a PHEMA network is expressed in terms of weight percentage relative to the wet weight W by [61]:

$$WC = 100 \times (W - W_0)/W \ \% \qquad (10.1)$$

where W_0 is the dry weight measured after the specimen had cooled to 25 C at the completion of the TMA test. The sample weights were determined using a Mettler M3 microbalance.

The ageing behaviour of partially and fully hydrated PHEMA specimens were investigated. Three partially hydrated specimens containing 7.5 %, 8.5 % and 11.7 % water were tested. These specimens were cooled at a rate of 2 C/min from 20 C to -50 C, and heated from -50 C to 150 C at 2 C/min under a constant load of 0.1 N. Fully-hydrated specimens had a more complicated thermal history: they were initially dried at 160 C for 30 minutes and then quenched in liquid nitrogen for 10 minutes. The quenched specimens were quickly transferred to a dessicator and was allowed to warm to 25 C over a period of 8-9 hours. The specimens were immersed in deionised water at 25 C for long periods between 18 to 409 hours until each specimen had a water content of 40%. The hydrated specimens were heated from -100 C to 160 C at a rate of 2 C/min under a static load of 0.1 N. A TMA scan of a dry and quenched PHEMA specimen was also carried out.

*10.2.3 Preparation of PHEMA-KBR Specimens**

Cast PHEMA specimens were initially dried in a vacuum oven at 50 C until a constant weight was achieved. The dry specimens were then soaked in KBr solutions of different concentrations for 2 weeks at ambient temperature and atmospheric pressure. Water was removed from these specimens by drying at ambient temperature for a period of one month followed by vacuum drying for 1 week at 50 C until the weight of the polymer was constant. The KBr concentrations are listed in Table 10.1 as a fraction of the polymer weight.

TABLE 10.1

Concentrations of potassium bromide in poly(hydroxy ethyl methacrylate) specimens

KBr solution (mol/dm^3)	[KBr] (moles/g)	[KBr] (g/g)
0.50	1.69×10^{-4}	0.0201
0.75	2.92×10^{-4}	0.0347
1.00	3.52×10^{-4}	0.0419

The PHEMA-KBr specimens were thermally equilibrated at 145 C for 10 minutes followed by quenching in liquid nitrogen for 10 minutes. In order to prevent any uptake of moisture, the specimen was quickly transferred from the liquid nitrogen bath to the TMA in which the specimen was allowed to warm to 25 C under dry nitrogen. The weight of the specimen was measured before and after thermal equilibration at 145 C to ascertain the amount of KBr which may have been removed during heating. Weight losses of less than 1.0% indicated that a negligible amount of KBr was lost during equilibration at 145 C, hence the KBr concentrations of Table 10.1 in the quenched PHEMA-KBr specimens were assumed to be unchanged prior to thermal analysis. The specimens were heated in the TMA at a constant rate of 2 C/min under a static load of 0.1 N from 25 C to 160 C.

*10.2.4 Preparation of Poly(HEMA-co-EGDMA) Specimens**

Crosslinked PHEMA specimens containing 3, 7 and 31 mol/mol % EGDMA were cast according to the method described in Section 10.2.1. For the mixture containing 31 % EGDMA, a postcure of 120 C for one hour was required to ensure the fullest cure possible. DSC measurements of crosslinked specimens indicate no evidence of undercure, even though solid-state NMR [84-85] results showed that tight networks such as PEGDMA, PDEGMA and PTetEGDMA still contained residual monomer and pendant double bonds.

Water was removed from these specimens by heating at 160 C for 15 minutes, followed by quenching in liquid nitrogen for 10 minutes. The specimens were placed inside a dessicator to warm to 25 C to prevent the uptake of moisture. The specimens were then heated in the TMA at a constant rate of 2 C/min under a static load of 0.1 N from 25 C to 160 C.

(PHEMA and poly(HEMA-co-EGDMA) specimens were prepared by Darrell Bennett while the PHEMA-KBr specimens were prepared by Darren Miller).*

10.3 RESULTS AND DISCUSSION

10.3.1 Physical Ageing of Dry and Partially-Hydrated PHEMA

The ΔL-T plots of dry PHEMA and partially-hydrated PHEMA containing 7.5, 8.5 and 11.7 % water are presented in Figure 10.5. In quenched dry PHEMA the onset of contraction is observed at 89 C, while the attainment of equilibrium, as determined by expansion in the liquid phase, occurs above 119 C. Dynamic mechanical measurements of dry

FIGURE 10.5 PHYSICAL AGEING IN DRY AND PARTIALLY HYDRATED PHEMA (the percentage weight of water absorbed is shown in the legend)

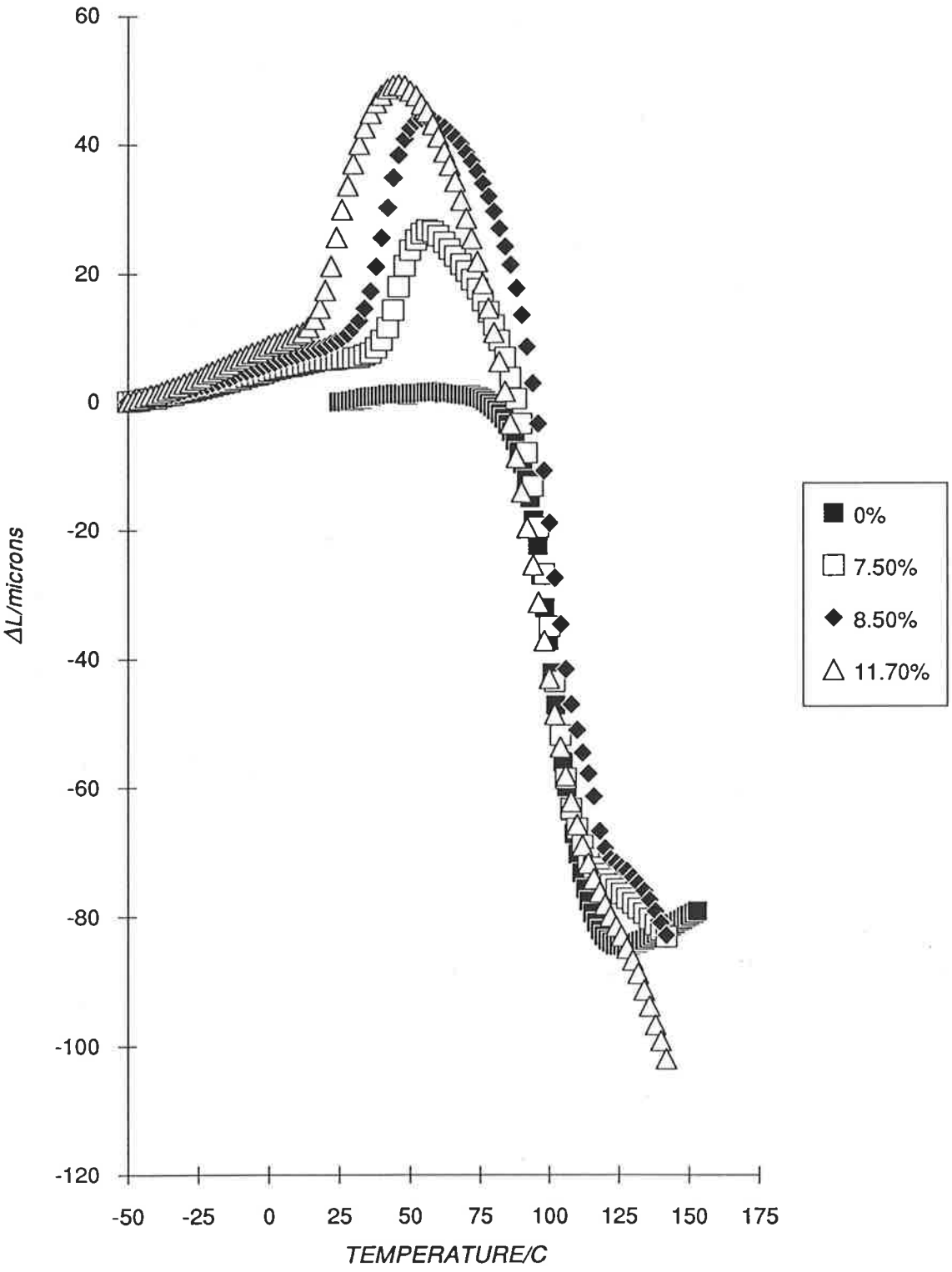

PHEMA [46] indicated the existence of three relaxations: the lowest temperature relaxation at -133 C is presumed to arise from internal rotations of the hydroxy group, the second relaxation at 27 C has been ascribed to the partial rotation of the $COOCH_2CH_2OH$ group, and the third relaxation observed at 103 C is ascribed to the glass transition of PHEMA. A higher T_g of 125 C was obtained by Allen *et al.* [62] from torsion pendulum tests. The onset of length contraction has been associated with the onset of cooperative segmental motion, which suggests that the T_g obtained by Kolarik [46] is more appropriate. The length contraction (ΔL_z) of 86.1 x 10^{-9} m yields a free volume of 3.59 x 10^{-9} m^3 and a free volume fraction of 0.085.

The ΔL-T plots of Figure 10.5 also show an abrupt expansion in the range 18-40 C, and the temperature at which the sudden expansion is observed is lowered with increasing water content. On the other hand, the magnitude of the expansion increases with water content, reaching a maximum ΔL_z of *ca* 50 x 10^{-9} m at 11.7 % water. These observations indicate that the dimensional changes of PHEMA are significantly modified by the presence of moisture. Separate measurements of dimensional changes of fully hydrated PHEMA (containing 40 % water) suggest that the abrupt expansion may be caused by the formation of hydrogen-bonded (bound) water which swells the PHEMA specimen.

It is suggested that the formation of more bound water molecules (caused by the diffusion of unbound water which facilitates the formation of hydrogen bonds) results in the swelling of PHEMA. Allen *et al.* [61] observed that the percentage of water accommodated in voids rises to a maximum of 7.2 % during the early stages of sorption, but declines to only 1.2 % when the EWC was reached. These observations suggest that the distribution of water in PHEMA is not dependent only on the water content but also on the storage time. Hydrated PHEMA specimens that are stored for long periods are thus expected to contain a higher proportion of hydrogen bonded water than unbound water. On the other hand, unbound and bound water may coexist in PHEMA at relatively short time immersion times.

Length contraction is observed for all partially-hydrated PHEMA specimens in the range 45-60 C. It is observed that the plots of partially-hydrated PHEMA overlap the plot of dry PHEMA in the contraction phase at about 90 C (Fig. 10.5a), which suggests that the observed contraction in partially-hydrated PHEMA is due to ageing. On the other hand, the loss of water during heating arises as another possible explanation for the contraction. This explanation attributes the contraction to the de-swelling of PHEMA as bound water molecules

FIGURE 10.5A PHYSICAL AGEING IN DRY AND PARTIALLY HYDRATED PHEMA (the percentage weight of water absorbed is shown in the legend)

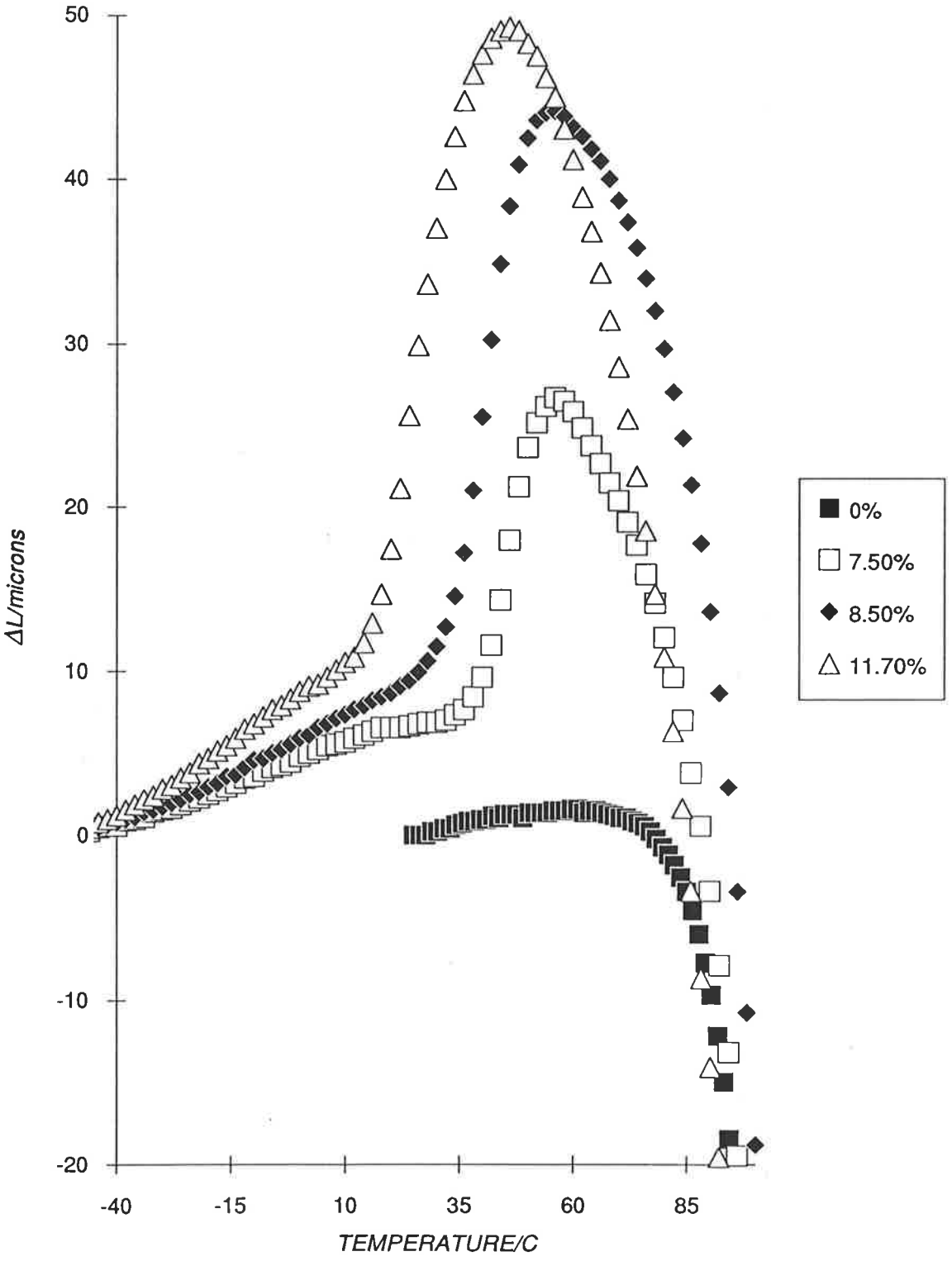

are released from the PHEMA network during the course of the experiment. However, as physical ageing and the loss of diluent both result in contraction, the contraction in partially-hydrated PHEMA could well be caused by ageing and by the loss of water.

The linear glass expansion coefficient α'_g is also affected by moisture, rising from 42.1 x 10^{-6} K^{-1} for dry PHEMA to 74.4 x 10^{-6} K^{-1} at 11.7 % water content. The glass expansivity of partially-hydrated PHEMA were measured at about -25 C, while α'_g of dry PHEMA was obtained at *ca* 35 C. The relevant data are presented in Table 10.2.

It has been shown in Chapter 8 that the free volume fractions of plasticised PMMA are generally higher than that of unplasticised PMMA, and that the free volume fraction and α'_g increases with increasing plasticiser concentration (Table 8.3). The increase in α'_g with water content suggests that the presence of water molecules in the PHEMA network increases the free volume fraction of PHEMA. This observation is thus consistent with the plasticising action of water [86-90].

TABLE 10.2

Thermal analysis data of dry and hydrated poly(2-hydroxyethyl methacrylate) specimens

WC (%)	α'_g (10^{-6} K^{-1})	Onset Temp. of Expansion (C)
0	42.1	not observed
7.5	63.9	40
8.5	64.7	33
11.7	74.4	18

Although these results represent a preliminary investigation of the effect of moisture on the dimensional changes of PHEMA, there is sufficient evidence to suggest that the nature and distribution of water molecules in PHEMA may be elucidated from future work involving TMA measurements. Further work investigating the dimensional changes of fully-hydrated PHEMA specimens (containing EWC of 40 % water) are currently in progress.

10.3.2 Effect of Crosslinking on Physical Ageing of Dry PHEMA

The length-temperature curves of quenched PHEMA copolymerised with 3, 7 and 24 mole fraction percentage of EGDMA are shown in Figure 10.6. The lowering of segmental mobility of a crosslinked polymer is reflected by the decrease in length contraction with increasing EGDMA concentration. A featureless scan was observed for 24 % EGDMA, except for a hint of expansion at about 190 C which may an indication of a glass-rubber transition. Accompanying the reduction in length contraction is a decrease in free volume fraction, from 0.085 for uncrosslinked PHEMA to 0.054 at 7 % EGDMA. The free volume fraction at 31 % EGDMA could not be measured as length contraction was not observed.

The thermal expansivities α'_g, α'_l and the free volume expansivity, $3(\alpha'_l - \alpha'_g)$, of poly(HEMA-co-EGDMA) show an increase up to 7 % EGDMA, and decreases with further increments in EGDMA concentration. This behaviour was observed for poly(MMA-co-EGDMA) (Figs. 9.7-9.9), except for α'_g which decreased monotonically for poly(MMA-co-EGDMA). The glass expansivity at 3 % EGDMA could not be accurately determined due to an anomalous contraction below T_g. The expansivities of the two copolymer systems are plotted as a function of EGDMA concentration in Figures 10.7-10.9. The relevant data of poly(HEMA-co-EGDMA) are presented in Table 10.3.

TABLE 10.3

Thermal expansion coefficients (10^{-6} K^{-1}) and free volume fractions of poly(HEMA-co-EGDMA) copolymers

Mole % EGDMA	α'_g	α'_l	$3(\alpha'_l - \alpha'_g)$	V_f (m^3)	f
0	42.1	128.4	258.9	3.59×10^{-9}	0.085
3	-2.8	162.1	351.3	2.53×10^{-9}	0.074
7	49.8	172.7	368.7	1.80×10^{-9}	0.054
24	48.0	163.5	346.5	*	*
100	42.6	152.6	330.0	*	*

* not measured as length contraction was not observed

FIGURE 10.6 PHYSICAL AGEING IN QUENCHED POLY(HEMA-co-EGDMA) COPOLYMERS (numbers adjacent to the curves indicate the mole fraction percentage of EGDMA)

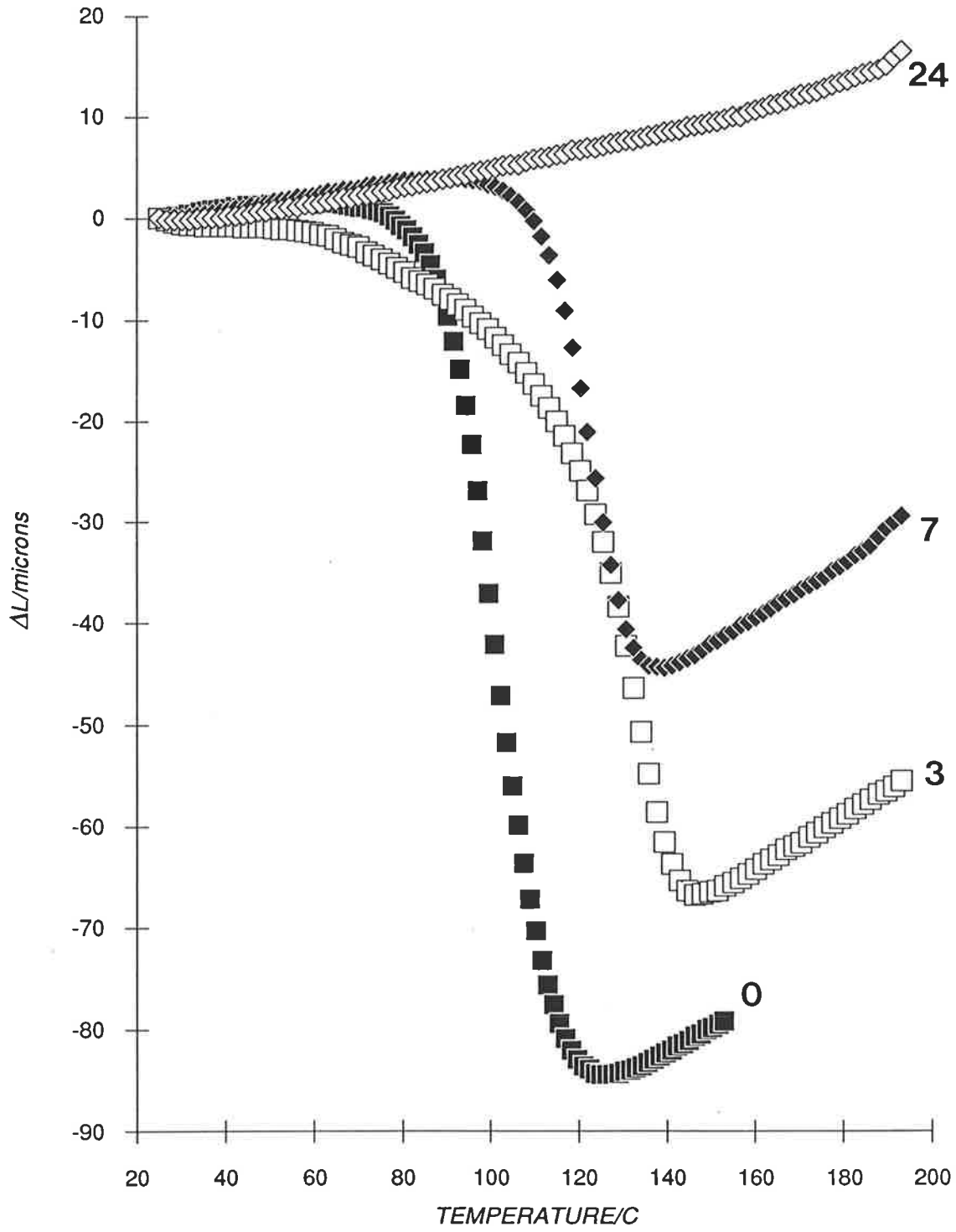

FIGURE 10.7 VARIATION OF GLASS EXPANSIVITY WITH EGDMA CONCENTRATION (the expansivity of -2.8 ppm/K at 3 % EGDMA is not shown for P(HEMA-co-EGDMA))

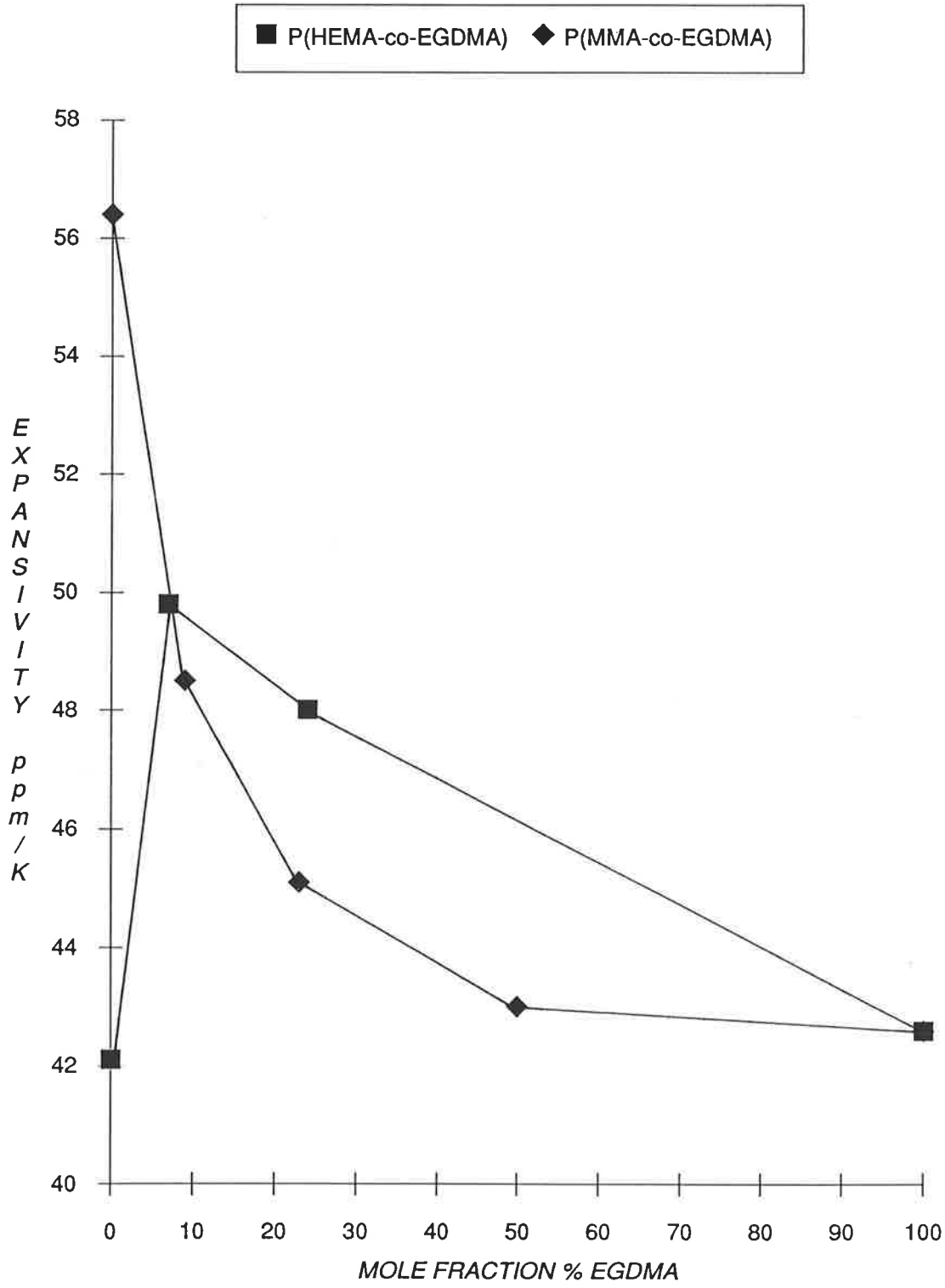

FIGURE 10.8 VARIATION OF LIQUID EXPANSIVITY WITH EGDMA CONCENTRATION

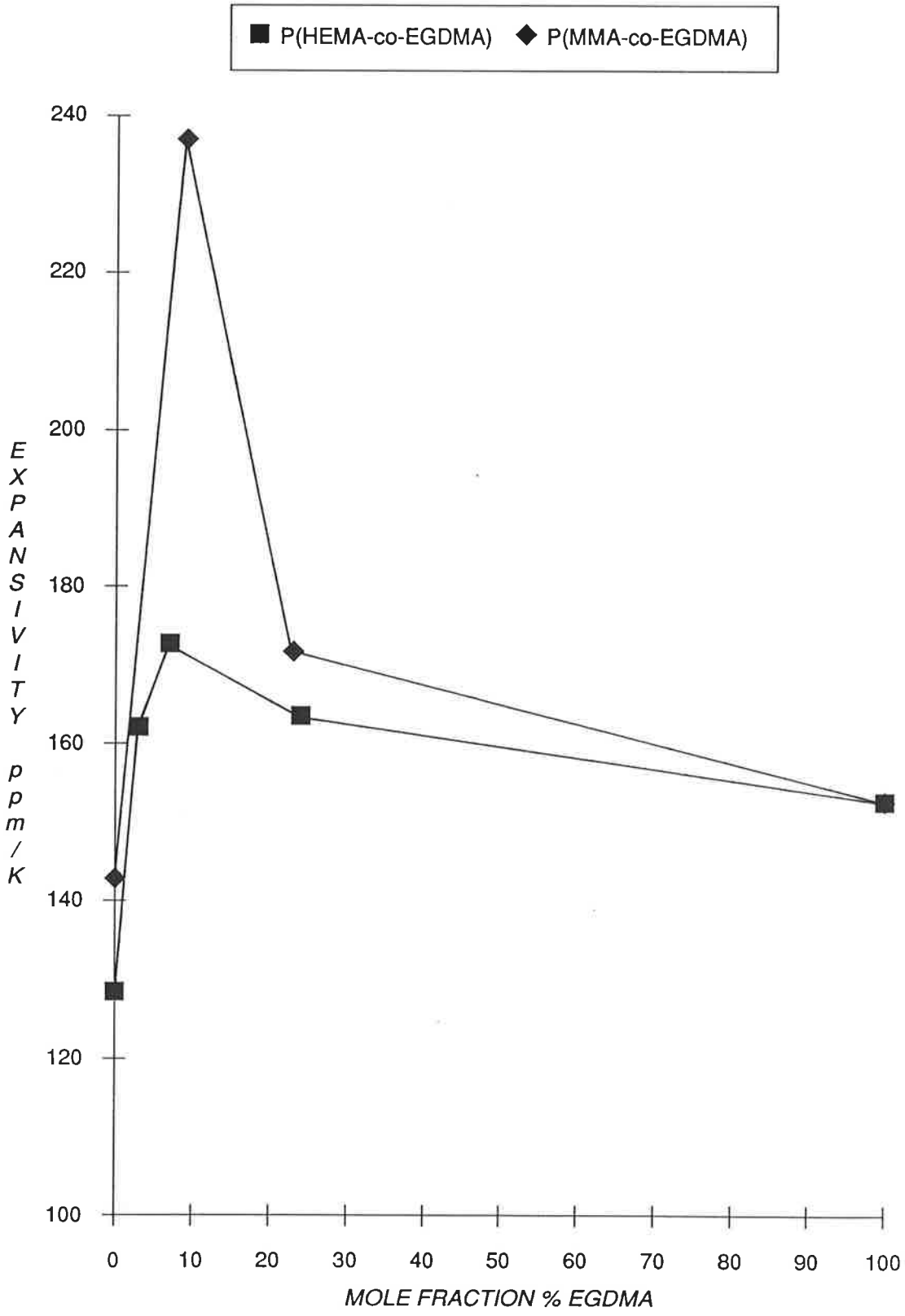

FIGURE 10.9 VARIATION OF FREE VOLUME EXPANSIVITY WITH EGDMA CONCENTRATION

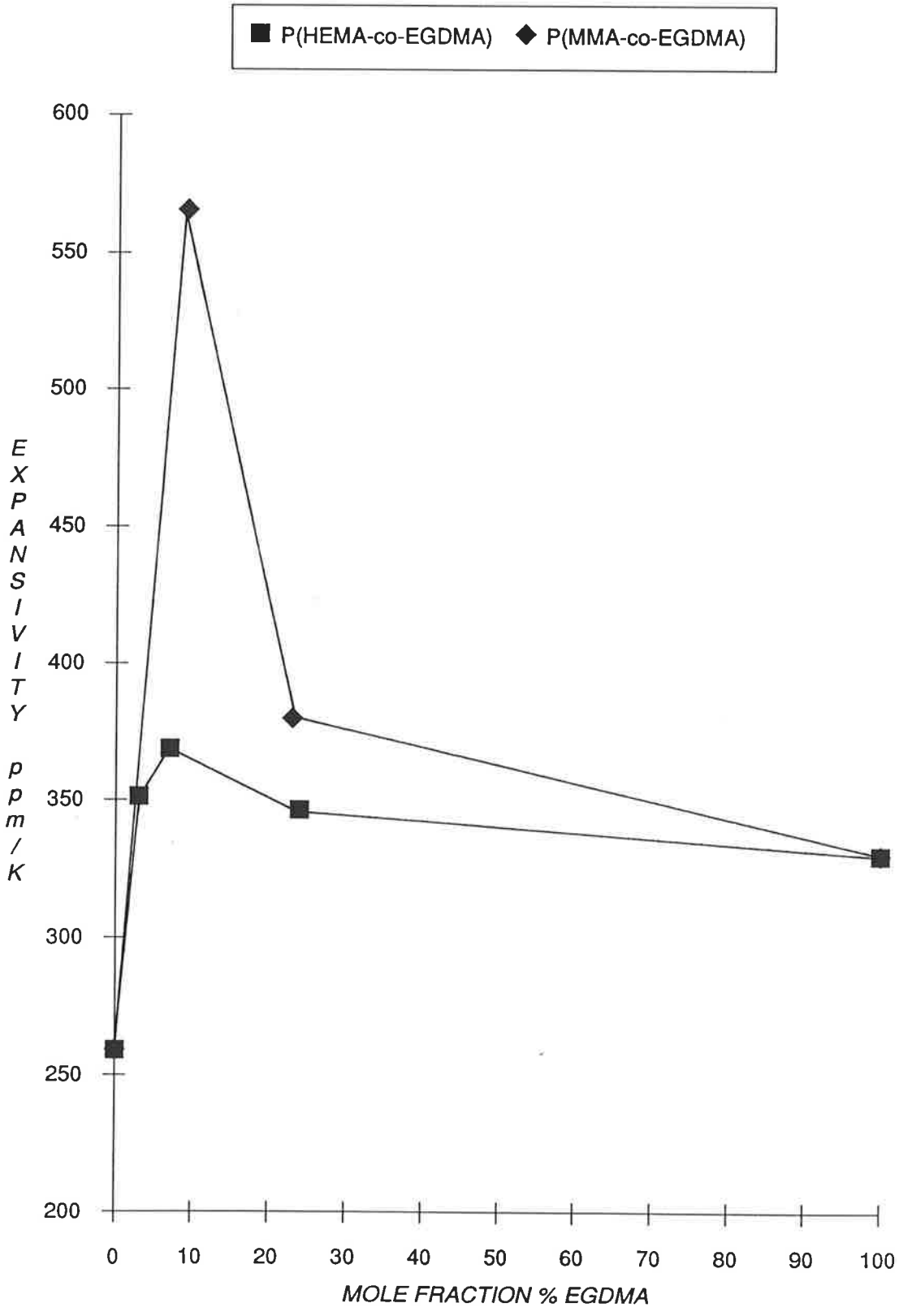

The initial increase in expansivity indicates that the free volume of PHEMA increases with crosslinking at small EGDMA concentrations. This observation is in accordance with the results of Figure 9.8, where α'_g of pure crosslinked poly(dimethacrylates) are observed to have larger values than that obtained for uncrosslinked PMMA.

However, one arrives at a different conclusion if free volume fractions obtained from length contractions are considered (Fig. 10.6 and Table 10.3). It has been acknowledged (Chapter 9) that the reduction in contraction is a consequence of the lowering of segmental mobility with increasing crosslinker concentration, suggesting that the process of physical ageing may be less significant at higher crosslink densities. It is already apparent that the free volume fraction of highly crosslinked specimens (e.g. PEGDMA and PTriEGDMA) cannot be determined with a high degree of accuracy as these specimens exhibit very little contraction. The same problem is also encountered with specimens which undergo viscoelastic deformation above T_g (e.g. highly plasticised PMMA and low-molecular weight PMMA).

Nevertheless, length measurements remain a sensitive technique in which the segmental mobility of a polymer specimen can be monitored. Segmental mobility becomes progressively restricted by the tightening of a crosslinked copolymer network. This is reflected by the decrease in contraction in crosslinked PMMA and PHEMA upon increasing the concentration of EGDMA.

10.3.3 Physical Ageing of Dry PHEMA-KBr Polymers

The ΔL-T plots of PHEMA-KBr polymers (Fig. 10.10) show that length contraction decreases with increasing concentration of KBr. This observation is consistent with the hypothesis [71] that the adsorption of the polymer onto filler molecules restrict segmental motion and increases the T_g of the filled polymer. The increase in T_g is reflected by the increase in the onset and endset temperatures of contraction (T_{on} and T_{end}) with increasing KBr concentration. The liquid expansion coefficient, α'_l, is also observed to increase with KBr concentration, in accordance with the results of Trostyanskaya *et al.* [76]. The relevant data are listed in Table 10.4.

It has been shown [75, 91] that the rate of ageing of filled polymers is generally lowered by the presence of filler and that the enthalpy of relaxation (determined by the area of the DSC endotherm peak on heating from below to above T_g) decreases with increasing filler

FIGURE 10.10 PHYSICAL AGEING OF DRY AND QUENCHED PHEMA WITH DIFFERENT KBr CONCENTRATIONS (wt/wt %)

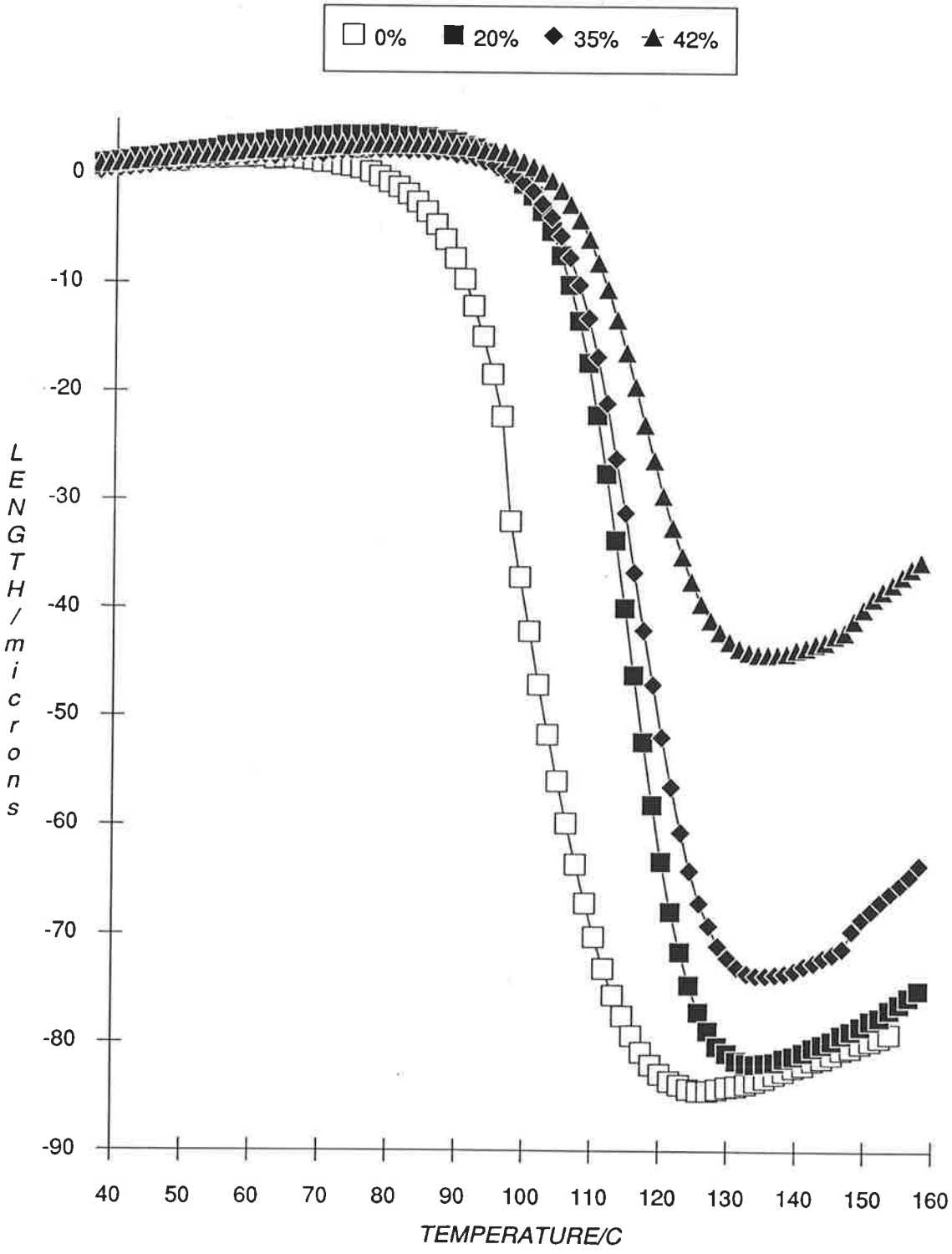

concentration [75]. These observations are supported by the curves in Figure 10.10 which show that length contraction of PHEMA decreases with increasing KBr concentration (Table 10.5). The initial specimen lengths L_z and $L_{x,y}$ of PHEMA and PHEMA-KBr were approximately 1.9029 x 10^{-3} m and 4.90 x 10^{-3} m respectively. It is suggested that the restricted mobility of polymer segments in PHEMA-KBr result in the the collapse of a smaller free volume fraction leading to lower values of ΔL_z. This suggestion implies that the remaining free volume fraction which has not been annihilated by ageing can facilitate cooperative segmental motion and thus account for the large values of α'_l.

TABLE 10.4

Thermal expansion coefficients (10^{-6} K^{-1}) and onset and endset temperatures of contraction of PHEMA-KBr polymers

[KBr] (g/g %)	α'_g	α'_l	T_{on} (C)	T_{end} (C)
0	42.1	128.4	88	114
2.0	44.1	253.1	103	126
3.5	40.7	332.3	105	128
4.2	44.0	341.8	105	129

TABLE 10.5

Length contraction and free volume fractions of PHEMA and PHEMA-KBr polymers

[KBr] (g/g %)	ΔL_z (10^{-6} K^{-1})	V_f (m^3)	f
0	86.1	3.59 x 10^{-9}	0.085
20	85.6	3.57 x 10^{-9}	0.084
35	76.1	3.18 x 10^{-9}	0.075
42	47.1	1.98 x 10^{-9}	0.045

Table 10.4 shows that the introduction of KBr ions into PHEMA had resulted in a shift in the contraction range of about +15 C but the temperature range of contraction, T_{end} - T_{on}, remained relatively unchanged at 23-26 C. These observations suggest that the

distribution of free volume in PHEMA had not been altered by the KBr ions. The shift of T_{on} and T_{end} to higher temperatures is consistent with Struik's [67] observation that filled polymers have been shown to age at temperatures above the T_g of the unfilled polymer. The similar values of α'_g of PHEMA and PHEMA-KBr polymers supports the suggestion that the KBr ions had little effect on the free volume fraction of PHEMA.

10.4 SUMMARY

(1) Preliminary studies on dimensional changes of hydrated PHEMA suggested that these changes were influenced both by the amount of water absorbed by the polymer and by the length of time at which the water was resident in the polymer network. A bi-partite model was used to describe the distribution of water in PHEMA, in which unbound water occupied voids while bound water formed hydrogen bonds with the polymer.

(2) Physical ageing of PHEMA-KBr polymers indicated that the onset and endset temperatures of contraction of PHEMA had been increased by the presence of KBr. However, the temperature range of contraction was found to be similar for filled and unfilled PHEMA hence it was assumed that the KBr ions had little effect on the magnitude and distribution of free volume of PHEMA.

(3) It was observed that length contraction of PHEMA-KBr decreased with increasing KBr concentration. The decrease in contraction in filled PHEMA was attributed to the lower segmental mobility as a result of polymer-filler interactions. This proposal suggested that the presence of unaged free volume in PHEMA facilitated cooperative motion above T_g which accounted for unusually large values of α'_l.

Chapter 10

1. P.H. Corkhill, A.M. Jolly, C.O. Ng and B.J. Tighe, *Polymer* **28**, 1758 (1987).
2. S.M. Aharoni and S.F. Edwards, *Macromolecules* **22**, 3361 (1989).
3. O. Wichterle and D. Lim, *Nature* **185**, 117 (1960).
4. O. Wichterle and D. Lim, *U.S. Patents* 2 976 576 (1961); 3 220 960 (1965).
5. M.F. Refojo and H.J. Yasuda, *J. Appl. Polym. Sci.* **9**, 2425 (1965).

6. H.J. Yasuda, M. Gichin and W. Stone Jr., *J. Polym. Sci. Polym. Phys. Ed.* **4**, 2913 (1966).

7. M.F. Refojo, *J. Polym. Sci. Polym. Chem. Ed.* **5**, 3103 (1967).

8. M. Illasky and W. Prins, *Macromolecules* **3**, 415 (1970).

9. J.H. Gouda, K. Provodator, T.C. Warren and W. Prins, *J. Polym. Sci.* **B8**, 225 (1970).

10. K. Dusek and B. Sedlacek, *Eur. Polym. J.* **7**, 1275 (1971).

11. B.D. Ratner and I.F. Miller, *J. Polym. Sci. Polym. Chem. Ed.* **10**, 2425 (1972).

12. H.B. Lee, M.S. Jhon and J.D. Andrade, *J. Coll. Interface Sci.* **51**, 225 (1975).

13. D.G. Pedley and B.J. Tighe, *Br. Polym. J.* **11**, 130 (1979).

14. S.P. Rowland ed., *Water in Polymers, ACS Symposium Series* **127**, (1980).

15. J.H. Collett, D.E.M. Spillane and E.J. Pywell, *Polym. Prepr.* **28**, 141 (1987).

16. S. Sevcik, J. Stamberg and P. Schmidt, *J. Polym. Sci.* **C16**, 821 (1967).

17. J. Stamberg and S. Sevcik, *Coll. Czech. Chem. Comm.* **31**, 1009 (1966).

18. D.G. Pedley, P.J. Skelley and B.J. Tighe, *Br. Polym. J.* **12**, 99 (1980).

19. B.J. Tighe, *Contact Lenses,* A. Phillips and J. Stone eds., Vol **2**, Butterworth, London (1980), 2nd Ed. p377.

20. J.R. Larke and B.J. Tighe, *British Patent* 1 395 501 (1975).

21. J.R. Larke, D.G. Pedley and B.J. Tighe, *British Patent* 1 478 455 (1977).

22. J.R. Larke, D.G. Pedley and B.J. Tighe, *British Patent* 1 500 692 (1978).

23. A.S. Hoffman, T.A. Horbett and B.D. Ratner, *Ann. N. Y. Acad. Sci.* **283**, 372 (1977).

24. T. Nakashima, K. Takakura and Y. Komoto, *J. Biomed. Mater. Res.* **11**, 787 (1977).

25. T.A. Jadwin, A.S. Hoffman and W.R. Vieth, *J. Appl. Polym. Sci.* **14**, 1339 (1970).

26. J. Kopecek and J. Vacik, *Coll. Czech. Chem. Comm.* **38**, 854 (1973).

27. A.S. Hoffman, M. Modell and P. Pan, *J. Appl. Polym. Sci.* **14**, 285 (1970).

28. J. Vacik, M. Czakora, J. Exner, J. Kalal and J. Kopecek, *Coll. Czech. Chem. Comm.* **42**, 2786 (1977).

29. J. Kopecek, J. Vacik and D. Lim, *J. Polym. Sci. A-1* **9**, 2801 (1971).

30. M. Tollar, M. Stol and K. Kliment, *J. Biomed. Mater. Res.* **3**, 305 (1969).

31. J.N. LaGuerre, H. Kay, S.M. Lazarus, W.S. Calem, S.R. Weinberg and B.S. Levowitz, *Surg. Forum* **19**, 522 (1968).

32. S.M. Lazarus, J.N. LaGuerre, H. Kay, S.R. Weinberg and B.S. Levowitz, *J. Biomed. Mater. Res.* **5**, 129 (1971).

33. G.M. Zenter, J.R. Cardinal and S.W. Kim, *J. Pharm. Sci.* **67**, 1347, 1352 (1978).

34. R. Langer and J. Folkman, *Nature* **263**, 797 (1976).

35. J.D. Andrade ed., *Hydrogels for Medical and Related Applications, ACS Symposium Series* **31**, (1976).

36. W. Heitz, W. Krappitz, C. Stutzel-Bilbao and B. Neumann, *Angew. Makromol. Chem.* **123/124**, 147 (1984).

37. M. Rosenberg, P. Bartl and J. Lesko, *J. Ultrastruc. Res.* **4**, 298 (1960).

38. L. Allen, *Polym. Prepr.* **15**, 395 (1974).

39. B.D. Ratner and A.S. Hoffman, in reference 35, p1.

40. C.E. Gregonis, C.M. Shen and J.D. Andrade, in reference 35, p88.

41. Y. Taniguchi and S. Horigome, *J. Appl. Polym. Sci.* **19**, 706 (1975).

42. M.N. Sarbolouki, *J. Appl. Polym. Sci.* **17**, 2407 (1973).

43. A. Higuchi and T. Iijima, *Polymer* **26**, 1833 (1985).

44. R.E. Dehl, *Science* **170**, 738 (1970).

45. J. Kolarik and J. Janecek, *J. Polym. Sci. A-2* **10**, 11 (1972).

46. J. Kolarik, *Adv. Polym. Sci.* **46**, 119 (1982).

47. M.S. Jhon and J.D. Andrade, *J. Biomed. Mater. Res.* **7**, 509 (1973).

48. H. Yasuda, H.G. Olf, C.E. Lamaze and A. Peterlin, *Water Structure at The Water-Polymer Interface,* H.H.G. Jellinik ed., Plenum Press, New York (1975), p39.

49. S. Krishnamurthy, D. McIntyre, E.R. Santee and C.W. Wilson, *J. Polym. Sci. Polym. Phys. Ed.* **11**, 427 (1973).

50. Y.K. Sung, D.E. Gregonis, M.S. Jhon and J.D. Andrade, *J. Appl. Polym. Sci.* **26**, 3719 (1981).

51. K. Nakamura, T. Hatakeyama and H. Hatakeyama, *Polymer* **24**, 871 (1983).

52. T. Hatakeyama, A. Yamauchi and H. Hatakeyama, *Eur. Polym. J.* **20**, 61 (1984).

53. M. Frommer, M. Shporer and R. Messalem, *J. Appl. Polym. Sci.* **17**, 2263 (1973).

54. M. Shporer and M. Frommer, *J. Macromol. Sci. Phys.* **B10**, 529 (1974).

55. M. Frommer and D. Lancet, *J. Appl. Polym. Sci.* **16**, 1295 (1972).

56. R.A. Nelson, *J. Appl. Polym. Sci.* **21**, 645 (1977).

57. M. Froix and R.A. Nelson, *Macromolecules* **8**, 726 (1975).

58. G. Smyth, F.X. Quinn and W.J. McBrierty, *Macromolecules* **21**, 3198-3204 (1988).

59. S.W. Kim, J.R. Cardinal, S. Wisniewski and G.M. Zentner, in reference 14, p347.

60. J. Janecek and J. Hasa, *Coll. Czech. Chem. Comm.* **31**, 2186 (1966).

61. P.E.M. Allen, D.J. Bennett and D.R.G. Williams, *Eur. Polym. J.* **28(4)**, 347 (1992).

62. P.E.M. Allen, D.J. Bennett and D.R.G. Williams, *Water in Methacrylates: II Dynamic Mechanical Properties of Swollen (2-Hydroxyethyl Methacrylate-co-Glycol Dimethacrylate) Networks,* submitted for publication, *Eur. Polym. J.* (1992).

63. P.E.M. Allen, D.J. Bennett and D.R.G. Williams, *Water in Methacrylates: IV Structures and Organisation in Poly(2-Hydroxyethyl Methacrylate-co-Glycol Dimethacrylate) Networks,* submitted for publication, *Eur. Polym. J.* (1992).

64. E.S.W. Kong, *Adv. Polym. Sci.* **80**, 126 (1986).

65. D.T. Turner, *Polymer* **23**, 197 (1982).

66. R.J. Young and P.W. Beaumont, *J. Mat. Sci.* **11**, 777 (1976).

67. L.C.E. Struik, *Physical Ageing in Amorphous Polymers and Other Materials,* Elsevier, Amsterdam (1978).

68. I.N. Razinskaya, B.P. Shtarkman, V.A. Izvokchik, N.Y. Averbakh and I.M. Monich, *Vysokomol. Soyed.* **A26(8)**, 1617 (1984).

69. J. Shen, C.C. Chen and J.A. Sauer, *Abracts IUPAC,* Macro '85, *Structure and Properties,* Bucharest (1984), Section 4, p279.

70. P.E.M. Allen, S. Hagias, G.P. Simon, E.H. Williams and D.R.G. Williams, *Polym. Bull.* **15**, 359-362 (1986).

71. G.J. Howard and R.A. Shanks, *J. Appl. Polym, Sci.* **26**, 3099-3102 (1981).

72. G.J. Howard and R.A. Shanks, *J. Macromol. Sci. Phys.* **B19**, 167 (1981).

73. G.J. Howard and R.A. Shanks, *J. Macromol. Sci. Chem.* **A17**, 287 (1982).

74. R.A. Shanks, *Polym. Prepr.* **25**, 134 (1984).

75. R.A. Shanks, *Br. Polym. J.* **18(2)**, 75 (1986).

76. E.B. Trostyanskaya, A.M. Poimanov, E.F. Nosov and A.R. Belnik, Translated from *Mekh. Polim.* **6**, 1018 (1969).

77. P. Peyser and W.D. Bascom, *J. Macromol. Sci. Phys.* **B13**, 597 (1977).

78. S. Hagias, Unpublished results.

79. G.F. Cowperthwaite, J.J. Foy and M.A. Malloy, *Biomedical and Dental Applications of Polymers,* C.G. Geblen and F.F. Koblitz eds., Plenum Press, New York (1981), p387.

80. D.J. Bennett, *Ph.D. Thesis,* University of Adelaide, South Australia (1991).

81. *Chemical Engineers Handbook,* J. Perry ed., McGraw-Hill, New York (1934).

82. *Handbook of Chemistry and Physics,* R.C. Weast and S.M. Selby eds., The Chemical Rubber Company, Ohio (1966).

83. L.S.A. Smith and V. Schmitz, *Polymer* **29**, 1871 (1988).

84. P.E.M. Allen, G.P. Simon, D.R.G. Williams and E.H. Williams, *Macromolecules* **22**, 809 (1989).

85. P.E.M. Allen, D.J. Bennett, S. Hagias, A.M. Hounslow, G. Ross, G.P. Simon, D.R.G. Williams and E.H. Williams, *Eur. Polym. J.* **25**, 785 (1989).

86. C.E. Browning, *Polym. Eng. Sci.* **18**, 16 (1978).

87. R.J. Morgan, J.E. O'Neal and D.L. Fanter, *J. Mater. Sci.* **15**, 751 (1980).

88. W.W. Wright, *Composites* **12**, 201 (1981).

89. T.S. Ellis and F.E. Karasz, *Polymer* **25**, 644 (1984).

90. L.W. Jelinski, J.J. Dumais, R.E. Stark, T.S. Ellis and F.E. Karasz, *Macromolecules* **16**, 1019 (1983).

91. Y. Long and R.A. Shanks, *Proceedings of the Asia Pacific Composites Congress,* Adelaide, June (1989), p1.

GLOSSARY OF SYMBOLS

α'_g	Linear Glass Expansion Coefficient
α'_l	Linear Liquid Expansion Coefficient
EWC	Equilibrium Water Content
f	Free Volume Fraction
L_z, $L_{x,y}$	Initial Specimen Lengths
ΔL_z	Length Change
RH	Relative Humidity
T_g	Glass Transition Temperature
T_{on}	Onset Temperature of Contraction
T_{end}	Endset Temperature of Contraction
V_f	Free Volume
W	Wet Weight Measured at 25 C
W_0	Dry Weight Measured at 25 C
WC	Water Content

CHAPTER 11
EFFECT OF SUBSTITUENTS ON PHYSICAL AGEING OF ACRYLATE POLYMERS

11.1 INTRODUCTION 216

11.2 EXPERIMENTAL 217

11.3 RESULTS AND DISCUSSION

11.3.1 Length Contraction 217

11.3.2 Thermal Expansion Coefficient 220

11.4 SUMMARY 222

BIBLIOGRAPHY 223

CHAPTER 11

11.1 INTRODUCTION

It was first observed by Rogers and Mandelkern [1] in 1957 that the glass and liquid expansion coefficients (α_g and α_l) of a series of poly(*n*-alkyl methacrylates) increased with increasing length of the ester side-chain. A few years later, Simha and Boyer [2] (SB) derived two emprirical equations which related the free volume fraction to α_g and α_l, viz. $\alpha_l.T_g = 0.164$ and $(\alpha_l - \alpha_g).T_g = 0.113$. These equations were found to be tolerably well-obeyed by most polymers studied in reference [2], but the latter equation was found to fail with the poly(*n*-alkyl methacrylates) series. This was also found to be the case with other polymer systems with long flexible side chains, such as poly(*n*-alkyl acrylates) [3-4], poly(vinyl-*n*-alkyl ethers) [5-6] and poly(α-olefins) [7].

Poly(alkyl methacrylates) have been found [8-12] to exhibit transitions at cryogenic temperatures (~-100 C) below T_g. Sub-T_g transitions have likewise been observed for a number of polymer systems with flexible side chains [13-14]. Simha and Boyer [2] proposed that the side chains retained excess free volume on cooling below T_g, leading to unusually high values of α_g. It was further proposed that the relevant free volume quantity should be $(\alpha_l - \alpha_g').T_g$, where $\alpha_g' \leq \alpha_g$ is the expansion coefficient below the low temperature transition. The incorporation of α_g' was found [6, 11] to restore the free volume fractions of homologous polymer series to values close to the "universal" free volume fraction of 0.113. The SB [2] proposal appears to be well-accepted since recent publications alluding to the effect of side groups on the fractional free volume of polymers could not be found. The effect of side chains appears to be similar to that of chain ends, where free volume may be generated by the freezing of chain end motion [15-16].

The purpose of this chapter is to present a study of the effect of side groups on the free volume and physical ageing behaviour of a number of linear amorphous acrylate polymers. The side groups were varied in length, ranging from poly(methyl acrylate) to poly(benzyl methacrylate), and polarity, e.g. poly(2-hydroxyethyl methacrylate). Free volume fractions were determined from measurements of length contraction and were used to examine the results of Simha *et al.* [2, 11].

11.2 EXPERIMENTAL

The casting of polymers are described in the experimental section of Chapter 3. The abbreviations of systematic names of polymers are also listed in Chapter 3. The polymers which were investigated were PMA, PMMA, PEMA, PIBMA, PBzylMA and PHEMA.

A preliminary heating run was performed on as-cast specimens to determine the temperature range of interest. The polymer specimens were thermally equilibrated at *ca* 40-50 C above the onset temperature of contraction for 15-20 minutes and then quenched in liquid nitrogen for 10 minutes. Specimens which required subambient starting temperatures (e.g. PIBMA and PBzylMA) were quickly transferred to the thermomechanical analyser (TMA) to prevent any uptake of moisture. The TMA was programmed to maintain a constant subambient temperature, such that the quenched specimen was allowed to warm to the starting temperature with minimal ageing taking place. Polymer specimens which do not require subambient starting temperatures (e.g. PMMA, PHEMA) were allowed to warm to room temperature (22 C) inside a dessicator.

A period of 20 minutes [17] was allowed to elapse after quenching to minimise any irreproducibility which may occur as a result of cooling stresses [18-19]. The TMA was continually flushed with high-purity nitrogen gas which maintained a dry and inert environment throughout the experiment. The specimens were heated at a constant rate of 2 C/min under a static applied load of 0.1 N.

11.3 RESULTS AND DISCUSSION

11.3.1 Length Contraction

The ΔL-T plots of the six quenched polymers are shown in Figures 11.1-11.2. Figure 11.1 shows that the magnitude of length contraction increases in the following order: PHEMA < PMMA < PEMA << PMA. The absence of the α-methyl group in PMA yields a larger free volume fraction of 0.259 than the value of 0.109 obtained for PMMA (Table 11.1), suggesting that the macromolecular chains of PMA occupy greater volume at equilibrium. The larger frozen-in free volume fraction of quenched PMA is also reflected by large values of thermal expansivities (α'_g = 270 x 10^{-6} K^{-1} and α'_l = 560 x 10^{-6} K^{-1} [21]) (Table 11.2).

FIGURE 11.1 PHYSICAL AGEING OF QUENCHED ACRYLATE POLYMERS

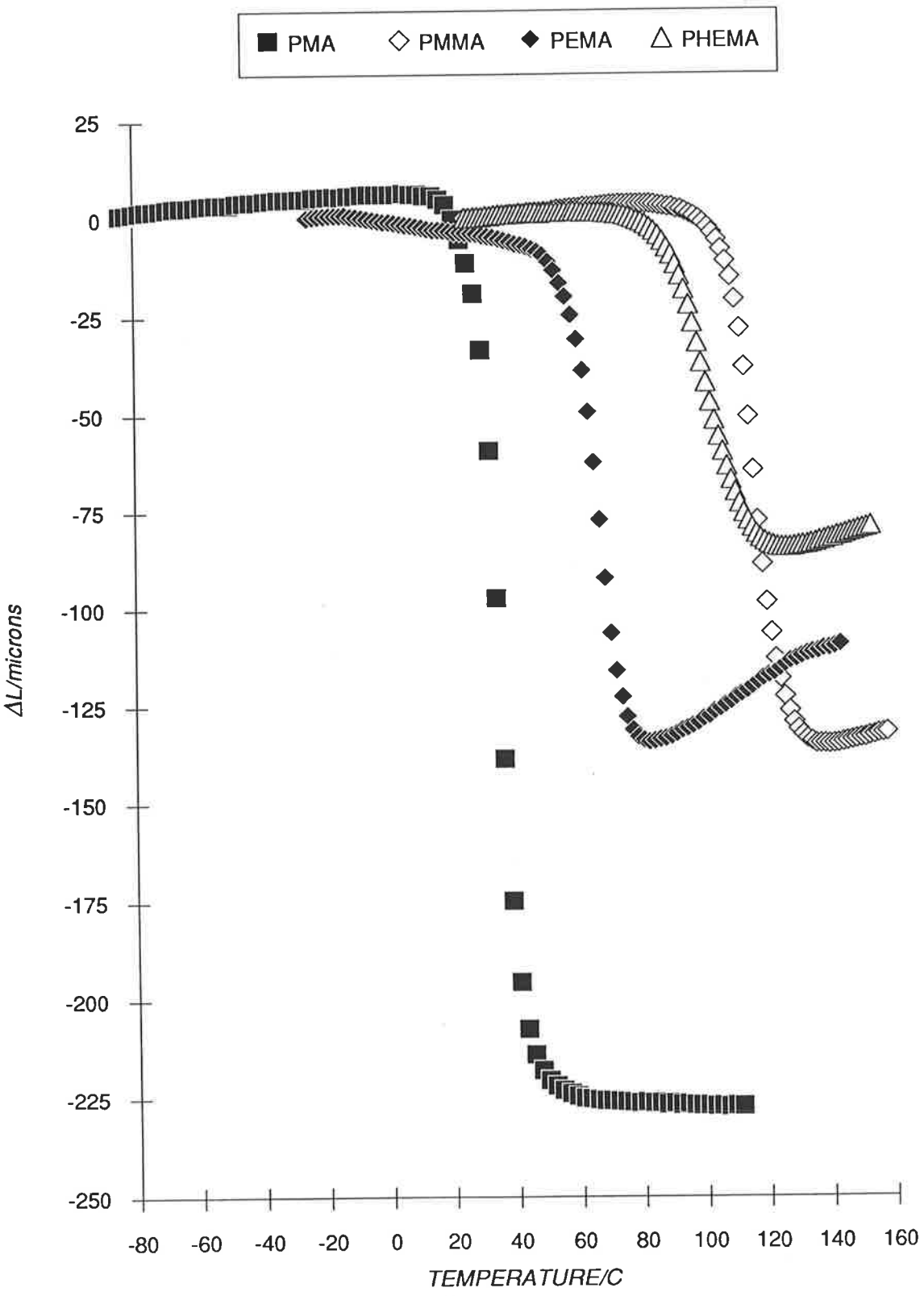

FIGURE 11.2 PHYSICAL AGEING OF QUENCHED ACRYLATE POLYMERS

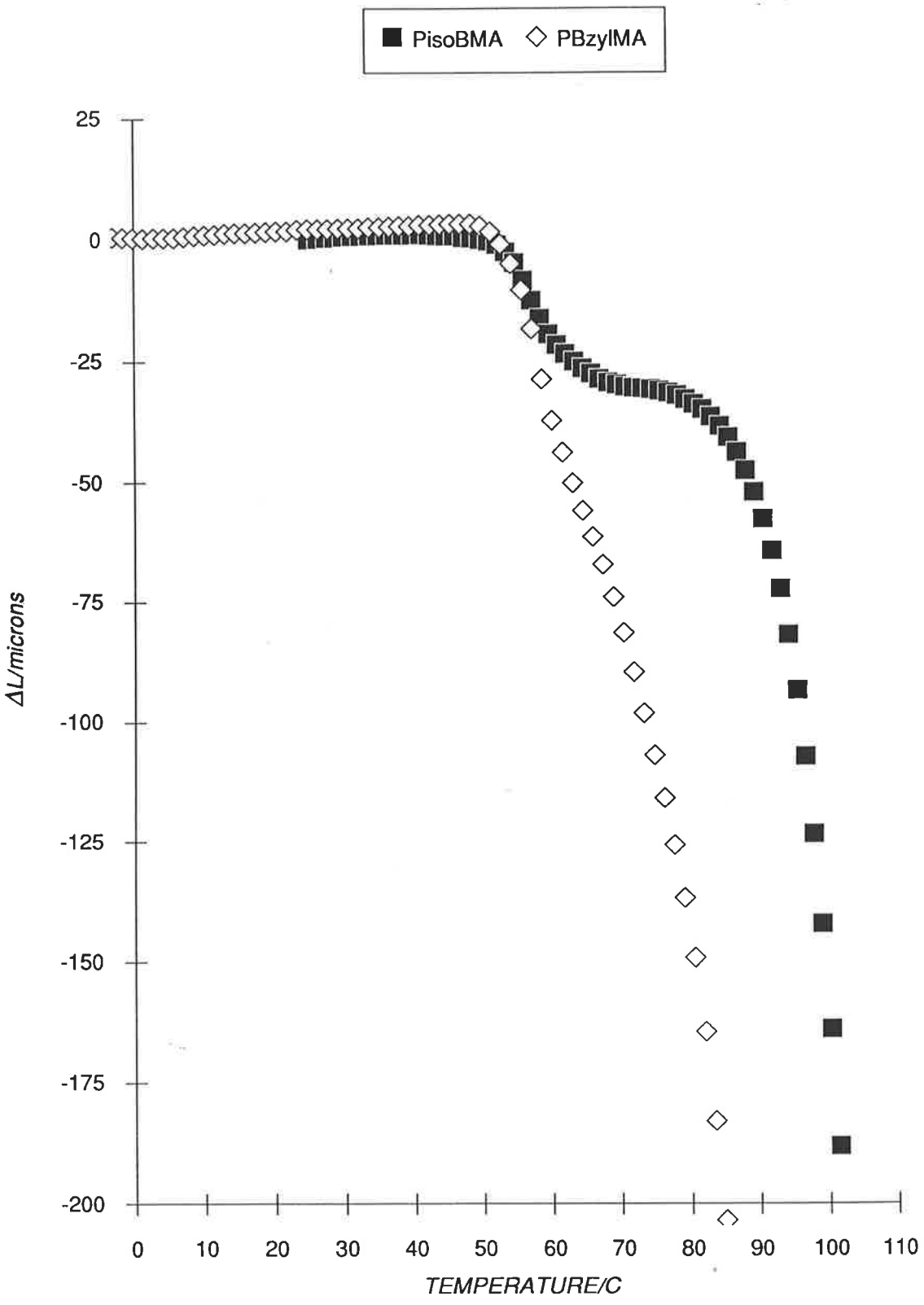

These observations are related to the fact that the α-methyl group on the backbone chain is known [9, 30] to cause significant differences in the molecular mobility of polymethacrylates and polyacrylates. Molecular mechanics calculations [31-32] have shown that the presence of the α-methyl group causes a three-fold increase in the energy barrier to rotation of the ester side group, that is, α-methyl groups of adjacent repeating units hinder the rotation of the $-COOCH_3$ in PMMA [33-35]. In addition, mechanical relaxation studies of copolymers of methyl acrylate and methyl methacrylate [35-36] have shown that the α-relaxation shifts to shorter times as the proportion of MA in the copolymer increases, suggesting that the incorporation of the more flexible acrylate units into the methacrylate chain increases the chain mobility of the copolymer [9]. Therefore, it may be concluded that the lack of steric hindrance and the flexible polymer chains of PMA facilitates the process of ageing to a greater extent than in PMMA.

The lengthening the ester side-group by one CH_2 unit from PMMA to PEMA also results in a slight increase in free volume fraction from 0.109 to 0.139 for PEMA. It is suggested that a larger free volume fraction is generated by the freezing-in of the motion of the larger $-OOCCH_2CH_3$ side-group of PEMA than the $-OOCCH_3$ group of PMMA. This suggestion is consistent with the hypothesis [2, 11] that the amount of free volume trapped by the freezing-in of side-chain motion increases with the length of the side-chain. On the other hand, a comparison of the free volume fractions of PMA, PMMA and PEMA suggests that the main-chain α-substituent has a greater effect on the free volume that the substituents on the ester group. It is disappointing that PIBMA and PBzylMA undergo viscous flow above 50 C (T_g of both polymers are approximately 54 C [25]), which does not permit measurement of free volume of these polymers.

The addition of a hydroxy group to the ester moiety of PEMA is expected to yield a free volume fraction which is similar to that observed for PEMA. However, as a consequence of strong intramolecular hydrogen bonding, segmental mobility in PHEMA is restricted, thus resulting in a lower free volume fraction of 0.085 for quenched dry PHEMA. The T_g of PHEMA (86 C [11]) is also observed to be higher than for the corresponding alkyl polymer, poly(*n*-propyl methacrylate) (35 C [11]). In addition, α'_l of PHEMA is found to be lower (128×10^{-6} K^{-1}) than the values obtained for PMMA and PEMA (Table 11.2), suggesting that the expansion at equilibrium is lower for PHEMA than for polymers containing side groups of

similar size. It follows that the quenching of PHEMA from equilibrium to below T_g will freeze-in a smaller free volume.

TABLE 11.1

Transition temperatures and free volume fractions of acrylate polymers

Polymer	T_{on} (C)	T_g (C)	f	$3(\Delta\alpha.T_g)$
PMMA	104	105 [22]	0.109	0.093-0.120 [22-23]
PMA	30	9 [20-21]	0.259	0.082-0.101 [20-21]
PEMA	54	64 [11]	0.139	0.067-0.100 [1, 21]
PHEMA	88	86 [11]	0.085	0.037-0.052 [11, 24]
PIBMA	53	54 [11]	not measured	0.060-0.109 [1, 21]
PBzylMA	52	54 [25]	not measured	not available

However, with the exception of PMMA, Table 11.1 shows that literature values of free volume fraction obtained according to the SB equation are lower than the values obtained by length contraction. It has been admitted [2, 11] that the use of α'_g in the SB equation to measure the free volume fraction may produce unacceptably low values with polymers containing flexible side chains. It was mentioned in Chapter 1 that the lengthy experimental timescale involved in volume dilatometry may cause the specimen to age inside the dilatometer which leads to a lower free volume. A second explanation for the discrepancy is that the calculation of fractional free volumes using the SB equation involves the use of the thermal expansivities and T_g, which is normally taken to be the intersection of the glass and liquid lines of a V-T or L-T plot. The value of α_g has been known [2, 11] to be susceptible to changes in free volume fraction, in which an increase in free volume (e.g. generated by the freezing of side-chain motion) results in a corresponding increase in α_g. The assignment of T_g from V-T plots has been criticised by a number of authors [26-28] as to whether it is capable of reflecting the true physical meaning of the observed glass-rubber transition phenomena. Physical ageing of quenched polymers show a distinct length contraction in the glass transition region which does not allow the conventional assignment of T_g. In addition, the presence of a large free volume fraction facilitates segmental motion [29] which consequently lowers the T_g, for

example, T_g of PMMA is 105 C [22] whereas T_g of PMA decreases to 9 C [20-21]. Hence, the incorporation of T_g = 9 C for PMA yields a free volume fraction of only 0.082-0.101 [20-21], which contradicts the free volume theory [29] that a smaller free volume fraction will increase T_g. This example illustrates the inability of the SB equation to predict free volume changes in polymers.

The values of the onset temperature of contraction, T_{on}, are observed to compare favourably with literature values of T_g for the polymers listed in Table 11.1. This observation suggests that the onset of segmental motion responsible in the glass transition may be adequately represented by T_{on}. However, T_{on} of PMA (30 C) is about 20 C higher than its T_g of 9 C [20-21]. It is possible that the measurement of T_g may have been performed by volume dilatometry, which suggests that the ageing of the specimen during the experiment (as a result of the slow rate of heating in volume dilatometry) would yield a lower T_g.

The T_{on} of PEMA is observed at 54 C, which is in reasonable agreement with its T_g of 64 C [11]. Good correlation between T_{on} and literature values of T_g are also observed for PIBMA, PBzylMA and PHEMA. The origin and effects of *internal plasticisation* [9] has been discussed in Section 2.3.9, in which T_g of poly(*n*-alkyl methacrylates) decreases with increasing length of the *n*-alkyl side chain [2, 9, 11]. However, the presence of a bulky *iso*-butyl or a benzyl group causes an increase in T_g as the shorter and more rigid *iso*-butyl and benzyl groups are less effective at internal plasticisation, e.g. T_g of poly(*n*-butyl methacrylate) is only 19 C [21], while T_g of PIBMA is 54 C [11]. The high T_g (88 C) of PHEMA is attributed to the restricted mobility as a result of strong intramolecular hydrogen bonding.

11.3.2 Thermal Expansion Coefficient

The linear thermal expansivities, α'_g and α'_l, of the polymers are presented in Table 11.2 along with their respective T_{on}'s and free volume fractions. These values are compared with the results of Haldon and Simha [11] shown in Table 11.3. Data for PMA is taken from Fujita and Maekewa [20], while data for PBzylMA is not available.

Significant differences between experimental values and the values of Haldon and Simha [11] are observed for PEMA. Figure 11.1 showa an inexplicably low thermal expansion below T_g for PEMA, which lends justification to Haldon and Simha's value of 114 x 10^{-6} K^{-1} as a more appropriate value of α'_g for PEMA. However, no explanation could be offered at the

present time for the large difference between values of α'_l. A discrepancy in α'_g is also observed for PHEMA, although the values of α'_l are in good agreement. It is not fully understood why the literature value of 92 x 10^{-6} K^{-1} is twice as large as the experimental value of 42.1 x 10^{-6} K^{-1}.

TABLE 11.2

Thermal expansion coefficients (10^{-6} K^{-1}) of acrylate polymers

Polymer	α'_g	α'_l	$3(\alpha'_l - \alpha'_g)$	T_{on} (C)	f
PMA	74.5	196.8	366.9	30	0.259
PMMA	56.4	142.8	259.2	104	0.109
PEMA	47.2	289.9	728.1	54	0.139
PHEMA	42.1	128.4	258.9	88	0.085
PIBMA	105.0	not measured	not measured	53	not measured
PBzylMA	170.0	not measured	not measured	52	not measured

TABLE 11.3

Thermal expansivities (10^{-6} K^{-1}) of acrylate polymers obtained by Haldon and Simha [11]

Polymer	α'_g	α'_l	$3(\alpha'_l - \alpha'_g)$	T_g (C)	$3(\Delta\alpha.T_g)$
PMA [20]	90	187	291	9	0.082
PMMA	75	160	255	105	0.096
PEMA	114	180	198	64	0.067
PHEMA	92	126	102	86	0.037
PIBMA	134	195	183	54	0.060

A number of trends may be derived from the experimental values of Table 11.1 and 11.2. T_{on} decreases in magnitude according to the sequence: PMMA > PHEMA > PEMA ≈ PIBMA ≈ PBzylMA >> PMA, while the free volume fraction decreases according to: PMA > PEMA > PMMA > PHEMA. α'_g decreases from PBzylMA > PIBMA > PMA > PMMA > PEMA > PHEMA.

The low values of α'_g and f and the corresponding high T_{on} and T_g of PHEMA has already been attributed to intramolecular hydrogen bonding. The variation in α'_g appears to be consistent with the hypothesis that the magnitude of the glass expansivity reflects the free volume fraction existing in the polymer [11]. However, it has been noted that α'_g of PEMA is unusually low, as α'_g of PEMA would be expected to lie between the values of PMA and PMMA. The decrease in T_{on} with increasing free volume fraction suggests that segmental mobility is facilitated by the free volume available for cooperative motion. This result supports Struik's [29, 37] assertion that molecular mobility is essentially controlled by the free volume. Although only a limited number of acrylate polymers have been tested, measurements of length contraction appear to provide a sensitive indicator of the effect of the α- and ester side groups substituents on the free volume fraction.

11.4 SUMMARY

(1) The thermal expansion behaviour of a number of acrylate polymers have been investigated by measurements of linear dimensional changes. The onset temperature of contraction, free volume fraction and thermal expansivities of these polymers were measured and compared with the work of Simha *et al.* [2, 11].

(2) A good correlation between T_{on} and literature values of T_g was generally observed for all polymers. This observation suggested that the onset of the glass-rubber transition may be adequately represented by T_{on}.

(3) The free volume fractions obtained from length contraction were observed to be greater than the values obtained using the SB equation $f = 3(\alpha'_l - \alpha'_g).T_g$. The lower values obtained by the SB equation were due to the fact that polymers with flexible side chains retain excess free volume leading to large values of α'_g and thus small values of $(\alpha'_l - \alpha'_g)$. In addition, polymers containing large free volume fractions (e.g. PMA) have low T_g's, hence the incorporation of these values of T_g into the SB equation resulted in small free volume fractions.

(4) It was observed that the effect of a methyl group in the α-position on the properties of acrylate polymers was more pronounced than the substituents of the ester group. A two-fold increase in free volume fraction was observed between PMA and PMMA, whereas only a slight increase was observed between PMMA and PEMA. On the other hand, a large decrease in T_g and T_{on} were observed for PMA while T_g and T_{on} for PEMA, PIBMA and

PBzylMA were found to be similar. Strong intramolecular hydrogen bonding between polar hydroxy groups in PHEMA resulted in low values of α'_g and fractional free volume. This in turn, had the opposite effect on the transition temperatures, in which high values were observed for T_g and T_{on} of PHEMA.

Chapter 11

1. S.S. Rogers and L. Mandelkern, *J. Phys. Chem.* **61**, 985 (1957).
2. R. Simha and R.F. Boyer, *J. Chem. Phys.* **37(5)**, 1003 (1962).
3. L.A. Wood, *J. Polym. Sci.* **28**, 319 (1958).
4. K. Illers, *Kolloid-Z.* **190**, 16 (1963).
5. J. Lal and G.S. Trick, *J. Polym. Sci.* **A2**, 4559 (1964).
6. W.J. Schell, R. Simha and J.J. Aklonis, J. Macromol. Sci. Chem. **A3(7)**, 1297 (1969).
7. M.L. Dannis, *J. Appl. Polym. Sci.* **1**, 121 (1959).
8. E.A.W. Hoff, D.W. Robinson and A.H. Willbourn, *J. Polym. Sci.* **18**, 161 (1955).
9. N.G. McCrum, B.E. Read and G. Williams, *Anelastic and Dielectric Effects in Polymeric Solids,* Wiley, London (1967).
10. M.C. Shen, J.D. Strong and F.J. Matusik, *J. Macromol. Sci. Phys.* **B1**, 15 (1967).
11. R.A. Haldon and R. Simha, *J. Appl. Phys.* **39(3)**, 1890 (1968).
12. R.A. Haldon and R. Simha, *Macromolecules* **1(4)**, 340 (1968).
13. K. Schemieder and K. Wolf, *Kolloid-Z.* **134**, 149 (1953).
14. A.E. Woodward, J.A. Sauer and R.A.Wall, *J. Polym. Sci.* **50**, 117 (1967).
15. M.C. Shen and A.V. Tobolsky, Adv. Chem. Ser. 48, 27 (1965).
16. M.C. Shen and A. Eisenberg, *Progress in Solid State Chemistry* **3**, 407 (1966).
17. R. Diaz-Calleja, A. Ribes-Greus and J.L. Gomez-Ribelles, *Polymer* **30**, 1433 (1989).
18. L.C.E. Struik. Polym. Eng. Sci. **18(10)**, 799 (1978).
19. L.C.E. Struik, *Internal Stresses, Dimensional Instabilities and Molecular Orientations in Plastics,* Wiley, Chichester, (1990).
20. H. Fujita and E. Maekawa, *J. Phys. Chem.* **66**, 1053 (1966).
21. S.C. Sharma, L. Mandelkern and F.C. Stehling, J. Polym. Sci. Polym. Lett. **10**, 345-356 (1972).

22. S. Loshaek, *J. Polym. Sci.* **15**, 391 (1955).

23. J.C. Wittman and A.J. Kovacs, *J. Polym. Sci. C* **16**, 4443 (1969).

24. S. Krause, J.G. Gormley, N. Roman, J.A. Shetter and W.H. Watanabe, *J. Polym. Sci. A* **3**, 3573 (1965).

25. *Catalogue Handbook of Fine Chemicals,* Aldrich Chemical Company, Milwaukee (1990).

26. P. Meares, *Polymers, Structure and Bulk Properties,* Van Nostrand, London (1965).

27. M.J. Richardson, *Comprehensive Polymer Science,* Volume **1**, C. Booth and C. Price eds., Chapter 36 (1989).

28. H.H.D. Lee and F.J. McGarry, *J. Macromol. Sci. Phys.* **B29(1)**, 11-29 (1990).

29. L.C.E. Struik, *Physical Ageing in Amorphous Polymers and Other Materials,* Elsevier, Amsterdam (1978).

30. J. Kolarik, *Adv. Polym. Sci.* **46**, 120 (1982).

31. J. Heijboer, J.M.A. Bass, B. van de Graaf and M.A. Hoefnagel, *Polymer* **28**, 509 (1987).

32. J.M.G. Cowie and R. Ferguson, *Polymer* **28**, 30 (1987).

33. J. Heijboer, *Physics of Non-Crystalline Solids,* North-Holland, Amsterdam (1965).

34. J. Koppelmann, *Physics of Non-Crystalline Solids,* North-Holland, Amsterdam (1965).

35. J. Heijboer, *Kolloid Z.* **134**, 149 (1956); **148**, 36 (1956).

36. J. Heijboer, *Private Communication,* in reference 9.

37. L.C.E. Struik, *Polym. Eng. Sci.* **17(3)**, 165 (1977).

CONCLUSION

A technique has been developed in which the structural and conformational rearrangement of glassy polymers is characterised by linear dimensional changes using a thermomechanical analyser. The sensitivity of this technique to small dimensional changes enabled a detailed investigation of the mechanisms that are associated with a number of processes which affect the dimensional stability of a polymer. The major component of this thesis was devoted to the study of physical ageing, which is characterised by length contraction in the vicinity of the glass transition region as the polymer is heated from below to above T_g. The major success of this study was to establish that the contraction is directly related to the collapse of free volume, which provided an alternative method for the quantitative measurement of free volume fraction. The characterisation of physical ageing as a function of length contraction provides a more suitable technique over the conventional method of volume dilatometry for the study of physical ageing.

This technique was also applied to a number of related phenomena such as randomisation, viscous flow and the relief of internal stresses. Dimensional changes associated with these processes may occur simultaneously during ageing, hence it was important that the individual contribution of each phenomenon to the observed change in dimensions was recognised. This work has been successful in distinguishing the dimensional changes associated with randomisation, viscous flow and the relief of internal stresses, but the separation of the effects of physical ageing from those arising from the sorption and desorption of diluents requires further study.

The manifestation of dimensional contraction in the glass transition region arising from physical ageing raises doubts if the T_g can be properly represented by the intersection of the extrapolated glass and liquid lines of V-T of L-T plots. It was found that experimental ΔL-T curves were appropriately characterised by the temperature range of contraction, (in the range 20-30 C) which was bounded by the onset and endset temperatures of contraction (T_{on} and T_{end}). The temperature T_{on} was associated with the onset of cooperative motion responsible for the glass transition, whereas T_{end} represented the limiting temperature for the attainment of equilibrium. Although the value of T_{on} was found to vary with heating rate, the use of T_{on} as

an indicator of the onset of cooperative motion was supported by good correlation with literature values of T_g obtained from volumetric data. The proposal that the attainment of equilibrium at T_{end} was supported by the work of Lee and McGarry [1], who observed that the complete removal of frozen-in free volume (i.e. the attainment of equilibrium) in atactic polystyrene was achieved only at *ca* 20-30 C above the extrapolated T_g.

Reports which claim to anneal polymer specimens to equilibrium at temperatures below T_g for an arbitrary period of time are therefore questionable. It is possible that the absence of observable changes in properties after ageing below T_g had led some researchers to presume that the specimen had attained equilibrium. These reports suggest that the temperature range of physical ageing had reached a limiting stage below T_g, where subsequent increases in ageing period will not yield further relaxation. Isothermal ageing data indicates that although some contraction was observed below T_g, it is unlikely that equilibrium can be attained without the participation of main-chain motion. In addition, the data predicts a small increase in free volume at temperatures below T_β, in accordance with the hypothesis that excess free volume will be generated by the freezing of side group motions [2-3]. This result also supports the controversial proposal of Struik [4-5] that physical ageing does not occur below T_β. Although conflicting experimental evidence [6-10] exist, a closer inspection of some these reports found that the specimens were aged at the high temperature side of the secondary β-transition, thus a conclusive argument about the effects of ageing *below* T_β cannot be reached.

The semi-quantitative free volume theory proposed by Struik [4-5] was found to be most appropriate in verifying experimental observations. However, there are some doubts if segmental mobility is determined solely by the available free volume fraction. This question was raised in the case of glassy P(MMA-co-[oligo(ethylene glycol) dimethacrylate] copolymers, where length contraction was observed to decrease with increasing crosslinker concentration such that contraction could not be observed above 50 mole fraction % crosslinker. This observation was attributed to the lack of segmental mobility as a result of the incorporation of rigid crosslinks into the MMA backbone chains, rather than the suggestion (as implied by the absence of contraction) that highly crosslinked polymers contain negligible free volume fraction. Glass expansion coefficients of pure crosslinked dimethacrylates suggest that highly crosslinked polymers may retain unaged free volume above T_g as a consequence of restricted segmental mobility.

Poly(methyl acrylate) represents a second example in which doubts are raised concerning the hypothesis that segmental mobility is controlled by free volume. An increase in the length or size of the substituents of the side group of a number of homologous series has been shown [2-3, 11-14] to result in an increase in free volume and a decrease in T_g. If the same trend was applied to substituents in the α-position, then according to Struik's hypothesis [4-5], the replacement of an α-methyl group by a hydrogen atom in PMA should result in a lower free volume fraction and lower mobility. On the contrary, the free volume fraction of PMA was found to be more than twice as large as that of PMMA or PEMA. The reason for this discrepancy is that the α-methyl group on adjacent repeating units in PMMA hinders the motion of the ester side group [15-16], and increases the energy barrier for such motion [17-18]. Hence, T_{on} of PMMA is located at a much higher temperature (104 C) than that of PMA (30 C), and unlike PMMA, physical ageing in PMA is facilitated by the lack of steric hindrance.

Free volume fractions derived from length contractions were compared with the results of Williams, Landel and Ferry (WLF) [19] and Simha and Boyer (SB) [2]. Although the WLF and SB theories employ different definitions of free volume, both theories support the hypothesis that the free volume fraction is constant at T_g. However, results obtained in this work show that the free volume fraction is not constant and is affected by the thermal history and molecular structure of the polymer. Slow-cooled and annealed specimens which have been equilibrated above T_g exhibit smaller contractions than quenched specimens. In general, the free volume fraction increases with decreasing molecular weight and increasing side-chain length, plasticiser concentration and cooling rate past T_g. On the other hand, the presence of fillers in PHEMA-KBr specimens was found to decrease the free volume fraction.

A review of positron annihilation lifetime spectroscopy (PALS) studies of polycarbonate [20-23], poly(vinyl acetate) [24] and PMMA [25] showed that the average size and concentration of free volume may be represented by the lifetime parameters of the orthopositronium component. PALS represents a potentially powerful technique for investigating individual contributions to variations in free volume from changes in the average hole size and in the number of free volume holes. However, the results of Hill *et al.* [20-23] indicated that the free volume fraction remained constant during ageing. This represented a significant discrepancy since the collapse of free volume during physical ageing has been observed by many authors [1, 26-37], including experimental results contained in this thesis.

The investigation of the nature and structure of acrylic polymers was not restricted only to the observation of length contraction which is associated with physical ageing. Internal stresses caused by rapid cooling from above to below T_g also resulted in dimensional instability. Two peculiar characteristics were noted in ΔL-T plots of as-cast PMMA specimens, firstly, α_g was lower than for specimens which had been thermally equilibrated above T_g, and a sudden expansion was observed near T_{end}. Low values of α_g was attributed to frozen-in internal stresses, in which rapidly cooled polymers were found [38-41] to contain compressive stresses at the surface and tensile stresses in the interior. Curing stresses generated during monomer casting were also found [42-43] to be compressive in nature. The combination of contraction forces arising from cooling and curing stresses led to a lower expansion coefficient in the glass state.

Secondly, low values of α_g was also attributed to molecular orientation which was frozen-in during cooling of the mould from the postcure temperature of 125 C to ambient temperature. Randomisation, or the release of molecular orientation, was observed when compressed PMMA specimens were heated to above T_{end}. Length changes associated with randomisation was found to depend on the direction of measurement relative to the axis of orientation. In the case where the measurement was carried out parallel to the orientation axis, length contraction was observed in which the temperature range of randomisation was found to be between *ca* 125-135 C. On the other hand, length expansion is observed when the measurement was made perpendicular to the axis of orientation.

It was observed that physical ageing of crosslinked polymers become less significant at high crosslink densities as these polymers exhibited very little contraction. However, the glass and liquid expansion coefficients were found to reflect the thermal history of the polymer, in which polymers containing large free volume fractions tend to have larger glass expansivities than polymers with low free volume fractions. The observation of large values of expansivities in quenched polymers is attributed to the expansion of the free volume when the polymer is heated, e.g. α'_g of quenched PMMA (200.7×10^{-6} K^{-1}) is higher than the corresponding value of slow-cooled PMMA (153.6×10^{-6} K^{-1}) (Tables 4.5-4.6), while the free volume fraction of slow-cooled PMMA (0.0575) is smaller than that of quenched PMMA (0.107) (Tables 4.1-4.2) measured at 5 C/min.

The characterisation of structural rearrangement by length measurement is limited, however, in the case of polymers which undergo viscous flow above T_g. Examples of such polymers are low molecular weight PMMA and highly-plasticised (> 30 mol/mol % of plasticiser) PMMA. Viscous flow was recognised by continual contraction at temperatures well above T_g, which does not allow the measurement of liquid expansivity nor the free volume fraction. A preliminary study on the dimensional instability of partially hydrated PHEMA specimens suggested that measurements of dimensional changes may be used to deduce the nature and distribution of water molecules in PHEMA. It was suggested that the distribution of water in PHEMA was dependent on both the amount of water present and the duration in which the specimen was hydrated. Although the results of this investigation are tentative, the interesting nature of this study merits further research involving PHEMA specimens which contain larger amounts of water.

BIBLIOGRAPHY

1. H.H.D. Lee and F.J. McGarry, *J. Macromol. Sci. Phys.* **B29(1)**, 11-29 (1990); **B29(2&3)**, 185-202 (1990); **B29(2&3)**, 237-248 (1990).

2. R. Simha and R.F. Boyer, *J. Chem. Phys.* **37**, 1003 (1962).

3. R.A. Haldon and R. Simha, *J. Appl. Phys.* **39(3)**, 1890 (1968).

4. L.C.E. Struik, *Polym. Eng. Sci.* **17**, 165 (1977).

5. L.C.E. Struik, *Physical Ageing in Amorphous Polymers and Other Materials,* Elsevier, Amsterdam (1978).

6. V.E. Malpass, *Appl. Polym. Symp.* **12**, 267 (1969).

7. L. Guerdox and E. Marchal, *Polymer* **22**, 1199 (1981).

8. E. Ito, K., Tajima and Y. Kobayashi, *Polymer* **24**, 877 (1983).

9. E.J. Roche, *Polym. Eng. Sci.* **23**, 390 (1983).

10. G.P. Johari, *J. Chem. Phys.* **77**, 4619 (1982).

11. L.A. Wood, *J. Polym. Sci.* **28**, 319 (1958).

12. K.H. Illers, *Makromol. Chem.* **127**, 1 (1969).

13. J. Lal and G.S. Trick, *J. Polym. Sci.* **A2**, 4559 (1964).

14. M.L. Dannis, *J. Appl. Polym. Sci.* **1**, 121 (1959).

15. N.G. McCrum, B.E. Read and G. Williams, *Anelastic and Dielectric Effects in Polymeric Solids,* Wiley, London (1967).

16. J. Kolarik, *Adv. Polym. Sci.* **46**, 120 (1982).

17. J. Heijboer, J.M.A. Bass, B. van de Graaf and M.A. Hoefnagel, *Polymer* **28**, 509 (1987).

18. J.M.G. Cowie and R. Ferguson, *Polymer* **28**, 30 (1987).

19. M.L. Williams, R.F. Landel and J.D. Ferry, *J. Am. Chem. Soc.* **77**, 3701 (1955).

20. A.J. Hill, K.J. Heater and C.M. Agrawal, *J. Polym. Sci. Polym. Phys.* **28**, 387 (1990); *J. Mat. Sci. Lett.* **8**, 1414 (1989).

21. A.J. Hill and C.M. Agrawal, *J. Mat. Sci.* **25**, 5036 (1990).

22. A.J. Hill, *Materials Forum* **14**, 174-182 (1990).

23. A.J. Hill, I.M. Katz and P.L. Jones, *Polym. Eng. Sci.* **30(13)**, 762 (1990).

24. Y. Kobayashi, W. Zheng, E.F. Meyer, J.D. McGervey, A.M. Jamieson and R. Simha, *Macromolecules* **22**, 2302-2306 (1989).

25. Y.C. Jean, H. Nakanishi, L.Y. Hao and T.C. Sandreczki, *Phys. Rev. B* **42(15)**, 9705 (1990).

26. J. Perez, *Polymer* **29**, 483 (1988).

27. T.S. Chow, *Polym. Eng. Sci.* **79**, 4602 (1985); *Macromolecules* **17**, 2336 (1984).

28. A.J. Kovacs, J.J. Aklonis, J.M. Hutchinson and A.R. Ramos, *J. Polym. Sci. Polym. Phys. Ed.* **17**, 1097 (1979).

29. J.B. Enns and J.K. Gillham, *J. Appl. Polym. Sci.* **28**, 2831 (1983).

30. G. Goldbach and R. Rehage, *J. Polym. Sci.* **C16**, 2289 (1967); *Rheol. Acta* **6**, 30 (1967).

31. R.E. Robertson, *J. Polym. Sci. Symp.* **63**, 173 (1978); *J. Polym. Sci. Phys.* **17**, 597 (1979).

32. D.G. LeGrand, *J. Appl. Polym. Sci.* **13**, 2129 (1969).

33. L.C.E. Struik, *Rheol. Acta* **5**, 303 (1966); *Plast. Rubb. Process. Appl.* **2**, 41 (1982).

34. M.G. Wyzgoski, *Polym. Eng. Sci.* **16**, 265 (1976); *J. Appl. Polym. Sci.* **25**, 1443 (1980).

35. C.K. Chai and N.G. McCrum, *Polymer* **21**, 706 (1980).

36. G. Levita and T.L. Smith, *Polym. Eng. Sci.* **21**, 936 (1981).

37. M.R. Tant and G.L. Wilkes, *Polym. Eng. Sci.* **21**, 874 (1981).

38. L.C.E. Struik, *Polym. Eng. Sci.* **18(10)**, 799 (1978).

39. W.D. Callister Jr., *Materials Science and Engineering, An Introduction,* Wiley (1991),

40. P. So and L.J. Broutman, *Polym. Eng. Sci.* **16(21)**, 785 (1976).

41. L.E. Hornberger and K.L. Davies, *Polym. Eng. Sci.* **27(19)**, 1473 (1987).

42. M. Shimbo, M. Ochi and Y. Shigeta, *J. Appl. Polym. Sci.* **26**, 2265-2277 (1981).

43. A.R. Plepys and R.J. Farris, *Polymer* **31**, 1932 (1990).